

WITS
UNIVERSITY

Total synthesis of the analogues of pavettamine

Memory Zimuwandeyi

A thesis submitted to the Faculty of Science, University of the Witwatersrand, in fulfilment of the requirements of the Doctor of Philosophy

19 April 2020

Declaration

I declare that the work presented in this thesis was carried out exclusively by myself under the supervision of Prof Moira L. Bode and Prof Amanda Rousseau. It is being submitted for the degree of Doctor of Philosopy at the University of the Witwatersrand, Johannesburg. It has not been submitted before for any degree or any examination in any other University.



Memory Zimuwandeyi

19 April 2020

Abstract

Pavettamine, a plant toxin isolated from *Pavetta harborii*, was previously identified as a polyamine with C-2 symmetry and a 1,3-*syn*-diol moiety on a C-10 carbon backbone (one of very few to be isolated from nature). Biological studies have shown that this toxin is responsible for "quick disease" (gousiekte) in ruminant animals which causes inhibition of protein synthesis in the cardiovascular organs. The uniqueness of pavettamine coupled with its toxicological effects prompted this study, which aims to contribute towards the complete study of the structure activity relationships associated with its toxicity. To this end, the first total synthesis of the enantiomer of pavettamine was achieved together with the development of a suitable method for the synthesis of reduced functionality analogues.

The symmetrical structure of the molecule allows for the synthesis of two individual C_5 fragments to be coupled at a later stage. Retrosynthetic analysis identified commercially available *S*-malic acid as a suitable starting material for synthesis of the two individual C_5 fragments. This chiral hydroxyl acid from nature's pool constitutes a β-hydroxy ketone group. Several transformations of *S*-malic acid allowed for the addition of the *R*-methyl *p*-tolyl sulfoxide chiral auxiliary, facilitating stereoselective reduction of the ketone, and affording the desired 1,3-*syn*-diol functionality. A protecting group strategy was also developed for the orthogonal protection of the alcohol and amine functional groups as they were unveiled. From this point onwards the terminal carbon atoms of the separate C_5 fragments were functionalised, followed by coupling of the fragments via reductive amination revealing the C-10 carbon backbone. Deprotection of the alcohols and amines successfully provided the enantiomer of pavettamine as a TFA salt. Application of a similar synthetic protocol afforded acetonide protected pavettamine. A method was also developed for the synthesis of the reduced functionality analogues lacking certain hydroxyl groups.

List of abbrevations

APAO	acetylpolyamine oxidase
Bn	benzyl alcohol
BnBr	benzyl bromide
Boc	*tert*-butyloxycarbonyl
CAN	ceric ammonium nitrate
COSY	correlation spectroscopy
1,2-DCE	1,2-dichloroethane
DCM	dichloromethane
d.e.	diastereomeric excess
DEPT	distortioneless enhancement by polarisation transfer
DMAP	4-dimethylaminopyridine
DMP	Dess-Martin periodinane
DNA	deoxyribonucleic acid
2,4-DNP	2,4-dinitrophenylhydrazine
e.e	enantiomeric excess
EtOAc	ethyl acetate
Hex	hexane
HRMS	high resolution mass spectroscopy
IBX	2-iodoxybenzoic acid
iGluRs	ionotropic glutamic receptors
IR	infrared

LDA	lithium diisopropylamide
MeCN	acetonitrile
MeOH	methanol
NMDA	*N*-methyl D-aspartate
NMR	nuclear magnetic resonance
NOESY	nuclear Overhauser effect spectroscopy
ODC	ornithine decarboxylase
PA	polyamine
PAT	polyamine transporter
PCC	pyridinium chlorochromate
RNA	ribonucleic acid
SMO	spermine oxidase
SSAT	spermidine/spermine N^1 acetyltransferase
TBAF	*tetra*-*n*-butylammonium fluoride
TBS	*tert*-butyldimethylsilyl
TFAA	trifluoroacetic anhydride
TFA	trifluoroacetic acid
THF	tetrahydrofuran
TLC	thin layer chromatography
TMSCN	trimethylsilyl cyanide
TrCl	trityl chloride
TsCl	tosyl chloride

Acknowledgements

There is an African proverb which loosely translates to, ‘give people praises whilst they are still alive and not by their grave’ and that is the ethos I live by. I consider myself fortunate and blessed to have worked with my supervisor, Prof Moira Bode and co-supervisor Prof Amanda Rousseau. Their guidance, leadership, encouragement and support was priceless. In this regard, I sincerely thank my supervisors for carving out the chemist and leader in me and I will forever be grateful. I would also like to thank Prof C de. Koning, Prof J. Michael, Prof D. Brady and Dr M. Makatini for assistances they made for this project to be a success.

The accomplishments of this project were made possible by the contributions of; NRF, Wits University and the School of Chemistry for funding and provision of research workspace. A big thank you goes to all those who assisted with data analysis; Dr I. Kotze, Dr M. Johnson and Dr H. Henning for NMR spectroscopic analysis, Thapelo Mbhlele for HRMS analysis and Prof M. Fernandes for X-ray crystallographic analysis. I will cherish the supportive and fun members of the Wits organic research group; Charles, Jean, Donald, Songeziwe, Peter, Kennedy, Kamogelo, Adelaide, Mpumi and Fatema. You guys created a conducive working environment.

A special mention goes to my lunch friends Juanita, Nosipho, Izak, Myron and Siya for their continuous encouragement, which was vital for this journey. Your continuous reminder that I was the only one without a PhD made me work harder. To Yvonne and Kuda you were there from day zero, your support carried my through it all.

To my parents, I thank you for instilling the values that have carried me through this journey. To the rest of my family I thank you for your support you guys are amazing.

Finally to my husband Tapiwa, words fail me because your unwavering support was more than I could have ever hoped for. Your complete support, love and belief in my capabilities made this journey a ridable one. From the bottom of my heart, I thank you.

Ebenezer!

Table of contents

Declaration ..... **i**

Abstract ..... **ii**

List of abbrevations ..... **iii**

Acknowledgements ..... **v**

Table of contents ..... **vi**

Chapter 1: Introduction **1**

1.1 Polyamines 1

1.1.1 Biological functions of polyamines 2

1.1.2 The polyamine transporter (PAT) 3

1.2 Polyamine conjugates 4

1.2.1 Polyamine conjugates from spiders and wasps 4

1.2.2 Macrocyclic and linear alkaloid polyamines from plants 7

1.2.3 Polyamine alkaloids from marine organisms 8

1.3 Synthetic polyamine analogues 9

1.4 Hydroxylated natural polyamines 14

1.4.1 Pavettamine 15

1.5 Synthetic methods for 1,3-diols 17

1.5.1 Carbon-carbon bond forming reactions 17

1.5.2 Biocatalytic methods 22

1.5.3 Synthesis of 1,3-diols using the aldol reaction 24

1.5.4 Synthesis of 1,3-diols via stereoselective reduction of ketones 29

1.6 Hydroxy acids from the chiral pool 37

1.6.1 Malic acid carboxylic acid differentiation methods 40

1.7 Aims of the project 41

1.7.1 Retrosynthetic analysis 42
1.7.2 Proposed synthetic approach 43
Chapter 2: Results and Discussion 46
2.1 Introduction 46
2.2 Synthesis of the enantiomer of pavettamine 46
2.2.1 Synthesis of the 1,3-*syn*-diol intermediate 124 46
2.2.2 An alternative method for the synthesis of key intermediate 124 65
2.2.3 Synthesis of fragment 1 and fragment 2 76
2.2.4 A different approach to the synthesis of the enantiomer of pavettamine 112 90
2.3 Synthesis of pavettamine 101
2.4 Synthesis of the reduced functionality analogues. 112
Chapter 3: Conclusion and future work 136
Chapter 4: Experimental procedures 142
4.1 General Experimental Procedures 142
4.1.1 Purification of solvents and reagents 142
4.1.2 Chromatography 142
4.1.3 Spectroscopic and physical data 142
4.2 Experimental data 143
4.2.1 Preparation of (*S*)-4-(benzyloxy)-3-hydroxy-4-oxobutanoic acid 126 143
4.2.2 Preparation of (*S*)-dimethyl 2-hydroxysuccinate 128 143
4.2.3 Preparation of (*S*)-methyl 3,4-dihydroxybutanoate 129 144
4.2.4 Preparation of (S)-methyl 2-(2,2-dimethyl-1,3-dioxolan-4-yl)acetate 132 144
4.2.5 Preparation of (-)-(*S*)-menthyl *p*-toluene sulfinate 136 145
4.2.6 Preparation of (+)-(*R*)-methyl *p*-tolylsulfoxide 137 146
4.2.7 Preparation of (*S*(*R*),4*S*)-4,5-*O*-isopropylidene-1-*p*-tolylsulfinyl-2-pentanone 138 147

4.2.8 Preparation of (*S*(*R*),2*R*,4*S*)-4,5-*O*-isopropylidene-1-(*p*-tolylsulfinyl)-pentane-2,4,5-triol 139……147

4.2.9 Preparation of (*S*(*R*),2*R*,4*S*)-1-(*p*-tolylsulfinyl)-pentane-2,4,5-triol 140 148

4.2.10 Synthesis of (2*R*,4*S*)-1-((*S*)-*p*-tolylsulfinyl)-5-(trityloxy)pentane-2,4-diol 141 149

4.2.11 Synthesis of (4*R*,6*S*)-2,2-dimethyl-4-(((*S*)-*p*-tolylsulfinyl)methyl)-6-((trityloxy)methyl)-1,3-dioxane 124.....150

4.2.12 Synthesis of (*S*)-methyl 3-hydroxy-4-(trityloxy)butanoate 142 150

4.2.13 Synthesis of (*S*)-methyl 3-((*tert*-butyldimethylsilyl)oxy)-4-(trityloxy)butanoate 143 ……151

4.2.14 Sulfoxide addition to (S)-methyl 3-((tert-butyldimethylsilyl)oxy)-4-(trityloxy)butanoate 145.....151

4.2.15 Synthesis of (2*R*,4*S*)-4-((*tert*-butyldimethylsilyl)oxy)-1-((*R*)-*p*-tolylsulfinyl)-5-(trityloxy)pentan-2-ol 150.....153

4.2.16 Synthesis of (2*R*,4*S*)-1-((*S*)-*p*-tolylsulfinyl)-5-(trityloxy)pentane-2,4-diol 141 154

4.2.17 Synthesis of (4*R*,6*S*)-2,2-dimethyl-6-((trityloxy)methyl)-1,3-dioxane-4-carbaldehyde 151……154

4.2.18 Synthesis of *N*-benzyl-1-((4*R*,6*S*)-2,2-dimethyl-6-((trityloxy)methyl)-1,3-dioxan-4-yl)methanamine 152 155

4.2.19 Synthesis of (2*S*,4*R*)-5-aminopentane-1,2,4-triol 153 155

4.2.20 ((4*R*,6*S*)-2,2-dimethyl-6-((trityloxy)methyl)-1,3-dioxan-4-yl)methanamine 154 ...156

4.2.21 Synthesis of *tert*-butyl (((4*R*,6*S*)-2,2-dimethyl-6-((trityloxy)methyl)-1,3-dioxan-4-yl)methyl)carbamate 155.....156

4.2.22 Synthesis of *tert*-butyl (((4*R*,6*S*)-6-(hydroxymethyl)-2,2-dimethyl-1,3-dioxan-4-yl)methyl)carbamate 156.....157

4.2.23 Synthesis of ((4*S*,6*R*)-6-(((*tert*-butoxycarbonyl)amino)methyl)-2,2-dimethyl-1,3-dioxan-4-yl)methyl 4-methylbenzenesulfonate 157 157

4.2.24 Synthesis of *tert*-butyl (((4*R*,6*S*)-6-(azidomethyl)-2,2-dimethyl-1,3-dioxan-4-yl)methyl)carbamate 158.....158

4.2.25 Synthesis of *tert*-butyl (((4*R*,6*S*)-6-(aminomethyl)-2,2-dimethyl-1,3-dioxan-4-yl)methyl)carbamate 159.....159

4.2.26 Synthesis of *tert*-butyl (((4*R*,6*S*)-6-formyl-2,2-dimethyl-1,3-dioxan-4-yl)methyl)carbamate 160.....159

4.2.27 Synthesis of di-*tert*-butyl (((4*R*,4'*R*,6*S*,6'*S*)-6,6'-(azanediylbis(methylene))bis(2,2-dimethyl-1,3-dioxane-6,4-diyl))bis(methylene))dicarbamate 161.....160

4.2.28 Synthesis of (2*R*,2'*R*,4*S*,4'*S*)-5,5'-azanediylbis(1-aminopentane-2,4-diol) 112.....160

4.2.29 Synthesis of ((4*R*,6*S*)-2,2-dimethyl-6-((trityloxy)methyl)-1,3-dioxan-4-yl)methanol 162.....161

4.2.30 Synthesis of *tert*-butyl(((4*R*,6*S*)-2,2-dimethyl-6-((trityloxy)methyl)-1,3-dioxan-4-yl)methoxy)dimethylsilane 163.....161

4.2.31 Preparation of (2*S*,4*R*)-5-((*tert*-butyldimethylsilyl)oxy)pentane-1,2,4-triol 164.....162

4.2.32 Synthesis of ((4*S*,6*R*)-6-(((*tert*-butyldimethylsilyl)oxy)methyl)-2,2-dimethyl-1,3-dioxan-4-yl)methanol 165.....163

4.2.33 Synthesis of ((4*S*,6*R*)-6-(((*tert*-butyldimethylsilyl)oxy)methyl)-2,2-dimethyl-1,3-dioxan-4-yl)methyl 4-methylbenzenesulfonate 166.....163

4.2.34 Synthesis of (((4*R*,6*S*)-6-(azidomethyl)-2,2-dimethyl-1,3-dioxan-4-yl)methoxy)(*tert*-butyl)dimethylsilane 167.....164

4.2.35 Synthesis of ((4*S*,6*R*)-6-(((*tert*-butyldimethylsilyl)oxy)methyl)-2,2-dimethyl-1,3-dioxan-4-yl)methanamine 168.....164

4.2.36 (4*S*,6*R*)-6-(((*tert*-butyldimethylsilyl)oxy)methyl)-2,2-dimethyl-1,3-dioxane-4-carbaldehyde 170.....165

4.2.37 Synthesis of bis(((4*S*,6*R*)-6-(((*tert*-butyldimethylsilyl)oxy)methyl)-2,2-dimethyl-1,3-dioxan-4-yl)methyl)amine 171.....166

4.2.38 Synthesis of ((4*R*,4'*R*,6*S*,6'*S*)-6,6'-(azanediylbis(methylene))bis(2,2-dimethyl-1,3-dioxane-6,4-diyl))dimethanol 172.....166

4.2.39 Synthesis of ((4*R*,4'*R*,6*S*,6'*S*)-6,6'-((tosylazanediyl)bis(methylene))bis(2,2-dimethyl-1,3-dioxane-6,4-diyl))bis(methylene) bis(4-methylbenzenesulfonate) 173.....167

4.2.40 Synthesis of *N*,*N*-bis(((4*S*,6*R*)-6-(azidomethyl)-2,2-dimethyl-1,3-dioxan-4-yl)methyl)-4-methylbenzenesulfonamide 174 167

4.2.41 Synthesis of ((4*R*,6*S*)-2,2-dimethyl-6-((trityloxy)methyl)-1,3-dioxan-4-yl)methyl 4-methylbenzenesulfonate 175 168

4.2.42 Synthesis of (4*R*,6*S*)-4-(azidomethyl)-2,2-dimethyl-6-((trityloxy)methyl)-1,3-dioxane 176..... 168

4.2.43 Preparation of ((4*R*,6*S*)-2,2-dimethyl-6-((trityloxy)methyl)-1,3-dioxan-4-yl)methanamine 154 169

4.2.44 Preparation of bis(((4*R*,6*S*)-2,2-dimethyl-6-((trityloxy)methyl)-1,3-dioxan-4-yl)methyl)amine 177 169

4.2.45 Synthesis of ((4*S*,4'*S*,6*R*,6'*R*)-6,6'-(azanediylbis(methylene))bis(2,2-dimethyl-1,3-dioxane-6,4-diyl))dimethanol 179 170

4.2.46 Synthesis of ((4*S*,4'*S*,6*R*,6'*R*)-6,6'-((tosylazanediyl)bis(methylene))bis(2,2-dimethyl-1,3-dioxane-6,4-diyl))bis(methylene) bis(4-methylbenzenesulfonate) 180..... 171

4.2.47 Synthesis of ((4*S*,4'*S*,6*R*,6'*R*)-6,6'-(azanediylbis(methylene))bis(2,2-dimethyl-1,3-dioxane-6,4-diyl))dimethanol 181 172

4.2.48 Synthesis of ((4*S*,4'*S*,6*R*,6'*R*)-6,6'-((tosylazanediyl)bis(methylene))bis(2,2-dimethyl-1,3-dioxane-6,4-diyl))bis(methylene) bis(4-methylbenzenesulfonate) 182..... 172

4.2.49 Synthesis of *N*,*N*-bis(((4*R*,6*S*)-6-(azidomethyl)-2,2-dimethyl-1,3-dioxan-4-yl)methyl)-4-methylbenzenesulfonamide 183 173

4.2.50 Synthesis of bis(((4R,6S)-6-(aminomethyl)-2,2-dimethyl-1,3-dioxan-4-yl)methyl)amine 184 173

4.2.51 Synthesis of (*R*)-5-chloro-1-(*p*-tolylsulfinyl)pentan-2-one 192..... 174

4.2.52 Synthesis of (*R*)-5-azido-1-(*p*-tolylsulfinyl)pentan-2-one 193 174

4.2.53 Synthesis of (*R*)-5-hydroxy-1-(*p*-tolylsulfinyl)pentan-2-one 195 175

4.2.54 Synthesis of (*S*)-5-((tert-butyldimethylsilyl)oxy)-1-(*p*-tolylsulfinyl)pentan-2-one 196..... 175

4.2.55 Synthesis of (*R*)-5-((*tert*-butyldimethylsilyl)oxy)-1-((*S*)-*p*-tolylsulfinyl)pentan-2-ol 197…… 176

4.2.56 Synthesis of (*R*,*E*)-*tert*-butyldimethyl((5-(*p*-tolylsulfinyl)pent-3-en-1-yl)oxy)silane…….....177

4.2.57 (((*R*)-4-(benzyloxy)-5-((*R*)-*p*-tolylsulfinyl)pentyl)oxy)(*tert*-butyl)dimethylsilane 200…….....178

4.2.58 Synthesis of (*R*)-4-(benzyloxy)-5-((*R*)-*p*-tolylsulfinyl)pentan-1-ol 201.....178

4.2.59 Synthesis of (*R*)-4-(benzyloxy)-5-((*R*)-*p*-tolylsulfinyl)pentyl methanesulfonate 202…… 179

4.2.60 Synthesis of (*R*)-*N*-benzyl-4-(benzyloxy)-5-((*R*)-*p*-tolylsulfinyl)pentan-1-amine 203…….....180

4.2.61 Synthesis of (*R*)-2-(benzyloxy)-5-((*tert*-butyldimethylsilyl)oxy)pentanal 204 180

4.2.62 Synthesis of (*R*)-5-(benzylamino)-4-(benzyloxy)pentan-1-ol 205.....181

4.2.63 Synthesis of (*R*)-4-(benzyloxy)-5-(4-methylphenylsulfonamido)pentyl 4-methylbenzenesulfonate 182

4.2.64 Synthesis of (*R*)-*N*-(5-azido-2-(benzyloxy)pentyl)-4-methylbenzenesulfonamide 208…… 182

4.2.65 Synthesis of (*R*)-2-(benzyloxy)-5-((*tert*-butyldimethylsilyl)oxy)pentan-1-ol 210....183

4.2.66 Synthesis of (*R*)-2-(benzyloxy)-5-((*tert*-butyldimethylsilyl)oxy)pentyl 4-methylbenzenesulfonate 211 183

4.2.67 Synthesis of (*R*)-((5-azido-4-(benzyloxy)pentyl)oxy)(*tert*-butyl)dimethylsilane 212…… 184

4.2.68 Synthesis of (*R*)-2-(benzyloxy)-5-((*tert*-butyldimethylsilyl)oxy)pentan-1-amine 213…….....184

4.2.69 Synthesis of ((((*R*)-4-(benzyloxy)-5-((*S*)-*p*-tolylsulfinyl)pentyl)oxy)methanetriyl)tribenzene 214.....185

4.2.70 Synthesis of (*R*)-2-(benzyloxy)-5-(trityloxy)pentan-1-ol 215 186

4.2.71 (*R*)-2-(benzyloxy)-5-(trityloxy)pentyl 4-methylbenzenesulfonate 216.....186

4.2.72 Synthesis of (*R*)-(((5-azido-4-(benzyloxy)pentyl)oxy)methanetriyl)tribenzene 217…… 187

4.2.73 (*R*)-2-(benzyloxy)-5-(trityloxy)pentan-1-amine 218 187

4.2.74 Synthesis of (*R*)-2-(benzyloxy)-5-(trityloxy)pentanal 219.....188

4.2.75 Synthesis of (*R*)-bis((*R*)-2-(benzyloxy)-5-(trityloxy)pentyl)amine 220.....189

4.2.76 Synthesis of (4*R*,4'*R*)-5,5'-azanediylbis(4-(benzyloxy)pentan-1-ol) 221.....189

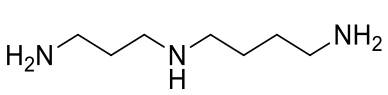
References ..... Error! Bookmark not defined.

Appendix.....197

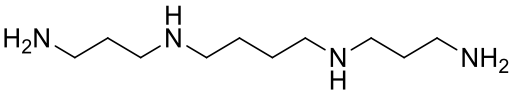
Chapter 1: Introduction

1.1 Polyamines

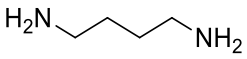
Research to date has uncovered a plethora of compounds that are vital for growth, development and sustenance of living organisms. Amongst this diverse group of compounds is a class of molecules named polyamines (PAs). Polyamines are described as aliphatic organic compounds with two or more primary amine substituents, connected by one or more methylene linkages within their structure.[1, 2] They were initially discovered in the 17th century although the elucidation of their chemical structure, knowledge of their biosynthesis and functions was not well understood until the 20th century.[3] Polyamines are ubiquitous; present in both eukaryotic and prokaryotic cells indicating the pivotal role they play in nature. The biogenic polyamines, putrescine, spermidine and spermine are the most fundamental molecules in this class of compounds (**Figure 1**).



spermidine



spermine



putrescine

Figure 1: Structure of basic polyamines

PAs also belong to an exclusive club of small organic compounds that are capable of interacting with the three natural biopolymers namely, polypeptides and proteins, nucleic acids and oligosaccharides. The observed interactions arise because of the amines' full protonation under physiological conditions. The resulting cationic factor enables these molecules to play different molecular roles in living organisms as shown in **Figure 2**, whilst allowing them to ionically bind to several anions in the cells including DNA, RNA, proteins and phospholipids, consequentially maintaining the structure of these macromolecules.[4]

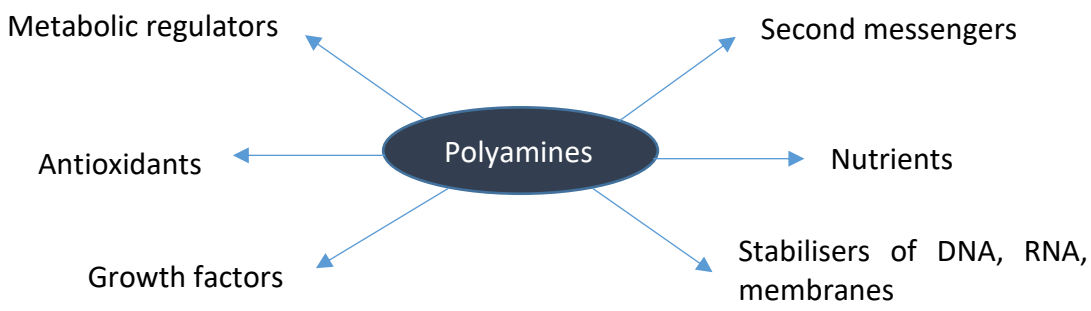


Figure 2: Biological functions of polyamines

1.1.1 Biological functions of polyamines

Comprehensive studies have shown that polyamines play an instrumental role in the promotion of cell growth, maintenance of chromatin conformation, regulation of specific gene expression, ion-channel regulation, maintenance of membrane stability and free radical scavenging.[5, 6, 7, 8] PAs are also involved in protein synthesis and in the differentiation of mammalian cells.[9] Interestingly, spermidine is also utilised as a precursor in the synthesis of the eukaryotic translation initiation factor 5A, the only protein known to contain the unusual amino acid hypusine.[10] Normal growth regulation is attributed to PAs and high concentrations of PAs are evident in fast multiplying animal tissues. Elevated levels of PAs are therefore required during development or tumour growth and this makes the biosynthesis of polyamines an important target for chemotherapeutic intervention. The charged nature of PAs facilitates interaction with various receptors e.g. *N*-methyl D-aspartate receptors (NMDA) and ion channels. The multiple studies of biogenic PAs have also revealed that interruption of the metabolic pathways provides targets for the design of therapeutic agents. These and other characteristics of PAs sparked an interest in their mechanism of action and the potential therapeutic uses of PA conjugates and synthetic analogues.

The ability of endogenous polyamines to play diverse functions within the biological systems resulted in studies being undertaken to understand their biosynthesis, metabolism and catabolism with the research spanning decades.[11] The synthetic pathway for polyamines in mammals, plants, fungi and many bacteria begins with the decarboxylation of the amino acid *L*-ornithine by ornithine decarboxylase (ODC) enzyme to afford putrescine as shown in **Figure 3**. ODC enzyme is therefore crucial in maintaining the levels of polyamines and it is highly regulated. Spermidine and spermine are synthesised from putrescine by the action of spermidine synthase and spermine synthase enzymes, respectively. The inherent feedback systems within the cells trigger the catabolic reactions when there is a higher demand or low concentration of either of the

polyamines.[12] Spermine can either undergo direct oxidation by spermine oxidase (SMO) or be acetylated by spermidine/spermine N^1 acetyltransferase (SSAT), followed by subsequent oxidation by acetylpolyamine oxidase (APAO) back to spermidine. Synthesis of putrescine follows the same pathway; whereby spermidine undergoes acetylation and oxidation using SSAT and APAO. Knowledge of the biosynthesis mechanism is useful in providing new targets for therapeutic treatment because several disorders arise as a result of a deficiency of the three polyamines.

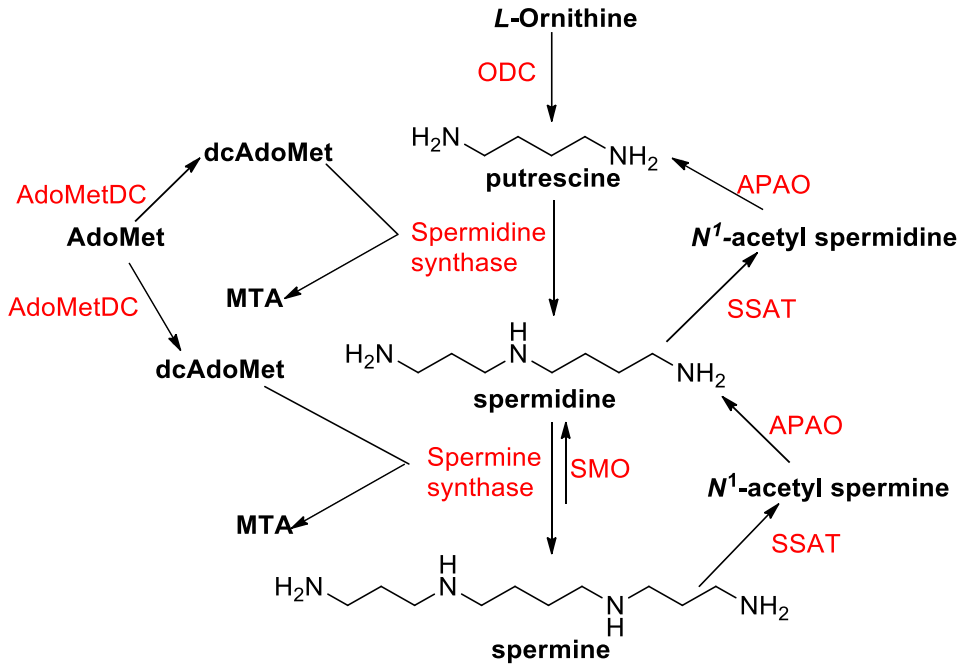


Figure 3: Biosynthesis and interconversion of polyamines (ODC – ornithine decarboxylase, AdoMetDC – *S*-adenosylmethionine decarboxylase, SMO – spermine oxidase, SSAT – spermidine/spermine N^1 acetyltransferase, APAO – acetylpolyamine oxidase)

1.1.2 The polyamine transporter (PAT)

Whilst the homeostasis and adjustment of intra-cellular concentrations of PAs is regulated by synthetic and catabolic reactions, delivery of PAs around the body and cellular entry is accomplished by a specific transport system known as the polyamine transporter (PAT).[8, 13, 14] The transport system is energy and temperature dependent and saturable, meaning it is carrier mediated. The recognition site of the transporter contains at least three negatively charged groups at a distance corresponding to the distance between the positively charged nitrogen atoms of spermidine.[13] This characteristic of the PAT implies that specific molecular recognition elements are required in order for molecules to utilise the PAT. Despite this, the polyamine has a surprisingly

broad structural tolerance. Current data attributes this to the fact that it is probable that there are multiple PAT systems in mammalian cells with differing specificities, allowing for the transportation of both natural compounds and a significant range of analogues.[15]

The polyamine transporter also serves as an adaptational response of cells to changes in polyamine requirements whereby enhanced growth rates are not only accompanied by accelerated rates of intracellular *de novo* synthesis but also by increased uptake of exogenous polyamines. Depletion of intracellular polyamines enhances their uptake seven-fold and this was proven by introducing ODC inactivators. This observation means that in principle the biosynthesis of PAs can be substituted by polyamine uptake from the environment. In addition to this since PAs are associated with proliferative responses and tumour promotion, research has identified polyamine regulation as an attractive target for a number of different anticancer chemotherapeutic strategies.[16, 15]

1.2 Polyamine conjugates

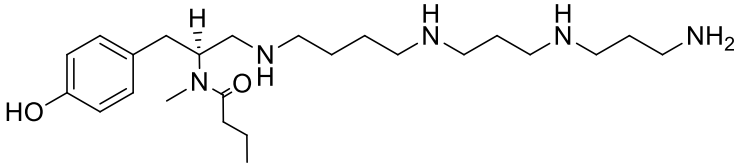
Apart from the three freely occurring biogenic PAs already mentioned, a multitude of PAs with different structural features have been isolated from various natural sources and their biological properties are under continual investigation.[1, 17, 18] These PAs are either linear or conjugated to various other moieties, including but not limited to aryl groups, amino acids, sugars and guanidine. A huge library of synthetic polyamine conjugates has also been developed and their biological effect assessed. These compounds are under ongoing investigation for their potential therapeutic activity against diseases such as cancer,[9, 19] malaria,[20] inflammation,[21] sleeping sickness,[22] Alzheimer's[23] and as antiproliferatives.[19] This list is by no means exhaustive but merely serves as an indicator of how widely varied the application of polyamines is. The sources of the naturally occurring polyamines are also varied and representative classes will be discussed in detail.

1.2.1 Polyamine conjugates from spiders and wasps

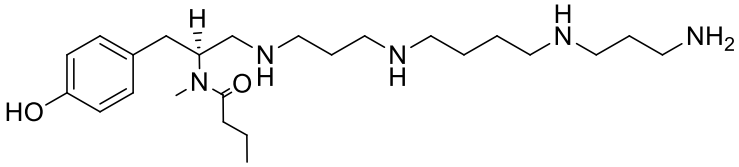
Venoms isolated from insects and amphibians contain polyamine toxins of extraordinary potency and selectivity. The interest in these toxins emanates from their usefulness in the discrimination of pharmacologically distinct receptor and ion channels in the nerves and muscles. Polyamine toxins isolated from spider and wasp venom act as potent antagonists of mammalian neuroexcitatory ionotropic glutamic acid receptors (iGluRs) and they inhibit nicotinic acetylcholine receptors.[24] Glutamate is the major excitatory amino acid neurotransmitter in the mammalian

central nervous system and acts through two classes of receptors, the ionotropic and metabotropic receptors. The polyamine toxins therefore act as pharmacological tools for examining the iGluRs due to their ability to distinguish between Ca^{2+} -permeable and – impermeable iGluR subtypes.[25] The distinction is necessary during diagnosis of neurodegenerative diseases.

Philanthus triangulum 433 (PhTX-4.3.3) is a polyamine that was isolated from the venom of *Philanthus triangulum*, a solitary parasitic wasp (**Figure 4**).[26] Investigations revealed that the toxin was an antagonist of Ca^{2+} permeable iGluR subtypes and kainate receptors, a characteristic that is useful for the determination of the subunit composition of these receptors.[27] Modification of the polyamine portion gave rise to philanthotoxins such as PhTX-3.4.3, with enhanced potency and selectivity at receptors.[28] The analogues were potent cation-channel blockers with uses as selective receptor probes for nicotinic acetylcholine and glutamate receptors for sodium and calcium channels.[29,30]



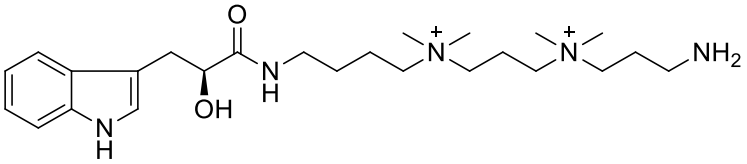
PhTX-4.3.3



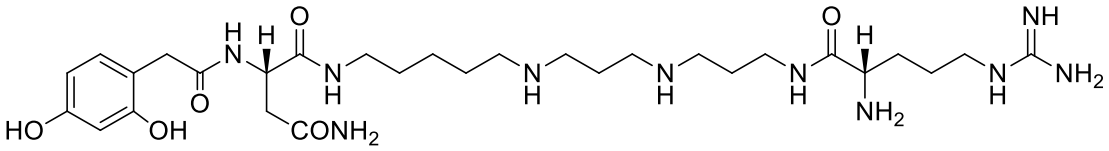
PhTX-3.4.3

Figure 4: Structures of PhTX-4.3.3 found in wasps and its analogue

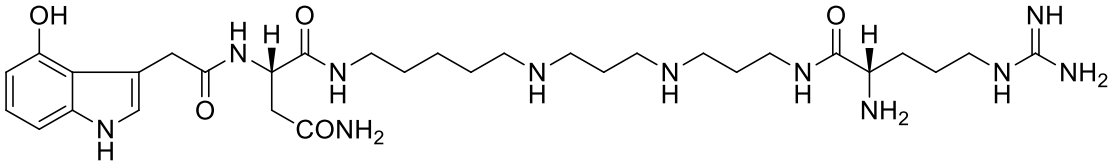
Compound MG30 (**Figure 5**) was isolated as the major component in the venom of the Hexathelidae spider *Macrothele gigas*.[31] Preliminary toxicological analysis of MG30 showed that it acted as an ion channel blocker. A huge library of toxins duly named acylpolyamines, because they share a common structure of an aromatic moiety at one end and either a primary amino or guanidine group at the other end, have been isolated from different species of spiders. These acylpolyamines exhibit neuromodulatory activity within the mammalian central nervous system; hence their application in investigating diseases such as stroke, Alzheimer's and epilepsy.[32]



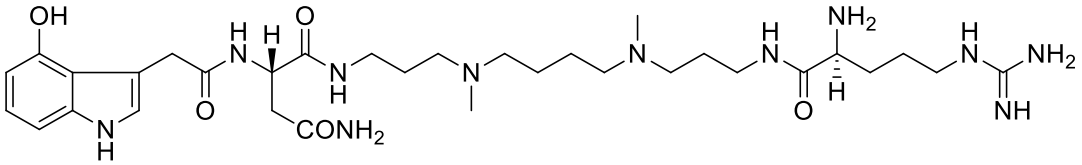
MG30



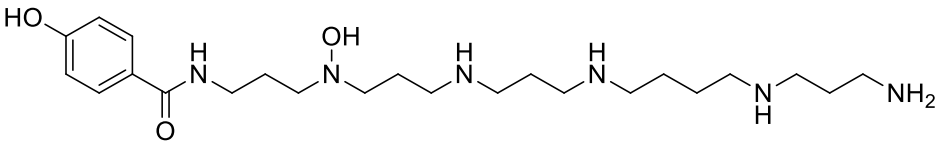
ArgTX-636



ArgTX-659



ArgTX-673



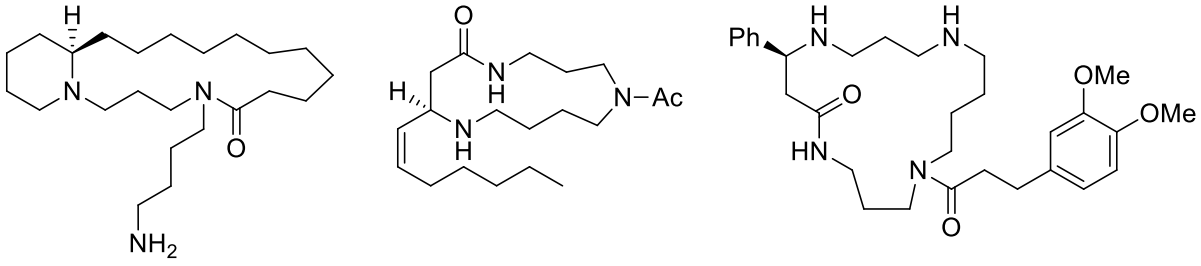
AGEL-452

Figure 5: Structures of PAs found in spiders

Another library of acylpolyamines isolated from different types of spiders, belonging to the argiotoxin class, are shown in **Figure 5**. Toxins ArgTX-636, ArgTX-659 and ArgTX-673 were isolated from the venom of the spider *Argiope aurantia.* AGEL-452 was isolated from the American funnel web spider *Agelenopsis aperta.*[33] Over fifty related polyamine toxins have been isolated and characterised from other species of spiders, and many of them have been synthesised.[12] Biological evaluation of these toxins and their analogues confirmed biological activity was through blocking neuromuscular junctions by primarily targeting the ionotropic glutamate receptors.[34] The interesting point to note about these polyamine toxins is that they contain methylene linkers having three or four carbon atoms without any substitution on the carbon chain backbone.

1.2.2 Macrocyclic and linear alkaloid polyamines from plants

A plethora of polyamine conjugates have also been isolated from plants and characterised, revealing both the macrocyclic and linear properties,[1, 5] with representative macrocyclic compounds shown in **Figure 6**. Oncinotine belongs to a group of alkaloid PAs isolated from the stem bark of *O. nitida*, a tree belonging to the genus *Oncinotis* (*Apocynaceae*).[35] Several other polyamine alkaloids were also isolated and characterised. *R*-Loesenerine was amongst a group of alkaloids isolated from *Maytenus loeseneri* containing a 13-membered lactam ring and total synthesis of the compound confirmed the stereochemistry.[36] *S*-Verbasitrine belongs to the protoverbine class of spermine alkaloids containing a 17-membered ring. This compound also contains a phenylpropionate unit which is contained in the antibacterial and cytotoxic spermine alkaloids.[1]



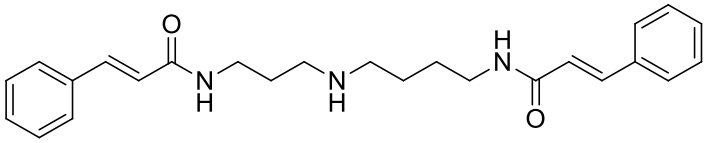
oncinotine **_R_-loesenerine** **_S_-verbasitrine**

Figure 6: Macrocyclic polyamines from plants

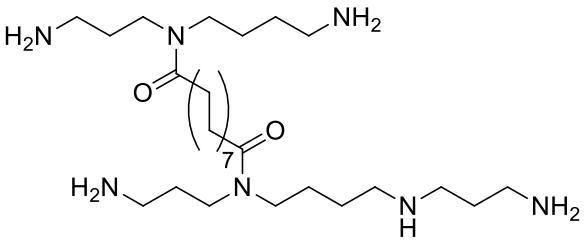
Biological analysis of the macrocyclic polyamine compounds revealed that the presence of the lone pairs of electrons on nitrogen enables the molecules to exhibit strong coordination ability towards different metal cations, forming coordination complexes.[37] Macrocyclic polyamines are tunable, allowing the creation of smart molecules with specific physical and chemical properties. These properties include, but are not limited to, chemical sensors and anion binders to a variety of compounds such as antibodies.[38] They can also cross-link with DNA and therefore act as anti-tumour agents and anti-protozoal agents.[39] Cyclic polyamines are used to prepare silica particles of controllable and uniform size in a procedure duly named the Stöber process.[40] A significant library of macrocyclic polyamines has been developed for studying their ability to form strong ion pairing complexes with phosphate-containing metabolites and to catalyse the dephosphorylation of ATP.[41] The polyamine complexes also find applications as chiral catalysts for organic reactions.

Other than the macrocyclic polyamines, plants also contain a variety of linear polyamines (**Figure 7**). Meytenine is an example of a linear PA that was isolated from the reproductive organs of many

higher plants as a conjugated spermidine.[5] Tenuilobine was isolated from the same source and is the first PA alkaloid containing both spermine and spermidine, cross-conjugated through a long aliphatic chain.[35] These toxins are known to act on invertebrates by antagonising ion-gated channel proteins in the muscle membrane.[42]



meytenine



tenuilobine

Figure 7: Linear polyamines from plants

1.2.3 Polyamine alkaloids from marine organisms

The ocean is a diverse ecosystem that has provided the human race with not only food and energy but chemotherapeutic agents as well. Marine sponges are known to be prolific producers of a wealth of diverse secondary metabolites including PAs. The wide array of structurally different polyamines that have been uncovered from these sponges require their own review because marine organisms provide an interesting and useful array of potentially therapeutic PA alkaloids. The structurally unique PA stellettadine A (**Figure 8**) was isolated from a marine sponge *Stelleta* sp. in 1996 and it was the first example of a polyamine alkaloid with the arcaine backbone (1,4-diguanidinobutane), which is connected to a norsesquiterpene moiety.[43] The compound was described as a metamorphosis inducer in ascidians. Crambescidin 826, belonging to the crambrescidin family, was isolated from the sponge *Monanchora* sp.[44] This PA alkaloid features a polycyclic guanidine core coupled to modified spermidine. Biological studies showed HIV-1 fusion inhibition properties, and thus this molecule represented an interesting lead structure for potentially new anti-HIV therapeutics.

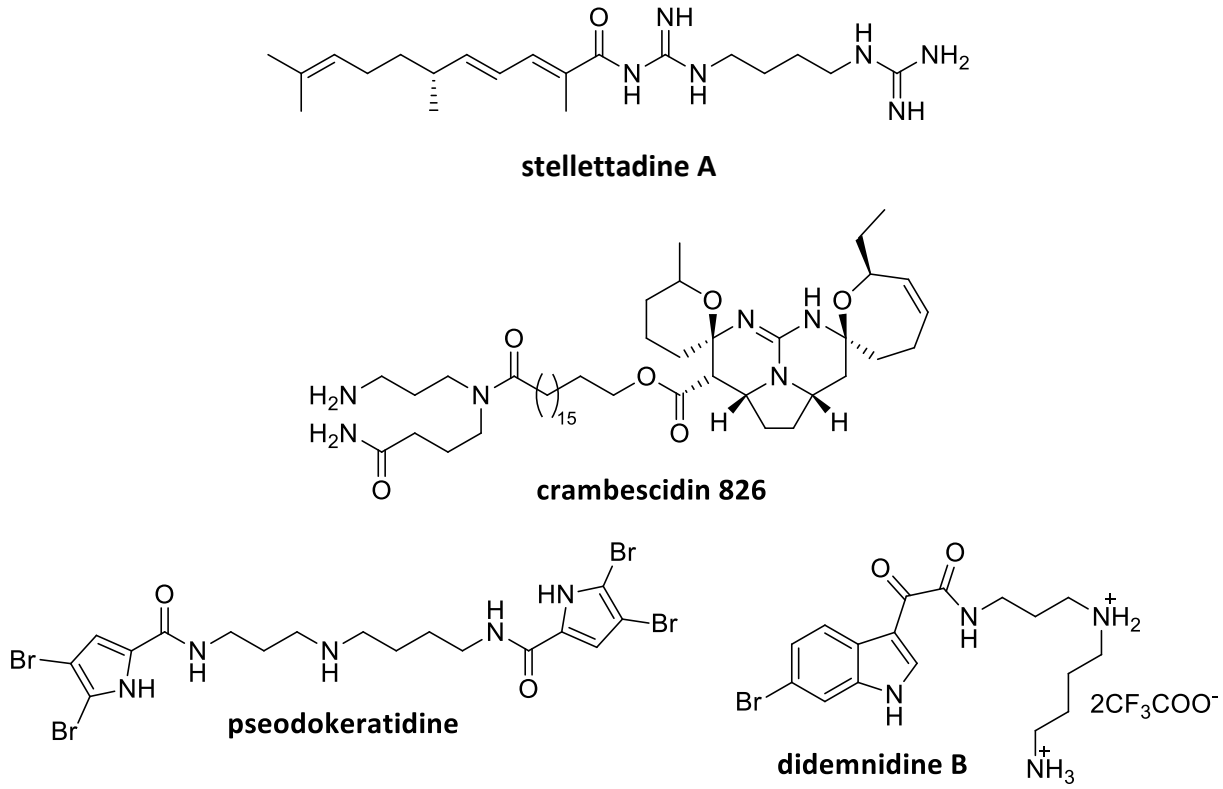


Figure 8: Polyamine alkaloids from marine organisms

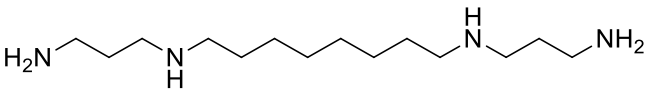
Pseudokeratidine, a halogenated PA conjugate, was isolated from marine sponges and displayed antifouling and antimicrobial activities making it of considerable interest as a component of antifouling paints.[26] Didemnidine B was isolated from *Didemnum* sp. together with several other similar PAs which contain an indole-3-glyoxylamide moiety linked to the N^1 position of spermidine.[45] This PA was found to be mildly active against the malarial parasite *Plasmodium falciparum* with an IC_{50} value of 8.4 µM.

1.3 Synthetic polyamine analogues

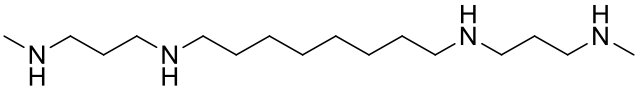
The positive results from biological assays of the naturally occurring polyamine conjugates provided the platform for a new research area of synthetic analogues. Initial studies involving synthesis of unnatural polyamines was targeted at understanding the influence of charge, length and flexibility of the polyamine backbone structure on biological activity. Since the polyamine biosynthetic pathway of mammalian organisms had been studied extensively, it had been shown that some pathogenic organisms possess enzymes involved in polyamine metabolism that were not present in the host.[6] This knowledge provided a need to design specific therapeutic agents targeting the PA in the pathogens. Research has already highlighted the importance of PAs in living organisms, and the continuous discovery of PAs from various natural sources with different

structural features provided the launch pad for research on polyamines. The initial working theory was that the terminal nitrogens of the linear polyamines are most important for biological activity.

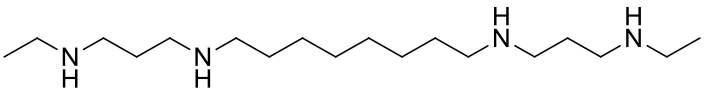
The first synthetic polyamines involved simple modifications of the natural polyamines i.e they possessed terminal primary or secondary amine groups with small alkyl substituents and differed only in the length of the central carbon chain.[16] Compounds **1** – **3** (**Figure 9**), with an eight carbon spacer generally showed significant antitumour activity. These results supported the theory that analogues with altered pK_a values at the terminal nitrogens, comparison of compound **1** to compound **2** and **3**, could disrupt polyamine metabolism and potentially provide therapeutic benefit. Of the initial benzyl analogues, compound **4** was the only one to act as an active antiproliferative agent, exhibiting an IC_{50} value of 50 µm against L1210 leukemia. Subsequently, the compound was shown to possess excellent antimalarial activity *in vitro* and *in vivo* but unfortunately no further investigations were performed on similar sets of analogues.[46]



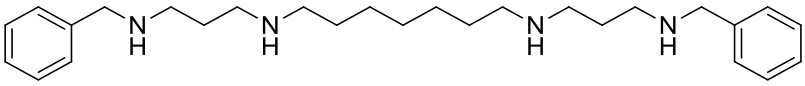
1



2



3



4

Figure 9: Early polyamine analogues

The early findings of the effects of synthetic polyamine analogues led to the design of symmetrical, terminally substituted bis(alkyl) polyamines. The analogues featured terminal secondary amines to explore the relationship between altered pKa and cellular function and the utilisation of the PA transporter by the modified polyamines. From a representative library, **Figure 10** shows synthetic analogues **5** – **8** which were shown to slow down the synthesis of biogenic polyamines through downregulation of constitutive biosynthetic enzymes, although they did not support the cellular

functions of the endogenous polyamines.[6] Treatment of tumour cells with micromolar concentrations of the analogues initiated cell death via apoptosis. These symmetrically substituted analogues are amongst the most successful as they have been shown to possess a wide variety of therapeutic effects.[11]

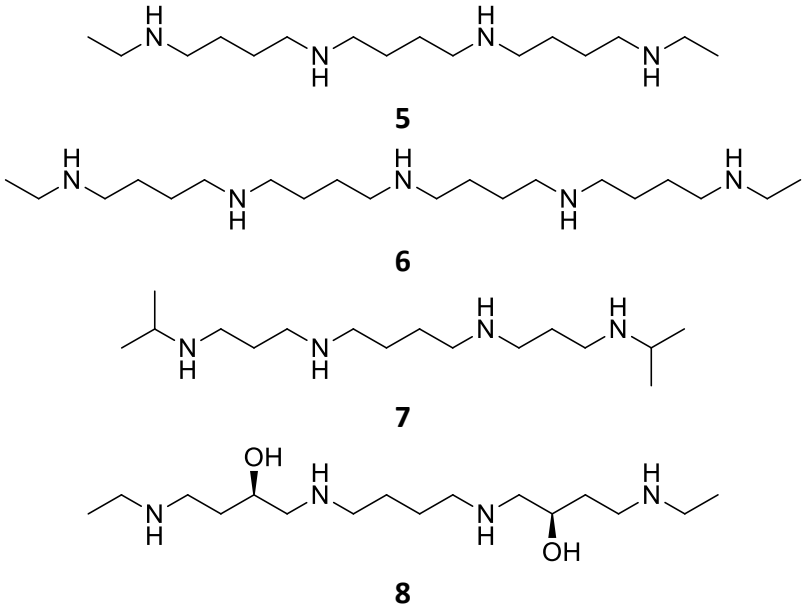
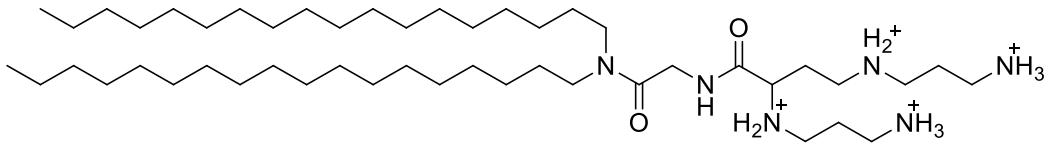


Figure 10: Structures of bis(ethyl) and isopropyl polyamines

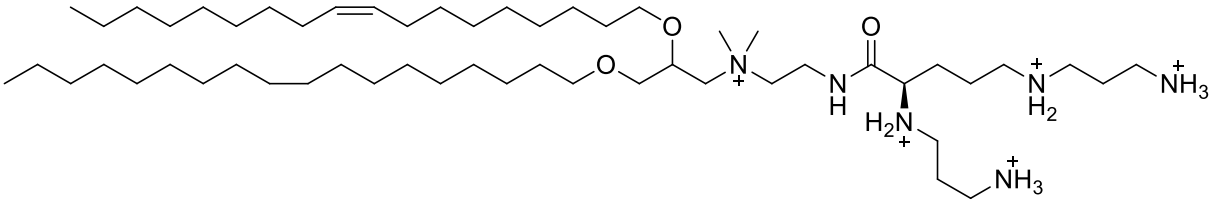
The synthesis of these symmetrical polyamines was straightforward and easily scalable which favoured further investigations. BEHSpm **5** was proven to be a useful antidiarrhoeal agent, although phase 2 clinical trials were halted due to neuro-toxicity and hepatotoxicity issues.[19, 47] The observed toxicity issues were reduced by the introduction of hydroxyl groups into the intermediate chain, giving rise to compound **8**. The reduction in toxicity of the hydroxylated analogue was probably due to the fact that the analogues were cleared through phase 2 metabolism.[42]

The positive results from the biological studies of the analogues of the naturally occurring polyamines prompted studies into conjugates of these PAs with other biologically active motifs. Applications of synthetic PA conjugates are as diverse as the sources of the naturally occurring ones, from being used as drug vectors, where they are attached to therapeutic drugs for cell delivery, or new drugs against neglected tropical diseases and chemotherapy against different types of cancer, the applications are endless. The similarity in structure of the synthetic PAs to the endogenous PAs enables them to efficiently utilise the PAT for uptake by cells, whilst they are metabolically stable.

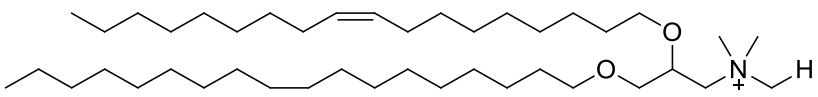
The sequencing of the human genome availed the possibility of the treatment of hereditary diseases and cancers through gene therapy. Successful application of gene therapy is dependent on the efficient transfer of DNA to specific cells *in vivo* to silence a bad gene,[48] turn on a needed gene[49] or install a new gene to address particular cellular defects.[50] Traditionally viral vectors were employed for this function but the method suffered from several setbacks such as immunogenicity and only a limited size of the DNA could be transferred.[51] Continual improvement in new vector design coupled with the knowledge of PAs led Behr to incorporate polyamines into liposomes after realizing that naturally occurring polyamines could efficiently compact DNA.[52] This led to the successful synthesis of the first transfection vector DOGS (**Figure 11**) by incorporating a branched polyamine.[53] Since then, the polyamine vectors have been shown to be superior as compared to the traditional vectors because of their low toxicity and immunogenicity, and they possess the ability to transfer large strands of DNA, accompanied by simple synthetic preparation.[54] Currently DOSPA and DOTMA (**Figure 11**) are commercially available PA vectors sold as a 3:1 mixture known as Lipofectamine.[54]



DOGS



DOSPA



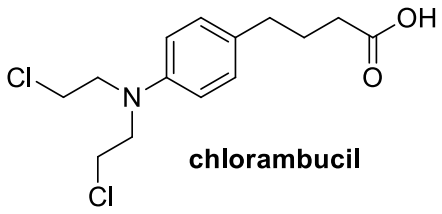
DOTMA

Figure 11: Synthetic polyamine vectors

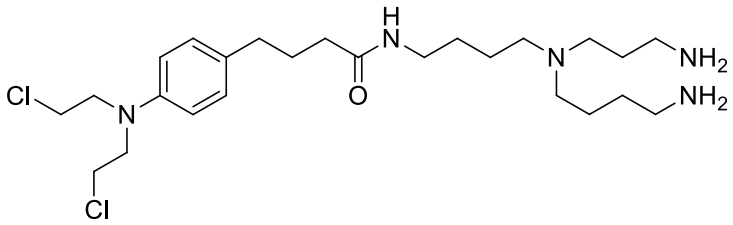
Cancer targeting using synthetic PAs is also an active research field because many cancer cells are unable to produce enough PAs to sustain their growth rate and therefore rely heavily upon polyamine import to grow. The enhanced cellular need for the three basic polyamines coupled with the structural tolerance of the PAT allows for the importation of non-native polyamines in order to meet the high demand. Considering the heavy reliance of rapidly dividing cancer cells on

PA import it was shown that drug-polyamine conjugates have enhanced cytotoxicity to cancer cells.[55] PA analogues can mimic some of the self regulatory functions of biogenic polyamines but are unable to substitute natural polyamines in their growth-promoting role.

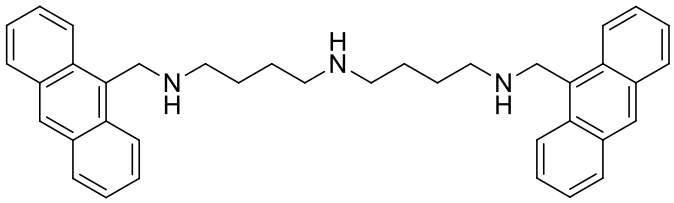
Chlorambucil (**Figure 12**) is a chemotherapeutic drug used for the treatment of chronic lymphocytic leukemia, low-grade non-Hodgkin's lymphoma, Hodgkin's lymphoma and ovarian cancer. Kaur *et al*. reported good results in targeting tumour cells with the chlorambucil-spermidine conjugate **9**, with a 10 000 fold increase in activity when compared with chlorambucil because of the ability of the conjugate to form cross-links with naked DNA.[56] *N*-Anthracene-substituted polyamines like **10** were shown to be 150 times more toxic to Chinese hamster ovary (CHO) cells when compared to a mutant PAT-deficient CHO cell line (CHO-MG).[55]



chlorambucil



9

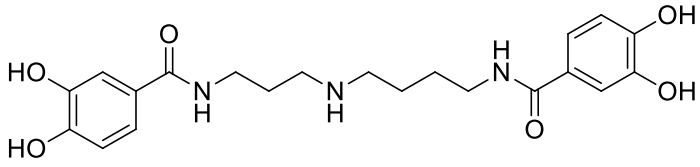


10

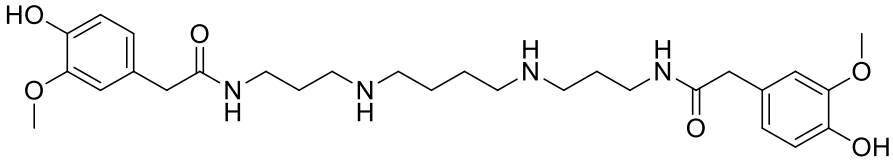
Figure 12: Polyamine drug conjugates

The continual search for antimalarial drugs also led to the development of polyamine conjugate-based lead compounds in an attempt to discover new targets in the pathogen. Pistillarin (**Figure 13**), isolated from the fungus *R. subaurantiaca*, was shown to inhibit the growth of a drug sensitive *P. falciparum* line (3D7) with an IC_{50} value of 1.9 µM and displayed no cytoxicity against NFF cells at 100 µM.[57] A library of several modified pistillarin analogues showed significant activity against *P. falciparum* in the micromolar range. In a separate investigation two analogues, compound **11**

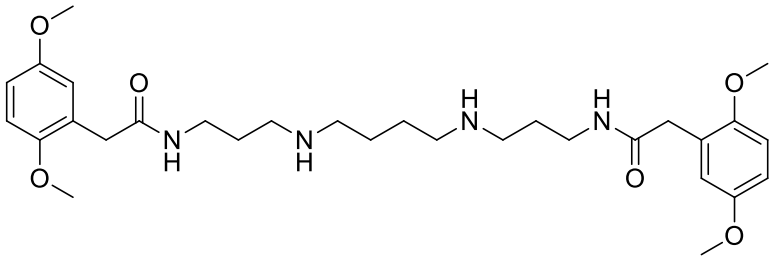
and **12**, were synthesised based on diamide orthidine and showed potent antimalarial activity. Nanomolar activity was reported for compound **11** and compound **12**, with values of 19.0 nM and 8.6 nM, respectively, against the *P. falciparum* K1 line.[20]



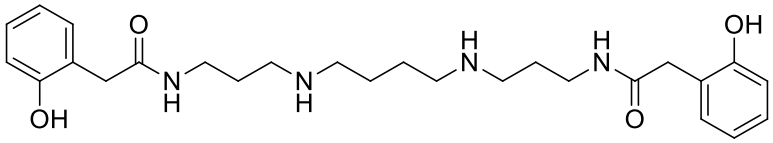
pistillarin



diamide orthidine



11



12

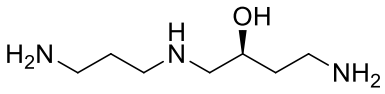
Figure 13: Lead antimalarial polyamine structures

Different synthetic polyamine analogues are being synthesised as potential therapeutic agents based on different types of naturally occurring PAs because of their promising activity. The need for continual drug development means all promising leads are explored until every possible outcome is exhausted. Given this fact, the examples discussed here so far are by no means an exhaustive list of the findings and work that has already been published, but merely serve to highlight the importance of this class of compounds as therapeutic agents.

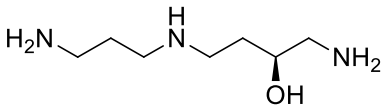
1.4 Hydroxylated natural polyamines

The class of polyamines of interest to this PhD are those with a hydroxylated methylene backbone. For all the naturally occurring PAs shown thus far, there have not been many naturally occurring polyamine examples in which the methylene backbone itself is substituted. The only available

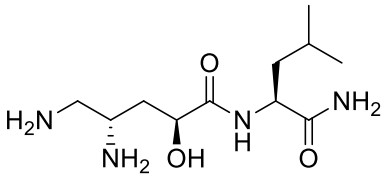
examples were for the synthetic analogues shown in **Figure 10**, where hydroxylation of the methylene backbone was introduced as a way of reducing the toxic effects of a potentially therapeutic synthetic polyamine. The absence of methylene linkage substitution is attributed to the sensitivity of PAT to substitution of the methylene linkages. The discovery of an exception to rules in nature always attracts much attention and generates interest in synthesis and possible biological effects/applications. To date only a few methylene-substituted polyamine compounds have been isolated from various natural sources. The first to be isolated were the triamines *S*-6- and *S*-7-hydroxyspermidine (**Figure 14**).[58] *S*-2-hydroxyspermidine is a component of several alkaloids isolated from marine microorganisms, whilst *S*-7-hydroxyspermidine occurs free in *Pseudomonas* species.[5]



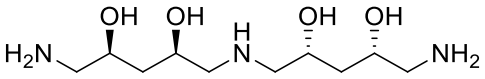
***S*-6-hydroxyspermidine**



***S*-7-hydroxyspermidine**



13



pavettamine

Figure 14: Methylene substituted polyamines

Compound **13** was recently isolated from *Streptomyces* sp. and fully characterised, but biological assays revealed no significant inhibitory activity against a few cancer cell lines.[59] To the best of our knowledge, the total synthesis of this compound has not yet been reported. The compound of interest for this work is pavettamine, another naturally occurring hydroxylated polyamine which was isolated from Rubiaceae species.

1.4.1 Pavettamine

The toxic properties of plants of the Rubiaceae species have been known for over a century. During the early 1900's farmers in South Africa lost considerable livestock and they noticed that death occurred after the animals had consumed plants from the Rubiaceae family namely *Vangueria* (syn. *Pachystigm*a) *pygmaeum*, *V. thamnus*, *V. latifolium*, *Pavetta harborii*, *P. schumanniana* and *Fadogia homblei*.[60] The resulting plant toxicoses named Gousiekte or 'quick disease' is characterised by the sudden death of animals without warning due to cardiac failure,

usually after a physical activity. A number of cardio dynamic changes coupled with myocardial lesions consisting of myofilaments, replacement of myocytes with collagenous tissue, lengthening of sarcomeres and cardiac dilation have been reported for animals after consuming the plants.[61] Dedicated research by Fourie *et al*. led to the first isolation of the causal toxin which was duly named pavettamine.[61]

It is noteworthy that pavettamine is the only natural polyamine to be implicated in livestock poisonings. This polyamine stimulated our interest because of its uniqueness in the polyamine class of compounds, coupled with its occurrence in plants indigenous to Southern Africa. The importance of livestock to this part of the world cannot be overstated because they are a vital source of wealth combined with social status and hence the effects of poisonous plants are detrimental to this critical part of the economy. Plant poisoning of livestock causes considerable losses annually and authorities estimate that during certain years, up to 25% of stock losses occur as a result of plant poisonings.[62]

Bode *et al*. identified and published the structure of pavettamine after performing the first and only total synthesis of this unusual polyamine shown in **Figure 14**.[63] It is the only polyamine with a five-carbon linker having a 1,3-*syn*-diol functionality to be isolated from nature. Pavettamine also possesses a C-2 symmetry. The synthetic toxin was found to be more potent than the isolated natural product, probably due to the difference in purity levels of the isolated material in comparison to the synthesised compound. Toxicological studies of the naturally occurring toxin revealed that pavettamine inhibits protein synthesis in the cardiac muscle of rats, but it had no effect on other tissues.[61] This observation was in agreement with results published earlier which stated that dried leaves of the toxic plants induced heart failure in sheep and rats.

Given what has been discussed so far regarding the role of polyamines in living organisms, it is evident that pavettamine is responsible for apoptosis in the cells of cardiovascular organs, hence the cardiac syndrome that is observed in the animals. The toxin is likely to be selectively transported by the cardiovascular organs using the PAT into the cells where it disrupts the normal functions of the endogenous polyamines, thus initiating cell death. Further investigations still need to be performed to establish the actual mechanism of action because the observed selectivity is intriguing. In general, the stereochemistry of a molecule has significant implications on its biological activity. Thus, synthesis of the enantiomer of pavettamine and the reduced

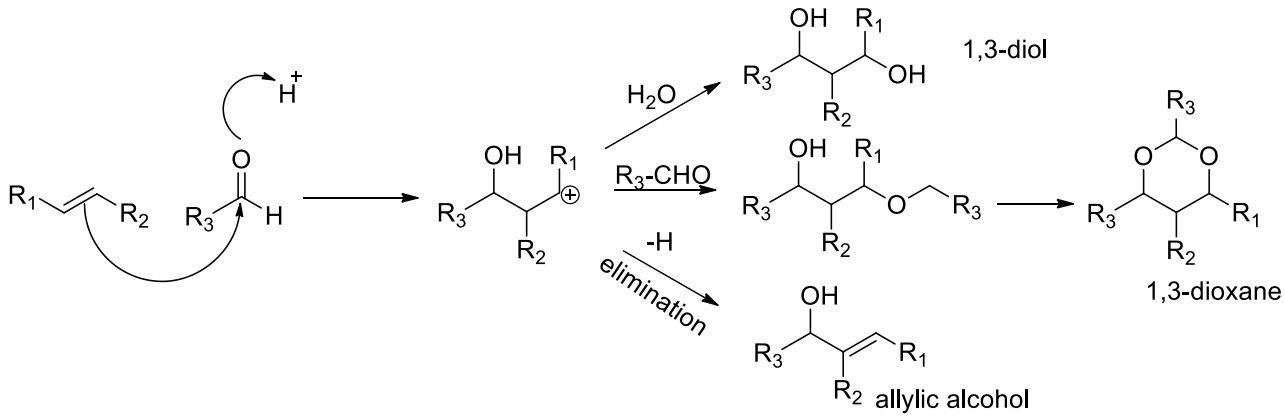
functional analogues with different stereochemical conformations forms the basis of this research work.

1.5 Synthetic methods for 1,3-diols

One of the most potent classes of biological compounds known to man is the polyketide class, which possesses broad structural diversity and many of these compounds contain a 1,3-diol unit. Due to the importance of the 1,3-diol subunit, the synthetic access to this active moiety has been of interest to organic chemists for decades, therefore a variety of synthetic methodologies targeting this moiety have been developed.[64, 65, 66, 67] Thus, because of the presence of a 1,3-diol system in compounds of interest to this project, synthetic methods targeting the synthesis of the 1,3-diol motif are going to be discussed in greater detail.

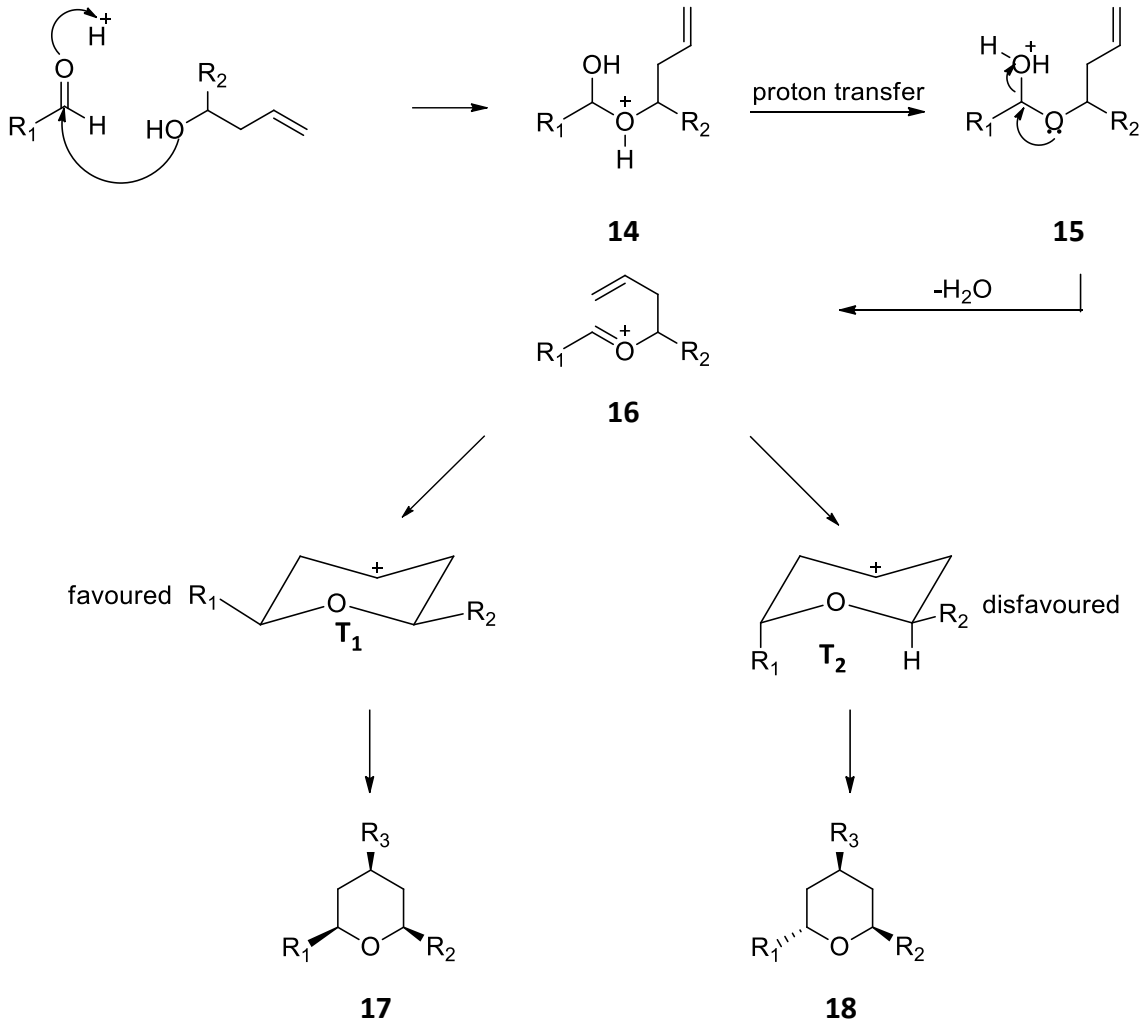
1.5.1 Carbon-carbon bond forming reactions

Synthesis of *syn*- and *anti*-1,3-diols can be achieved by carbon-carbon bond forming reactions, and depending on the substrates, reagents and conditions both conformations of the diol can be recovered. One such reaction is the Prins reaction, involving an acid catalysed condensation of an aldehyde with an alkene. The product of the reaction depends on the substrate and the reaction conditions, resulting in a mixture of products namely a 1,3-diol, 1,3-dioxane or an allylic alcohol (**Scheme 1**). The reaction has very limited chemo- and regio-selectivity, which restricts its applications in organic synthesis. The lack of stereo-control arises from the fact that nucleophilic addition to the carbocation intermediate that is formed lacks any kind of selectivity. Even if chirally pure compounds are used as starting material, the newly formed carbon-carbon bond always lacks selectivity. As a result of this, the reaction was not popular in natural product synthesis until useful modifications of the reactions were developed.



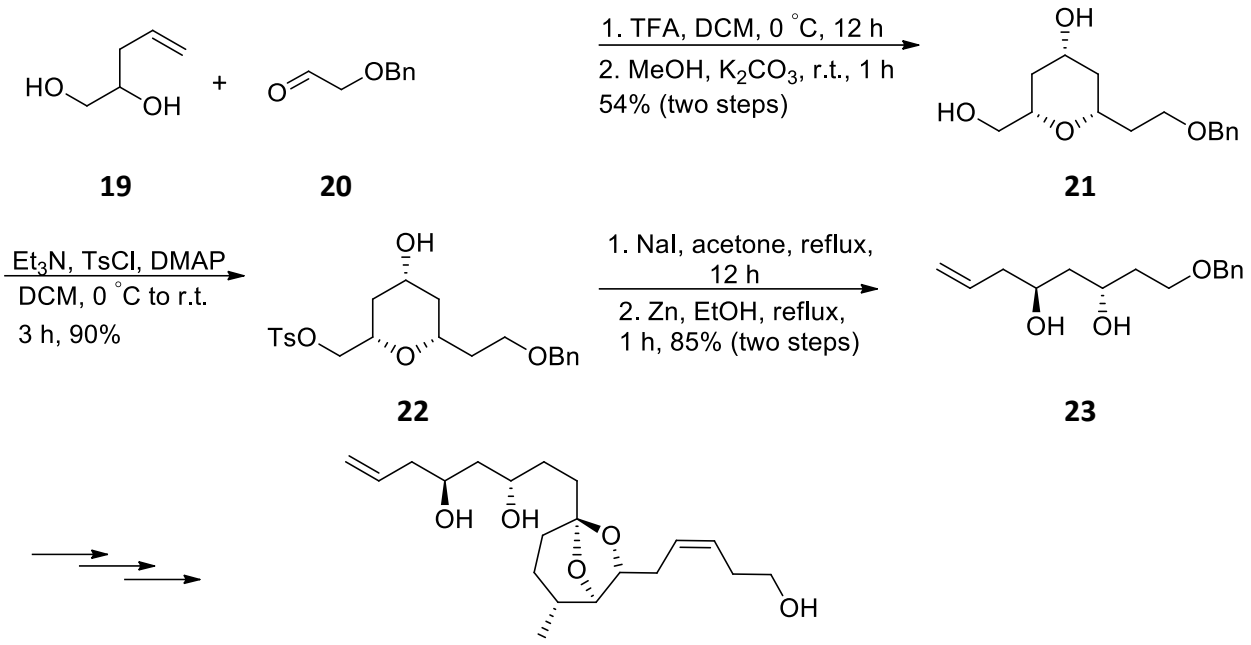
Scheme 1: Prins reaction

Continuous investigations unearthed a useful modification of the Prins reaction, which enabled the synthesis of many chiral heterocyclic compounds, suitably named the Prins-type cyclisation reaction. In the modified Prins reaction, a homo allylic alcohol reacts with a carbonyl compound, mainly an aldehyde, under acidic conditions as shown **Scheme 2** giving rise to an intermediate **14**.[68] Appending the alkene or π-nucleophile to the alcohol facilitates the cyclisation after the addition step. Intramolecular proton transfer of **14** gives rise to intermediate **15** which loses a water molecule yielding an oxocarbenium ion **16**. The oxocarbenium ion rearranges via intramolecular addition of a π-nucleophile from an alkene to an oxocarbenium ion or related species to generate a ring through carbon-carbon bond formation. There are two possible chair transition states $\mathbf{T_1}$ and $\mathbf{T_2}$ arising from this intramolecular reaction. The most favourable state is $\mathbf{T_1}$ because the substituents at the 2nd and 6th positions assume equatorial positions resulting in a stable conformer. In contrast, the $\mathbf{T_2}$ state is disfavoured because of the severe 1,3-diaxial interactions that exist between groups at the 2nd and 6th positions. Hence the nucleophilic attack to form the favoured transition state will occur from the equatorial position forming *cis* products such as **17** as the main stereoisomer with **18** being formed as the minor product. Although oxocarbenium ions undergo conformational changes, the energy barrier is sufficiently high that free rotation does not occur at low temperatures, such that the transformation occurs with excellent and predictable stereocontrol. The high degree of stereocontrol arising from the configurational predictability of oxocarbenium ions and cyclisation states, allows for multiple applications in natural product synthesis.



Scheme 2: Prins cyclisation

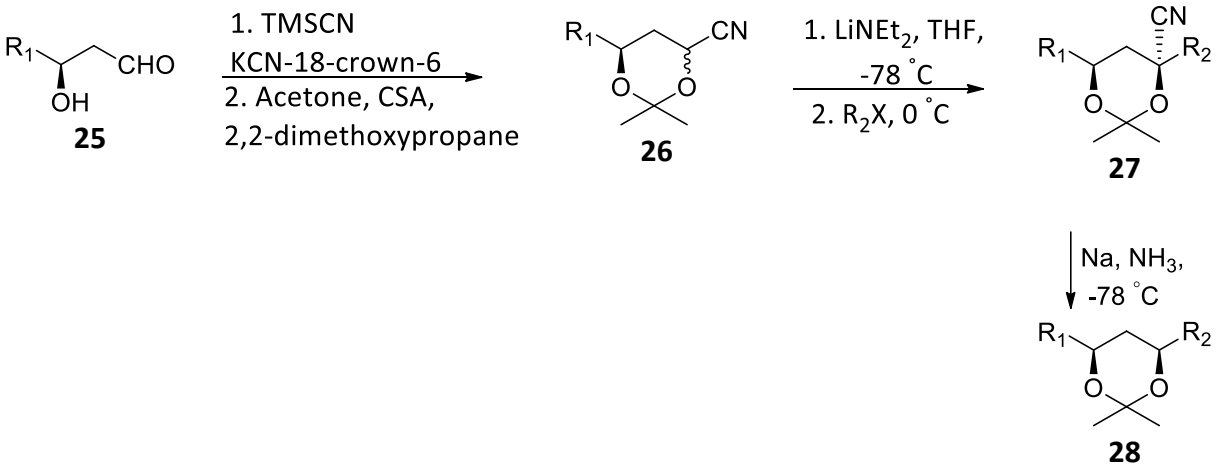
Yadav *et al*. successfully employed the Prins cyclisation when they developed a general route for the synthesis of various polyketide precursors containing *anti*-1,3-diols from a common pyran system (**Scheme 3**).[67] In one of their successful syntheses, *S*-homoallylic alcohol **19** was subjected to the Prins cyclisation with 2-benzyloxypropanal **20** in the presence of TFA. Subsequent hydrolysis afforded a trisubstituted tetrahydropyrandiol **21** in excellent de. Regioselective tosylation of the primary alcohol yielded compound **22** followed by ring opening to furnish an *anti*-diol **23**. Further transformation of the diol allowed for the successful synthesis of a major fragment, incorporated in the synthesis of the natural product attenol B **24**. They proved this novel method to be versatile for the synthesis of an *anti*-1,3-diol framework with high stereoselectivity.



19 **20** **21** **22** **23** **24**

Scheme 3: Synthesis of 1,3-diols using Prins cyclisation

In their quest to develop new methods for assembling polyol chains, Rychnovsky *et al*. developed a method for the convergent synthesis of polyol chains based on the generation and alkylation of *cis*- or *trans*-6-alkyl-2,2-dimethyl-4-litho-1,3-dioxanes.[69] In one example, treatment of β-hydroxy aldehyde **25** with TMSCN and potassium cyanide-18-crown-6 complex, followed by treatment with acetone, 2,2-dimethoxy propane and an acid catalyst converted aldehyde **25** to cyanohydrin **26** (**Scheme 4**). The resultant cyanohydrin was produced in a 1:1 mixture of the *syn*- and *anti*-1,3-isomers. Recovery of a single *syn* product **27** was reported after deprotonation of the cyanohydrin with lithium diethylamide followed by alkylation.

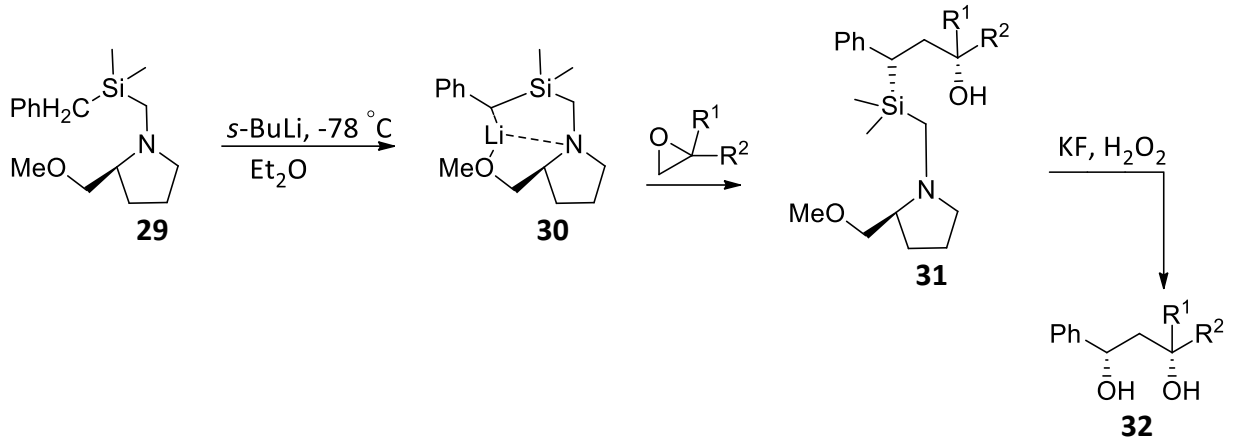


25 **26** **27** **28**

Scheme 4: Synthesis of *syn*-1,3-diols acetonides by reductive decyanation of cyanohydrins

The high stereochemical outcome of the protocol is as a result of the configurational control of the intermediate generated from cyanohydrin **26**. The lithium reagent generates a radical intermediate with a six membered ring. The ring adopts a much more stable chair conformation where the axial radical is formed as opposed to an equatorial radical. Thus, both isomers of cyanohydrin **26** form the same axial radical intermediate. Axial radical formation is favoured because, the oxygen lone pair of electrons overlap with the axial radical stabilising it while the lone pair of electrons is not accessible to the equatorial radical. Consequently, because both isomers follow the same reaction pathway, the same product is recovered. In this case a 1,3-*syn*-diol is recovered after alkylation yielding **27**. Reductive cyanation proceeds without loss of stereochemistry at the secondary alcohol centres yielding compound **28**. The 1,3-dioxane structure contributes towards the configurational rigidity of intermediates which in turn protects the stereochemistry.

Chiral 1,3-diols were prepared in high enantiomeric purity from the reactions of the chiral silycarbanion formed from **29** with epoxides. Aliphatic epoxide addition to the carbanion **30** furnished a crucial intermediate **31**, followed by oxidative cleavage of the carbon-silicon bond with peroxide at low temperatures, yielding the diol **32** (**Scheme 5**).[70] This approach proved to be of high enantioselectivity and diastereoselective when achiral aliphatic epoxides were employed. However, poor diastereoselectivity was detected when epoxides with an existing chiral centre were used. Nevertheless, the resulting two diastereomers could be easily separated by column chromatography. This sequence was used for phenyl-substituted diols but it is applicable on different types of systems. 1,3-diols have also been reported to be synthesised from 2,3 epoxy alcohols using a Ti(III) mediated ring opening with excellent diastereoselectivity.[34] Similar methods have been used for 1,3-diol synthesis, each with its own set of limitations, and choosing the best approach is best based on the type of target molecule.[64]

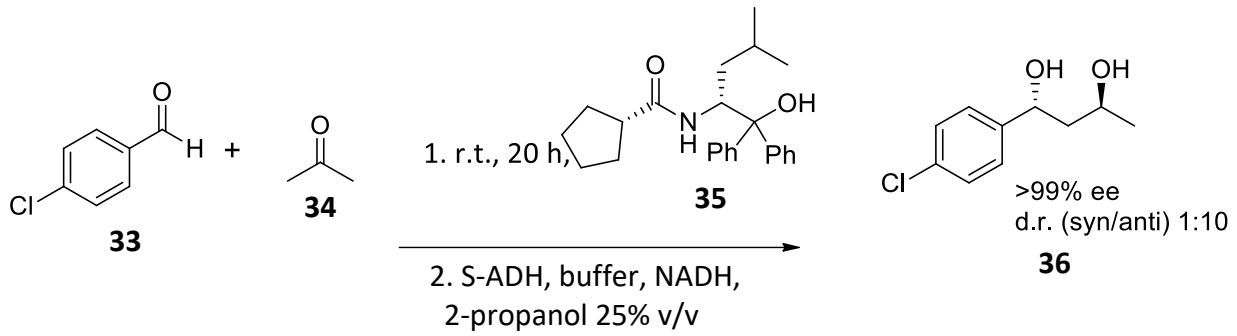


Scheme 5: Asymmetric synthesis of chiral 1,3-diols using chiral organosilicon compounds

1.5.2 Biocatalytic methods

Due to the growing need and demand for greener methods in organic synthesis for research and industrial processes, biocatalysis has grown rapidly as a method of choice for synthesis in the past decade.[71, 72] One of the main advantages for incorporating enzymes in synthesis is their ability to generate chirally pure compounds under non-toxic conditions. However, because enzymes are not versatile, a library of enzymes always needs to be assayed before finding an enzyme best suited for the desired transformation. Examples of the enantioselective synthesis of 1,3-diols using enzymes as isolated or co-catalysts have been reported in literature, but in most cases a huge library of enzymes had to be assayed first.

Chemo-enzymatic methods are currently being used as a convenient and environmentally friendly way of synthesising a 1,3-diol unit (**Scheme 6**) for fragments of pharmaceutical importance. Baer *et al*. demonstrated the applicability of enzymes for the synthesis of 1,3-diols with excellent ee.[73] An aldol reaction between aldehyde **33** and acetone **34**, utilising an organocatalyst **35**, gave rise to an aldol product which was diastereoselectively reduced to the diol **36** by using biocatalysts in a modified one pot synthesis. This approach also allowed for the synthesis of all possible stereoisomers of the diol by changing the configuration of the organocatalyst **35**. The high ee and the environmentally friendly conditions makes this approach very desirable. However, enzymes tend to be substrate specific in terms of both activity and selectivity.

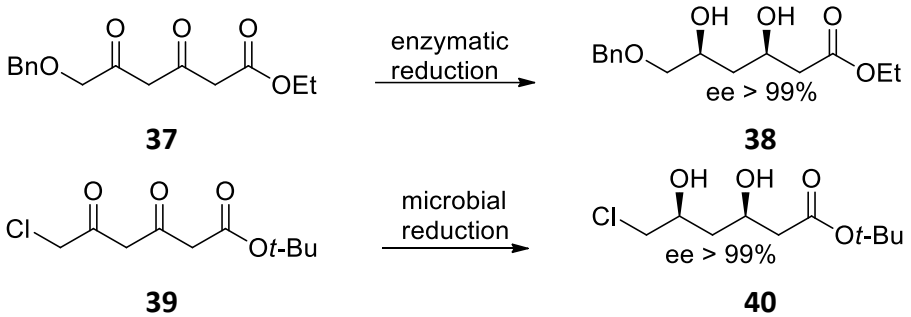


33 **34** **35** **36**

Scheme 6: Enzymatic kinetic resolution of an aldol product

1,3-Diols can also be recovered from the enzymatic reduction of 1,3-diketones, although double site reduction in a single operational step is seldom achieved. In general, β-hydroxyketones are commonly recovered as the primary products and reduction of the second keto group is either very slow or does not occur owing to stabilisation of the β-hydroxyketone by hydrogen bonding.[74]

A few notable examples of bi-keto enzymatic reduction in a single step have been reported. Patel *et al*. reported that the stereoselective microbial reduction of 3,5-dioxo-6-benzyloxyhexanoic acid ethyl ester **37**, yielded a key chiral intermediate, 3,5-dihydroxy-6-benzyloxyhexanoic acid ethyl ester **38** (**Scheme 7**).[75] Excellent yield and optical purity of the desired product was achieved even though a significant library of microbial cultures had to be evaluated. The recovered diol was a key intermediate in the chemical synthesis of an anti-cholesterol drug that acts by inhibition of hydroxyl methyl glutaryl coenzyme A (HMG CoA) reductase. Since then, various statins have been approved by the FDA and due to the presence of the 1,3-diol motif in all of them, various biocatalysts have been developed to achieve the required high yields and ee.[76] Successful *syn*-selective reduction of the chlorinated diketoester **39** to dihydroxyester **40** was also achieved by whole cells of *Lactobacillus kefir* with excellent enantioselecivity.[64]



37 **38** **39** **40**

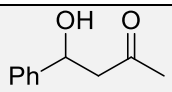
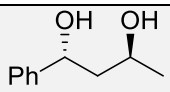
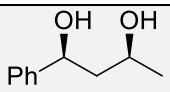
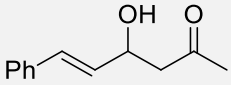
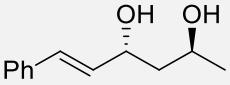
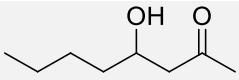
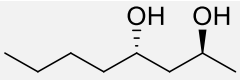
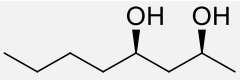
Scheme 7: Asymmetric reduction of 1,3-diketones

The desire for concomitant one pot preparations of 1,3-diols also led to the investigation of bakers' yeast reductions after it had shown promising results for such transformations.[65] The

motivation behind this investigation was the possibility of employing an enzymatic protocol for obtaining synthons for the preparation of natural products.

Bakers' yeast fermentation of a representative library of β-hydroxyketones shown in **Table 1** afforded products with high enantioselectivity, albeit in low yields.[77] Fermentation of *rac*- **41** gave rise to both the *syn* and *anti* products but *anti*- **42** was formed in excess, whilst for *rac*- **43** only a single diastereomer, compound **44**, was recovered. *rac*- **45** was the only compound that had a slight excess of the *syn*-diol **46** but in general, the *anti*-diol was always in excess for all the tested substrates. It is interesting to note that the enantioselectivity always gave rise to a new stereogenic centre with an *S*-configuration. The diastereomeric excesses ranged from 43% – 99% depending on the substrate. Despite the promising results, the yields of the reactions were still quite low and long reaction times were required. The variability of enzymes in yeast also makes its use problematic because it lacks repeatability.

Table 1: Bakers' yeast reductions of β-hydroxyketones to afford diols.

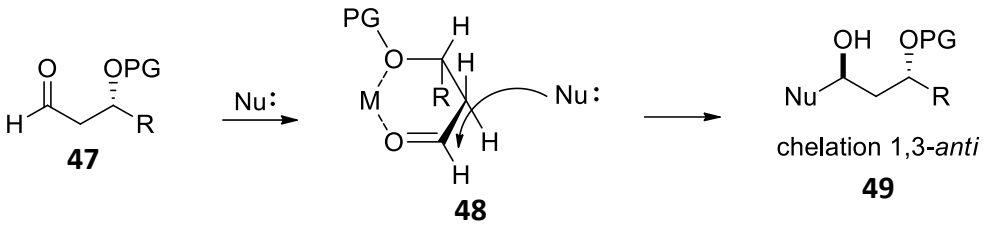
Substrate	Yield (time)	*anti*-diol	*syn*-diol	*anti*/*syn*
	40% (48 h)			5.7/1
rac- **41**		*anti*- **42** *ee* = 98%	*syn*- **42** *ee = 98%*	
	23% (48 h)			
rac- **43**		**44** o.p > 99%		
	44% (72 h)			1/1.2
rac- **45**		*anti*- **46** o.p > 99%	*syn*- **46** o.p > 99%	

1.5.3 Synthesis of 1,3-diols using the aldol reaction

The discovery of cross-aldol reactions with silyl ethers by Mukaiyama in the early 1970's brought utility to the aldol reaction.[78] Traditionally aldol addition reactions had been used to gain access to the 1,3-diol moiety but the approach had insufficient stereoselectivity. Mukaiyama conceived that coordination of the carbonyl oxygen atom of an aldehyde to a Lewis acid would make the carbonyl atom more electrophilic. After investigations of the effect of various Lewis acids, $BF_3.OEt_2$ was identified as the most effective. Consequentially, the effect of the Lewis acids on

stereoselectivity at the newly formed stereogenic centre was also investigated.[79] The Mukaiyama aldol reaction was further investigated to reveal various features such as diastereoselectivity and competency of other Lewis acids. Evans later developed a diastereoselective aldol reaction by introducing chiral auxiliaries.[80] The synthetic approach was then the subject of many variations of 1,3-diol syntheses with significant success.[81, 82]

Following his accomplishments in 1,3-diol diastereoselective synthesis, Evans undertook an extensive mechanistic study which explained the stereochemical outcome of the aldol reactions.[83] Initially, 1,3-diol synthesis via aldol reactions of β-alkoxy aldehydes were established to be controlled by Felkin-Anh with low stereocontrol (**Scheme 8**). When an aldehyde with an alcohol on the β-position **47** is employed, the aldehyde face selectivity for 1,3-induction involves internal chelation to a β-heteroatom substituent. The resulting favoured transition state **48** favours nucleophilic attack on the less hindered face of the conformationally locked and internally locked intermediate. The preferred product **49** is the 1,3-*anti* diastereomer which is consistent with the transition state. For meaningful chelation control, the chelating metal centre must possess a minimum of two open coordination sites to simultaneously complex both the carbonyl and ether oxygen. NMR spectroscopic experiments performed by Keck established that the oxygen protecting group (PG) should also allow effective bidentate complexation of the chelating metal between the carbonyl and ether oxygen.[84, 85]



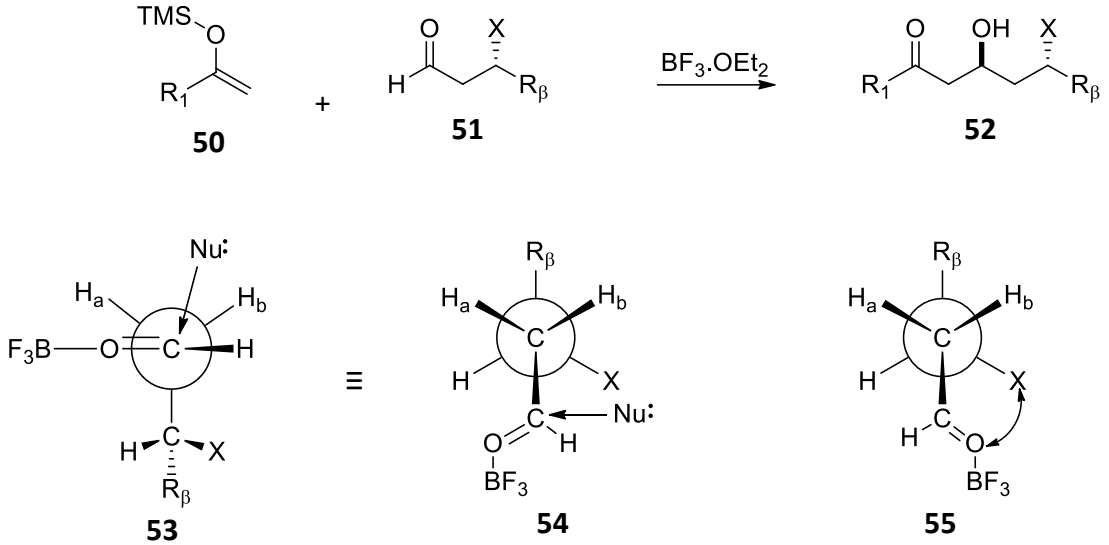
Scheme 8: Chelation controlled 1,3-asymmetric induction model

Further work revealed that the $BF_3.OEt_2$ mediated Mukaiyama aldol reaction with R-unsubstituted, alkoxy aldehydes afforded good levels of 1,3-*anti* induction in the absence of internal aldehyde chelation.[83] Several assumptions common to the Felkin-Anh model were still incorporated for explanation of the observed outcome in this model. At the outset, it was assumed that torsional effects dictated that the aldehyde adopted staggered conformations between the forming bonds and the aldehyde α-substituents. The second assumption was that the principal addition product evolved from the reactant-like transition structure wherein the β-stereogenic centre of the aldehyde is oriented *anti*, rather than *gauche* to the forming bond. This geometry

reduces non-bonded interactions between the aldehyde α-substituents and the incoming nucleophile.

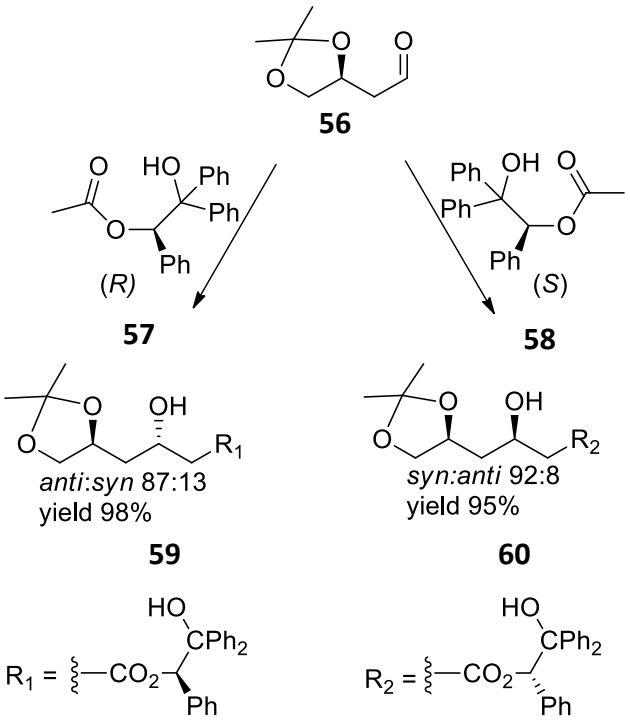
After taking all the assumptions into account, the researchers concluded that the aldehyde face selectivity is governed by steric and electrostatic effects in the aldehyde that originate from interactions between the β-substituents and the carbonyl reaction centre (**Scheme 9**). Accordingly, the incoming nucleophile **50** will approach the aldehyde **51** on the path that offers the minimal electrostatic and steric repulsion yielding product **52**. The preferred transition state is illustrated in two different perspectives **53** and **54**, which show that the preferred resulting product is a 1,3-*anti* diastereomer.

The staggered conformation of the α-substituents with respect to the incoming nucleophile is clearly illustrated in **53** whilst **54** depicts the favoured orientation of the β-stereocentre relative to the coordinated carbonyl moiety. Coordination of aldehyde to BF_3 results in a constrained conformer in the transition state which contributes to the observed outcome. Steric interactions are expected to be minimised when the β-alkyl substituent R_β is oriented *anti* to the C_α-C=O bond. Therefore, of all the possible conformations for the staggered arrangement, **53** is the most stable and it can also be stabilised by an attractive electrostatic interaction between the β heteroatom X and the polarised carbonyl carbon.[86, 87] The destabilised staggered *gauche* conformer one example is represented by **55**, leads to the 1,3-*syn* diastereomer. However, the conformers arising from this staggered arrangement are not favoured because of the steric and electrostatic repulsion emanating from the $R_\beta \leftrightarrow$ C=O, X ↔ C=O and to a lesser extend H ↔ R_β interactions.



Scheme 9: 1,3-Asymmetric induction polar model

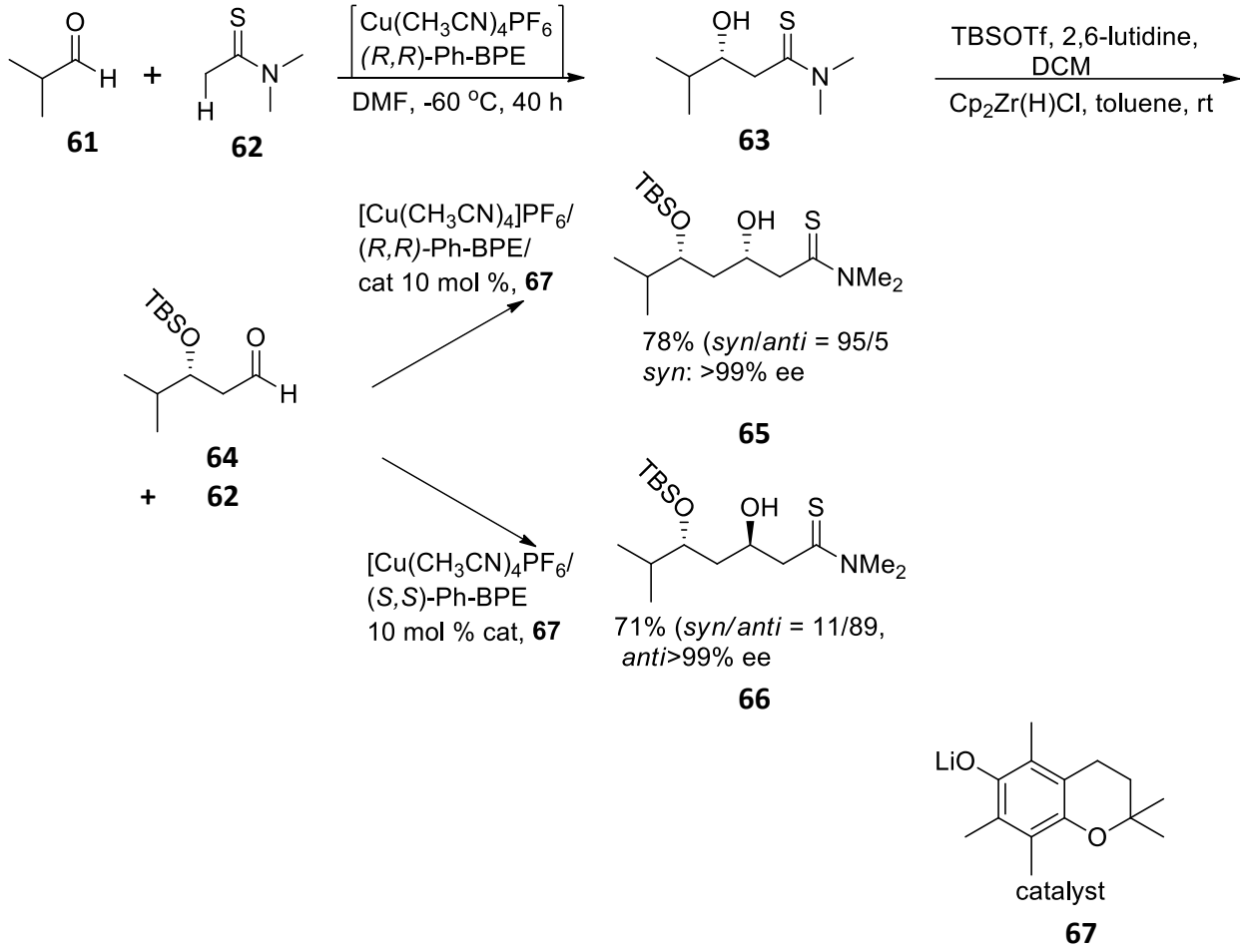
Armed with this knowledge, Mahler *et al*. established an improved diastereoselective method for developing 1,3-*syn* and 1,3-*anti*-diols, and they successfully applied the procedure for the synthesis of various substrates.[88] They demonstrated that when an enantiomerically pure β-alkoxy aldehyde **56** reacted with both enantiomers of the acetate enolate 2-hydroxy-1,2,2-triphenylethyl acetate **57** and **58**, diastereofacial selectivity was observed. The acetate enolate facilitated either a matched or mismatched pair effect by utilising the inherent selectivity of the aldehydes. This gave rise to a mismatched major product **59** when the *R*-enolate **57** was used and the matched pair major product **60** when the *S*-enolate **58** was used.



Scheme 10: Reagent-controlled aldol reaction of 2-hydroxy-1,2,2-triphenylethyl acetate with chiral aldehydes

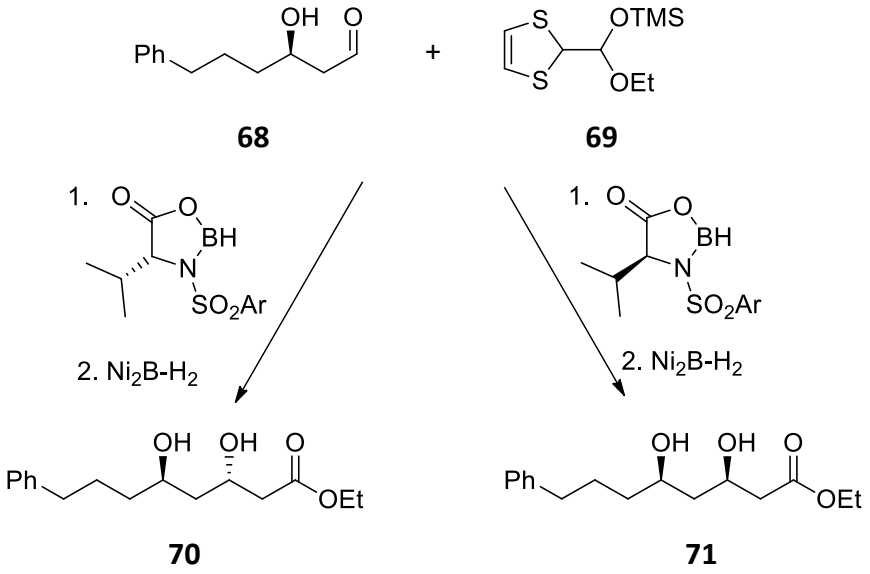
The presence of the 1,3-polyol system structural motif in a plethora of biologically active natural products means that nature already has an efficient way of achieving this stereoselectively. Polyketide synthases are harnessed in nature to enable efficient, iterative elongation of a thioester-activated C_2 unit through a decarboxylative Claisen condensation coupled with an enzymatic stereoselective reduction of ketones to provide 1,3-polyol arrays. Iwata *et al*. reported an efficient approach imitating this natural enzymatic approach for 1,3-diol asymmetric induction by employing a catalysed aldol reaction (**Scheme 11**).[89] They demonstrated that a catalytic asymmetric aldol reaction between aldehyde **61** and thioacetamide **62** yielded an aldol product **63** with an ee of 94%. TBS protection and reduction of the thioamide functionality with the

Schwartz reagent converted **63** to a chiral aldehyde **64** with a β-hydroxyl group. Iterative installation of thioacetamide **62** under catalytic conditions yielded both the *syn*-product **65** and the *anti*-product **66** by changing the ligand and catalyst **67** combination with both the recovered products having ee > 99%. The approach was applicable to a variety of substrates and excellent enantiomeric excesses were recovered.



Scheme 11: Catalyst controlled direct catalytic asymmetric aldol reaction for the synthesis of 1,3 diols

After reporting the aldol reaction of aldehydes with TBDMS ketene acetals in the presence of a chiral borane complex, Kaneko *et al*. disclosed a direct enantioselective synthesis of *syn*-1,3-diols under similar conditions.[90] A modification of the procedure composed of a chiral oxazaborodinone-promoted aldol reaction of a β-chiral aldehyde **68** with a silyl ketene acetal **69** (**Scheme 12**). The aldol reaction yielded *anti*-product **70** diastereoselectively when the *S*- chiral borane auxiliary was used and the *syn*-product **71** when the *R*-borane was used, with excellent ee after desulfurisation.[91] The results of this procedure indicate that the chiral centre at the β-position of the ester has no effect on the stereoselection at the newly-generated stereogenic centre.

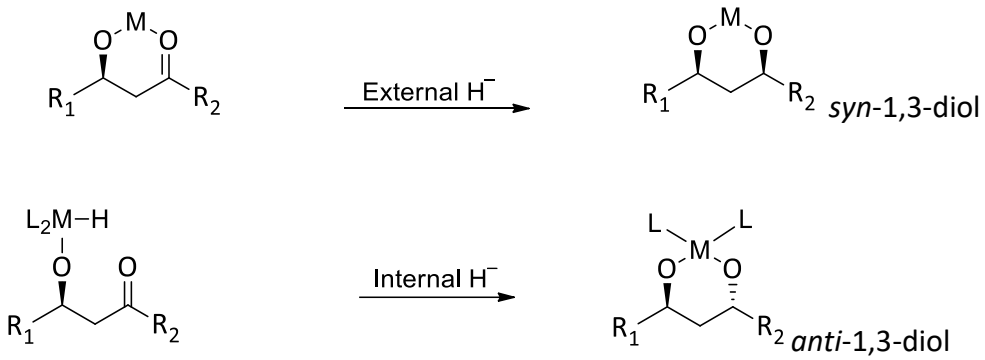


Scheme 12: Oxazaborolidinone-promoted aldol reaction of silyl ketene acetal with a β-chiral aldehyde

1.5.4 Synthesis of 1,3-diols via stereoselective reduction of ketones

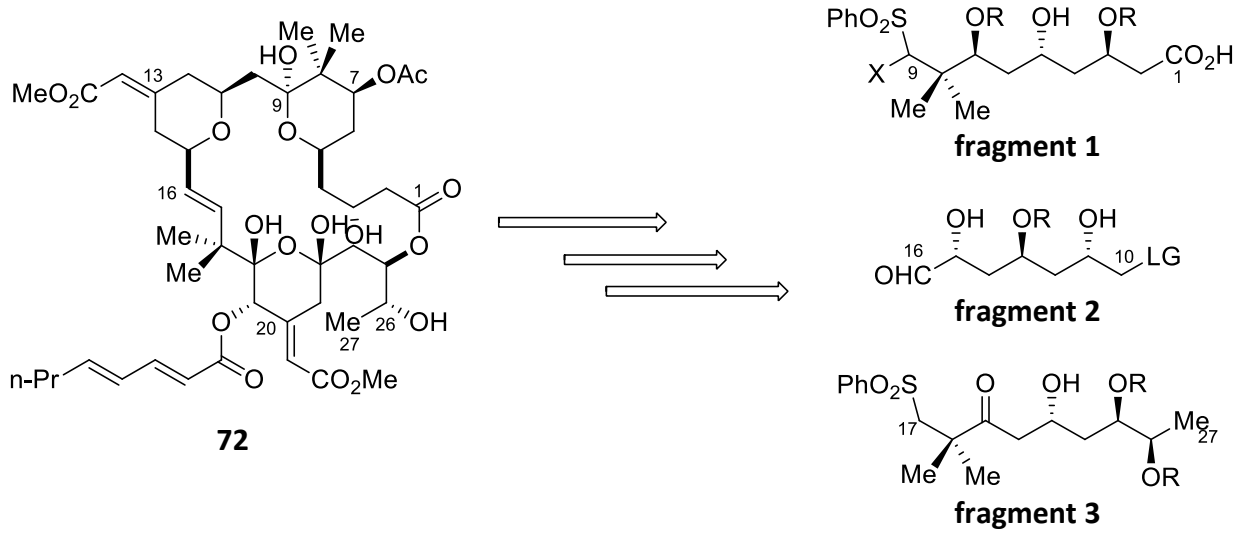
The versatility of chiral auxiliaries means they have a wide range of applications in organic synthesis. Their application in enantioselective synthesis as already discussed in **1.5.3**, has enabled the synthesis of chiral natural products. Incorporation of chiral auxiliaries in the 1,3-asymmetric reduction of β-hydroxyketones is another effective method that addresses the diastereoselective synthesis of the 1,3-diol motif. The direct enantioselective synthesis from achiral starting compounds is intrinsically more attractive because of substrate availability, but employing optically active β-hydroxyketone synthons is more common. An added advantage of the stereoselective reduction of acyclic β-hydroxyketones is that both *syn*- and *anti*-diols can easily be synthesised from the same starting material by change of reagents and reaction conditions.

Depending on the type of reducing agent used, the *anti*-diol is preferred when the reducing agent possesses the capacity to bind to the hydroxyl function, followed by intramolecular transfer of the hydride (**Scheme 13**).[92] In contrast a *syn*-diol is preferred when a chelating agent is employed to preorganise the substrate prior to the addition of the reducing agent. Thus several researchers have reported success using different types of chiral auxiliaries for selective reduction of ketones to 1,3-diols.[64]



Scheme 13: Stereoselective reduction of β-hydroxyketones via chelate control to yield *syn* products and intramolecular hydride transfer to yield *anti* products

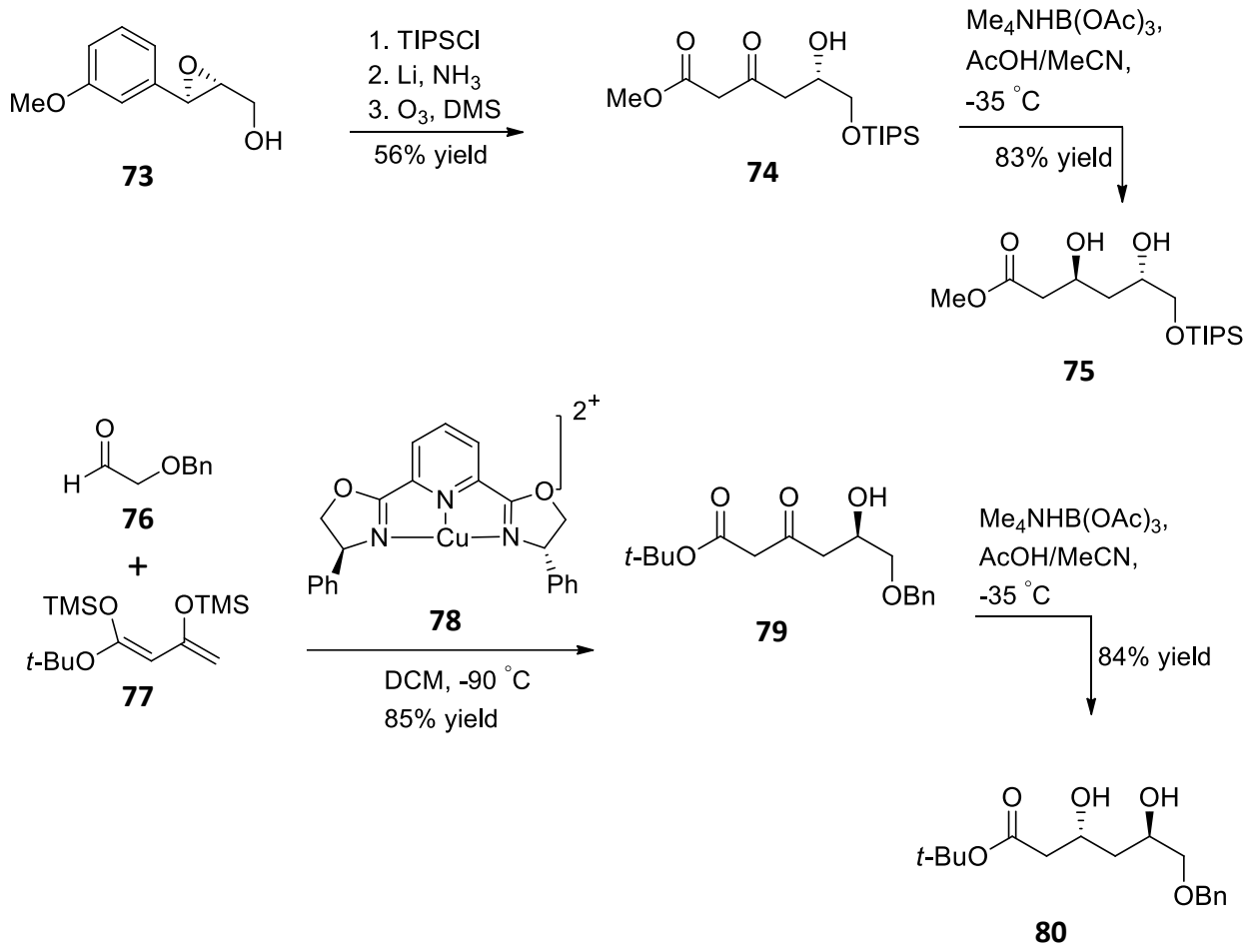
For the total synthesis of the macrolide bryostatin 1 **72**, a potent a antitumor agent[93], Evans *et al*. retrosynthetic analysis broke down the molecule into three main fragments[94]. The three fragments all possessed the 1,3-diol moiety (**Scheme 14**), which meant that stereoselective synthesis of the alcohols became a crucial part of the project. The presence of the irregular arrangement of the alcohols served as the impetus for the development of a fitting method for the stereoselective reduction of β-hydroxyketones.



Scheme 14: Retrosynthetic analysis for bryostatin 1, 72

To achieve this, aldol based strategies were combined with reduction chemistry in the synthesis of the three acyclic fragments, because of the convergent and flexible approach that these two methods offered. Synthesis of fragment 2 began with subjecting an epoxystyrene **73** to a Sharpless asymmetric epoxidation[95], followed by protection, Birch reduction and ozonolysis revealing the β-hydroxyketone **74** in 93% ee (**Scheme 15**). By using an internally binding reducing agent, the desired 1,3-*anti*-diol **75** was recovered in a diastereomeric ratio of 91:9. The alternative route for synthesis of the β-hydroxyketone for fragment 3, began with an aldol reaction between aldehyde

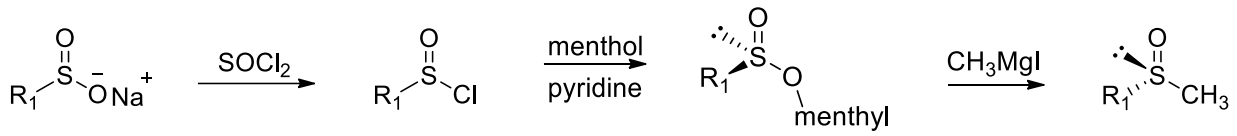
76 and the silyl enolate **77**. Chiral induction of the reaction was provided by catalytic amounts of the copper complex **78**, affording compound **79** in an excellent ee of 99%. The previously described reduction protocol gave rise to the *anti*-diol with a diastereomeric ratio of 94:6. Both these fragments were further transformed into the desired compound and the established chirality was used for chiral induction in some of the synthetic steps.



Scheme 15: Synthesis of the target fragments for total synthesis of bryostatin 1

Other examples of the stereoselective reduction of 1,3-diketones involve attaching chiral auxiliaries to the ketone, which in turn provides the chiral induction with moderate to excellent de and ee being achieved.[64, 96] The success of the chiral auxiliaries is dependent on whether they can be synthesised in chirally pure form and chiral sulfoxides form an important subclass of this category. The past three decades have seen an explosion in interest in the synthesis and utility of molecules containing a stereogenic sulfur center[97, 98, 99]. The sulfoxide auxiliary can be easily prepared by what is generally referred to as the Anderson method, starting from the sodium salt of *p*-toluenesulfinic acid **81** (**Scheme 16**), although different starting sulfinates can be used. Once treated with thionyl chloride, the salt is converted to intermediate **82** followed by a nucleophilic

substitution with menthol to afford **83**. Finally, a Grignard reaction leads to the chiral auxiliary **84** which is easily reacted with β-hydroxyesters. Though this structural motif is typically represented in Lewis structures as analogous to a carbonyl moiety, the sulfur atom of the sulfoxide **84** is in fact a stereogenic center when two different groups apart from oxygen are attached.

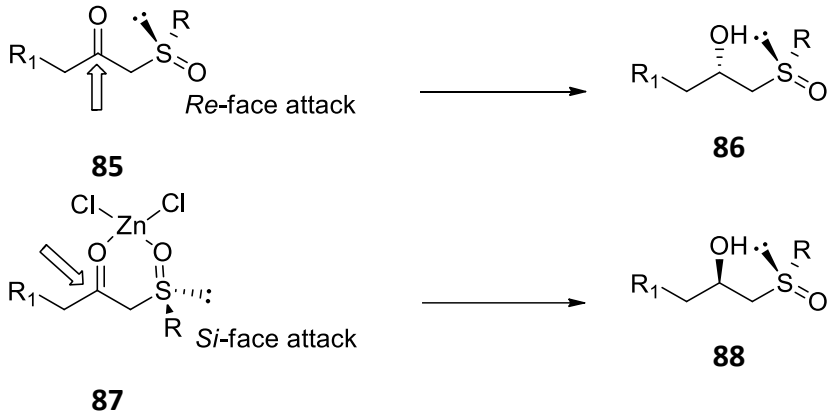


81 **82** **83** **84**

Scheme 16: Synthesis of sulfoxide, Anderson method

The oxygen and sulfur do not share a typical *p*-orbital *pi* bond which would enforce a planar conformation, but rather the oxygen donates electron density from a lone pair into a d-orbital of sulfur. This d-π bonding allows the sulfur to assume tetrahedral sp^3 hybridization, with a lone pair of electrons from sulfur as "place holders" in the fourth quadrant resulting in the observed chirality. Sulfoxides are conformationally stable at room temperature and therefore can be separated into pure diastereomers when a substituent, like menthol, with inherent chirality is attached. The barrier to inversion via a bipyramidal intermediate for most sulfoxide compounds is in the range of 38-41 kcal/mol. As such, sulfoxides will only racemise under rather harsh conditions, including temperatures in excess of 200 °C, irradiation to induce C-S bond scission, and radical transfer reagents.

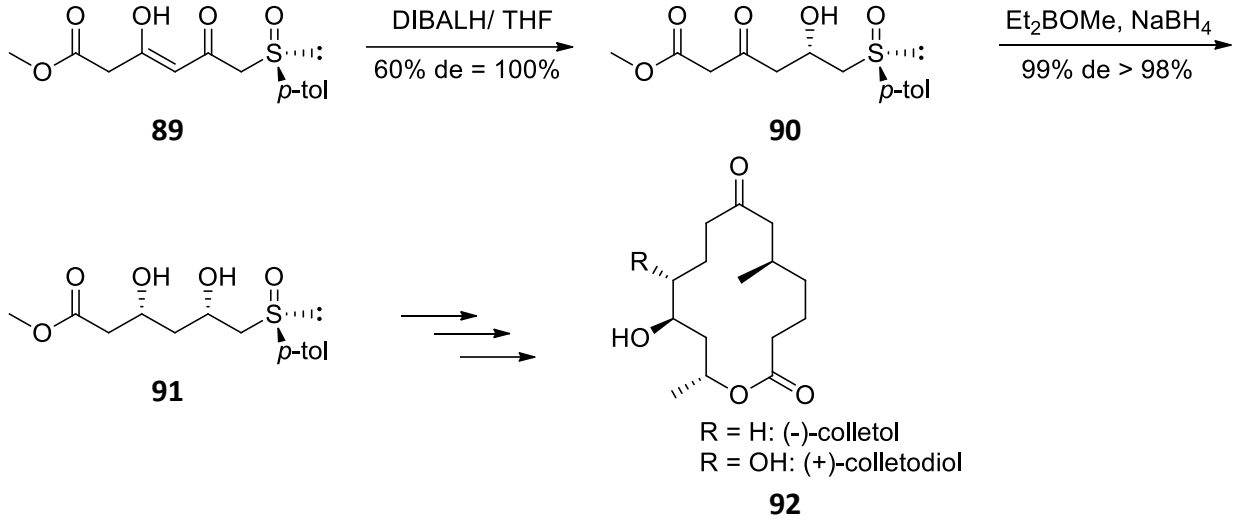
When the sulfoxide chiral auxiliary is added to a molecule possessing either a β- or δ- ketone it transfers chirality to the newly formed stereogenic centre during reduction of the carbonyl groups. The bulky R-group attached to the sulfur atom provides steric hindrance coupled with electronic effects during the reduction. The electronic effects arise from the electrostatic repulsion between the incoming nucleophile and the substituent of the sulfoxide. Reduction of substrate **85** means that the hydride will only be delivered on the *Re*-face of the ketone because the *Si*-face is blocked by the R-group on the sulfoxide group resulting in product **86** with an *S*-configuration at the newly formed stereogenic centre (**Scheme 17**). Introduction of a Lewis acid like $ZnCl_2$ results in the chelation of the ketone and the sulfur oxygen affording an intermediate **87**. The locked conformation of the molecule blocks the *Re*-face meaning the hydride can only be delivered from the *Si*-face yielding a substrate **88** with an *R*-configuration. By using the sulfoxide auxiliary both enantiomers can be easily synthesised which is not easily achieved with other methods.



85 **86** **87** **88**

Scheme 17: Selective reduction of sulfoxides

The sulfoxide protocol has been incorporated into the synthesis of various biologically important molecules with much success. A general synthetic strategy for the antifungal natural products (-)-colletol and (+)-colletodiol **92** was developed, and the method successfully incorporated a sulfoxide auxiliary for chiral induction.[100] Synthesis of a crucial 1,3-*syn*-diol fragment involved the iterative stereo-controlled reduction of the sulfoxide **89** yielding the hydroxyketone **90** in a de of 100% (**Scheme 18**). Successive reduction of the δ carbonyl using the Narasaka-Prasad protocol ensured the recovery of a 1,3-*syn*-diol **91** in an excellent de of 98%.[100] The simplicity of the synthesis of the sulfoxide auxiliary and the high de of the recovered secondary alcohols made this an ideal procedure for the synthesis of the desired compounds.

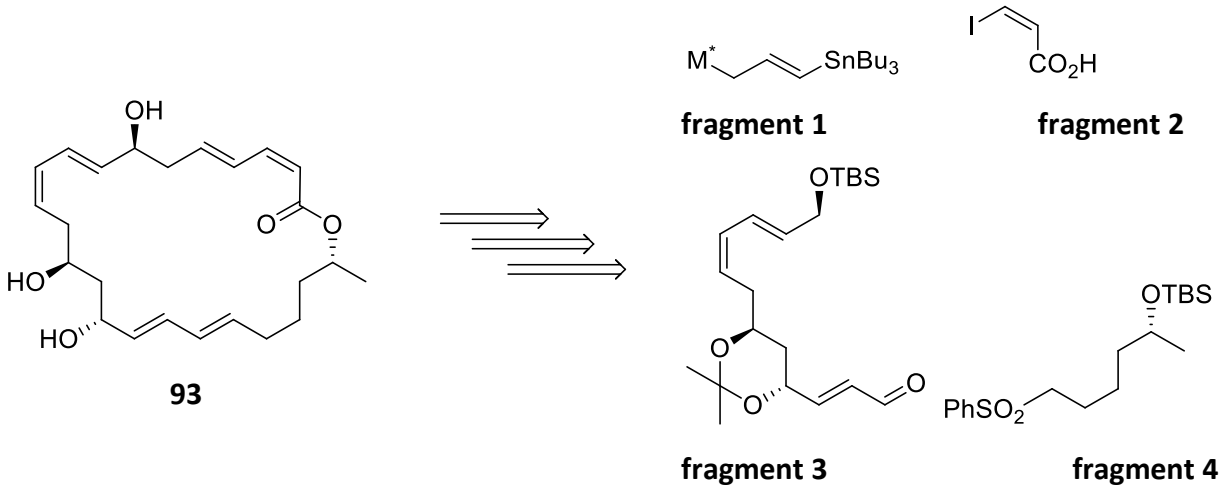


89 **90** **91** **92**

Scheme 18: Synthesis of (-)-colletol and (+)-colletodiol

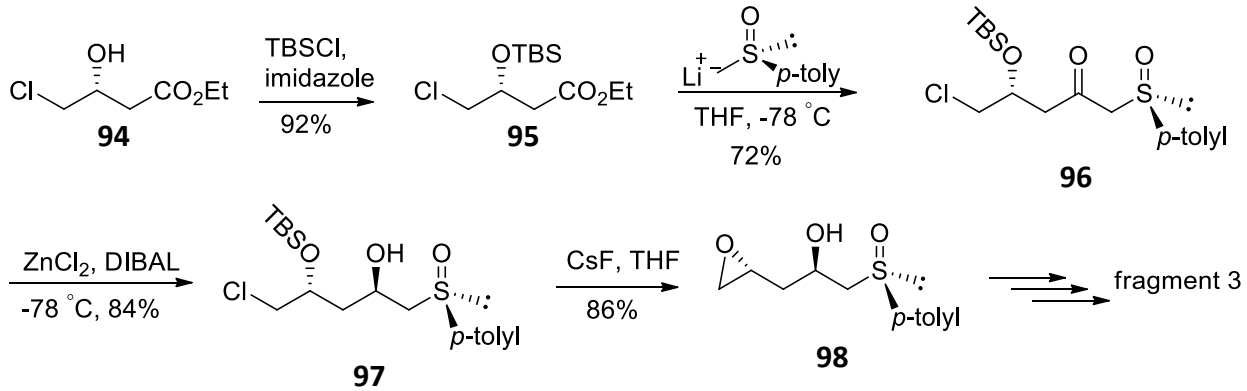
Macrolactin **93** is a potent antiviral and antitumour agent which was isolated from metabolites of deep-sea bacteria.[101] The unique structural architecture and the potential for broad therapeutic application of the macrolactin led to the development of a synthetic methodology for this compound. Of the four components identified by retrosynthetic analysis (**Scheme 19**), fragment

3 contained the 1,3-*anti*-diol synthon which was crucial in the synthesis of the target compound. For the synthesis of analogues of compound **93** they needed to employ a method which furnished different 1,3-diol conformations. Thus, the sulfoxide auxiliary was chosen because it allowed for the synthesis of the targeted diastereomers.



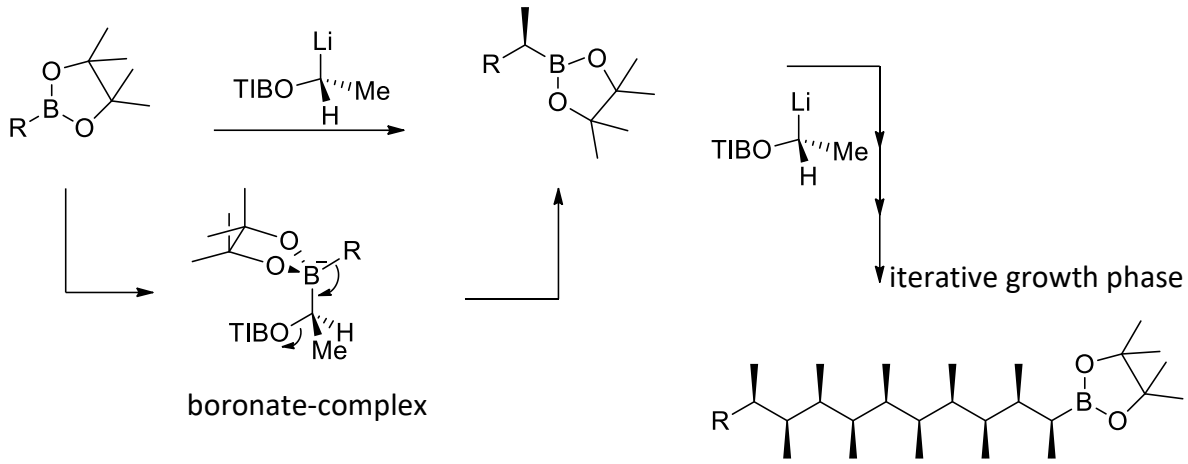
Scheme 19: Retrosynthesis for macrolactin 93

The requisite fragment was prepared according to **Scheme 20**. The β-hydroxyester **94** was TBS protected yielding compound **95** which was subsequently subjected to the addition of the sulfoxide auxiliary. The β-ketosulfoxide **96** was recovered in a good yield of 72% with high de. In order to recover the *anti*-1,3-diol during the stereoselective reduction, a chelating agent $ZnCl_2$ was added prior to the introduction of the reducing agent. The desired product **97** was recovered as a single diastereomer after recrystallisation. Epoxide **98** was easily recovered after treatment of the diol with cesium (I) fluoride in THF. All four possible diastereomers of this motif were successfully synthesised using this protocol by varying the reaction conditions. Subsequent chemical transformations allowed for the synthesis of the target fragment 3.



Scheme 20: Synthesis of macrolactin's fragment 3

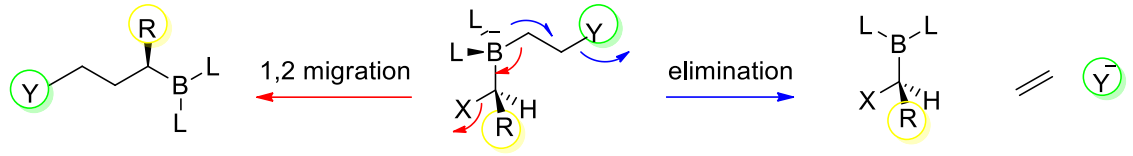
Apart from the syntheses of 1,3-diols already described, there are many more methods that have been developed that incorporate various synthetic strategies.[64] The fact that the 1,3-diol unit is present as a repeating unit in molecules of biological importance, created the need for iterative synthetic methods such as homologation of boronic esters. This method has been demonstrated to be a useful procedure for the iterative synthesis of chiral compounds because it presents full stereocontrol, exemplified by the application of the method in the synthesis of (+)-10-hydroxyphthioceranic acid (**Scheme 21**).[102]



Scheme 21: Iterative homologation of esters for the synthesis of permethylated carbon chains

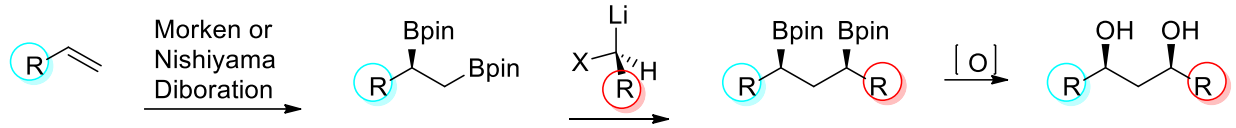
The homologation proceeds via addition of a suitable boronic ester to a starting fragment followed by a 1,2-migration of the boronic ester to generate a new boronic ester. Unfortunately application of boronic esters to the synthesis of 1,3-hydroxy groups was hindered by the formation of the intermediate boronate complex shown in **Scheme 22**. The complex can either undergo the desired 1,2 migration or the undesired β-elimination. In order to circumvent the problem, the β-alkoxy group was masked with another boron atom because 1) the β-boronic ester does not undergo elimination 2) oxygen functionality can be readily generated from the boron intermediate and 3) the required 1,2-bis(boronic esters) are readily available through Morken/Nishiyama catalytic asymmetric diboration of alkenes.

1. Limitation of homologation of organoboron compounds



Y = halogen, oxygen, nitrogen group

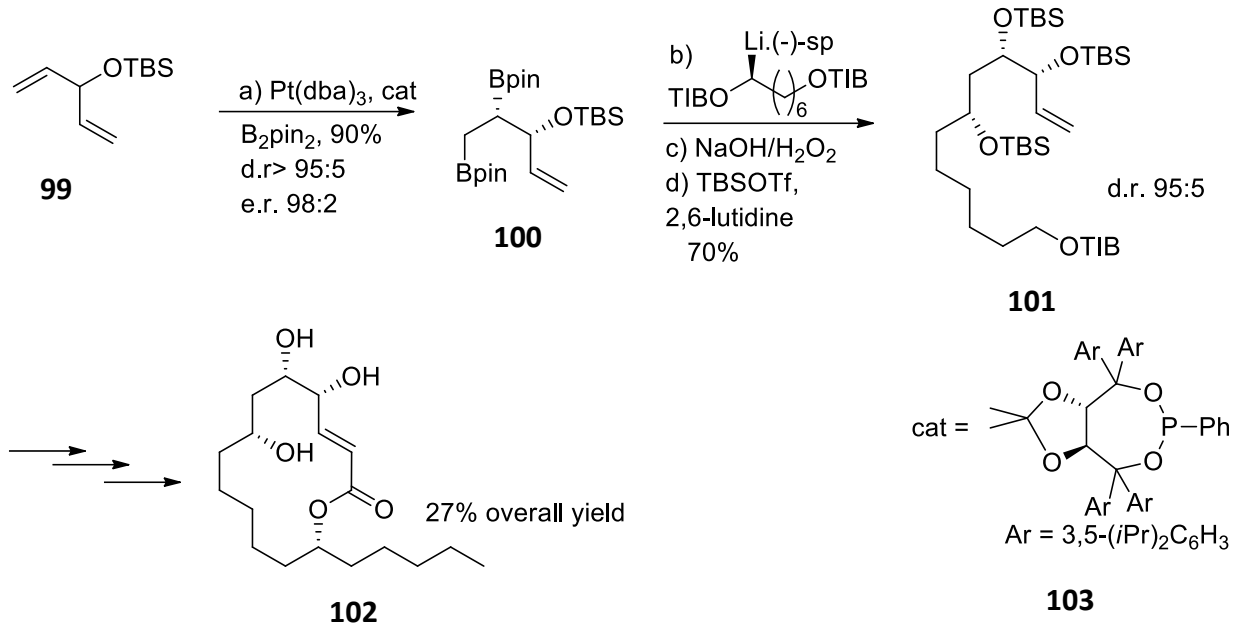
2. Regioselective homologation of 1,2 bis(boronic esters)



Scheme 22: Homologation of organoboron compounds

The modified method was first successfully tested on several substrates for the regio- and stereoselective homologation of 1,2-bis(boronic esters).[103] A diverse library of both *syn*- and *anti*-1,3-diols was prepared in high selectivity which culminated in the preparation of a TBS-protected derivative of the lipid lowering drug atorvastatin in good yields and excellent levels of stereoselectivity. To further showcase the versatility of the methodology Fawcett *et al.* applied the homologation method in the concise total synthesis of the 14-membered lactone Sch 725674 isolated from *Aspergillus* sp. The lactone exhibits moderate antifungal activity. Using Morken's conditions on the divinyl carbinol *O*-silyl derivative **99** furnished a single-diboration product **100** in 90% yield with excellent stereoselectivity.

The 1,2-boronic ester was converted to the TBS-protected triol **101** and the diastereoselectivity of the transformation was approximately 95:5 revealing the desired 1,3-diol motif in the process (**Scheme 23**). Subjecting the protected triol to a few of the remaining steps afforded the desired product **102** in an overall yield of 27%. The chiral catalyst **103** plays a crucial role in controlling the stereochemistry of **100**. The homologation method has been shown to be applicable for both the stereoselective synthesis of 1,3-diol systems and chiral secondary hydroxyl groups.



Scheme 23: Total synthesis of Sch 725674 (102)

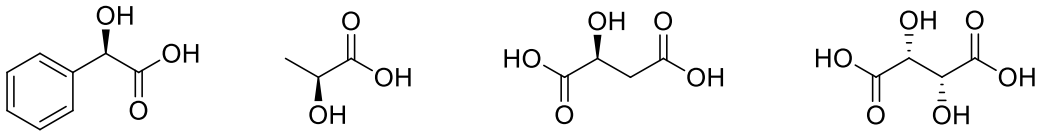
Although the described methods for the synthesis of 1,3-diols are not close to the total number of available methods, the list is representative and highlights how the moiety can be synthesised. The described methods also highlight which starting materials, are compatible with the respective methods.

1.6 Hydroxy acids from the chiral pool

The total synthesis of biologically active chiral molecules is characterised by the need for absolute regio- and stereo-chemical control. A crucial aspect in the design of the synthetic route is the decision relating to the stage at which it is most economical to work with enantiomerically pure compounds. Resolution of racemic mixtures at the final stage is undesirable because half of the yield is sacrificed. Another option is starting the synthesis from chiral synthons which necessitates stereocontrol at every subsequent step, especially when new elements are introduced.

Given the fact that this work involves stereoselective synthesis involving chiral hydroxy compounds it is prudent that a chiral synthon is selected as the starting material. Chiral synthons can either be synthesised or used from the library provided by nature's pool. The four main chiral synthons from nature best suited for application in this work are the α-hydroxy acids, namely mandelic acid, lactic acid, malic acid and tartaric acid (**Figure 15**).[104] These four acids are commonly used as precursors in enantioselective synthesis because they assist in minimising the

need for chiral resolution or asymmetric catalysis. For the work under investigation a chiral synthon with 1) a chiral secondary alcohol 2) functional group which allows for the stereo controlled introduction of a second alcohol group at the β-position and 3) terminal carbon atoms possessing functional groups that could be modified into amine groups, would be the most ideal.



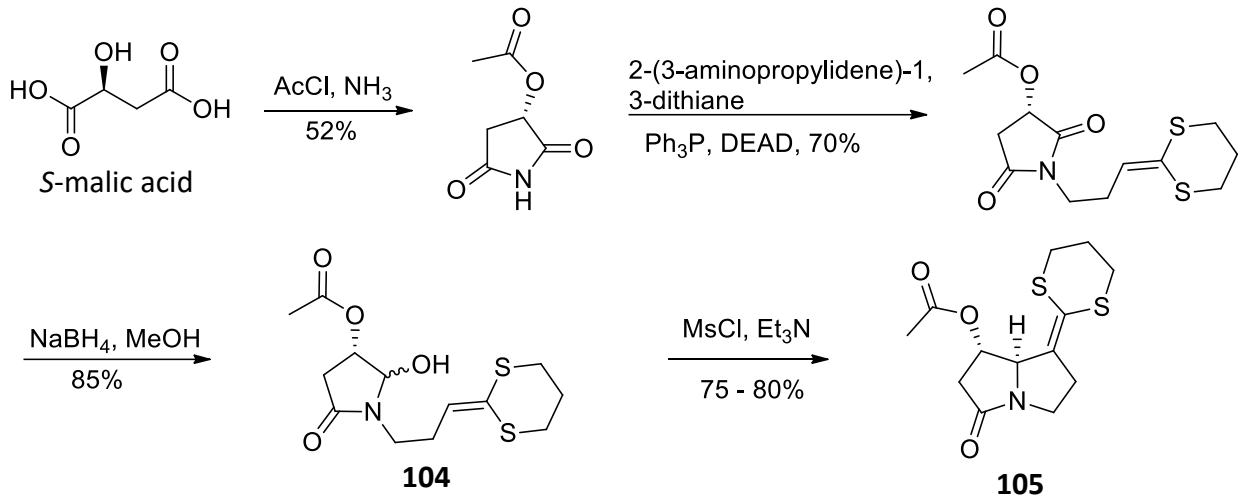
mandelic acid **lactic acid** **malic acid** **tartaric acid**

Figure 15: Naturally occurring α-hydroxy acids

Of the four acids listed, malic acid is best suited for the synthesis of the C_5 fragment because of the inherent chiral hydroxyl group, with a carbonyl group β to the alcohol and the terminal carbon atoms are carboxylic acids which are easily manipulated to afford other functional groups. Malic acid has been widely used as a chiral synthon in the synthesis of medicinal agents, natural products and agrochemicals. Despite possessing two nearly identical carboxylic acid groups, there are various techniques available to manipulate them individually. As a result of this differentiation it will be possible to add the chiral sulfoxide auxiliary to malic acid which would then be used to stereoselectively reduce the carbonyl group using established methods.[105]

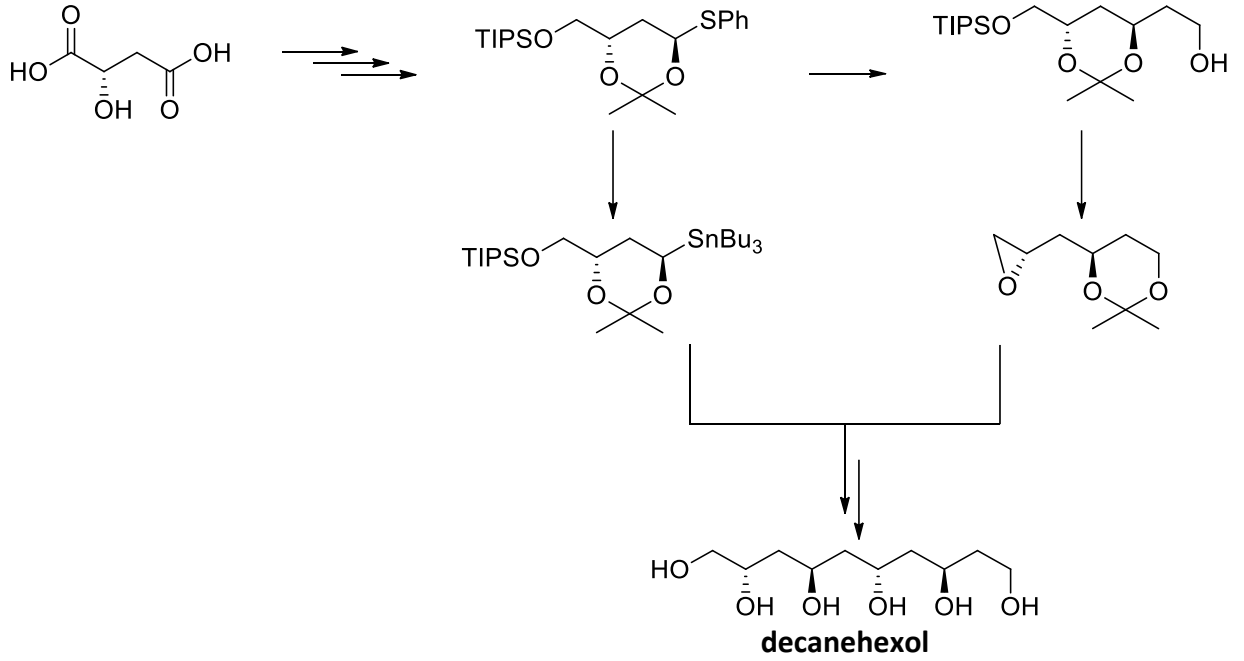
Literature is awash with the total synthesis of chiral molecules that integrated malic acid as a chiral synthon for preparation of chiral products.[106] Herein a few representative examples from literature are going to be highlighted.

In their quest for finding chirally pure intermediates for the synthesis of pyrrolizidines, Chamberlain *et al.* proved that employing both enantiomers of malic acid facilitated the progression of the reactions with high selectivity (**Scheme 24**).[107] Their initial attempts were unsuccessful because they yielded a complex mixture of products because the final ring closing step lacked control. However, after choosing malic acid as the starting material, ring closing of **104** proceeded with high selectivity to yield the desired intermediate **105**. The regioselectivity was due to the steric effects of the inherent chirality afforded by the acetyl group, from the hydroxyl functionality of malic acid. They were able to synthesis the enantiomer of **105** by using *R*-malic acid.



Scheme 24: Stereoselective synthesis of a pyrrolizidine intermediate 105 from malic acid

Other researchers like Burton *et al.*, were only able to synthesis (+)-laurencin in its enantiomerically pure form after using *R*-malic acid as the starting material.[108] Rychnovsky successfully designed a convergent method for the synthesis of polyol chains from malic acid after using the inherent chirality for inducing chirality of new stereogenic centres (**Scheme 25**).[109] The method also required far fewer steps when compared to previously used methods. The recovered decanehexol is a fragment of the antibacterial agent lienomycin. Previous methods were longer and resulted in a mixture of products. Malic acid was incorporated in the synthesis of many other oxo-polyene macrolide antibiotics as highlighted in a review by Rychnovsky.[110]

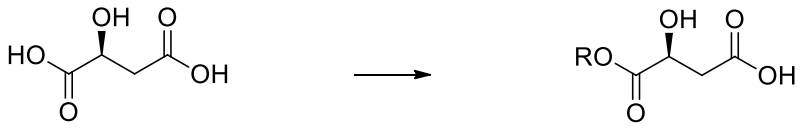


Scheme 25: Synthesis of the polyol, decanehexol

1.6.1 Malic acid carboxylic acid differentiation methods

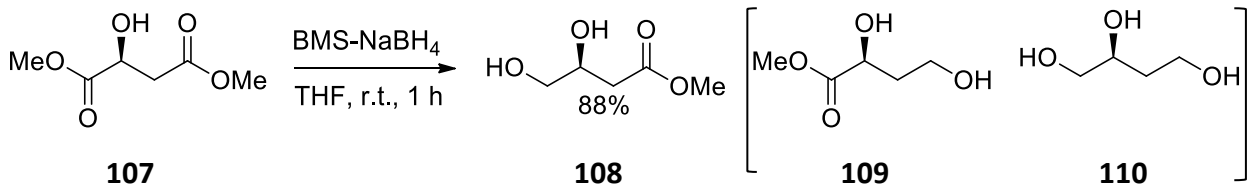
One of the initial steps when employing malic acid as a chiral starting material would involve differentiation of the two carboxylic acid groups. Several methods are available for the selective esterification of the carboxylic acid α to the hydroxyl group. Most methods capitalise on procedures that form intermediates with a preference for the formation of 5-membered rings as opposed to six membered rings. The rings form via the chelation of the carbonyl and hydroxyl group.

Houston *et al*. published a protocol for the selective esterification of α-hydroxycarboxylic acids without causing significant esterification of the other carboxylic acids in the presence of boric acid.[111] Between 10 – 20% of the boric acid in the chosen alcohol was sufficient to effect the desired transformation yielding a mono ester **106** (**Scheme 26**). About 10% of the diester was recovered when the malic acid concentration was greater than 0.25 M. Compound **106** can also be recovered by the treatment of malic acid with either 2 equivalents of TFAA or DCC to form an anhydride.[112] Quenching of the ensuing anhydride with the desired alcohol yields the monoester. Enzymatic methods have also been successfully used for the differentiation of the acid groups by means of *Candida antarctica* lipase esterification.[113]



Scheme 26: Selective esterification of malic acid

Another method for differentiation of the terminal carbon atoms involves initially esterifying the acid to recover the diester **107**, followed by the selective reduction of the ester α to the hydroxyl group in the presence of BMS-$NaBH_4$ (**Scheme 27**).[114] There were three possible products from this reaction but only compound **108** was recovered in a yield of 88%. The other possible products, **109** and **110**, were not recovered.



Scheme 27: Selective reduction of esterified malic acid

1.7 Aims of the project

In order to achieve a comprehensive study of the structure activity relationships of pavettamine **111**, this study aims to synthesise the unnatural enantiomer of pavettamine **112** and analogues with reduced functionality, **113** – **116** (**Figure 16**). The interest in pavettamine arises from the fact that it is a toxin which affects the livelihood of people in Southern Africa and establishing structure activity relationships might help in the prevention or treatment of the "quick disease" and in developing compounds with possible therapeutic and pharmaceutical applications. Comparison of the toxicology test results of our target compounds with those that have already been synthesised will provide a broad overview in understanding of the activity of pavettamine.

The 1,3-diol functionality unique to pavettamine is also present in the most potent biologically active compounds, which makes this rare polyamine and its analogues potentially potent. The sheer interest and applications of polyamines and compounds with 1,3-diol functionality means there are a plethora of methods which can be used for the synthesis of the target compounds. The general approach to synthesising polyamines involves two main steps, namely the synthesis of the individual methylene linkers and combining the linkers, usually via reductive amination.

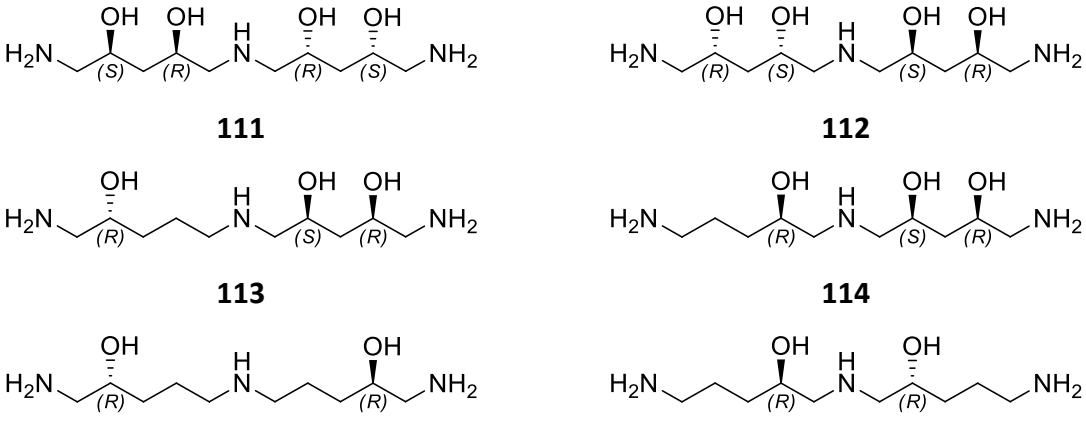


Figure 16: Pavettamine, enantiomer of pavettamine and its analogues

The proposal for this project is to synthesise the compounds shown in **Figure 16** because to the best of our knowledge, these compounds have not yet been synthesized, with the exception of pavettamine. Organic synthesis is a creative science that entails the design and execution of proposed synthetic routes for the preparation of compounds. In order to design a plausible synthetic route for the target compound a retrosynthetic analysis was performed.

1.7.1 Retrosynthetic analysis

Retrosynthetic analysis is a problem solving technique for transforming the structure of a synthetic target molecule to a sequence of progressively simpler structures along a pathway that ultimately leads to simple or commercially available starting materials. Pavettamine is a molecule with C_2 symmetry with a central C-N bond which can be disconnected after a series of functional group transformations into a single C_5 unit (**Figure 17**). This approach allows the synthesis of the target compound to be accomplished by the preparation of a common C_5 subunit using malic acid as the starting material. The presence of both hydroxyl and primary amino groups presents a challenge which requires an orthogonal protection strategy taking into consideration the subsequent reaction conditions. The synthesis of polyamines is generally plagued with problems regarding the selective protection or the directed reaction of the various primary and secondary amino functionalities. It is therefore of vital importance that the protecting groups selected are versatile, and non-labile under most reaction conditions, whilst being easily cleavable at the end of the reaction sequence. Selectivity can be achieved by use of protecting groups capable of differentiating between primary and secondary amines and alcohols.

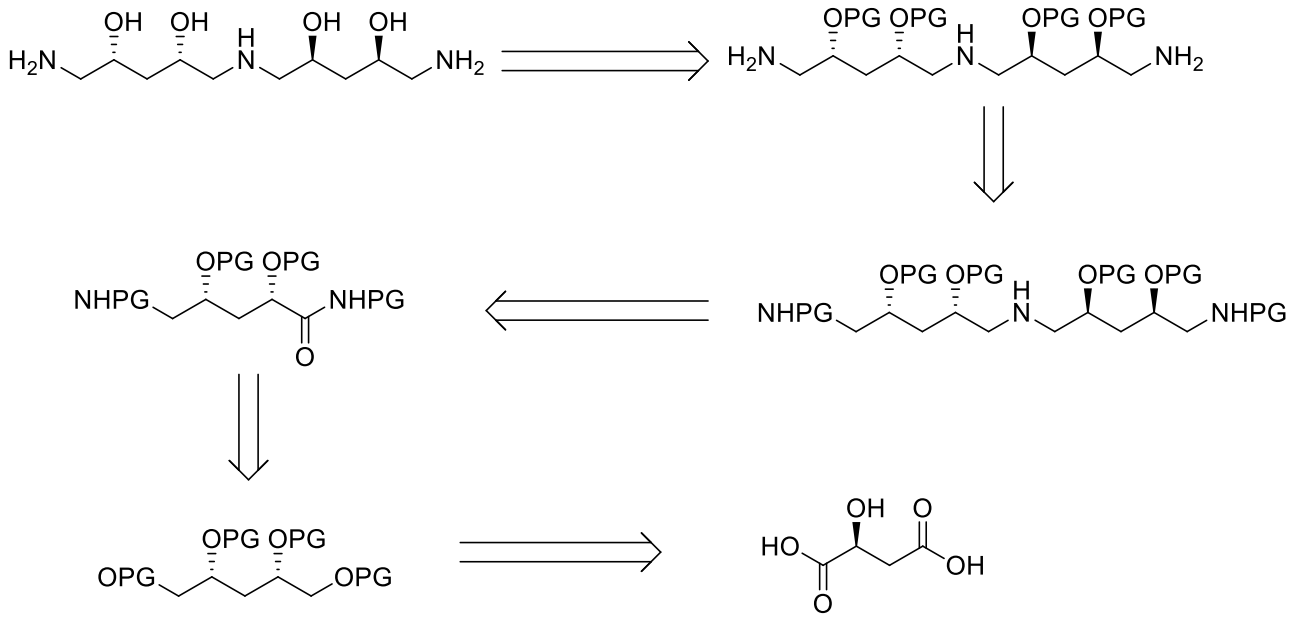


Figure 17: Retrosynthetic analysis the enantiomer of pavettamine

To accomplish differentiation between amines and alcohols, a modular construction of the polyamine backbone will be undertaken, allowing for the stepwise introduction of the alcohol and amine groups. This strategy generally results in complex synthetic schemes and is limited by the number of orthogonal amino/alcohol protection groups which are compatible with this type of

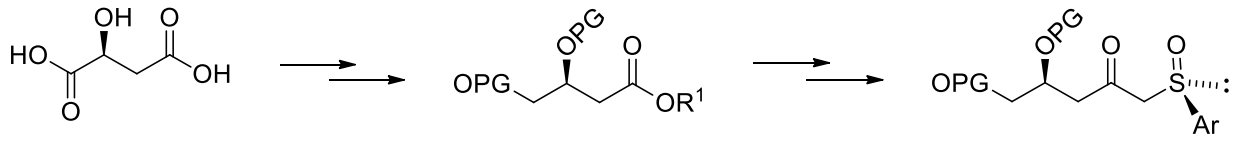
approach. Work-up and purification of both products and intermediates is generally tedious and complicated because of high substrate polarities. Purification on silica gel requires large volumes of polar solvents such as methanol, adversely increasing the amount of impurities resulting from the solubilisation of the silica gel.

One way of circumventing the above-mentioned problems is to immobilise the starting substrate on resin because it eliminates the need for excess reagents accompanied by simple washing steps. However, the method is not without its own set of problems. Usually more than 90% of the reaction site is located inside the resin bead and only solvents that swell the bead can be applied. The resin is also sensitive to mechanical stress and reaction conditions like high temperatures and aggressive reagents destroy the matrix. Monitoring the reaction is more difficult because techniques like thin layer chromatography are not directly accessible. Harsh conditions are normally used for the removal of the resin which can potentially compromise the stereochemical integrity of the desired product.

Given the pros and cons of the two different approaches for the synthesis of polyamines, modular construction of the C_5 methylene backbone would be the best for synthesising the desired compounds. The two C_5 units can be coupled using reductive amination between a primary amine and a carboxylic acid or aldehyde. The primary amines can be synthesised from the conversion of the hydroxyl groups using already published methods. What remains after retrosynthetic analysis is a C_5 unit with a 1,3-hydroxyl functionality which can be derived from malic acid.

1.7.2 Proposed synthetic approach

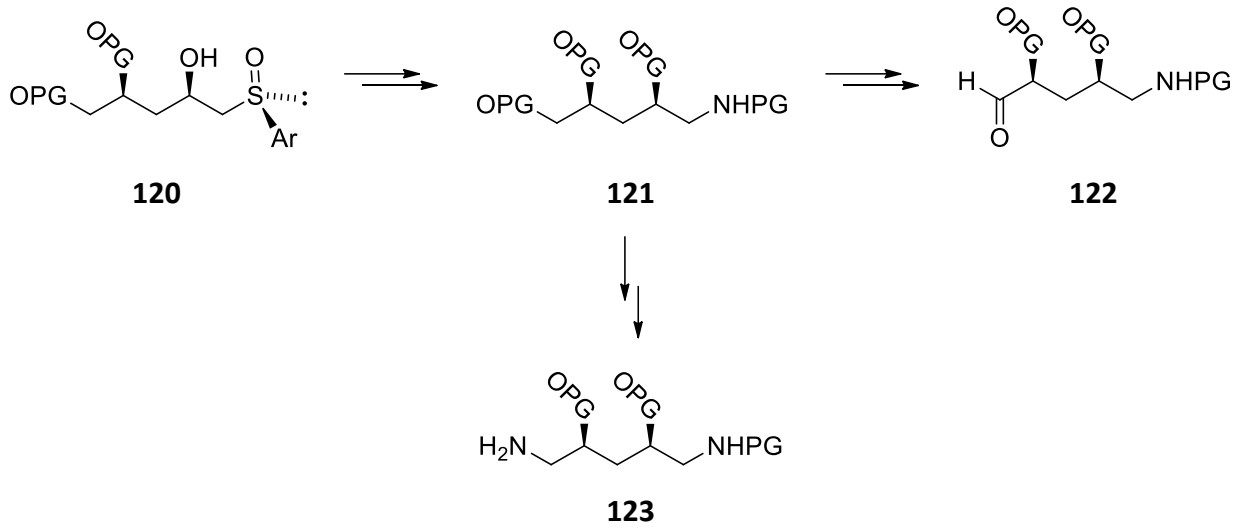
A key feature for the synthesis of pavettamine and the analogues is the sequential construction of the hydroxyl stereogenic centres. Malic acid **117** was identified as the ideal starting material because it already contains an enantiomerically pure β-hydroxyketone moiety. Having selected the starting material combined with the already discussed methods of 1,3-chiral induction, part of the proposed synthetic strategy is shown in **Scheme 28**. Protection of the alcohol to afford **118** coupled with addition of the sulfoxide chiral auxiliary will yield compound **119**. The added advantage of employing methyl *p*-tolyl sulfoxide as a chiral auxiliary is the elongation of the carbon chain from C-4 of malic acid to the desired C-5. The C-2 symmetry of the target molecules allows for the synthesis of one subunit followed by functionalisation of the terminal carbon atoms at a later stage to facilitate the coupling step and introduce the amine groups.



117 **118** **119**

Scheme 28: Proposed synthetic strategy 1

After several transformations of malic acid, the sulfoxide auxiliary present in compound **119** will enable the stereoselective reduction of the carbonyl group with the anticipated diastereoselectivity yielding substrate **120**. In principle either the *syn*- or 1,3-*anti*-diol for substrate **120** can be prepared depending on the reaction conditions of the reduction step. Once the second hydroxyl functionality is introduced, careful consideration will have to be given to which protecting group strategy will be applied. The sulfoxide moiety is easily transformed using the Pummerer rearrangement[115] and the ensuing product will be converted to an amine giving rise to substrate **121.** From this point, attention will be focused on the functionalisation of the terminal carbon atoms at the ends where coupling of the two fragments will occur. For illustration purposes, the penultimate crucial step for the synthesis of compound **112** would involve converting the alcohol on substrate **121** to the aldehyde **122** for fragment 1 and to the amine **123** for fragment 2.

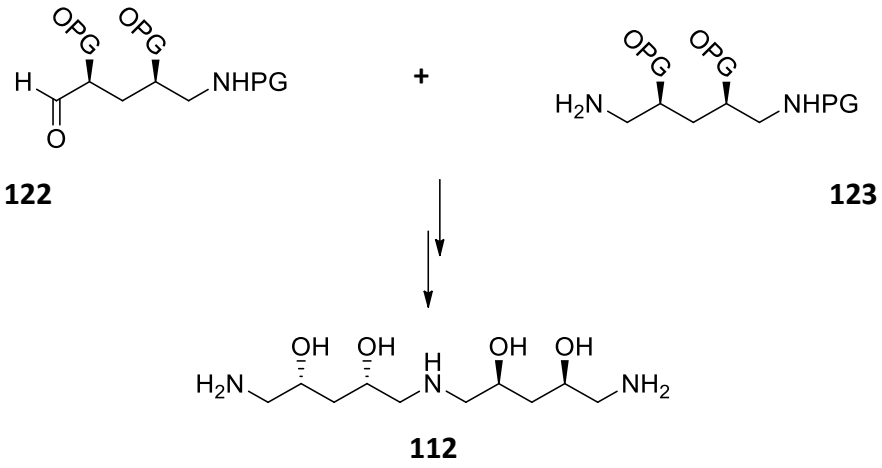


120 **121** **122**

123

Scheme 29: Proposed synthetic strategy

Once the two C_5 fragments have been synthesised they can be coupled together using reductive amination (**Scheme 30**), followed by the removal of the protecting groups to reveal the desired product. The synthesis of all the other analogues will be based on this synthetic strategy. The C_5 fragment for reduced functionality analogues **113** – **116** will be synthesised using the sulfoxide protocol employing substrates such as 4-chlorobutyric acid and y-butyrolactone.



122 **123**

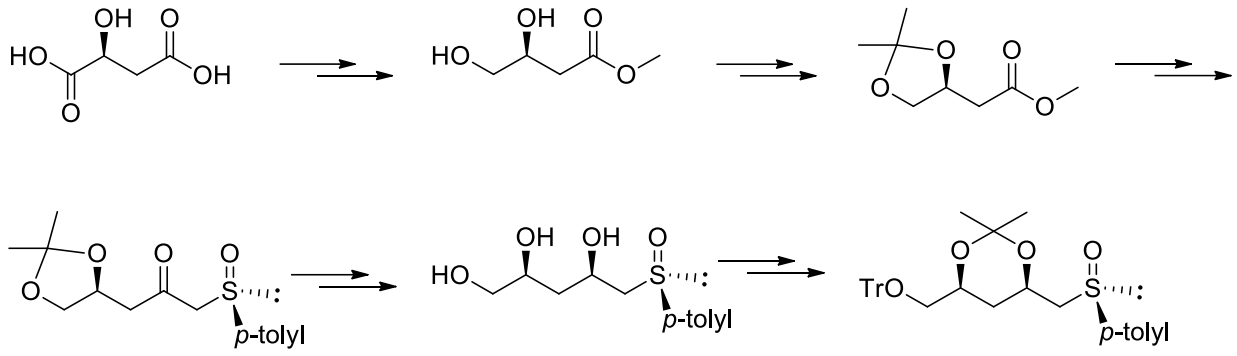
112

Scheme 30: Coupling of the two C-5 fragments

Chapter 2: Results and Discussion

2.1 Introduction

Using the naturally occurring malic acid as the starting material, synthesis of pavettamine and its analogues was undertaken using a modular design approach. It was envisioned that using this protocol would allow for a quick entry into the library of desired compounds in a reasonable number of steps. As already discussed in **Chapter 1** (retrosynthetic analysis), the major steps of the synthetic route involve the synthesis of the chiral auxiliary and the stereo-controlled introduction of the alcohol functionality by use of a sulfoxide chiral auxiliary. Thirdly, choosing the right protecting groups for the amine and alcohol groups was critical as it would have a huge influence on how the final compound would be isolated. Use of malic acid reduced the complexity of the synthetic process for pavettamine and its enantiomer. For the first part of the synthesis, the two carboxylic acids of malic acid were differentiated, and the 1,3-diol functionality was introduced and protected as shown in **Scheme 31**.



124

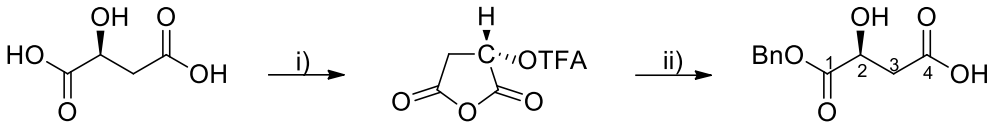
Scheme 31: Introduction of the 1,3-*syn*-diol functionality to *S*-malic acid

2.2 Synthesis of the enantiomer of pavettamine

2.2.1 Synthesis of the 1,3-*syn*-diol intermediate 124

Commencement of the synthesis began by the selective esterification of 2*S*-malic acid (**Scheme 32**) using benzyl alcohol. This approach allowed for the differentiation of the two terminal carboxylic acids, which in turn expedited the stepwise functionalisation of the starting material towards the target fragments. The acid was treated with two equivalents of TFAA over an ice bath, followed by the evaporation of excess TFAA and TFA formed.[116, 117] This step provided the

corresponding trifluoroacetate of malic anhydride, **125** as an intermediate in quantitative yield. The intermediate was not isolated but treated with an excess of benzyl alcohol and the reaction was left stirring overnight at room temperature. Purification of the product afforded compound **126** in a yield of 61% as a yellow oil.



Malic acid **125** **126**

Scheme 32: i) TFAA, 0 °C, 2 h; ii) benzyl alcohol, r.t., overnight, 61% overall yield

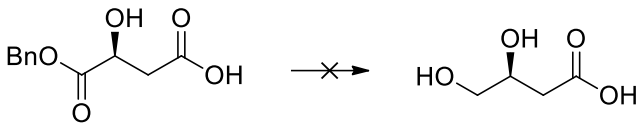
Characterisation of the recovered product was accomplished by means of NMR spectroscopy. As expected, the aromatic protons at δ 7.39 – 7.27 integrating for 5 protons and the benzylic CH_2 protons which appeared as a singlet at δ 5.19 integrating for two protons were observed in the ^1H NMR spectrum. The presence of these signals confirmed the successful mono-benzylation of malic acid, as opposed to the potential dibenzyl product. The H-2 proton signal was at δ 4.62 – 4.48 whilst the H-3 protons were observed as doublets of doublets at δ 2.89 (*J* = 16.7, 4.2 Hz) and δ 2.80 (*J* = 16.8, 6.2 Hz). The ^{13}C NMR spectrum showed the characteristic carbonyl carbon signals 1 and 4 at δ 175.5 and δ 173.2 respectively. The difference in chemical shifts is because the carbonyl carbon for the carboxylic acid experiences a greater shielding effect due to delocalisation of electrons of the carboxylic acid. The rest of the signals were as expected. IR spectroscopy showed signals for both the alcohol at 3534 cm^{-1} and the broad carboxylic acid signal at 3274 cm^{-1}.

Having achieved the terminal carbon differentiation, the next step involved selectively reducing the ester group in the presence of the carboxylic acid group (**Scheme 33**). Several reports for this procedure are available in literature but none of them were successfully employed for the selective ester reduction of compound **126**.[118, 119] Initially the reduction was performed using a mild reducing agent $NaBH_4$ in the presence of LiCl in diglyme at a refluxing temperature of 150 °C.[120] TLC showed total consumption of the starting material but the expected product was unrecoverable after workup.

Two factors could have been responsible for the observed outcome; firstly, the expected product compound **127** is polar and therefore water-soluble. Due to the water solubility, the desired product would likely be lost to the aqueous layer during workup and secondly, the reduction could

have occurred at both the ester and the carboxylic acid functional groups. The aqueous workup was necessary for removing the diglyme and for quenching the reducing agent. Realising the complexity of product purification due to aqueous solubility of the desired product, the reaction was performed in toluene, which is a much easier solvent to remove, and only stoichiometric amounts of $KHSO_4$ were used during workup. However, there was no change in the observed outcomes. Varying the temperatures and the reaction times did not yield the desired product either.

After several failed attempts at selectively reducing the benzyl ester, a supposedly more selective method was chosen (**Scheme 33**) involving the use of $LiBH_4$ as the reducing agent, as reported by Blacklock *et al*.[118, 121] The mechanism for the procedure involved lithium coordinating with the alcohol and the carbonyl on the α-carbon before delivering the hydride. The hydroxyl group provided anchimeric assistance, forming a stable and more favourable complex as opposed to the complex formed resulting from lithium coordinating the alcohol and the carbonyl on the β-carbon, which makes this procedure more selective. Unfortunately, as with the other procedures neither the starting material nor the expected product were recovered. THF was replaced with diethyl ether as solvent and the reaction was left stirring for up to 2 days whilst observing the reaction by TLC. Unfortunately the desired product was not recovered after workup despite the recovery of a side product emanating from the benzyl group of compound **126**.

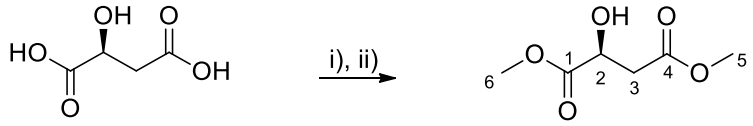


126 **127**

Scheme 33: $LiBH_4$, THF, reflux, overnight

Realising that compound **127** would be difficult to isolate because of the aqueous work up, converting the carboxylic acid of compound **126** to a Weinreb amide seemed a possible way of reducing the polarity.[122] Even though Weinreb amides are reducible, conditions exist where selective reduction of the benzyl ester is possible in the presence of the amide. Unfortunately, the synthesis of the Weinreb amide was not successful despite varying the experimental conditions. Following these series of unsuccessful experiments, a different approach for malic acid differentiation was chosen.

The second approach involved the esterification of both the carboxylic acid groups of 2*S*-malic acid using thionyl chloride and methanol (**Scheme 34**) as the first step.[123] In this reaction thionyl chloride acts as an electrophile at the sulfur atom due to the presence of the 2 chlorine atoms and the oxygen atom attached. The sulfur is then attacked by the carboxylic acid to give an unstable and highly electrophilic intermediate, which disintegrates in the presence of methanol resulting in the acyl chloride, HCl and SO_2. The release of SO_2 was evidenced by effervescence as the thionyl chloride was being slowly added. The activated acyl chloride reacted with the methanol yielding the expected diester, compound **128**, in a yield of 77% as a colourless oil.



Malic acid **128**

Scheme 34: i) $SOCl_2$, MeOH, 0 °C, 1 h; ii) r.t., 12 h, 77%

The recovered yield of 77% for malic acid dimethyl ester **128** was lower than the literature value of 98% as reported by Borjesson *et al*.[123] This could have resulted from using slightly wet methanol, which meant any water present easily hydrolysed the acyl chloride formed back to the carboxylic acid. Formation of the product was confirmed by ^{1}H NMR spectroscopy evidenced by the presence of the methoxy proton signals (H-5 and H-6) at δ 3.81 and δ 3.72. The OH signal was observed at δ 3.58 as a doublet with a coupling constant of 6.0 Hz, and this signal was confirmed by the D_2O exchange experiment as shown in **Figure 18**. All the ^{13}C NMR spectroscopic signals were as expected and the IR spectrum showed the characteristic OH and C=O signals at 3478 cm^{-1} and 1730 cm^{-1}, respectively.

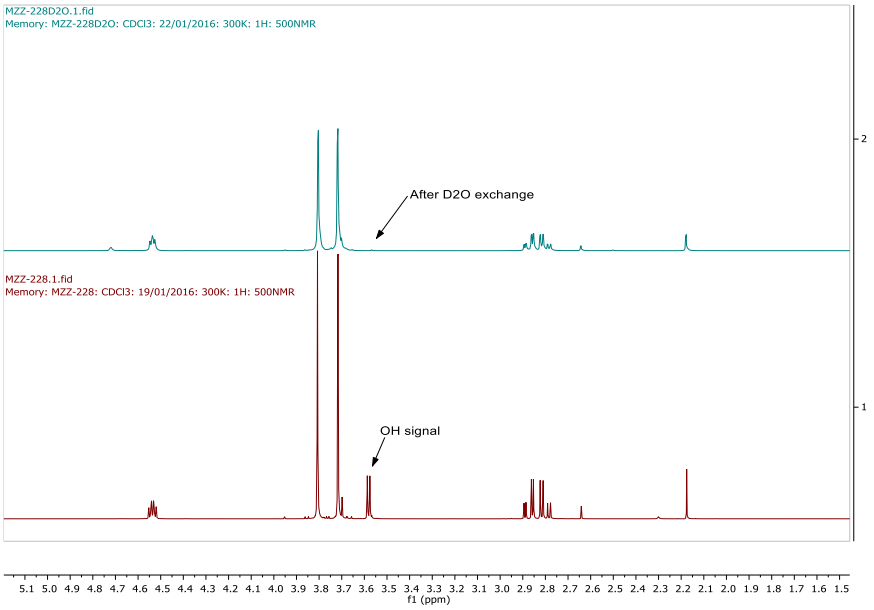
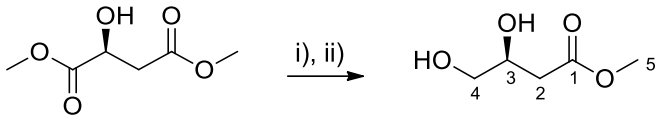


Figure 18: D_2O exchange ^1H NMR spectra for compound 128

Malic acid dimethyl ester **128** was subsequently subjected to the selective reduction of the ester alpha to the hydroxyl group (**Scheme 35**). Borane dimethyl sulfide was slowly added to a stirring solution of the diester in THF at room temperature.[114] This step was characterised by effervescence of the H_2 as the borane chelated to the alcohol oxygen and the carbonyl of the alpha ester. After gas evolution had subsided, $NaBH_4$ addition at 0 °C completed the reduction with the release of the odoriferous dimethyl sulfide gas. Finally, addition of MeOH dissociated the resulting complex formed between the substrate and borane yielding the desired diol **129** in a yield of 91%.

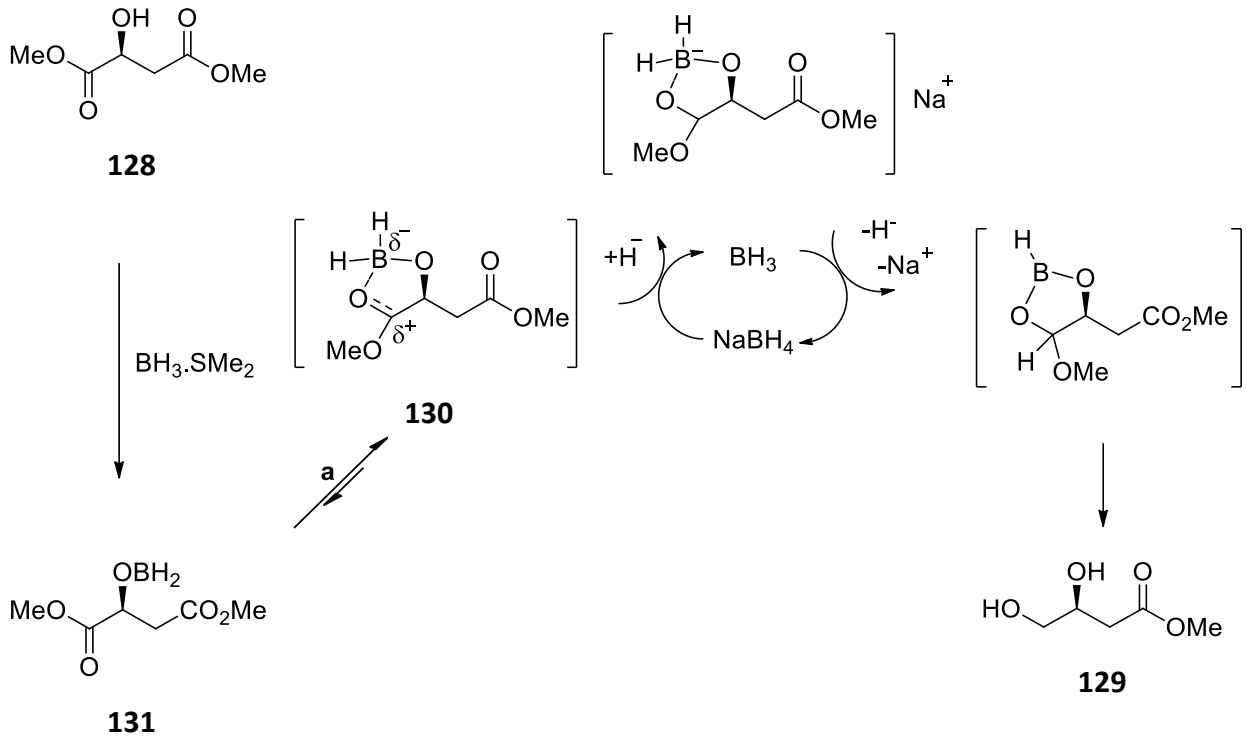


128 **129**

Scheme 35: i) BMS, THF, r.t., 4 h; ii) 0 °C, $NaBH_4$, 1 h, 91%

The initial study by Saito *et al*. concluded that the reduction of compound **128** occurs exclusively at the alpha carboxylic acid.[114] Once added, BMS reacts with the alcohol yielding intermediate **131** and this step is characterised by effervesce as the dimethyl sulfide is released (**Scheme 36**). The boron atom intramolecularly coordinates to the α-carbonyl to form the five membered intermediate **130**. The probability of neighbouring group participation is dependent on the ring size formed in a transition state.[124, 125] In general, neighbouring group participation is most favoured when five membered rings are formed as a result of the balance between strain energy

and entropy factors under kinetically controlled conditions.[124] For this mechanism, the six membered transition state is less favoured because of severe 1,3-diaxial interaction between the ester-alkoxy group and the hydrogen on the boron atom due to the short boron-oxygen bond length. The $NaBH_4$ is necessary to complete the reduction whilst the methanol releases the desired compound from the boron complex to furnish the diol **129**.



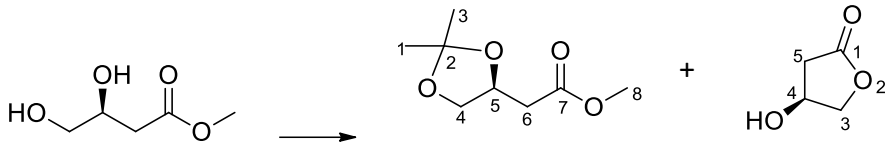
Scheme 36: Reaction mechanism for the reduction of compound 128

The measured specific optical rotation of $[\alpha]^{20}_{D}$ -23.7 (c 1.83, $CHCl_3$) of the diol was comparable to the published literature value of $[\alpha]^{22}_{D}$ –26.9 (c 1.3, $CHCl_3$).[126] The IR spectrum showed the presence a single carbonyl signal visible at 1719 cm^{-1} and the OH signal appeared at 3372 cm^{-1} as a broad peak. In the ^1H NMR spectrum, two alcohol signals were observed at δ 4.28 as a doublet with a coupling constant of 4.7 Hz and as a triplet at δ 4.01 with *J* = 5.9 Hz for compound **129**. H-2 protons appeared as a multiplet at δ 2.56 – 2.46 integrating for 2 protons, while the H-3 signal was observed at δ 4.16 – 4.09 as a multiplet. H-4 proton signals were observed as two multiplets at δ 3.66 – 3.60 and δ 3.54 – 3.47. The H-4 protons are diastereotopic as a consequence of their alpha position to the stereogenic centre at C-3 hence the observed splitting pattern. The remaining methoxy signal was observed at δ 3.71 integrating for 3 protons. The characteristic carbonyl carbon signal, C-1 was observed at δ 172.8 with the remaining C-2, C-3, C-4 and methoxy carbon signals at δ 37.9, 68.8, 65.8 and 51.9, respectively, visible in the ^{13}C NMR spectrum.

At this stage, careful consideration of the choice of alcohol protecting groups for compound **129** was taken. Selective functionalisation and protection of different alcohols (and later amines) was a critical component and desirable attribute in the synthesis of the target compounds. Unfortunately, each protecting group incorporated increases the synthesis by two non-productive steps and this no doubt reduces the overall yield and efficiency of the synthesis. Nevertheless the most ideal groups had to be chosen which, 1) readily and selectively protected the desired functional group, 2) formed a derivative (without generating a new stereogenic centre) easily separated from side products formed during protection/deprotection 3) was stable and resistant to all the reagents and reaction conditions in the subsequent steps and 4) was selectively removed under mild conditions. For this work, an orthogonal strategy was necessary for the protection and deprotection of the amine and hydroxyl groups.

Protecting groups for alcohols comprise of ethers and esters. Ether protecting groups can further be subdivided into acetal protecting groups and silyl protecting groups. Ethers are generally ideal for 'permanent' protection when removal is only necessary at the late stages of a synthesis. They are stable to basic reaction conditions and therefore tolerate metallating reagents such as Grignard reagents, nucleophilic reducing reagents such as $LiAlH_4$, oxidising reagents such us pyridinium chlorochromate (PCC), Wittig reagents and strong bases.[127] Esters and silyl groups are commonly used for temporary protection of hydroxyl groups that require unveiling during synthesis. Acetonides are preferred for protection of 1,2-diols and 1,3-diols because of the ease of protection and deprotection whilst they are relatively inert to most reaction conditions.

Given the above reasons, the acetonide group was chosen for the protection of compound **129** because of its relative stability under the envisioned conditions of the subsequent reactions. The procedure involved dissolving compound **129** in acetone, followed by the addition of excess dimethoxypropane (**Scheme 37**).[126, 67] A catalytic amount of *p*-toluenesulfonic acid (*p*-TsOH) was added to the reaction which was complete in 4 hours. Purification via column chromatography enabled the separation of the major product from the unwanted side products, affording the expected acetonide protected diol **132** in a yield of 86% and a lactone side product **133** in a yield of 8%.



129 **132** **133**

Scheme 37: 2,2 Dimethoxypropane, acetone, *p*-toluene sulfonic acid, r.t., 4 h, 86% yield

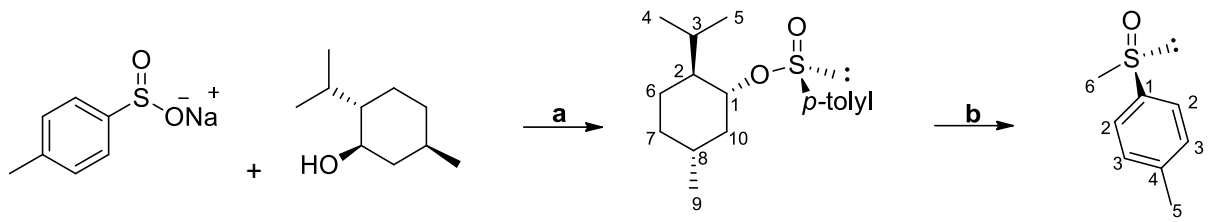
NMR and IR spectroscopy confirmed the identity and purity of compound **132** meaning that purification had successfully separated out the unwanted side product. The presence of the acetonide in compound **132** was evidenced by the presence of two methyl peaks at δ 1.41 and δ 1.35 with a total integration of 6 protons in the ^{1}H NMR spectrum. H-4 protons are diastereotopic and the H-4_{trans} signal was observed at δ 4.16 as a doublet of doublets with coupling constant values of 8.4 and 6.0 Hz. The H-4_{cis} signal was at δ 3.65 with *J*-values of 8.4 and 6.4 Hz. These signals are well separated owing to the 5-membered ring of the acetonide adopting an envelope twist conformation. Despite the fact that 5 membered rings have a high conformational flexibility, one conformation might be favoured owing to the presence of the bulky methyl groups which makes the rapid interchange between conformations much slower, hence the observed splitting pattern.[128] There is not much difference between the *cis* and *trans* vicinal coupling of H-4 and H-5 protons with the values being 6.0 and 6.4 Hz respectively. The H-5 signal was observed at δ 4.50 – 4.44 as a multiplet owing to the neighbouring diastereotopic H-4 and H-6 protons. The methoxy H-8 protons appeared as singlet at δ 3.70 with the remaining H-6 signals also appearing as a set of doublets of doublets at δ 2.72 (*J* = 15.9, 6.4 Hz) and δ 2.53 (*J* = 15.9, 7.1 Hz). The ^{13}C NMR spectrum showed all the signals as expected with the characteristic C-7 carbonyl signal at δ 171.0, C-5 at δ 72.1 and C-8 at δ 51.8. The purity of the compound was confirmed by optical rotation with $[\alpha_D]^{20}$ for compound **132** being +20.1 (c 1.3, $CHCl_3$) which was comparable to literature values.[63]

Lactonisation of compound **129** under the acidic conditions resulted in the recovered side product **133** in a yield of 8%. This has been reported in literature and the two products isolated from this reaction are formed as a result of the competing lactonisation and the protection of the diol, but under the given conditions the protection step is more favourable.[126] ^{1}H NMR spectroscopy confirmed the identity of **133**, whereby signals for H-3_a were observed at δ 4.43 (td, *J* = 9.0, 2.1 Hz, 1H, H-3_a). The expected splitting pattern was doublet of doublets but a triplet of doublets was observed due to a strong AB system, the doublets collapsed into a triplet. The doublet splitting

arises from coupling with the H-5_a proton. The H-3_b signal was observed at δ 4.24 (ddd, *J* = 10.4, 9.2, 6.1 Hz, 1H). The doublets of doublets of doublets arises from both vicinal and geminal coupling plus coupling to the H-5_b signal. Although rare, ^4J couplings are only seen where there is a favourable geometric orbital alignment along the H-C-C-C-H chain, referred to as 'W-coupling'. Conformational arrangement of the 5-membered lactone ring evidently favours W-coupling. The OH signal was observed at δ 4.39 as a broad singlet and the rest of the signals were as expected. The remaining H-5 signals were observed at δ 2.61 (dddd, *J* = 12.6, 8.2, 6.1, 2.0 Hz, 1H, H-5_a) and at δ 2.28 (dtd, *J* = 12.7, 10.3, 8.7 Hz, 1H, H-5_b) In the ^{13}C NMR spectrum, C-1, C-4, C-3 and C-5 were observed at δ 178.5, 67.4, 65.5, and 30.9 respectively.

With the synthesis of the ester substrate complete, the next step involved synthesis of the sulfoxide chiral auxiliary, to be added to compound **132**. Use of the sulfoxide as a chiral auxiliary is a widely published and well established protocol.[129, 130] Two factors favoured the choice of the sulfoxide chiral auxiliary, firstly addition of the sulfoxide creates a new C-C bond elongating the fragment to the desired C-5 carbon length. Secondly, use of the sulfoxide auxiliary for asymmetric induction has been reported to yield products with high diastereoselective excesses.[131]

Synthesis of the chiral sulfoxide employed the Andersen method which was developed in the early 1960's (**Scheme 38**).[132] Sodium *p*-toluenesulfinate **134** was dried overnight, to drive out all the moisture, cooled and then slowly added to thionyl chloride at 0 °C with continuous stirring until all the solid had dissolved. This step activated the sulfur for nucleophilic substitution with menthol **135**. Excess thionyl chloride was removed as an azeotropic mixture with toluene to dryness, followed by the dropwise addition of menthol in a pyridine solution at 0 °C. This condensation step is not selective and produces two diastereomers, one crystalline and the other an oil, meaning the maximum recoverable yield for desired crystalline diasteromer would be 50%. Faced with this challenge G Solladie *et al*., improved the yield by developing an epimerisation equilibration method achieved by acidification of the mother liquor after recovering the first batch of crystals, which afforded an increase in the yield of the desired diastereomer.[133] Employing the improved method gave *S*-menthyl *p*-toluenesulfinate **136** as spiky white crystals, in a combined yield of 77%, with a melting point of 102 – 103 °C. Optical rotation was confirmed to be $[\alpha_D]^{20}$ = -196 (c 2, acetone) which is identical to the value reported in literature indicating a high level of enantiomeric purity.[133] Single crystal X-ray crystallography (**Figure 19**) further confirmed the identity and configuration of the product.



134 **135** **136** **137**

Scheme 38: a) i) $SOCl_2$, 0 °C, 1 h; ii) pyridine, 0 °C – r.t., 1 h, 77%; b) CH_3MgI, ether, 0 – 10 °C, 73%

For the synthesis of the sulfoxide auxiliary **137**, methyl magnesium iodide was used to displace the mentholate from the menthol sulfinate ester with a clean inversion at the sulfur centre. The synthesis of the Grignard reagent was only successful when carried out in dry Et_2O, with a condenser attached to minimise solvent loss. Purification of the desired product was achieved by column chromatography followed by recrystallisation in hot hexane and diethyl ether, affording *R*-methyl *p*-tolylsulfoxide **137** in a yield of 73% with a melting point of 73 – 74 °C. The low average yield was due to product loss during the recrystallisation step, however the reaction proceeded as expected.

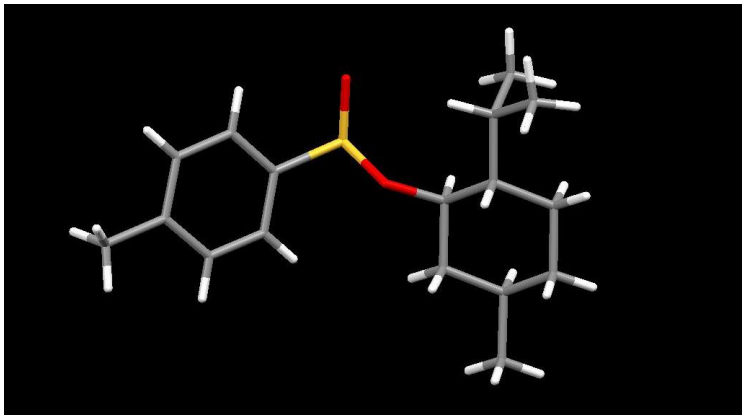


Figure 19: Crystal structure for compound 136

The importance of working with optically pure reagents and substrates for this work cannot be overstated. This meant that effort was made to obtain as much data relating to the optical purity of the synthesised molecules as possible. The recovered crystals for sulfoxide **137** were analysed, and the single crystal structure obtained by X-ray crystallography is shown in **Figure 20**. This data provided extra information needed for the confirmation of the absolute configuration of (+)-*R*-methyl *p*-tolylsulfoxide. The specific optical rotation was as expected with a value of $[\alpha_D]^{20}$ = +148 (c 2, acetone) comparable to the literature value of $[\alpha_D]^{21}$ = +146 (c 2, acetone).[133]

In the ^{1}H NMR spectrum, the aromatic protons were observed as two slightly distorted doublets at δ 7.54 (d, *J* = 8.2 Hz, H-2) and δ 7.33 (d, *J* = 7.9 Hz, H-3) integrating for two protons each. The distortion in the shape of the doublets is as a result of magnetic inequivalence of both the H-2 and the H-3 protons. The *para* substitution of the aromatic ring introduces symmetry resulting in the H-2 protons being both chemically and magnetically equivalent by chemical shift criterion, and the same is true for H-3 protons. However, because the H-2 protons have different spatial and connectivity relations to H-3 protons, they are magnetically inequivalent by coupling criterion. This relationship is also true with respect to the coupling relationship of H-3 protons to H-2 protons. This inequivalence gives rise to the distortion of the observed doublets because the observed signals are a summation of two individual doublets. The remaining methyl protons gave rise to singlets at δ 2.70 for H-5 and δ 2.42 for H-6. The aromatic carbon signals appeared at δ 142.6, 141.5, 130.0 and 123.5 whilst the signals for C-6 appeared at δ 44.0, and the C-5 was visible at δ 21.4 in the ^{13}C NMR spectrum confirming the identity of the desired compound.

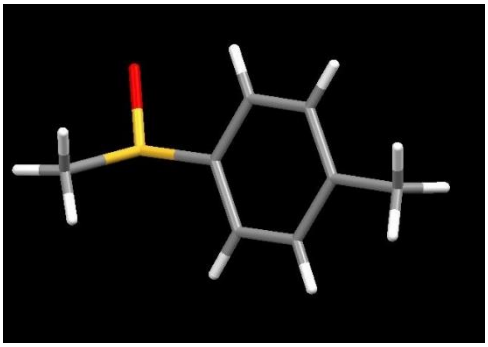
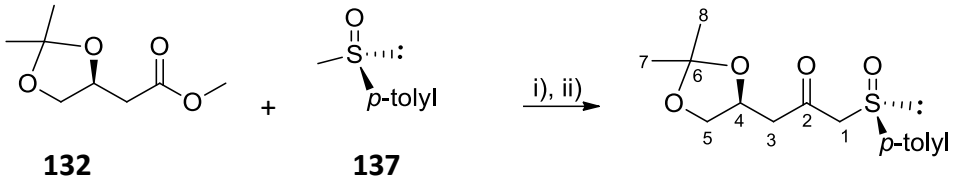


Figure 20: Crystal structure for compound 137

After confirmation of the formation of both the pure chiral auxiliary, and the ester substrate **132**, the next step involved addition of (+)-(*R*)-methyl *p*-tolylsulfoxide to compound **132**. This protocol is well researched and has been widely used, with much success (**Scheme 39**).[134, 98, 135] Using the established methodology, a cooled solution of the sulfoxide at -40 °C was slowly added to freshly prepared LDA at -78 °C. An intense yellow colour was observed as the anion was generated and the reaction was left stirring for 30 minutes. Allowing the reaction to proceed for longer time decreased the yields of the desired product significantly.

In a separate two-necked flask, the protected diol was cooled to -40 °C under N_2 followed by the slow addition of the sulfoxide mixture via cannula. The yellow colour disappeared with each addition until excess amounts were added. The generated anion of the chiral auxiliary was added

to compound **132** as opposed to the ester being added to the anion, because when compound **138** is generated an acidic proton at position 1 can be easily deprotonated by the excess base yielding a rearranged product. It is for this reason that two equivalents of *R*-methyl *p*-tolylsulfoxide were initially used in this reaction. However, because of low recoverable yields the reaction was performed using different equivalents of the sulfoxide in an attempt to optimise the reaction.



132 **137** **138**

Scheme 39: i) LDA (1.5 equiv), THF, -78 °C; 30 min; ii) compound 137 (1.2 equiv), THF, -40 °C – r.t., 2 h, 64%

For workup, the reaction was quenched with a saturated aqueous solution of NH_4Cl, followed by adjustment of the pH to 6 in order to quench the excess base. The highest yield obtained for this reaction was 64% despite adjusting the reaction conditions, with several attempts resulting in low yields of less than 40% (**Table 2**). The low average yields are attributed to product loss due to the side reaction between the product and the excess base, coupled with co-elution of the desired product and the sulfoxide during purification. The rearranged product was recovered but could not be fully characterised.

Table 2: Yields for compound 138 under different conditions

Optimised reaction conditions	% yield for compound 138
2.5 equiv freshly prepared LDA, 2.0 equiv sulfoxide	48
2.5 equiv Sigma bought LDA, 2.0 equiv sulfoxide	61
2.0 equiv freshly prepared LDA, 1.5 equiv sulfoxide	52
1.5 equiv freshly prepared LDA, 1.2 equiv sulfoxide	64
1.4 equiv freshly prepared LDA, 1.4 equiv sulfoxide	36
1.2 equiv freshly prepared LDA, 1.2 equiv sulfoxide	36

The optical rotation for compound **138** was confirmed to be $[\alpha_D]^{20}$ = +151.1 (c 1.2, $CHCl_3$) which is comparable to the literature value.[63] The expected new signals of C=C-H and S=O functional groups were observed at 3147 cm^{-1} and 1033 cm^{-1} respectively, in the IR spectrum. Analysis of the

^{1}H NMR spectrum revealed the presence of (*S*(*R*),4*S*)-4,5-*O*-isopropylidene-1-(*p*-tolylsulfinyl-2-pentanone **138**. Despite H-1 protons being diastereotopic because of their α position to the chiral sulfur centre, a singlet signal was observed integrating for two protons at δ 3.88 in the ^{1}H NMR spectrum. Interesting roof top effects were observed for the H-3 proton signals as shown in **Figure 21**. Signals for H-3 protons appeared as a set of doublets of doublets at δ 2.96 with coupling constants of 17.2 Hz and 6.3 Hz and δ 2.64 with *J* being 17.2 Hz and 6.5 Hz. The chemical shift difference of 96 Hz between the H-3 signals in comparison to the geminal coupling constant of 17.2 Hz is indicative of a second-order AM system of the protons which are clearly neither chemically nor magnetically equivalent. This chemical shift system gives rise to the observed roof top or leaning effects. The H-4 signal was observed as a pentet at δ 4.40 with *J* = 6.4 Hz.

The chemical shifts for the H-5 protons showed an AX coupling system as the signals appeared as doublets of doublets at δ 4.10 with *J* = 8.4 Hz and 6.0 Hz and at δ 3.46 with *J* = 8.4 Hz and 6.5 Hz. The geminal coupling constant of 8.4 Hz is much smaller in comparison to the chemical shift difference between the two H-5 proton signals of 192 Hz. The dioxane 5-membered ring provides restricted rotation which causes one of the H-5 protons to be in an axial position and the other in an equatorial position. The fixed conformational arrangement results in the protons experiencing significantly different magnetic fields hence the observed large chemical shift difference between the signals. In the ^{13}C NMR spectrum the aromatic signals at δ 142.3, 139.4, 130.1 and 124.1 further confirmed the successful addition of the sulfoxide. The tosyl methyl carbon appeared at δ 21.4, and with the absolute conformation of compound **138** established, work began on the synthesis of the triol via chelation-controlled reduction of the ketone in compound **138**.

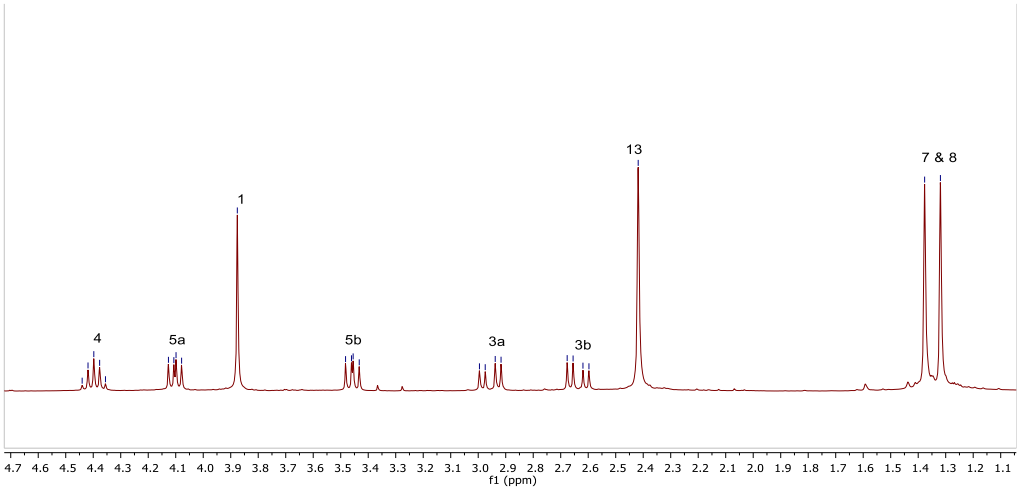
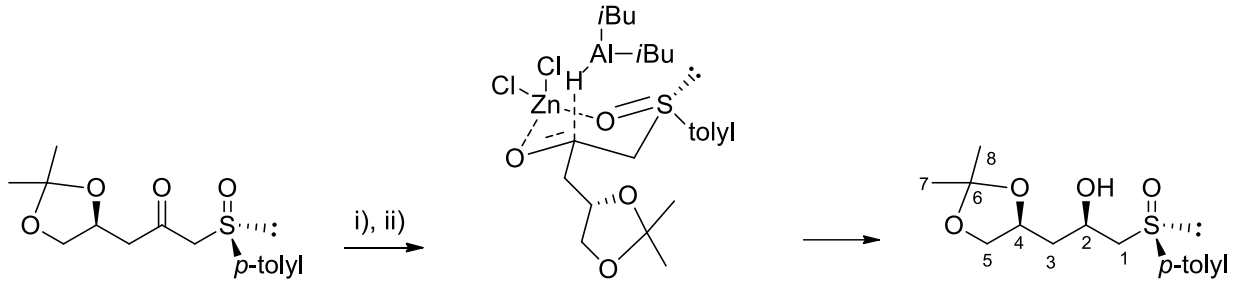


Figure 21: ^{1}H NMR spectrum for compound 138

Chelation controlled reduction of (*S*(*R*),4*S*)-4,5-*O*-isopropylidene-1-*p*-tolylsulfinyl-2-pentanone **138** was afforded by employing $ZnCl_2$ as a Lewis acid (**Scheme 40**). The chelation step of the reaction was left stirring for 2 h at room temperature, ensuring quantitative yields of the intermediate complex **138a**. The chelated substrate was cooled to -78 °C prior to the addition of the reducing agent, otherwise product decomposition was observed. The zinc-chelated complex locks the conformation of the substrate. Thus when the reducing agent is introduced, the presence of the bulky *p*-tolyl group blocks the *si* face of the carbonyl, therefore the hydride from the DIBALH which is equally bulky prefers to be delivered from the *re* face so as to minimise steric repulsion. The crucial transition state **138a,** depicted in **Scheme 40** clearly illustrates how the stereo-controlled reduction is induced by the steric encumbrance of the bulky groups.



138 **138a** **139**

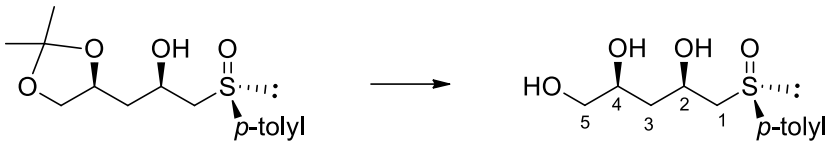
Scheme 40: i) $ZnCl_2$ (4 equiv), THF, r.t., 2 h; ii) DIBALH (2 equiv), -78 °C – r.t., 2 h, 79%

The rigidity of the transition state and the steric repulsions of the *iso*-butyl groups on aluminium and the tosyl group ensures that very little of the other diastereomer is formed. For this work only the desired diastereomer, compound **139**, was recovered as a white solid in a yield of 79%. A significant amount of the product was lost during work up because the by-product of the DIBAL adduct forms a viscous emulsion with NH_4Cl, which is onerous to extract.

The measured melting point of the product was 78 – 79 °C which is lower than the literature value of 87 – 89 °C.[63] This variance is likely to be because of different moisture and solvent content levels. The specific optical rotation was +73.3 in $CHCl_3$ when the concentration was 0.3 which is comparable to literature values.[63] The optical rotation value confirmed that the correct diastereomer was recovered without epimerisation of either of the stereogenic centres. For IR spectroscopy, the characteristic alcohol signal confirming the reduction of the carbonyl group was observed as a broad peak at 3382 cm^{-1}.

In the ^{1}H NMR spectrum the OH proton was observed as a broad singlet at δ 3.99 whilst a new signal for the H-2 proton, overlapping with H-4 protons was observed as a multiplet at δ 4.36 – 4.24 integrating for two protons. The singlet signal for protons at the α-position to the sulfur in compound **138** had disappeared. The H-1_a proton for compound **139** was observed at δ 3.08 as a doublet of doublets with *J* of 13.2 Hz and 7.9 Hz and the H-1_b proton was observed at δ 2.85 with *J* of 13.2 Hz and 3.8 Hz. The newly formed stereogenic centre at C-2 enhanced the diastereotopic nature of the H-1 protons because they are not magnetically equivalent and a large geminal coupling constant of 13.2 Hz was observed. In the ^{13}C NMR spectrum the carbonyl signal previously observed at δ 199.5 had disappeared and was replaced by a new C-2 signal at δ 74.1. This further confirmed the identity of our desired product since the new signal appeared in the characteristic region for C-O carbon atoms. The C-1 signal had migrated from δ 68.0 to δ 63.0 showing that there was a conformational change and chemical transformation, causing a shielding effect at the alpha position to the S atom.

Once the 1,3-*syn*-diol functionality had been introduced, attention moved to protecting the diols and functionalising the terminal carbon atoms. The first step involved acetonide deprotection of compound **139** via hydrolysis, at elevated temperatures under acidic conditions (**Scheme 41**). As a consequence of the high polarity of the resulting triol (compound **140**) it was water soluble, and recovery of the desired product from the aqueous layer was achieved by continuous extraction with ethyl acetate (EtOAc) over 2 days. A white solid with a melting point of 113 – 114 °C, in a below par yield of 63%, was recovered as the desired compound.



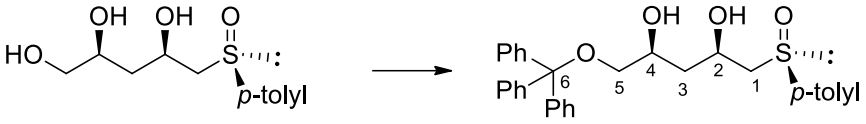
139 **140**

Scheme 41: 5% *p*-TsOH, MeOH, H_2O, 60 °C, 4 h, 63%

Not much change besides a shift in the position of the signals was observed in the IR spectrum. A much broader and more intense signal was observed at 3230 cm^{-1} representing all the OH groups. The first indication of a successful deprotection step was the disappearance of the two acetonide methyl group signals previously observed at δ 1.41 and δ 1.34 in the ^{1}H NMR spectrum. The only methyl signal observed was for the *p*-tolyl group at δ 2.41 integrating for three protons. The acetonide methyl peaks had also disappeared from the ^{13}C NMR spectrum together with the

quaternary acetonide signal previously observed at δ 109.4. Not much change in chemical shift was observed for the rest of the signals of the molecule.

With both the primary and secondary alcohols revealed, the trityl group was used to selectively protect the primary alcohol, because use of this group for the protection of primary alcohols is kinetically favourable over secondary alcohols at room temperature (**Scheme 42**).[136] The mechanism of the protection follows a simple S_N1 nucleophilic substitution reaction whereby the primary alcohol, after deprotonation by DMAP, attacks the electrophilic tertiary carbon of trityl chloride. The chloride leaving group forms HCl which in turn is neutralised by pyridine. The reagents were added together and left stirring overnight and the desired diol **141** was easily recoverable by column chromatography in an average yield of 65% as a white solid. Unfortunately, the protecting and deprotecting steps resulted in significant product loss despite attempts to optimise the reaction conditions. The melting point of **141** was determined to be 65 – 66 °C with a specific optical rotation of +118.6 (c 0.98, acetone) comparable to the published values.[63]



140 **141**

Scheme 42: DMAP, trityl chloride, pyridine, DCM, r.t., 24 h, 65%

In the ^{1}H NMR spectrum there was an increase in the total integration of protons in the aromatic region because of the addition of trityl group, and the representative three multiplets were visible at δ 7.55 – 7.52, δ 7.43 – 7.37 and δ 7.35 – 7.20. A total integration of nineteen protons accounted for all the expected aromatic protons. The H-2 and H-4 protons appeared as separate multiplet signals at δ 4.42 – 4.35 and δ 4.08 – 4.01 respectively, with a combined integration of two. The two alcohol signals were observed as two separate signals; a singlet at δ 4.31 and the second signal appeared as a doublet at δ 3.15 with a coupling constant of 2.7 Hz. The COSY NMR spectrum showed that the OH coupling was with the H-4 proton. The H-5 protons appeared as a doublet at δ 3.11 with *J* of 5.6 Hz. The observed splitting pattern suggests that the two protons are magnetically equivalent despite being diastereotopic. The H-5 protons are chemically equivalent by virtue of being attached to the same carbon atom but they are expected to be magnetically inequivalent. Conformational arrangement of diastereotopic protons means that they experience slightly different magnetic fields.

The ^{13}C NMR spectrum also showed an increase in signals in the aromatic region due to the trityl group. The characteristic quaternary C-6 signal was observed at δ 86.8, which is a significantly deshielded position for a C-O carbon. This is because this carbon atom is attached to 3 phenyl groups which have a withdrawing effect and an electronegative oxygen atom resulting in the deshielding effect observed. The quaternary carbon atom identity was further confirmed by DEPT135 NMR spectroscopy as shown in **Figure 22**. The comparison of the ^{13}C NMR spectrum and DEPT135 NMR spectrum also assisted in identifying CH and CH_2 carbon signals. The C-1, C-2, C-3, C-4 and C-5 signals were observed at δ 62.9, 68.3, 39.4, 70.6 and 67.4 respectively.

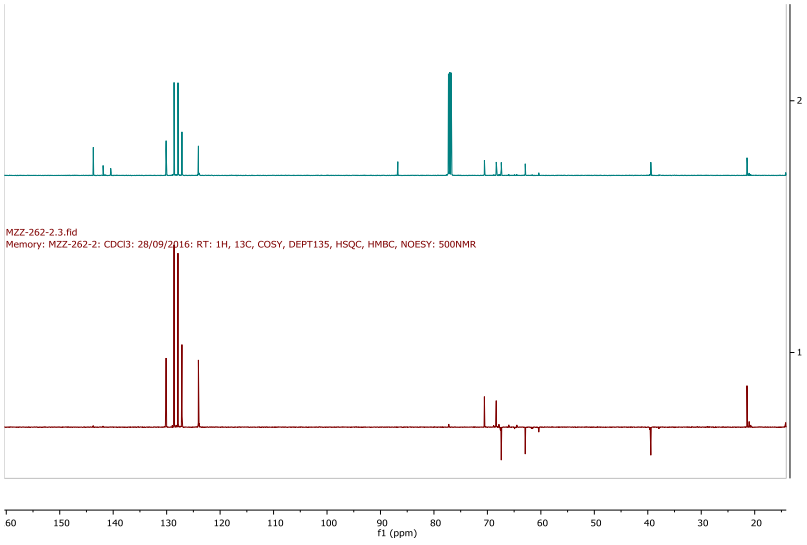
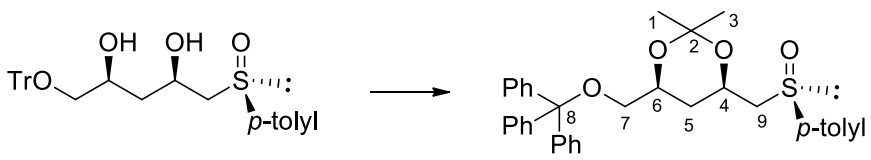


Figure 22: ^{13}C NMR and DEPT135 NMR spectra for compound 141

After the primary alcohol protection, the next step involved protection of the 1,3-diol functionality. Since no further transformations were planned to occur at these two stereogenic centres, the idea was to select a protecting group that would be stable under the successive reaction conditions (**Scheme 43**). The group also had to minimise or preferably eliminate the chance of racemisation of the stereogenic centres. The acetonide group was chosen due to its stability and ease of deprotection which is well documented in carbohydrate and sugar chemistry where chiral integrity is of high importance.[104]



141 **124**

Scheme 43: 5 % *p*-TsOH, 2,2-dimethoxypropane, acetone, r.t., 1 h, 86%

The same experimental procedure employed for the synthesis of compound **132** was used for the synthesis of compound **124** as shown in **Scheme 43**. For this procedure, the reaction was complete in 2 hours, and extended reaction times resulted in loss of product due to loss of the trityl group under the acidic conditions, resulting in product decomposition. The reaction was high yielding and 86% of the expected product was recovered as a white solid with a melting point of 164 – 165 °C. The specific optical rotation was determined to be +28.1 in acetone (c 1.09) which is comparable to literature values, confirming that the diastereomer with the desired stereochemistry had been synthesised.[63] For IR spectroscopy, the broad signal indicative of alcohols had disappeared and only the anticipated signals were observed. The aromatic C-H stretch signal was observed at 3036 cm^{-1} and the C=C stretch was visible at 1597 cm^{-1}. Three C-O signals were observed at 1161 cm^{-1}, 1100 cm^{-1} and 1078 cm^{-1}.

Fortuitously, crystals of the product were recovered, which allowed for the determination of the single crystal X-ray structure as shown in **Figure 23**. The *syn*-1,3-diol functionality was clearly evident and the six membered dioxane ring adopted a chair conformation as a result of the acetonide group. This is because the bulky trityl and tosyl groups prefer adopting the less hindered equatorial positions. The chair conformation clearly has an influence on the chemical shift and splitting patterns in NMR spectroscopy. In the ^{1}H NMR spectrum the new acetonide methyl groups were observed as two singlets at δ 1.33 and δ 1.30 integrating for six protons. The first H-5 proton appeared as a doublet of triplets at δ 1.75 with a geminal coupling constant of 12.8 Hz and a vicinal coupling constant to H-4 and H-6 protons, of 2.5 Hz. The second H-5 proton appeared as a multiplet at δ 1.40 – 1.34. 2D NMR spectroscopy was used to distinguish and correctly assign the remaining signals.

In order to assign the H-4 and H-6 signals, the H-7 and H-9 signals were assigned first using 2D NMR spectroscopy. Looking at all the signals, it is evident that H-7 protons are CH_2 protons that are attached to the most deshielded carbon because oxygen is more electronegative than sulfur. Analysis of the HSQC NMR spectrum shown in **Figure 24** shows that the H-7 protons are at δ 3.23 as a doublet of doublets with J = 9.3 Hz and 5.2 Hz, 1H for H-7_a and at δ 2.96 with J = 9.3Hz and 6.0 Hz for H-7_b. The assignment of the H-6 signal was achieved by performing a COSY NMR spectroscopic experiment since it was the only signal that would show coupling with H-5 and H-7 signals. The proton was assigned to the signal at δ 3.97 (dtd, J = 11.4, 5.6, 2.4 Hz) integrating for one proton. With the H-6 and H-7 protons assigned the rest of the signals were easier to assign.

The H-4 signal was observed at δ 4.13 – 4.06 and the H-9 peaks were at δ 3.15 (dd, *J* = 13.1, 6.8 Hz) and δ 2.76 (dd, *J* = 13.1, 5.4 Hz). The remaining aromatic proton signals were as expected with an integration of nineteen protons.

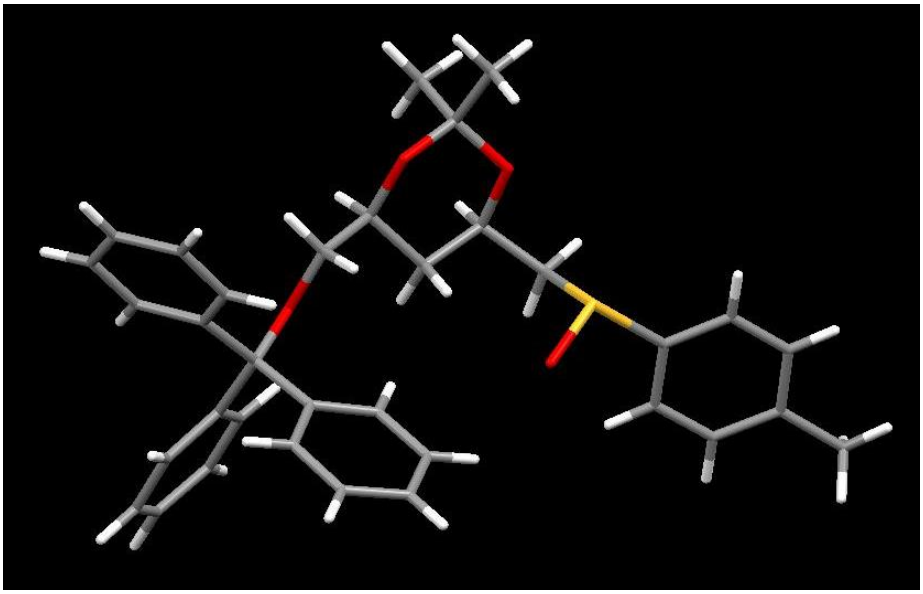


Figure 23: Crystal structure for compound 124

For the ^{13}C NMR spectrum the most important signal indicating the acetonide protection, the C-2 signal, was observed at δ 98.9. The reason for this importance is because an extensive NMR spectroscopy investigation for acetonide protected 1,3-diols performed by Scott D. Rychnovsky *et al*., proved that the stereochemistry of the alcohols is determinable by NMR spectroscopy.[69] Since *syn*-1,3 diols are not conformationally flexible molecules, the methyl groups do not interact in space which has an influence on their chemical shift. In their study they established the ^{13}C NMR spectroscopic chemical shifts of *syn*-1,3-diol acetonides which exist in a chair confirmation. The experimental results showed that the axial methyl group gives rise to a signal at 19 ppm, the equatorial methyl group appeared as a signal at 30 ppm and the quaternary carbon was visible at 98 ppm. The signal for the quaternary carbon signal was never observed above 100 ppm. On contrary, the *anti*-1,3-diols exist in a twist conformation to avoid 1,3-diaxial interactions which would be present in a chair conformation. Both the methyl signals in an *anti* system were observed at 25 ppm whilst the quaternary carbon signal was at 109 ppm and always above 100 ppm.

The observed results in this work concurred with this conclusion as the axial methyl (C-1) of **124** was observed at δ 19.6 and the equatorial methyl (C-3) was observed at δ 29.7. From these results, it was evident that the relative stereochemistry of the molecule had been maintained thus far.

For the subsequent reactions, the chemical shifts of these signals were closely monitored to ensure that epimerisation of the stereogenic centres had not occurred. C-4, C-5, C-6, C-7, C-8 and C-9 signals were observed at δ 68.2, 33.6, 63.9, 67.0, 86.5 and 63.1 respectively.

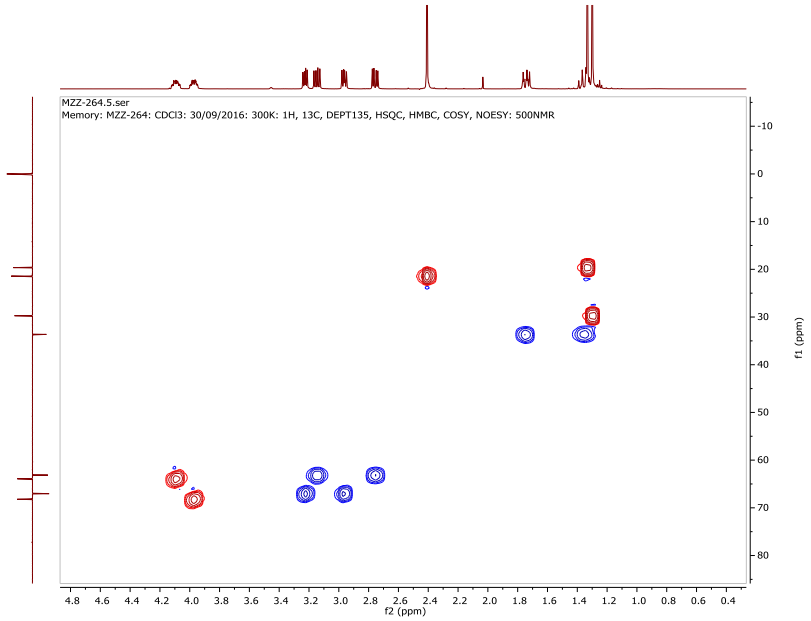
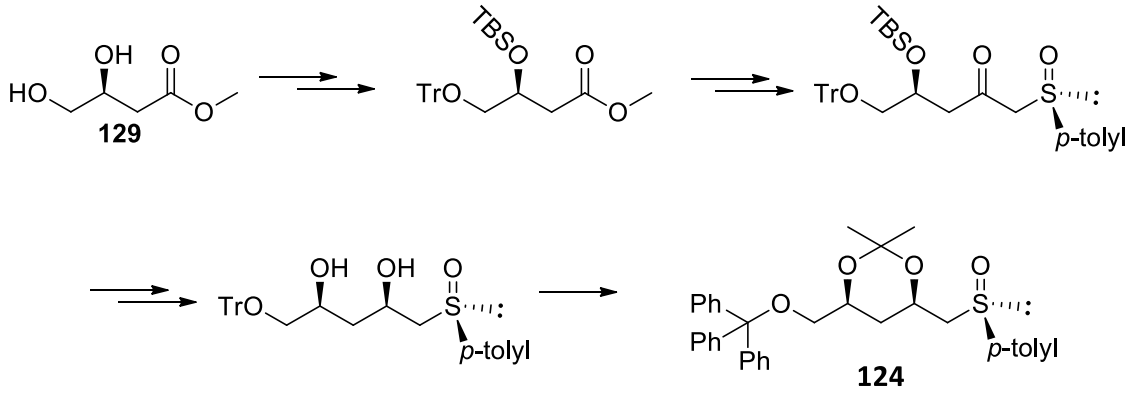


Figure 24: HSQC NMR spectrum for compound 124

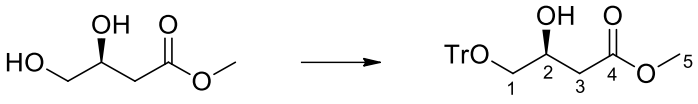
2.2.2 An alternative method for the synthesis of key intermediate 124

Before proceeding further with the synthesis, the synthetic approach towards intermediate **124** was reinvestigated for two main reasons (**Scheme 44**). Firstly, there was a need to improve yields since the synthesis of compound **138** was low yielding. Secondly, there was a need to eliminate the continuous extraction step for recovering compound **140** because of the energy requirements and the long extraction times. Given the fact that malic acid had already been established as a suitable starting material, the route change occurred from the diol **129**. Orthogonal protection of the alcohol groups ensured that the two stated problems observed with the current synthetic route were addressed.



Scheme 44: Alternative synthesis for compound 124

Since the diol, compound **129**, has two alcohol functional groups, the primary alcohol was chemoselectively protected by using the trityl group (**Scheme 45**). The reaction was performed under basic conditions, overnight and a quantitative yield of compound **142**, was obtained as a viscous yellow oil after purification by column chromatography. Attempted purification by recrystallisation in a chloroform/methanol (9:1) was low yielding, and the single crystal X-ray structure for compound **142** is shown in **Figure 25**. In general the product was a viscous oil at room temperature and was pure by NMR spectroscopy after column chromatography. The crystal exists as a dimer in each unit cell due to intermolecular hydrogen bonding between the free hydroxyl groups. Recrystallisation in the bi-solvent mixture probably allowed the molecules to pack linearly because of the strong hydrogen bonding between the alcohols, allowing the growth of the crystals.



129 **142**

Scheme 45: TrCl, DMAP, pyridine, r.t., overnight, quantitative yield

IR spectroscopy revealed a new C=C-H signal at 3058 cm^{-1} due to the phenyl rings and an alcohol signal was observed as a broad singlet at 3469 cm^{-1}, confirming that only mono protection had occurred. The recovered crystals had a melting point of 129 – 130 °C. The mass spectroscopy results for the trityl protected alcohol **142** were as expected with a measured mass of 399.1561 $(M+Na)^+$ being similar to the calculated mass of 399.1567 $(M+Na)^+$. The recovered product was optically active with a measured specific optical rotation of -15.0 (c 1.05, $CHCl_3$).

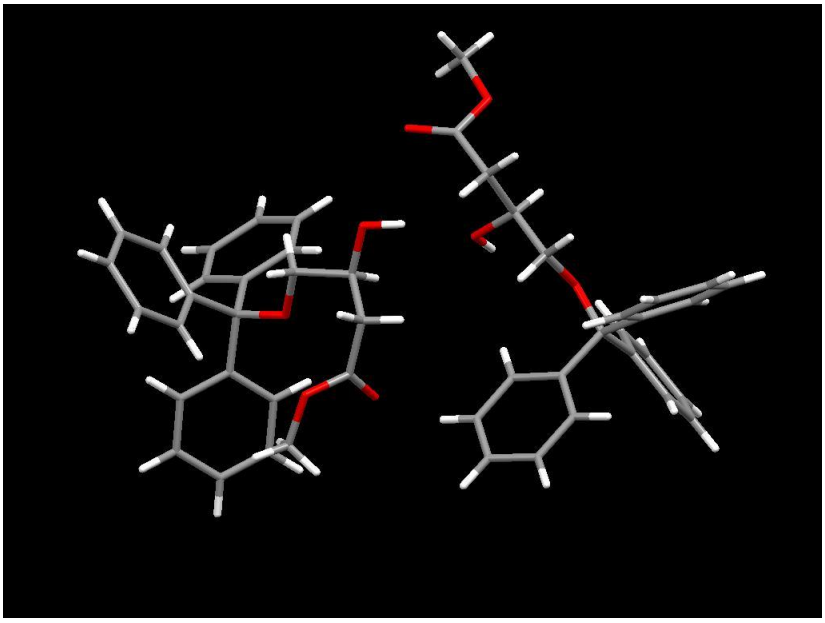
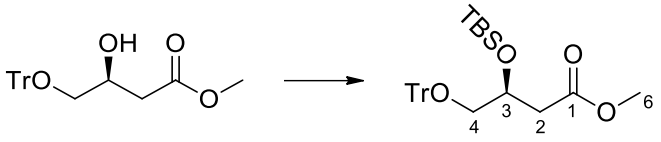


Figure 25: Crystal structure of compound 142

A broad OH signal was observed at 3469 cm^{-1} in the IR spectrum indicating that trityl protection had only occurred at the primary alcohol. The expected new aromatic proton signals were observed at δ 7.47 – 7.39 and δ 7.33 – 7.16 as a set of multiplets with a combined integration of fifteen protons in the ^{1}H NMR spectrum. H-4 protons were observed as a doublet at δ 3.16 with a coupling constant of 5.4 Hz. A doublet signal at δ 3.02 with a coupling constant of 4.6 Hz was assigned to the OH proton after correlation analysis in both the COSY NMR and HSQC spectra. Both the H-3 and H-2 signals were observed as multiplets at δ 4.28 – 4.16 and δ 2.64 – 2.43 respectively. The remaining singlet signal at δ 3.63 was assigned to the remaining methoxy protons. The carbon signals for the trityl group were observed at δ 143.7, 128.4, 127.7 and 126.9 in the ^{13}C NMR spectrum and the rest of the signals were as expected.

Subsequent protection of the secondary alcohol on compound **142** with the *tert*-butyldimethylsilyl (TBS) protecting group (**Scheme 46**) followed the tritylation step. The TBS protecting group was chosen because of the simplicity of the protection and deprotection procedures without the reaction conditions affecting the rest of the functionality of the molecule. In fact, the synthesis of compound **142** and compound **143** could have been performed in tandem, in a single pot. However, because full characterisation of the two products was required, compound **142** was isolated and characterised prior to the next step. The reagents were added sequentially to a stirring solution of the substrate and left stirring overnight.[117] Purification afforded the desired compound **143** as a white waxy precipitate in a combined yield of 65%, much lower than expected

yield even though no starting material was recovered. IR spectroscopy showed the disappearance of the alcohol peak at 3469 cm^{-1}, which further confirmed the successful protection of the alcohol.

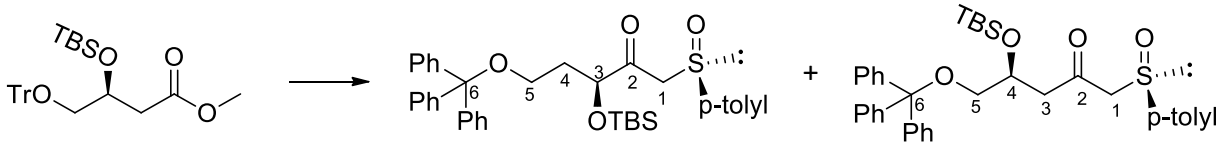


142 **143**

Scheme 46: DMAP, imidazole, TBS, DCM, r.t., 12 h, 65% yield

^{1}H NMR spectroscopy indicated the presence of compound **143** evidenced by the TBS-$(CH_3)_3$ peak visible at δ 0.80 with an integration of nine protons. The dimethyl protons of the TBS group were observed as singlets at δ -0.02 and -0.08, with each signal integrating for 3 protons. The rest of the ^{1}H NMR signals were as expected. In the ^{13}C NMR spectrum the TBS methyl *tert*-butyl carbon signals were observed at δ 25.7 and δ 17.9 for the quaternary carbon atom. The two silyl methyl carbons were observed at δ -4.6 and δ -5.2 indicating their non equivalence because of their proximity to the stereogenic centre.

Once the protected ester precursor **143** had been successfully synthesised, the next step involved addition of the sulfoxide chiral auxiliary. Due to the change in the protecting groups on the ester substrate, it was reasoned that the trityl and TBS protecting groups would provide steric stability to the desired product. This extra stability would minimise the secondary reaction of the product once formed under the basic reaction conditions, consequentially increasing the yield of the desired compound. A similar procedure to that employed for the synthesis of compound **138** was employed for the addition of the chiral auxiliary to compound **143** and similar colour changes were observed (**Scheme 47**).



143 **144** **145**

Scheme 47: LDA, *R*-methyl *p*-tolyl sulfoxide, THF, -78 °C – r.t., 2.5 h, 24% compound 144, 55% compound 145

TLC analysis showed two new major products which had close R_f values and fortunately purification by column chromatography using gradient elution enabled the separation and recovery of the products, **144** and **145**. Both products were light yellow solids with the same

melting point of 115 – 116 °C and a specific optical rotation of +91.4 for compound **144** and +67.0 for compound **145** in $CHCl_3$ (c 1.3). Mass spectrometry confirmed the masses of the recovered products to be the same, with a measure value of 635.2631 $(M+Na)^+$ for compound **144** and 635.2614 $(M+Na)^+$ for compound **145**. Consequently, because the masses of the two products were the same and similar to that of the expected product, it proved that they were structural isomers. At this point it was crucial to conclusively characterise the recovered products using both X-ray crystallography and NMR spectroscopy so as to identify the desired product.

After several recrystallisation attempts of both products, using different solvents at varying temperatures, it was sheer joy when crystals for compound **144** were recovered, and the single crystal X-ray structure is shown in **Figure 26**. Surprisingly the crystal structure showed the O-TBS group on the carbon atom α to the carbonyl group. For the desired compound, the O-TBS was expected on the carbon atom β to the carbonyl carbon. These results were puzzling as the reasons behind the recovery of this product were not immediately obvious. Once the structure and molecular weight of compound **144** had been confirmed, its yield was determined to be 24%.

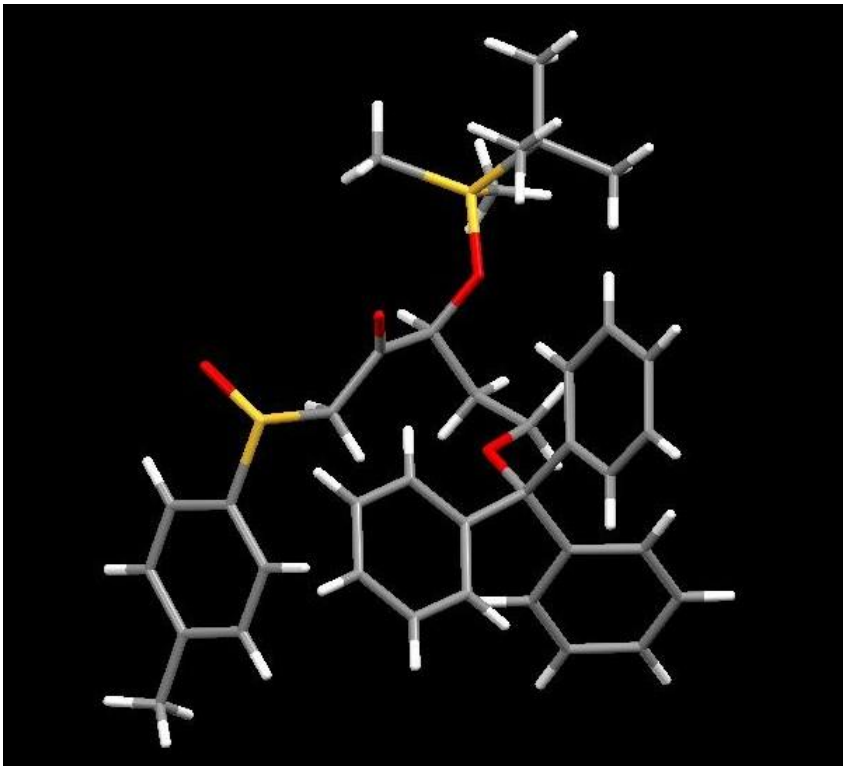


Figure 26: Crystal structure for compound 144

NMR spectroscopy also further confirmed the identity of compound **144**. Firstly total integration of the aromatic protons increased from fifteen to nineteen in the ^1H NMR spectrum. The signals

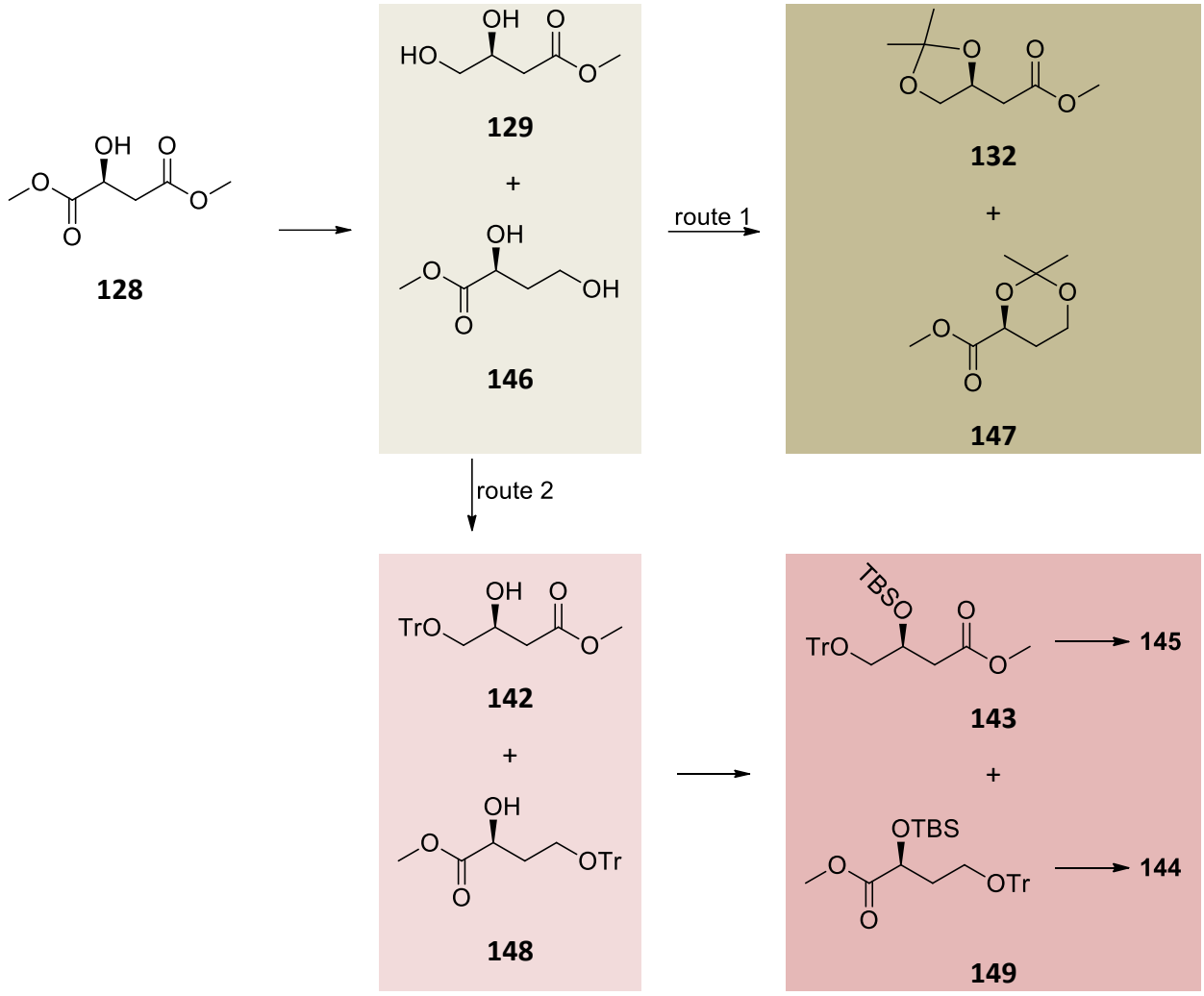
were observed as three multiplets at δ 7.56 – 7.50 (2H), δ 7.41 – 7.34 (6H) and δ 7.33 – 7.16 (11H). A new methyl singlet signal was observed for H-7 protons at δ 2.40. H-5 protons were observed as a set of multiplets at δ 3.32 – 3.18 and δ 3.17 – 3.04 and the H-4 proton signal was also a set of multiplets at δ 2.12 – 1.95 and δ 1.90 – 1.75. A triplet signal was observed for the H-3 proton at δ 4.18 with a coupling constant of 5.5 Hz. The set of doublets for H-1 protons at δ 4.07 and δ 3.92 with a geminal coupling constant of 14.8 Hz exhibited the rooftop effects. In the ^{13}C NMR spectrum the C-5 signal was at δ 58.7 which is a very shielded position for a C-O carbon signal. This observation might be attributed to conformational effects. COSY NMR, HSQC NMR and DEPT135 NMR spectra were used to conclusively assign all the signals.

After confirmation of the identity of compound **144**, significant effort was placed in establishing the source of this product. The structure of the compound raised the question of whether a different side reaction on the expected product resulting in a 1,2-*O*-migration was at play**.** Under the given reaction conditions, the sulfoxide auxiliary had already been shown to be very stable, and if either of the chiral centres had racemised, a more complex mixture of products would have been recovered. Further investigation from several articles only point to the possibility of a 1,2-silyl migration in the presence of a strong base like LDA as opposed to a 1,2-*O*-silyl migration.[137, 138] The phenomenon has well been studied and is duly named the Brook rearrangement, after the researcher who first published it.[139] The bulky silyl protecting groups like the TBS group are generally stable under many chemical transformations, and typically the worst that can happen is a deprotection. As an example, the TBS group was used as one of the protecting groups in the total synthesis of olivine, and no migration nor deprotection was observed after subjecting a TBS protected intermediate to LDA.[140, 141, 142] Several other stereochemical synthetic procedures have employed the TBS protecting group without any deprotection problems, when protected substrates were subjected to strongly basic conditions using LDA.[143, 144, 145]

After establishing that a 1,2-migration of the O-TBS group was impossible, the next probability was that compound **144** was as a result of a side product carried through from an earlier step in the synthesis. All the reactions performed thus far were critically analysed in order to establish whether there was contaminant that had been missed that could be the source of the unwanted side product. After careful examination and literature review, it was revealed that the reduction of compound **128** did not selectively yield compound **129** (**Scheme 48**). A revised article by Saito *et al.* revealed that the reduction does not occur exclusively at the carboxylic acid alpha to the

alcohol but it also occurred at the beta carboxylic acid yielding compound **146** albeit in a 99:1 ratio.[146]

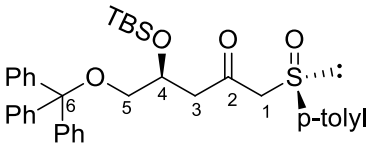
Due to the similarity in polarity, compound **129** and **146** are not separable by column chromatography. Re-evaluation of the ^{1}H NMR spectrum of compound **129** did not conclusively reveal the signals for compound **146** except for a small methoxy signal in a ratio of 9:1. Since the reduction step had been performed a few times, all the NMR spectra were re-evaluated to establish whether the ratio of the two products was constant. It was discovered that the ratio ranged from approximately 1:3 to 1:21. In the ^{13}C NMR spectrum, the signals for compound **146** were slightly more visible although the intensity was relatively less in comparison to those of the desired compound. The recovered products from acetonide protection of the diols, **132** and **147** were separable by column chromatography, hence the reason why the presence of compound **146** had not been detected earlier.



Scheme 48: Scheme showing the source of compound 144

By comparison, the products recovered after trityl protection of the diol compound, **142** and **148**, were unfortunately not separable by column chromatography. The polarity of the two compounds is very similar because a single spot was visualised on TLC for the two products. Methoxy signals established the approximate ratio of the two products (compound **142**:compound **148**) to be 9:1. Similarly the products recovered after TBS protection, compound **143** and **149**, were still not separable by column chromatography. However the ratio of the methoxy signals had changed to 6:1 suggesting that the TBS protection step was quantitative for compound **148** but not for compound **142**. At this point it was now evident that the recovered side product **144** had formed by addition of the chiral sulfoxide to compound **149**, originating from 1,3-diol **146** and its subsequent products being carried through several reactions (**Scheme 48**).

Given this revelation, the only way of minimising the unwanted side products would be to eliminate the formation of compound **146** during the reduction step as the two products are evidently formed as a result of competing reactions.



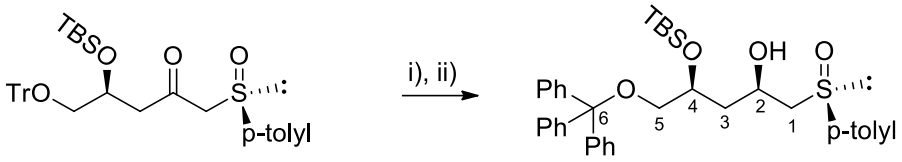
145

Figure 27: Structure for compound 145

After successfully characterising and establishing the source of compound **144**, attention shifted to the desired product of the reaction in **Scheme 47**, which was identified to be compound **145** by NMR spectroscopy. Firstly, the total aromatic integration was nineteen as expected in the ^{1}H NMR spectrum, and the signals were observed at δ 7.45 (d, *J* = 7.9 Hz, 2H), δ 7.42 – 7.36 (m, 6H,) and δ 7.32 – 7.17 (m, 11H). The methyl singlet signal from the tolyl group was at δ 2.36. The diastereotopic H-1 proton signals were a set of doublets at δ 3.88 and δ 3.76 both with a coupling constant of 14.0 Hz. A multiplet at δ 2.80 – 2.62 integrating for two protons was assigned to H-3 protons, while two sets of doublet of doublets at δ 3.10 (*J* = 9.3, 4.6 Hz, 1H, H-5_a) and 2.95 (*J* = 9.3, 6.8 Hz, 1H, H-5_b) were assigned to H-5 protons. Assignment of the H-3 and H-5 protons was based on the fact that H-5 proton signals will be more deshielded because they are attached to a C-O carbon atom. This is the most distinguishing factor because both protons show coupling to the H-3 proton and they are attached to a CH_2 carbon atom. The remaining singlet signals for the TBS group were observed at δ 0.79 (9H), δ -0.02 (3H) and δ -0.09 (3H).

Assignment of the carbon atoms was accomplishment by analysis of the HSQC NMR spectrum. In the ^{13}C NMR spectrum, the C-1 signal was observed at δ 69.9 whilst the carbonyl signal observed at δ 200.5 was assigned to C-2. The C-3 carbon atom was evidently experiencing strong deshielding effects because the signal was observed downfield at δ 50.0, which is uncharacteristic for a saturated CH_2 atom that is not directly attached to a heteroatom. C-4 and C-5 signals were within the expected range at δ 68.3 and δ 67.1 respectively. The remaining signals were as expected. With both the mass spectrometry results and the NMR spectroscopic assignments, it was evident that the desired compound had been recovered and it was subjected to subsequent reactions.

Since attempts to isolate crystals of compound **145** for X-ray crystallography were unfruitful, the relative stereochemistry was assumed at this stage and it was only proved by further transforming to the known compound **124** which was also the target molecule. In order to achieve this, compound **145** was subjected to the chelation controlled reduction using the previously described procedure as shown in **Scheme 49**. A good yield of 87% was achieved for the desired compound **150** as an optically active yellow solid with a specific rotation of +43.0 (c 1.3, $CHCl_3$). IR spectroscopy showed the alcohol signal at 3339 cm^{-1} whilst the previously observed carbonyl signal had totally disappeared. This confirmed the success of the reduction of the carbonyl group.

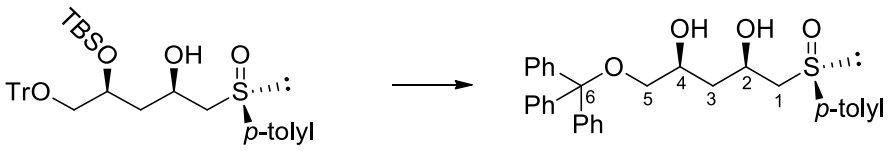


145 **150**

Scheme 49: i) $ZnCl_2$, r.t., 2 h; ii) DIBALH, THF, -78 °C – r.t., 2 h, 87%

Further confirmation of the identity of the product was afforded by NMR spectroscopic analysis. In the ^1H NMR spectrum, the H-2 signal at the newly generated stereogenic centre was observed as a multiplet at δ 4.24 – 4.07. The H-4 signal was observed at δ 3.97 – 3.87 overlapping with the OH signal, integrating for 2 protons. In the ^{13}C NMR spectrum, the carbonyl signal had totally disappeared and was replaced by a new C-2 signal at δ 66.3 whilst the H-4 signal was at δ 70.2. A huge chemical shift change was observed for the C-3 signal from δ 50.0 to δ 41.7 because the carbonyl group exerts greater anisotropic effects to the alpha position resulting in a deshielding effect when compared to alcohol group. The rest of the signals were as expected and HRMS confirmed the expected mass for compound **150** of 637.6729 $(M+Na)^+$.

Compound **150** was successively subjected to TBS deprotection using TBAF for 2 hours revealing the already known triol compound **141** in a yield of 87% as shown in **Scheme 50**. Allowing the reaction to proceed for longer resulted in the loss of the trityl group as well. The measured specific optical rotation of the recovered product was +83.3 at a concentration of 1 which is comparable to the literature value.[63] The measured polarity confirms that indeed the correct enantiomer of diol **141** had been recovered by employing the alternative route.



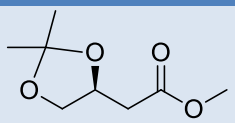
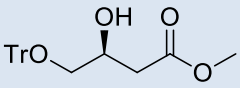
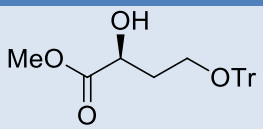
150 **141**

Scheme 50: TBAF, THF, 0 °C, 4 h, 87%

Further confirmation of the identity of the recovered product was achieved by comparison of NMR spectroscopic data with that from previously prepared diol **141**. Acetonide protection of the recovered diol yielded the target intermediate **124** as described previously in **Scheme 43** and the measured specific optical rotation of +27.3 confirmed the recovery of the desired enantiomer. The NMR spectroscopic results also supported the identity of the product to be compound **124**, and the chemical shifts for the acetonide group indicate that a 1,3-*syn*-diol system was present.[147] Since the recovered product was indeed the desired product, it confirmed the identity and stereochemistry of compound **145**.

After synthesising compound **124** by employing the two different approaches a comparison from diol **129** was made to establish which route was higher yielding. Both routes had six steps and the best overall yield for route **1** was 8% whilst for route **2** the best overall yield was 16%. For route **1** the minor side product resulting from compound **146** after the acetonide protection (compound **147**) was easily removed via column chromatography. On contrary, for route **2** the minor product resulted in compound **148** and it was carried through the subsequent reactions only to be separated after the sulfoxide addition step.

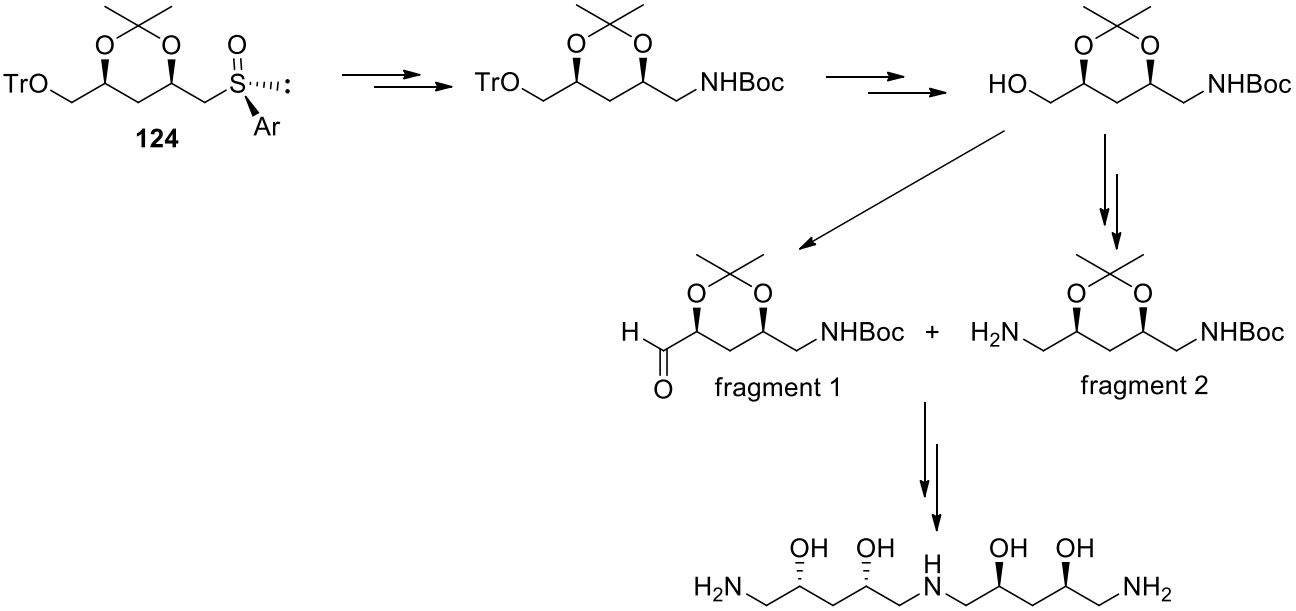
Table 3: Comparison of route 1 and route 2 employed for the synthesis of intermediate 124

	Route 1	Route 2	
Key intermediates	 **132**	 **142**	 **148**
Number of steps to compound 124 from diol 129	6	6	
Overall yield of compound 124 from compound 129	8%	16%	
Yield of the sulfoxide addition reaction	64%	73%	94%

Yields for the sulfoxide intermediate were more interesting, for route **1** the sulfoxide product **138** was recovered in a best yield of 64%. Unfortunately, the presence of the side product for route **2** provided competing reactions because the results indicate that there was complete conversion of compound **149** to **144**. However, the desired compound **145** was recovered in a best yield of 73%. The observed yields for route 2 suggest that there is complete conversion of both compound **143** and **149** to compound **145** and **144** respectively. However, once the products are formed the acidity of the protons alpha to the sulfur for compound **145** in the presence of the sulfoxide anion and excess base probably results in product decomposition. In comparison, the absence of the acidic protons for compound **144** makes it more stable and recoverable in quantitative yields. Nevertheless, it was exciting that employing route 2 doubled the recoverable yield of compound **124**. The route also eliminated the tedious continuous extraction step needed for the recovery of the triol **140**. If formation of the side product **146** is minimised and the subsequent steps are optimised, route 2 offers the greater potential for increasing the overall yield for compound **124**.

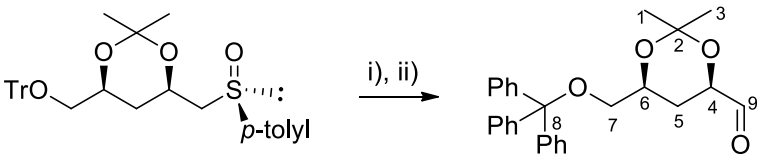
2.2.3 Synthesis of fragment 1 and fragment 2

Once the 1,3-diol core had been synthesised, work started on functionalising the terminal carbons, which would facilitate the differentiation of the two fragments prior to coupling them. For synthesis of the enantiomer of pavettamine, parallel reactions were performed starting with intermediate **124**. For fragment 1 the alcohol on C-5 was converted to an aldehyde whilst the second set of reactions were for converting the alcohol on the C-5 carbon atom to an amine yielding fragment 2, followed by coupling of the fragments as shown in **Scheme 51**.



Scheme 51: Planned synthesis of fragment 1 and fragment 2

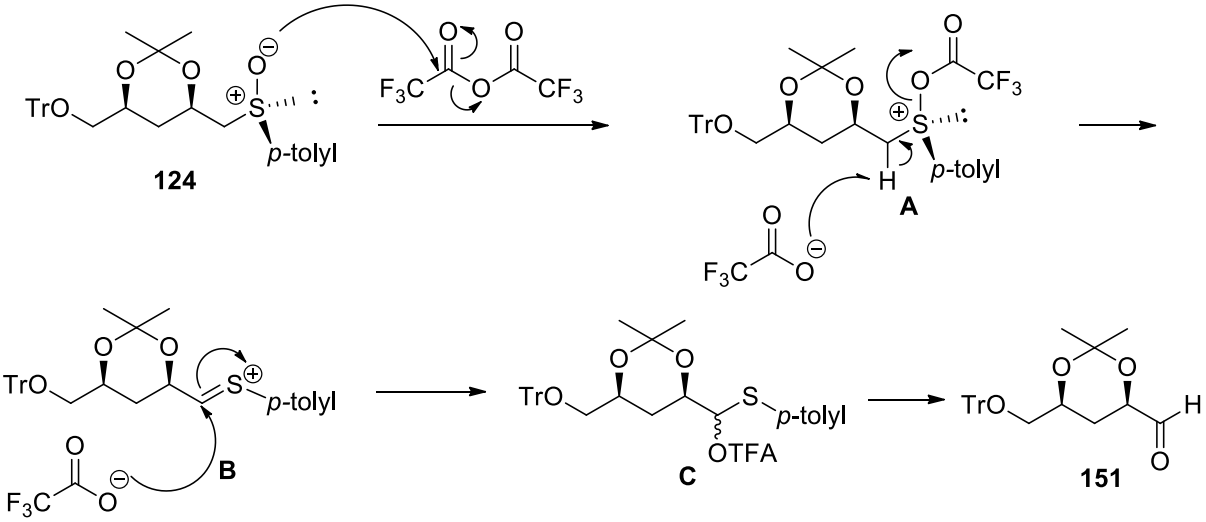
Compound **124** was subjected to the interrupted Pummerer rearrangement using TFAA as the acid with collidine as a base to furnish the aldehyde **151** (**Scheme 52**).[115, 148] The reaction was complete in under 30 minutes, quenching was afforded with water and excess base. The quenched reaction was left stirring for a further 30 min revealing the desired aldehyde as compound **151**. The Pummerer rearrangement mechanism has been well studied and the most accepted mechanism is shown in **Scheme 53**.[97, 149]



124 **151**

Scheme 52: i) TFAA, collidine, 0 °C, 30 min; ii) K_2CO_3, r.t., 30 min, 99%

The first step in the mechanism involves the acetylation of the nucleophilic sulfoxide oxygen by the trifluoroacetic anhydride giving rise to the intermediate **A**. This step yields a trifluoroacetate anion which in turn deprotonates the acidic proton at the α-carbon to the sulfur resulting in a sulfonium ion intermediate **B**. The trifluoroacetate ion from the generated acetic ion released in the previous step then traps the sulfonium intermediate by adding to the double bond generating an α-acyloxy thioether intermediate **C**, which is hydrolysed by water yielding the desired compound **151**. The overall reaction reaches completion in approximately one hour, which is ideal because short reaction times are desirable for total syntheses procedures. The rearrangement method increases the desirability of the sulfoxide as a chiral auxiliary because it allows for the removal of sulfur whilst introducing the aldehyde moiety, which can be easily converted to other functional groups.

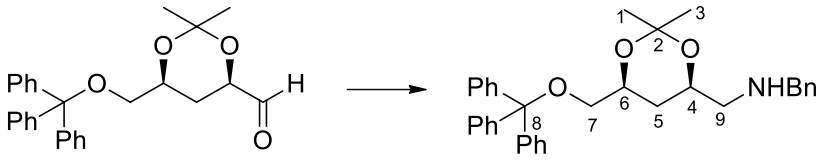


Scheme 53: Pummerer rearrangement mechanism

Product **151** was recovered in quantitative yields as a white solid. Product racemisation was always a concern because of the increased acidity of the aldehydic proton that is alpha to a C-O stereocentre. In order to acquire clean NMR spectra, purification was performed on a 50 mg sample using a very short column. The rest of the crude product was used as is in the next step. Successful synthesis of the product was confirmed by the characteristic aldehyde peak, observed at δ 9.58 as a singlet integrating for one proton in the ^{1}H NMR spectrum. There were no significant changes in any of the other chemical shifts. In the ^{13}C NMR spectrum the carbonyl signal for C-9 was observed at δ 201.1. The chemical shifts for the C-1, C-2 and C-3 carbon atoms were observed at δ 29.6, δ 99.0 and δ 19.4, respectively just as expected for acetonide protected 1,3-*syn* alcohols.

This confirmed that there was no epimerisation during the Pummerer rearrangement step and the relative stereochemistry had been conserved.[69]

The aldehyde **151** was subjected to a reductive amination procedure with benzylamine in the presence of sodium triacetoxyborohydride, in the presence of 3Å molecular sieves (**Scheme 54**).[150, 151, 152] The rationale for employing this approach was that the procedure introduced the desired amine functionality already benzyl protected. In the reaction, the reduction of the aldehyde competes with the reductive amination step, therefore to minimise this unwanted side reaction the amine was always added in excess. The amine and aldehyde were left stirring for at least 30 minutes prior to the addition of the reducing agent. Low yields were obtained when a 1:1 DCE/THF solvent mixture was used without molecular sieves. Yield optimisation was achieved with at least a 1:9 THF/DCE solvent ratio in the presence of molecular sieves that acted as a dehydrating agent.



151 **152**

Scheme 54: Benzylamine, DCE, THF, sodium triacetoxyborohydride, N_2, r.t., 24 h, 60%

Despite all the yield optimisation protocols, compound **152** was recovered in a below average yield of 60% as a colourless thick gel. The optical rotation was measured to be -16.8° in chloroform at a concentration of 0.9 g/ml. The ^{1}H NMR spectrum showed an increase in the number of aromatic protons from fifteen to twenty, with the signals observed as multiplets at δ 7.54 – 7.48 and δ 7.40 – 7.24. The expected new signal for the H-9 protons was at δ 2.77 – 2.66 as a multiplet, whilst the benzylic CH_2 protons were observed at δ 3.85 as a singlet. Despite compound **152** being a viscous oil at room temperature, the compound crystallised in a chloroform/methanol mixture, and the structure is shown in **Figure 28**. The 1,3-*syn*-diol moiety was shown to be still intact, agreeing with the observed ^{13}C NMR chemical shifts for the dioxane methyl groups and the quaternary carbon atom.

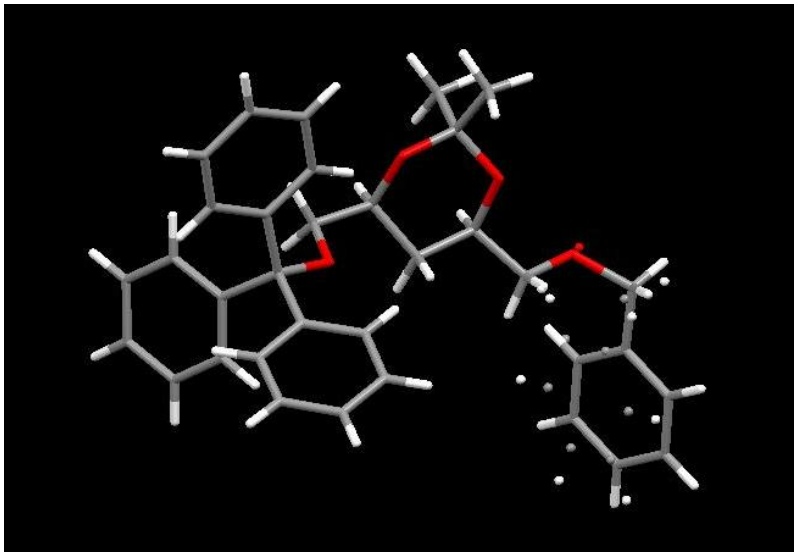


Figure 28: Crystal structure of compound 152

With the first amine functionality introduced, the next steps involved differential functionalisation of the C-7 carbon atom of compound **152** in order to generate two separate fragments. The proposed plan was to selectively deprotect the trityl group in the presence of the benzyl group, revealing the primary alcohol, which in turn would be converted into an aldehyde for fragment 1 and an amine for fragment 2. Thus the two fragments would be subsequently coupled via reductive amination. Although the benzyl group and the trityl group are generally deprotected under similar conditions, there are several examples in literature where the trityl group was selectively removed in the presence of a benzyl-protected amine.[153] The anticipated selectivity was based on the premise that the trityl functionality forms a more stable cation intermediate because of the stabilising effect of the phenyl rings. The stability of the intermediate results in trityl deprotection being kinetically more favourable than that of the benzyl protected amine.

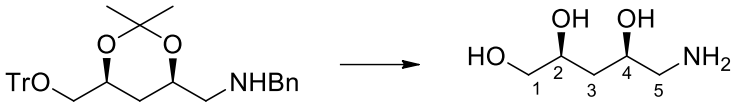
The first attempt at selective trityl deprotection employed a freshly prepared heterogeneous catalyst of $NaHSO_4.SiO_2$ in a DCM/MeOH (9:1) solvent mixture. This procedure had not only been shown to be selective for the trityl group, but was also proven to be a mild deprotecting agent in the presence of acid and base sensitive groups.[153] Unfortunately, the desired alcohol was not recovered even after slightly increasing the temperature of the reaction. Changing the inorganic salt to ceric ammonium nitrate (CAN-SiO_2) did not yield the desired product either.[154] Only the starting material was recovered which suggests that the substrate was unreactive under the tested experimental conditions

Further investigations into other possible deprotection procedures revealed that mild Lewis acids can also be used for the selective deprotection of the trityl group.[155] This procedure utilises Lewis acids such as $ZnBr_2$, and it was shown to be selective for the trityl group whilst other *N*-acyl protecting groups namely isobutyryl, benzoyl and anisoyl remained unaffected. For this work, the efficacy of both $ZnBr_2$ and $ZnCl_2$ was tested but the desired molecular transformation was not realised. From the mechanism, the trityl ethereal oxygen acts as an electron donor to the $ZnBr_2$ resulting in a stable trityl carbenium ion. The stability of the intermediate should then act as a driving force for the reaction but this was not achieved. The desired product was also not recovered even after refluxing compound **152** with LiCl in THF and only the starting was recovered.[156]

After the failed deprotection attempts employing Lewis acids, attention shifted to the use of protic acids being cognisant of the potential competing reactions. Based on the work published by Bessods *et al*., a mixture of formic acid and diethyl ether (1:1) can be successfully used for the selective cleavage of the trityl group in the presence of acid sensitive groups.[157] The authors reported good yields in times ranging from 10 – 40 minutes with minimal or no effect on the acetonide groups. Given the reported success, the same procedure was tested for the selective deprotection of the trityl group on compound **152**, and the procedure utilised a 1:1 mixture of dry diethyl ether and formic acid under anhydrous conditions to minimise hydrolysis of the acetonide. The reaction was monitored using TLC but there was no observable change even after one and a half hours reaction time. The starting material was recovered intact even after varying the experimental conditions.

All the attempted protocols thus far had capitalised on the formation of the stable trityl carbocation as the driving force behind the selectivity. A quick search in Theodora Green's, "Protective Groups in Organic Synthesis" revealed that hydrogenation under a Pd/C catalyst readily deprotects both O-trityl and *N*-benzyl groups under slightly different conditions.[158] As a way of capitalising on the different deprotection conditions, a few drops of formic acid were added to catalyse the hydrogenation reaction just to establish whether the acidic conditions would result in selectivity (**Scheme 55**). The reaction was left stirring at atmospheric pressure and instead of the desired product, a completely deprotected compound **153** was recovered. This was certainly the first time acetonide deprotection under acidic hydrogenation conditions had been

observed, at least to the best of our knowledge. Although this was not the desired outcome, the result opened the door to other possibilities.

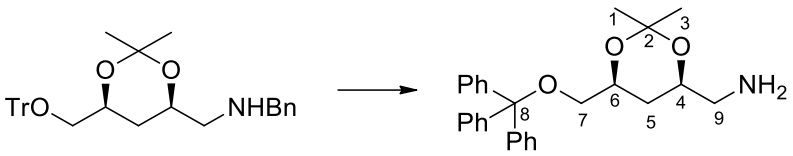


152 **153**

Scheme 55: Formic acid, ethanol, H_2, 10% Pd/C, overnight, 24 h, 90%

Confirmation of the structure of the recovered product was achieved by NMR spectroscopic analysis. In the ^{1}H NMR spectrum, H-2 and H-4 signals were observed as multiplets at δ 4.03 – 3.89 and δ 3.82 – 3.68 respectively. The H-1 signal was observed at δ 3.52 – 3.32 as a multiplet integrating for two protons, whilst the H-3 proton signal was at δ 1.73 – 1.51. In the ^{13}C NMR spectrum only five signals were observed with the C-2 and C-4 signals at δ 70.5 and δ 67.1 whilst the C-1, C-3 and C-5 signals were observed at δ 66.9, δ 39.0 and δ 46.0. There was no evidence of aromatic signals in both spectra. Although this was not the desired result a more controlled hydrogenolysis procedure could prove to be selective for the benzyl group instead of the trityl group.

The hydrogenation reaction was repeated under neutral conditions at atmospheric pressure for 24 hours in order to determine if these conditions were selective for a single protecting group (**Scheme 56**). The procedure resulted in the selective debenzylation of the amine in the presence of *O*-trityl. Primary amine **154** was recovered in a yield of 84% as a white amorphous product, with a specific optical rotation of -24.6 (c 1.0 $CHCl_3$) which was comparable to the literature value.[63] From the ^{1}H NMR spectrum, the total integration for the aromatic protons had reduced to fifteen, with the signals observed as multiplets at δ 7.48 – 7.42 and δ 7.32 – 7.18. The singlet signal for the benzylic protons which had previously been at δ 3.85 had disappeared. A new broad singlet signal for the amine, integrating for two protons was observed at δ 1.65. No correlation in the HSQC or coupling in the COSY NMR spectrum was observed for this signal, confirming that the signal was for NH_2 protons.



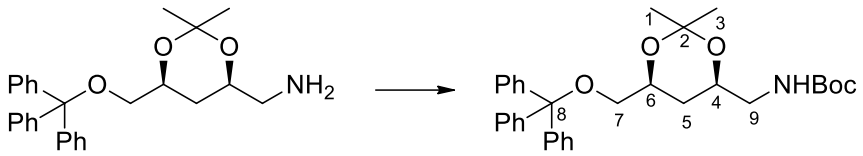
152 **154**

Scheme 56: ethanol, 10% Pd/C, H_2, r.t., 24 h, 84%

As expected only four carbon signals were observed in the aromatic region of the ^{13}C NMR spectrum at δ 144.0, δ 128.7, 127.7 and 126.9 whilst the quaternary trityl C-8 signal was at δ 86.5. The benzylic carbon signal had also disappeared with only the C-9 signal being detected at δ 47.4. The relative stereochemical integrity of the compound was confirmed by the chemical shifts of C-1 and C-3 signals at δ 30.0 and δ 19.9 whilst C-2 was at δ 98.6.

Before proceeding with the synthesis, an evaluation of protecting group compatibility was conducted. Up to this point all the reaction conditions employed for the selective deprotection of the trityl group had been unsuccessful. One procedure with guaranteed success was the Birch reduction methodology but it had not been employed as yet because the reaction conditions are not selective in the presence of the benzyl group.[158] The mechanism of the reaction proceeds via a single electron transfer to the trityl moiety forming a radical which is quenched during workup, revealing the alcohol. The Birch reduction is mainly used for aromatic ring and alkene reductions but is also useful for the removal of aromatic protecting groups.[159] Carbamates, alkyl ethers and silyl groups are the only stable protecting groups under these reduction conditions.

Subjecting amine **154** to trityl deprotection without protecting the primary amine would have yielded a polar product most likely difficult to purify. After careful consideration of the trityl deprotection conditions and the remaining synthetic steps, Boc protection was chosen for the amine group as shown in **Scheme 57**. The reagents were left stirring overnight, and after work up the desired product was recovered quantitatively as a white precipitate. No column chromatography was necessary because all the side products were either volatile or dissolved in the aqueous layer during workup.

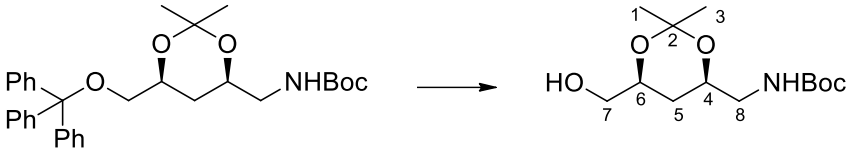


154 **155**

Scheme 57: Boc anhydride, DMAP, THF, r.t., overnight, 100%

The specific optical rotation of compound **155** was confirmed to be -20.3 (c 1.0 $CHCl_3$) showing that, the Boc group had little effect on the magnitude and sign of rotation when compared with that of the free amine. Confirmation of the product structure was achieved by NMR spectroscopic analysis. The ^1H NMR spectrum showed the disappearance of the broad singlet for the NH_2 protons, and appearance of a new broad singlet at δ 4.88 for the NH proton. The methyl Boc proton singlet signal was observed at δ 1.45 whilst the acetonide methyl singlets were detected at δ 1.43 and δ 1.38 giving a total integration of fifteen protons. The new characteristic Boc carbonyl signal was observed at δ 156.0 in the ^{13}C NMR spectrum with the remaining Boc signals at δ 79.3 and δ 25.6.

With the Boc-protected amine in hand the next step involved detritylation of compound **155** under Birch reduction conditions (**Scheme 58**). The ammonia was first refluxed over sodium, ensuring anhydrous conditions evidenced by a deep blue colour prior to the addition of the substrate. The reaction was allowed to proceed for an hour, after which work up and product purification using column chromatography yielded compound **156**. The detritylated product was recovered in a yield of 81% as a yellow oil with a specific optical rotation of -10.7 (c 0.6 $CHCl_3$).



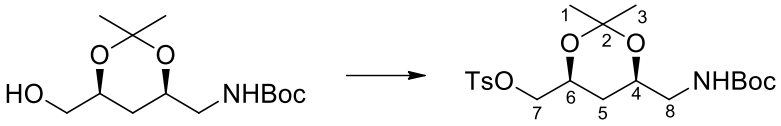
155 **156**

Scheme 58: Na, NH_3, THF, -60 °C, 1 h, 81%

IR spectroscopy revealed a broad signal at 3324 cm^{-1} indicating the presence of both the OH and NH groups. In the ^1H NMR spectrum no aromatic signals were observed but two broad singlets which showed no coupling to any other protons or carbon correlations in the COSY and HSQC NMR spectra were observed at δ 4.95 and δ 2.41. These signals were attributed to the OH and NH protons, respectively. As expected, the Boc group was not affected by the Birch reduction protocol, and the proton signals were overlapping with the H-1 protons at δ 1.47 – 1.43 giving rise

to a total integration of twelve protons. Likewise, in the ^{13}C NMR spectrum there was no evidence of aromatic carbon signals. Since it was critical to monitor the stereochemical integrity of the compound as the synthesis progressed, the chemical shifts for C-1, C-2 and C-3 were as usual used for confirmation of the relative stereochemistry. The signals were observed at δ 98.8 for C-2 and δ 29.9 and δ 19.9 for C-3 and C-1, indicating that the product was still a 1,3-*syn* product.

At this point compound **156** was apportioned into two parts, to synthesise the two fragments separately by converting the alcohol to an amine for one fragment and an aldehyde for the second fragment. These two fragments would be coupled by reductive amination, and subjected to Boc and acetonide deprotection to reveal the desired compound. The first step began by converting the alcohol to an amine by tosylating the primary alcohol as shown in **Scheme 59** using a standard established procedure.[160, 161] Tosylates are versatile substrates for substitution reactions because they are good leaving groups.



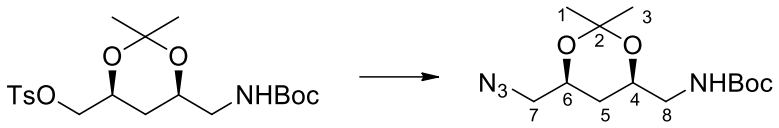
156 **157**

Scheme 59: TsCl, DMAP, DCM, r.t., 24 h, 83%

Compound **157** was recovered in a yield of 83% as a yellow oil with a specific optical rotation of - 3.6 (c 0.5, $CHCl_3$). The expected aromatic proton signals for the tosyl group were observed as sets of doublets at δ 7.78 (*J* = 8.3 Hz) and 7.34 (*J* = 7.9 Hz) each integrating for two protons in the ^1H NMR spectrum. The tosyl-methyl protons were observed at δ 2.45 as a singlet. In the ^{13}C NMR spectrum, the aromatic carbon signals were visible at δ 144.9, δ 132.9, δ 129.8 and δ 128.0 with the tosyl-methyl carbon signal at δ 19.6. The rest of the signals were as expected and the NMR spectroscopic assignments confirmed the successful tosylation procedure. For this reaction, the tosylation of the amine was not likely, as it is a carbamate, so not very nucleophilic. As a result tosylation of the amine was not detected in the recovered product.

The tosyl group on compound **157** was displaced by an azide via an S_N2 type substitution reaction because azide is a strong nucleophile, and the substrate is unlikely to form a stable cation.[162, 163] Both the substrate and sodium azide were dissolved in DMF and heated at 80 °C for 3 hours (**Scheme 60**). Heating at higher temperatures and leaving the reaction going on for longer resulted in decomposition of the product. The desired compound **158** was recovered in a yield of 75% as a

yellow oil with a specific optical rotation of -2.59 (c 0.5, $CHCl_3$). The initial success of the formation of the azide was confirmed by IR spectroscopy due to the presence of the characteristic azide signal at 2098 cm^{-1}.

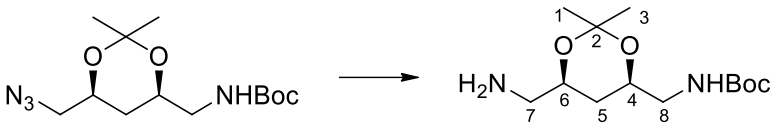


157 **158**

Scheme 60: NaN_3, DMF, reflux 80 °C, 3 h, 75%

Further verification of the success of the azide substitution reaction was established by the disappearance of the tosyl signals from the ^1H NMR spectrum. There was an observable shift for the H-7 proton signal from δ 4.02 – 3.85, where it overlapped with the H-4 signal for compound **157** to δ 3.40 – 3.15 for compound **158** overlapping with a single H-8 proton signal. The upfield chemical shift was expected because oxygen is more electronegative than nitrogen therefore CH_2O protons appear more downfield than CH_2N protons. The chemical shift change due to a change in the heteroatom was also apparent as well in the ^{13}C NMR spectrum. The C-7 signal had migrated from δ 72.2 for compound **157** to δ 55.1 for compound **158**. Mass spectrometry also confirmed the identity of the desired compound with a measured mass of 323.1619 $(M+H)^+$.

The final step for the synthesis of fragment 1 was the reduction of the azide to the amine using hydrogenation conditions under pressure as shown in **Scheme 61**. Reduction was only successful at a pressure of 4 atm, otherwise only the starting material was recovered. No further purification was necessary for compound **159** apart from filtration to remove the catalyst. Quantitative yields of the product were recovered as a brown oil with the IR spectrum showing a broad NH_2 peak at 3353 cm^{-1} and the disappearance of the previously observed azide signal.



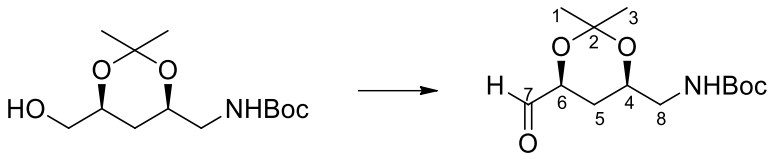
158 **159**

Scheme 61: 10% Pd/C, H_2, ethanol, 4 atm, r.t., overnight, quantitative yield

Validation of the product's identity was accomplished by both ^1H and ^{13}C NMR spectroscopy. The C-7 proton signal migrated from δ 3.40 – 3.15 for compound **158** to δ 2.80 – 2.52 for compound **159**. The C-7 carbon signal also migrated from δ 55.1 to δ 47.4. The observed change in the

chemical shift corresponds with the change in the functional group at C-7. The azide group is more electronegative than the amine group, giving rise to the observed chemical shifts.

With fragment 1 synthesised, attention was focused on converting alcohol **156** to aldehyde **160**. The first attempt employed MnO_2 in DCM but even after stirring for 24 h, only the starting material was recovered. The second attempt utilised PCC ground together with silica as the oxidant in dry DCM.[164, 165] A green oil was recovered after work up and was not purified further for fear of racemization of the product due to the acidity of the aldehydic proton. However, ^{1}H NMR spectroscopic analysis showed a very small signal for the aldehyde proton, and ^{13}C NMR spectroscopy showed two signals in the aldehyde region. The acetonide peaks suggested that racemisation had occurred at the position α to the carbonyl because there were both signals for the *anti*-1,3 diol system and signals for the *syn*-1,3-diol system. Oxidation using PCC was therefore abandoned. Fortunately, successful oxidation was achieved by using 2-iodoxybenzoic acid (IBX) in DMSO as shown in **Scheme 62**. Due to the suspected poor stability of the product, it was not purified further, but used immediately in subsequent reactions.



156 **160**

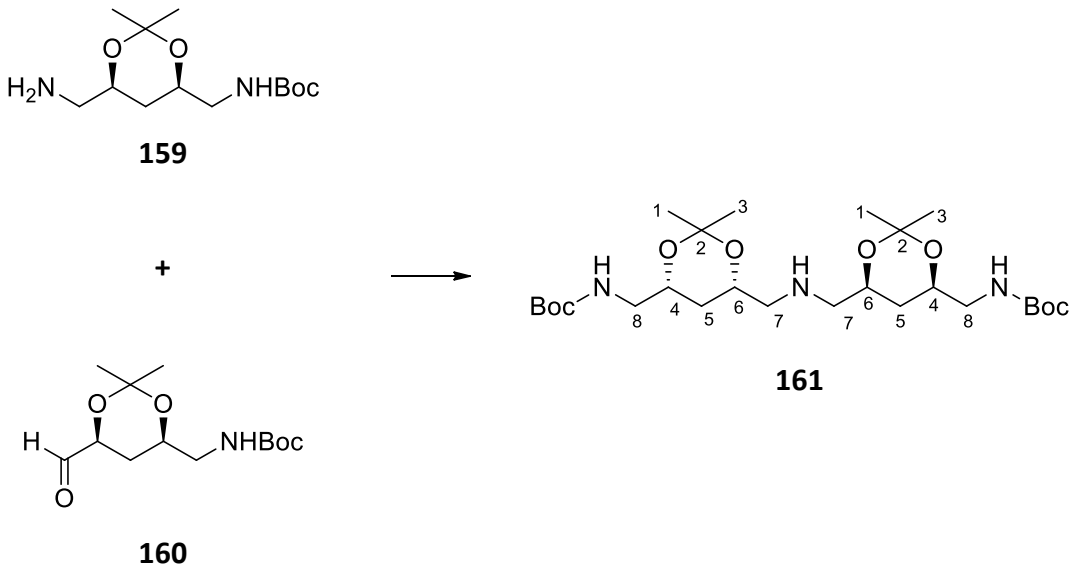
Scheme 62: IBX, DMSO, r.t., overnight, quantitative yield

Confirmation of the desired product **160** was achieved by staining the TLC plate in 2,4-dinitrophenylhydrazine (2,4-DNPH). The recovered compound stained yellow on an orange background indicating the presence of the aldehyde. In the IR spectrum the characteristic carbonyl signal was evident at 1710 cm^{-1}. The ^{1}H NMR spectrum of the crude material showed the aldehyde peak in the expected region at δ 9.58 as a singlet with an integration of one. The broad singlet for the amine peak was observed at δ 4.93 and the rest of the signals were as expected. Mass spectrometry also confirmed the recovery of the desired product with a measured mass of 274.1647 $(M+H)^{+}$.

With the two fragments synthesised, the next step involved coupling compound **159** and compound **160** via reductive amination as previously described in **Scheme 63** to afford the pavettamine backbone. Product purification via column chromatography furnished compound

161 as a yellow viscous oil in a yield of 95%. The optical rotation of the product was measured to be -10.1 in chloroform at a concentration of 1.03 g/ml. Spectroscopic analysis confirmed the identity of the product. IR spectroscopy showed a signal at 3362 cm^{-1}, indicative of the presence of an NH group. In the ^{1}H NMR spectrum, the signals for the H-1 acetonide methyl protons, Boc groups and H-5_a were overlapping and the multiplet was observed at δ 1.48 – 1.42 integrating for twenty six protons. Two separate peaks for the amines were observed, at δ 4.94 and δ 2.07. The difference in chemical shifts of the amine signals is because of the difference in hydrogen bonding levels between the carbamates at C-8 and the connecting amine at C-7. Amines that appear more upfield experience a greater degree of hydrogen bonding as opposed to those that appear downfield.

The ^{13}C NMR spectrum showed the quaternary C-2 at δ 98.8 whilst the C-1 and C-3 signals were observed at δ 19.9 and δ 30.0. The chemical shifts for these signals show that the *syn*-1,3 configuration is still present, therefore racemisation at the α-position had not occurred. The C-7 and C-8 signals were at δ 55.0 and δ 45.4 respectively, which is the expected range for C-N carbon signals. Only two signals were visible in the C-O range of the NMR spectrum at δ 68.2 and δ 67.9 for the C-4 and C-6 carbons, as expected. The Boc group and C-5 signals were in the expected regions as well.



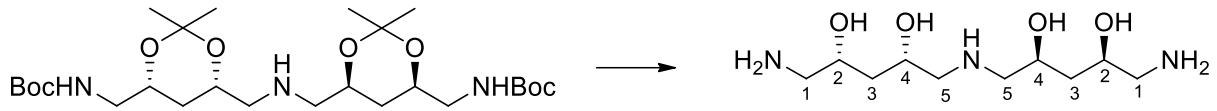
Scheme 63: Sodium triacetoxyborohydride, 1,2-DCE, THF, r.t., 24 h, 95%

Elated that the protected pavettamine enantiomer was in hand, the syntheses set about the removal of the protecting groups. The final deprotection step was unfortunately not straight forward as expected, given the fact that both the acetonide and Boc groups are cleavable under

acidic conditions. Literature is awash with different methods for Boc deprotection, and the conditions employed also generally favour the removal of acetonide groups.[166, 167] In the steps preceding the final step, we had discovered that the acetonide groups had been deprotected (**Scheme 55**) under acidic hydrogenation conditions, therefore the deprotection step was attempted under similar conditions. Unfortunately, only the starting material was recovered despite changing the reaction conditions by increasing the pressure up to 7 atm and lowering the pH with a few drops of HCl instead of formic acid. The second attempt involved stepwise deprotection, by first removing the acetonide via hydrolysis with *p*-TsOH as the acid catalyst. Despite refluxing at 60 °C for over 48 hours the desired product was not recovered, only the starting material was recovered. Treating compound **161** with 20 equivalents of TFA in DCM for 12 hours did not furnish the desired product either and only the starting material was recovered.

A routine deprotection step was turning out to be one of the most complicated steps of the synthesis. Further literature research showed that CAN has been used effectively to cleave the Boc and acetonide groups in carbohydrate chemistry.[168, 169] Ceric ammonium nitrate functions as a one electron transfer catalyst in the deprotection procedures and all the acid sensitive groups remain unaffected. However, use of CAN as a catalyst under reflux conditions for the removal of the Boc groups from compound **161** did not furnish the desired product. Deprotection attempts under microwave conditions also failed to yield the desired product.[166]

After the series of failed attempts, a procedure typically used for Boc deprotection in peptide synthesis was employed utilizing trifluoroacetic acid (TFA) and triisopropylsilane (TIPS), with the assumption that, even though the substrate was not a peptide it was just as polar as a peptide, and the protocol might be successful. The reagents were added together and left stirring at room temperature overnight as shown in **Scheme 64**. To our delight, TLC monitoring showed total consumption of the starting material and formation of a new polar product. The high polarity of the desired polyamine **112** under the acidic reaction conditions complicated the work up procedure. The reaction was initially diluted with methanol, and excess solvent and TFA were removed *in vacuo*. The residue was re-dissolved in methanol, followed by the removal of solvent under reduced pressure. After leaving the product to completely dry in the fume-hood, a yellow oily residue was recovered in quantitative yield.



161 **112**

Scheme 64: 95% TFA, 2.5% H_2O, 2.5% triisopropylsilane, r.t., overnight, quantitative yield

Confirmation of the structure of the desired polyamine **112** was performed using NMR spectroscopy. Both the acetonide and Boc group signals were missing from the ^{1}H NMR spectrum indicating that the deprotection had been successful. A multiplet signal for H-4 and H-2 protons was observed at δ 4.19 – 4.10 and δ 4.07 – 3.99 respectively, whilst the H-5_a signal was observed at δ 3.22 – 3.14. The H-1_a and H-5_b signals were overlapping at δ 3.10 – 3.00 with a total integration of four protons. The H-1_b signal was a doublet of doublets at δ 2.88 (*J* = 12.8, 8.9 Hz) and the remaining H-3 multiplet signal was at δ 1.78 – 1.62.

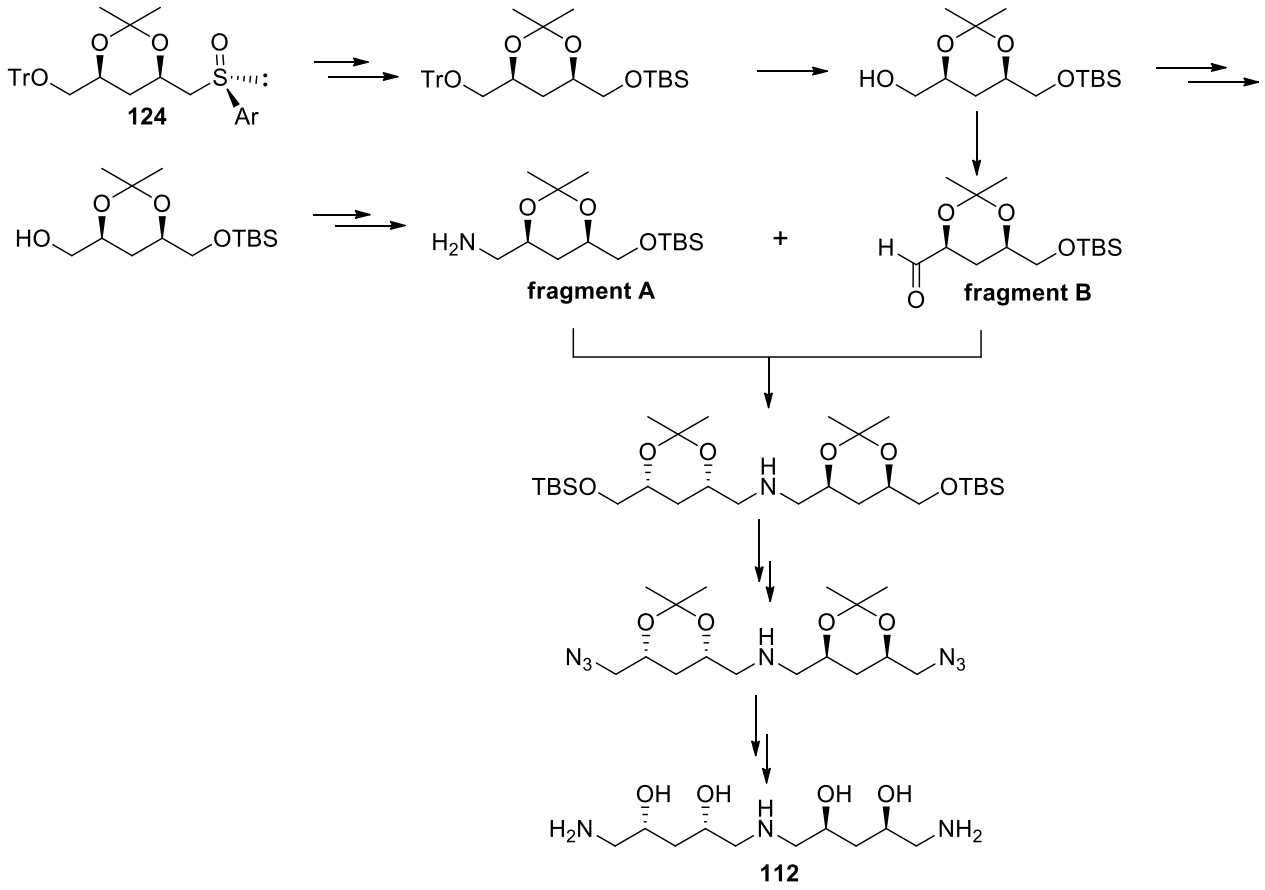
As expected both the acetonide and the Boc group signals were not present in the ^{13}C NMR spectrum. However, a distorted quartet was observed at δ 163.7 and δ 120.3 indicative of the presence of TFA, suggesting that the desired product was recovered as a TFA salt. This is a strong possibility because of the basicity of the amine groups present in the product. ^{19}F NMR spectroscopy confirmed the presence of TFA. The remaining C-2, C-4, C-5, C-1 and C-3 signals were observed at δ 64.6, δ 63.7, δ 52.3, δ 44.4 and δ 38.9, respectively. All the NMR spectroscopic proton and carbon signals are comparable to the literature values for pavettamine, even though for the literature experimental data was acquired in D_2O.[63] High resolution mass spectrometry confirmed the mass of the enantiomer of pavettamine **112** to be 252.1912 $(M+H)^+$ which is comparable to the expected mass of 252.1918 $(M+H)^+$. The TFA fragment ion was also present with a confirmed mass of 115.1227 $(M+H)^+$. Since the enantiomer of pavettamine was recovered as a TFA salt, a comparative analysis of the specific optical rotation between pavettamine and its enantiomer was not performed. Attempts to neutralise the salt were unsuccessful, and reprotection with benzyl groups resulted in product decomposition.

Nevertheless, the conclusive characterisation of the enantiomer of pavettamine was met with sheer joy and excitement because this was the first reported total synthesis of this compound. This work also shows that the same starting material, malic acid can be used for the syntheses of both pavettamine and its enantiomer. The low overall yield was as a result of material being lost

during optimisation of several steps. However, high yields can probably be recovered by employing the optimised reaction conditions.

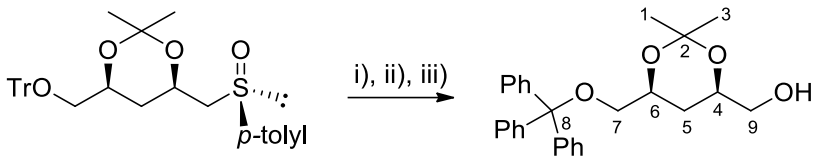
2.2.4 A different approach to the synthesis of the enantiomer of pavettamine 112

Given the successful synthesis of polyamine **112**, the synthetic approach was changed in an attempt to recover the product as a neutral product, which would allow for comparison of biological results with those for the naturally occurring enantiomer. The major problem with the previous synthetic route, was the difficulty faced in recovering the desired product in neutral form, due to acidic conditions employed in the final deprotection step. In an attempt to recover polyamine **112** in a neutral form, the synthetic route was redesigned from compound **124** (**Scheme 65**). The new design was in such a way that the final deprotection step would constitute hydrogenation under neutral conditions to reveal the neutral polyol. In order to avoid the amine deprotection step, the coupling of the two C-5 fragments occurred prior to the introduction of the terminal amine groups.



Scheme 65: Alternative synthetic route to compound 112

Instead of converting intermediate **124** to the aldehyde as was done previously, the Pummerer rearrangement was performed to reveal the alcohol followed by protection of the alcohol with a TBS group, stable under Birch reduction conditions. The Pummerer rearrangement procedure shown in **Scheme 66**, was employed to recover the alcohol **162** in quantitative yields as already described in literature.[170] In order to recover the alcohol, the aldehyde reduction was accomplished *in situ* by adding $NaBH_4$ after neutralising the excess acid with K_2CO_3. The product was recovered as a white solid with an optical rotation of -20.4 when the concentration was 0.7 g/ml in chloroform. A broad peak at 3489 cm^{-1} in the IR spectrum signified the presence of an alcohol, confirming that the rearrangement step was a success.



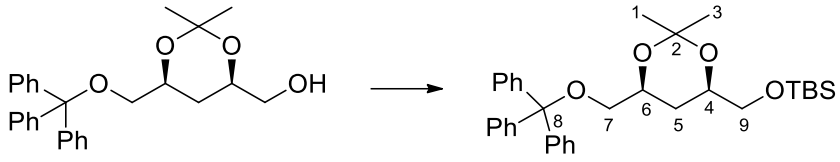
124 **162**

Scheme 66: i) TFAA, 2,4,6-collidine, MeCN, 0 °C, 30 min; ii) H_2O, K_2CO_3, r.t., 30 min; iii) $NaBH_4$, r.t., 40 min, 99%

From the ^1H NMR spectroscopic analysis, a reduction in the integration of aromatic protons from nineteen to fifteen for the multiplet signals at δ 7.48 – 7.40 and δ 7.33 -7.16, pointed to the removal of the tosyl group. The methyl signal for the sulfoxide moiety had also disappeared, and instead a broad signal for the OH proton was observed at δ 2.14. The rest of the signals were as expected. In the ^{13}C NMR spectrum, there were only four aromatic signals for the trityl group that were observed at δ 144.0, 128.7, 127.7 and 127.0. The methyl signal for the sulfoxide moiety had also disappeared. The change in the heteroatom attached to C-9 from S to a more electronegative O resulted in a downfield shift of the signal from δ 63.1 to δ 66.1. As expected the chemical shifts for C-1, C-2 and C-3, observed at δ 19.9, δ 98.7 and δ 29.9 were all consistent with a 1,3-*syn*-diol functionality.

Given the challenges encountered with the removal of the Boc group, a different approach was employed at this point, which allowed the penultimate step to be the acetonide removal and the final step to be the reduction of the azide groups at the terminal carbon atoms. A quick search of the literature on alcohol protecting groups that could withstand the Birch reduction conditions used for the removal of the trityl group revealed that the TBS group was the most appropriate.[158]

Compound **162** was therefore TBS protected as shown in **Scheme 67**, yielding compound **163** as a colourless oil in a yield of 97%.



162 **163**

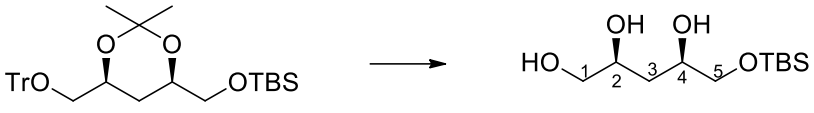
Scheme 67: TBSCl, DMAP, imidazole, DCM, r.t., overnight, 97%

IR spectroscopy revealed the disappearance of the broad OH signal previously observed at 3489 cm^{-1}. The newly introduced TBS group signals were observed as a singlet at δ 0.90 for the *tert*-butyl group and overlapping singlet signals were observed at δ 0.07 and δ 0.06 for the two methyl groups in the ^{1}H NMR spectrum. The carbon signals for the TBS group were at δ 25.9 and δ 18.4 for the *tert*-butyl and δ 5.1 and δ 5.3 for the dimethyl groups.

The first attempt for the removal of the trityl group employed boron trichloride as the Lewis acid. Use of BCl_3 was identified as a mild and expeditious method for removal of the trityloxy protecting group by Jones *et al*.[171] The procedure proved to be fruitful in selectively unmasking trityloxy ethers of differentially protected alcohols. These results prompted the application of the method for the selective trityl deprotection of compound **163** (**Scheme 68**). Due to the presence of potentially liable acetonide and TBS groups only 0.6 equivalents of the boron trichloride were used and the reaction only proceeded for 15 minutes in an attempt to increase the selectivity.

TLC analysis showed the presence of single product, which was more polar than the starting material indicating completion of the reaction. Unfortunately, purification by column chromatography yielded the triol **164** instead of the desired product showing that the deprotection was not as selective as anticipated. Confirmation of the compound structure was achieved by both mass spectroscopy and NMR spectroscopic analysis. Mass spectrometry confirmed the mass to be 251.1670 $(M+H)^{+}$. Both aromatic signals and acetonide signals had disappeared from the ^{1}H NMR spectrum but the TBS signals were still present at δ 0.92 (s, 9H) and δ 0.10 (br s, 6H). Similarly there were no aromatic or acetonide signals present in the ^{13}C NMR spectrum which shows that both trityl and acetonide deprotection had occurred. The signals from the TBS group were visible at δ 26.2, δ 18.6, δ -5.0 and δ -5.1. Considering that the reaction had

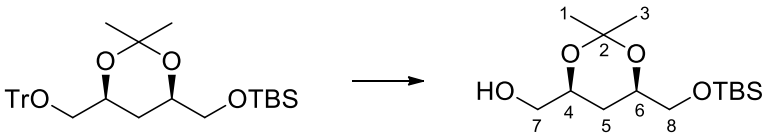
been performed at a low temperature and for a short period of time, but still deprotected both trityl and acetonide groups, shows that the use of BCl_3 is not selective.



163 **164**

Scheme 68: BCl_3, DCM, -30 °C, 5 min, 66%

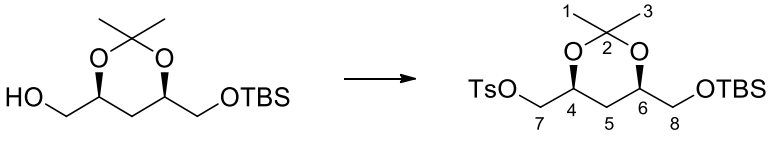
Given the failure of the BCl_3 deprotection, the selective detritylation was achieved by employing the Birch reduction using the previously discussed procedure, as shown in **Scheme 69**. The reaction furnished compound **165** in a yield of 80% as a yellow oil. Both the ^{13}C NMR and the ^{1}H NMR spectra confirmed the complete removal of the trityl group because aromatic signals were not detectable. The TBS group was unaffected by the Birch reduction conditions as evidenced by the fact that the groups signals were detected in both spectra. IR spectroscopy showed a broad signal at 3441 cm^{-1} indicative of the alcohol. Mass spectrometry also confirmed the desired mass of compound **165** to be 291.1985 $(M+H)^+$, which confirms a structure with $C_{11}H_{26}O_4Si$.



163 **165**

Scheme 69: Na, liquid NH_3, THF, -60 °C, 1 h, 80%

With compound **165** in hand, synthesis progressed to the formation of the two desired fragments **A** and **B** (**Scheme 65**) as before, starting with the synthesis of the amine. Conversion of the primary alcohol into a good leaving group via tosylation, in preparation for a nucleophilic substitution reaction using an azide, gave rise to the tosylated compound **166** (**Scheme 70**). The desired product **166** was recovered in quantitative yields as a colourless viscous oil.



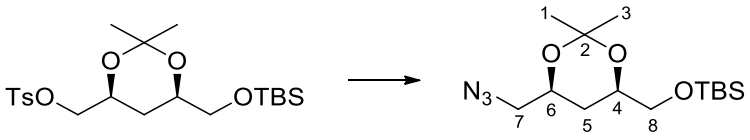
165 **166**

Scheme 70: TsCl, DMAP, DCM, r.t., overnight, 99%

Confirmation of the success of the tosylation procedure was achieved via IR spectroscopic analysis. The previously observed OH signal had disappeared from the spectrum and a new signal

for S=O was observed at 1356 cm^{-1}. The ^{1}H NMR spectrum further confirmed the success of the reaction due to the presence of the aromatic signals from the tosyl group at δ 7.82 – 7.76 and δ 7.37 – 7.31. Each multiplet integrated for 2 protons, whilst the tosyl-methyl group appeared as a singlet at δ 2.44. There was no significant change observed for the chemical shift of the remaining signals. In the ^{13}C NMR spectrum the aromatic carbon signals were observed at δ 144.8, δ 133.0, δ 129.8 and δ 128.0, whilst the tosyl-methyl carbon signal appeared at δ 21.6. Epimerisation was not detected in this procedure because the acetonide signals were within the expected range.

The tosylated tetraol **166** was subjected to a nucleophilic substitution protocol using sodium azide as shown in **Scheme 71**. Normally this procedure is performed at temperatures above 80 °C, but in this instance any temperature above 75 °C degraded both the reactant and the product and therefore the reaction was carried out at 75 °C. The desired azide **167** was recovered as a yellow oil in a yield of 75%, a much lower than expected yield. Product loss could have occurred during the process of continuous aqueous extraction of DMF, when the diluted reaction mixture had to be repeatedly washed with brine for complete removal of the solvent.



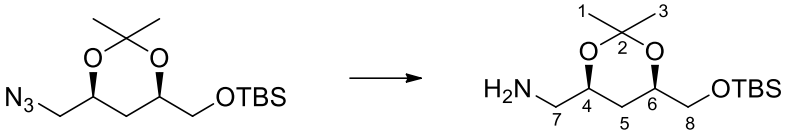
166 **167**

Scheme 71: NaN_3, DMF, 75 °C, 4 h, 75%

For IR spectroscopic analysis the azide signal appeared at 2098 cm^{-1}, confirming the success of the substitution procedure. In the ^{1}H NMR spectrum the aromatic signals had disappeared and the multiplet signal for H-7 protons at δ 4.02 – 3.94 in compound **166** had migrated to a multiplet at δ 3.34 – 3.20 in compound **167**, showing that there had been a heteroatom change to a less electronegative atom. In the ^{13}C NMR spectrum the aromatic signals had disappeared as well, and the C-7 signal had migrated from δ 72.4 to δ 55.2. This was the expected chemical shift change because the C-N signals generally appear at chemical shifts below 60 ppm.

Attempts at reducing the azide group under hydrogenation conditions were unsuccessful. The recovered products could not be characterised, suggesting that the product had decomposed. This observation did not come as a total surprise, because as already discussed, previous hydrogenation attempts of substrates possessing the acetonide protected 1,3-diol functionality

had yielded unexpected products which were sometimes completely deprotected. After the failed attempt, the reduction was successfully effected by employing $LiAlH_4$ under anhydrous conditions (**Scheme 72**). All the side products generated after work up of the reaction precipitated, and they were removed by filtration with the sodium sulfate. This meant that the desired product was not purified any further because column chromatography of primary aliphatic amines is tedious and they tend to have long retention times.



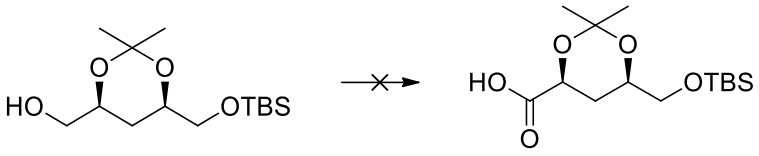
167 **168**

Scheme 72: $LiAlH_4$, Et_2O, r.t., 2 h, quantitative yield

The IR spectrum showed the desired NH_2 signal at 3444 cm^{-1} and the complete disappearance of the azide signal. There was a chemical shift change in the H-7 proton signals in the ^1H NMR spectrum from a multiplet at δ 3.34 – 3.20 for compound **167** to a multiplet signal at δ 2.76 – 2.67. A similar trend was observed in the ^{13}C NMR spectrum because of the greater shielding effect that an amine group has as a result of strong hydrogen interactions, in comparison to the azide group. The C-7 carbon signal shifted from δ 55.2 for compound **167** to δ 45.1 for compound **168**. The chemical shifts of the acetonide signals still agreed with what is expected for a 1,3-*syn*-diol system, confirming that the relative stereochemical integrity of the compound had been upheld to this point.

With the synthesis of the amine fragment successful, the next step involved synthesis of the second fragment as either a carboxylic acid or as an aldehyde which would allow for the coupling to be achieved by amidation or reductive amination, respectively. The initial attempt involved oxidising compound **165** to the carboxylic acid which meant the coupling step would be via amide bond formation. Given the varied options of possible reaction conditions that could be used for this transformation and the observed results of this work, possible optimal conditions were selected as shown in **Scheme 73**.[172, 173] The choice of reagents was based on the inertness of the other functional groups under the mild reaction conditions. The procedure would generate the aldehyde *in situ*, which would be oxidised to the carboxylic acid in tandem.[174] Compound **165** was subjected to the oxidation conditions, and monitoring by TLC revealed the formation of a new product. Considering the high polarity of carboxylic acids, purification was afforded by filtering

the reaction mixture through a plug of silica. Unfortunately, the recovered product was not the desired compound but rather a mixture of oxidized products contaminated with Tempo.



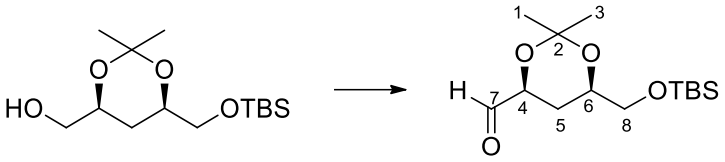
165 **169**

Scheme 73: $Fe(NO_3)_3.9H_2O$, Tempo, KCl, O_2, 1,2-dichloroethane, r.t., overnight

It was becoming very evident during this PhD work that despite the extensive investigations and methods for performing routine organic chemistry transformations, a lot of these methods are substrate specific. For some of these methods one can preempt potential problems given the required reaction conditions and avoid the methods altogether, but for some of the methods it is impossible to judge the outcome. Given these findings, it became a matter of trial and error until the most suitable method was found.

The synthesis of the carboxylic acid was abandoned, and instead aldehyde **170** was synthesised, because of the relative success in synthesis of a similar substrate (**Scheme 74**). Previously employed methods comprising the use of MnO_2, PCC, IBX and the more popular Swern oxidation did not yield the expected product.[175] NMR spectroscopic analysis of the recovered material, for each of the attempts, was for either the starting material or the decomposed product with TBS signals missing.

After all the trial and error attempts, Dess-Martin periodinane (DMP) was chosen as a milder oxidant with the assumption that the desired chemical transformation would be achieved (**Scheme 74**). DMP is has stability problems and risk of explosions therefore the oxidant was freshly prepared from 2-iodobenzoic acid. The use of DMP is considered to be superior for sensitive substrates because the reactions are performed under mild and neutral conditions. TLC analysis, using 2,4- DNPH visualisation confirmed the presence of an aldehyde and, after work up, the product was not purified further for fear that it might decompose on silica gel.

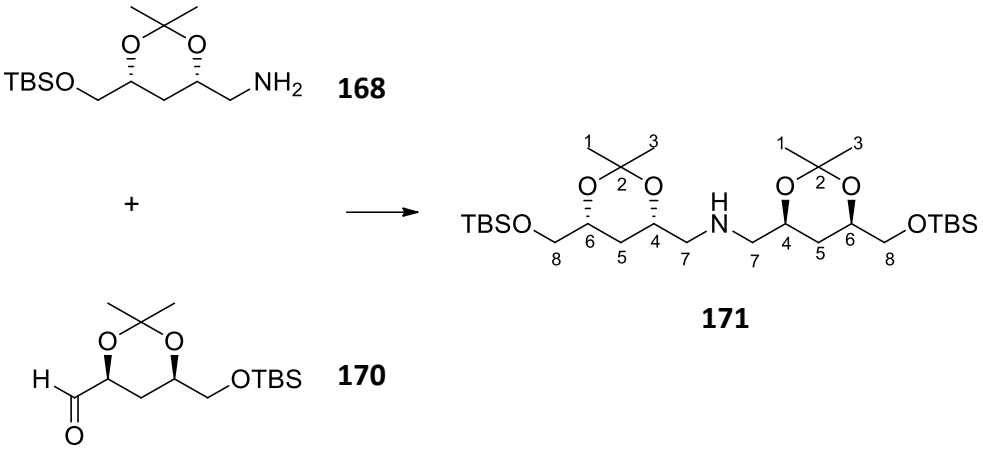


165 **170**

Scheme 74: DMP, DCM, r.t., overnight, quantitative yield

The aldehydic proton signal was observed at δ 9.60 in the ^{1}H NMR spectrum, confirming the formation of the desired product. There were also residual signals from the DMP visible, although the concentration of DMP was relatively smaller than that of aldehyde **170**. The carbonyl signal was at δ 201.1 in the ^{13}C NMR spectrum, as expected, confirming the successful synthesis of the desired fragment **B**.

Once synthesised, the two desired fragments, amine **168** and aldehyde **170** were subjected to reductive amination for 24 hours under inert conditions with the amine in excess (**Scheme 75**). Addition of excess amine is necessary because in the presence of sodium triacetoxy borohydride the aldehyde can be reduced back to the alcohol. Given the competing reaction, excess amine ensures that the desired reductive amination reaction is favoured. After purification the desired compound was recovered as a yellow oil in a yield of 73%.



168

171

170

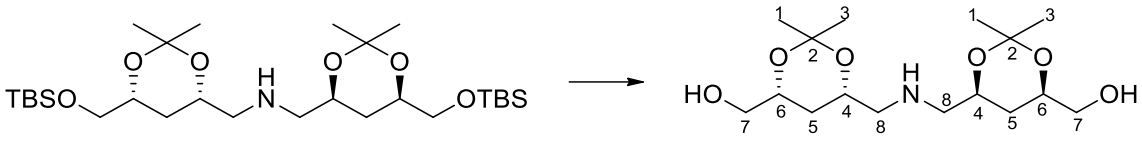
Scheme 75: Sodium triacetoxyborohydride, 1,2-dichloroethane, r.t., 24 h, 73%

Due to the symmetry of the recovered compound **171**, a single set of signals was expected in the NMR spectra. The broad NH signal was at δ 1.99 in the ^{1}H NMR spectrum whilst the H-7 protons were observed as a set of doublets of doublets at δ 2.68 (dd, *J* = 12.0, 7.4 Hz) and 2.60 (dd, *J* = 12.0, 4.0 Hz). The H-8 proton signals appeared further downfield as expected because they are attached to a carbon attached to oxygen. The presence of a chiral centre on the α-carbon results

in the H-8 protons being diastereotopic, hence the reason why they were also observed as separate doublet of doublet signals at δ 3.65 (dd, *J* = 10.1, 5.2 Hz) and δ 3.46 (dd, *J* = 10.2, 6.0 Hz).

In the ^{13}C NMR spectrum, the signals of great importance were the acetonide signals because they confirm the stereochemical integrity of compound **171**. The C-1 and C-3 signals were observed at δ 19.9 and δ 30.0 whilst the C-2 signal was at δ 98.6. The acetonide chemical shift values confirmed the presence of the 1,3-*syn*-diol system in the recovered product. The C-7 signal was at δ 55.1, and since there was no evidence of the aldehydic carbon signal for compound **170** and no sign of the C-7 signal for compound **168** at δ 45.1, the coupling was a success. The rest of the carbon signals were as expected.

The remaining steps proved to be the rate determining steps of the whole project, because of significant product losses during purification, due to the high polarity of the compounds. Removal of the TBS group was easily achieved by employing TBAF in THF in under 4 hours (**Scheme 76**). Work up of the reaction involved quenching the reaction with ammonium chloride, followed by recovering the desired compound **172** by extracting the aqueous layer with DCM. Unfortunately, only the TBS side product was recovered in the organic layer whilst the desired product remained in the aqueous layer. On the second attempt, work up of the reaction was achieved by adding a slight excess of ammonium chloride. The reaction mixture was dried over Na_2SO_4, and the mixture was extracted with DCM. After the removal of excess solvent, the crude product was not purified any further.



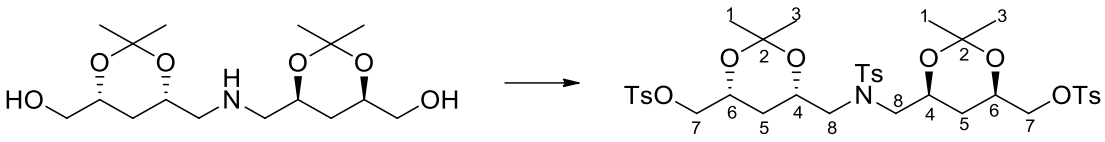
171 **172**

Scheme 76: TBAF, THF, 0 °C, 4 h

^{1}H NMR spectroscopic analysis was not conclusive as the side product signals from the TBAF were more dominant in the spectrum and the signals also overlapped with those from the desired compound. It should be noted that there were no TBS signals that were visible, suggesting that the deprotection procedure had been successful. The ^{13}C NMR spectrum was more enlightening and showed the desired signals, with the C-2 signal at δ 99.3, C-6 at δ 69.2, C-8 at δ 65.3, C-4 at δ

64.4, C-7 at δ 51.7, C-5 at δ 30.3, and C-1 and C-3 at δ 29.8 and δ 20.2. These results, although not conclusive, provided some confidence that the desired product had been recovered.

By this stage only a small quantity of the product was recovered but there was hope that the end of the synthetic route could be reached with the amount of product that was recovered. Crude compound **172** was tosylated using the already described procedure as shown in **Scheme 77**. Purification of the desired compound **173** allowed for the successful removal of the side products from the previous step. When the ninhydrin stain was used for amine visualisation, the desired compound tested negative which suggested that tosylation had occurred on both the amine and hydroxyl groups. The desired compound was recovered in a yield of 76% whilst IR spectroscopy did not indicate the presence of either the alcohol or the amine groups.



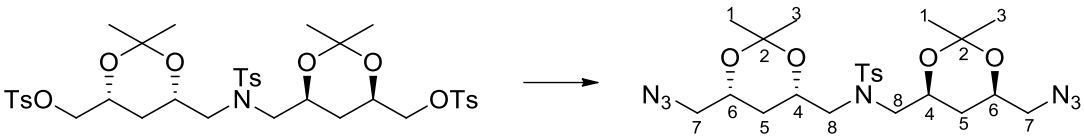
172 **173**

Scheme 77: TsCl, DMAP, DCM, r.t., 24 h, 76%

In the ^{1}H NMR spectrum, two sets of aromatic signals were observed for the tosyl protons as a multiplet at δ 7.96 – 7.90, and a doublet at δ 7.41 with *J* of 8.2 Hz for the *O*-tosyl and a total integration of eight protons. The *N*-tosyl signals were at δ 7.82 – 7.75 and δ 7.34 as a doublet with *J* = 7.9 Hz giving rise to a total integration of four protons. The tosyl-methyl singlet signals were observed as singlets at δ 2.49 and δ 2.45. In the ^{13}C NMR spectrum, the tosyl methyl signals were at δ 21.6 and δ 21.5. The characteristic C-2 signal was still in the expected range at δ 98.9 whilst the C-7 signals showed the downfield migration from δ 64.3 in compound **172** to δ 72.1 in compound **173**.

Approximately 18 mg of compound **173** was recovered and the tosylated product was subjected to a nucleophilic substitution reaction with sodium azide as shown in **Scheme 78**. After removal of excess DMF only minute quantities of the crude product were recoverable and NMR spectroscopy was performed on the crude material to assess whether the desired compound was present. The ^{1}H NMR spectrum was not conclusive at all and there were more signals observed than was expected for compound **174**. The ^{13}C NMR spectrum showed the expected characteristic signals for the desired product plus many more unidentified signals in the aliphatic region. Generally for the nucleophilic substitution reaction of the tosyl group with azide, the side products

generated are extracted in the aqueous layer. From the crude NMR spectrum it was evident that other side reactions had occurred and any attempts to purify the minute quantities of product did not change the outcome. At this stage of the project, we were faced with a difficult decision of changing the route, synthesising more starting material or postponing for future work.



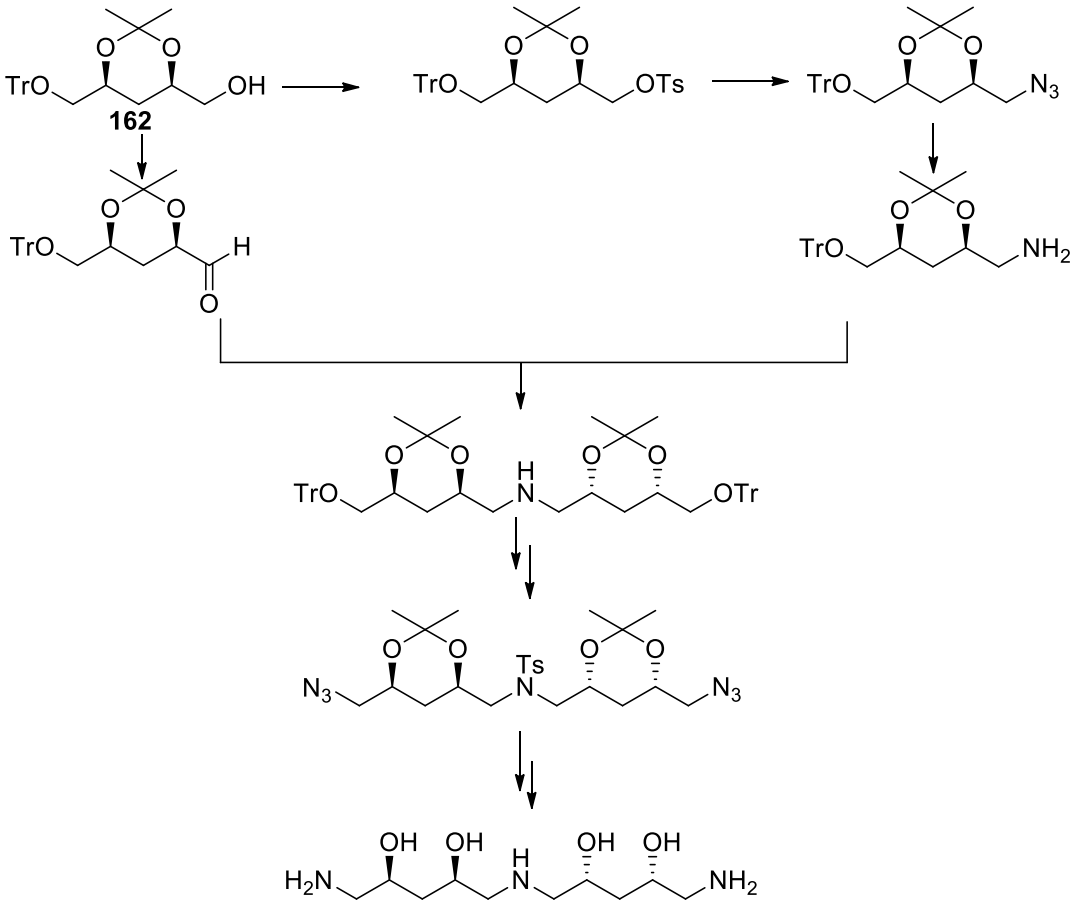
173 **174**

Scheme 78: NaN_3, DMF, 75 °C, 4 h

Despite not being able to recover the desired enantiomer the alternative route proved viable as well and there is definitely room for optimising some of the steps. Further attempts at synthesising a neutral enantiomer of pavettamine were postponed for future work.

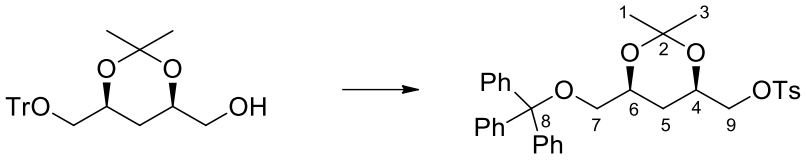
2.3 Synthesis of pavettamine

The synthetic approach of the C-10 pavettamine backbone developed in this work was also applied for the synthesis of pavettamine, to ascertain whether the recoverable yield could be improved. Synthesis of pavettamine started from compound **162**, transforming the substrate into two fragments by converting the alcohol into an amine for fragment 1 and an aldehyde for fragment 2 (**Scheme 79**). The two fragments were coupled by reductive amination followed by transforming the alcohols on the terminal carbons into amines.



Scheme 79: Synthetic route for pavettamine

The synthesis of pavettamine also utilised malic acid as the basic starting material, and a similar synthetic protocol was employed for synthesis of the two fragments up to compound **162**. Fragment differentiation occurred on the C-9 side of compound **175**. To achieve this, the amine was synthesised by first tosylating compound **162** as shown in **Scheme 80** ensuring that the OH becomes a good leaving group. Tosylated alcohol **175** was recovered in a yield of 75% as a white solid and the IR spectrum showed the total disappearance of the alcohol signal at 3489 cm^{-1} confirming the success of the tosylation step.

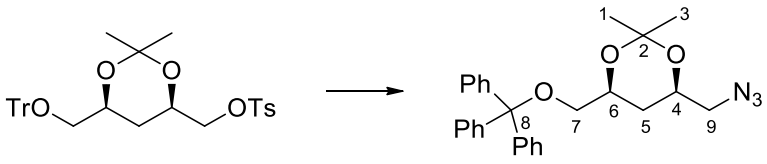


162 **175**

Scheme 80: TsCl, DMAP, DCM, r.t., 24 h, 75%

In the ^{1}H NMR spectrum, there was an increase in the integration of the aromatic signals from 15 protons to 19 protons whilst the expected methyl singlet for the tosyl group was at δ 2.42. The ^{13}C NMR spectrum also showed an increase in the number of aromatic signals, whilst the C-9 signal migrated from δ 66.1 in compound **162** to δ 72.4 in compound **175**. The chemical shift indicates that the C-9 carbon is now experiencing a greater deshielding effect due to the increasing electrophilicity of the carbon atom. This increase in electrophilicity of the carbon atom, coupled with the good leaving tendencies of *O*-tosyl enables nucleophilic substitutions to proceed quite easily. The remaining newly introduced methyl carbon signal for the tosyl group was observed at δ 21.6.

After tosylation, compound **175**, the tosyl group was easily substituted by azide, using the already described synthetic protocol as shown in **Scheme 81**, yielding compound **176** in a yield of 97%. The IR spectrum showed the characteristic azide signal at 2096 cm^{-1}, confirming the success of the substitution reaction. The total integration of the aromatic signals decreased from nineteen protons to fifteen in the ^{1}H NMR spectrum, indicating the removal of the tosyl group. The previously observed methyl signal at δ 2.42 had also disappeared. Instead, a chemical shift change for the H-9 signals was detected from δ 4.03 – 3.88 for compound **175**, to a multiplet at δ 3.37 – 3.19, and a doublet of doublets at δ 3.05 for azide **176**. The observed chemical shift change is as a result of the change in heteroatom from oxygen to nitrogen.



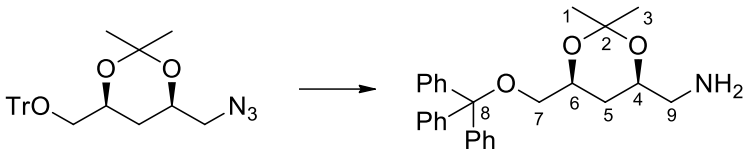
175 **176**

Scheme 81: NaN_3, DMF, 95 °C, 4 h, 97%

In the ^{13}C NMR spectrum, a reduced number of aromatic signals were observed, and only the four signals expected for the trityl group were found at δ 144.0, δ 128.7, δ 127.8 and δ 127.0. The

previously observed methyl signal from the tosyl group at δ 21.6 was not detected. Given the heteroatom change on the C-9 carbon, the expected chemical shift change was observed from δ 72.4 for compound **175** to δ 55.2 for azide **176**.

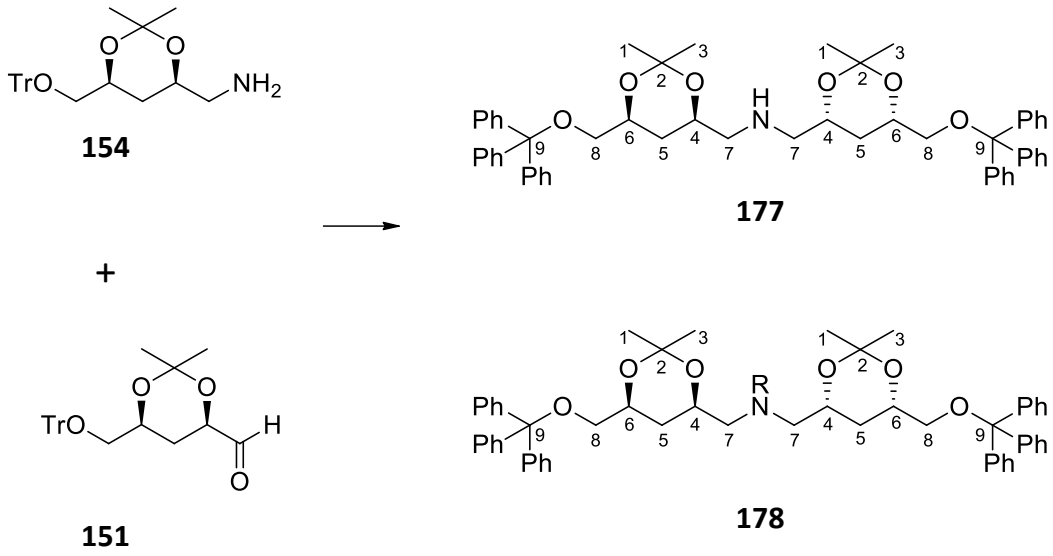
The final step for revealing the amine fragment involved reduction of the azide using $LiAlH_4$ under anhydrous conditions as shown in **Scheme 82**, yielding the desired primary amine **154**, in a yield of 94%. The described method was chosen for the synthesis of primary amine **154**, as opposed to the previously employed approach shown in **Scheme 52** to **Scheme 56**, because the procedure was shorter and higher yielding. Comparison of the spectroscopic data from the IR and NMR spectra of the products from the two procedures showed that the same compound had been synthesised.



176 **154**

Scheme 82: $LiAlH_4$, Et_2O, r.t., 2 h, 94%

After the successful synthesis of the amine and aldehyde fragments, aldehyde **151** and primary amine **154** were coupled via reductive amination as shown in **Scheme 83**, yielding compound **177** and compound **178**. The synthetic approach had proved to be dependable as shown in the previous reactions hence it was decided that there was no need to change a winning formula half way through the game. The reaction was carried out in the presence of molecular sieves as a dehydrating agent, preventing the hydrolysis of the imine intermediate. Reductive amination reactions are generally slow, therefore the reaction was allowed to proceed for 48 hours. The reaction was repeated a few times so as to increase the quantity of material before proceeding further and it was shown to be reproducible. TLC analysis of the reaction mixture showed formation of two new products, with one product being significantly more polar than the other. The products were purified and separated by column chromatography, giving a combined best yield of 78%.



Scheme 83: Sodium triacetoxyborohydride, 1,2-dichloroethane, r.t., 2 d, 78%

The specific optical rotation for compound **178**, with the higher R_f value was determined to be - 11.1 in chloroform when the concentration was 1.0 g/100 ml which is significantly different from the literature value of -33.5.[63] An optical rotation of -16.6 (c 0.87) was measured for compound **177**, with the lower R_f value, which was still much lower than the expected literature value. These results were puzzling considering the fact that no racemisation of the precursors had been observed up to this point, even when the reductive amination procedure was employed for the synthesis of compound **161** and compound **171**. Where racemisation had been observed sufficient care was taken to exclude the undesirable epimers from the synthesis by changing the synthetic approach.

The characteristic NH signal was not detectable in the IR spectrum, despite the positive response for amines when the TLC was stained in ninhydrin for both compounds. NMR spectroscopic analysis of the recovered compounds confirmed formation of new products because the observed chemical shifts were neither for the starting amine, aldehyde nor for the alcohol. Comparative analysis of the ^{1}H NMR spectra for the two compounds shown in **Figure 29** revealed the main difference between the two compounds to be for the H-7 protons. They were observed as a set of doublets of doublets at δ 2.72 (J = 13.7, 6.3 Hz) and δ 2.60 (J = 13.7, 4.6 Hz) for compound **178**, whilst for compound **177** a multiplet signal was observed at δ 2.77 – 2.63. The observed chemical shifts for both compounds are in the expected region for protons attached to a carbon atom carrying N and the remaining signals were not significantly different.

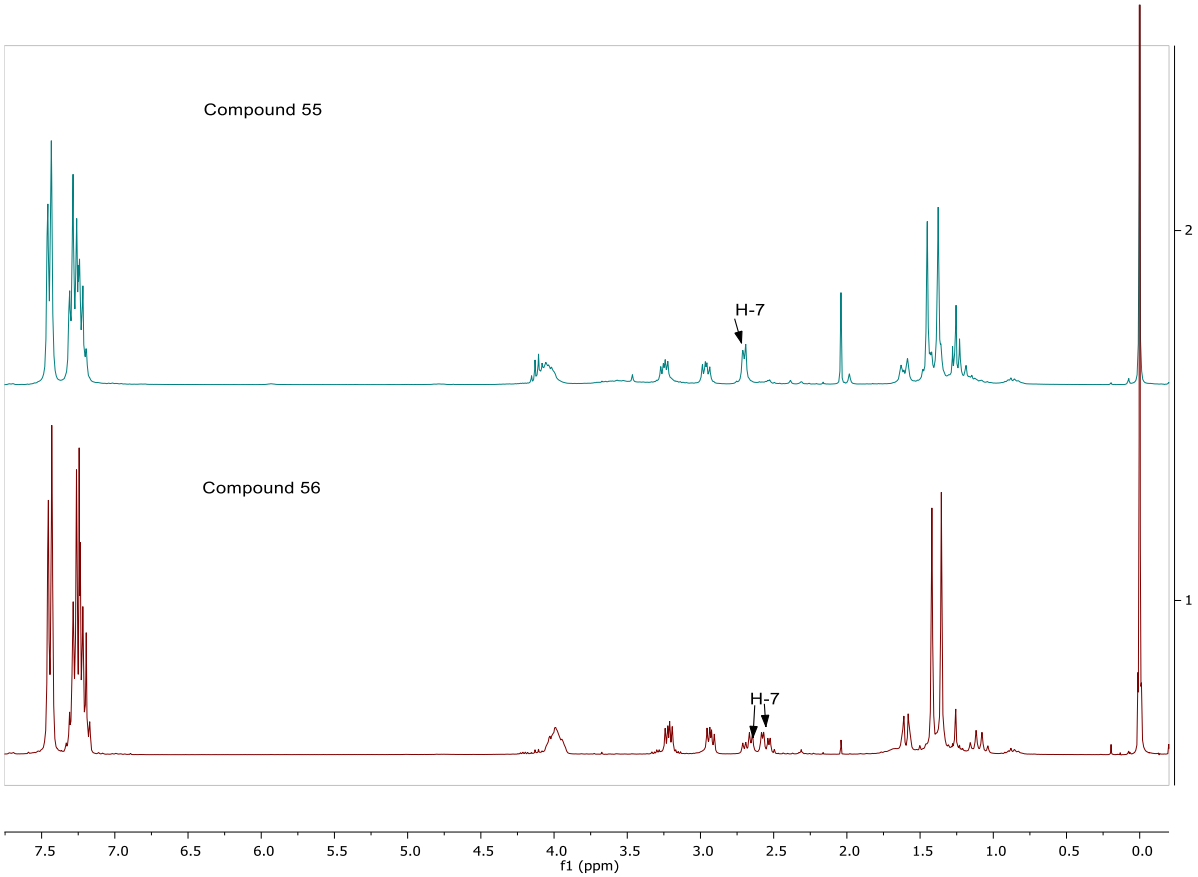


Figure 29: Stacked ^{1}H NMR spectra for compound 177 and compound 178

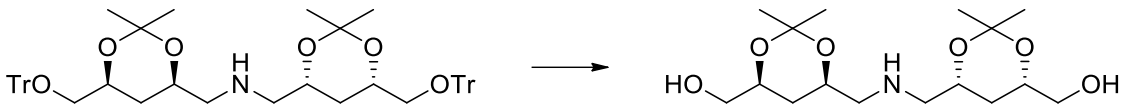
However, marked differences were observed between the chemical shifts of the two recovered products in the ^{13}C NMR spectra as shown in **Table 4**. The greatest difference observed was between the C-7 signals whereby the signal was significantly downfield at δ 62.4, a value uncharacteristic for CN carbon signals, for compound **178** and at δ 54.2 for compound **177**. Comparison of the experimental data with the literature values showed that compound **177** was the desired compound because the rest of the other signals were as expected.[63] It is not clear why the specific optical rotation was lower than expected, as all other experimental data supported the structure for compound **177**. All the experimental results presented a new challenge of fully identifying compound **178** and establishing why it was being formed.

Table 4: A comparison for ^{13}C NMR shifts for compound 177 and compound 178

	C-1	C-2	C-3	C-4	C-5	C-6	C-7	C-8
Compound **177** - δ	19.9	98.7	29.9	68.2	32.1	67.3	54.2	67.2
Compound **178** - δ	20.0	98.3	30.2	69.0	32.6	68.6	62.4	67.6

Mass spectrometric analysis also confirmed the expected mass of the desired compound **177** to be 818.4421 $(M+H)^+$. Analysis of the fragmentation pattern for compound **178** showed the expected base peak of the desired mass 818.4407 $(M+H)^+$, along with other fragments which could not be explicitly identified. From these results it was evident that nitrogen was bonded or coordinated to another atom. Predictive ^{13}C NMR spectroscopic data suggested that the nitrogen in compound **178** was attached to a boron atom and this hypothesis was loosely supported by the HRMS results. High Resolution ESI-MS showed two major fragments, one for the expected molecular weight of the desired compound **177**, 818.4407 $(M+H)^+$, plus a second fragment with a mass of 846.4720 $(M+H)^+$. The difference between the two masses is equivalent to the molecular mass of a B_2H_6 fragment, agreeing with what was suggested by predictive ^{13}C NMR data. To eliminate the possibility that the nitrogen was attached to a metal, a sample of compound **178** was treated with TMEDA for two days. The recovered product was analysed using NMR spectroscopy but there was no observable change in the chemical shift of the C-7 carbon signal. From this point onwards, the two compounds were treated separately towards the synthesis of pavettamine.

Removal of the trityl groups on compound **177** was not as trivial as expected and the recovery of the free alcohol was nearly impossible. Despite the considerable number of deprotection procedures available, only a few methods were applicable for this substrate because the rest would have deprotected the acetonide groups as well. The first attempt employed hydrogenation, but the desired product was not recovered even after increasing the pressure to 5 atm. All the other reaction conditions employing the use of CAN, $ZnBr_2$, $ZnCl_2$, $NaHSO_4.SiO_2$ etc., did not avail the trityl-deprotected alcohol. Successful deprotection was only achieved under Birch reduction conditions, as shown in **Scheme 84**.



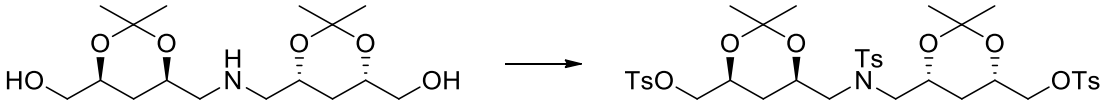
177 **179**

Scheme 84: Na, NH_3, THF, -60 °C, 1 h

Unfortunately, compound **179** was recovered in minute quantities despite recovering quantitative yields of the trityl alcohol side product. The high polarity of the product contributed to the difficulty of the recovery process regardless of the absence of aqueous media during workup. Even

though the precipitate recovered after quenching the reaction with solid NH_4Cl was washed with copious amounts of DCM the desired compound could not be recovered in meaningful yields. The experiment was repeated three times, varying the workup conditions, but only the trityl side product was recovered.

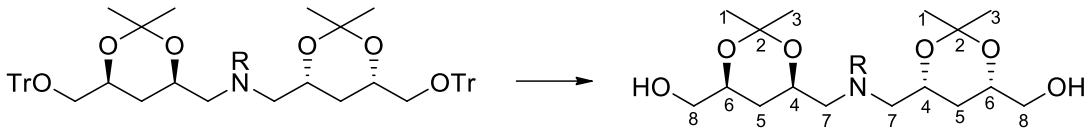
It was evident that the deprotection step proceeded successfully but the desired product was unrecoverable from the reaction matrix. NMR spectroscopic analysis revealed the desired signals plus the presence of other side products. Instead of attempting to isolate compound **179**, the crude mixture was treated with tosyl chloride in the presence of base (**Scheme 85**). The reasoning behind this strategy was that the alcohol groups on compound **179** would be tosylated, yielding the less polar compound **180**. Indeed the approach yielded promising results, but the best recoverable yield from this procedure was only 28%. Structure confirmation was achieved by NMR spectroscopic analysis. ^{1}H NMR spectrum showed aromatic signals as multiplets at δ 7.82 – 7.74 (m, 4H), 7.74 – 7.62 (m, 2H) and 7.38 – 7.15 (m, 6H). The total number of aromatic protons indicate that tosylation had occurred on both the alcohol groups and the nitrogen atom. After three failed attempts of improving the yield, it was evident that a different trityl-deprotection approach would be more appropriate. Due to the low quantities of the product no further transformations were performed on compound **180**



179 **180**

Scheme 85: TsCl, DMAP, DCM, r.t., 24 h, 28%

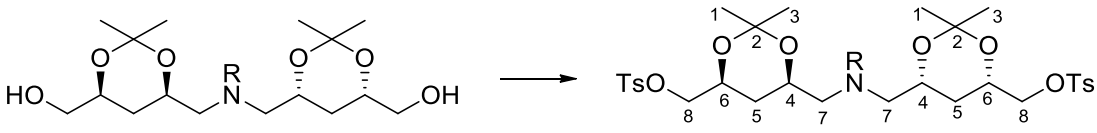
In an attempt to determine the nature of the moiety attached to the central nitrogen atom of compound **178**, the substrate was subjected to subsequent reactions with the assumption that the group would either fall off or would be transformed into a group that could be easily removed. Compound **178** was subjected to trityl deprotection using previously described methods as shown in **Scheme 86**. The desired product was recovered in a dismal yield of 35% despite quantitative yields of the trityl alcohol side product being recovered as well. This suggested that product losses were incurred during work up and purification of the reaction due to the high polarity of the compound, or that the compound decomposed in the process. The same recovery problems were encountered in the synthesis of the enantiomer compound **172** and compound **179**.



178 **181**

Scheme 86: Na, liquid NH_3, THF, -60 °C, 1 h, 35%

The broad peak indicative of OH was visible at 3421 cm^{-1} in the IR spectrum, and confirmed the successful removal of the trityl groups. ^{1}H NMR spectroscopy revealed complete disappearance of aromatic signals, whilst the H-8 signal was observed as a multiplet at δ 3.65 – 3.45 and the H-7 signals were at δ 2.88 – 2.63 and δ 2.61 – 2.48 as two multiplets overlapping with the alcohol peaks. In the ^{13}C NMR spectrum the C-8 signal was at δ 66.0 and a slight change in the chemical shift was observed for C-7 from δ 62.4 to δ 61.8 for compound **181**. The group attached to the amine was still intact and it is also critical to mention that there were no extra carbon or proton signals observed, which eliminated the possibility of alkylation of the amine being responsible for the anomalous results. From here onward, the yields were calculated based on measured mass.

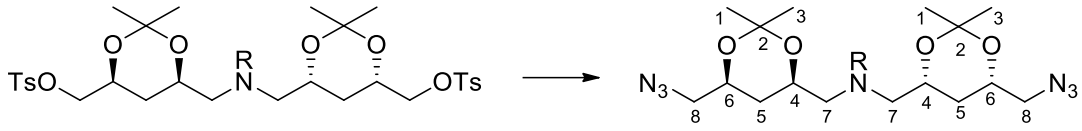


181 **182**

Scheme 87: TsCl, DMAP, DCM, r.t., 24 h, 98%

The primary alcohols of **181** were tosylated as shown in **Scheme 87** in preparation for the nucleophilic substitution reaction with azide. As expected, the reaction proceeded without any hindrance and a quantitative yield of the tosylated product **182** was recovered. A new set of aromatic signals was observed in the ^{1}H NMR spectrum representative of the tosyl group as doublets at δ 7.78 (*J* = 7.8 Hz) and δ 7.34 (*J* = 8.3 Hz). A single tosyl-methyl singlet was evident at δ 2.44 and the H-7 signals were observed as a doublet of doublet δ 2.66 (*J* = 13.5, 5.9 Hz) and a multiplet at δ 2.59 – 2.47. The ^{13}C NMR spectrum also showed a single set of aromatic signals at δ 145.0, 132.9, 129.9 and 128.0 and the methyl signal from the tosyl groups was observed at δ 21.6. From the NMR spectroscopic analysis it is evident that tosylation only occurred on the alcohols and not on the amine suggesting that the group attached to the nitrogen had not been displaced by the tosyl group.

Subsequent nucleophilic substitution of the tosylated product with the azide (**Scheme 88**) made way for the introduction of the amine functionality at the terminal carbon atoms. The reaction proceeded as expected, however a low yield of 48% was recovered after work up. Removal of DMF by repeatedly washing with a saturated brine solution could have resulted in azide **183** dissolving in the aqueous layer. The group attached to the amine could have increased the polarity of the desired product, increasing the chances of the product being extracted into the aqueous layer.

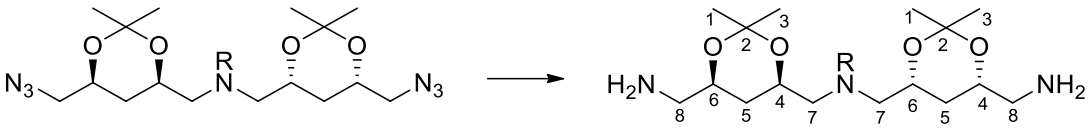


182 **183**

Scheme 88: NaN_3; DMF, 95 °C, 4 h, 48%

There was no indication of aromatic signals or the tosyl methyl signal in the ^{1}H NMR spectrum, confirming the success of the substitution reaction. There was an observable change in the chemical shift of the H-8 proton signals from a multiplet at δ 4.03 – 3.87 for compound **182**, to a more upfield chemical shift value of δ 3.23 as a doublet with a coupling constant of 5.1 Hz for azide **183**. For the ^{13}C NMR spectroscopic analysis, just as for the ^{1}H NMR spectrum, no aromatic signals were detected. The C-8 peak had migrated from δ 72.4 for the precursor molecule to δ 55.1 for compound **183**. The observed change in the chemical shift is indicative of a heteroatom change from *O* to *N* at the C-8 carbon centre.

During the course of this research, the acetonide group had been removed under hydrogenation conditions on two separate occasions, under both acidic and neutral conditions. An assumption was made that the same outcome was going to be achieved in the experiment shown in **Scheme 89**. However, only the azide was reduced under neutral conditions, while the acetonide groups remained intact, to our disappointment. The reasoning behind this approach was that if the reduction and the removal of the acetonide groups could occur under hydrogenation conditions the desired product could be easily isolated in neutral form. All the by-products could then be removed by either filtration, or by evaporation under reduced pressure, allowing for the recovery of the desired product under neutral conditions. Acidic hydrogenation conditions did not furnish the desired product either.



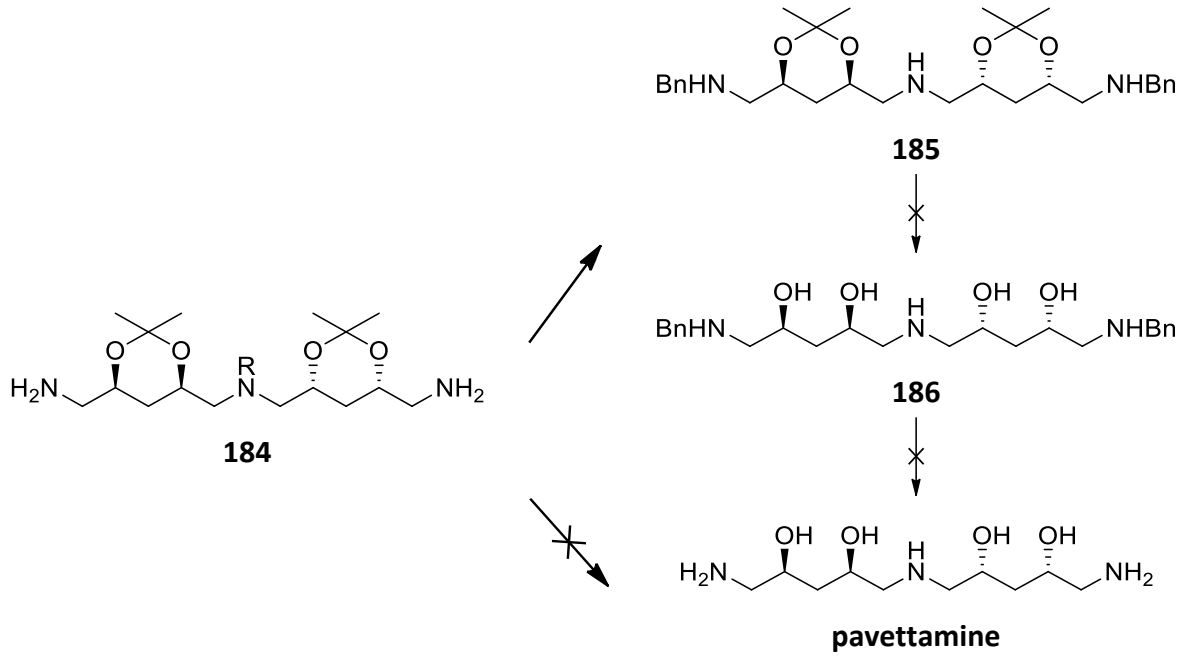
183 **184**

Scheme 89: 10% Pd/C, H_2, ethanol, 5 atm, r.t., 5 h, quantitative

NMR spectroscopic analysis showed that the acetonide group was still present. In the ^{1}H NMR spectrum the acetonide methyl group peaks were overlapping with the H-5 proton signals at δ 1.51 – 0.82. Surprisingly, the C-2 signal was at δ 100. 6 but as shown by Rychnovsky *et al*.[69] and the results for this work the chemical shift for the C-2 signal is expected to appear under 100 ppm in the ^{13}C NMR spectrum. However, the C-1 and C-3 signals were at δ 20.2 and δ 30.4 characteristic for a 1,3-*syn*-diol. The only explanation that can be offered at this point is that the group attached on the central nitrogen atom might have an influence on the chemical shift of C-2. The chemical shifts for C-1 and C-3 confirmed integrity of the relative chemistry of the diols which eliminated the possibility of the presence of an *anti* relative stereochemistry. The C-8 signal was observed at δ 44.8 from δ 55.1 which shows that the reduction of the azide group had been successful. The chemical shift of the C-7 signal had not changed whilst the rest of the signals were as expected.

Based on the NMR spectroscopic results it was evident that acetonide deprotection, once the 1,3-diol moiety with a C-2 symmetry has been introduced, was proving to be a challenge again. Based on the results from the synthesis of pavettamine and its enantiomer it is safe to conclude that once the terminal amines have been introduced, removal of the acetonide group becomes increasingly difficult.

Compound **184** was subjected to two different protocols in an attempt to recover pavettamine in neutral form. The first attempt involved hydrolysis with catalytic amounts of acid as shown in **Scheme 90** but despite extended reaction time and slightly elevated temperatures only the starting material was recovered. The second option was a longer route involving benzyl protection of the primary amines to give compound **185**. The crude product would be subjected to stepwise deprotection beginning with the acetonide but, unfortunately, the reaction was not successful. The product decomposed and only the benzyl signals were evident after NMR spectroscopic analysis. It was becoming increasingly obvious that once the dimer has been synthesised, the acetonide groups need to be removed before introduction of the amine groups, otherwise harsher conditions would be required or the acetonide groups could not be removed.

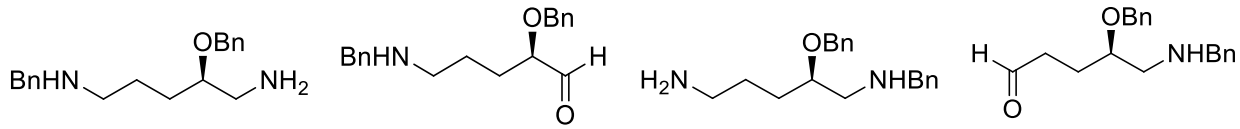


Scheme 90: Attempted deprotection of compound 184

At this stage of the project with potential pavettamine in hand, efforts shifted focus to the synthesis of the reduced functionality analogues. By now, methods for the synthesis of pavettamine and its enantiomer had been developed and could be modified for the syntheses of the analogues.

2.4 Synthesis of the reduced functionality analogues.

For a structure and activity study of pavettamine there is a need to synthesise reduced functionality analogues. The targeted reduced functionality analogues comprised of one hydroxyl group on the C-5 backbone, and the synthesis incorporated synthetic methods already described in this project in sections **2.2** and **2.3**. The synthesis was first broken down into preparation of four target fragments all possessing a hydroxyl mono-substituted C-5 linker, with an *R* configuration at the stereogenic centre from the same starting material (**Figure 30**). All of the compounds **187**, **188**, **189** and **190** could be easily synthesised from the same starting material, which in turn would significantly reduce the number of synthetic steps. It was envisioned that once the fragments had been synthesised, coupling to form the polyamines with the C-10 pavettamine backbone would easily be accomplished via reductive amination. Given the difficulty associated with deprotection of amines and alcohols once the C-10 pavettamine backbone was unveiled, benzyl protection was chosen for both amines and alcohols. It would allow for the simultaneous deprotection of the amines and the alcohols in a single step, revealing the desired compounds.



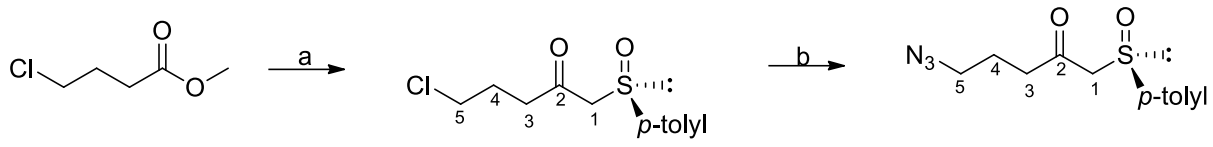
187 **188** **189** **190**

Figure 30: Reduced functionality fragments

Methyl-4-chlorobutyrate **191** was initially chosen as a suitable starting material because it allowed for the sequential functionalisation towards the reduced functionality fragments. The chloride group could be easily substituted with either an azide group, which would be reduced to unveil the desired amine, or substituted with the hydroxyl group, which would be oxidised to reveal the aldehyde. The ester functionality acted as a handle for the addition of the chiral sulfoxide auxiliary, which would be used for chiral induction during the reduction of the carbonyl group. As already discussed, the sulfoxide group would allow for further functionalisation of the molecule.

The initial step involved addition of *R*-methyl-*p*-tolylsulfoxide **137** to methyl-4-chlorobutyrate **191** at -40 °C and the rest of the experiment was carried out as previously described (**Scheme 91**). TLC analysis showed formation of a new product but the spot was co-eluting with the sulfoxide spot. Varying the mobile phases did not result in any change, which meant that purification of the desired product yielded compound **192** as a white solid in a very low yield of 14%, with a melting

point of 116 – 117 °C. The low yield could also be as a result of the acidic H-1 protons which could potentially react with the excess base present. An intramolecular reaction would ensue whereby the generated anion would attack the electrophilic C-5 carbon, resulting in formation of another product. HRMS confirmed the presence of the desired product with a measured mass of 258.0558, as expected. IR spectroscopy showed the characteristic aromatic C=C-H signal at 3016 cm^{-1} indicating the successful addition of the sulfoxide.



191 **192** **193**

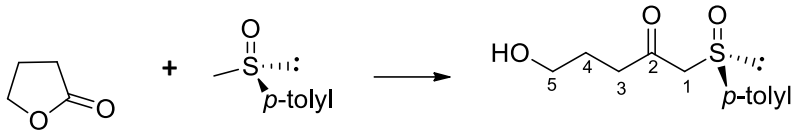
Scheme 91: a) *R*-methyl-*p*-tolyl sulfoxide, LDA, THF, -78 °C – r.t., 2 h, 14%; b) NaN_3, DMF, 95 °C, 4 h, 16%

In the ^{1}H NMR spectrum of the chlorinated sulfoxide **192**, the aromatic protons from the sulfoxide group appeared as two doublets at δ 7.53 (*J* = 8.3 Hz) and δ 7.35 (*J* = 8.0 Hz) whilst the methyl singlet from the tolyl group was at δ 2.42. The set of doublets indicative of the H-1 protons showed strong second order effects and the signals were visible at δ 3.86 (*J* = 13.3 Hz) and δ 3.79 (*J* = 13.3 Hz). The rest of the signals were as expected. Aromatic signals were observed at δ 142.3, 139.5, 130.2 and 124.0 whilst the tosyl methyl carbon peak was at δ 21.5 in the ^{13}C NMR spectrum, confirming the success of the sulfoxide addition. The characteristic carbonyl peak was in the expected range at δ 200.4.

Despite the dismal yields, compound **192** was subjected to nucleophilic substitution with sodium azide under reflux, and compound **194** was recovered in a poor yield of 16%. After purification, apart from the desired product, a significant number of side products which could not be identified, together with a sulfoxide side product were recovered, but no starting material was observed. NMR spectroscopy was used to confirm the identity of azide **194**. There was a slight upfield shift in the ^{1}H NMR spectrum for the H-5 triplet signal, from δ 3.51 to δ 3.26 for azide **194**, with a coupling constant of 6.6 Hz. The set of doublets previously observed for the H-1 protons was now a singlet at δ 3.61. In the ^{13}C NMR spectrum the expected change in chemical shift for the C-5 signal, because of the heteroatom change, was observed from δ 43.9 for compound **193** to δ 44.5 for compound **194**. However, the biggest chemical shift change observed was for the C-1 signal, from δ 67.9 to δ 44.5, but the reason for the huge shift is not very clear given the fact that the heteroatom change occurred 4-bonds away. The only explanation that can be offered is

that there is a conformational arrangement change which causes the C-1 to be in a shielded zone perhaps of the newly-installed azide functional group.

Instead of pursuing this approach and attempting to optimise yields, an alternative route was chosen at this early stage. For the new synthetic route, γ-butyrolactone **194** was used as the starting ester for the addition of the sulfoxide auxiliary as shown in **Scheme 92**. Alternatively, ring opening of the lactone under basic conditions can occur first in a separate step. The recovered carboxylate salt is subjected to methylation revealing the ester followed by the addition of the sulfoxide auxiliary.[176] For this work, however, the ring opening of γ-butyrolactone **194** and sulfoxide addition to reveal compound **195** was achieved in a single step, with recoverable yields of approximately 63% (**Scheme 92**). The reaction yield was probably higher, but the sulfoxide and compound **195** have similar R_f values, complicating the recovery process to the extent that even gradient elution could not completely separate the two compounds.



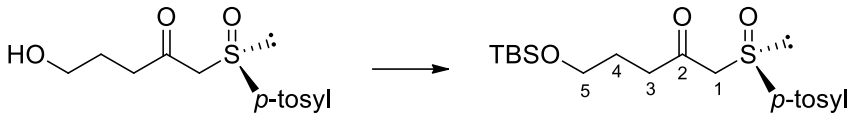
194 **137** **195**

Scheme 92: LDA, THF, -78 °C – r.t., 2.5 h, 63%

Despite the difficulty in product isolation, reasonable product yields were recovered. Confirmation of the product identity was achieved firstly by the broad OH signal at 3392 cm^{-1}, and the carbonyl signal at 1710 cm^{-1} in the IR spectrum. The ^{1}H NMR spectrum showed the aromatic tosyl protons as two multiplets, due to slight contamination with residual methyl *p*-tolylsulfoxide, at δ 7.58 – 7.49 and δ 7.37 – 7.27, giving rise to a total integration of four protons. The tosylmethyl singlet was visible at δ 2.40, integrating for three protons. A broad singlet peak for the alcohol group was at δ 5.58 and the remaining signals were as expected. In the ^{13}C NMR spectrum the aromatic signals from the di-substituted tosyl ring were at δ 142.2, δ 141.9, δ 124.1 and δ 124.0, and the tosyl-methyl peak (C-6) was observed at δ 21.4. The characteristic carbonyl carbon signal was at δ 202.2 whilst the C-1 and C-5 signals were at δ 67.8 and δ 68.3, respectively.

The primary alcohol of **195** was TBS protected (**Scheme 93**) yielding compound **196** in a poor yield of 50% as a viscous oil, probably as a result of the presence of side products carried through from the previous reaction. However, because of the orthogonal protection requirements of the

alcohol and amine groups for this synthetic route, there were limited options of compatible groups, forcing the use of the TBS group. IR spectroscopic analysis showed the disappearance of the broad OH peak previously seen at 3392 cm^{-1}. The HRMS data confirmed the desired mass to be 355.1754 as the $(M+H)^+$ ion.



195 **196**

Scheme 93: TBSCl, imidazole, DMAP, r.t., overnight, 50%

The newly added TBS *tert*-butyl proton signals were observed at δ 0.87 as a singlet integrating for nine protons, and the dimethyl signal was also a singlet at δ 0.02 integrating for six hydrogens. An interesting observation was noted for the H-1 proton signal as shown in **Figure 31**. The peak looks like a quartet but measuring the coupling constants shows that there are two doublets with a coupling constant of 13.6 Hz exhibiting strong second order effects because of the diastereotopic nature of the H-1 protons. In the ^{13}C NMR spectrum the TBS *tert*-butyl signal was at δ 25.9, the TBS-quaternary carbon signal at δ 18.3 and the remaining TBS-Si(CH_3) at δ -5.4. The rest of the remaining signals were as expected.

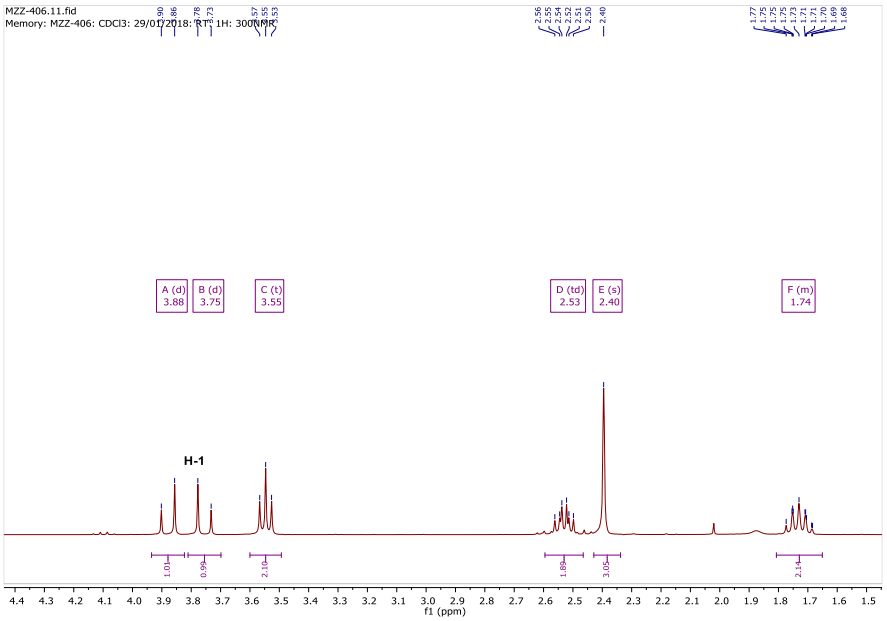
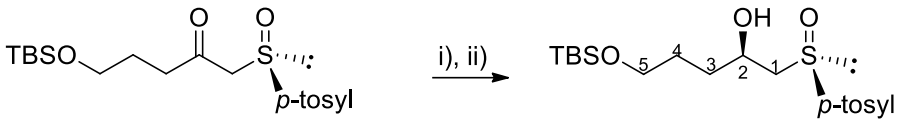


Figure 31: ^1H NMR spectrum for compound 196

The TBS protected alcohol was subsequently subjected to chelation controlled stereo-selective reduction, using DIBALH as the reducing agent (**Scheme 94**), giving the alcohol **197** in an excellent

yield of 95%. Scaling up the reaction from a gram to 5.00 g reduced the average yield to 67% and therefore, the reductions were not performed on a scale greater than 1.00 g. The optical rotation of the product was measured to be +115.0°, when the concentration was 1.0 g/100 ml in chloroform, showing that at least the recovered product was not a racemic mixture. A broad peak evident at 3337 cm^{-1} in the IR spectrum signified the presence of an alcohol in the recovered compound.

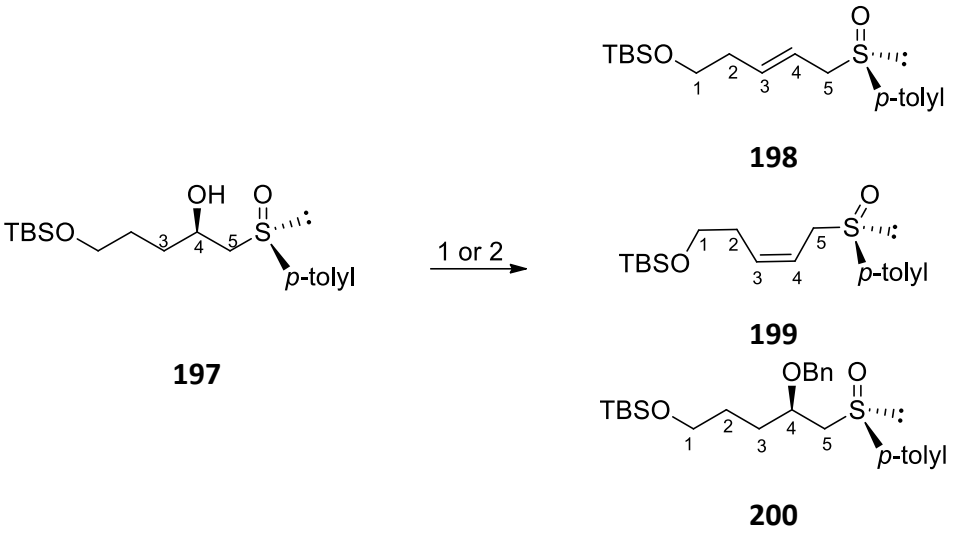


196 **197**

Scheme 94: i) $ZnCl_2$, r.t., 2 h; ii) DIBALH, THF, -78 °C – r.t., 2 h, 95%

^{1}H NMR spectroscopic analysis was performed, to confirm whether the observed alcohol signal was as a result of TBS deprotection, or a successful reduction procedure. The spectrum showed the presence of the TBS signals at δ 0.89 as a singlet integrating for nine protons, and overlapping singlets at δ 0.050 and δ 0.052 integrating for six protons. The newly revealed multiplet signal for the H-2 proton was evident at δ 4.21 – 4.08 and a doublet was observed for the OH signal at δ 4.24 (*J* = 2.3 Hz). The COSY NMR spectrum showed that the doublet was as a result of the OH coupling with the H-2 proton. The H-1 signals were now a set of doublets of doublets at δ 3.03 (*J* = 13.1, 8.8 Hz), and at δ 2.78 (*J* = 13.0, 3.1 Hz). In the ^{13}C NMR spectrum the carbonyl signal for C-2 had been replaced by a signal at δ 68.1 signifying a carbon atom attached to oxygen, and the remaining signals were just as expected.

After the selective reduction of compound **196** had been achieved, the next step involved benzyl protection of the secondary alcohol using benzyl bromide, as shown in **Scheme 95**. Before settling on NaH as the preferred base, other milder bases such as K_2CO_3 under reflux were employed to no avail, as only the starting material was recovered. Employing NaH at room temperature gave rise to the elimination products **198** and **199** together with 26% of the desired product **200**.



197

Scheme 95: 1. NaH, BnBr, THF, r.t. 12 h, 26% yield for compound 200; 2. NaH, BnBr, THF, 0 °C, 96% for compound 200

The identity of the elimination products was confirmed by ^{1}H NMR spectroscopy, firstly by the presence of the alkenyl protons in the expected range. In general, the *trans* isomer olefinic protons are more deshielded than for the *cis* isomer. Unfortunately coupling constants of the H-4 signals of the isomers could not be used for *cis*-*trans* assignment because they were not clearly resolved. Therefore, compound **198** was assigned to be the *trans* isomer because the H-4 signal was more downfield at δ 5.87 – 5.72, and compound **199** to be the cis isomer because the H-4 signal was more upfield at δ 5.65 – 5.61. The elimination mechanism is not clear but it is suspected that elimination occurs on the desired product **200**. The recovered alkenes were not the expected elimination products. The H-5 protons for compound **200** are susceptible to deprotonation by virtue of being α to an electropositive carbon atom whilst the OBn becomes a leaving group. This should result in an elimination product with conjugation to the S=O bond however, it was therefore surprising not to recover an alkene conjugated to S=O. As already mentioned the reason behind this outcome is not clear at this stage. The olefinic carbon assignments were confirmed by HSQC NMR spectroscopy as shown in **Figure 32**.

Table 5: ^{1}H and ^{13}C NMR spectroscopic chemical shifts for compound 198 and compound 199

	H-3	H-4	C-3	C-4
Compound 198	δ 5.44 – 5.27	δ 5.87 – 5.72	δ 117.6	δ 135.1
Compound 199	δ 5.42 – 5.27	δ 5.65 – 5.51	δ 118.8	δ 136.8

The HRMS results for the two isomers were similar as expected, 339.1807 $(M+H)^+$ for compound **198** and 339.1814 $(M+H)^+$ for compound **199**, both with a calculated mass of 339.1809 but the specific optical rotation for the two isomers was significantly different. The *trans*-isomer was not pure because of co-elution problems with an unidentified side product, and the measured specific optical rotation value was +29.8 (c 2.05) in chloroform. The *cis*-isomer was recovered in pure form, therefore the specific optical rotation value is more accurate, and it was measured to be +1.90 (c 2.10) in chloroform. The elimination of the alcohol group meant that the recovered products were no longer of any use in the synthesis of the desired compounds.

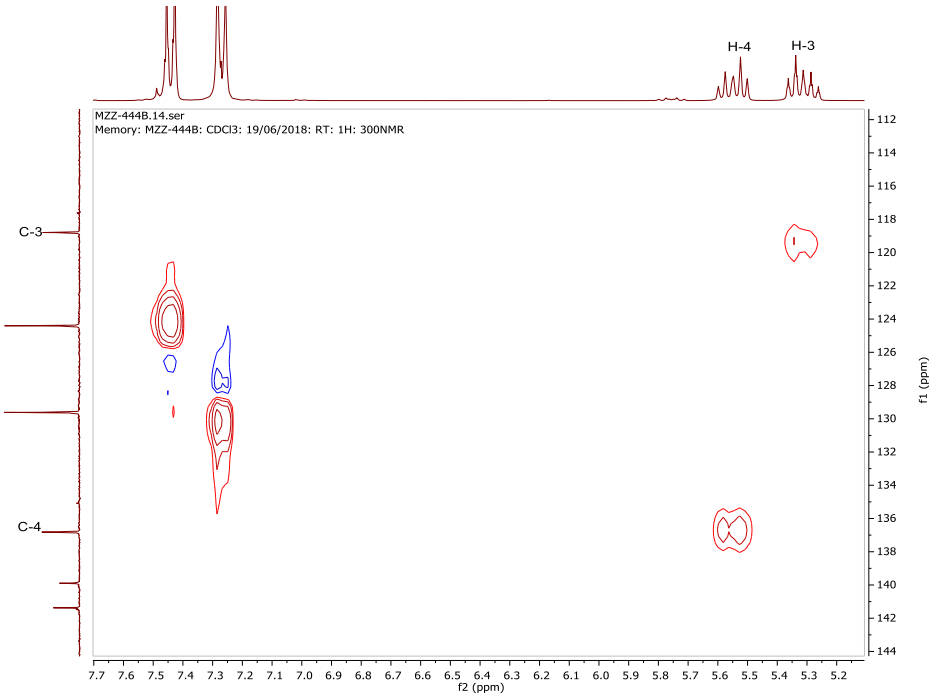
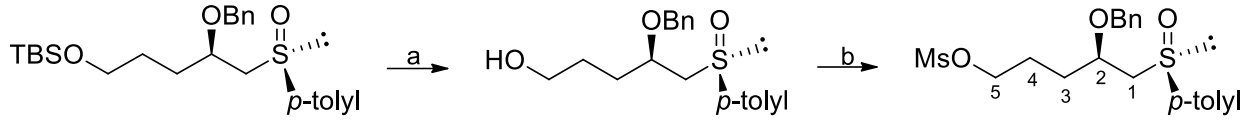


Figure 32: HSQC NMR spectrum for compound 199

A modified reaction was carried out at 0 °C on a one-gram scale. The desired product **200**, was recovered in an excellent yield of 96%, as a colourless oil with a measured specific optical rotation of +85.2 (c 0.56) indicating optical activity. There was a marked increase in the integration of aromatic protons to nine hydrogens, the total sum of the benzyl and the tosyl group protons, in the ^{1}H NMR spectrum. The fact that the benzylic protons are 2 bonds away from a stereogenic centre means that they are chemically equivalent by virtue of being attached to the same carbon atom but not magnetically equivalent because they couple differently to the H-2 proton. This effect gives rise to the second order coupling observed in the ^{1}H NMR spectrum for the benzylic protons at δ 4.38 and δ 4.48 as two sets of doublets with a coupling constant of 11.5 Hz. The

benzylic carbon signal was at δ 70.8 in the ^{13}C NMR spectrum and the rest of the signals were as expected.

The successful synthesis of the benzyl protected alcohol **200**, provided a common starting material for all the reduced functionality fragments. Thus, work began on the synthesis of the target fragments beginning with compound **187** and compound **188** (**Figure 30**). In order to achieve this the TBS group was removed revealing the primary alcohol, to give compound **201**. The product was subsequently mesylated to compound **202** (**Scheme 96**) prior to a nucleophilic substitution with benzylamine. Mesylates have two advantages over tosylates, namely; stability against hydrolysis and reduced steric hindrance for a nucleophilic attack by benzylamine.



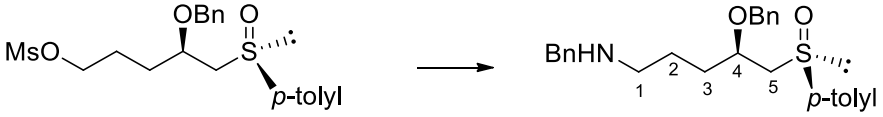
200 **201** **202**

Scheme 96: a) TBAF, THF, 0 °C, 4 h, 71%; b) MsCl, Et_3N, DCM, 0 °C – r.t., overnight, 82%

A broad signal for OH at 3395 cm^{-1} in the IR spectrum confirmed the successful removal of the TBS group, revealing the primary alcohol in compound **201**. Both the ^1H and ^{13}C NMR spectra showed the disappearance of the TBS signals, confirming the success of the deprotection step. Successful synthesis of compound **202** was confirmed by HRMS with a measured mass of 411.1295 $(M+H)^+$, and the IR spectrum showed the disappearance of the broad alcohol signal previously visible at 3395 cm^{-1}. In the ^1H NMR spectrum, the new methyl singlet signal from the mesylate group was at δ 2.98, whilst the carbon signal for this group was at δ 24.9 in the ^{13}C NMR spectrum.

Once the mesylate had been synthesised, it was subjected to a nucleophilic substitution reaction with benzylamine, as shown in **Scheme 97**. The reaction was left stirring for 2 days, but only 22% of the desired product was recovered. Change of the solvent to DCM, and increasing the temperature to 50 °C did not increase the yield of the desired product. Confirmation of the product was done by NMR spectroscopy and HRMS, with a measured mass of 422.2148 $(M+H)^+$ observed when compared to a calculated mass of 422.2149. The ^1H NMR spectrum showed the total disappearance of the mesylate methyl signal and an increase in the aromatic protons with a total integration of fourteen at δ 7.52 – 7.45 (m, 2H) and δ 7.40 – 7.21 (m, 12H). The *O*-benzylic protons were observed at δ 4.50 – 4.34, whilst the *N*-benzylic protons were observed as a singlet

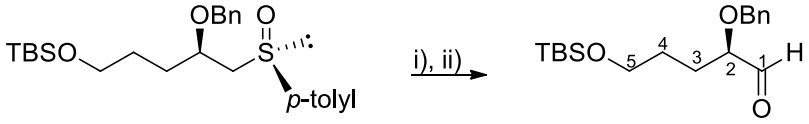
at δ 3.82. The corresponding carbon signals were evident at δ 70.9 and δ 53.6, respectively, in the ^{13}C NMR spectrum and the rest of the signals were as expected.



202 **203**

Scheme 97: Benzylamine, THF, r.t., 2 d, 22%

Due to the problematic nature of further transformations on **203** and the low yielding nature of the amination of compound **202**, the synthetic approach was abandoned and a different synthetic route chosen. A route that would afford all the desired fragments was chosen. Synthesis began by transformation of compound **200** to the aldehyde via the Pummerer rearrangement (**Scheme 98**). The desired compound **204**, was recovered in a crude yield of 88% because purification by column chromatography did not separate all the undesired sulfoxide side products. The specific optical rotation of the aldehyde was measured to be +27.4 in chloroform when the concentration was 0.53 g/100 ml, and the carbonyl signal was evident at 1735 cm^{-1} in the IR spectrum.



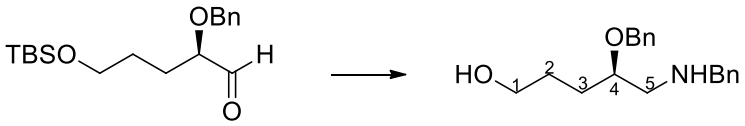
200 **204**

Scheme 98: i) TFAA, 2,4,6-collidine, MeCN, 0 °C, 30 min; ii) H_2O, K_2CO_3, r.t., 1 h, 88%

From NMR spectroscopic analysis it was evident that the sulfoxide side product and residual 2,4,6-collidine were still present as contaminants even after purification. However, only the signals for the desired compound are reported in the experimental section. The aldehyde signal was observed as a doublet at δ 9.64 (J = 2.0 Hz) in the ^1H NMR spectrum. The observed multiplicity was as a result of the H-1 proton coupling with the H-2 proton, and this relationship was confirmed by COSY NMR spectroscopy. The aldehydic carbon signal was observed at δ 203.5 and there was no extra C-O signal which would have suggested partial TBS deprotection. HRMS results also confirmed the desired mass of the product to be 323.2036 $(M+H)^+$ with a molecular formula of $C_{18}H_{30}O_3Si$ and a calculated mass of 323.2037.

Despite the aldehyde not being pure, the compound was subjected to a reductive amination procedure as a way of introducing the amine functionality to the C-1 carbon as shown in **Scheme**

99. It was hoped that the unwanted side products would either be separable from the benzylated amine or converted to other more easily separable products. The experiment proceeded as expected, but unfortunately TBS deprotection was also observed and alcohol **205** was recovered in a low yield of 44%. The high polarity of the compound added to loss in product yield due to purification difficulty, as a high polarity mobile phase of $CHCl_3$/MeOH (4:1) was used for column chromatography. Reasons behind the unexpected deprotection of the TBS group could not be established, because the reaction conditions employed are not known to result in the deprotection of the TBS group. The presence of the side products from the previous reaction might have contributed to the formation of compound **205**.



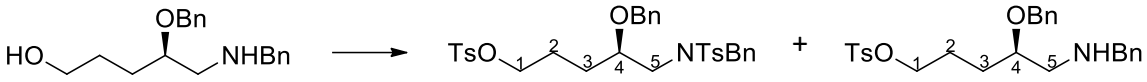
204 **205**

Scheme 99: Benzylamine, $NaBH(OAc)_3$, 1,2-DCE, N_2, r.t., 18 h, 44%

Confirmation of the structure was achieved by NMR spectroscopy. Firstly, in the ^1H NMR spectrum, there was no evidence of the TBS signals, but there was an extra methyl signal at δ 2.41 integrating for three protons, likely to be the sulfoxide side product from the Pummerer rearrangement (**Scheme 98**) being carried through. The integration for the aromatic protons showed more protons than expected suggesting the presence of the tosyl side product, which was still not separable by column chromatography. Apart from the unexpected signals from the contaminants, the H-1 signal for compound **205** was observed as a triplet at δ 3.58 with a coupling constant of 6.2 Hz. The H-4 signal was evident at δ 4.03 (*J* = 5.2 Hz) as a pentet, whilst the two sets of doublets of doublets for the H-5 protons were at δ 3.46 (*J* = 14.6, 5.9 Hz) and δ 3.22 (*J* = 14.5, 5.1 Hz). Unfortunately, the broad signals expected from both the OH and the NH protons were not visible in the spectrum. Mass spectrometry also showed the presence of the recovered alcohol with a measured mass of 300.1958 $(M+H)^+$ and a molecular formular of $C_{19}H_{26}NO_2$ when the calculated mass was 300.1958.

In the ^{13}C NMR spectrum the C-1, O-CH_2 and C-4 signals were at δ 62.3, δ 71.4 and δ 73.4 respectively, whilst the C-5 and N-CH_2 signals were at δ 43.7 and δ 60.6. Assignment of all the signals was possible by analysis of the 2D NMR spectra obtained from COSY and HSQC experiments. The resultant alcohol was tosylated as before as shown in **Scheme 100**. The

recovered material after purification suggested a mixture of products, where tosylation had occurred on both the alcohol and the amine groups for **206**, the desired product **207** and residual tosyl chloride. The product recovered from further transformation of the mixture supported this suggestion.



205 **206** **207**

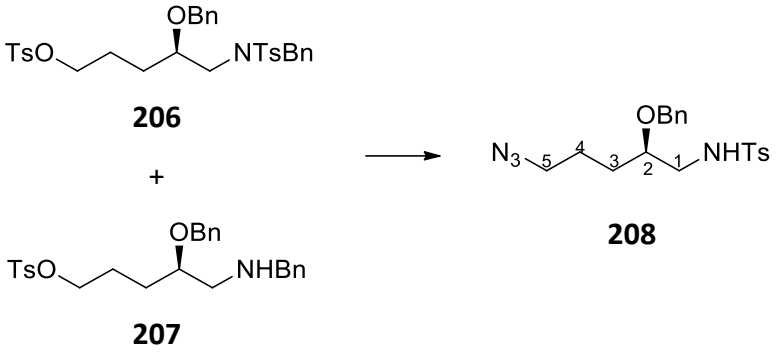
Scheme 100: TsCl, DMAP, DCM, r.t., overnight

Due to the small quantity of material present no further attempts were made at separating the mixture. Explicit characterisation of the two products could not be conclusively determined from NMR spectroscopic analysis. However, 2D spectroscopic analysis strongly suggested the presence of compound **206** and compound **207**. The presence of the two products was also suggested by the doubling of all signals in the ^{13}C NMR spectrum except the C-1 signal. The difference between the two compounds is the tosylation of the amine group therefore atoms closer to the C-5 atom are expected to show slightly different chemical shifts while a single signal was observed for the C-1 atom because it is six bonds away from *N.*

The recovered products were then subjected to the nucleophilic substitution reaction as a mixture, because the molecular difference was not expected to have an impact on the desired transformation. Excess sodium azide was added to the dissolved substrates in DMF, and refluxed at 80 °C for up to 4 hours (**Scheme 101**), whilst monitoring the progress of the reaction by TLC. Purification afforded compound **208** as the only product and surprisingly the amine was benzyl deprotected. None of the expected products from the conversion of either of the starting materials were isolated from the reaction.

There is no precedent to the observed results and it is not clear whether both **206** and **207** were converted to azide **208**. A possibility is that the substitution might have occurred on both substrates but the azide formed from **207** might have been benzyl deprotected during the reaction and the resulting amine lost to the aqueous layer during rigorous aqueous workup due to the high polarity of amines. Azide **208** was recoverable because the amine was tosylated which reduced polarity. Benzyl deprotection had definitely occurred during the nucleophilic substitution reaction with the azide because the precursor showed the presence of the *N*-benzyl group. An azide signal

was observed at 2094 cm^{-1} in the IR spectrum for the recovered product but unfortunately compound **208** was not stable enough to measure the base peak in HRMS.



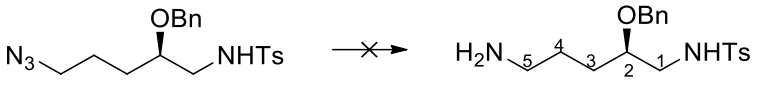
Scheme 101: NaN_3, DMF, 80 °C, 4 h

Structure confirmation of the recovered product was accomplished by NMR spectroscopic analysis. In the ^1H NMR spectrum, the total integration for the aromatic protons was nine, showing that only a single benzyl and a single tosyl group were present. The Bn-CH_2 signals were at δ 4.45 (d, *J* = 11.4 Hz) and 4.39 (d, *J* = 11.4 Hz, 1H) as two doublets which almost appeared as a quartet, whilst the H-2 signal was a pentet at δ 3.99 (*J* = 5.5 Hz). A doublet of doublets signal for a single H-1 proton was observed at δ 3.45 with coupling constants of 14.6 Hz and 5.5 Hz. The remaining H-1 signal overlapped with the H-5 signal and the multiplet was evident at δ 3.25 – 3.15. As has been the case up to this point, the multiplet signal for the H-3 and H-4 protons was at δ 1.83 – 1.50. The remaining singlet signal at δ 2.42 integrating for three protons was for the Ts-CH_3 protons. The previously observed contaminants were not observable in the NMR spectra.

In the ^{13}C NMR spectrum the signals for the aromatic carbons for the benzyl and tosyl groups were at δ 144.8, δ 137.3, δ 137.0, δ 129.9, δ 128.4, δ 127.91, δ 127.88 and δ 127.85. The previously observed doubling of signals in the spectrum was not visible, confirming that only one compound had been recovered. The C-2 signal was at δ 72.9, whilst the Bn-CH_2 signal was at δ 71.4. A significant deshielding effect was being experienced by the C-1 carbon, because the signal was at δ 60.6, which is further downfield than the usually expected range for a C-N signal. The C-5 signal was observed in the characteristic region for C-N carbon signals at δ 51.1. All assignments were done using 2D NMR spectroscopy and DEPT135 experiments.

Following the successful synthesis of the azide **208**, the product was subjected to a reduction procedure using $LiAlH_4$, but unfortunately the desired product was not recovered. The recovered material could not be fully characterised. Had the procedure been successful, compound **209**

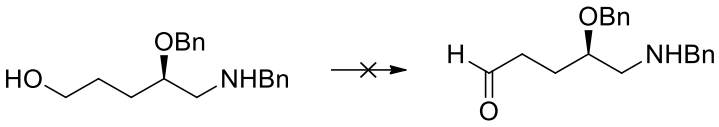
would have been the *N*-tosylated equivalent of compound **189** which could have been easily converted to compound **187**.



208 **209**

Scheme 102: $LiAlH_4$, Et_2O, N_2, r.t., overnight

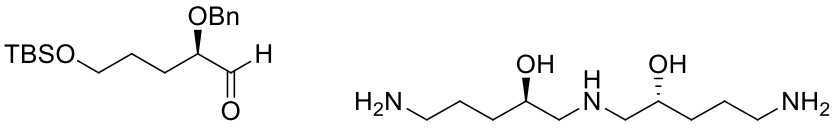
Alcohol **205** was then subjected to oxidation in an attempt to recover fragment **190**. Synthesis of the aldehyde **190** involved treating alcohol **205** with DMP as the oxidant in DCM at room temperature (**Scheme 103**). The reaction was monitored by TLC analysis and total consumption of the starting material was observed after 7 hours, but workup of the reaction did not yield the desired product **190**. A crude NMR spectroscopic analysis was performed but the spectrum was not conclusive and the characteristic aldehyde signal was not observed. The unexpected results were probably as a result of a possible intermolecular reaction between the aldehyde as it forms and the secondary amine. Possible solutions to circumvent the observed problem are to either reduce the reaction time or consider oxidising the alcohol to the carboxylic acid.



205 **190**

Scheme 103: DMP, DCM, r.t., overnight

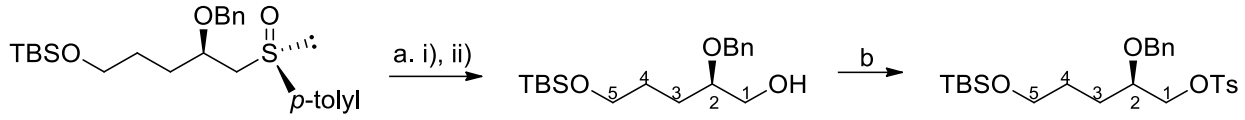
Given the complexity brought about by the introduction of the amine group at an early stage in the synthesis, the synthetic route was changed, and this time the aim was to introduce the terminal amine after the coupling of the two fragments to form the C-10 backbone. Since aldehyde **204** had already been synthesised it was prudent for the amine compound of a similar substrate to be synthesised for coupling to form one of the reduced functionality analogues **116**.



204 **116**

Figure 33: Structures of compound 204 and 116

For the synthesis of the amine, compound **200** was first subjected to the Pummerer rearrangement revealing the alcohol **210** which in turn was tosylated to yield compound **211** (**Scheme 104**). The alcohol **210** was recovered in an average yield of 74%, and IR spectroscopy confirmed its formation by the presence of a signal at 3403 cm^{-1}. The measured mass of the recovered product was 325.2194 $(M+H)^+$ comparable to an expected mass of 325.2193. The tosylated alcohol **211** was recovered in quantitative yields.



200 **210** **211**

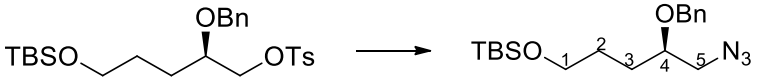
Scheme 104: a) i) 2,4,6-collidine, TFAA, 0 °C, 30 min; ii) $NaBH_4$, MeCN, r.t., 1 h, 74%; b) TsCl, DMAP, DCM, r.t., 12 h, quantitative yield

In the ^1H NMR spectrum of compound **210**, the total integration for the aromatic protons had reduced to five, whilst the methyl signal for the tosyl group previously observed at δ 2.39 had disappeared. Formerly observed doublet of doublet signals for the H-1 protons were replaced by a set of overlapping multiplet signals for H-1 and H-5 protons at δ 3.64 – 3.46. The observed overlapping of signals is expected because these protons are both attached to carbon atoms carrying oxygen, and the rest of the signals were as expected. In the ^{13}C NMR spectrum, the tosyl methyl signal had disappeared as expected, whilst the C-1 signal had migrated from δ 62.4 to δ 64.2. The greatest observed chemical shift change was for the C-2 signal which jumped from δ 73.6 to δ 79.5. Such a chemical shift difference is a result of the heteroatom change, since oxygen exerts greater deshielding effects than sulfur.

Confirmation of the tosylated product **211** was easily achieved by conducting both IR and NMR spectroscopy. The broad alcohol signal previously observed at 3403 cm^{-1} had completely disappeared from the IR spectrum, and the only other change observed was in the fingerprint region as a result of the S=O bond. In the ^1H NMR spectrum, the previously observed broad alcohol signal had completely disappeared, to be replaced by a new singlet at δ 2.43 for the tosyl methyl. A single doublet for the aromatic signal from the tosyl group was observed at δ 7.78 (J = 8.0 Hz), whilst the second doublet overlapped with the multiplet signal for the benzyl aromatic protons at δ 7.35 – 7.22. The total integration for the two sets of signals was nine, as expected. The major changes observed in the ^{13}C NMR spectrum were the increase in the number of aromatic signals as a result of the aromatic tosyl carbon atoms and the tosylmethyl carbon signal that was observed

at δ 21.6. Chemical shift changes were also observed for the remaining signals, but all were accounted for.

The successful tosylation step was followed by the general facile nucleophilic substitution introducing the azide moiety (**Scheme 105**). A light brown oil, with a specific optical rotation of -15.4 when the concentration was 0.55 g/100 ml in chloroform, was recovered as compound **212** in a reasonable yield of 73%. The characteristic azide signal was visible at 2097 cm^{-1} in the IR spectrum, which confirmed the success of the substitution reaction. Mass spectrometry also confirmed the mass to be 350.2260 $(M+H)^+$ comparable to a calculated mass of 350.2258.



211 **212**

Scheme 105: NaN_3, DMF, 75 °C, 4 h, 73%

In the ^1H NMR spectrum of azide **212**, the previously observed doublet for the tosyl aromatic protons had disappeared and the total integration of the aromatic signals had reduced from nine to five. This is consistent with the total expected number of aromatic protons in the desired molecule from the benzyl group. The obvious absence of the singlet representative of the tosyl methyl group, also confirmed the complete substitution of the tosyl group. Unfortunately, an inexplicable doubling of the signals from the TBS group was observed, with the total integration being half the expected number of protons. The Bn-CH_2 signal also showed the doubling effect although an integration of two as expected was observed. Only the integration of the TBS protons was a mismatch. This suggested that there was partial deprotection of the TBS group however; this theory was not supported by the IR data because no signal indicative of the alcohol group was observed. The second possibility is that the conformation of the molecule is restricted which gives rise to two observable conformers detectable by NMR spectroscopy. Probably all the other signals overlap except the TBS signals in the ^1H NMR spectrum. The remaining signals were all observed as multiplets at δ 3.67 – 3.56 (H-2 and H-5), δ 3.40 – 3.29 (H-1) and δ 1.75 – 1.51 (H-3 and H-4), but with the expected integration.

The ^{13}C NMR spectrum for compound **212** also showed doubling of all the signals. This was unexpected because the recovered compound only has one stereogenic centre therefore if racemisation occurs only enantiomers are expected. Enantiomers have the same physical

properties, resulting in identical chemical shifts. Doubling of signals is only expected in the event of diastereomers. Secondly, the compound does not possess any sp^2 centres which could cause restricted rotation and result in rotamers, which consequently could give rise to doubling of signals. For illustration purposes, a portion of the ^{13}C NMR spectrum is shown in **Figure 34**. Only the expected signals were observed in the spectrum which eliminated the possibility of the presence of a side product. All the other analytical tools for product characterisation had alluded to the presence of a single compound except NMR spectroscopy, thus complicating the determination of why the doubling of signals was being observed in the NMR spectra. The only explanation that can be offered at this point is that maybe the conformational arrangement of the molecule gave rise to the observed anomaly but exactly how this occurs is still unclear.

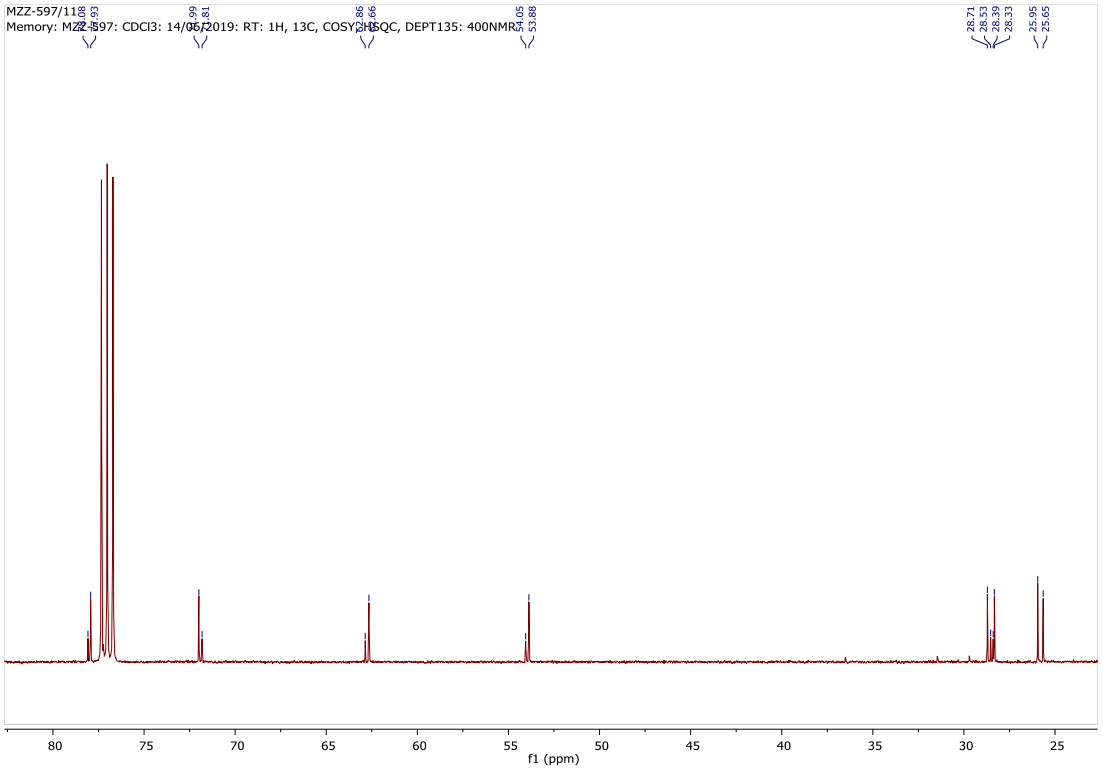
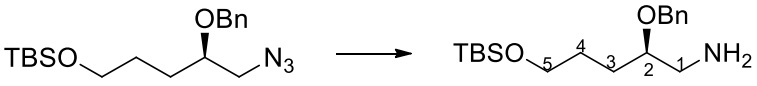


Figure 34: ^{13}C NMR spectrum for compound 212

In an attempt to establish the nature of the observed anomaly, azide **212** was transformed into the corresponding amine **213**. Reduction of the azide was achieved using a previously described method as shown in **Scheme 106**, and the desired amine **213** was recovered in a low yield of 14%. NMR spectroscopy of the recovered product indicated the same doubling of signals observed in the NMR spectrum for compound **212**. Additional signals were also present in the spectra although they could not be fully identified. Due to the tailing nature of amines during TLC analysis,

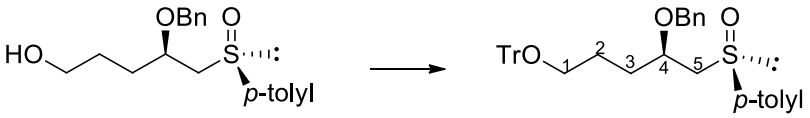
it could not be established how many other side products were present by TLC visualisation. Instead of continuing with a substrate whose identity was not confirmed, the synthetic approach for the reduced functional analogues was reconsidered.



212 **213**

Scheme 106: $LiAlH_4$, Et_2O, r.t., 3 h, 14%

Evaluation of all the results up to this point led to the conclusion that introduction of the terminal amines of the target compounds for this work at an early stage, coupled with the presence of the TBS group, gave rise to undesirable side reactions and products. To overcome this limitation, the synthetic route was changed, by replacing the TBS group on compound **200** with a trityl group, and subjecting the substrate to the same chemical transformations. Thus, the primary alcohol of compound **201** was trityl protected under basic conditions for 12 hours (**Scheme 107**). Use of DMAP alone failed to yield the desired product, however, success was achieved by the use of a combination of Et_3N and a catalytic amount of DMAP, furnishing compound **214** in an excellent yield of 84%.



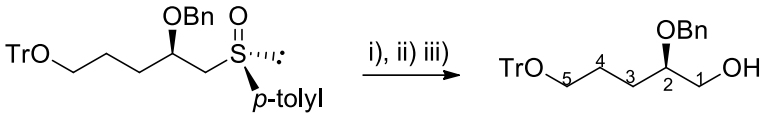
201 **214**

Scheme 107: TrCl, DMAP (cat), Et_3N, DCM, r.t., 12 h, 84%

The measured optical rotation of **214** was +43.1 in chloroform at a concentration 0.45 g/100 ml, indicating that at least the product was not a racemic mixture. The previously observed broad signal indicative of an alcohol had disappeared from the IR spectrum thus confirming that the protection of the primary alcohol had been successful. In the ^1H NMR spectrum, there was a marked increase in the integration of the aromatic protons as a result of the added aromatic protons from the trityl group. The H-1 proton signal was a distinct triplet at δ 3.07, with a coupling constant of 6.1 Hz. The H-4 proton signal was a pentet at δ 3.69 with a coupling constant of 5.8 Hz. As already observed for similar substrates, the benzyl CH_2 signals appeared as two doublets at δ 4.42 and δ 4.36 both with a coupling constant of 11.5 Hz.

The major change in the ^{13}C NMR spectrum was the increase in the number of aromatic carbon signals. The C-1 signal had also migrated from δ 62.0 for compound **201** to δ 63.2 for compound **214** owing to the slight deshielding effect of the trityl group. A new signal was observed at δ 86.4, which is consistent with the expected chemical shift for the quaternary trityl ether carbon. The rest of the signals were as expected, and the measured mass of the product was consistent with the desired mass of 597.2434 $(M+Na)^+$.

Instead of converting sulfoxide **214** directly to the aldehyde, the substrate was converted to the alcohol first. The alcohol was later converted to an amine for one of the fragments and oxidized to the aldehyde for the second fragment. Subjecting compound **214** to the Pummerer rearrangement (**Scheme 108**) yielded compound **215** in an excellent yield of 94%, as a yellowish/greenish oil. IR spectroscopy showed a broad peak at 3442 cm^{-1} that is consistent with an O-H stretch. Staining the TLC plate in $KMnO_4$ gave a yellow spot on a purple background for the single spot that had an R_f value of 0.37 (EtOAc/Hex, 3:7) and this was used to identify the desired product from the side products. The measured mass using HRMS was consistent with the expected mass of 475.2239 $(M+Na)^+$.



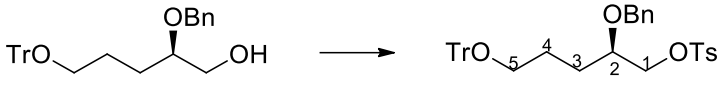
214 **215**

Scheme 108: i) TFAA, 2,4,6-collidine, MeCN, 0 °C, 30 min; ii) H_2O, K_2CO_3, r.t., 30 min; iii) $NaBH_4$, r.t., 1 h, 94%

Further confirmation of the recovery of the desired alcohol was achieved using NMR spectroscopy. In the ^1H NMR spectrum, the singlet signal for the tolyl methyl protons, coupled with the reduction in integration of the aromatic protons pointed to the successful removal of the sulfoxide moiety. A broad singlet signal at δ 2.04, which did not show any correlation to carbon atoms in the HSQC spectrum, confirmed the presence of the hydroxyl group. The heteroatom change at C-1 resulted in a downfield shift of the H-1 proton signals, appearing as a set of doublets of doublets at δ 3.65 (J = 11.2, 3.1 Hz). The second doublet of doublets signal overlapped with the H-2 signal and appeared as a multiplet at δ 3.55 – 3.42 with a total integration of two. The second order effects of the benzylic CH_2 protons gave rise to two doublets at δ 4.55 and δ 4.49 each with a coupling constant of 11.6 Hz, appearing as a quartet.

In the ^{13}C NMR spectrum there was a significant reduction in the number of aromatic carbon signals owing to the removal the sulfoxide group. The methyl signal from the tolyl group previously observed at δ 21.4 had also disappeared. A chemical shift change of the C-1 signal was observed from δ 62.5 to δ 64.2 because of the functional group change from the sulfoxide to the more electronegative oxygen. The rest of the signals were as expected.

The alcohol **215** was tosylated (**Scheme 109**) in preparation for the nucleophilic substitution reaction with azide. The desired product **216** was recovered in an excellent yield of 94% giving rise to a yellow oil. Recovery of the product was only achieved when the reaction was carried out at 0 °C otherwise decomposition occurred. In order to establish the success of the tosylation step, IR spectroscopic analysis was performed which revealed the disappearance of the alcohol signal previously observed at 3442 cm^{-1}. Optical activity of the product was confirmed by a measured specific rotation value of +10.4 g/100 ml in chloroform.



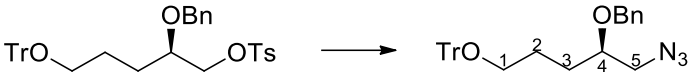
215 **216**

Scheme 109: TsCl, DMAP, Et_3N, DCM, r.t., 6 h, 94%

The ^1H NMR spectrum showed an increase in the total integration of the aromatic protons to a total of twenty four as expected, due to the added aromatic protons from the tosyl group. Another signal used to affirm the identity of the recovered product was the new singlet observed at δ 2.39, signaling the presence of the methyl substituent of the tosyl group. A further downfield shift was observed for the H-1 protons, when compared to the chemical shift of H-1 in compound **215**, as the signal was now a multiplet at δ 4.06 – 3.98 with a total integration of two. In the ^{13}C NMR spectrum, the Ts-CH_3 signal was observed at δ 21.5. A downfield shift was also observed for C-1, from δ 64.2 for compound **215**, to δ 71.4 for compound **216**. The observed downfield chemical shift was a result of the O-Ts group exerting a greater deshielding effect, due to its stronger electron withdrawing capability, than the OH group.

With the tosylation step confirmed, synthesis progressed to the nucleophilic substitution of the OTs group with azide (**Scheme 110**). As discussed previously the reaction was only heated to 75 °C, otherwise product decomposition occurred. Compound **217** was recovered in a yield of 98% as a light brown oil. The optical rotation was measured to be +1.17° in chloroform (c 0.6).

Formation of the azide was confirmed by the appearance of a signal at 2096 cm^{-1} in the IR spectrum. HRMS measured the mass of the product to be 500.2301 $(M+Na)^+$ as expected.

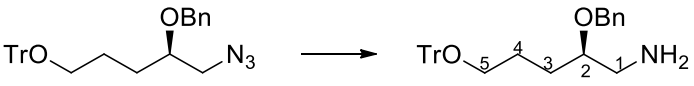


216 **217**

Scheme 110: NaN_3, DMF, 75 °C, 4 h, 98%

The previously observed doubling of signals of the TBS protected equivalent **212** was not observed in the NMR spectra for azide **217**. In the ^1H NMR spectrum, all the signals from the tosyl group had disappeared, and the total integration of the aromatic hydrogens was now twenty. In the ^{13}C NMR spectrum, the tosyl signals had also disappeared, coupled with a reduction in the number of aromatic signals. A sure sign of the success of the substitution reaction was the presence of a new signal at δ 54.0, duly assigned to C-5. The chemical shift correlated with the expected chemical shift for C-N signals and no such signal was present in the spectrum of the precursor.

Following the synthesis of the azide **217**, the substrate was successfully subjected to reduction under anhydrous conditions using $LiAlH_4$ (**Scheme 111**). The primary amine **218** was recovered in quantitative yield as a yellow oil, with a specific optical rotation of -7.56 in chloroform (c 0.37). Only an N-H vibrational signal for the N-H bond was observed at 1596 cm^{-1} in the IR spectrum. Mass spectrometry results showed the presence of the desired product with a measured value of 452.2590 $(M+H)^+$.



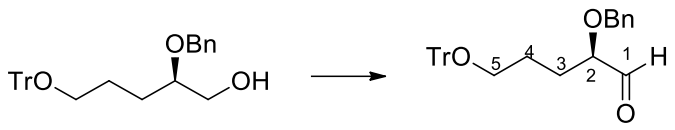
217 **218**

Scheme 111: $LiAlH_4$, Et_2O, N_2, r.t., 6 h, 100%

There were no significant changes for most of the chemical shifts of the signals in the ^1H NMR spectrum, except the H-1 signals for compound **218**. The signal was observed as a multiplet at δ 3.32 – 3.22 for compound **217**, but in the spectrum for compound **218** the H-1 signal was a doublet of doublets at δ 2.81 (*J* = 13.3, 3.9 Hz), and δ 2.70 (*J* = 13.3, 6.3 Hz). When lone pairs of electrons on a heteroatom are *anti* to a C-H bond the proton signal is shifted upfield, and there is thus a conformational dependence of chemical shifts of protons α to nitrogen. This characteristic explains the observed chemical shift changes. Analysis of the ^{13}C NMR spectrum revealed two

significant chemical shift changes. The C-1 signal had shifted upfield from δ 54.0 for compound **217** to δ 45.0 for compound **218** due to the same conformational dependence described for the proton shift. The C-2 signal shifted downfield from δ 78.0 for compound **217** to δ 80.6 for compound **218** due to anisotropic effects of the amine group.

Having successfully synthesised the amine, focus shifted to the synthesis of the aldehyde **219** from the alcohol **215** as shown in **Scheme 112**. The chemical transformation was easily achieved by using DMP as the oxidant, and leaving the reaction overnight. Product purification afforded compound **219** as a white viscous oil in an average yield of 75%. A specific optical rotation value of +35.5 (c 0.2) in chloroform confirmed the optical activity of the aldehyde. IR spectroscopy showed the disappearance of the alcohol signal and the presence of a new carbonyl signal at 1731 cm^{-1}, confirming the success of the oxidation step.

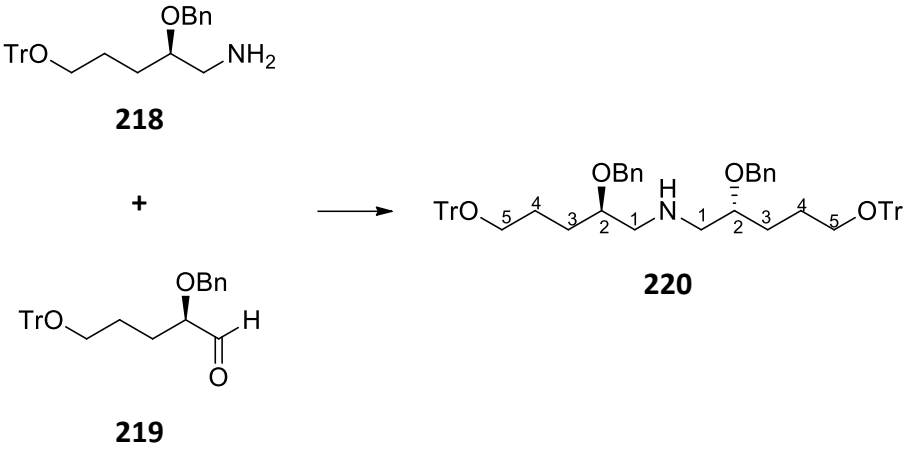


215 **219**

Scheme 112: DMP, DCM, r.t., overnight, 75%

In the ^{1}H NMR spectrum the characteristic aldehydic proton signal appeared as a doublet at δ 9.61 with a coupling constant of 2.1 Hz. Correlation between the H-1 signal and the H-2 signal in the COSY NMR spectrum confirmed coupling between the two protons, giving rise to the observed doublet. The C-1 signal was in the characteristic region at δ 203.5 in the ^{13}C NMR spectrum, a clear indication that indeed the aldehyde had been successfully synthesised.

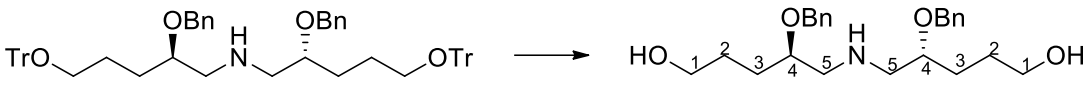
Now that the amine **218** and the aldehyde **219** had been successfully prepared, the next step involved coupling of the two fragments via reductive amination. The reaction was carried out in neat 1,2-dichloroethane and the desired product, compound **220**, was recovered in a good yield of 89% as a viscous yellow oil. The product spot stained positive for amines when the TLC plate was stained in ninhydrin. The specific optical rotation of the compound **220** was measured to be -22.7 (c 0.45) in chloroform, whilst analysis of the IR spectrum revealed the absence of the carbonyl signal from the aldehyde.



Scheme 113: $NaBH(CH_3COO)_3$, 1,2-DCE, N_2, r.t., 36 h, 89%

Due to the inherent symmetry of compound **220** only a single set of signals was observed in the NMR spectra. The H-1 signal was observed as a doublet of doublets at δ 2.76 (*J* = 12.3, 7.1 Hz) and δ 2.68 (*J* = 12.3, 4.0 Hz), because they are diastereotopic protons due to the stereogenic centre at the α-carbon. A multiplet signal was observed at δ 3.62 – 3.52 for the H-2 proton. The signal was easily distinguishable because it is the only proton signal which coupled to a CH carbon signal in the HSQC spectrum. The set of doublets for the benzylic CH_2 was at δ 4.57 and δ 4.52 with a coupling constant of 11.5 Hz displaying strong second order effects. In the ^{13}C NMR spectrum the C-1 signal was at δ 53.2 which is significantly downfield compared to the chemical shift for the starting amine. The carbonyl signal had completely disappeared. Although the alcohol **215** is a potential side product emanating from the probable reduction of the aldehyde, NMR spectroscopy did not indicate the presence of the alcohol.

Following the successful linking of the fragments, attention shifted to functionalising the terminal carbon atoms from alcohols to amines. Successful detritylation of compound **220** under acidic conditions revealed the free primary diol **221**, in an excellent yield of 88% (**Scheme 114**). The success of the procedure was most welcome because these were the only reaction conditions employable for the selective removal of the trityl group in the presence of the benzyl groups. All previous attempts at employing this trityl deprotection procedure on different substrates had been unfruitful. Purification of the desired product was not trivial because of its high polarity; therefore a highly polar mobile phase was used during chromatography. Thus the product was recovered contaminated with residual *p*-TsOH and Et_3N and the signals are evident in the NMR spectra.



220 **221**

Scheme 114: *p*-TsOH, MeOH, reflux, 4 h, 88%

^{1}H NMR spectroscopy confirmed the removal of the trityl group by the absence of the trityl aromatic signals. The multiplet for the benzylic aromatic signals was at δ 7.26 – 7.18 giving a total integration of ten protons. The amine signal was not detected in the spectrum suggesting that compound **221**, was isolated as a *p*-TsOH salt. This narrative is supported by the relative integration of the tosylate signals when compared to the product signals in the ^{1}H NMR spectrum. The H-1 protons for compound **221** were experiencing a greater deshielding effect after the removal of the trityl group. The multiplet signal migrated from δ 3.16 – 3.09 for compound **220** to δ 3.52 for compound **221** were it was observed as a triplet with a coupling constant of 6.0 Hz.

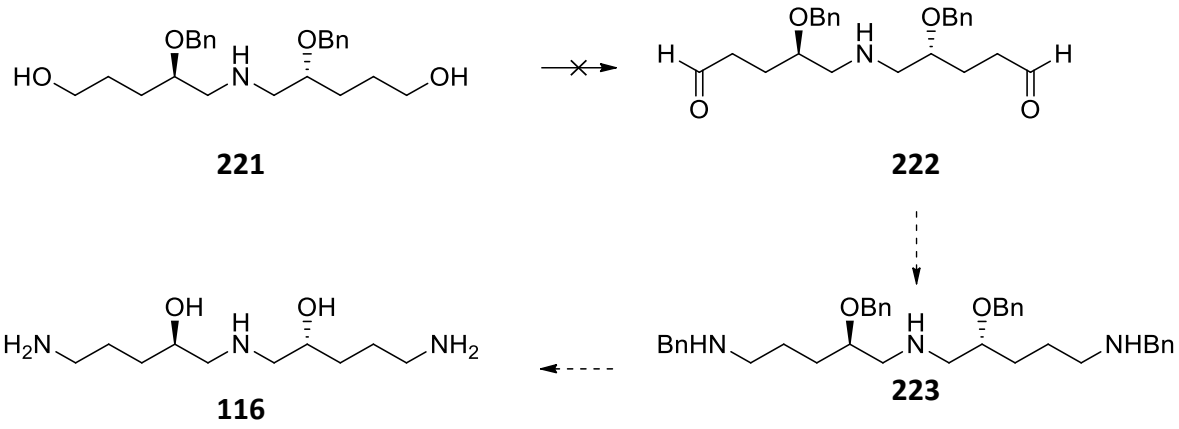
In the ^{13}C NMR spectrum, the trityl signals had disappeared, evidenced by the absence of the characteristic etherate quaternary signal previously observed at δ 86.4. The C-1 signal did not show a large chemical shift change with the signal appearing at δ 61.8, whilst the C-5 signal was observed at δ 50.5. Optical activity of the product was confirmed by the measured specific optical rotation of -10.0 (c 0.44) in chloroform. The intense broad alcohol signal was visible in the IR spectrum at 3414 cm^{-1}.

At this point, several methods for introducing the amine could be employed. The already established method of alcohol tosylation, followed by nucleophilic substitution with azide and reduction to reveal the amine was a possibility. However, tosylation would also occur on the nitrogen, and this would introduce an extra deprotection step. *N*-tosyl deprotection generally occurs under harsh conditions, and would result in the deprotection of the benzyl groups. If this happened, the resulting product would be polar and difficult to purify. Thus this option was not chosen. Amine synthesis could also be achieved by substituting the tosyl group with phthalimide, followed by deprotection to reveal the amine. However, added potential problems could arise, because liberation of the primary amine, from phthalimide, occurs under either acidic or basic conditions, meaning the desired product would be isolated as a salt.

A potentially less problematic approach was chosen. The method involved first converting the primary alcohols to aldehyde groups followed by reductive animation with benzyl amine (**Scheme**

115). Both the *N*-benzyl and *O*-benzyl are removable by hydrogenation under neutral conditions. Unfortunately, compound **222** could not be isolated. The reaction mixture turned orange after 30 minutes coupled with formation of an insoluble precipitate. Monitoring the reaction by TLC showed total consumption of the starting material. However, staining the TLC plate with 2,4-DNPH did not test positive for aldehydes. The reaction was immediately quenched, and the crude product analysed. The ^{1}H NMR spectrum showed neither the starting material nor the desired product or fragments thereof.

A possible explanation based on the absence of both reactant and product signals in the ^{1}H NMR spectrum is that the oxidation of the alcohols was successful. However, as soon as the aldehyde was formed, either an inter- or intramolecular amidation reaction between the aldehyde and the secondary amine occurred, resulting in a polymeric substance. This explains the observed insoluble precipitate from the reaction and the absence of signals in the NMR spectrum.

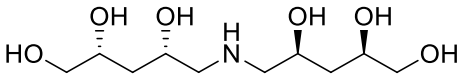


Scheme 115: DMP, DCM, r.t., 30 min

At this point, we had run out of both time and starting material but it was exciting that synthesis of the desired reduced analogue **116** was only three steps away. The whole process had highlighted the importance of protecting group compatibility and how huge a difference changing a protecting group has on several reactions. A new route for the synthesis of the reduced functionality analogues of pavettamine had also been established. The successful method development of the C-5 fragments could be applied to synthesise the enantiomers of each fragment, which would enable the development of a larger library.

Chapter 3: Conclusion and future work

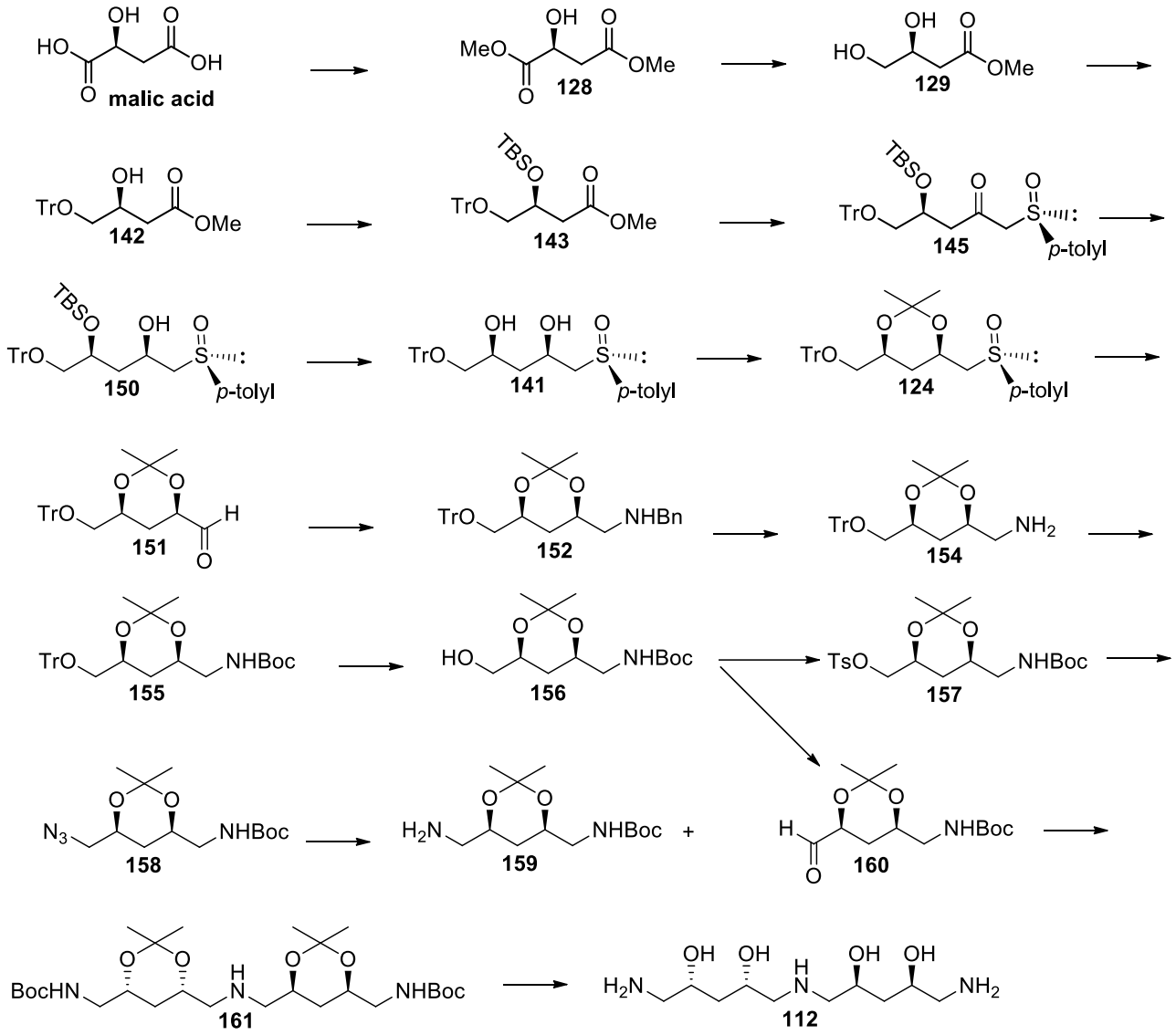
This research aimed to synthesise pavettamine, a ten-carbon polyamine toxin with C-2 symmetry and a 1,3-*syn*-diol moiety, and its analogues in order to perform a structure activity relationship study. Synthesis began with the enantiomer of pavettamine **112** (**Figure 35**), which was successfully synthesised and recovered as a TFA salt. The unveiling of this polyamine heralded the first reported total synthesis of the enantiomer of pavettamine. The introduction of the 1,3-*syn*-diol moiety was achieved with a fair degree of effort with the main challenge being protecting group compatibility. The proposed method involved stereoselective synthesis of the 1,3-*syn*-diol and selective protection and deprotection of both primary and secondary alcohols and primary and secondary amines. The similarity in reactivity of these functional groups resulted in difficulty in differentiation but fortunately, after trial and error, a suitable sequence was established. The developed synthetic protocol clearly highlighted the importance of substrate specificity when it came to protection and deprotection of both alcohols and amines. Product polarity also became a challenge to purification once the amine functionality was introduced, and this resulted in product loss during purification. Nevertheless, all these snags were surmounted and the polyamine of interest was recovered.



112

Figure 35: Structure of the enantiomer of pavettamine

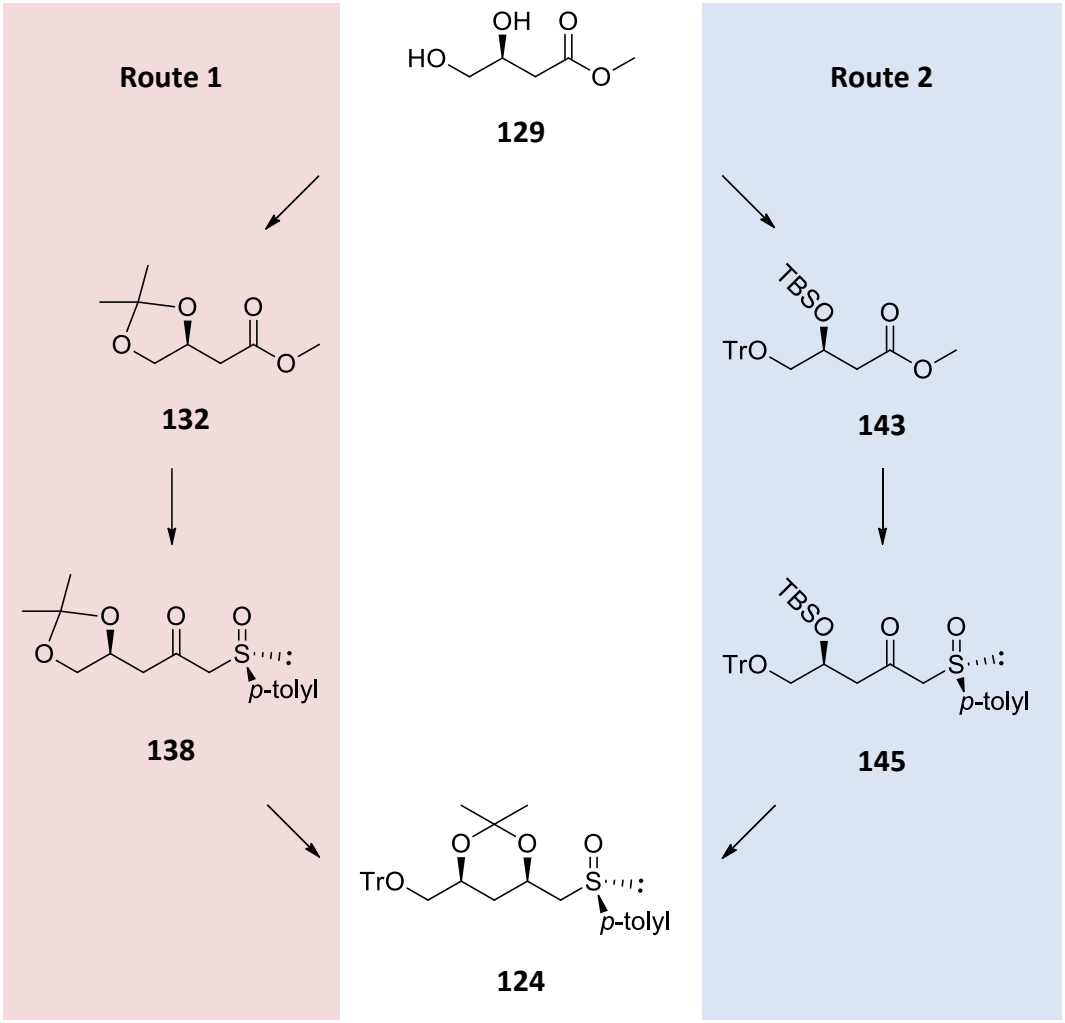
Several synthetic routes and methodologies were tested and the highest yielding overall synthetic route employed is shown in **Scheme 116**. *S*-Malic acid, identified as a suitable starting material in the retrosynthetic analysis, was first converted into a versatile fragment **124**. This intermediate was crucial in that it possessed the required 1,3-*syn*-diol moiety and allowed for the synthesis of two separate C-5 fragments which were later coupled together to unveil the C-10 carbon backbone for polyamine **112**. Other reactions of importance included functional group differentiation, selective protection and deprotection of alcohols and amines and introduction of terminal amine groups.



Scheme 116: Synthetic scheme for the total synthesis of the enantiomer of pavettamine 112

Two approaches furnished intermediate **124**, a previously reported route (Route **1**, **Scheme 117**) and a novel route (Route **2**, **Scheme 117**) developed in this work, each with its own set of pros and cons. Work began by first converting *S*-malic acid into *S*-dimethyl 2-hydroxysuccinate followed by selective reduction of the ester α to the hydroxyl group. Reduction favoured the formation of the desired *S*-methyl 3,4-dihydroxybutanoate **129** over a side product *S*-methyl 2,4-dihydroxybutanoate, from a competing reaction in an average ratio of 9:1. Yield of the desired diol can definitely be improved by carefully monitoring the reaction conditions. For this work the presence of the undesired diol only became apparent at a much later stage. Conversion to the C-5 fragment was achieved by attaching the chiral auxiliary, (+)-*R*-methyl *p*-tolylsulfoxide, to the transformed malic acid, either ester **132** or **143**, followed by stereoselective reduction,

deprotection and reprotection of the alcohols. The overall yield from *S*-methyl 3,4-dihydroxybutanoate **129** to intermediate **124** for route **1** was 8% but employing route **2** successfully doubled the overall yield to 16%. The lowest yielding step for both routes was the addition of the chiral auxiliary, *R*-methyl *p*-tolysulfoxide, to both compound **132** and **143** to give compound **138** and **145** respectively (**Scheme 117**).



Scheme 117: Synthetic route towards compound 124

The lower than expected yields were attributed to a possible side reaction which occurs once the desired product is formed. The auxiliary reaction occurs under strongly basic conditions therefore once the product has formed, an acidic CH_2 proton α to sulfur can be removed and the molecule can rearrange to give a different product. This was the case in the synthesis of compound **138** but the rearranged product was not conclusively identified. From these results it is evident that compound **145** was more stable than compound **138**, under the basic reaction conditions, hence the observed increase in the overall yield. In order to optimise the yield of compound **124**, a

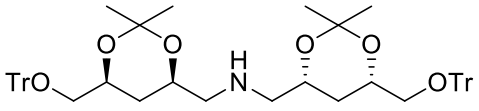
different protection protocol for both the primary and secondary alcohol of compound **143** could be investigated.

From here onwards attention shifted towards functionalisation of the terminal carbon atoms: firstly, Pummerer rearrangement and reductive amination of intermediate **124** gave rise to compound **152**. At this point meticulous steps were taken to selectively deprotect the primary alcohol of **152**, in the presence of benzyl protected amine. Several attempts at selectively removing the trityl group in the presence of the acetonide and *N*-benzyl were unfruitful and in the end, the benzyl group was selectively removed and replaced with a Boc group. Only then was the trityl group selectively removed under Birch reduction conditions affording the alcohol **156**.

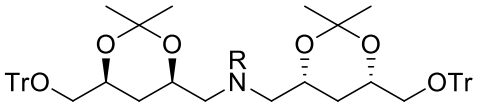
In turn, the alcohol was transformed to the amine **159** and the aldehyde **160**. The two fragments were fruitfully coupled via reductive amination and the desired dimer was recovered in an excellent yield of 95%, revealing the C-10 carbon backbone with C-2 symmetry. To our delight, the relative stereochemistry had been conserved up to this point. Great difficulty accompanied the acetonide and Boc deprotection step and because the starting material was recovered in most of the reactions, it alluded to the unreactive nature of **161**. This unreactive characteristic of the compound **161** was attributed to its conformational arrangement because of the presence of two 1,3-dioxane moieties that adopt a stable chair conformation. Several deprotection conditions were tested but only a solution of TFA:H_2O:triisoproplyamine afforded the desired polyamine **112** as a TFA salt in 100% crude yield and the polyamine was not purified further.

A similar protocol was applied for the synthesis of pavettamine and reductive amination was used for coupling of the C-5 fragments as opposed to the amidation method reported in literature. Surprisingly two products were recovered, the desired product **178** and a second product **179** (**Figure 36**). It is noteworthy that the presence of two products was not detected in the synthesis of polyamine **112** after the coupling of the C-5 fragments. The group attached to the central nitrogen atom for **179** could not be conclusively identified but mass spectroscopic analysis suggested the group to be B_2H_5. Further transformations of **179** led to the furnishing of acetonide protected pavettamine **185**. At this stage it was discovered that once the terminal primary amines had been unveiled, it was very difficult to deprotect the acetonide protected secondary alcohols. A suitable acetonide deprotection method could not be established which suggested the high

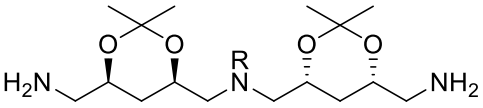
stability of the compound. Overall, throughout the project the protection and deprotection strategy was shown to be substrate dependent and it needed to be optimised for each step.



178



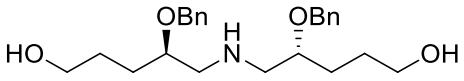
179



185

Figure 36: Structures for the precursors to pavettamine

For the synthesis of the reduced functionality analogues, two possible synthetic strategies were developed starting from either methyl 4-chlorobutanoate or y-butyrolactone. The approach employing y-butyrolactone was shown to be malleable to the aims of the project, after a matter of finding the most suitable amine and alcohol protecting groups. Despite establishing a suitable protocol for the synthesis of the reduced functionality analogues, the final compounds could not be isolated but precursor **223** (**Figure 37**) was recovered in good yields.



223

Figure 37: Structure of compound 223

In the end, the enantiomer of pavettamine **112**, acetonide protected pavettamine **185** and a precursor to the reduced functionality analogues **223** were successfully synthesised. A larger library of analogues will have to be developed before subjecting all the compounds to a comprehensive structure activity relationship biological assay. From this research work it is evident that synthesis of the 1,3-*syn*-diol functionality was achieved with a fair degree of difficulty. Major challenges were faced once the amine functionality had been introduced which increased the polarity of the substrates, resulting in routine procedures being more problematic. The art of selective protection and deprotection of amines and alcohols also played a significant role in the success of this project. Reaction conditions proved to be substrate specific and at each interval an investigation was performed to find the most suitable and applicable protocol. Nevertheless, the enantiomer of pavettamine was synthesised and a method for the synthesis of the reduced

functional analogues was developed. The fundamentals of synthesis of the polyamines were established and from here onwards, it will be much easier to build a library of compounds.

Chapter 4: Experimental procedures

4.1 General Experimental Procedures

4.1.1 Purification of solvents and reagents

All solvents used for reactions and column chromatography were purified by distillation and when required solvents were stored over activated molecular sieves (4Å) under a nitrogen atmosphere. THF, diethyl ether and toluene were dried over sodium wire and distilled, with benzophenone as indicator. DCM and MeCN were distilled from calcium hydride. All other reagents and solvents were obtained from commercial sources and used without further purification.

4.1.2 Chromatography

Thin layer chromatography was carried out using aluminium-backed Machery-Nagel ALUGRAMSil G/UV_{254} plates pre-coated with 0.25 mm silica gel 60. Column chromatography was performed on Merck silica gel of particle size 0.035 – 0.070 mm employing different types of solvents.

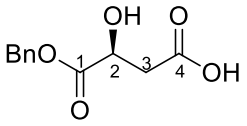
4.1.3 Spectroscopic and physical data

All melting points were obtained using a Stuart SMP10 melting point apparatus and are uncorrected. Infrared spectra were obtained using a Bruker Vector 22 spectrometer where measurements were made by directly loading the sample onto the diamond cell. All signals are reported on the wavenumber scale (v/cm^{-1}). ^{1}H NMR and ^{13}C NMR spectroscopy was performed using a Bruker Avance-300, Bruker Avance-400 or a Bruker Avance-500 spectrometer at 300 MHz, 400 MHz and 500 MHz respectively for ^{1}H NMR. The frequencies for ^{13}C NMR were recorded at 75 MHz, 100 MHz and 125 MHz. Chemical shifts are reported in parts per million and referenced against the internal standard, tetramethylsilane (TMS), which occurs at zero parts per million and coupling constants are given in Hertz. ^{13}C NMR chemical shifts are reported to 1 decimal place in general but they were also reported to 2 decimal places were necessary, and ^{1}H NMR shifts are reported to 2 decimal places. High resolution mass spectra (HRMS) were recorded on a Bruker Compact Q-TOF High Resolution Mass Spectrometer. All data was quoted in (m/z). Numbering of atoms followed the IUPAC format for nomenclature, but other numbering was used for discussion and illustration purpose only. Specific optical rotation was performed on a JASCO P-2000 polarimeter.

4.2 Experimental data

4.2.1 Preparation of (*S*)-4-(benzyloxy)-3-hydroxy-4-oxobutanoic acid 126

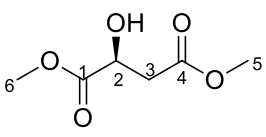
S-malic acid (20.00 g, 0.149 mol) was cooled to 0 °C followed by the addition of TFAA (15 ml, 0.149 mol). The suspension was stirred for 2 h whilst gradually warming to room temperature until all the solid had dissolved and the clear solution had turned milky. Excess TFAA and TFA were removed *in vacuo* and a white residue was recovered. The precipitate was re-dissolved in benzyl alcohol (15 ml) and left stirring overnight under N_2. The reaction mixture was diluted with EtOAc (200 ml), washed with water and the organic layer separated. The aqueous layer was acidified using 2 M HCl and washed with 2 portions of EtOAc (200 ml). The combined organic layers were washed with saturated brine (200 ml) and dried over anhydrous $MgSO_4$ and the solvent was removed under reduced pressure. Purification of the product was achieved by column chromatography (EtOAc/Hex, 1:1) yielding compound **126** (20.32 g, 61%) as a yellow oil.



R_f = 0.34 (1:1 EtOAc/Hex); **IR**: ν_{max}(cm^{-1}): 3534 (OH), 3274 (COOH, C=C-H), 1745 (C=O), 1164 (C-O); **^{1}H NMR (300 MHz, $CDCl_3$)** δ 7.39 – 7.27 (m, 5H, Ar-H), 7.06 (br-s, 2H, 2xOH), 5.19 (s, 2H, Bn-CH_2), 4.62 – 4.48 (m, 1H, H-2), 2.89 (dd, *J* = 16.7, 4.2 Hz, 1H, H-3_a), 2.80 (dd, *J* = 16.8, 6.2 Hz, 1H, H-3_b); **^{13}C NMR (75 MHz, $CDCl_3$)** δ 175.5 and 173.2 (C-1 and C-4), 134.8, 128.66, 128.65 and 128.4 (Ar-C), 67.9 (C-2), 67.2 (Bn-$\underline{C}H_2$), 38.3 (C-3).

4.2.2 Preparation of (*S*)-dimethyl 2-hydroxysuccinate 128

S-malic acid (20.00 g, 0.149 mol) was dissolved in MeOH (400 ml) and cooled to 0 °C. Thionyl chloride (24 ml, 0.328 mol) was added to the stirring solution dropwise, over a 1 h period. The reaction was allowed to proceed for 12 h whilst the temperature gradually increased to r.t. in air. Upon completion of the reaction, excess solvent and thionyl chloride were removed *in vacuo* almost to dryness and the residue was partitioned between DCM (200 ml) and a saturated aqueous solution of Na_2CO_3 (200 ml). The organic layer was separated, dried over anhydrous $MgSO_4$ followed by the removal of excess solvent. Purification of the product was achieved by column chromatography (EtOAc/Hex, 1:1) affording compound **128** (18.56 g, 77%) as a colourless oil.

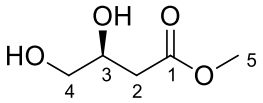


R_f = 0.59 (EtOAc/Hex, 1:1); **$[\alpha_D]^{20}$** -8.8 (c 1.0, MeOH); **IR**: ν_{max}(cm^{-1}): 3478 (OH), 2922 (C-H), 1730 (C=O), 1166 and 1102 (C-O); **^{1}H NMR (500 MHz,**

$CDCl_3$) δ 4.56 – 4.51 (m, 1H, H-2), 3.81 and 3.72 (2 x s, 6H, H-5 and H-6), 3.58 (d, *J* = 6.0 Hz, 1H, OH), 2.87 (dd, *J* = 16.4, 4.4 Hz, 1H, H-3_a) and 2.80 (dd, *J* = 16.4, 6.4 Hz, 1H, H-3_b); **^{13}C NMR (126 MHz, $CDCl_3$)** δ 173.8 and 171.1 (C-1 and C-4), 67.4 (C-2), 52.8 and 52.0 (C-5 and C-6), 38.6 (C-3).

4.2.3 Preparation of (*S*)-methyl 3,4-dihydroxybutanoate 129

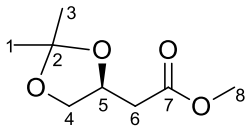
To a stirring solution of (*S*)-dimethyl 2-hydroxysuccinate **128** (17.75 g, 0.109 mol) in THF (300 ml) was added BH_3·Me_2S (12 ml, 0.120 mol) dropwise for 4 h. The reaction mixture was cooled to 0 °C in an ice bath, followed by the addition of $NaBH_4$ (53.90 mg, 1.425 mmol). After stirring for 10 min, the reaction was warmed to r.t. and stirred for an additional 1 h. Upon completion, the dropwise addition of MeOH (100 ml) and solid *p*-TsOH quenched the reaction. The reaction mixture was concentrated and purified by column chromatography (EtOAc), yielding diol **129** (13.34 g, 91%), as a colourless oil.



Compound 5: R_f = 0.30 (EtOAc); **$[\alpha_D]^{20}$** -23.7 (c 1.83, $CHCl_3$); **IR:** ν_{max}(cm^{-1}): 3372 (OH), 2955 (C-H), 1719 (C=O), 1167 (C-O); **^{1}H NMR ($CDCl_3$, 500 MHz)** δ 4.28 (d, *J* = 4.7 Hz, 1H, OH), 4.16 – 4.09 (m, 1H, H-3), 4.01 (t, *J* = 5.9 Hz, 1H, OH) 3.71 (s, 3H, H-5), 3.66 – 3.60 (m, 1H, H-4_a), 3.54 – 3.47 (m, 1H, H-4_b), 2.56 – 2.46 (m, 2H, H-2); **^{13}C NMR (126 MHz, $CDCl_3$)** δ 172.8 (C-1), 68.8 (C-3), 65.8 (C-4), 51.9 (C-5), 37.9 (C-2).

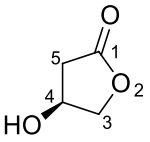
4.2.4 Preparation of (*S*)-methyl 2-(2,2-dimethyl-1,3-dioxolan-4-yl)acetate 132

(*S*)-Methyl 3,4-dihydroxybutanoate **129** (13.08 g, 97.5 mmol), 2,2 dimethoxypropane (18.0 ml, 0.146 mol) and catalytic amounts of *p*-TsOH (200 mg) were added together in acetone (20 ml) and left stirring at r.t. in air for 4 h. After completion of the reaction, addition of a few drops of Et_3N facilitated quenching of the reaction. The reaction mixture was filtered through silica gel, and washed with Et_2O (100 ml). Excess solvent was removed *in vacuo*, and the product was purified by column chromatography (EtOAc/Hex, 3:2) yielding compound **132** (13.13 g, 86%) as a yellow oil together with compound **133** as a side product.



R_f = 0.25 (EtOAc/Hex, 3:2); **$[\alpha_D]^{20}$** +20.1 (c 1.3, CH_2Cl_2); **IR:** ν_{max}(cm^{-1}): 2988 (C-H), 1735 (C=O), 1205 (C-O); **^{1}H NMR ($CDCl_3$, 500 MHz)** δ 4.50 – 4.44 (m, 1H, H-5), 4.16 (dd, *J* = 8.4, 6.0 Hz, 1H, H-4_a), 3.70 (s, 3H, H-8), 3.65 (dd, *J* = 8.4, 6.4 Hz, 1H, H-4_b), 2.72 (dd, *J* = 15.9, 6.4 Hz, 1H, H-6_a), 2.53 (dd, *J* = 15.9, 7.1 Hz, 1H, H-6_b), 1.41 and 1.35 (2 x s, 6H, H-1 and H-3); **^{13}C NMR (126 MHz, $CDCl_3$)** δ 171.0 (C-7), 109.2 (C-2), 72.1 (C-5), 69.2 (C-4), 51.8 (C-8), 38.8 (C-6), 26.9 and 25.5 (C-1 and C-3).

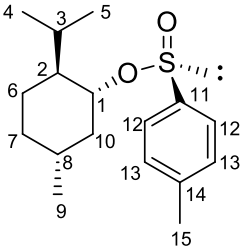
(*S*)-4-hydroxydihydrofuran-2(3H)-one 133



^{1}H NMR (500 MHz, $CDCl_3$) δ 4.56 (dd, *J* = 10.2, 8.3 Hz, 1H, H-4), 4.43 (td, *J* = 9.0, 2.1 Hz, 1H, H-3_a), 4.39 (br-s, 1H, OH), 4.24 (ddd, *J* = 10.4, 9.2, 6.1 Hz, 1H, H-3_b), 2.61 (dddd, *J* = 12.6, 8.2, 6.1, 2.0 Hz, 1H, H-5_a), 2.28 (dtd, *J* = 12.7, 10.3, 8.7 Hz, 1H, H-5_b); **^{13}C NMR (126 MHz, $CDCl_3$)** δ 178.5 (C-1), 67.4 (C-4), 65.4 (C-3), 30.9 (C-5).

4.2.5 Preparation of (-)-(*S*)-menthyl *p*-toluene sulfinate 136

Sodium *p*-toluenesulfinate (80 g, 0.449 mol) was dried overnight at 100 °C before being used in the reaction. Excess $SOCl_2$ (100 ml) was cooled to 0 °C, and sodium *p*-toluenesulfinate was added in small portions over a 1 h period. The reaction was warmed to r.t., and left stirring for a further 30 min, and the mixture had turned very viscous. The excess $SOCl_2$ was removed as an azeotropic mixture with toluene under vacuum. The residue was diluted with anhydrous diethyl ether (250 ml) resulting in a white precipitate (NaCl), and cooled to 0 °C. Menthol (77.18 g, 0.494 mol) was dissolved in pyridine (100 ml), and added dropwise to the cooled solution. After complete addition of the menthol, the reaction was stirred for 1 h at r.t., after which it was hydrolysed with water (300 ml). The organic layer was separated and washed with 10% HCl (300 ml) followed by saturated brine (300 ml). The organic layer was dried over sodium sulfate, and excess solvent was removed *in vacuo* leaving a yellowish oily residue. The residue was dissolved in hot acetone and allowed to crystallise overnight at -20 °C. After collection by filtration, the first crop of crystals was recrystallised from acetone and the initial yield was recorded separately. The mother liquor was concentrated, followed by the addition of a few drops of concentrated HCl. The solution was allowed to crystallise again at -20 °C and the procedure was repeated 5 times, whilst harvesting crystals at every stage. Finally the individual batches of product were combined and recrystallised from acetone yielding compound **136** (40.20 g, 61%) first crop before racemisation, (102.11 g, 77%) total yield after racemisation as white crystals.

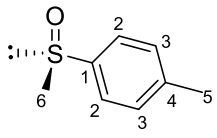


R_f = 0.35 (EtOAc/Hex, 3:2); **$[\alpha_D]^{20}$** = -196.0 (c 2, acetone); **M.p.** = 102 – 103 °C (Lit[133], **M.p.** = 105 – 107 °C); **IR:** ν_{max}(cm^{-1}): 2948 (C-H), 2846 (C-H), 1131 (S=O), 981, 952, 778; **^{1}H NMR ($CDCl_3$, 500 MHz)** δ 7.60 (d, *J* = 8.2 Hz, 2H, H-12), 7.32 (d, *J* = 7.9 Hz, 2H, H-13), 4.12 (1H, td, *J* = 10.8, 4.5 Hz, H-1), 2.41 (3H, s, H-15), 2.31 – 2.25 (1H, m, H-10_a), 2.13 (septet of doublets, *J* = 7.0, 2.6 Hz, 1H, H-3), 1.71 – 1.65 (m, 2H, H-6_a, H-7_a), 1.54 – 1.43 (m, 1H, H-8), 1.35 (ddt, *J* = 13.8, 10.6, 3.1 Hz,

1H, H-2), 1.26 – 1.18 (m, 1H, H-10_b), 1.11 – 0.99 (1H, m, H-7_b), 0.96 (3H, d, *J* = 6.6 Hz, H-9), 0.92 – 0.81 (4H, m, H-4 and H-6_b), 0.72 (3H, d, *J* = 6.9 Hz, H-5); **^{13}C NMR (126 MHz, $CDCl_3$)** δ 143.2 and 142.4 (C-11 and C-14), 129.6 (C-13) and 125.0 (C-12), 80.1 (C-1), 47.9 (C-2), 42.9 (C-10), 34.0 (C-6), 31.7 (C-8), 25.2 (C-3), 23.2 (C-7), 22.1 (C-9), 21.5 (C-15), 20.9 (C-4), 15.5 (C-5).

4.2.6 Preparation of (+)-(*R*)-methyl *p*-tolyl sulfoxide 137

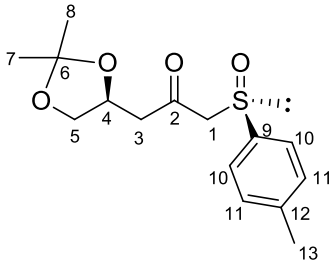
Mg (6.38 g, 0.263 mol) was placed in a 250 ml two necked round bottomed flask, one neck connected to N_2 and the other sealed with a rubber septum. The flask was heat sealed under vacuum ensuring complete dryness. Dry Et_2O (300 ml) was added to the flask containing Mg, followed by the dropwise addition of MeI (13.0 ml, 0.210 mol). The solution immediately turned milky accompanied by vigorous effervescence. After 15 min, the reaction mixture turned clear, and it was left stirring for a further 15 min after the complete addition of MeI. Meanwhile in a separate 500 ml two-necked round bottomed flask, (-)-*S*-menthyl *p*-toluenesulfinate **136** (51.65 g, 0.145 mol) was dissolved in dry toluene (300 ml) under N_2. The solution was cooled to between 0 – 10 °C, after which the MeMgI solution was slowly added. After complete addition of the Grignard reagent, the reaction was left stirring at r.t. for 2 h and was then quenched with saturated aqueous NH_4Cl solution (200 ml). The aqueous solution was extracted with Et_2O (200 ml) and the organic layer was washed with a saturated brine (100 ml), and dried over sodium sulfate. Excess solvent was removed *in vacuo* yielding a yellowish residue. The product was purified using column chromatography (EtOAc/Hex, 9:1) resulting in an off-white solid. The product was re-dissolved in hot ether, followed by the addition of hot hexane until the formation of a light cloudy precipitate was observed. Crystallisation was allowed to occur overnight at -20 °C, after which the crystals were filtered and dried yielding compound **137** (19.68 g, 73%) as an off-white solid.



R_f = 0.31 (EtOAc/Hex, 9:1); **$[\alpha_D]^{20}$** = +146.3 (c 2, acetone); **M.p.** = 73 – 74 °C (Lit[133], **M.p.** = 73 – 74 °C); **IR:** ν_{max}(cm^{-1}): 3052 (C=C-H), 2906 (C-H), 1104 (S=O); **^{1}H NMR ($CDCl_3$, 500 MHz)** δ 7.54 (d, *J* = 8.2 Hz, 2H, H-2), 7.33 (d, *J* = 7.9 Hz, 2H, H-3), 2.70 (s, 3H, H-5), 2.42 (s, 3H, H-6); **^{13}C NMR (126 MHz, $CDCl_3$)** δ 142.6 and 141.5 (C-1 and C-4), 130.0 (C-3), 123.5 (C-2), 44.0 (C-6), 21.4 (C-5).

4.2.7 Preparation of (*S*(*R*),4*S*)-4,5-*O*-isopropylidene-1-*p*-tolylsulfinyl-2-pentanone 138

n-Butyllithium (1.6 M in hexanes, 105 ml, 0.168 mol) was added to a solution of diisopropylamine (20 ml, 0.147 mol) in dry THF (100 ml) under N_2 at -78 °C. The reaction mixture was stirred for 30 min before the temperature was allowed to warm to -30 °C. *R*(+)-Methyl *p*-tolylsulfoxide **137** (19.5 g, 0.126 mol) in dry THF (50 ml) was added to the stirring mixture, and the solution turned bright yellow. The reaction mixture was allowed to stir for an additional 30 min, whilst warming to 0 °C, after which the reaction was cooled to -40 °C, and stirred for a further 10 min. (*S*)-methyl 2-(2,2-dimethyl-1,3-dioxolan-4-yl)acetate **132** (12.00 g, 0.105 mol), in THF (150 ml) was slowly added to the cooled solution, and the reaction was allowed to reach r.t. upon complete addition. After 2 h of stirring at r.t., the reaction was quenched by the addition of a saturated NH_4Cl solution (200 ml), and acidified to pH 6 using 1 M HCl. The mixture was extracted with EtOAc (3 x 100 ml). Combined organic layers were washed with H_2O (50 ml), followed by saturated brine (200 ml) and dried over anhydrous Na_2SO_4. Excess solvent was removed *in vacuo* yielding a brownish oil, which was purified by column chromatography (EtOAc/Hex, 1:1). Gradient elution was employed for eluting the desired product starting from a ratio of 1:1 and thereafter increasing the ratio to 4:1. The desired product **138** (20.0 g, 64%), was recovered as a light yellow solid.

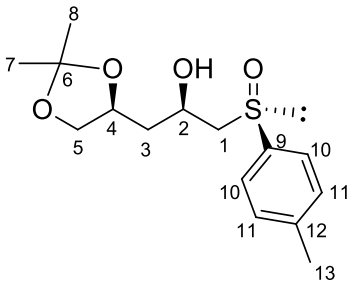


R_f = 0.46 (EtOAc/Hex, 4:1); **$[\alpha_D]^{20}$** = +151.1 (c 1.2, $CHCl_3$); **M.p.** = 78 – 79 °C (Lit[63], **M.p.** = 77 – 79 °C); **IR:** $\nu_{max}(cm^{-1})$: 3147 (C=C-H), 2916 (C-H), 1758 (C=O), 1598 and 1494 (C=C), 1033 (S=O)), 808 (C=C bending); **^{1}H NMR ($CDCl_3$, 300 MHz)** δ 7.53 (d, *J* = 8.2 Hz, 2H, H-10), 7.34 (d, *J* = 7.8 Hz, 2H, H-11), 4.40 (p, *J* = 6.4 Hz, 1H, H-4), 4.10 (dd, *J* = 8.4, 6.0 Hz, 1H, H-5_a), 3.88 (s, 2H, H-1), 3.46 (dd, *J* = 8.4, 6.5 Hz, 1H, H-5_b), 2.96 (dd, *J* = 17.2, 6.3 Hz, 1H, H-3_a), 2.64 (dd, *J* = 17.2, 6.5 Hz, 1H, H-3_b), 2.42 (s, 3H, H-13), 1.38 and 1.32 (2 x s, 6H, H-7 and H-8); **^{13}C NMR (75 MHz, $CDCl_3$)** δ 199.5 (C-2), 142.3 (C-12), 139.4 (C-9), 130.1 (C-11), 124.1 (C-10), 109.11 (C-6), 71.2 (C-4), 69.1 (C-5), 68.0 (C-1), 49.5 (C-3), 26.8 and 25.5 (C-7 and C-8), 21.4 (C-13).

4.2.8 Preparation of (*S*(*R*),2*R*,4*S*)-4,5-*O*-isopropylidene-1-(*p*-tolylsulfinyl)-pentane-2,4,5-triol 139

$ZnCl_2$ (16.9 g, 125 mmol) was flame dried under vacuum in a 500 ml 2-necked round bottomed flask, cooled and dissolved in dry THF (200 ml). (*S*(*R*),4*S*)-4,5-*O*-isopropylidene-1-(*p*-tolylsulfinyl-2-pentanone **138** (9.24 g, 31.2 mmol) was dissolved in dry THF (100 ml) and added to the $ZnCl_2$

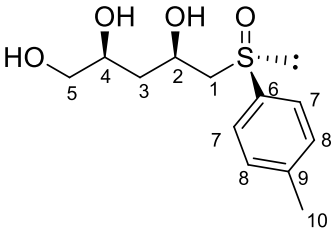
solution, and the mixture was left stirring under N_2 at r.t. for 2 h. The reaction mixture was cooled to -78 °C, and left stirring for a further 10 min, followed by the slow addition of DIBALH (1.0 M, 63.0 ml, 62.4 mmol). After the complete addition of the DIBALH, the stirring reaction was slowly warmed to r.t., and allowed to proceed for a further 2 h, after which the temperature was reduced to -78 °C. The reaction was quenched by the slow addition of a saturated solution of NH_4Cl until effervescence had stopped. Excess solvent was removed *in vacuo*, and the residue was extracted with EtOAc (3 x 150 ml). The combined organic layer was washed with saturated brine (150 ml), dried over anhydrous Na_2SO_4, and an oily residue was recovered after removal of solvent. The desired product was purified by column chromatography (EtOAc/Hex, 4:1), to afford the compound **139** (7.38 g, 79%) as a white solid.



R_f = 0.30 (EtOAc/Hex, 4:1); **$[\alpha_D]^{20}$** = +73.3 (c 0.3, $CHCl_3$); **M.p.** = 78 – 79 °C (Lit[63], **M.p.** = 87 – 89 °C); **IR:** $\nu_{max}(cm^{-1})$: 3382 (OH), 3040 (C=C-H), 2897 (C-H), 1493 (C=C), 1067 (C-OH), 1029 (S=O) (; **^{1}H NMR (500 MHz, $CDCl_3$)** δ 7.59 – 7.53 (m, 2H, H-10), 7.34 (d, *J* = 7.9 Hz, 2H, H-11), 4.36 – 4.24 (m, 2H, (H-2 and H-4), 4.09 (dd, *J* = 8.2, 6.0 Hz, 1H, H-5_a), 3.99 (br-s, 1H, OH), 3.66 – 3.57 (m, 1H, H-5_b), 3.08 (dd, *J* = 13.2, 7.9 Hz, 1H, H-1_a), 2.85 (dd, *J* = 13.2, 3.8 Hz, 1H, H-1_b), 2.42 (s, 3H, H-13), 1.96 – 1.82 (m, 2H, H-3), 1.41 and 1.34 (2 x s, 6H, H-7 and H-8); **^{13}C NMR (126 MHz, $CDCl_3$)** δ 141.9 and 140.5 (C-9 and C-12), 130.1 (C-11), 124.1 (C-10), 109.4 (C-6), 74.1 (C-2), 69.4 (C-5), 66.9 (C-4), 63.0 (C-1), 40.0 (C-3), 26.9 and 25.7 (C-7 and C-8), 21.4 (C-13).

4.2.9 Preparation of (*S*(*R*),2*R*,4*S*)-1-(*p*-tolylsulfinyl)-pentane-2,4,5-triol 140

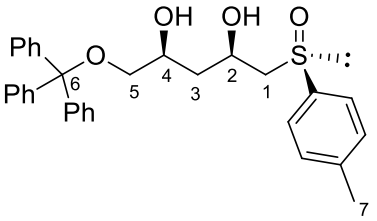
(*S*(*R*),2*R*,4*S*)-4,5-*O*-isopropylidene-1-(*p*-tolylsulfinyl)-pentane-2,4,5-triol **139** was dissolved in MeOH (200 ml) and water (50 ml), followed by the addition of *p*-TsOH (0.44 g, 2.33 mmol). The reaction was heated under reflux for 4 h, whilst monitoring the progress of the reaction by TLC. Upon completion of the reaction, Et_3N (1 ml) was added to neutralize the acid, and excess solvent was removed under reduced pressure. The residue was dissolved in water (50 ml), and extracted once with EtOAc (150 ml) for the removal of any residual organic compounds and starting material. The aqueous layer was continuously extracted with EtOAc (150 ml) for 2 days. The EtOAc solution was dried over anhydrous Na_2SO_4 and the solvent was removed under reduced pressure leaving (*S*(*R*),2*R*,4*S*)-1-(*p*-tolylsulfinyl)-pentane-2,4,5-triol **140** (3.77 g, 63%) as a white solid.



R_f = 0.22 (EtOAc/Hex, 4:1); **$[\alpha_D]^{20}$** = +258.0 (c 0.53, acetone); **M.p.** = 133 – 134 °C (Lit[63], **M.p.** = 140 – 142 °C); **IR:** ν_{max}(cm^{-1}): br-3230 (OH), 3056 (C=C-H), 2870 (C-H), 1460 (C=C), 1386, 1346 and 1317 (C-O), 1009 (S=O); **^{1}H NMR (300 MHz, $CDCl_3$)** δ 7.57 – 7.51 (m, 2H, H-7), 7.37 – 7.29 (m, 2H, H-8), 4.83 (s, 1H, OH), 4.51 – 4.39 (m, 1H, H-2), 4.18 (s, 1H, OH), 4.04 – 3.93 (m, 1H, H-4), 3.69 – 3.57 (m, 1H, H-5_a), 3.55 – 3.40 (m, 2H, H-5_b and OH), 3.19 – 3.05 (m, 1H, H-1_a), 2.83 (dd, *J* = 13.2, 3.8 Hz, 1H, H-1_b), 2.41 (s, 3H, H-10), 1.87 – 1.68 (m, 2H, H-3); **^{13}C NMR (75 MHz, $CDCl_3$)** δ 142.1 (C-6), 140.0 (C-9), 130.2 (C-8), 124.1 (C-7), 71.3 (C-4), 67.8 (C-2), 66.4 (C-5), 63.2 (C-1), 39.2 (C-3), 21.5 (C-10).

4.2.10 Synthesis of (2*R*,4*S*)-1-((*S*)-*p*-tolylsulfinyl)-5-(trityloxy)pentane-2,4-diol 141

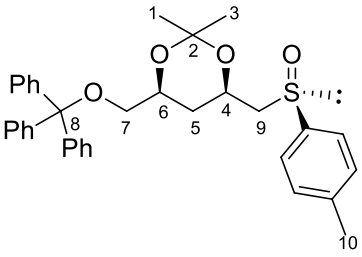
DMAP (0.34 g, 2.79 mmol) and trityl chloride (4.28 g, 15.4 mmol) were added to a stirring solution of compound **140** (3.61 g, 13.9 mmol) in DCM (60 ml) and pyridine (4.5 ml). The reaction was left stirring for 24 h, whilst monitoring the completion of the reaction using TLC analysis. After completion of the reaction, the mixture was washed with 1 M HCl (4 x 100 ml) followed by saturated brine (100 ml). The organic layer was separated and dried over anhydrous Na_2SO_4 and excess solvent was then removed *in vacuo* leaving a very viscous oil. The product was purified using column chromatography (EtOAc/Hex, 4:1) to afford compound **141** (4.52 g, 65%), as a white solid.



R_f = 0.38 (EtOAc/Hex, 4:1); **$[\alpha_D]^{21}$** = +118.6 (c 0.98, acetone); **M.p.** = 65 – 66 °C (Lit[63], **M.p.** = 74 – 76 °C); **IR:** ν_{max}(cm^{-1}): br-3355 (OH), 3056 (C=C-H), 2918 (C-H), 1596 (C=C), 1221 (C-O), 1083 (C-O), 1030 (S=O); **^{1}H NMR (500 MHz, $CDCl_3$)** δ 7.55 – 7.52 (m, 2H, Ar-H), 7.43 – 7.37 (m, 6H, Ar-H), 7.35 – 7.20 (m, 11H, Ar-H), 4.42 – 4.35 (m, 1H, H-2), 4.31 (s, 1H, OH), 4.08 – 4.01 (m, 1H, H-4), 3.15 (d, *J* = 2.7 Hz, 1H, OH), 3.11 (d, *J* = 5.6 Hz, 2H, H-5), 3.03 (dd, *J* = 13.2, 8.2 Hz, 1H, H-1_a), 2.79 (dd, *J* = 13.2, 3.4 Hz, 1H, H-1_b), 2.41 (s, 3H, H-7), 1.77 – 1.67 (m, 2H, H-3); **^{13}C NMR (126 MHz, $CDCl_3$)** δ 143.7, 141.9, 140.5, 130.1, 128.6, 127.9, 127.1 and 124.1 (Ar-C), 86.8 (C-6), 70.6 (C-4), 68.3 (C-2), 67.4 (C-5), 62.9 (C-1), 39.4 (C-3), 21.4 (C-7).

4.2.11 Synthesis of (4*R*,6*S*)-2,2-dimethyl-4-(((*S*)-*p*-tolylsulfinyl)methyl)-6-((trityloxy)methyl)-1,3-dioxane 124

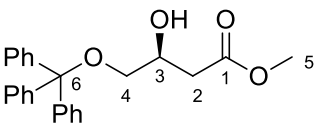
Compound **141** (4.40 g, 8.79 mmol), 2,2-dimethoxypropane (30 ml, 19.2 mmol) and *p*-toluene sulfonic acid (125 mg) were dissolved in acetone (40 ml). The mixture was then left stirring for 1 h after which a few drops of Et_3N were added to neutralise the acid. Excess solvent was removed *in vacuo*, and a white precipitate was recovered. Purification of the desired product by column chromatography (EtOAc/Hex, 1:1) afforded compound **124** (4.08 g, 86%) as a white solid.



R_f = 0.46 (EtOAc/Hex, 1:1); **$[\alpha_D]^{21}$** = +28.1 (c 1.09, acetone); **M.p.** = 164 – 165 °C (Lit[63], **M.p.** = 167 – 168 °C); **IR:** $\nu_{max}(cm^{-1})$: 3036 (C=C-H), 2925 (C-H), 1597 (C=C), 1161, 1100 and 1078 (C-O), 1047 (S=O); **^{1}H NMR (500 MHz, $CDCl_3$)** δ 7.55 – 7.52 (m, 2H, Ar-H), 7.45 – 7.41 (m, 6H, Ar-H), 7.33 – 7.19 (m, 11H, Ar-H), 4.13 – 4.06 (m, 1H, H-4), 3.97 (dtd, *J* = 11.4, 5.6, 2.4 Hz, 1H, H-6), 3.23 (dd, *J* = 9.3, 5.2 Hz, 1H, H-7_a), 3.15 (dd, *J* = 13.1, 6.8 Hz, 1H, H-9_a), 2.96 (dd, *J* = 9.3, 6.0 Hz, 1H, H-7_b), 2.76 (dd, *J* = 13.1, 5.4 Hz, 1H, H-9_b), 2.41 (s, 3H, H-10), 1.75 (dt, *J* = 12.8, 2.5 Hz, 1H, H-5_a), 1.40 – 1.34 (m, 1H, H-5_b), 1.33 and 1.30 (2 x s, 6H, H-1 and H-3); **^{13}C NMR (126 MHz, $CDCl_3$)** δ 143.9, 141.6, 140.3, 129.8, 128.7, 127.8, 127.0 and 124.4 (Ar-C), 98.9 (C-2), 86.5 (C-8), 68.2 (C-4), 67.0 (C-7), 63.9 (C-6), 63.1 (C-9), 33.6 (C-5), 29.7 (C-3), 21.4 (C-10), 19.6 (C-1).

4.2.12 Synthesis of (*S*)-methyl 3-hydroxy-4-(trityloxy)butanoate 142

Compound **129** (3.77 g, 28.1 mmol) was dissolved in pyridine (9 ml) and DCM (30 ml) followed by the addition of DMAP (1.72 g, 14.1 mmol) and trityl chloride (8.62 g, 30.9 mmol), and the reaction was left stirring overnight. TLC analysis showed total consumption of the starting material. The reaction mixture was washed with 1 M HCl (4 x 100 ml) followed by saturated brine (200 ml). The organic layer was dried over Na_2SO_4 and excess solvent was removed *in vacuo*. Purification of the product by column chromatography (EtOAc/Hex, 3:7) afforded compound **142** (10.55 g, 100%) as a yellow oil.

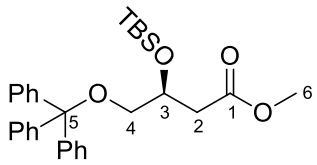


R_f = 0.42 (EtOAc/Hex, 3:7); **$[\alpha_D]^{20}$** = -15.0 (c 1.05, $CHCl_3$); **M.p**: 129 – 130 °C **IR**: $\nu_{max}(cm^{-1})$: 3469 (OH), 3058 (C=C-H), 2951 (C-H), 1732 (C=O), 1597 (C=C), 1216 (C-O); **^{1}H NMR (300 MHz, $CDCl_3$)** δ 7.47 – 7.39 (m, 6H, Ar-H), 7.33 – 7.16 (m, 9H, Ar-H), 4.28 – 4.16 (m, 1H, H-3), 3.63 (s, 3H, H-5), 3.16 (d, *J* = 5.4 Hz, 2H,

H-4), 3.02 (d, *J* = 4.6 Hz, 1H, OH), 2.64 – 2.43 (m, 2H, H-2); **^{13}C NMR (75 MHz, $CDCl_3$)** δ 172.5 (C-1), 143.7, 128.4, 127.7 and 126.9 (Ar-C), 86.7 (C-6), 67.5 (C-3), 66.6 (C-4), 51.7 (C-5), 38.4 (C-2); **HRMS** (m/z), calculated for $C_{24}H_{24}NaO_4$: 399.1567, found $(M+Na)^+$: 399.1561.

4.2.13 Synthesis of (*S*)-methyl 3-((*tert*-butyldimethylsilyl)oxy)-4-(trityloxy)butanoate 143

To a stirring solution of compound **142** (10.40 g, 27.8 mmol) in DCM was added, 1.5 equiv of TBSCl (5.03 g, 33.4 mmol), imidazole (1.5 equiv, 2.84 g, 41.7 mmol) and DMAP (5.12 g, 41.7 mmol) sequentially. TLC showed total consumption of the starting material after 12 h. Work up of the reaction by washing the reaction mixture with H_2O (300 ml), saturated brine (300 ml), and drying the organic layer over Na_2SO_4, followed by the removal of excess solvent *in vacuo* afforded the crude product. Purification was achieved by column chromatography (EtOAc/Hex, 1:9) yielding compound **143** (8.82 g, 65%) as a white precipitate.

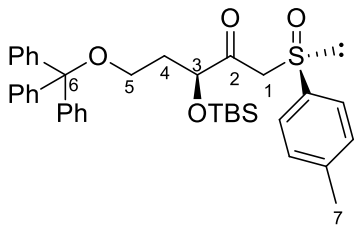


R_f = 0.38 (EtOAc/Hex, 1:9); **$[\alpha_D]^{20}$** = -13.4 (c 1.00, $CHCl_3$); **M.p**: 70 – 71 °C **IR**: ν_{max}(cm^{-1}): 3058 (C=C-H), 2928 (C-H), 1738 (C=O), 1598 (C=C), 1123, 1074 and 1031 (C-O); **^{1}H NMR (300 MHz, $CDCl_3$)** δ 7.49 – 7.38 (m, 6H, Ar-H), 7.35 – 7.16 (m, 9H, Ar-H), 4.31 – 4.19 (m, 1H, H-3), 3.63 (s, 3H, H-6), 3.18 – 3.09 (m, 1H, H-4_a), 3.06 – 2.96 (m, 1H, H-4_b), 2.75 (dd, *J* = 14.9, 4.5 Hz, 1H, H-2_a), 2.47 (dd, *J* = 14.9, 8.1 Hz, 1H, H-2_b), 0.80 (s, 9H, TBS-C(CH_3)$_3$), -0.02 and -0.08 (2 x s, 6H, TBS-Si(CH_3)$_2$); **^{13}C NMR (75 MHz, $CDCl_3$)** δ 172.2 (C-1), 143.9, 128.7, 127.8 and 127.0 (Ar-C), 86.7 (C-5), 68.9 (C-3), 67.2 (C-4), 51.4 (C-6), 40.7 (C-2), 25.7 (TBS-C($\underline{C}H_3$)$_3$), 17.9 (TBS-$\underline{C}$(CH_3)$_3$), -4.6 and -5.2 (TBS-Si(CH_3)$_2$); **HRMS** (m/z), calculated for $C_{30}H_{38}NaO_4Si$: 513.2432, found $(M+Na)^+$: 513.2422.

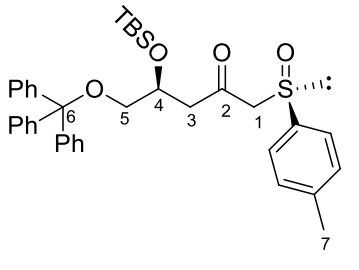
4.2.14 Sulfoxide addition to (*S*)-methyl 3-((tert-butyldimethylsilyl)oxy)-4-(trityloxy)butanoate 145

LDA (1.0 M in hexanes, 26 ml, 26.0 mmol) was added to dry THF (100 ml) under N_2 at -78 °C, followed by the addition of *R*(+)-methyl *p*-tolyl sulfoxide **137** (3.21 g, 20.8 mmol) in dry THF (50 ml). The reaction proceeded for 30 min, during which the solution turned bright orange whilst the temperature was slowly raised to -40 °C. In a separate two-necked flask, (*S*)-methyl 2-(2,2-dimethyl-1,3-dioxolan-4-yl)acetate **143** (5.10 g, 10.4 mmol) was dissolved in dry THF (100 ml), and cooled to -40 °C. The methyl sulfoxide solution was added dropwise using a cannula needle to the stirring solution of compound **143**, and the reaction was allowed to reach r.t. upon complete

addition. After 2 h of stirring at r.t. the reaction was quenched by the addition of saturated aqueous NH_4Cl solution (200 ml), and acidified to pH 6 using 1 M HCl. The mixture was extracted with EtOAc (3 x 100 ml). The combined organic layers were washed with H_2O (100 ml), followed by saturated brine solution (100 ml), and dried over anhydrous Na_2SO_4. TLC showed two products of potential significance. Excess solvent was removed *in vacuo* yielding a brownish oil, which was purified by column chromatography. Gradient elution was used for separating the desired products starting from (EtOAc/Hex, 1:1) and then increasing the ratio to 4:1. The separated compound **144** (1.50 g, 24%), and compound **145** (3.49 g, 55%) were recovered as pale yellow solids.



Compound 144 : (*S*)-3-((tert-butyldimethylsilyl)oxy)-1-((*R*)-*p*-tolylsulfinyl)-5-(trityloxy)pentan-2-one: R_f = 0.48 (EtOAc/Hex, 3:7); $[\alpha_D]^{20}$ = +91.4 (c 1.3, $CHCl_3$); **M.p.** = 115 – 116 °C; **IR**: ν_{max}(cm^{-1}): 3056 (C=C-H), 2951 (C-H), 1716 (C=O), 1083 (C-O), 1067 (S=O); **^{1}H NMR (300 MHz, $CDCl_3$)** δ 7.56 – 7.50 (m, 2H, Ar-H), 7.41 – 7.34 (m, 6H, Ar-H), 7.33 – 7.16 (m, 11H, Ar-H), 4.18 (t, *J* = 5.5 Hz, 1H, H-3), 4.07 (d, *J* = 14.8 Hz, 1H, H-1_a), 3.92 (d, *J* = 14.8 Hz, 1H, H-1_b), 3.32 – 3.18 (m, 1H, H-5_a), 3.17 – 3.04 (m, 1H, H-5_b), 2.40 (s, 3H, H-7), 2.12 – 1.95 (m, 1H, H-4_a), 1.90 – 1.75 (m, 1H, H-4_b), 0.75 (s, 9H, TBS-C(CH_3)$_3$), -0.07 and -0.13 (2 x s, 6H, TBS-Si(CH_3)$_2$); **^{13}C NMR (75 MHz, $CDCl_3$)** δ 204.7 (C-2), 143.8, 141.9, 141.0, 130.0, 128.6, 127.8, 127.0 and 124.3 (Ar-C), 87.3 (C-6), 76.2 (C-3), 65.3 (C-1), 58.7 (C-5), 34.5 (C-4), 25.7 (TBS-C($\underline{C}H_3$)$_3$), 21.4 (C-7), 17.9 (TBS-$\underline{C}$(CH_3)$_3$), -5.0 and -5.1 (TBS-Si(CH_3)$_2$); **HRMS** (m/z), calculated for $C_{37}H_{44}NaO_4SSi$: 635.2622, found $(M+Na)^+$: 635.2621.

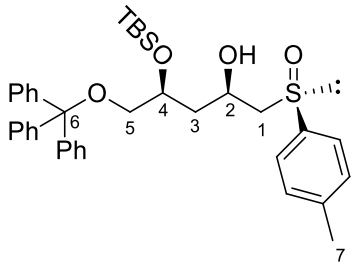


Compound 145 : (*S*)-4-((*tert*-butyldimethylsilyl)oxy)-1-((*R*)-*p*-tolylsulfinyl)-5-(trityloxy)pentan-2-one: R_f = 0.46 (EtOAc/Hex, 3:7); $[\alpha_D]^{20}$ = +67.0 (c 1.3, $CHCl_3$); **M.p.** = 115 – 116 °C; **IR**: ν_{max}(cm^{-1}): 3064 (C=C-H), 2950 (C-H), 1712 (C=O), 1080 (C-O), 1050 (S=O); **^{1}H NMR (300 MHz, $CDCl_3$)** δ 7.45 (d, *J* = 7.9 Hz, 2H, Ar-H), 7.42 – 7.36 (m, 6H, Ar-H), 7.32 – 7.17 (m, 11H, Ar-H), 4.28 – 4.17 (m, 1H, H-4), 3.88 (d, *J* = 14.0 Hz, 1H, H-1_a), 3.76 (d, *J* = 14.0 Hz, 1H, H-1_b), 3.10 (dd, *J* = 9.3, 4.6 Hz, 1H, H-5_a), 2.95 (dd, *J* = 9.3, 6.8 Hz, 1H, H-5_b), 2.80 – 2.62 (m, 2H, H-3), 2.36 (s, 3H, H-7), 0.79 (s, 9H, TBS-C(CH_3)$_3$), -0.02 and -0.09 (2 x s, 6H, TBS-Si(CH_3)$_2$); **^{13}C NMR (75 MHz, $CDCl_3$)** δ 200.5 (C-2), 143.7, 142.0, 140.0, 130.0, 128.6, 127.8, 127.1 and 124.1 (Ar-C), 86.9 (C-6), 69.9 (C-1), 68.3 (C-4), 67.1 (C-5), 50.0 (C-3), 25.7 (TBS-C($\underline{C}H_3$)$_3$), 21.4

(C-7), 17.9 (TBS-C(CH$_3$)$_3$), -4.7 and-5.0 (TBS-Si(CH$_3$)$_2$); **HRMS** (m/z), calculated for $C_{37}H_{44}NaO_4SSi$: 635.2622, found $(M+Na)^+$: 635.2616.

4.2.15 Synthesis of (2*R*,4*S*)-4-((*tert*-butyldimethylsilyl)oxy)-1-((*R*)-*p*-tolylsulfinyl)-5-(trityloxy)pentan-2-ol 150

$ZnCl_2$ (3.25 g, 23.8 mmol) was flame dried under vacuum in a 500 ml 2-necked round bottomed flask, cooled and dissolved in dry THF (200 ml). (*S*)-4-((*tert*-butyldimethylsilyl)oxy)-1-((*R*)-*p*-tolylsulfinyl)-5-(trityloxy)pentan-2-one **145** (3.65 g, 5.96 mmol) was dissolved in dry THF (100 ml) and added to the $ZnCl_2$ solution and the mixture was left stirring under N_2 at r.t. for 2 h. The reaction mixture was cooled to -78 °C, left stirring for 10 min followed by the dropwise addition of DIBALH (1.0 M, 9.0 ml, 9.0 mmol). After the complete addition of the DIBALH, the stirring reaction was warmed to r.t. and allowed to proceed for a further 2 h after which the temperature was reduced to -78 °C. The reaction was then quenched by the slow addition of a saturated aqueous solution of NH_4Cl until effervescence had stopped. Excess solvent was removed *in vacuo* and the residue was extracted with EtOAc (3 x 150 ml). The combined organic layers were washed with saturated brine (150 ml), dried over anhydrous Na_2SO_4 and an oily residue was recovered after removal of solvent. Purification of the desired compound was afforded by column chromatography (EtOAc/Hex, 3:7) yielding the compound **150** (3.20 g, 87%) as a yellow solid.



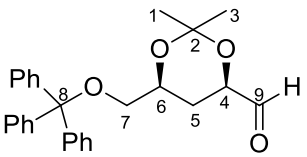
R$_f$ = 0.27 (EtOAc/Hex, 3:7); **[α$_D$]^{20}** = +43.0 (c 1.3, $CHCl_3$); **M.p.** = 45 – 46 °C; **IR**: ν_{max}(cm^{-1}): 3339 (OH), 3058 (C=C-H), 2952 (C-H), 1251, 1155, 1083 (C-O), 1029 (S=O); **^{1}H NMR (500 MHz, CDCl$_3$)** δ 7.55 (d, *J* = 8.2 Hz, 2H, Ar-H), 7.46 – 7.38 (m, 6H, Ar-H), 7.35 – 7.19 (m, 11H, Ar-H), 4.24 – 4.07 (m, 1H, H-2), 3.97 – 3.87 (m, 2H, H-4 and OH), 3.15 – 3.00 (m, 3H, H-1$_a$ and H-5), 2.77 (dd, *J* = 13.0, 3.1 Hz, H-1$_b$), 2.42 (s, 3H, H-7), 1.95 (dt, *J* = 14.2, 4.7 Hz, 1H, H-3$_a$), 1.89 – 1.77 (m, 1H, H-3$_b$), 0.80 (s, 9H, TBS-C(CH$_3$)$_3$), -0.04 and -0.10 (2 x s, 6H, TBS-Si(CH$_3$)$_2$); **^{13}C NMR (126 MHz, CDCl$_3$)** δ 143.8, 141.8, 140.7, 130.0, 128.7, 127.9, 127.1 and 124.2 (Ar-C), 86.9 (C-6), 70.2 (C-4), 67.3 (C-5), 66.3 (C-2), 63.7 (C-1), 41.7 (C-3), 25.8 (TBS-C(CH$_3$)$_3$), 21.5 (C-7), 17.9 (TBS-C(CH$_3$)$_3$), -4.4 and -4.9 (TBS-Si(CH$_3$)$_2$); **HRMS** (m/z), calculated for $C_{37}H_{46}NaO_4SSi$: 637.6722, found $(M+Na)^+$: 637.6729.

4.2.16 Synthesis of (2*R*,4*S*)-1-((*S*)-*p*-tolylsulfinyl)-5-(trityloxy)pentane-2,4-diol 141

To a solution of compound **150** (2.90 g, 4.71 mmol) in dry THF (150 ml) was added TBAF (1.5 equiv, 7.00 ml) under N_2 at 0 °C. The reaction was stirred for 4 h until completion, whilst monitoring by TLC. Quenching of the reaction was achieved by addition of saturated aqueous NH_4Cl solution (50 ml), followed by washing with saturated brine (100 ml). The organic layer was separated and dried over anhydrous Na_2SO_4 and excess solvent was removed *in vacuo*. Purification of the desired product using column chromatography (EtOAc/Hex, 4:1) yielded the desired product as a white precipitate, compound **141** (2.08 g, 87%), **$[\alpha_D]^{20}$** = +83.3 (c 1.00, $CHCl_3$). See compound **141** for the rest of the NMR spectroscopic data.

4.2.17 Synthesis of (4*R*,6*S*)-2,2-dimethyl-6-((trityloxy)methyl)-1,3-dioxane-4-carbaldehyde 151

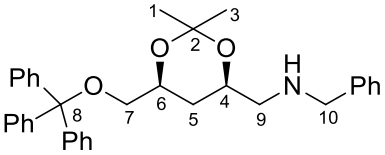
Compound **124** (3.38 g, 6.26 mmol) was dissolved in dry MeCN (20 ml) followed by the subsequent addition of collidine (2.48 ml, 18.77 mmol) and TFAA (4.35 ml, 31.28 mmol) at 0 °C. The reaction proceeded for 30 min until total consumption of the starting material was detected, before quenching with water (1 ml) followed by solid K_2CO_3 until the reaction mixture was neutral. Stirring of the reaction continued for a further 30 min at room temperature after which it was diluted with EtOAc (250 ml), washed with saturated aqueous NH_4Cl solution (200 ml), 1M HCl (100 ml), saturated $NaHCO_3$ solution (200 ml) and saturated brine solution (250 ml). The organic layer was separated, and dried over anhydrous Na_2SO_4 and excess solvent was removed *in vacuo*. Purification of the desired product was achieved by column chromatography employing gradient elution (EtOAc/Hex, 1:9 to 1:1) yielding compound **151** (2.59 g, 99%), as a white solid.



R_f = 0.30 (EtOAc/Hex, 1:1); **M.p.**: 61 – 62 °C; **IR**: ν_{max}(cm^{-1}): 3059 (C=C-H), 2991 (C-H), 1736 (C=O), 1258, 1165, 1076 (C-O) **^{1}H NMR (300 MHz, $CDCl_3$)** δ 9.58 (s, 1H, H-9), 7.50 – 7.40 (m, 6H, Ar-H), 7.34 – 7.17 (m, 9H, Ar-H), 4.30 (dd, *J* = 12.3, 3.0 Hz, 1H, H-4), 4.09 – 3.96 (m, 1H, H-6), 3.26 (dd, *J* = 9.4, 5.2 Hz, 1H, H-7_a), 3.02 (dd, *J* = 9.4, 6.1 Hz, 1H, H-7_b), 1.88 (dt, *J* = 13.0, 2.8 Hz, 1H, H-5_a), 1.462 and 1.457 (2 x s, 6H, H-1 and H-3), 1.43 – 1.32 (m, 1H, H-5_b); **^{13}C NMR (75 MHz, $CDCl_3$)** δ 201.1 (C-9), 143.9, 128.7, 127.8 and 127.0 (Ar-C), 99.0 (C-2), 86.6 (C-8), 73.8 (C-4), 67.9 (C-6), 66.9 (C-7), 29.6 (C-3), 28.6 (C-5), 19.4 (C-1).

4.2.18 Synthesis of *N*-benzyl-1-((4*R*,6*S*)-2,2-dimethyl-6-((trityloxy)methyl)-1,3-dioxan-4-yl)methanamine 152

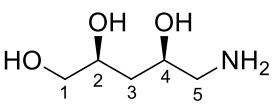
A solution of benzylamine (774 µl, 7.08 mmol) in 1,2-dichloroethane (18 ml) was added to a solution of compound **151** (2.27 g, 5.44 mmol) in THF (2 ml) stirring under N_2. The mixture was treated with sodium triacetoxyborohydride (1.61 g, 7.61 mmol) in one portion and the reaction was allowed to proceed for 24 h whilst monitoring by TLC. Quenching of the reaction was achieved by addition of 1 M NaOH (20 ml) followed by extraction of the organic layer with DCM (100 ml). The organic layer was washed with saturated brine solution (100 ml), and dried over anhydrous Na_2SO_4, followed by solvent removal *in vacuo.* Purification by column chromatography (EtOAc/Hex, 1:1) yielded the desired product **152** (1.65 g, 60%) as a colourless thick gel.



R_f = 0.38 (EtOAc/Hex, 1:1); **$[\alpha_D]^{20}$** = -16.8 (c 0.9, $CHCl_3$); **IR**: ν_{max}(cm^{-1}): 3316 (NH), 3060 (C=C-H), 2986 (C-H), 1092 (C-O); **^{1}H NMR (400 MHz, $CDCl_3$)** δ 7.54 – 7.48 (m, 6H, Ar), 7.40 – 7.24 (m, 14H, Ar-H), 4.16 – 4.00 (m, 2H, H-4 and H-6), 3.85 (s, 2H, H-10), 3.30 (dd, *J* = 9.2, 5.3 Hz, 1H, H-7_a), 3.02 (dd, *J* = 9.2, 6.0 Hz, 1H, H-7_b), 2.77 – 2.66 (m, 2H, H-9), 2.08 (br-s, 1H, NH), 1.64 (dt, *J* = 12.8, 2.5 Hz, 1H, H-5_a), 1.50 and 1.44 (2 x s, 6H, H-1 and H-3), 1.36 – 1.23 (m, 1H, H-5_b); **^{13}C NMR (75 MHz, $CDCl_3$)** δ 144.0, 140.3, 128.7, 128.3, 128.1, 127.7 and 126.9 (Ar-C), 98.6 (C-2), 86.4 (C-8), 68.34 and 68.27 (C-4 and C-6), 67.3 (C-7), 54.6 (C-9), 53.9 (C-10), 32.1 (C-5), 30.0 and 19.9 (C-3 and C-1); **HRMS** (m/z), calculated for $C_{14}H_{37}NO_3$: 508.2866, found $(M+H)^+$: 508.2865.

4.2.19 Synthesis of (2*S*,4*R*)-5-aminopentane-1,2,4-triol 153

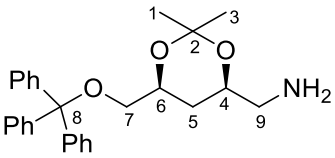
Compound **152** (0.490 g, 0.965 mmol) was dissolved in ethanol (5 ml) followed by the addition of Pd/C (0.050 g, 10%) and a few drops of formic acid. The reaction was left stirring overnight under H_2 at atmospheric pressure. After reaction completion, the crude product was filtered over celite, and excess solvent was removed under reduced pressure. Purification of the product was afforded by column chromatography ($CHCl_3$/MeOH, 4:1) yielding compound **153** (0.152 g, 90%) as a yellow oil.



R_f = 0.28 ($CHCl_3$/MeOH, 9:1); **^{1}H NMR (300 MHz, MeOD**) δ 4.03 – 3.89 (m, 1H, H-4), 3.82 – 3.68 (m, 1H, H-2), 3.52 – 3.32 (m, 2H, H-1), 3.13 – 2.96 (m, 1H, H-5_a), 2.86 – 2.72 (m, 1H, H-5_b), 1.73 – 1.51 (m, 2H, H-3); **^{13}C NMR (75 MHz, MeOD**) δ 70.5 (C-2), 67.1 (C-4), 66.9 (C-1), 46.0 (C-5), 39.0 (C-3).

4.2.20 ((4*R*,6*S*)-2,2-dimethyl-6-((trityloxy)methyl)-1,3-dioxan-4-yl)methanamine 154

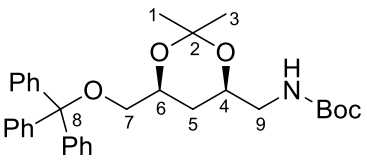
Compound **152** (1.04 g, 2.05 mmol) was dissolved in ethanol (10 ml) and left stirring under N_2 for 15 min, followed by the addition of Pd/C (1.00 g, 10%). The reaction was left stirring for a further 15 min before introducing H_2. Completion of the reaction was observed after 24 h of regular monitoring using TLC. The mixture was filtered through a celite plug and excess solvent was removed *in vacuo*. Purification of the desired product was achieved by column chromatography (DCM/MeOH, 95:5) yielding compound **154** (0.71 g, 84%) as a white gluey viscous oil.



R_f = 0.27 (DCM/MeOH, 1:1); **$[\alpha_D]^{20}$** = -24.6 (c 1.0, $CHCl_3$); **IR**: ν_{max}(cm^{-1}): 3319 (NH), 3057 (C=C-H), 2924 (C-H), 1052 (C-O); **^{1}H NMR (300 MHz, $CDCl_3$)** ^{1}H NMR (300 MHz, $CDCl_3$) δ 7.48 – 7.42 (m, 6H, Ar-H), 7.32 – 7.18 (m, 9H, Ar-H), 4.03 (dtd, *J* = 11.5, 5.6, 2.5 Hz, 1H, H-6), 3.92 – 3.78 (m, 1H, H-4), 3.25 (dd, *J* = 9.2, 5.3 Hz, 1H, H-7_a), 2.96 (dd, *J* = 9.2, 6.0 Hz, 1H, H-7_b), 2.80 – 2.62 (m, 2H, H-9), 1.65 (br-s, 2H, NH_2), 1.58 (dt, *J* = 12.7, 2.5 Hz, 1H, H-5_a), 1.45 and 1.39 (2 x s, 6H, H-1 and H-3), 1.29 – 1.10 (m, 1H, H-5_b), **^{13}C NMR (75 MHz, $CDCl_3$)** δ 144.0, 128.7, 127.7 and 126.9 (Ar-C), 98.6 (C-2), 86.5 (C-8), 70.5 (C-4), 68.2 (C-6), 67.3 (C-7), 47.4 (C-9), 31.6 (C-5), 30.0 and 19.9 (C-3 and C-1); **HRMS** (m/z), calculated for $C_{27}H_{32}NO_3$: 418.2377, found $(M+H)^+$: 418.2376.

4.2.21 Synthesis of *tert*-butyl (((4*R*,6*S*)-2,2-dimethyl-6-((trityloxy)methyl)-1,3-dioxan-4-yl)methyl)carbamate 155

Compound **154** (0.68 g, 1.63 mmol) was dissolved in THF (50 ml), followed by the addition of Boc anhydride (0.43 g, 1.96 mmol) and DMAP (10 mg, 0.082 mmol). The reaction was left stirring overnight and TLC showed total consumption of the starting material. Work up of the experimental mixture was achieved by diluting with DCM (100 ml) followed by washing with H_2O (100 ml) and saturated brine solution (150 ml). The organic layer was separated, dried over anhydrous Na_2SO_4 and excess solvent was removed *in vacuo*. The desired product **155** was recovered as a white solid (0. 85 g, 100%).

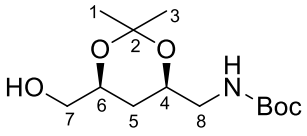


R_f = 0.30 (EtOAc/Hex, 1:9); **$[\alpha_D]^{20}$** = -20.3 (c 1.0, $CHCl_3$); **IR**: ν_{max}(cm^{-1}): 3330 (NH), 3057 (C=C-H), (C-H), 1686 (C=O), 1091 (C-O); **^{1}H NMR (300 MHz, $CDCl_3$)** δ 7.49 – 7.40 (m, 6H, Ar-H), 7.34 – 7.13 (m, 9H, Ar-H), 4.88 (br-s, 1H, NH), 4.11 – 3.89 (m, 2H, H-4 and H-6), 3.40 – 3.19 (m, 2H, H-7_a and H-9_a), 3.07 – 2.91 (m, 2H, H-7_b and H-9_b), 1.58 (dt, *J* = 12.8, 2.5 Hz, 1H, H-5_a), 1.45 (s, 9H, Boc-C(CH_3)$_3$)),

1.43 and 1.38 (2xs, 6H, H-1 and H-3), 1.28 – 1.13 (m, 1H, H-5_b); **^{13}C NMR (75 MHz, $CDCl_3$)** δ 156.0 (Boc-C=O), 144.0, 128.7, 127.8 and 127.0 (Ar-C), 98.7 (C-2), 86.5 (C-8), 79.3 (Boc-$\underline{C}(CH_3)_3$), 68.2 and 68.1 (C-4 and C-6), 67.2 (C-7), 45.5 (C-9), 31.2 (C-5) 29.9 (C-3), 28.4 (Boc-C($\underline{C}H_3)_3$), 19.9 (C-1); **HRMS** (m/z), calculated for $C_{32}H_{39}NNaO_5$: 540.2720, found $(M+Na)^+$: 540.2711.

4.2.22 Synthesis of *tert*-butyl (((4*R*,6*S*)-6-(hydroxymethyl)-2,2-dimethyl-1,3-dioxan-4-yl)methyl)carbamate 156

A 500 ml two-necked round bottomed flask was heat sealed before being connected to a cold finger condenser under N_2. Na (729 mg, 31.7 mmol) was added in one portion and the flask was cooled to -60 °C with the condenser also at -60 °C. Liquid NH_3 (50 ml) was introduced to the flask and it was allowed to reflux for 15 min ensuring that the colour remained deep blue. Compound **155** (820 mg, 1.58 mmol) was dissolved in dry THF (20 ml), cooled, and added to the ammonia solution. There was no colour change observed, and the reaction proceeded for a further 1 h. Quenching was achieved by slow addition of ethanol (10 ml) over 10 min until the blue colour had disappeared completely. Solid NH_4Cl (4 g) was then added in one portion and the reaction was left stirring open at ambient temperature until all the NH_3 had evaporated. The reaction mixture was diluted with saturated aqueous NH_4Cl solution (100 ml), and the organic layer was extracted with DCM (200 ml), dried over anhydrous Na_2SO_4 and excess solvent was removed *in vacuo*. Purification of the desired compound was achieved by column chromatography (DCM/MeOH, 95:5) yielding compound **156** (353 mg, 81%) as a yellow oil.

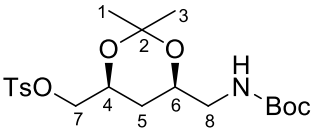


R_f = 0.30 (DCM/MeOH, 95:5); **$[\alpha_D]^{20}$** = -10.7 (c 0.6, $CHCl_3$); **IR**: $\nu_{max}(cm^{-1})$: 3324-br (OH and NH), 2923 (C-H), 1023 (C-O); **^{1}H NMR (300 MHz, $CDCl_3$)** δ 4.95 (br-s, 1H, NH), 4.03 – 3.95 (m, 2H, H-4 and H-6), 3.60 (dd, *J* = 11.5, 3.4 Hz, 1H, H-7_a), 3.51 (dd, *J* = 11.5, 6.2 Hz, 1H, H-7_b), 3.36 – 3.27 (m, 1H, H-8_a), 3.04 (ddd, *J* = 13.8, 6.9, 5.1 Hz, 1H, H-8_b), 2.41 (br-s, 1H, OH), 1.47 – 1.43 (m, 12H, Boc-C($CH_3)_3$ and H-1), 1.40 (s, 3H, H-3), 1.40 – 1.30 (m, 2H, H-5), **^{13}C NMR (75 MHz, $CDCl_3$)** δ 156.1 (Boc-C=O), 98.8 (C-2), 79.4 (Boc-$\underline{C}(CH_3)_3$), 69.3 and 67.9 (C-4 and C-6), 65.9 (C-7), 45.4 (C-8), 29.9 (C-3), 29.2 (C-5), 28.4 (Boc-C($\underline{C}H_3)_3$), 19.9 (C-1); **HRMS** (m/z), calculated for $C_{13}H_{26}NO_5$: 276.1805, found $(M+H)^+$: 276.1806.

4.2.23 Synthesis of ((4*S*,6*R*)-6-(((*tert*-butoxycarbonyl)amino)methyl)-2,2-dimethyl-1,3-dioxan-4-yl)methyl 4-methylbenzenesulfonate 157

Compound **156** (198 mg, 0.719 mmol), was dissolved in DCM (10 ml), followed by the addition of DMAP (527 mg, 4.31 mmol) and TsCl (822 mg, 4.31 mmol). The reaction was left stirring for 24 h

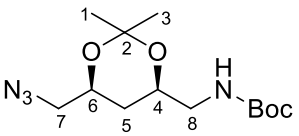
until TLC showed complete disappearance of the starting material. Work up of the reaction was performed by diluting the reaction with water (100 ml), followed by extraction of the desired compound with DCM (150 ml), followed by washing with saturated brine (100 ml). The organic layer was separated and dried over anhydrous Na_2SO_4 and excess solvent was removed *in vacuo*. Purification of the product was achieved by column chromatography (EtOAc/Hex, 3:7) yielding compound **157** (256 mg, 83%) as a yellow oil.



R_f = 0.32 (EtOAc/Hex, 3:7); **$[\alpha_D]^{20}$** = -3.2 (c 1.02, $CHCl_3$); **IR**: $\nu_{max}(cm^{-1})$: 3403 (NH), 2980 (C-H), 1598 (C=C), 1363 (S=O), 1168 (C-N), 1097 (C-O); **^{1}H NMR (300 MHz, $CDCl_3$)** δ 7.78 (d, *J* = 8.3 Hz, 2H, Ar-H), 7.34 (d, *J* = 7.9 Hz, 2H, Ar-H), 4.91 (br-s, 1H, NH), 4.17 – 4.04 (m, 1H, H-6), 4.02 – 3.85 (m, 3H, H-4 and H-7), 3.34 – 3.19 (m, 1H, H-8_a), 3.02 (ddd, *J* = 13.8, 6.7, 5.3 Hz, 1H, H-8_b), 2.45 (s, 3H, Ar-CH_3), 1.44 (s, 9H, Boc-$C(CH_3)_3$), 1.36 and 1.30 (2 x s, 6H, H-1 and H-3), 1.28 – 1.10 (m, 2H, H-5); **^{13}C NMR (75 MHz, $CDCl_3$)** δ 156.0 (Boc-C=O), 144.9, 132.9, 129.8 and 128.0 (Ar-C), 99.0 (C-2), 79.4 (Boc-$\underline{C}(CH_3)_3$), 72.2 (C-7), 67.7 (C-4), 66.6 (C-6), 45.2 (C-8), 29.6 (C-3), 29.5 (C-5), 28.4 (Boc-$C(CH_3)_3$), 21.6 (Ts-CH_3), 19.6 (C-1).

4.2.24 Synthesis of *tert*-butyl (((4*R*,6*S*)-6-(azidomethyl)-2,2-dimethyl-1,3-dioxan-4-yl)methyl)carbamate 158

Compound **157** (240 mg, 0.559 mmol), was dissolved in DMF (6 ml) followed by the addition of NaN_3 (182 mg, 2.79 mmol) and the reaction was refluxed at 80 °C for 3 h. After TLC analysis showed complete disappearance of the starting material the reaction was cooled and diluted with Et_2O (100 ml) and washed with saturated brine. The brine layer in turn was extracted once with Et_2O (100 ml). The combined Et_2O solutions were washed with saturated brine (7 x 150 ml), dried over Na_2SO_4 and evaporated to afford the crude product. Purification by column chromatography (EtOAc/Hex, 3:7) yielded the desired product **158** (125 mg, 75%) as a yellow oil.

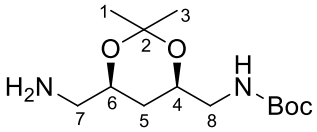


R_f = 0.35 (EtOAc/Hex, 3:7); **$[\alpha_D]^{20}$** = -5.4 (c 0.5, $CHCl_3$); **IR**: $\nu_{max}(cm^{-1})$: 3358 (NH), 2979 (C-H), 2098 (N=N=N), 1703 (C=O), 1164 (C-O); **^{1}H NMR (300 MHz, $CDCl_3$)** δ 4.92 (br-s, 1H, NH), 4.12 – 3.91 (m, 2H, H-4 and H-6), 3.40 – 3.15 (m, 3H, H-7 and H-8_a), 3.06 (ddd, *J* = 13.9, 6.9, 5.2 Hz, 1H, H-8_b), 1.50 – 1.43 (m, 12H, Boc-$C(CH_3)_3$ and H-1), 1.41 (s, 3H, H-3), 1.41 – 1.23 (m, 2H, H-5); **^{13}C NMR (75 MHz, $CDCl_3$)** δ 156.1 (Boc-C=O), 99.1 (C-2), 79.4 (Boc-$\underline{C}(CH_3)_3$), 68.2 (C-6), 68.0 (C-4), 55.1 (C-7), 45.3 (C-8), 30.6 (C-5), 29.8

(C-3), 28.4 (Boc-C($\underline{C}H_3)_3$), 19.8 (C-1); **HRMS** (m/z), calculated for $C_{13}H_{24}NaN_4O_4$: 323.1690, found $(M+H)^+$: 323.1691.

4.2.25 Synthesis of *tert*-butyl (((4*R*,6*S*)-6-(aminomethyl)-2,2-dimethyl-1,3-dioxan-4-yl)methyl)carbamate 159

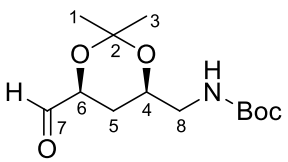
Pd/C (30 mg, 10 mol%) was added to a stirring solution of compound **158** (112 mg, 0.373 mmol) in ethanol (5 ml) under H_2. The reaction was allowed to proceed overnight at 4 atm until TLC showed total consumption of the starting material. The reaction mixture was then filtered over celite and evaporated yielding the desired compound **159** as a brown oil in quantitative yield. It was not purified any further.



R_f = 0.14 (DCM/MeOH, 9:1); **IR**: $\nu_{max}(cm^{-1})$: 3353 (NH), 2978 (C-H), 1696 (C=O), 1160 (C-O); **^{1}H NMR (300 MHz, $CDCl_3$)** δ 5.00 (br-s, 1H, NH), 4.09 – 3.91 (m, 1H, H-4), 3.89 – 3.79 (m, 1H, H-6), 3.39 – 3.22 (m, 1H, H-8_a), 3.04 (ddd, *J* = 13.8, 6.9, 5.0 Hz, 1H, H-8_b), 2.80 – 2.52 (m, 2H, H-7), 1.45 (s, 12H, Boc-C$(CH_3)_3$ and H-1), 1.41 – 1.35 (m, 4H, H-3 and H-5_a), 1.31 – 1.15 (m, 1H, H-5_b); **^{13}C NMR (75 MHz, $CDCl_3$)** δ 156.1 (Boc-C=O), 98.8 (C-2), 79.3 (Boc-$\underline{C}(CH_3)_3$), 70.3 (C-4), 68.1 (C-6), 47.4 (C-7), 45.4 (C-8), 30.9 (C-5), 30.0 (C-3), 28.4 (Boc-C($\underline{C}H_3)_3$), 20.0 (C-1); **HRMS** (m/z), calculated for $C_{13}H_{27}N_2O_4$: 275.1965, found $(M+H)^+$: 275.1975.

4.2.26 Synthesis of *tert*-butyl (((4*R*,6*S*)-6-formyl-2,2-dimethyl-1,3-dioxan-4-yl)methyl)carbamate 160

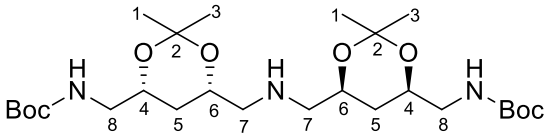
Compound **156** (196 mg, 0.712 mmol) and IBX (797 mg, 2.85 mmol) were added to DMSO (10 ml) and left stirring overnight. TLC analysis showed formation of an aldehyde using a 2,4 DNP as a visualisation agent. The reaction mixture was diluted with DCM (100 ml), followed by washing with water (2 x 100 ml), saturated brine (100 ml) and evaporation of excess solvent. Quantitative yield of the crude aldehyde **160** was recovered as an oil and was not purified further.



R_f = 0.34 (DCM/MeOH, 95:5); **IR**: $\nu_{max}(cm^{-1})$: 3382 (NH), 2922 (C-H), 1710 (C=O), 1164 (C-O); **^{1}H NMR (300 MHz, $CDCl_3$)** δ 9.58 (s, 1H, H-7), 4.93 (s, 1H, NH), 4.49 (dd, *J* = 12.2, 2.9 Hz, 0.34H) and 4.32 (dd, *J* = 12.2, 3.1 Hz, 0.41H, H-6), 4.15 – 3.84 (s, 1H, H-4), 3.43 – 3.18 (m, 1H, H-8_a), 3.15 – 3.00 (m, 1H, H-8_b), 1.77 – 0.99 (m, 17H, H-1, H-3, H-5 and Boc-C$(CH_3)_3$); **HRMS** (m/z), calculated for $C_{13}H_{24}NO_5$: 274.1649, found $(M+H)^+$: 274.1647.

4.2.27 Synthesis of di-*tert*-butyl (((4*R*,4'*R*,6*S*,6'*S*)-6,6'-(azanediylbis(methylene))bis(2,2-dimethyl-1,3-dioxane-6,4-diyl))bis(methylene))dicarbamate 161

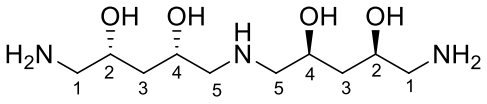
Compound **159** (101 mg, 0.370 mmol) and compound **160** (84 mg, 0.307 mmol) were dissolved in THF (3 ml) under N_2 followed by the addition of 1,2-dichloroethane (5 ml) and sodium triacetoxyborohydride (109 mg, 0.518 mmol) in one portion. After stirring at room temperature for 24 h over molecular sieves (3Å) the reaction was quenched with 1 M NaOH (5 ml), washed with DCM (50 ml) and saturated brine (50 ml). The organic layer was separated and dried over anhydrous Na_2SO_4 and excess solvent was removed *in vacuo*. Purification by column chromatography ($CHCl_3$/MeOH, 9:1) yielded compound **161** (155 mg, 95%) as a viscous yellow oil.



R_f = 0.40 (DCM/MeOH, 9:1); **$[\alpha_D]^{20}$** = -10.1 (c 1.03, $CHCl_3$); **IR** ν_{max}(cm^{-1}) : 3362 (NH), 2977 (C-H), 1694 (C=O), 1163 (C-O); **^{1}H NMR (500 MHz, $CDCl_3$)** δ 4.94 (s, 1H, NH), 4.05 – 3.91 (m, 4H, H-4 and H-6), 3.36 – 3.23 (m, 2H, H-8_a), 3.08 – 2.99 (m, 2H, H-8_b), 2.75 – 2.55 (m, 4H, H-7), 2.07 (br-s, 2H, NH), 1.48 – 1.42 (m, 26H, 2 x Boc-C(CH_3)$_3$, H-1 and H-5_a), 1.38 (s, 3H, H-3), 1.30 – 1.21 (m, 1H, H-5_b); **^{13}C NMR (126 MHz, $CDCl_3$)** δ 156.1 (Boc-C=O), 98.8 (C-2), 79.3 (Boc-C(CH_3)$_3$), 68.2 and 67.9 (C-4 and C-6), 55.0 (C-7), 45.4 (C-8), 31.6 (C-5), 30.0 (C-3), 28.4 (Boc-C(CH_3)$_3$), 19.9 (C-1); **HRMS** (m/z), calculated for $C_{26}H_{50}N_3O_8$: 532.3592, found $(M+H)^+$: 532.3592.

4.2.28 Synthesis of (2*R*,2'*R*,4*S*,4'*S*)-5,5'-azanediylbis(1-aminopentane-2,4-diol) 112

Compound **161** (65 mg, 0.122 mmol) was dissolved in a TFA:H_2O:Triisopropylsilane mixture (95%:2.5%:2.5%, 3 ml) and left stirring at ambient temperature. The reaction mixture was diluted with MeOH (100 ml) and excess solvent was removed under reduced pressure. The residue was redissolved in methanol (50 ml) followed by the addition of a few drops of Et_3N. The excess solvent was removed *in vacuo*. The desired polyamine **112** was not purified any further and it was recovered as a yellow oil in quantitative yield.

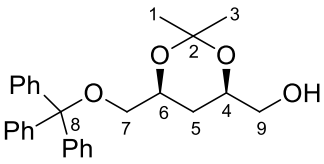


R_f = 0.35 (IPA/AcOH/H_2O, 9:1); **$[\alpha_D]^{20}$** = -1.61 (c 0.13, MeOH); **IR**: ν_{max}(cm^{-1}): 3220 – 2810 (NH_2, OH and C-H); **^{1}H NMR (500 MHz, MeOD)** δ 4.19 – 4.10 (m, 2H, H-4), 4.07 – 3.99 (m, 2H, H-2), 3.22 – 3.14 (m, 2H,

H-5_a), 3.10 – 3.00 (m, 4H, H-1_a and H-5_b), 2.88 (dd, *J* = 12.8, 8.9 Hz, 2H, H-1_b), 1.78 – 1.62 (m, 4H, H-3); ^{13}C **NMR (126 MHz, MeOD)** δ 163.8 (q, *J* = 33.4 Hz), 120.3 (q, *J* = 291.3 Hz) 64.6 (C-2), 63.7 (C-4), 52.3 (C-5), 44.4 (C-1), 38.9 (C-3); **HRMS** (m/z), calculated for $C_{10}H_{26}N_3O_4$: 252.1918, found $(M+H)^+$: 252.1912.

4.2.29 Synthesis of ((4*R*,6*S*)-2,2-dimethyl-6-((trityloxy)methyl)-1,3-dioxan-4-yl)methanol 162

To a stirring solution of compound **124** (400 mg, 0.740 mmol) in MeCN (6 ml) at 0 °C were added collidine (586 µl, 1.48 mmol) and TFAA (1.00 ml, 1.48 mmol) successively. The reaction was stirred for 30 min before being hydrolysed with H_2O (1 ml) followed by adjusting the pH to neutral using solid K_2CO_3 at ambient temperature. After stirring for 30 min $NaBH_4$ (168 mg, 1.48 mmol) was added in one portion, and the reaction continued to stir for a further 40 min before quenching with saturated aqueous NH_4Cl solution (20 ml). The reaction mixture was extracted using EtOAc (150 ml), washed successively with 1 M HCl (10 ml), saturated $NaHCO_3$ (20 ml) and saturated brine (100 ml). The organic layer was dried over anhydrous Na_2SO_4 before excess solvent was removed under reduced pressure. Purification using column chromatography (EtOAc/Hex, 3:7) yielded compound **162** (310 mg, 99%) as a white solid.

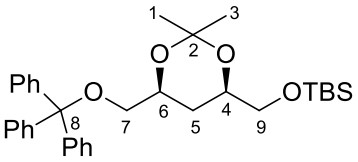


R_f = 0.31 (EtOAc/Hex, 3:7); **$[\alpha_D]^{20}$** = -20.4 (c 0.7, $CHCl_3$); **IR**: ν_{max}(cm^{-1}): 3489 (OH), 3058 (C=C-H), 2989 (C-H), 1030 (C-O); **^{1}H NMR (300 MHz, $CDCl_3$)** δ 7.48 – 7.40 (m, 6H, Ar-H), 7.33 – 7.16 (m, 9H, Ar-H), 4.08 – 3.93 (m, 2H, H-4 and H-6), 3.59 (dd, *J* = 11.4, 2.6 Hz, 1H, H-9_a), 3.49 (dd, *J* = 11.3, 6.3 Hz, 1H, H-9_b), 3.26 (dd, *J* = 9.2, 5.4 Hz, 1H, H-7_a), 2.97 (dd, *J* = 9.1, 6.1 Hz, 1H, H-7_b), 2.14 (br-s, 1H, OH), 1.58 – 1.50 (m, 1H, H-5_a), 1.45 and 1.39 (2 x s, 6H, H-1 and H-3), 1.32 – 1.20 (m, 1H, H-5_b); **^{13}C NMR (75 MHz, $CDCl_3$)** δ 144.0, 128.7, 127.7 and 127.0 (Ar-C), 98.7 (C-2), 86.5 (C-8), 69.5 (C-4), 68.0 (C-6), 67.3 (C-7), 66.1 (C-9), 29.9 (C-3), 29.8 (C-5), 19.9 (C-1).

4.2.30 Synthesis of *tert*-butyl(((4*R*,6*S*)-2,2-dimethyl-6-((trityloxy)methyl)-1,3-dioxan-4-yl)methoxy)dimethylsilane 163

Compound **162** (290 mg, 0.693 mmol) was dissolved in DCM (20 ml) followed by the addition of imidazole (47 mg, 1.04 mmol), DMAP (128 mg, 1.04 mmol) and TBSCl (125 mg, 0.831 mmol). After stirring overnight the reaction mixture was washed with H_2O (100 ml) and extracted with DCM (100 ml). The organic layer was separated and dried over anhydrous Na_2SO_4 and excess solvent

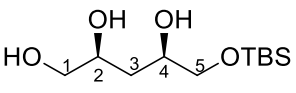
was removed under reduced pressure. Product purification was afforded by column chromatography (EtOAc/Hex, 1:9) to give compound **163** (358 mg, 97%) as a viscous colourless oil.



R_f = 0.74 (EtOAc/Hex, 1:9); **$[\alpha_D]^{20}$** = -11.6 (c 0.31, $CHCl_3$); **IR**: ν_{max}(cm^{-1}): 3059 (C=C-H), 2991 (C-H), 1108 (C-O); **^{1}H NMR (300 MHz, $CDCl_3$)** δ 7.49 – 7.42 (m, 6H, Ar-H), 7.32 – 7.18 (m, 9H, Ar-H), 4.04 (dtd, *J* = 11.6, 5.9, 2.5 Hz, 2H, H-4), 3.93 (dtd, *J* = 11.5, 5.8, 2.5 Hz, 2H, H-6), 3.67 (dd, *J* = 10.2, 5.2 Hz, 1H, H-7_a), 3.48 (dd, *J* = 10.2, 6.1 Hz, 1H, H-7_b), 3.24 (dd, *J* = 9.1, 5.3 Hz, 1H, H-9_a), 2.98 (dd, *J* = 9.1, 6.1 Hz, 1H, H-9_b), 1.78 (dt, *J* = 12.9, 2.6 Hz, 1H, H-5_a), 1.44 and 1.37 (2 x s, 6H, H-1 and H-3), 1.27 – 1.14 (m, 1H, H-5_b), 0.90 (s, 9H, TBS-C(CH_3)$_3$), 0.07 and 0.06 (2 x overlapping singlets, 6H, TBS-Si(CH_3)$_2$); **^{13}C NMR (75 MHz, $CDCl_3$)** δ 144.1, 128.8, 127.7 and 126.9 (Ar-C), 98.4 (C-2), 86.4 (C-8), 69.7 (C-6), 68.4 (C-4), 67.3 (C-9), 67.0 (C-7), 31.4 (C-5), 29.9 (C-3), 25.9 (TBS-C($\underline{C}H_3$)$_3$) , 19.8 (C-1), 18.4 (TBS-$\underline{C}$(CH_3)$_3$), -5.1 and -5.3 (TBS-Si($\underline{C}H_3$)$_2$); **HRMS** (m/z), calculated for $C_{33}H_{44}NaO_4Si$: 555.2901, found $(M+Na)^+$: 555.2895.

4.2.31 Preparation of (2*S*,4*R*)-5-((*tert*-butyldimethylsilyl)oxy)pentane-1,2,4-triol 164

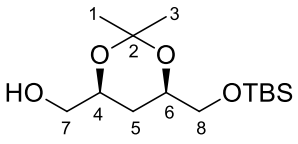
Compound **163** (60 mg, 0.111 mmol) was dissolved in dry DCM (1 ml) and cooled to -30 °C under N_2 followed by the dropwise addition of 1 M BCl_3 in hexanes (67 µl, 0.0666 mmol). The reaction was allowed to proceed for 15 min before quenching with anhydrous MeOH (5 ml). The solution was poured into a saturated $NaHCO_3$ solution (5 ml) and stirred for 5 min. The organic layer was separated and washed with saturated brine (5 ml), dried over anhydrous $MgSO_4$ and concentrated under reduced pressure. Product purification was afforded by column chromatography ($CHCl_3$/MeOH, 9:1) yielding compound **164** (17 mg, 66% yield) as a colourless oil.



R_f = 0.24 (EtOAc); **IR**: ν_{max}(cm^{-1}): 3261 (OH), 2906 (C-H), 1242 C-O); **^{1}H NMR (300 MHz, $CDCl_3$)** δ 4.05 – 3.89 (m, 3H, OH, H-2 and H-4), 3.69 – 3.58 (m, 2H, H-5), 3.56 – 3.45 (m, 2H, H-1), 3.29 (br-s, 1H, OH), 3.06 (br-s, 1H, OH), 1.68 – 1.52 (m, 2H, H-3), 0.92 (s, 9H, TBS-C(CH_3)$_3$), 0.10 (br-s, 6H, TBS-Si(CH_3)$_2$); **^{13}C NMR (75 MHz, $CDCl_3$)** δ 71.94 and 71.90 (C-2 and C-4), 67.5 and 66.9 (C-1 and C-5), 35.7 (C-3), 26.2 (TBS-C($\underline{C}H_3$)$_3$), 18.6 (TBS-$\underline{C}$(CH_3)$_3$), -5.0 and -5.1 (TBS-Si(CH_3)$_2$); **HRMS** (m/z), calculated for $C_{11}H_{27}O_4Si$: 251.1673, found $(M+H)^+$: 251.1670.

4.2.32 Synthesis of ((4*S*,6*R*)-6-(((*tert*-butyldimethylsilyl)oxy)methyl)-2,2-dimethyl-1,3-dioxan-4-yl)methanol 165

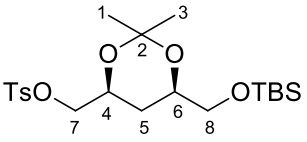
A 250 ml two-necked round bottomed flask was heat-sealed before being connected to a cold finger condenser under N_2. Na (258 mg, 11.0 mmol) was added in one portion and the flask was cooled to -60 °C with the condenser also at -60 °C. Liquid NH_3 (25 ml) was introduced to the flask and it was allowed to reflux for 15 min ensuring that the colour remained deep blue. Compound **163** (320 mg, 0.600 mmol) was dissolved in dry THF (10 ml) and added to the ammonia solution. There was no colour change observed, and the reaction proceeded for a further 1 h. Quenching was achieved by the slow addition of ethanol (10 ml) over 10 min until the blue colour had disappeared completely. Solid NH_4Cl (4 g) was then added in one portion and the reaction was left stirring open at ambient temperature until all the NH_3 had evaporated. The reaction mixture was diluted with saturated aqueous NH_4Cl (100 ml), and the organic layer was extracted with DCM (200 ml), dried over anhydrous Na_2SO_4 and excess solvent was removed *in vacuo*. Purification of the desired compound using column chromatography (DCM/MeOH, 95:5) gave rise to alcohol **165** (140 mg, 80%) as a yellow oil.



R_f = 0.16 (EtOAc/Hex, 9:1); **IR**: ν_{max}(cm^{-1}): 3441 (OH), 2993 (C-H), 1109 (C-O); **^{1}H NMR (500 MHz, $CDCl_3$)** δ 4.06 – 3.93 (m, 2H, H-4 and H-6), 3.72 – 3.67 (m, 1H, H-7_a), 3.66 – 3.61 (m, 1H, H-7_b), 3.57 – 3.47 (m, 2H, H-8), 2.13 (br-s, 1H, OH), 1.56 – 1.50 (m, 1H, H-5_a), 1.48 and 1.41 (2 x s, 6H, H-1 and H-3), 1.33 – 1.23 (m, 1H, H-5_b), 0.91 (s, 9H, TBS-C(CH_3)$_3$), 0.08 and 0.02 (2 x s, 6H, TBS-Si(CH_3)$_2$); **^{13}C NMR (126 MHz, $CDCl_3$)** δ 98.7 (C-2), 69.5 and 69.4 (C-4 and C-6), 66.9 (C-7), 66.2 (C-8), 29.9 (C-3), 29.3 (C-5), 25.9 (TBS-C($\underline{C}H_3$)$_3$), 19.9 (C-1), 18.3 (TBS-$\underline{C}$(CH_3)$_3$), -5.2 and -5.3 (TBS-Si(CH_3)$_2$); **HRMS** (m/z), calculated for $C_{14}H_{31}O_4Si$: 291.1986, found $(M+H)^+$: 291.1985.

4.2.33 Synthesis of ((4*S*,6*R*)-6-(((*tert*-butyldimethylsilyl)oxy)methyl)-2,2-dimethyl-1,3-dioxan-4-yl)methyl 4-methylbenzenesulfonate 166

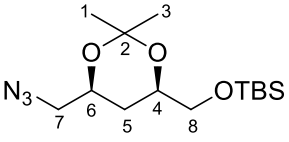
Compound **165** (140 mg, 0.482 mmol) was dissolved in DCM (10 ml) followed by the addition of DMAP (426 mg, 2.89 mmol) and TsCl (552 mg, 2.89 mmol). After stirring overnight, the reaction was quenched with H_2O (50 ml) and diluted with DCM (100 ml). The organic layer was separated, and dried over anhydrous Na_2SO_4 followed by evaporation of excess solvent under reduced pressure. Purification of the desired product was afforded by column chromatography using (EtOAc/Hex, 3:7) as the eluent to afford compound **166** (200 mg, 99%) as a colourless oil.



R_f = 0.39 (EtOAc/Hex, 3:7); **IR**: ν_{max}(cm^{-1}): 2987 (C-H), 1356 (S=O), 1170 (C-O); **^{1}H NMR (300 MHz, $CDCl_3$)** δ 7.82 – 7.76 (m, 2H, Ar-H), 7.37 – 7.31 (m, 2H, Ar-H), 4.16 – 4.05 (m, 1H, H-4), 4.02 – 3.94 (m, 2H, H-7), 3.93 – 3.83 (m, 1H, H-6), 3.63 (dd, *J* = 10.3, 5.2 Hz, 1H, H-8_a), 3.44 (dd, *J* = 10.3, 6.0 Hz, 1H, H-8_b), 2.44 (s, 3H, Ts-CH_3), 1.57 (dt, *J* = 12.7, 2.6 Hz, 1H, H-5_a), 1.37 and 1.30 (2 x s, 6H, H-1 and H-3), 1.20 – 1.05 (m, 1H, H-5_b), 0.88 (s, 9H, TBS-C(CH_3)$_2$), 0.04 (br-s, 6H, TBS-Si(CH_3)$_2$); **^{13}C NMR (75 MHz, $CDCl_3$)** δ 144.8, 133.0, 129.8 and 128.0 (Ar-C), 98.7 (C-2), 72.4 (C-7), 69.2 (C-6), 66.8 (C-4), 66.7 (C-8), 29.6 (C-5 and C-3), 25.9 (TBS-C($\underline{C}H_3$)$_3$), 21.6 (Ts-CH_3), 19.6 (C-1), 18.3 (TBS-$\underline{C}$(CH_3)$_3$), -5.2 and -5.3 (TBS-Si(CH_3)$_2$.

4.2.34 Synthesis of (((4*R*,6*S*)-6-(azidomethyl)-2,2-dimethyl-1,3-dioxan-4-yl)methoxy)(*tert*-butyl)dimethylsilane 167

Compound **166** (199 mg, 0.480 mmol), was dissolved in DMF (6 ml) followed by the addition of NaN_3 (156 mg, 2.40 mmol) and the reaction was refluxed at 75 °C for 4 h. After TLC analysis showed complete disappearance of the starting material the reaction was cooled down and diluted with Et_2O (100 ml) and washed with saturated brine (100 ml). The brine layer in turn was extracted once with Et_2O (100 ml). The combined Et_2O solutions were washed with saturated brine (7 x 150 ml), dried over anhydrous Na_2SO_4 and evaporated to afford the desired azide **167** (125 mg, 75%) as an orange oil.

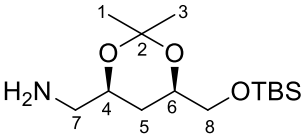


R_f = 0.40 (EtOAc/Hex, 3:7); **IR**: ν_{max}(cm^{-1}): 2992 (C-H), 2098 (N=N=N), 1253 (C-N), 1108 (C-O); **^{1}H NMR (300 MHz, $CDCl_3$)** δ 4.11 (dddd, *J* = 11.8, 6.2, 4.2, 2.6 Hz, 1H, H-4), 4.03 – 3.93 (m, 1H, H-6), 3.71 (dd, *J* = 10.2, 5.1 Hz, 1H, H-8_a), 3.52 (dd, *J* = 10.2, 6.2 Hz, 1H, H-8_b), 3.34 – 3.20 (m, 2H, H-7), 1.60 (dt, *J* = 12.7, 2.6 Hz, 1H, H-5_a), 1.50 and 1.44 (2 x s, 6H, H-1 and H-3), 1.37 – 1.26 (m, 1H, H-5_b), 0.92 (s, 9H, (TBS-C(CH_3)$_3$)), 0.10 and 0.09 (2 x overlapping singlets, 6H, TBS-Si(CH_3)$_2$; **^{13}C NMR (126 MHz, $CDCl_3$)** δ 98.8 (C-2), 69.5 (C-4), 68.5 (C-6), 66.8 (C-8), 55.2 (C-7), 30.8 (C-5), 29.8 (C-1), 25.9 (TBS-C($\underline{C}H_3$)$_3$), 19.7 (C-3), 18.3 (TBS-$\underline{C}$(CH_3)$_3$), -5.2 and -5.3 (TBS-$\underline{C}$(CH_3)$_3$).

4.2.35 Synthesis of ((4*S*,6*R*)-6-(((*tert*-butyldimethylsilyl)oxy)methyl)-2,2-dimethyl-1,3-dioxan-4-yl)methanamine 168

Compound **167** (100 mg, 0.317 mmol) was dissolved in dry Et_2O (20 ml) followed by the addition of $LiAlH_4$ (24 mg, 0.634 mmol) in one portion. The reaction was complete in 2 h (TLC control), and the reaction was quenched by dropwise addition of 2 M NaOH until a white precipitate formed.

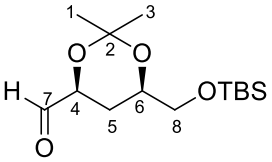
Anhydrous Na_2SO_4 was added and the mixture was filtered. The solid white residue was extracted twice with EtOAc (50 ml) and the combined organic solutions were evaporated to give compound **168** as an oil in quantitative yield. The product was not purified further.



R_f = 0.37 ($CHCl_3$/MeOH, 9:1); **IR**: ν_{max}(cm^{-1}): 3444 (NH), 2993 (C-H), 1108 (C-O); **^{1}H NMR (400 MHz, $CDCl_3$)** δ 3.98 – 3.89 (m, 1H, H-6), 3.88 – 3.81 (m, 1H, H-4), 3.67 (dd, *J* = 10.2, 5.2 Hz, 1H, H-8_a), 3.48 (dd, *J* = 10.2, 6.1 Hz, 1H, H-8_b), 2.76 – 2.67 (m, 2H, H-7), 1.60 – 1.50 (m, 3H, H-5_a and NH_2), 1.45 and 1.39 (2xs, 6H, H-1 and H-3), 1.22 – 1.09 (m, 1H, H-5_b), 0.89 (s, 9H, TBS-C(CH_3)$_3$), 0.061 and 0.058 (2 x overlapping singlets, 6H, TBS-Si(CH_3)$_2$); **^{13}C NMR (101 MHz, $CDCl_3$)** δ 98.6 (C-2), 70.6 (C-4), 69.6 (C-6), 67.0 (C-8), 47.5 (C-7), 31.0 (C-5), 30.0 (C-3), 25.9 (TBS-C(<u>C</u>H_3)$_3$), 19.9 (C-1), 18.4 (TBS-<u>C</u>(CH_3)$_3$), -5.2 and -5.3 (TBS-Si(CH_3)$_2$); **HRMS** (m/z), calculated for $C_{14}H_{32}NO_3Si$: 290.2146, found $(M+H)^+$: 290.2154

4.2.36 (4*S*,6*R*)-6-(((*tert*-butyldimethylsilyl)oxy)methyl)-2,2-dimethyl-1,3-dioxane-4-carbaldehyde 170

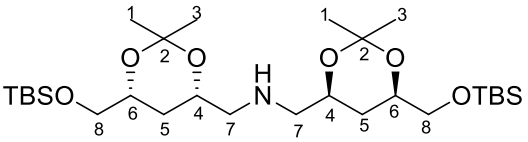
Compound **165** (138 mg, 0.476 mmol) was dissolved in DCM (5 ml) at ambient temperature, followed by the addition of DMP (225 mg, 0.153 mmol) in one portion. The reaction was left stirring overnight and TLC analysis showed formation of an aldehyde using 2,4-DNPH visualisation. Work-up of the reaction was achieved by washing with 2 M NaOH (10 ml) followed by saturated brine. The organic layer was separated and dried over anhydrous $MgSO_4$, and excess solvent was removed under reduced pressure yielding a colourless oil **170** as the desired product. No further purification was performed.



R_f = 0.37 (EtOAc/Hex, 3:2); **IR**: ν_{max}(cm^{-1}): 2992 (C-H), 1735 (C=O), 1103 (C-O); **^{1}H NMR (400 MHz, $CDCl_3$)** δ 9.60 (s, 1H, H-7), 4.32 (dd, *J* = 12.3, 3.0 Hz, 1H, H-4), 4.04 – 3.85 (m, 1H, H-6), 3.72 – 3.62 (m, 1H, H-8_a), 3.55 – 3.45 (m, 1H, H-8_b), 1.84 (dt, *J* = 13.0, 2.8 Hz, 1H, H-5_a), 1.48 and 1.47 (2 x s, 6H, H-1 and H-3), 1.38 – 1.28 (m, 1H, H-5_b), 0.89 (s, 9H, TBS-C(CH_3)$_3$), 0.061 and 0.059 (2 x overlapping singlets, 6H, TBS-Si(CH_3)$_2$); **^{13}C NMR (101 MHz, $CDCl_3$)** δ 201.1 (C-7), 99.0 (C-2), 73.8 (C-4), 69.2 (C-6), 66.5 (C-8), 29.6 (C-3), 28.0 (C-5), 25.9 (TBS-C(<u>C</u>H_3)$_3$), 19.5 (C-1), 18.3 (TBS-<u>C</u>(CH_3)$_3$), -5.26 and -5.32 (TBS-Si(CH_3)$_2$).

4.2.37 Synthesis of bis(((4*S*,6*R*)-6-(((*tert*-butyldimethylsilyl)oxy)methyl)-2,2-dimethyl-1,3-dioxan-4-yl)methyl)amine 171

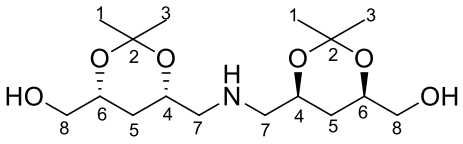
Compound **170** (101 mg, 0.281 mmol) was dissolved in dry 1,2-dichloroethane (5 ml) under N_2 followed by the addition of compound **168** (118 mg, 0.408 mmol) dissolved in 1,2-dichloroethane (2 ml) and sodium triacetoxyborohydride (118 mg, 0.562 mmol) was added in one portion. The reaction was left stirring for 24 h over molecular sieves (3Å) (TLC control). Upon completion, the reaction was quenched by the washing with 1 M NaOH (10 ml), separating the organic layer and drying over $MgSO_4$. Excess solvent was removed under reduced pressure. Purification of the desired product was performed by column chromatography ($CHCl_3$/MeOH, 9:1) yielding compound **171** (61 mg, 73%) as a yellow oil.



R_f = 0.32 (EtOAc/Hex, 4:1); **$[\alpha_D]^{20}$** = +10.4 (c 0.56, $CHCl_3$) **IR**: ν_{max}(cm^{-1}): 2293 (C-H), 1253 (C-N), 1157, 1106 and 1044 (C-O); **^{1}H NMR (400 MHz, $CDCl_3$)** δ 4.07 – 3.98 (m, 2H, H-4), 3.96 – 3.88 (m, 2H, H-6), 3.65 (dd, *J* = 10.1, 5.2 Hz, 2H, H-8_a), 3.46 (dd, *J* = 10.2, 6.0 Hz, 2H, H-8_b), 2.68 (dd, *J* = 12.0, 7.4 Hz, 2H, H-7_a), 2.60 (dd, *J* = 12.0, 4.0 Hz, 2H, H-7_b), 1.99 (br-s, 1H, NH), 1.55 (dt, *J* = 12.8, 2.7 Hz, 2H, H-5_a), 1.44 and 1.37 (2 x s, 12H, H-1 and H-3), 1.23 – 1.11 (m, 2H, H-5_b), 0.88 (s, 18H, TBS-C(CH_3)$_3$), 0.07 – 0.02 (m, 12H, TBS-Si(CH_3)$_2$); **^{13}C NMR (101 MHz, $CDCl_3$)** δ 98.6 (C-2), 69.7 (C-6), 68.1 (C-4), 67.0 (C-8), 55.1 (C-7), 31.7 (C-5), 30.0 (C-3), 25.9 (TBS-C($\underline{C}H_3$)$_3$), 19.9 (C-1), 18.4 (TBS-$\underline{C}$(CH_3)$_3$), -5.2 and -5.3 (TBS-Si($\underline{C}H_3$)$_2$); **HRMS** (m/z), calculated for $C_{28}H_{60}NO_6Si_2$: 562.3954, found $(M+H)^+$: 562.3973.

4.2.38 Synthesis of ((4*R*,4'*R*,6*S*,6'*S*)-6,6'-(azanediylbis(methylene))bis(2,2-dimethyl-1,3-dioxane-6,4-diyl))dimethanol 172

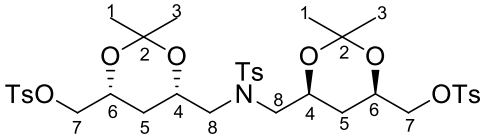
To a solution of compound **171** (60 mg, 0.108 mmol) in dry THF (3 ml) was added TBAF (161 µl, 0.161 mmol) under N_2 at 0 °C. The reaction was allowed to stir for 4 h until completion whilst monitoring by TLC. Quenching of the reaction was achieved by addition of a few drops of saturated aqueous NH_4Cl followed by drying over anhydrous Na_2SO_4. The mixture was filtered and excess solvent was removed *in vacuo*. The crude product **172** was used without further purification in the next step.



R_f = 0.28 ($CHCl_3$/MeOH, 9:1); **^{13}C NMR (101 MHz, $CDCl_3$)** δ 99.3 (C-2), 69.2 (C-6), 65.3 (C-8), 64.4 (C-4), 51.7 (C-7), 30.3 (C-5), 29.8 (C-3), 20.2 (C-1).

4.2.39 Synthesis of ((4*R*,4'*R*,6*S*,6'*S*)-6,6'-((tosylazanediyl)bis(methylene))bis(2,2-dimethyl-1,3-dioxane-6,4-diyl))bis(methylene) bis(4-methylbenzenesulfonate) 173

Compound **172** (27 mg, 0.108 mmol), was dissolved in DCM (3 ml), followed by the addition of TsCl (101 mg, 0.540 mmol) and DMAP (66 mg, 0.540 mmol). The reaction was left stirring for 24 h until TLC showed complete disappearance of the starting material. Work up of the reaction was performed by diluting the reaction with water (10 ml), followed by extraction of the desired compound with DCM (50 ml). The organic layer was separated and dried over anhydrous Na_2SO_4 and excess solvent was removed *in vacuo*. Purification of the product was achieved by column chromatography (EtOAc/Hex, 3:7) yielding compound **173** (18 mg, 21%) as a white solid.

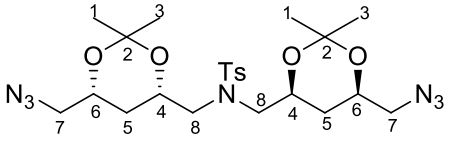


R_f = 0.38 (EtOAc/Hex, 1:1); **IR**: ν_{max}(cm^{-1}): 2993, 2929 (C-H), 1379 (S=O), 1200 (C-O); **^{1}H NMR (400 MHz, $CDCl_3$)** δ 7.96 – 7.90 (m, 4H), 7.82 – 7.75 (m, 2H), 7.41 (d, *J* = 8.2 Hz, 4H) and 7.34 (d, *J* = 7.9 Hz, 2H, Ar-H), 4.14 – 4.00 (m, 4H, H-4 and H-6), 3.99 – 3.86 (m, 4H, H-7), 3.30 (dd, *J* = 14.9, 4.2 Hz, 2H, H-8_a), 3.20 (dd, *J* = 14.9, 7.2 Hz, 2H, H-8_b), 2.49 (s, 6H) and 2.45 (s, 3H, Ar-CH_3), 1.47 (dt, *J* = 12.8, 2.5 Hz, 2H, H-5_a), 1.28 – 1.20 (m, 12H, H-1 and H-3), 1.13 – 1.03 (m, 1H, H-5_b); **^{13}C NMR (101 MHz, $CDCl_3$)** δ 144.9, 143.4, 137.3, 132.8, 129.8, 129.7, 128.0 and 127.2 (Ar-C), 98.9 (C-2), 72.1 (C-7), 67.8 and 66.7 (C-4 and C-6), 54.2 (C-8), 30.1 (C-5), 29.7 (C-3), 21.6 and 21.5 (Ts-CH_3), 19.4 (C-1).

4.2.40 Synthesis of *N*,*N*-bis(((4*S*,6*R*)-6-(azidomethyl)-2,2-dimethyl-1,3-dioxan-4-yl)methyl)-4-methylbenzenesulfonamide 174

Crude compound **173** was dissolved in DMF (3 ml) followed by the addition of NaN_3 (112 mg, 1.72 mmol) and the reaction was refluxed at 75 °C for 4 h. After TLC analysis showed complete disappearance of the starting material the reaction was cooled and diluted with Et_2O (100 ml) and washed with brine. The brine layer in turn was extracted once with Et_2O (100 ml). The combined Et_2O solutions were washed with saturated brine (7 x 150 ml), dried over anhydrous Na_2SO_4 and evaporated under reduced pressure, to afford the crude product. Purification of the desired

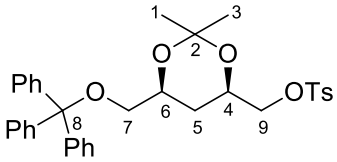
product was achieved by column chromatography (EtOAc/Hex, 3:7) but a complex mixture of product was recovered.



R_f = 0.34 (EtOAc/Hex, 3:7); **^{13}C NMR (126 MHz, $CDCl_3$)** δ 99.0 (C-2), 68.4 and 68.2 (C-4 and C-6), 55.0 and 53.7 (C-7 and C-8), 31.1 (C-5), 29.8 (C-3), 21.5 (Ts-CH_3), 19.5 (C-1).

4.2.41 Synthesis of ((4*R*,6*S*)-2,2-dimethyl-6-((trityloxy)methyl)-1,3-dioxan-4-yl)methyl 4-methylbenzenesulfonate 175

Compound **162** (146 mg, 0.349 mmol), was dissolved in DCM (5 ml), followed by the addition of DMAP (51 mg, 0.419 mmol) and TsCl (67 mg, 0.349 mmol). The reaction was left stirring for 24 h until TLC showed complete disappearance of the starting material. Work up of the reaction was performed by diluting the reaction with water (10 ml), followed by extraction of the desired compound with DCM (20 ml). The organic layer was separated and dried over anhydrous Na_2SO_4 and excess solvent was removed *in vacuo*. Purification of the product was achieved by column chromatography (EtOAc/Hex, 3:7) yielding compound **175** (149 mg, 75%) as a white solid.

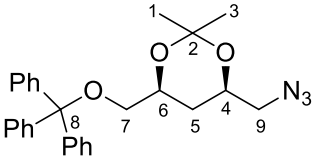


R_f = 0.28 (EtOAc/Hex, 3:7); **IR**: ν_{max}(cm^{-1}): 3065 (C=C-H), 2986 (C-H), 1378 (S=O), 1181 (C-O); **^{1}H NMR (300 MHz, $CDCl_3$)** δ 7.79 (d, *J* = 8.3 Hz, 2H, Ar-H), 7.48 – 7.38 (m, 6H, Ar-H), 7.33 – 7.18 (m, 11H, Ar-H), 4.17 – 4.04 (m, 1H, H-6), 4.03 – 3.88 (m, 3H, H-4 and H-9), 3.21 (dd, *J* = 9.3, 5.3 Hz, 1H, H-7_a), 2.94 (dd, *J* = 9.3, 6.0 Hz, 1H, H-7_b), 2.42 (s, 3H, Ar-CH_3), 1.60 (dt, *J* = 12.7, 2.6 Hz, 1H, H-5_a), 1.37 and 1.30 (2 x s, 6H, H-1 and H-3), 1.21 – 1.07 (m, 1H, H-5_b); **^{13}C NMR (75 MHz, $CDCl_3$)** δ 144.8, 143.9, 133.0, 129.8, 128.7, 128.0, 127.8 and 127.0 (Ar-C), 98.8 (C-2), 86.5 (C-8), 72.4 (C-9), 67.8 (C-4), 67.0 (C-7), 66.9 (C-6), 30.2 (C-5), 29.7 (C-3), 21.6 (Ts-CH_3), 19.6 (C-1).

4.2.42 Synthesis of (4*R*,6*S*)-4-(azidomethyl)-2,2-dimethyl-6-((trityloxy)methyl)-1,3-dioxane 176

Compound **175** (197 mg, 0.345 mmol) was dissolved in DMF (6 ml) followed by the addition of NaN_3 (112 mg, 1.72 mmol) and the reaction was refluxed at 95 °C for 4 h. After TLC analysis showed complete disappearance of the starting material the reaction was cooled, diluted with Et_2O (100 ml) and washed with saturated brine (100 ml). The brine layer in turn was extracted once with Et_2O (100 ml). The combined Et_2O layers were washed with saturated brine (7 x 150 ml), dried over anhydrous Na_2SO_4 and evaporated the afford our crude product. Purification of the desired

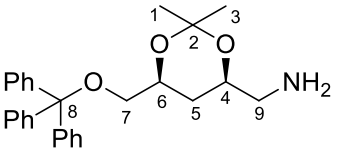
product was achieved by column chromatography (EtOAc/Hex, 3:7) affording azide **176** (148 mg, 97%) as a yellow oil.



R_f = 0.46 (EtOAc/Hex, 3:7); **IR**: ν_{max}(cm^{-1}): 3059 (C=C-H), 2992 (C-H), 2096 (N=N=N), 1380 (C-N), 1168 (C-O); **^{1}H NMR (400 MHz, $CDCl_3$)** δ 7.54 – 7.48 (m, 6H, Ar-H), 7.39 – 7.25 (m, 9H, Ar-H), 4.16 – 4.04 (m, 2H, H-4 and H-6), 3.37 – 3.19 (m, 3H, H-7 and H-9_a), 3.05 (dd, *J* = 9.3, 6.0 Hz, 1H, H-9_b), 1.66 (dt, *J* = 12.7, 2.6 Hz, 1H, H-5_a), 1.51 and 1.47 (2 x s, 6H, H-1 and H-3), 1.41 – 1.28 (m, 1H, H-5_b); **^{13}C NMR (101 MHz, $CDCl_3$)** δ 144.0, 128.7, 127.8 and 127.0 (Ar-C), 98.9 (C-2), 86.5 (C-8), 68.5 (C-4), 68.1 (C-6), 67.2 (C-7), 55.2 (C-9), 31.3 (C-5), 29.8 and 19.7 (C-1 and C-3).

4.2.43 Preparation of ((4*R*,6*S*)-2,2-dimethyl-6-((trityloxy)methyl)-1,3-dioxan-4-yl)methanamine 154

Compound **176** (115 mg, 0.260 mmol) was dissolved in dry Et_2O (10 ml) under N_2 followed by the addition of $LiAlH_4$ (10 mg, 0.260 mmol) in one portion. The reaction was allowed to proceed at room temperature for 2 h before being quenched by the dropwise addition of 2 M NaOH to give a white precipitate. After the addition of anhydrous Na_2SO_4 (2.00 g) the solids were collected by filtration and extracted twice with Et_2O (20 ml). The combined organic layers were evaporated to give the desired amine **154** (102 mg, 94%) as a white solid.

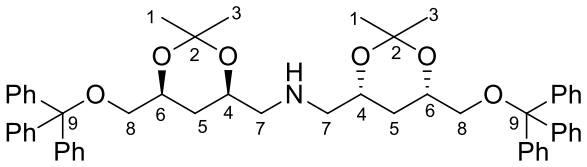


R_f = 0.27 (DCM/MeOH, 1:1); **$[\alpha_D]^{20}$** = -24.6 (c 1.0, $CHCl_3$); **IR**: ν_{max}(cm^{-1}): 3319 (NH), 3057 (C=C-H), 2924 (C-H), 1052 (C-O); **^{1}H NMR (300 MHz, $CDCl_3$)** δ 7.49 – 7.41 (m, 6H, Ar-H), 7.33 – 7.17 (m, 9H, Ar-H), 4.09 – 3.97 (m, 1H, H-6) , 3.97 – 3.84 (m, 1H, H-4), 3.25 (dd, *J* = 9.2, 5.3 Hz, 1H, H-7_a), 2.97 (dd, *J* = 9.2, 6.0 Hz, 1H, H-7_b), 2.74 (br s, 2H, NH_2), 1.58 (dt, *J* = 12.8, 2.5 Hz, 1H, H-5_a), 1.45 and 1.39 (2 x s, 6H, H-1 and H-3), 1.29 – 1.11 (m, 1H, H-5_b). See **section 4.2.20** for the rest of the experimental data.

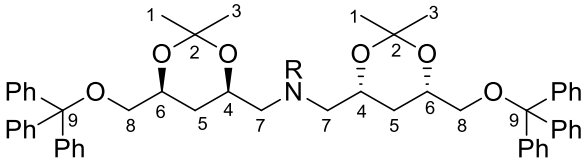
4.2.44 Preparation of bis(((4*R*,6*S*)-2,2-dimethyl-6-((trityloxy)methyl)-1,3-dioxan-4-yl)methyl)amine 177

Compound **151** (138 mg, 0.331 mmol) and compound **154** (102 mg, 0.245 mmol) were dissolved in THF (3 ml) under N_2 followed by the addition of 1,2-dichloroethane (5 ml) and sodium triacetoxyborohydride (105 mg, 0.497 mmol) in one portion. After stirring at room temperature for 2 d over molecular sieve (3Å) the reaction was quenched with 1 M NaOH (5 ml), extracted with

DCM (50 ml) and washed with saturated brine (50 ml). The organic layer was separated and dried over anhydrous Na_2SO_4 and excess solvent was removed *in vacuo*. Purification by column chromatography ($CHCl_3$/MeOH: 9:1) yielded compound **177** (157 mg, 78%) as a viscous yellow oil and compound **178** (40 mg, 19%) as an off-white viscous oil.



Compound 177 R_f = 0.31 (EtOAc/Hex, 4:1); **$[\alpha_D]^{20}$** = -16.6 (c 0.6, $CHCl_3$); **IR**: ν_{max}(cm^{-1}): 3058 (C=C-H), 2991 (C-H), 1378 (C-N), (1077 (C-O); **^{1}H NMR (300 MHz, $CDCl_3$)** δ 7.50 – 7.40 (m, 12H, Ar-H), 7.34 – 7.16 (m, 18H, Ar-H), 4.14 – 3.93 (m, 4H, H-4 and H-6), 3.29 – 3.21 (m, 2H, H-8_a), 2.96 (dd, *J* = 9.2, 5.9 Hz, 2H, H-8_b), 2.77 – 2.63 (m, 4H, H-7), 1.66 – 1.56 (m, 2H, H-5_a), 1.45 and 1.38 (2xs, 12H, H-1 and H-3), 1.30 – 1.20 (m, 2H, H-5_b); **^{13}C NMR (75 MHz, $CDCl_3$)** δ 144.0, 128.7, 127.8 and 127.0 (Ar-C), 98.7 (C-2), 86.5 (C-9), 68.2 and 67.3 (C-4 and C-6), 67.2 (C-8), 54.2 (C-7), 32.1 (C-5), 29.9 (C-3) and 19.9 (C-1); **HRMS** (m/z), calculated for $C_{54}H_{60}NO_6$: 818.4415, found $(M+H)^+$: 818.4421.

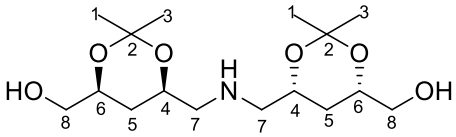


Compound 178 R_f = 0.29 (EtOAc/Hex, 3:2); **$[\alpha_D]^{20}$** = -11.1 (c 1.0, $CHCl_3$); **IR**: ν_{max}(cm^{-1}): 3059 (C=C-H), 2992 (C-H), 1379 (C-N), 1077 (C-O); **^{1}H NMR (500 MHz, $CDCl_3$)** δ 7.53 – 7.45 (m, 12H) and 7.38 – 7.22 (m, 18H, Ar-H), 4.10 – 3.96 (m, 4H, H-4 and H-6), 3.26 (dd, *J* = 9.3, 5.4 Hz, 2H, H-8_a), 2.98 (dd, *J* = 9.3, 5.6 Hz, 2H, H-8_b), 2.72 (dd, *J* = 13.7, 6.3 Hz, 2H, H-7_a), 2.60 (dd, *J* = 13.6, 4.6 Hz, 2H, H-7_b), 1.68 – 1.61 (m, 2H, H-5_a), 1.46 and 1.40 (2 x s, 12H, H-1 and H-3), 1.19 – 1.10 (m, 2H, H-5_b); **^{13}C NMR (126 MHz, $CDCl_3$)** δ 144.1, 128.8, 127.8 and 127.0 (Ar-C), 98.3 (C-2), 86.5 (C-9) , 69.0 and 68.6 (C-4 and C-6), 67.6 (C-8), 62.4 (C-7), 32.6 (C-5), 30.2 (C-3), 20.0 (C-1); **HRMS** (m/z), calculated for $C_{54}H_{60}NO_6$: 818.4415, found $(M+H)^+$: 818.4407, 846.4720.

4.2.45 Synthesis of ((4*S*,4'*S*,6*R*,6'*R*)-6,6'-(azanediylbis(methylene))bis(2,2-dimethyl-1,3-dioxane-6,4-diyl))dimethanol 179

A 250 ml two-necked round bottomed flask was heat-sealed before connecting to a cold finger condenser at -60 °C under N_2. Na (138 mg, 6.02 mmol) was added in one portion and the flask was cooled to -60 °C. Liquid NH_3 (25 ml) was introduced to the flask and allowed to reflux for 15 min until a permanent deep blue was achieved. Compound **177** (246 mg, 0.301 mmol) was dissolved

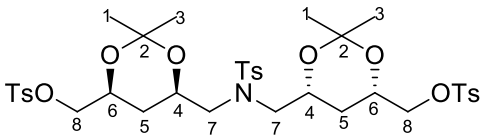
in dry THF (10 ml) and added to the ammonia solution. There was no colour change observed, and the reaction proceeded for a further 1 h. Quenching of the reaction was achieved by dropwise addition of ethanol (10 ml) over 10 min until the blue colour had disappeared completely. Solid NH_4Cl (4.00 g) was then added in one portion and the reaction was left stirring open at ambient temperature until all the NH_3 had evaporated. The reaction mixture was extracted with DCM (100 ml) and excess solvent was removed *in vacuo*. No further purification was performed and compound **179** was recovered as a crude product.



R_f = 0.28 ($CHCl_3$/MeOH, 9:1); **^{1}H NMR (300 MHz, $CDCl_3$)** δ 4.30 – 3.88 (m, 1H), 3.78 – 3.31 (m, 3H), 3.02 – 2.47 (m, 1H), 1.58 – 1.00 (m, 7H); ^{13}C NMR (75 MHz, $CDCl_3$) δ 99.1 (C-2), 69.4, 67.4 and 66.0 (C-4, C-6 and C-8), 54.3 (C-7), 30.3 (C-5), 30.0 (C-3), 20.2 (C-1).

4.2.46 Synthesis of ((4*S*,4'*S*,6*R*,6'*R*)-6,6'-((tosylazanediyl)bis(methylene))bis(2,2-dimethyl-1,3-dioxane-6,4-diyl))bis(methylene) bis(4-methylbenzenesulfonate) 180

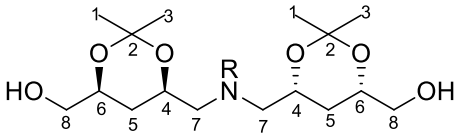
Compound **179** (60 mg, 0.179 mmol) was dissolved in DCM (5 ml) followed by the addition of DMAP (130 mg, 1.07 mmol) and TsCl (130 mg, 1.07 mmol). The reaction proceeded at room temperature for 24 h (TLC control) before being diluted with water (20 ml). The organic layer was separated and dried over anhydrous Na_2SO_4 followed by the removal of excess solvent under reduced pressure. The desired compound was purified by column chromatography (EtOAc/Hex, 9:1) yielding compound **180** (38 mg, 28%) as a yellow oil.



R_f = 0.31 (EtOAc/Hex, 9:1); **IR**: ν_{max}(cm^{-1}): 2925 (C-H), 1669 (C=C), 1152 (C-O); **^{1}H NMR (400 MHz, $CDCl_3$)** δ 7.82 – 7.74 (m, 4H, Ar-H), 7.74 – 7.62 (m, 2H, Ar-H), 7.38 – 7.15 (m, 6H, Ar-H), 4.20 – 3.73 (m, 8H, H-4, H-6 and H-7), 3.34 – 3.11 (m, 2H) and 2.99 – 2.77 (m, 2H, 2.49 – 2.39 (m, 6H), 1.51 – 1.01 (m, 10H); **^{13}C NMR (101 MHz, $CDCl_3$)** δ 144.9, 143.4, 137.3, 129.8, 129.7, 128.0 and 127.2 (Ar-C), 98.9 (C-2), 72.1 (C-8), 67.8 and 66.7 (C-4 and C-6), 54.2 (C-7), 30.1 (C-5), 29.7 (C-3), 21.7 and 21.5 (Ts-CH_3), 19.4 (C-1).

4.2.47 Synthesis of ((4*S*,4'*S*,6*R*,6'*R*)-6,6'-(azanediylbis(methylene))bis(2,2-dimethyl-1,3-dioxane-6,4-diyl))dimethanol 181

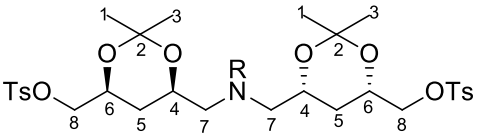
A heat-sealed 250 ml two-necked round bottomed flask connected to a cold finger condenser at -78 °C under N_2 was charged with Na (332 mg, 14.4 mmol) in one portion and the flask was cooled to -60 °C. Liquid NH_3 (25 ml) was introduced to the flask and allowed to reflux for 15 min ensuring that the colour remained deep blue. Compound **178** (598 mg, 0.720 mmol) was dissolved in dry THF (10 ml) and added to the ammonia solution. There was no colour change observed, and the reaction proceeded for a further 1 h. Quenching of the reaction was achieved by dropwise addition of ethanol (50 ml) over 10 min until total dissolution of sodium and disappearance of the blue colour. Solid NH_4Cl (4 g) was then added in one portion and the reaction was left stirring open at ambient temperature until all the NH_3 had evaporated. The reaction mixture was extracted with DCM (100 ml) and excess solvent was removed *in vacuo*. Purification of the desired compound using column chromatography (DCM/MeOH, 95:5) gave rise to compound **181** (85 mg, 35%) as a yellow oil.



R_f = 0.33 (DCM/MeOH, 95:5); **IR**: ν_{max}(cm^{-1}): 3421 (OH), 2993 (C-H), 1262 (C-N), 1199 (C-O) **^{1}H NMR (500 MHz, $CDCl_3$)** δ 4.07 – 3.94 (m, 4H, H-4 and H-6), 3.65 – 3.45 (m, 4H, H-8), 2.88 – 2.63 (m, 4H, OH and H-7_a), 2.61 – 2.48 (m, 2H, H-7_b), 1.54 – 1.48 (m, 2H, H-5_a), 1.46 and 1.39 (2 x s, 12H, H-1 and H-3), 1.32 – 1.18 (m, 2H, H-5_b); **^{13}C NMR (126 MHz, $CDCl_3$)** δ 98.6 (C-2), 69.6 and 67.8 (C-4 and C-6), 66.0 (C-8), 61.8 (C-7), 30.9 (C-5), 30.1 (C-3) 19.9 (C-1); **HRMS** (m/z), calculated for $C_{16}H_{32}NO_6$: 334.2224, found $(M+H)^+$: 334.2202.

4.2.48 Synthesis of ((4*S*,4'*S*,6*R*,6'*R*)-6,6'-((tosylazanediyl)bis(methylene))bis(2,2-dimethyl-1,3-dioxane-6,4-diyl))bis(methylene) bis(4-methylbenzenesulfonate) 182

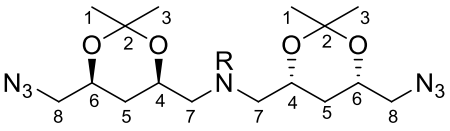
Compound **181** (80 mg, 0.239 mmol) was dissolved in DCM (5 ml) followed by the addition of DMAP (180 mg, 1.48 mmol) and tosyl chloride (282 mg, 1.48 mmol). The reaction was left to stir at room temperature for 24 h (TLC control) before being diluted with water (20 ml). The organic layer was separated and dried over anhydrous Na_2SO_4 followed by the removal of excess solvent under reduced pressure. The desired compound was purified by column chromatography (EtOAc/Hex, 9:1) yielding compound **182** (154 mg, 98%) as a colourless oil.



R_f = 0.44 (EtOAc/Hex, 9:1); **IR**: ν_{max}(cm^{-1}): 3101 (C=C-H), 2951 (C-H), 1645 (C=C), 1161 (C-O); **^{1}H NMR (300 MHz, $CDCl_3$)** δ 7.78 (d, *J* = 7.8 Hz, 4H, Ar-H), 7.34 (d, *J* = 8.3 Hz, 4H, Ar-H), 4.19 – 4.04 (m, 2H, H-6), 4.03 – 3.87 (m, 6H, H-4 and H-8), 2.66 (dd, *J* = 13.5, 5.9 Hz, 2H, H-7_a), 2.59 – 2.47 (m, 2H, H-7_b), 2.44 (s, 6H, Ar-CH_3), 1.61 – 1.50 (m, 2H, H-5_a), 1.37 and 1.28 (2 x s, 12H, H-1 and H-3), 1.19 – 1.02 (m, 2H, H-5_b); **^{13}C NMR (75 MHz, $CDCl_3$)** δ 145.0, 132.9, 129.9 and 128.0 (Ar-H), 98.8 (C-2), 72.4 (C-8), 67.6 (C-4), 67.0 (C-6), 61.5 (C-7), 30.9 (C-5), 29.8 (C-3), 21.6 (Ts-CH_3), 19.6 (C-1).

4.2.49 Synthesis of *N*,*N*-bis(((4*R*,6*S*)-6-(azidomethyl)-2,2-dimethyl-1,3-dioxan-4-yl)methyl)-4-methylbenzenesulfonamide 183

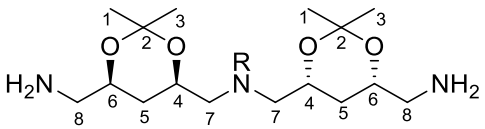
Compound **182** (154 mg, 0.239 mmol) was dissolved in DMF (6 ml) followed by the addition of NaN_3 (5 equiv, 77 mg). The reaction was refluxed for 4 h (TLC control) at 95 °C, until total consumption of the starting material was observed. The reaction mixture was diluted with Et_2O (20 ml) and washed with saturated brine (100 ml). The mixture was separated and the aqueous layer was washed once with Et_2O (50 ml). The combined organic layers were washed with saturated brine (7 x 50 ml) followed by drying over anhydrous Na_2SO_4. Excess solvent was removed *in vacuo* and the product **183** (44 mg, 48%) was not purified any further.



R_f = 0.32 (EtOAc/Hex, 4:1); **^{1}H NMR (300 MHz, $CDCl_3$)** δ 4.14 – 3.93 (m, 4H, H-4 and H-6), 3.23 (d, *J* = 5.1 Hz, 4H, H-8), 2.80 – 2.67 (m, 2H, H-7_a), 2.62 – 2.50 (m, 2H, H-7_b), 1.48 – 1.52 (m, 2H, H-5_a), 1.46 and 1.40 (2 x s, 12H, H-1 and H-3), 1.30 – 1.22 (m, 2H, H-5_b); **^{13}C NMR (75 MHz, $CDCl_3$)** δ 98.8 (C-2), 68.6 and 68.1 (C-4 and C-6), 61.8 (C-7), 55.1 (C-8), 32.1 (C-5), 30.0 and 19.7 (C-1 and C-3).

4.2.50 Synthesis of bis(((4R,6*S*)-6-(aminomethyl)-2,2-dimethyl-1,3-dioxan-4-yl)methyl)amine 184

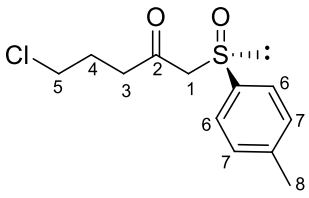
Compound **183** (40 mg, 0.104 mmol) was dissolved in ethanol (2 ml), followed by the addition of a few drops of acetic acid and Pd/C (1 equiv, 11 mg). The reaction proceeded under H_2 at 5 atm for 5 h (TLC control). The reaction mixture was filtered and excess solvent removed *in vacuo*, and it was not purified any further yielding compound **184** as an oil.



R_f = 0.20 ($CHCl_3$/MeOH, 9:1); **IR**: ν_{max}(cm^{-1}): 3400 (NH_2), 2986 (C-H); **^{1}H NMR (300 MHz, MeOD)** δ 4.24 – 3.72 (m, 4H, H-4 and H-6), 2.98 – 2.47 (m, 8H, H-7 and H-8), 1.51 – 0.82 (m, 16H, H-1, H-3 and H-5); **^{13}C NMR (75 MHz, MeOD)** δ 100.6 (C-2), 67.1 and 67.0 (C-4 and C-6), 61.4 (C-7), 44.9 (C-8), 32.5 (C-5), 30.4 (C-3) and 20.2 (C-1).

4.2.51 Synthesis of (*R*)-5-chloro-1-(*p*-tolylsulfinyl)pentan-2-one 192

Diisopropylamine (9.63 ml, 68.7 mmol) was added to THF (100 ml) under N_2 and cooled to -78 °C. *N*-butyllithium (46.0 ml, 68.7 mmol) was added slowly and the reaction was left stirring for 1 h before the addition of the methyl *p*-tolylsulfoxide **137**. The reaction mixture turned bright yellow, and after 30 min methyl-4-chlorobutyrate **191** (7.0 ml, 45.8 mmol) was added in one portion and the reaction stirred for a further 1 h. Saturated aqueous NH_4Cl (50 ml) was added to quench the reaction, followed by adjusting the pH to 6 using 1 M HCl. The reaction mixture was diluted with EtOAc (100 ml). The organic layer was separated, and washed with saturated brine (100 ml), dried over anhydrous Na_2SO_4 and excess solvent was removed *in vacuo*. Product purification was afforded by column chromatography (EtOAc/Hex, 3:2) yielding compound **192** (1.70 g, 14%) as a white precipitate.

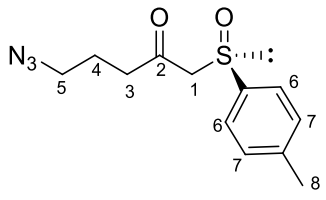


R_f = 0.39 (EtOAc/Hex, 3:2); **$[\alpha_D]^{20}$** = +213.0 (c 1, $CHCl_3$); **M.p** = 116 – 117 °C; **IR**: ν_{max}(cm^{-1}): 3016 (C=C-H), 2955 (C-H), 1701 (C=O), 1041 (S=O); **^{1}H NMR (300 MHz, $CDCl_3$)** δ 7.53 (d, *J* = 8.3 Hz, 2H, H-6), 7.35 (d, *J* = 8.0 Hz, 2H, H-7), 3.86 (d, *J* = 13.3 Hz, 1H, H-1_a), 3.79 (d, *J* = 13.3 Hz, 1H, H-1_b), 3.51 (t, *J* = 6.3 Hz, 2H, H-5), 2.69 (td, *J* = 6.8, 2.0 Hz, 2H, H-3), 2.42 (s, 3H, H-8), 2.00 (p, *J* = 6.7 Hz, 2H, H-4); **^{13}C NMR (75 MHz, $CDCl_3$)** δ 200.4 (C-2), 142.3 and 139.5 (Ar-C), 130.2 (C-7) 124.0 (C-6), 67.9 (C-1), 43.9 (C-5), 41.9 (C-3), 25.8 (C-4), 21.5 (C-8); **HRMS** (m/z), calculated for $C_{12}H_{16}ClO_2S$: 259.0554, found $(M+H)^+$: 259.0558.

4.2.52 Synthesis of (*R*)-5-azido-1-(*p*-tolylsulfinyl)pentan-2-one 193

Compound **192** (1.00 g, 3.86 mmol), was dissolved in DMF (10 ml) followed by the addition of NaN_3 (1.26 g, 19.3 mmol) and the reaction was refluxed at 95 °C for 4 h. After TLC analysis showed complete disappearance of the starting material, the reaction was cooled, diluted with Et_2O (200 ml) and washed with saturated brine. The brine layer in turn was extracted once with Et_2O (100 ml). The combined Et_2O layers were washed with saturated brine (7 x 250 ml), dried over

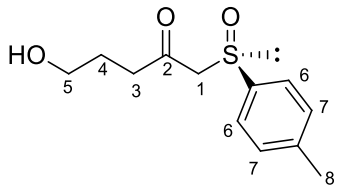
anhydrous Na_2SO_4 and evaporated to afford the crude product. Purification of the desired product was achieved by column chromatography (EtOAc/Hex, 3:2) affording compound **193** (166 mg, 16%) as a yellow oil.



R_f = 0.46 (EtOAc/Hex, 3:7); **^{1}H NMR (300 MHz, $CDCl_3$)** δ 7.29 – 7.22 (m, 2H, H-6), 7.15 – 7.07 (m, 2H, H-7), 3.61 (s, 2H, H-1), 3.26 (t, *J* = 6.6 Hz, 2H, H-5), 2.68 (t, *J* = 7.0 Hz, 2H, H-3), 2.31 (s, 3H, H-8), 1.82 (p, *J* = 6.8 Hz, 2H, H-4); **^{13}C NMR (75 MHz, $CDCl_3$)** δ 204.5 (C-2), 137.4 and 130.7 (Ar-C), 130.5 (C-7), 130.0 (C-6), 50.6 (C-5), 44.5 (C-1), 37.1 (C-3), 23.0 (C-4), 21.0 (C-8).

4.2.53 Synthesis of (*R*)-5-hydroxy-1-(*p*-tolylsulfinyl)pentan-2-one 195

LDA (1.0 M in hexanes, 98 ml) was added to THF (100 ml) under N_2 and cooled to -78 °C before the slow addition of the methyl sulfoxide **137** (15.1 g, 97.6 mmol). The reaction mixture turned bright yellow and after 30 min γ-butyrolactone **194** (5.0 ml, 65.0 mmol) slowly added in one portion and the reaction stirred for a further 2 h. Solid NH_4Cl (50 ml) was added to quench the reaction followed by adjusting the pH to 6 using 1 M HCl. The reaction mixture was diluted with EtOAc (100 ml) and the organic layer was separated, washed with saturated brine (100 ml) and dried over anhydrous Na_2SO_4 and excess solvent was removed *in vacuo*. Product purification was afforded by column chromatography (EtOAc/Hex, 3:2) yielding compound **195** (9.84g, 63%) as a colourless oil.

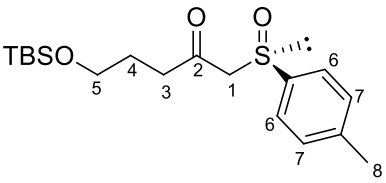


R_f = 0.46 (EtOAc/Hex, 4:1); **IR**: ν_{max}(cm^{-1}): 3392 (OH), 2924 (C-H), 1710 (C=O), 1596 (C=C), 1085 (C-O), 1012 (S=O); **^{1}H NMR (500 MHz, $CDCl_3$)** δ 7.58 – 7.49 (m, 2H, H-6), 7.37 – 7.27 (m, 2H, H-7), 5.58 (br-s, 1H, OH), 4.15 – 4.05 (m, 1H, H-5_a), 4.02 – 3.91 (m, 2H, H-5_b and H-1_a), 3.84 (d, *J* = 14.0 Hz, 1H, H-1_b), 2.40 (s, 3H, H-8), 2.22 – 2.06 (m, 2H) and 2.02 – 1.81 (m, 2H, H-3 and H-4); **^{13}C NMR (126 MHz, $CDCl_3$)** δ 202.2 (C-2), 142.2, 141.9, 124.1 and 124.0 (Ar-C), 68.3 (C-5), 67.8 (C-1), 38.4 (C-3), 24.6 (C-4), 21.4 (C-6).

4.2.54 Synthesis of (*S*)-5-((tert-butyldimethylsilyl)oxy)-1-(*p*-tolylsulfinyl)pentan-2-one 196

A crude mixture of compound **195** (1.82 g, 7.56 mmol) was dissolved in DCM (20 ml) followed by the successive addition of TBSCl (1.71 g, 11.3 mmol), imidazole (0.77 g, 11.3 mmol) and DMAP (1.39 g, 11.3 mmol). The reagents were left stirring in air at room temperature overnight (TLC

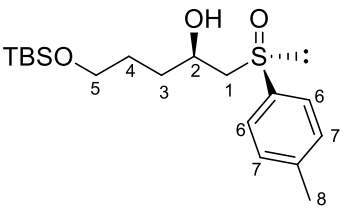
control). Upon completion, the reaction mixture was diluted with H_2O (50 ml). The organic layer was separated, washed with a saturated brine solution (50 ml), dried over Na_2SO_4 and excess solvent was removed *in vacuo*. The desired product was purified by column chromatography (EtOAc/Hex, 3:2) yielding compound **196** (1.33 g, 50%) as a viscous oil.



R_f = 0.37 (EtOAc/Hex, 3:2); **$[\alpha_D]^{20}$** = +116.7 (c 2.00, $CHCl_3$); **IR**: $\nu_{max}(cm^{-1})$: 2934 (C-H), 1711 (C-O), 1251 (C-O); **^{1}H NMR (300 MHz, $CDCl_3$)** δ 7.54 (d, *J* = 8.2 Hz, 2H, H-6), 7.33 (d, *J* = 8.0 Hz, 2H, H-7), 3.90 (d, *J* = 13.6 Hz, 1H, H-1_a), 3.78 (d, *J* = 13.6 Hz, 1H, H-1_b), 3.57 (t, *J* = 6.0 Hz, 2H, H-5), 2.59 – 2.51 (m, 2H, H-3), 2.42 (s, 3H, H-8), 1.75 (p, *J* = 6.6 Hz, 2H, H-4), 0.87 (s, 9H, TBS-C(CH_3)$_3$), 0.02 (s, 6H, TBS-Si(CH_3)$_2$); **^{13}C NMR (75 MHz, $CDCl_3$)** δ 201.6 (C-2), 142.1 and 139.8 (Ar-C), 130.1 (C-7), 124.1 (C-6), 68.3 (C-1), 61.8 (C-5), 41.5 (C-3), 26.4 (C-4), 25.9 (TBS-C($\underline{C}H_3$)$_3$), 21.5 (C-8), 18.3 (TBS-$\underline{C}$(CH_3)$_3$), -5.4 (TBS-Si($\underline{C}H_3$)$_2$); **HRMS** (m/z), calculated for $C_{18}H_{31}O_3SSi$: 355.1785, found $(M+H)^+$: 355.1754.

4.2.55 Synthesis of (*R*)-5-((*tert*-butyldimethylsilyl)oxy)-1-((*S*)-*p*-tolylsulfinyl)pentan-2-ol 197

Compound **196** (0.95 g, 14.1 mmol) in dry THF (50 ml) was added to a stirring solution of $ZnCl_2$ (1.46 g, 10.7 mmol) in THF (100 ml) for 2 h. The mixture was cooled -78 °C for 10 min before adding DIBALH (1.0 M in hexanes, 5.46 ml) and the reaction was allowed to proceed for a further 2 h whilst slowly warming to room temperature. Work up of the reaction was achieved by the slow addition of saturated aqueous NH_4Cl (100 ml), after cooling the reaction back to -78 °C. The reaction mixture was extracted with EtOAc (2 x 200 ml), followed by separation of the organic layer which in turn was washed with saturated brine (200 ml), separated, dried over anhydrous Na_2SO_4 followed by removal of solvent under reduced pressure. Purification of the product was afforded by column chromatography (EtOAc/Hex, 1:1) yielding compound **197** (0.93 g, 95%) as a white solid.

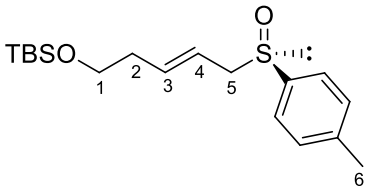


R_f = 0.39 (EtOAc/Hex, 1:1); **$[\alpha_D]^{20}$** = +115.0 (c 1.00, $CHCl_3$); **M.p.** = 69 – 70 °C; **IR**: $\nu_{max}(cm^{-1})$: 3337 (OH), 3052 (C=C-H), 2928 (C-H), 1251 (C-O), 1059 (S=O); **^{1}H NMR (300 MHz, $CDCl_3$)** δ 7.56 (d, *J* = 8.2 Hz, 2H, H-6), 7.33 (d, *J* = 7.9 Hz, 2H, H-7), 4.24 (d, *J* = 2.3 Hz, 1H, OH), 4.21 – 4.08 (m, 1H, H-2), 3.70 – 3.61 (m, 2H, H-5), 3.03 (dd, *J* = 13.1, 8.8 Hz, 1H, H-1_a), 2.78 (dd, *J* = 13.0, 3.1

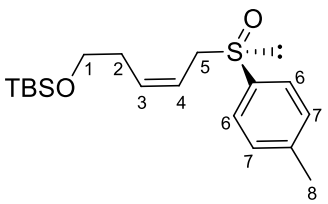
Hz, 1H, H-1_b), 2.42 (s, 3H, H-8), 1.75 – 1.57 (m, 4H, H-3 and H-4), 0.89 (s, 9H, TBS-C(CH_3)$_3$), 0.052 and 0.050 (2 x overlapping singlets, 6H, TBS-Si(CH_3)$_2$); **^{13}C NMR (75 MHz, $CDCl_3$)** δ 141.8 and 140.6 (Ar-C), 130.1 (C-7) 124.1 (C-6), 68.1 (C-2), 63.2 and 63.1 (C-1 and C-5), 34.4 and 28.7 (C-3 and C-4), 25.9 (TBS-C($\underline{C}H_3$)$_3$), 21.4 (C-8), 18.3 (TBS-$\underline{C}$(CH_3)$_3$), -5.4 (TBS-Si(CH_3)$_2$); **HRMS** (m/z), calculated for $C_{18}H_{33}O_3SSi$: 357.1914, found $(M+H)^+$: 357.1917.

4.2.56 Synthesis of (*R*,*E*)-*tert*-butyldimethyl((5-(*p*-tolylsulfinyl)pent-3-en-1-yl)oxy)silane

Compound **197** (3.21 g, 9.00 mmol) was dissolved in THF (20 ml) under inert conditions, followed by the addition of NaH (0.26 g, 10.8 mmol) in one portion. The reaction was stirred at room temperature for 30 min before addition of BnBr (2.14 ml, 18.0 mmol). The stirring reaction was allowed to proceed until total consumption of starting material was observed as determined by TLC analysis. Quenching of the reaction was achieved by dropwise addition of methanol (20 ml). The organic layer was diluted with EtOAc (100 ml), washed with saturated brine (100 ml), separated and dried over anhydrous Na_2SO_4 before removing excess solvent under reduced pressure. Purification of the desired product was afforded by column chromatography (EtOAc/Hex, 3:7) yielding two different products **198** and **199**.



Compound 198: R_f = 0.29 (EtOAc/Hex, 1:1); **$[\alpha_D]^{20}$** = +29.8 (c 2.05, $CHCl_3$); **IR**: ν_{max}(cm^{-1}): 3029 (C=C-H), 2953 (C-H), 1086 (C-O), 1046 (S=O), 834 (C=C bending); **^{1}H NMR (300 MHz, $CDCl_3$)** δ 7.60 – 7.42 (m, 2H, Ar-H), 7.37 – 7.20 (m, 2H, Ar-H), 5.87 – 5.72 (m, 1H, H-4), 5.44 – 5.27 (m, 1H, H-3), 3.66 – 3.42 (m, 4H, H-1 and H-5), 2.40 (s, 3H, H-6), 2.14 – 2.10 (m, 2H, H-2), 0.98 – 0.78 (m, 9H, TBS-C(CH_3)$_3$), 0.07 – 0.01 (m, 6H, TBS-Si(CH_3)$_2$); **^{13}C NMR (75 MHz, $CDCl_3$)** δ 141.5, 140.0 (Ar-C), 135.1 (C-4), 129.7 and 124.4 (Ar-C), 117.6 (C-3), 62.2 (C-1), 55.5 (C-5), 31.2 (C-2), 25.9 (TBS-C($\underline{C}H_3$)$_3$), 21.4 (C-6), 18.3 (TBS-$\underline{C}$(CH_3)$_3$), -5.3 (TBS-Si(CH_3)$_2$); **HRMS** (m/z), calculated for $C_{18}H_{31}O_2SSi$: 339.1809, found $(M+H)^+$: 339.1807.

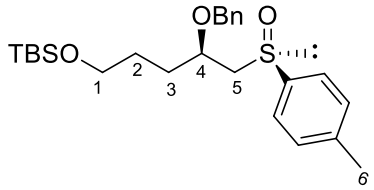


Compound 199: **R_f** = 0.27 (EtOAc/Hex, 1:1); **$[\alpha_D]^{20}$** = +1.90 (c 2.10, $CHCl_3$); **IR**: ν_{max}(cm^{-1}): 3034 (C=C-H), 2953 (C-H), 1661 (C=C), 1086 (C-O), 1045 (S=O), 833 (C=C bending); **^{1}H NMR (300 MHz, $CDCl_3$)** δ 7.47 (d, *J* = 7.9 Hz, 2H, H-6), 7.30 (d, *J* = 8.0 Hz, 2H, H-7), 5.65 – 5.51 (m, 1H, H-4), 5.42 – 5.27 (m, 1H, H-3), 3.56 (t, *J* = 6.8 Hz, 2H, H-1), 3.47 (d, *J* = 7.5 Hz, 2H, H-5), 2.41 (s, 3H,

H-8), 2.28 – 2.18 (m, 2H, H-2), 0.89 – 0.86 (m, 9H, TBS-C(CH_3)$_3$), 0.03 (s, 6H, TBS-Si(CH_3)$_2$); **^{13}C NMR (75 MHz, $CDCl_3$)** δ 141.4 and 139.9 (Ar-C), 136.8 (C-4), 129.6 (C-7), 124.4 (C-6), 118.8 (C-3), 62.4 (C-1), 60.4 (C-5), 36.2 (C-2), 25.9 (TBS-C($\underline{C}H_3$)$_3$), 21.4 (C-6), 18.3 (TBS-$\underline{C}$(CH_3)$_3$), -5.3 (TBS-Si($\underline{C}H_3$)$_2$); **HRMS** (m/z), calculated for $C_{18}H_{31}O_2SSi$: 339.1809, found $(M+H)^+$: 339.1814.

4.2.57 (((*R*)-4-(benzyloxy)-5-((*R*)-*p*-tolylsulfinyl)pentyl)oxy)(*tert*-butyl)dimethylsilane 200

Compound **197** (0.700 g, 1.96 mmol) was dissolved in THF (20 ml) at 0 °C under inert conditions, followed by the addition of NaH (94.0 mg, 2.36 mmol) in one portion. The reaction was stirred for 30 min before addition of BnBr (0.466 ml, 3.92 mmol). The stirring reaction was allowed to proceed until total consumption of starting material was observed by TLC analysis whilst gently warming to room temperature. Quenching of the reaction was achieved by dropwise addition of methanol (20 ml) at 0 °C. The organic layer was diluted with EtOAc (100 ml), washed with saturated brine (100 ml), separated and dried over Na_2SO_4 before removing excess solvent under reduced pressure. Purification of the desired product was afforded by column chromatography (EtOAc/Hex, 3:7) yielding compound **200** (0.844 g, 96%) as a colourless oil.

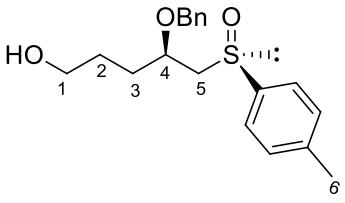


R_f = 0.37 (EtOAc/Hex, 3:7); **$[\alpha_D]^{20}$** = +85.2 (c 0.56, $CHCl_3$); **IR**: ν_{max}(cm^{-1}): 3032 (C=C-H), 2952 (C-H), 1597 (C=C), 1087 (C-O), 1042 (S=O); **^{1}H NMR (300 MHz, $CDCl_3$)** δ 7.52 – 7.45 (m, 2H, Ar-H), 7.37 – 7.23 (m, 7H, Ar-H), 4.48 (d, *J* = 11.5 Hz, 1H, (Bn-CH_2)$_a$), 4.38 (d, *J* = 11.5 Hz, 1H, (Bn-CH_2)$_b$), 3.72 (p, *J* = 6.0 Hz, 1H, H-4), 3.59 (t, *J* = 6.2 Hz, 2H, H-1), 3.23 (dd, *J* = 13.3, 5.8 Hz, 1H, H-5$_a$) 2.86 (dd, *J* = 13.3, 6.1 Hz, 1H, H-5$_b$), 2.39 (s, 3H, H-6), 1.92 – 1.51 (m, 4H, H-2 and H-3), 0.89 (s, 9H, TBS-C(CH_3)$_3$), 0.04 (s, 6H, TBS-Si(CH_3)$_2$); **^{13}C NMR (75 MHz, $CDCl_3$)** δ 141.6, 140.9, 137.9, 130.0, 128.3, 127.8, 127.7 and 124.2 (Ar-H), 73.6 (C-4), 70.8 (Bn-CH_2), 62.7 (C-1), 62.4 (C-5), 30.1 and 28.0 (C-2 and C-3), 26.0 (TBS-C($\underline{C}H_3$)$_3$), 21.4 (C-6), 18.3 (TBS-$\underline{C}$(CH_3)$_3$), -5.3 (TBS-Si($\underline{C}H_3$)$_2$); **HRMS** (m/z), calculated for $C_{25}H_{39}O_3SSi$: 447.2384, found $(M+H)^+$: 447.2377.

4.2.58 Synthesis of (*R*)-4-(benzyloxy)-5-((*R*)-*p*-tolylsulfinyl)pentan-1-ol 201

Compound **200** (0.730 g, 1.63 mmol) was dissolved in dry THF (20 ml) under N_2 at 0 °C, followed by the addition of TBAF (2.45 ml, 2.45 mmol). The reaction was left for 4 h before quenching with saturated aqueous NH_4Cl (50 ml) and dilution with EtOAc (50 ml). The organic layer was separated

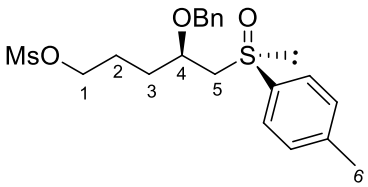
and washed with saturated brine (50 ml) followed by the removal of excess solvent under reduced pressure. Purification of the desired product was achieved by column chromatography (EtOAc) yielding compound **201** (0.388 g, 71%) as a colourless oil.



R_f = 0.21 (EtOAc); **$[\alpha_D]^{20}$** = +121.7 (c 0.63, $CHCl_3$); **IR**: ν_{max}(cm^{-1}): 3395 (OH), 3031 (C=C-H), 2922 (C-H), 1085 (C-O), 1026 (S=O); **^{1}H NMR (300 MHz, $CDCl_3$)** δ 7.50 – 7.43 (m, 2H, Ar-H), 7.36 – 7.20 (m, 7H, Ar-C), 4.44 (d, *J* = 11.5 Hz, 1H) and 4.37 (d, *J* = 11.5 Hz, 1H, Bn-CH_2), 3.73 (p, *J* = 6.1 Hz, 1H, H-4), 3.64 – 3.52 (m, 2H, H-1), 3.21 (dd, *J* = 13.4, 5.4 Hz, 1H, H-5_a), 3.14 (br-s, 1H, OH), 2.89 (dd, *J* = 13.4, 6.3 Hz, 1H, H-5_b), 2.38 (s, 3H, H-6), 1.97 – 1.52 (m, 4H, H-2 and H-3); **^{13}C NMR (75 MHz, $CDCl_3$)** δ 141.7, 140.4, 137.8, 130.0, 128.3, 127.8, 127.7 and 124.2 (Ar-C), 73.6 (C-4), 70.8 (Bn-CH_2), 62.0 (C-1), 61.7 (C-5), 30.4 and 28.0 (C-2 and C-3), 21.4 (C-6); **HRMS** (m/z), calculated for $C_{19}H_{25}O_3S$: 333.1525, found $(M+H)^+$: 333.1530.

4.2.59 Synthesis of (*R*)-4-(benzyloxy)-5-((*R*)-*p*-tolylsulfinyl)pentyl methanesulfonate 202

Compound **201** (0.380 g, 1.14 mmol) was dissolved in dry DCM (10 ml) at 0 °C under an inert atmosphere followed by the addition of Et_3N (318 µl, 2.28 mmol). The reaction was left stirring for 10 min before mesyl chloride (176 µl, 2.28 mmol) was added dropwise. The reaction was left to gradually reach room temperature, stirring overnight. After the total consumption of the starting material as determined by TLC analysis, the reaction was quenched by saturated aqueous $NaHCO_3$ (10 ml) and diluted with DCM (10 ml). The organic layer was separated and washed with saturated brine (10 ml) and dried over Na_2SO_4 followed by the removal of excess solvent *in vacuo*. Purification of the desired product was afforded by column chromatography (EtOAc/Hex, 4:1) yielding compound **202** (0.385 g, 82%) as a colourless oil.

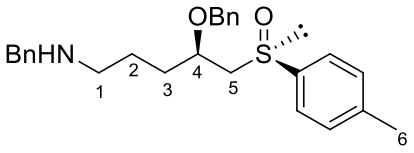


R_f = 0.35 (EtOAc/Hex, 4:1); **IR**: ν_{max}(cm^{-1}): 3029 (C=C-H), 2936 (C-H), 1350 (O=S=O), 1171 and 1085 (C-O); **^{1}H NMR (500 MHz, $CDCl_3$)** δ 7.54 – 7.47 (m, 2H, Ar-H), 7.37 – 7.24 (m, 7H, Ar-H), 4.48 – 4.39 (m, 2H, Bn-CH_2), 4.25 – 4.18 (m, 2H, H-1), 3.83 – 3.76 (m, 1H, H-4), 3.22 – 3.15 (m, 1H, H-5_a), 2.98 (s, 3H, Ms-CH_3), 2.91 – 2.83 (m, 1H, H-5_b), 2.42 (s, 3H, H-6), 2.01 – 1.77 (m, 4H, H-2 and H-6; **^{13}C NMR (126 MHz, $CDCl_3$)** δ 141.7, 140.6, 137.6, 130.1, 128.5, 127.92, 127.91

(Ar-C) 124.1, 73.1 (C-4), 71.1 (Bn-CH_2), 69.7 (C-1), 61.5 (C-5), 37.4 (Ms-CH_3), 30.2 (C-3), 24.9 (C-2), 21.4 (C-6); **HRMS** (m/z), calculated for $C_{20}H_{27}O_5SSi$: 411.1294, found $(M+H)^+$: 411.1295.

4.2.60 Synthesis of (*R*)-*N*-benzyl-4-(benzyloxy)-5-((*R*)-*p*-tolylsulfinyl)pentan-1-amine 203

Compound **202** (0.301 g, 0.731 mmol) was dissolved in dry THF (5 ml) at 0 °C under N_2 followed by the addition of a cooled benzylamine (1.30 ml, 11.6 mmol) solution in THF (5 ml). The reaction was allowed to warm to room temperature and left stirring for 2 d. The reaction mixture was then diluted with EtOAc (10 ml), saturated aqueous $NaHCO_3$ (10 ml) and saturated brine (10 ml). The organic layer was dried over Na_2SO_4 and excess solvent was removed *in vacuo*. Product purification was afforded by column chromatography (EtOAc/Hex, 4:1) to yield compound **203** (67 mg, 22%) as an oil.

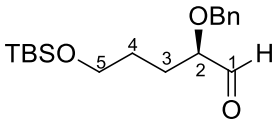


R_f = 0.25 (EtOAc/Hex, 4:1); **IR**: $\nu_{max}(cm^{-1})$: 3296 (NH), 3029 (C=C-H), 2923 (C-H), 1663 (C=C), 1085 (C-O); **^{1}H NMR (500 MHz, $CDCl_3$)** δ 7.48 (d, *J* = 7.8 Hz, 2H, Ar-H), 7.40 – 7.21 (m, 12H, Ar-H), 4.50 – 4.34 (m, 2H, Bn-O-CH_2), 3.82 (s, 2H, Bn-N-CH_2), 3.72 (s, 1H, H-4), 3.28 – 3.15 (m, 1H, H-5_a), 2.96 – 2.81 (m, 1H, H-5_b), 2.73 – 2.56 (m, 2H, H-1), 2.41 (s, 3H, H-6), 1.90 – 1.54 (m, 4H, H-2 and H-3); **^{13}C NMR (126 MHz, $CDCl_3$)** δ 141.6, 140.7, 138.3, 137.9, 130.0, 128.7, 128.5, 128.4, 127.9, 127.8, 127.7 and 124.3 (Ar-C), 73.6 (C-4), 70.9 (Bn-O-CH_2), 61.9 (C-5), 53.6 (Bn-N-CH_2), 48.8 (C-1), 31.6 (C-3), 25.1 (C-2), 21.4 (C-6); **HRMS** (m/z), calculated for $C_{26}H_{32}NO_2S$: 422.2149, found $(M+H)^+$: 422.2148.

4.2.61 Synthesis of (*R*)-2-(benzyloxy)-5-((*tert*-butyldimethylsilyl)oxy)pentanal 204

To a stirring solution of compound **200** (0.424 g, 0.948 mmol) at 0 °C in MeCN (3 ml), 2,4,6-collidine (0.63 ml, 4.74 mmol) was added followed by TFAA (0.66 ml, 4.74 mmol) and the reaction was left stirring for 30 min. The solution turned yellow and it was quenched by H_2O (1 ml) and solid K_2CO_3 until the solution was neutral. Stirring continued for a further 1 h at room temperature followed by work up with saturated aqueous NH_4Cl (10 ml) and 1 M HCl (10 ml). The organic layer was separated and washed with saturated aqueous $NaHCO_3$ (10 ml) and saturated brine (10 ml). The organic layer was separated, dried over anhydrous Na_2SO_4 and excess solvent was removed under

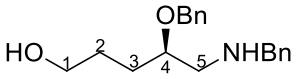
reduced pressure. Product purification was afforded by column chromatography (EtOAc/Hex, 1:9) yielding compound **204** (0.258 g, 88%) as a yellow oil.



R_f = 0.45 (EtOAc/Hex, 1:9); **$[\alpha_D]^{20}$** = +27.4 (c 0.53, $CHCl_3$); **IR**: $\nu_{max}(cm^{-1})$: 3029 (C=C-H), 2956 (C-H), 1735 (C=O), 1492 (C=C), 1091 (C-O); **^{1}H NMR (400 MHz, $CDCl_3$)** δ 9.64 (d, *J* = 2.0 Hz, 1H, H-1), 7.46 – 7.21 (m, 5H, Ar-H), 4.67 (d, *J* = 11.6 Hz, 1H) and 4.53 (d, *J* = 11.7 Hz, 1H, Bn-CH_2), 3.81 – 3.75 (m, 1H, H-2), 3.60 (t, *J* = 6.1 Hz, 3H, H-5), 1.89 – 1.45 (m, 4H, H-3 and H-4), 0.94 – 0.86 (m, 9H, TBS-C$(CH_3)_3$), 0.06 – 0.01 (m, 6H, TBS-Si$(CH_3)_2$); **^{13}C NMR (101 MHz, $CDCl_3$)** δ 203.5 (C-1), 137.3, 132.1, 129.8, 128.5 and 128.0 (Ar-C), 83.2 (C-2), 72.4 (Bn-CH_2), 62.5 (C-5), 27.9 and 26.5 (C-3 and C-4), 25.9 (TBS-C($\underline{C}H_3)_3$), 18.3 (TBS-$\underline{C}(CH_3)_3$), -5.3 (TBS-Si$(CH_3)_2$); **HRMS** (m/z), calculated for $C_{18}H_{31}O_3Si$: 323.2037, found $(M+H)^+$: 323.2036.

4.2.62 Synthesis of (*R*)-5-(benzylamino)-4-(benzyloxy)pentan-1-ol 205

To a stirring solution of compound **204** (92 mg, 0.288 mmol) in 1,2-DCE (3 ml) was added benzylamine (63 µl, 0.576 mmol) in one portion. The reaction was left stirring for 1 h prior to the addition of $NaBH(OAc)_3$ (122 mg, 0.576 mmol). TLC analysis showed formation of a new product after 18 h and the reaction was washed with 1 M NaOH (10 ml) and saturated brine (20 ml) and the organic layer was separated and dried over anhydrous Na_2SO_4. Excess solvent was removed under reduced pressure and product purification was achieved by column chromatography ($CHCl_3$/MeOH, 9:1) yielding compound **205** (38 mg, 44%) as a yellow oil.



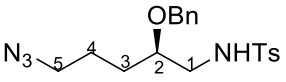
R_f = 0.45 ($CHCl_3$/MeOH, 9:1); **$[\alpha_D]^{20}$** = +27.4 (c 0.53, $CHCl_3$); **IR**: $\nu_{max}(cm^{-1})$: 3344 (NH and OH), 3032 (C=C-H), 2927 (C-H); **^{1}H NMR (500 MHz, $CDCl_3$)** δ 7.37 – 7.21 (m, 10H, Ar-H), 4.43 – 4.40 (m, 4H, Bn-N-CH_2 and Bn-O-CH_2), 4.03 (p, *J* = 5.2 Hz, 1H, H-4), 3.58 (t, *J* = 6.2 Hz, 2H, H-1), 3.46 (dd, *J* = 14.6, 5.9 Hz, 1H, H-5_a), 3.22 (dd, *J* = 14.5, 5.1 Hz, 1H, H-5_b), 1.84 – 1.50 (m, 4H, H-2 and H-3); **^{13}C NMR (126 MHz, $CDCl_3$)** δ 137.4, 137.1, 129.8, 128.7, 128.3, 127.9, 127.8 and 127.5 (Ar-C), 73.4 (C-4), 71.4 (Bn-O-CH_2), 62.3 (C-1), 60.6 (Bn-N-CH_2), 43.7 (C-5), 30.9 and 27.7 (C-2 and C-4); **HRMS** (m/z), calculated for $C_{19}H_{26}NO_2$: 300.1958, found $(M+H)^+$: 300.1958.

4.2.63 Synthesis of (*R*)-4-(benzyloxy)-5-(4-methylphenylsulfonamido)pentyl 4-methylbenzenesulfonate

Compound **205** (38 mg, 0.105 mmol) was dissolved in DCM (3 ml) followed by the addition of DMAP (44 mg, 0.361 mmol) and TsCl (69 mg, 0.361 mmol). The reagents were left stirring overnight and TLC analysis showed total consumption of the starting material. Work up of the reaction was achieved by diluting with H_2O (10 ml) and saturated brine (10 ml), followed by drying of the organic layer over anhydrous Na_2SO_4. Excess solvent was removed under reduced pressure. The crude product was purified by column chromatography (EtOAc/Hex, 4:1) yielding compound **206** and compound **207** as a mixture of products. $\mathbf{R_f}$ = 0.45 (EtOAc/Hex, 4:1); $\mathbf{[\alpha_D]^{20}}$ = +27.4 (c 0.53, $CHCl_3$).

4.2.64 Synthesis of (*R*)-*N*-(5-azido-2-(benzyloxy)pentyl)-4-methylbenzenesulfonamide 208

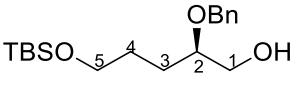
The crude mixture of compound **206** and compound **207** (54 mg) was dissolved in DMF (3 ml) followed by the addition of NaN_3 (47 mg, 0.720 mmol) in one portion. The reaction was left to reflux at 80 °C for 4 h until TLC analysis showed total consumption of the starting material. The reaction was diluted with Et_2O (10 ml) and H_2O (5 ml) followed by separation of the organic layer. The aqueous layer was washed once with Et_2O (3 ml) and separated. The combined organic layers were further washed with saturated brine (7 x 20 ml), dried over anhydrous Na_2SO_4 and excess solvent was removed under reduced pressure. A crude product **208** (26 mg) was recovered as a brown oil and was not purified further.



$\mathbf{R_f}$ = 0.33 (EtOAc/Hex, 9:1); **IR**: ν_{max}(cm^{-1}): 3354 (NH), 3033 (C=C-H), 2928 (C-H), 2094 (C-N=N=N), 1295 (C-O); **^{1}H NMR (400 MHz, $CDCl_3$)** δ 7.77 (d, *J* = 8.1 Hz, 2H, Ar-H), 7.39 – 7.23 (m, 5H, Ar-H), 7.19 – 7.13 (m, 2H, Ar-H), 4.45 (d, *J* = 11.4 Hz, 1H) and 4.39 (d, *J* = 11.4 Hz, 1H, Bn-CH_2), 3.99 (p, *J* = 5.5 Hz, 1H, H-2), 3.45 (dd, *J* = 14.6, 5.5 Hz, 1H, H-1_a), 3.25 – 3.15 (m, 3H, H-5 and H-1_b), 2.42 (s, 3H, Ar-CH_3), 1.83 – 1.50 (m, 4H, H-3 and H-4); **^{13}C NMR (101 MHz, $CDCl_3$)** δ 144.8, 137.3, 137.0, 129.9, 128.4, 127.91, 127.88 and 127.85 (Ar-C), 72.9 (C-2), 71.4 (Bn-CH_2), 60.6 (C-1), 51.1 (C-5), 31.8 (C-3), 24.2 (C-4), 21.6 (Ar-CH_3).

4.2.65 Synthesis of (*R*)-2-(benzyloxy)-5-((*tert*-butyldimethylsilyl)oxy)pentan-1-ol 210

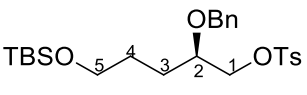
To a stirring solution of compound **200** (480 mg, 1.07 mmol) was added 2,4,6-collidine (710 µl, 573 mmol) followed by TFAA (746 µl, 5.37 mmol) at 0 °C for 30 min. The reaction was quenched with a saturated solution of $NaHCO_3$ (1 ml) and solid K_2CO_3. $NaBH_4$ (243 mg, 6.42 mmol) was added after the reaction had been left stirring at room temperature for 30 min. The reaction was allowed to proceed for a further 1 h before being washed with saturated aqueous NH_4Cl (10 ml), followed by 1 M HCl (10 ml). The organic layer was separated and washed with a saturated aqueous $NaHCO_3$ (10 ml) followed by saturated brine (10 ml) and dried over anhydrous Na_2SO_4. Excess solvent was removed *in vacuo* and the desired product was purified by column chromatography (EtOAc/Hex, 3:7) yielding compound **210** (244 mg, 70%) as a yellow oil.



R_f = 0.34 (EtOAc/Hex, 3:7); **$[\alpha_D]^{20}$** = -15.4 (c 0.55, $CHCl_3$); **IR**: $\nu_{max}(cm^{-1})$: 3403 (OH), 3032 (C=C-H), 2954 (C-H), 1475 (C=C), 1254 (C-O); **^{1}H NMR (400 MHz, $CDCl_3$)** δ 7.40 – 7.21 (m, 5H, Ar-H), 4.62 (d, *J* = 11.6 Hz, 1H) and 4.54 (d, *J* = 11.5 Hz, 1H, Bn-CH_2), 3.74 – 3.65 (m, 1H, H-2), 3.64 – 3.46 (m, 4H, H-1 and H-5), 2.12 (br-s, 1H, OH), 1.73 – 1.45 (m, 4H, H-3 and H-4), 0.89 (s, 9H, TBS-C(CH_3)$_3$)), 0.05 (s, 6H, TBS-Si(CH_3)$_2$); **^{13}C NMR (101 MHz, $CDCl_3$)** δ 138.4, 128.5, 127.8 and 127.7 (Ar-C), 79.5 (C-2), 71.4 (Bn-CH_2), 64.2 (C-1), 63.0 (C-5), 28.5 and 27.1 (C-3 and C-4), 26.0 (TBS-C($\underline{C}H_3$)$_3$), 18.3 (TBS-$\underline{C}$(CH_3)$_3$), -5.3 (TBS-Si(CH_3)$_2$); **HRMS** (m/z), calculated for $C_{30}H_{33}O_3Si$: 325.2193, found $(M+H)^+$: 325.2194.

4.2.66 Synthesis of (*R*)-2-(benzyloxy)-5-((*tert*-butyldimethylsilyl)oxy)pentyl 4-methylbenzenesulfonate 211

To a stirring solution of compound **210** (214 mg, 0.689 mmol) in DCM (5 ml) was added TsCl (394 mg, 2.07 mmol) and DMAP (253 mg, 2.07 mmol). After 12 h of stirring TLC analysis showed total consumption of the starting material and the reaction mixture was diluted with H_2O (10 ml). The organic layer was separated and washed with saturated brine (10 ml). Drying over anhydrous $MgSO_4$ was followed by the removal of excess solvent under reduced pressure. Product purification was afforded by column chromatography (EtOAc/Hex, 1:9) yielding compound **211** (300 mg, 97% yield) as a yellow oil.

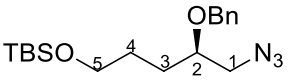


R_f = 0.29 (EtOAc/Hex, 1:9); **IR**: $\nu_{max}(cm^{-1})$: 3058 (C=C-H), 2948 (C-H), 1274 and 1173 (C-O); **^{1}H NMR (400 MHz, $CDCl_3$)** δ 7.78 (d, *J* = 8.0 Hz, 2H, Ar-

H), 7.35 – 7.22 (m, 7H, Ar-H), 4.55 (d, *J* = 11.5 Hz, 1H) and 4.47 (d, *J* = 11.5 Hz, 1H, Bn-CH_2), 4.10 – 4.00 (m, 2H, H-1), 3.68 – 3.60 (m, 1H, H-2), 3.57 – 3.50 (m, 2H, H-5), 2.43 (s, 3H, Ts-CH_3), 1.62 – 1.44 (m, 4H, H-3 and H-4), 0.87 (s, 9H, TBS-C(CH_3)$_3$), 0.02 (s, 6H, TBS-Si(CH_3)$_2$); **^{13}C NMR (101 MHz, $CDCl_3$)** δ 144.8, 138.0, 132.9, 129.8, 128.3, 127.9, 127.8 and 127.7 (Ar-C), 76.3 (C-2), 72.2 (Bn-CH_2), 71.6 (C-1), 62.7 (C-5), 28.2 and 27.8 (C-3 and C-4), 25.9 TBS-C($\underline{C}H_3$)$_3$), 21.6 (Ar-CH_3), 18.3 (TBS-$\underline{C}$(CH_3)$_3$), -5.3 (TBS-Si(CH_3)$_2$).

4.2.67 Synthesis of (*R*)-((5-azido-4-(benzyloxy)pentyl)oxy)(*tert*-butyl)dimethylsilane 212

Compound **211** (310 mg, 0.648 mmol) was dissolved in DMF (3 ml) followed by the addition of sodium azide (224 mg, 3.45 mmol). The stirring mixture was refluxed at 75 °C for 4 h until the starting material had completely reacted as determined by TLC analysis. The reaction mixture was diluted with Et_2O (20 ml) followed by washing with saturated brine (5 x 50 ml). The organic layer was dried over anhydrous Na_2SO_4 and excess solvent was removed under reduced pressure. The desired azide **212** (166 mg, 73%) was recovered as a light brown oil and was not purified any further. The quoted yield is approximate.

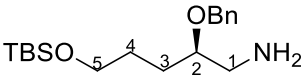


R_f = 0.30 (EtOAc/Hex, 1:9); **$[\alpha_D]^{20}_{589}$** = -15.4 (c 0.55, $CHCl_3$); **IR**: ν_{max}(cm^{-1}): 2949 (C-H), 2097 (CN); **^{1}H NMR (400 MHz, $CDCl_3$)** δ 7.40 – 7.27 (m, 5H, Ar-H), 4.70 – 4.53 (m, 2H, Bn-CH_2), 3.67 – 3.56 (m, 3H, H-2 and H-5), 3.40 – 3.29 (m, 2H, H-1), 1.75 – 1.51 (m, 6H, H-3 and H-4), 0.91 and 0.89 (2 x s, 4H, TBS-C(CH_3)$_3$), 0.10 (s, 1H) and 0.04 (s, 2H, TBS-Si(CH_3)$_2$); **^{13}C NMR (101 MHz, $CDCl_3$)** δ 138.1, 137.8, 128.5, 128.4, 128.0, 127.9, 127.9 and 127.7 (Ar-H), 78.1 and 77.9 (C-2), 72.0 and 71.8 (Bn-CH_2), 62.9 and 62.7 (C-5), 54.1 and 53.9 (C-1), 28.7, 28.5, 28.4 and 28.3 (C-3 and C-4), 25.9 and 25.6 (TBS-C($\underline{C}H_3$)$_3$), 18.3 and 18.0 (TBS-$\underline{C}$(CH_3)$_3$), -3.6 and -5.3 (TBS-Si(CH_3)$_2$); **HRMS** (m/z), calculated for $C_{18}H_{32}N_3O_2Si$: 350.2258, found $(M+H)^+$: 350.2260.

4.2.68 Synthesis of (*R*)-2-(benzyloxy)-5-((*tert*-butyldimethylsilyl)oxy)pentan-1-amine 213

Compound **212** (146 mg, 0.418 mmol) was dissolved in dry Et_2O (3 ml) followed by addition of $LiAlH_4$ (34 mg, 0.896 mmol) in one portion. The reaction was allowed to proceed for 3 h before quenching with a few drops of 2 M NaOH to give a white precipitate. After addition of solid Na_2SO_4,

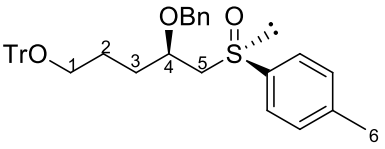
the solids were collected by filtration and extracted twice with Et_2O (5 ml). The combined organic solutions were evaporated yielding amine **213** (55 mg, 14% yield) as a colourless oil.



R_f = 0.34 ($CHCl_3$/MeOH, 9/1); **IR**: ν_{max}(cm^{-1}): 3338 (NH_2), 3033 (C=C-H), 2930 (C-H), 1295 (C-O); **^{1}H NMR (400 MHz, $CDCl_3$)** δ 7.40 – 7.27 (m, 5H, Ar-H), 4.72 – 4.48 (m, 2H, Bn-CH_2), 3.69 – 3.55 (m, 2H, H-5), 3.49 – 3.28 (m, 1H, H-2), 2.92 – 2.67 (m, 2H, H-1), 2.10 – 1.49 (m, 4H, H-3 and H-4), 0.95 – 0.77 (m, 9H, TBS-C(CH_3)$_3$), 0.12 – 0.02 (m, 6H, TBS-Si(CH_3)$_2$); **^{13}C NMR (101 MHz, $CDCl_3$)** δ 138.7, 128.4, 127.8 and 127.6 (Ar-H), 80.5 and 80.3 (C-2), 72.0 and 71.8 (Bn-CH_2) 63.1, 62.8 and 62.6 (C-5), 44.9, 44.6 (C-1), 28.6, 28.1 and 27.9 (C-3 and C-4), 26.0, 25.9 and 25.7 (TBS-C($\underline{C}H_3$)$_3$), 18.3 and 18.0 (TBS-$\underline{C}$(CH_3)$_3$), -3.6 and -5.3 (TBS-Si(CH_3)$_2$).

4.2.69 Synthesis of ((((*R*)-4-(benzyloxy)-5-((*S*)-*p*-tolylsulfinyl)pentyl)oxy)methanetriyl)tribenzene 214

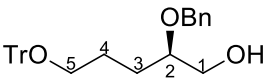
Compound **201** (0.378 mg, 1.14 mmol) was dissolved in DCM (5 ml) followed catalytic amounts of DMAP (30 mg, 0.228 mmol) and Et_3N (238 µl, 1.71 mmol). The reaction was left stirring overnight and the complete disappearance of the starting material was detected after 12 h. Work up of the reaction was achieved by washing with H_2O (20 ml) followed by saturated brine (20 ml). The organic layer was separated, dried over Na_2SO_4, and excess solvent was removed *in vacuo*. Product purification was afforded by column chromatography (EtOAc/Hex, 3:7) yielding compound **214** (547 mg, 84% yield) as a viscous colourless oil.



R_f = 0.34 (EtOAc/Hex, 3:7); **$[\alpha_D]^{20}$** = +43.1 (c 0.45, $CHCl_3$); **IR**: ν_{max}(cm^{-1}): 3057 and 3031 (C=C-H), 2921 and 2868 (C-H), 1492 (C=C), 1086 (C-O), 1066 (S=O); **^{1}H NMR (400 MHz, $CDCl_3$)** δ 7.49 – 7.37 (m, 9H, Ar-H), 7.34 – 7.17 (m, 15H, Ar-H), 4.42 (d, *J* = 11.5 Hz, 1H) and 4.36 (d, *J* = 11.5 Hz, 1H, Bn-CH_2), 3.69 (p, *J* = 5.8 Hz, 1H, H-4), 3.21 (dd, *J* = 13.3, 5.7 Hz, 1H, H-5$_a$), 3.07 (t, *J* = 6.1 Hz, 2H, H-1), 2.84 (dd, *J* = 13.3, 6.1 Hz, 1H, H-5$_b$), 2.38 (s, 3H, Ar-CH_3), 1.93 – 1.62 (m, 4H, H-2 and H-3); **^{13}C NMR (101 MHz, $CDCl_3$)** δ 144.3, 141.6, 140.8, 137.9, 130.0, 128.6, 128.3, 127.72, 127.67 126.9 and 124.2 (Ar-C), 86.4 (Tr-C), 73.6 (C-4), 70.8 (Bn-CH_2), 63.2 (C-1), 62.3 (C-5), 30.6 (C-3), 25.4 (C-2), 21.4 (Ar-CH_3); **HRMS** (m/z), calculated for $C_{38}H_{38}NaO_3S$: 597.2434, found $(M+Na)^+$: 597.2434.

4.2.70 Synthesis of (*R*)-2-(benzyloxy)-5-(trityloxy)pentan-1-ol 215

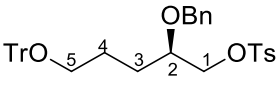
Compound **214** (547 mg, 0.952mmol) was dissolved in cooled MeCN (3 ml) at 0 °C, followed by the sequential addition of 2,4,6-collidine (503 µl, 3.80 mmol) and TFAA (528 µl, 3.80 mmol). The reaction proceeded for 30 min before a saturated solution of aqueous $NaHCO_3$ (1 ml) was added together with solid K_2CO_3 until neutral conditions were achieved. Stirring continued for a further 30 min after which $NaBH_4$ (227 mg, 6.00 mmol) was added and the reaction was allowed to proceed for a further hour. Quenching of the excess base was achieved by adding saturated aqueous NH_4Cl (20 ml). The organic layer was separated and washed with 1M HCl (10 ml), saturated aqueous $NaHCO_3$, saturated brine (100 ml), dried over anhydrous $MgSO_4$. Excess solvent was removed under reduced pressure. Product purification was achieved by column chromatography (EtOAc/Hex, 3:7) yielding compound **215** (406 mg, 94% yield) as a yellow/greenish oil.



R_f = 0.37 (EtOAc/Hex, 3:7); **$[\alpha_D]^{20}$** = -1.50 (c 0.2, $CHCl_3$); **IR**: ν_{max}(cm^{-1}): 3442 (OH), 3059 and 3032 (C=C-H), 2926 and 2870 (C-H), 1066 (C-O); **^{1}H NMR (400 MHz, $CDCl_3$)** δ 7.46 – 7.39 (m, 6H, Ar), 7.34 – 7.16 (m, 14H, Ar-H), 4.55 (d, *J* = 11.6 Hz, 1H) and 4.49 (d, *J* = 11.6 Hz, 1H, Bn-CH_2), 3.65 (dd, *J* = 11.2, 3.1 Hz, 1H, H-1_a), 3.55 – 3.42 (m, 2H, H-1_b and H-2), 3.08 (t, *J* = 5.9 Hz, 2H, H-5), 2.04 (br-s, 1H, OH), 1.73 – 1.54 (m, 4H, H-3 and H-4); **^{13}C NMR (101 MHz, $CDCl_3$)** δ 144.3, 138.4, 128.6, 128.4, 127.72, 127.70 and 126.8 (Ar-C), 86.4 (Tr-C), 79.5 (C-2), 71.5 (Bn-CH_2), 64.2 (C-1), 63.4 (C-5), 27.5 and 25.8 (C-3 and C-4); **HRMS** (m/z), calculated for $C_{31}H_{32}NaO_3$: 475.2244, found $(M+Na)^+$: 475.2239.

4.2.71 (*R*)-2-(benzyloxy)-5-(trityloxy)pentyl 4-methylbenzenesulfonate 216

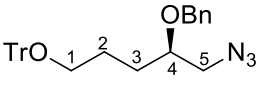
To a cooled solution of compound **215** (200 mg, 0.441 mmol) at 0 °C in DCM (3 ml) was added DMAP (32 mg, 0.265 mmol), Et_3N (92 µl, 0.662 mmol and TsCl (100 mg, 0.529 mmol). Total consumption of the starting material was observed after 6 h by TLC analysis and the reaction mixture was diluted with H_2O (10 ml) and DCM (10 ml).The organic layer was separated and washed with saturated brine (10 ml), dried over anhydrous Na_2SO_4 and excess solvent was removed under reduced pressure. Product purification was afforded by column chromatography (EtOAc/Hex, 1:9) yielding compound **216** (252 mg, 94% yield) as a yellow oil.



R_f = 0.24 (EtOAc/Hex, 1:9); **$[\alpha_D]^{20}$** = +10.4 (c 0.5, $CHCl_3$); **IR**: ν_{max}(cm^{-1}): 3059 and 3032 (C=C-H), 2948 and 2870 (C-H), 1633 (C=C), 1361 (S=O), 1157 (C-O); **^{1}H NMR (500 MHz, $CDCl_3$)** δ 7.76 (d, *J* = 8.3 Hz, 2H, Ar-H), 7.42 – 7.37 (m, 6H, Ar-H), 7.31 – 7.24 (m, 11H, Ar-H), 7.23 – 7.19 (m, 5H, Ar-H), 4.51 (d, *J* = 11.5 Hz, 1H) and 4.40 (d, *J* = 11.5 Hz, 1H, Bn-CH_2), 4.06 – 3.98 (m, 2H, H-1), 3.59 – 3.53 (m, 1H, H-2), 3.06 – 2.97 (m, 2H, H-5), 2.39 (s, 3H, Ar-CH_3), 1.72 – 1.50 (m, 4H, H-3 and H-4); **^{13}C NMR (126 MHz, $CDCl_3$)** δ 144.7, 144.2, 137.9, 132.8, 129.8, 129.7, 128.6, 128.5, 128.3, 127.9, 127.8, 127.6 and 126.8 (Ar-C), 86.3 (Tr-C), 76.1 (C-2), 72.1 (Bn-CH_2), 71.4 (C-1), 62.9 (C-5), 28.1 (C-3), 25.4 (C-4), 21.5 (Ar-CH_3).

4.2.72 Synthesis of (*R*)-(((5-azido-4-(benzyloxy)pentyl)oxy)methanetriyl)tribenzene 217

Compound **216** (251 mg, 0.415 mmol) was dissolved in DMF (3 ml), followed by the addition of NaN_3 (80 mg, 1.24 mmol). The reaction mixture was refluxed at 75 °C for 4 h after which TLC showed total consumption of the starting material. Et_2O (20 ml) was added and the mixture was washed once with saturated brine (20 ml) and the aqueous layer was separated. The aqueous layer was extracted with Et_2O (10 ml). The combined organic layers were washed with saturated brine (7 x 50 ml), dried over anhydrous Na_2SO_4 and excess solvent was removed *in vacuo*. The desired product **217** (193 mg, 98% yield) was not purified further and it was recovered as a light brown oil.

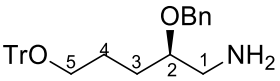


R_f = 0.25 (EtOAc/Hex, 1:9); **$[\alpha_D]^{20}$** = +1.17° (c 0.6, $CHCl_3$); **IR**: ν_{max}(cm^{-1}): 3060 and 3031 (C=C-H), 2925 and 2869 (C-H), 2096 (N=N=N), 1182 and 1066 (C-O); **^{1}H NMR (400 MHz, $CDCl_3$)** δ 7.45 – 7.40 (m, 6H, Ar-H), 7.33 – 7.24 (m, 11H, Ar-H), 7.24 – 7.18 (m, 3H, Ar-H), 4.58 (d, *J* = 11.5 Hz, 1H) and 4.50 (d, *J* = 11.5 Hz, 1H, Bn-CH_2), 3.56 – 3.48 (m, 1H, H-4), 3.32 – 3.22 (m, 2H, H-5), 3.11 – 3.01 (m, 2H, H-1), 1.74 – 1.56 (m, 4H, H-2 and H-3); **^{13}C NMR (101 MHz, $CDCl_3$)** δ 144.3, 138.1, 128.6, 128.4, 127.8, 127.7 and 126.9 (Ar-C), 86.4 (Tr-C), 78.0 (C-4), 71.8 (Bn-CH_2), 63.2 (C-1), 54.0 (C-5), 28.9 and 25.7 (C-2 and C-3); **HRMS** (m/z), calculated for $C_{31}H_{31}N_3NaO_2$: 500.2308, found $(M+Na)^+$: 500.2301.

4.2.73 (*R*)-2-(benzyloxy)-5-(trityloxy)pentan-1-amine 218

Compound **217** (190 mg, 0.398 mmol) was dissolved in dry Et_2O (3 ml) followed by $LiAlH_4$ (20 mg, 0.527 mmol) in one portion. The reaction was stirred under N_2 at room temperature for 6 h until TLC showed total disappearance of the starting material. 2 M NaOH was added dropwise until a

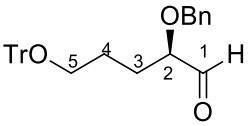
white precipitate was observed, followed by the addition of solid anhydrous Na_2SO_4. The reaction mixture was filtered and the filtrate was washed with dry Et_2O (2 x 20 ml) followed by the removal of excess solvent under reduced pressure. The crude amine **218** (164 mg, 100% yield) was not purified any further and it was recovered as a yellow oil.



R_f = 0.37 (EtOAc/Hex, 3:7); **$[\alpha_D]^{20}$** = -7.56 (c 0.37, $CHCl_3$); **IR**: ν_{max}(cm^{-1}): 3058 and 3031 (C=C-H), 2923 (C-H), 1596 (N-H), 1182 and 1066 (C-O); **^{1}H NMR (500 MHz, $CDCl_3$)** δ 7.47 – 7.38 (m, 6H), 7.35 – 7.18 (m, 14H, Ar-H), 4.54 (d, *J* = 11.5 Hz, 1H) and 4.49 (d, *J* = 11.5 Hz, 1H, Bn-CH_2), 3.37 – 3.31 (m, 1H, H-2), 3.08 (t, *J* = 6.0 Hz, 2H, H-5), 2.81 (dd, *J* = 13.3, 3.9 Hz, 1H, H-1_a), 2.70 (dd, *J* = 13.3, 6.3 Hz, 1H, H-1_b), 1.74 – 1.55 (m, 4H, H-3 and H-4), 1.26 (s, 2H, NH_2).; **^{13}C NMR (126 MHz, $CDCl_3$)** δ 144.4, 138.7, 128.7, 128.4, 127.74, 127.72 127.6 and 126.9 (Ar-C), 86.4 (Tr-C), 80.6 (C-2), 71.3 (Bn-CH_2), 63.5 (C-5), 45.0 (C-1), 28.4 and 25.9 (C-3 and C-4); **HRMS** (m/z), calculated for $C_{31}H_{34}NO_2$: 452.2584, found $(M+H)^+$: 452.2590.

4.2.74 Synthesis of (*R*)-2-(benzyloxy)-5-(trityloxy)pentanal 219

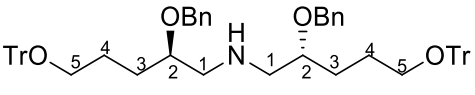
Compound **215** (200 mg, 0.442 mmol) was dissolved in DCM (3 ml) followed by the addition of DMP (225 mg, 0.530 mmol). The reaction was left stirring overnight. TLC showed total consumption of the starting material. The reaction was diluted with water (10 ml), the organic layer was separated and washed with saturated brine (10 ml), dried with Na_2SO_4 and excess solvent removed under reduced pressure. Product purification was afforded by column chromatography (EtOAc/Hex, 1:9) yielding compound **219** (150 mg, 75% yield) as a white viscous oil.



R_f = 0.28 (EtOAc/Hex, 1:9); **$[\alpha_D]^{20}$** = +35.5 (c 0.20, $CHCl_3$); **IR**: ν_{max}(cm^{-1}): 3058 and 3031 (C=C-H), 2924 (C-H), 1731 (C=O), 1069 (C-O**); ^{1}H NMR (400 MHz, $CDCl_3$)** δ 9.61 (d, *J* = 2.1 Hz, 1H, H-1), 7.44 – 7.38 (m, 6H, Ar-H), 7.35 – 7.15 (m, 14H, Ar-H), 4.61 (d, *J* = 11.7 Hz, 1H) and 4.46 (d, *J* = 11.7 Hz, 1H, Bn-CH_2), 3.74 – 3.68 (m, 1H, H-2), 3.14 – 2.99 (m, 2H, H-5), 1.94 – 1.58 (m, 4H, H-3 and H-4); **^{13}C NMR (101 MHz, $CDCl_3$)** δ 203.5 (C-1), 144.2, 137.3, 128.6, 128.5, 127.8, 127.7, 126.9 and 126.8 (Ar-C), 86.4 (Tr-C), 83.2 (C-2), 72.5 (Bn-CH_2), 62.8 (C-5), 26.9 and 25.3 (C-3 and C-4); **HRMS** (m/z), calculated for $C_{31}H_{30}NaO_3$: 473.2087, found $(M+H)^+$: 473.2076.

4.2.75 Synthesis of (*R*)-bis((*R*)-2-(benzyloxy)-5-(trityloxy)pentyl)amine 220

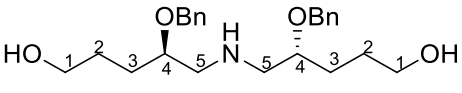
Compound **218** (150 mg, 0.332 mmol) was dissolved in 1,2-DCE (5 ml) in a two necked 50 ml round bottomed flask under N_2, followed by the addition of compound **219** (120 mg, 0.266 mmol) in 1,2-DCE (2 ml). The reaction was allowed to stir for 30 min before the addition of sodium triacetoxyborohydride (77 mg, 0.365 mmol) and the reaction was stirred for a further 36 h. For quenching the reaction, 2 M NaOH (2 ml) was added and the organic layer was separated and washed with saturated brine (10 ml), dried over anhydrous Na_2SO_4 and excess solvent was removed under reduced pressure. Purification of the product was afforded by column chromatography (EtOAc/Hex, 4:1) yielding compound **220** (210 mg, 89% yield) as a viscous yellow oil.



R_f = 0.28 (EtOAc/Hex, 4:1); **$[\alpha_D]^{20}$** = -22.7 (c 0.45, $CHCl_3$); **IR**: ν_{max}(cm^{-1}): 3059, 3031 (C=C-H), 2925, 2868 (C-H), 1065 (C-O); **^{1}H NMR (400 MHz, $CDCl_3$)** δ 7.52 – 7.45 (m, 12H, Ar-H), 7.38 – 7.21 (m, 28H, Ar-H), 4.57 (d, *J* = 11.5 Hz, 2H) and 4.52 (d, *J* = 11.5 Hz, 2H, Bn-CH_2), 3.62 – 3.52 (m, 2H, H-2), 3.16 – 3.09 (m, 4H, H-5), 2.76 (dd, *J* = 12.3, 7.1 Hz, 2H, H-1_a), 2.68 (dd, *J* = 12.3, 4.0 Hz, 2H, H-1_b), 1.80 – 1.57 (m, 8H, H-3 and H-4); **^{13}C NMR (101 MHz, $CDCl_3$)** δ 144.4, 138.7, 128.7, 128.3, 127.7, 127.7, 127.5 and 126.8 (Ar-C), 86.4 (Tr-C), 78.1 (C-2), 71.4 (Bn-CH_2), 63.6 (C-5), 53.2 (C-1), 29.0 and 25.9 (C-3 and C-4); **HRMS** (m/z), calculated for $C_{30}H_{33}NO_3$: 886.4830, found $(M+H)^+$: 886.4809.

4.2.76 Synthesis of (4*R*,4'*R*)-5,5'-azanediylbis(4-(benzyloxy)pentan-1-ol) 221

Compound **220** (200 mg, 0.226 mmol) was dissolved in MeOH (5 ml) followed by the addition of *p*-TsOH (42 mg, 0.226 mmol) in one portion. The reaction was refluxed, and total consumption of the starting material was observed by TLC analysis after 4 h. A few drops of Et_3N were added to neutralise the excess acid followed by the removal of excess solvent under reduced pressure. Product purification was afforded by column chromatography ($CHCl_3$/MeOH, 95:5) yielding compound **221** (80 mg, 88% yield) as a light brown viscous oil.



R_f = 0.20 ($CHCl_3$/MeOH, 95:5); **$[\alpha_D]^{20}$** = -10.0 (c 0.44, $CHCl_3$); **IR**: ν_{max}(cm^{-1}): br-3414 (OH and NH), 3028 (C=C-H, 2925, 2870 (C-H), 1220, 1166, 1121 (C-O) **^{1}H NMR (500 MHz, $CDCl_3$)** δ 7.26 – 7.18 (m, 10H, Ar-H), 4.47

(d, *J* = 11.3 Hz, 2H) and 4.39 (d, *J* = 11.4 Hz, 2H, Bn-CH_2), 3.93 – 3.86 (m, 2H, H-4), 3.52 (t, *J* = 6.0 Hz, 4H, H-1), 3.26 (dd, *J* = 12.9, 3.6 Hz, 2H, H-5_a), 3.01 (dd, *J* = 12.8, 8.1 Hz, 2H, H-5_b), 1.75 – 1.65 (m, 2H, H-3_a), 1.65 – 1.56 (m, 2H, H-3_b), 1.50 (p, *J* = 6.6 Hz, 4H, H-2); **^{13}C NMR (126 MHz, $CDCl_3$)** δ 142.4, 128.5, 128.0 and 127.8 (Ar-C), 74.1 (C-4), 71.2 (Bn-CH_2), 61.8 (C-1), 50.7 (C-5), 27.8 (C-3), 27.2 (C-2); **HRMS** (m/z), calculated for $C_{30}H_{33}O_3Si$: 401.2639, found $(M+H)^+$: 401.2633.

References

(1) Bienz, S.; Bisegger, P.; Guggisberg, A.; Hesse, M. *Natural Product Reports* **2005**, *22*, 647.
(2) Wallace, H. M. *European Journal of Clinical Investigation* **2000**, *30*, 1.
(3) Casero Jr, R. A.; Marton, L. J. *Nature Reviews Drug Discovery* **2007**, *6*, 373.
(4) Manku, S.; Laplante, C.; Kopac, D.; Chan, T.; Hall, D. G. *The Journal of Organic Chemistry* **2001**, *66*, 874.
(5) Karigiannis, G.; Papaioannou, D. *European Journal of Organic Chemistry* **2000**, 1841.
(6) Woster, P. M.; Casero, J. R. A. In *Polyamine Drug Discovery*; The Royal Society of Chemistry: **2012**, p 104.
(7) Castagnolo, D.; Schenone, S.; Botta, M. *Chemical Reviews* **2011**, *111*, 5247.
(8) Miller-Fleming, L.; Olin-Sandoval, V.; Campbell, K.; Ralser, M. *Journal of Molecular Biology* **2015**, *427*, 3389.
(9) Seiler, N.; Raul, F. *Journal of Cellular and Molecular Medicine* **2005**, *9*, 623.
(10) Park, M. H. *The Journal of Biochemistry* **2006**, *139*, 161.
(11) Casero, R. A.; Woster, P. M. *Journal of Medicinal Chemistry* **2001**, *44*, 1.
(12) Murray-Stewart, T.; Casero, R. A. In *Polyamines: A Universal Molecular Nexus for Growth, Survival, and Specialized Metabolism*; Kusano, T., Suzuki, H., Eds.; Springer Japan: Tokyo, **2015**, p 61.
(13) Seiler, N.; Dezeure, F. *International Journal of Biochemistry* **1990**, *22*, 211.
(14) Vanhoutte, R.; Kahler, J. P.; Martin, S.; van Veen, S.; Verhelst, S. H. L. *ChemBioChem* **2018**, *19*, 907.
(15) Cullis, P. M.; Green, R. E.; Merson-Davies, L.; Travis, N. *Chemistry & Biology* **1999**, *6*, 717.
(16) Edwards, M. L.; Prakash, N. J.; Stemerick, D. M.; Sunkara, S. P.; Bitonti, A. J.; Davis, G. F.; Dumont, J. A.; Bey, P. *Journal of Medicinal Chemistry* **1990**, *33*, 1369.
(17) Khan, F. A.; Ahmad, S.; Kodipelli, N.; Shivange, G.; Anindya, R. *Organic & Biomolecular Chemistry* **2014**, *12*, 3847.
(18) Umezawa, N.; Tsuji, K.; Sato, S.; Kikuchi, M.; Watanabe, H.; Horai, Y.; Yamaguchi, M.; Hisamatsu, Y.; Umehara, T.; Higuchi, T. *RSC Advances* **2018**, *8*, 36895.
(19) Bergeron, R. J.; Müller, R.; Huang, G.; McManis, J. S.; Algee, S. E.; Yao, H.; Weimar, W. R.; Wiegand, J. *Journal of Medicinal Chemistry* **2001**, *44*, 2451.
(20) Liew, L. P. P.; Kaiser, M.; Copp, B. R. *Bioorganic & Medicinal Chemistry Letters* **2013**, *23*, 452.
(21) Pearce, A. N.; Chia, E. W.; Berridge, M. V.; Maas, E. W.; Page, M. J.; Harper, J. L.; Webb, V. L.; Copp, B. R. *Tetrahedron* **2008**, *64*, 5748.
(22) Lizzi, F.; Veronesi, G.; Belluti, F.; Bergamini, C.; López-Sánchez, A.; Kaiser, M.; Brun, R.; Krauth-Siegel, R. L.; Hall, D. G.; Rivas, L.; Bolognesi, M. L. *Journal of Medicinal Chemistry* **2012**, *55*, 10490.
(23) Bolognesi, M. L.; Banzi, R.; Bartolini, M.; Cavalli, A.; Tarozzi, A.; Andrisano, V.; Minarini, A.; Rosini, M.; Tumiatti, V.; Bergamini, C.; Fato, R.; Lenaz, G.; Hrelia, P.; Cattaneo, A.; Recanatini, M.; Melchiorre, C. *Journal of Medicinal Chemistry* **2007**, *50*, 4882.
(24) Saccomano, N. A.; Volkmann, R. A.; Jackson, H.; Parks, T. N. In *Annual Reports in Medicinal Chemistry*; Allen, R. C., Ed.; Academic Press: **1989**; Vol. 24, p 287.
(25) Nørager, N. G.; Poulsen, M. H.; Strømgaard, K. *Journal of Medicinal Chemistry* **2018**, *61*, 8048.

(26) Blagbrough, I. S.; Carrington, S.; Geall, A. J. *Pharmacy and Pharmacology Communications* **1997**, *3*, 223.
(27) Kromann, H.; Krikstolaityte, S.; Andersen, A. J.; Andersen, K.; Krogsgaard-Larsen, P.; Jaroszewski, J. W.; Egebjerg, J.; Strømgaard, K. *Journal of Medicinal Chemistry* **2002**, *45*, 5745.
(28) Andersen, T. F.; Tikhonov, D. B.; Bølcho, U.; Bolshakov, K.; Nelson, J. K.; Pluteanu, F.; Mellor, I. R.; Egebjerg, J.; Strømgaard, K. *Journal of Medicinal Chemistry* **2006**, *49*, 5414.
(29) Jørgensen, M. R.; Olsen, C. A.; Mellor, I. R.; Usherwood, P. N. R.; Witt, M.; Franzyk, H.; Jaroszewski, J. W. *Journal of Medicinal Chemistry* **2005**, *48*, 56.
(30) Strømgaard, K.; Piazzi, L.; Olsen, C. A.; Franzyk, H.; Jaroszewski, J. W. *Magnetic Resonance in Chemistry* **2006**, *44*, 1013.
(31) Yamaji, N.; Horikawa, M.; Corzo, G.; Naoki, H.; Haupt, J.; Nakajima, T.; Iwashita, T. *Tetrahedron Letters* **2004**, *45*, 5371.
(32) Chesnov, S.; Bigler, L.; Hesse, M. *Helvetica Chimica Acta* **2001**, *84*, 2178.
(33) Moya, E.; Blagbrough, I. S. *Journal of Pharmacy and Pharmacology* **1996**, *48*, 179.
(34) Estrada, G.; Villegas, E.; Corzo, G. *Natural Product Reports* **2007**, *24*, 145.
(35) Doll, M. K.-H.; Guggisberg, A.; Hesse, M. *Helvetica Chimica Acta* **1996**, *79*, 973.
(36) Häusermann, U. A.; Linden, A.; Song, J.; Hesse, M. *Helvetica Chimica Acta* **1996**, *79*, 1995.
(37) Dietrich, B.; Hosseini, M. W.; Lehn, J.-M.; Sessions, R. B. *Helvetica Chimica Acta* **1983**, *66*, 1262.
(38) Vanbilloen, H. P.; Eraets, K.; Evens, N.; Terwinghe, C.; Rattat, D.; Bormans, G.; Mortelmans, L.; Verbruggen, A. M. *Journal of Labelled Compounds and Radiopharmaceuticals* **2005**, *48*, 1003.
(39) Wilson, J. M.; Giordani, F.; Farrugia, L. J.; Barrett, M. P.; Robins, D. J.; Sutherland, A. *Organic & Biomolecular Chemistry* **2007**, *5*, 3651.
(40) Masse, S.; Laurent, G.; Coradin, T. *Physical Chemistry Chemical Physics* **2009**, *11*, 10204.
(41) Bazzicalupi, C.; Bencini, A.; Lippolis, V. *Chemical Society Reviews* **2010**, *39*, 3709.
(42) Bergeron, R. J.; Weimar, W. R.; Wu, Q.; Feng, Y.; McManis, J. S. *Journal of Medicinal Chemistry* **1996**, *39*, 5257.
(43) Tsukamoto, S.; Kato, H.; Hirota, H.; Fusetani, N. *Tetrahedron Letters* **1996**, *37*, 5555.
(44) Chang; Whittaker, N. F.; Bewley, C. A. *Journal of Natural Products* **2003**, *66*, 1490.
(45) Finlayson, R.; Pearce, A. N.; Page, M. J.; Kaiser, M.; Bourguet-Kondracki, M.-L.; Harper, J. L.; Webb, V. L.; Copp, B. R. *Journal of Natural Products* **2011**, *74*, 888.
(46) Bitonti, A. J.; McCann, P. P.; Sjoerdsma, A. In *Progress in Polyamine Research: Novel Biochemical, Pharmacological, and Clinical Aspects*; Zappia, V., Pegg, A. E., Eds.; Springer US: Boston, MA, **1988**, p 717.
(47) Bergeron, R. J.; Wiegand, J.; Fannin, T. L. *Digestive Diseases and Sciences* **2001**, *46*, 2615.
(48) Sung, J. J.; Hopkins, M. M. *Technology Analysis & Strategic Management* **2006**, *18*, 345.
(49) Wang, D.; Zheng, F.; Holmberg, S.; Kohlhaw, G. B. *Journal of Biological Chemistry* **1999**, *274*, 19017.
(50) Chisaka, O.; Musci, T. S.; Capecchi, M. R. *Nature* **1992**, *355*, 516.
(51) Wheeler, C. J.; Felgner, P. L.; Tsai, Y. J.; Marshall, J.; Sukhu, L.; Doh, S. G.; Hartikka, J.; Nietupski, J.; Manthorpe, M.; Nichols, M.; Plewe, M.; Liang, X.; Norman, J.; Smith, A.; Cheng, S. H. *Proceedings of the National Academy of Sciences* **1996**, *93*, 11454.
(52) Behr, J.-P. *Tetrahedron Letters* **1986**, *27*, 5861.
(53) Behr, J. P.; Demeneix, B.; Loeffler, J. P.; Perez-Mutul, J. *Proceedings of the National Academy of Sciences* **1989**, *86*, 6982.

(54) Gardner, R. A.; Belting, M.; Svensson, K.; Phanstiel *Journal of Medicinal Chemistry* **2007**, *50*, 308.
(55) Gardner, R. A.; Delcros, J.-G.; Konate, F.; Breitbeil, F.; Martin, B.; Sigman, M.; Huang, M.; Phanstiel *Journal of Medicinal Chemistry* **2004**, *47*, 6055.
(56) Kaur, N.; Delcros, J.-G.; Imran, J.; Khaled, A.; Chehtane, M.; Tschammer, N.; Martin, B.; Phanstiel, O. *Journal of Medicinal Chemistry* **2008**, *51*, 1393.
(57) Choomuenwai, V.; Schwartz, B. D.; Beattie, K. D.; Andrews, K. T.; Khokhar, S.; Davis, R. A. *Tetrahedron Letters* **2013**, *54*, 5188.
(58) Ponasik, J. A.; Ganem, B. *Tetrahedron Letters* **1995**, *36*, 9109.
(59) Jaivel, N.; Uvarani, C.; Rajesh, R.; Velmurugan, D.; Marimuthu, P. *Journal of Natural Products* **2014**, *77*, 2.
(60) Van Elst, D.; Nuyens, S.; van Wyk, B.; Verstraete, B.; Dessein, S.; Prinsen, E. *Plant Physiology and Biochemistry* **2013**, *67*, 15.
(61) Hay, L.; Schultz, R. A.; Schutte, P. J. *Onderstepoort Journal of Veterinary Research* **2008**, *75*, 249.
(62) Penrith, M.-L.; Botha, C. J.; Tustin, R. C. *Journal of the South African Veterinary Association* **2015**, *86*, 01.
(63) Bode, M. L.; Gates, P. J.; Gebretnsae, S. Y.; Vleggaar, R. *Tetrahedron* **2010**, *66*, 2026.
(64) Bode, S. E.; Müller, M.; Wolberg, M. *Organic Letters* **2002**, *4*, 619.
(65) Gupta, P.; Mahajan, N.; Taneja, S. C. *Catalysis Science & Technology* **2013**, *3*, 2462.
(66) BouzBouz, S.; Cossy, J. *Organic Letters* **2000**, *2*, 501.
(67) Yadav, J. S.; Reddy, P. A. N.; Reddy, Y. J.; Meraj, S.; Prasad, A. R. *European Journal of Organic Chemistry* **2013**, 6317.
(68) Han, X.; Peh, G.; Floreancig, P. E. *European Journal of Organic Chemistry* **2013**, 1193.
(69) Rychnovsky, S. D.; Skalitzky, D. J. *Tetrahedron Letters* **1990**, *31*, 945.
(70) Chan, T. H.; Nwe, K. T. *The Journal of Organic Chemistry* **1992**, *57*, 6107.
(71) Schrittwieser, J. H.; Resch, V. *RSC Advances* **2013**, *3*, 17602.
(72) Chen, B.-S.; Ribeiro de Souza, F. Z. *RSC Advances* **2019**, *9*, 2102.
(73) Baer, K.; Kraußer, M.; Burda, E.; Hummel, W.; Berkessel, A.; Gröger, H. *Angewandte Chemie International Edition* **2009**, *48*, 9355.
(74) Fauve, A.; Veschambre, H. *Biocatalysis* **1990**, *3*, 95.
(75) Patel, R. N.; Banerjee, A.; McNamee, C. G.; Brzozowski, D.; Hanson, R. L.; Szarka, L. J. *Enzyme and Microbial Technology* **1993**, *15*, 1014.
(76) Müller, M. *Angewandte Chemie International Edition* **2005**, *44*, 362.
(77) Acetti, D.; Brenna, E.; Fuganti, C.; Gatti, F. G.; Serra, S. *European Journal of Organic Chemistry* **2010**, 142.
(78) Matsuo, J.-i.; Murakami, M. *Angewandte Chemie International Edition* **2013**, *52*, 9109.
(79) Nobuharu, I.; Teruaki, M. *Chemistry Letters* **1982**, *11*, 1441.
(80) Evans, D. A.; Bartroli, J.; Shih, T. L. *Journal of the American Chemical Society* **1981**, *103*, 2127.
(81) Kiyooka, S.-i.; Hena, M. A. *The Journal of Organic Chemistry* **1999**, *64*, 5511.
(82) Takeshi, Y.; Reiko, Y.; Satoshi, N.; Satoshi, M.; Ryoji, F.; Syun-ichi, K. *Bulletin of the Chemical Society of Japan* **2009**, *82*, 1528.
(83) Evans, D. A.; Dart, M. J.; Duffy, J. L.; Yang, M. G. *Journal of the American Chemical Society* **1996**, *118*, 4322.
(84) Keck, G. E.; Castellino, S.; Wiley, M. R. *The Journal of Organic Chemistry* **1986**, *51*, 5478.
(85) Keck, G. E.; Boden, E. P.; Wiley, M. R. *The Journal of Organic Chemistry* **1989**, *54*, 896.

(86) Lewis, M. D.; Kishi, Y. *Tetrahedron Letters* **1982**, *23*, 2343.
(87) Roush, W. R.; Hoong, L. K.; Palmer, M. A. J.; Straub, J. A.; Palkowitz, A. D. *The Journal of Organic Chemistry* **1990**, *55*, 4117.
(88) Mahler, U.; Devant, R. M.; Braun, M. *Chemische Berichte* **1988**, *121*, 2035.
(89) Iwata, M.; Yazaki, R.; Suzuki, Y.; Kumagai, N.; Shibasaki, M. *Journal of the American Chemical Society* **2009**, *131*, 18244.
(90) Kaneko, Y.; Matsuo, T.; Kiyooka, S.-i. *Tetrahedron Letters* **1994**, *35*, 4107.
(91) Kiyooka, S.-i.; Yamaguchi, T.; Maeda, H.; Kira, H.; Hena, M. A.; Horiike, M. *Tetrahedron Letters* **1997**, *38*, 3553.
(92) Evans, D. A.; Chapman, K. T.; Carreira, E. M. *Journal of the American Chemical Society* **1988**, *110*, 3560.
(93) Pettit, G. R.; Gao, F.; Blumberg, P. M.; Herald, C. L.; Coll, J. C.; Kamano, Y.; Lewin, N. E.; Schmidt, J. M.; Chapuis, J.-C. *Journal of Natural Products* **1996**, *59*, 286.
(94) Evans, D. A.; Carter, P. H.; Carreira, E. M.; Charette, A. B.; Prunet, J. A.; Lautens, M. *Journal of the American Chemical Society* **1999**, *121*, 7540.
(95) Gao, Y.; Klunder, J. M.; Hanson, R. M.; Masamune, H.; Ko, S. Y.; Sharpless, K. B. *Journal of the American Chemical Society* **1987**, *109*, 5765.
(96) Ohtsuka, Y.; Kubota, T.; Ikeno, T.; Nagata, T.; Yamada, T. *Synlett* **2000**, 535.
(97) Souza, F. B.; Shamim, A.; Argomedo, L. M. Z.; Pimenta, D. C.; Stefani, H. A. *Molecular Diversity* **2015**, *19*, 773.
(98) Pellissier, H. *Tetrahedron* **2006**, *62*, 5559.
(99) Walker, A. J. *Tetrahedron: Asymmetry* **1992**, *3*, 961.
(100) Solladié, G.; Gressot, L.; Colobert, F. *European Journal of Organic Chemistry* **2000**, 357.
(101) Marino, J. P.; McClure, M. S.; Holub, D. P.; Comasseto, J. V.; Tucci, F. C. *Journal of the American Chemical Society* **2002**, *124*, 1664.
(102) Balieu, S.; Hallett, G. E.; Burns, M.; Bootwicha, T.; Studley, J.; Aggarwal, V. K. *Journal of the American Chemical Society* **2015**, *137*, 4398.
(103) Fawcett, A.; Nitsch, D.; Ali, M.; Bateman, J. M.; Myers, E. L.; Aggarwal, V. K. *Angewandte Chemie International Edition* **2016**, *55*, 14663.
(104) Gary M. Coppola, H. F. S. *α-Hydroxy Acids in Enantioselective Syntheses*; A Wiley Company: Germany, **1997**.
(105) Izzo, I.; Crumbie, R.; Solladié, G.; Hanquet, G. *Tetrahedron: Asymmetry* **2005**, *16*, 1503.
(106) Magauer, T. In *Comprehensive Chirality*; Carreira, E. M., Yamamoto, H., Eds.; Elsevier: Amsterdam, **2012**, p 268.
(107) Chamberlin, A. R.; Chung, J. Y. L. *The Journal of Organic Chemistry* **1985**, *50*, 4425.
(108) Burton, J. W.; Clark, J. S.; Derrer, S.; Stork, T. C.; Bendall, J. G.; Holmes, A. B. *Journal of the American Chemical Society* **1997**, *119*, 7483.
(109) Rychnovsky, S. D. *The Journal of Organic Chemistry* **1989**, *54*, 4982.
(110) Rychnovsky, S. D. *Chemical Reviews* **1995**, *95*, 2021.
(111) Houston, T. A.; Wilkinson, B. L.; Blanchfield, J. T. *Organic Letters* **2004**, *6*, 679.
(112) Miller, M. J.; Bajwa, J. S.; Mattingly, P. G.; Peterson, K. *The Journal of Organic Chemistry* **1982**, *47*, 4928.
(113) Torres, C.; Bernabé, M.; Otero, C. *Enzyme and Microbial Technology* **1999**, *25*, 753.
(114) Seiki, S.; Takashi, H.; Masami, I.; Ryosuke, N.; Toshikazu, F.; Seiya, N.; Toshio, M. *Chemistry Letters* **1984**, *13*, 1389.
(115) Carreño, M. C.; Hernández-Torres, G.; Urbano, A.; Colobert, F. *European Journal of Organic Chemistry* **2008**, 2035.

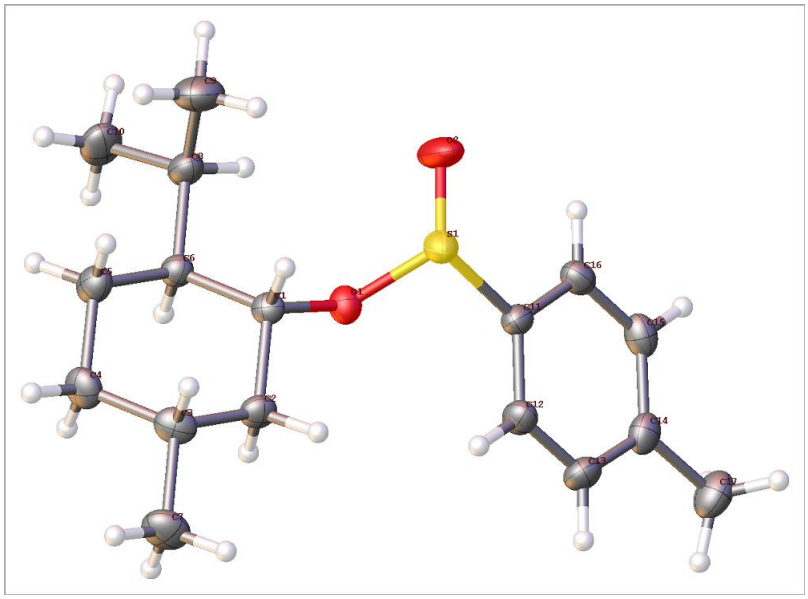
(116) Cammas, S.; Renard, I.; Boutault, K.; Guérin, P. *Tetrahedron: Asymmetry* **1993**, *4*, 1925.
(117) Solladié, G.; Arce, E.; Bauder, C.; Carreño, M. C. *The Journal of Organic Chemistry* **1998**, *63*, 2332.
(118) Jin, H.-X.; Liu, H.-H.; Zhang, Q.; Wu, Y. *The Journal of Organic Chemistry* **2005**, *70*, 4240.
(119) Brown, H. C.; Narasimhan, S. *The Journal of Organic Chemistry* **1982**, *47*, 1604.
(120) Zanka, A.; Ohmori, H.; Okamoto, T. *Synlett* **1999**, 1636.
(121) Hu, B.; Prashad, M.; Har, D.; Prasad, K.; Repič, O.; Blacklock, T. J. *Organic Process Research & Development* **2007**, *11*, 90.
(122) Solladié, G.; Hanquet, G.; Izzo, I.; Crumbie, R. *Tetrahedron Letters* **1999**, *40*, 3071.
(123) Börjesson, L.; Welch, C. J. *Tetrahedron* **1992**, *48*, 6325.
(124) Capon, B. *Quarterly Reviews, Chemical Society* **1964**, *18*, 45.
(125) Galli, C.; Mandolini, L. *European Journal of Organic Chemistry* **2000**, 3117.
(126) Dardonville, C.; Gilbert, I. H. *Organic & Biomolecular Chemistry* **2003**, *1*, 552.
(127) Plante, O. J.; Buchwald, S. L.; Seeberger, P. H. *Journal of the American Chemical Society* **2000**, *122*, 7148.
(128) Lambert, J. B.; Papay, J. J.; Khan, S. A.; Kappauf, K. A.; Magyar, E. S. *Journal of the American Chemical Society* **1974**, *96*, 6112.
(129) Solladie, G. *Heteroatom Chemistry* **2002**, *13*, 443.
(130) Oppolzer, W.; Froelich, O.; Wiaux-Zamar, C.; Bernardinelli, G. *Tetrahedron Letters* **1997**, *38*, 2825.
(131) Han, J.; Soloshonok, V. A.; Klika, K. D.; Drabowicz, J.; Wzorek, A. *Chemical Society Reviews* **2018**, *47*, 1307.
(132) Andersen, K. K. *Tetrahedron Letters* **1962**, *3*, 93.
(133) Solladié, G.; Hutt, J.; Girardin, A. *Synthesis* **1987**, *1987*, 173.
(134) Bauder, C. *European Journal of Organic Chemistry* **2015**, *2015*, 5402.
(135) Fernández, I.; Khiar, N. *Chemical Reviews* **2003**, *103*, 3651.
(136) Jarowicki, K.; Kocienski, P. *Journal of the Chemical Society, Perkin Transactions 1* **2001**, 2109.
(137) Inoue, K.; Nakura, R.; Okano, K.; Mori, A. *European Journal of Organic Chemistry* **2018**, 3343.
(138) Nakura, R.; Inoue, K.; Okano, K.; Mori, A. *Synthesis* **2019**, *51*, 1561.
(139) Moser, W. H. *Tetrahedron* **2001**, *57*, 2065.
(140) Dodd, J. H.; Weinreb, S. M. *Tetrahedron Letters* **1979**, *20*, 3593.
(141) Roush, W. R.; Michaelides, M. R.; Tai, D. F.; Chong, W. K. M. *Journal of the American Chemical Society* **1987**, *109*, 7575.
(142) Roush, W. R.; Michaelides, M. R.; Tai, D. F.; Lesur, B. M.; Chong, W. K. M.; Harris, D. J. *Journal of the American Chemical Society* **1989**, *111*, 2984.
(143) Tan, N. P. H.; Donner, C. D. *Tetrahedron Letters* **2008**, *49*, 4160.
(144) Tan, N. P. H.; Donner, C. D. *Tetrahedron* **2009**, *65*, 4007.
(145) Donner, C. D. *Tetrahedron* **2013**, *69*, 377.
(146) Saito, S.; Ishikawa, T.; Kuroda, A.; Koga, K.; Moriwake, T. *Tetrahedron* **1992**, *48*, 4067.
(147) Song, F.; Fidanze, S.; Benowitz, A. B.; Kishi, Y. *Organic Letters* **2002**, *4*, 647.
(148) Bur, S. K.; Padwa, A. *Chemical Reviews* **2004**, *104*, 2401.
(149) Feldman, K. S. *Tetrahedron* **2006**, *62*, 5003.
(150) Neelarapu, R.; Petukhov, P. A. *Tetrahedron* **2012**, *68*, 7056.
(151) Korošec, T.; Grdadolnik, J.; Urleb, U.; Kocjan, D.; Grdadolnik, S. G. *The Journal of Organic Chemistry* **2006**, *71*, 792.

(152) Abdel-Magid, A. F.; Carson, K. G.; Harris, B. D.; Maryanoff, C. A.; Shah, R. D. *The Journal of Organic Chemistry* **1996**, *61*, 3849.
(153) Das, B.; Mahender, G.; Sunil Kumar, V.; Chowdhury, N. *Tetrahedron Letters* **2004**, *45*, 6709.
(154) Hwu, J. R.; Jain, M. L.; Tsai, F.-Y.; Tsay, S.-C.; Balakumar, A.; Hakimelahi, G. H. *The Journal of Organic Chemistry* **2000**, *65*, 5077.
(155) Kohli, V.; Blöcker, H.; Köster, H. *Tetrahedron Letters* **1980**, *21*, 2683.
(156) Behloul, C.; Chouti, A.; Chabour, I.; Bey, H. B.; Guijarro, D.; Foubelo, F.; Nájera, C.; Yus, M. *Tetrahedron Letters* **2016**, *57*, 3526.
(157) Bessodes, M.; Komiotis, D.; Antonakis, K. *Tetrahedron Letters* **1986**, *27*, 579.
(158) Theodora W Greene, P. G. M. W. *Green's Protective Groups in Organic Synthesis*; 4th ed.; John Wiley and Sons: United States of America (New York), **2006**.
(159) Heravi, M. M.; Fard, M. V.; Faghihi, Z. *Current Organic Chemistry* **2015**, *19*, 1491.
(160) Kabalka, G. W.; Varma, M.; Varma, R. S.; Srivastava, P. C.; Knapp, F. F. *The Journal of Organic Chemistry* **1986**, *51*, 2386.
(161) Jia, H.; Li, Q.; Bayaguud, A.; She, S.; Huang, Y.; Chen, K.; Wei, Y. *Scientific Reports* **2017**, *7*, 12523.
(162) Edagwa, B.; Wang, Y.; Narayanasamy, P. *Bioorganic & Medicinal Chemistry Letters* **2013**, *23*, 6138.
(163) Martina, K.; Trotta, F.; Robaldo, B.; Belliardi, N.; Jicsinszky, L.; Cravotto, G. *Tetrahedron Letters* **2007**, *48*, 9185.
(164) Luzzio, F. A.; Fitch, R. W.; Moore, W. J.; Mudd, K. J. *Journal of Chemical Education* **1999**, *76*, 974.
(165) Hunsen, M. *Tetrahedron Letters* **2005**, *46*, 1651.
(166) Dandepally, S. R.; Williams, A. L. *Tetrahedron Letters* **2009**, *50*, 1071.
(167) Sartori, G.; Ballini, R.; Bigi, F.; Bosica, G.; Maggi, R.; Righi, P. *Chemical Reviews* **2004**, *104*, 199.
(168) Jih Ru, H.; Jain, M. L.; Shwu-Chen, T.; Hakimelahi, G. H. *Tetrahedron Letters* **1996**, *37*, 2035.
(169) Roy, S. J. S. C. *Indian Journal of Chemistry* **2007**, *46B*, 707.
(170) Adachi, M.; Hashimoto, H.; Sakakibara, R.; Imazu, T.; Nishikawa, T. *Synlett* **2014**, *25*, 2498.
(171) Jones, G. B.; Hynd, G.; Wright, J. M.; Sharma, A. *The Journal of Organic Chemistry* **2000**, *65*, 263.
(172) Jiang, X.; Zhai, Y.; Chen, J.; Han, Y.; Yang, Z.; Ma, S. *Chinese Journal of Chemistry* **2018**, *36*, 15.
(173) Rafiee, M.; Konz, Z. M.; Graaf, M. D.; Koolman, H. F.; Stahl, S. S. *ACS Catalysis* **2018**, *8*, 6738.
(174) Jiang, X.; Zhang, J.; Ma, S. *Journal of the American Chemical Society* **2016**, *138*, 8344.
(175) De Luca, L.; Giacomelli, G.; Porcheddu, A. *The Journal of Organic Chemistry* **2001**, *66*, 7907.
(176) Rival, N.; Hazelard, D.; Hanquet, G.; Kreuzer, T.; Bensoussan, C.; Reymond, S.; Cossy, J.; Colobert, F. *Organic & Biomolecular Chemistry* **2012**, *10*, 9418.

Appendix

Crystal Structures

Crystal structure for compound 136



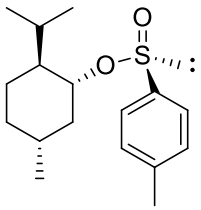


Table 1 Crystal data and structure refinement for 15m_mb2_memory2mzz216_0f.

Identification code	15m_mb2_memory2mzz216_0f
Empirical formula	$C_{17}H_{26}O_2S$
Formula weight	294.44
Temperature/K	173.15
Crystal system	monoclinic
Space group	$P2_1$
a/Å	8.2724(5)
b/Å	6.1759(4)
c/Å	16.4324(9)
α/°	90
β/°	91.941(4)
γ/°	90
Volume/Å^3	839.04(9)
Z	2
ρ_{calc}g/cm^3	1.165
μ/mm^{-1}	0.193
F(000)	320.0
Crystal size/mm^3	0.41 × 0.21 × 0.13
Radiation	MoKα (λ = 0.71073)
2Θ range for data collection/°	4.926 to 55.996
Index ranges	$-9 \le h \le 10$, $-8 \le k \le 8$, $-21 \le l \le 19$

Reflections collected	7354
Independent reflections	3973 [R_{int} = 0.0297, R_{sigma} = 0.0421]
Data/restraints/parameters	3973/1/185
Goodness-of-fit on F^2	1.083
Final R indexes [I>=2σ (I)]	R_1 = 0.0437, wR_2 = 0.1078
Final R indexes [all data]	R_1 = 0.0545, wR_2 = 0.1154
Largest diff. peak/hole / e $Å^{-3}$	0.40/-0.36
Flack parameter	-0.01(6)

Table 2 Fractional Atomic Coordinates (×10⁴) and Equivalent Isotropic Displacement Parameters (Å²×10³) for 15m_mb2_memory2mzz216_0f. U_{eq} is defined as 1/3 of of the trace of the orthogonalised U_{IJ} tensor.

Atom	*x*	*y*	*z*	U(eq)
C1	1219(4)	7113(4)	2197.0(17)	21.8(6)
C2	-362(4)	8291(5)	2001.2(19)	26.4(6)
C3	-90(4)	10416(5)	1557(2)	29.3(7)
C4	867(4)	10008(5)	794.8(19)	32.6(7)
C5	2448(4)	8820(5)	997(2)	31.4(7)
C6	2168(4)	6655(5)	1431.2(17)	23.5(6)
C7	-1685(5)	11568(6)	1359(2)	41.6(9)
C8	3716(4)	5321(5)	1591(2)	31.5(7)
C9	5011(5)	6503(8)	2093(3)	51.2(10)
C10	4400(4)	4515(8)	791(2)	44.1(9)
C11	-303(3)	2933(5)	3722.5(17)	24.9(6)
C12	-1878(4)	3668(5)	3584.5(19)	29.0(7)
C13	-3164(4)	2364(6)	3780(2)	32.0(7)
C14	-2911(4)	314(5)	4126.2(18)	30.7(7)
C15	-1324(4)	-375(6)	4263.1(16)	31.0(6)
C16	-10(4)	919(5)	4067.3(18)	28.5(7)
C17	-4319(5)	-1082(7)	4352(2)	42.2(9)
O1	800(3)	5024(3)	2568.7(11)	27.0(5)
O2	2807(3)	3320(5)	3571.6(18)	53.6(8)
S1	1355.2(9)	4689.3(13)	3519.3(4)	30.3(2)

Table 3 Anisotropic Displacement Parameters (Å²×10³) for 15m_mb2_memory2mzz216_0f. The Anisotropic displacement factor exponent takes the form: $-2\pi^2[h^2a^{*2}U_{11}+2hka^*b^*U_{12}+\ldots]$.

Atom	U_{11}	U_{22}	U_{33}	U_{23}	U_{13}	U_{12}
C1	22.0(14)	17.6(13)	25.8(14)	0.6(11)	0.4(11)	-1.4(10)
C2	24.0(15)	25.9(15)	29.5(15)	-2.5(12)	3.2(11)	5.4(11)
C3	32.7(17)	18.7(13)	36.1(16)	-4.4(12)	-3.4(13)	3.6(12)
C4	40.7(17)	22.6(16)	34.6(15)	7.5(13)	1.1(12)	4.2(14)
C5	30.0(16)	27.4(14)	37.2(16)	7.4(13)	6.9(13)	1.1(13)

C6	22.8(14)	22.3(14)	25.5(14)	1.1(11)	2.4(11)	1.9(12)
C7	42(2)	35.5(19)	47(2)	0.1(16)	-2.1(16)	15.6(17)
C8	23.9(15)	35.6(18)	35.3(16)	7.8(13)	5.7(12)	6.2(13)
C9	28.6(19)	69(3)	56(2)	2(2)	-5.0(16)	5.5(19)
C10	40.1(18)	49(2)	44.2(18)	5.0(19)	14.5(14)	19.4(19)
C11	20.3(15)	31.4(15)	23.1(13)	1.6(12)	1.5(11)	0.8(12)
C12	26.8(16)	27.3(15)	33.0(16)	7.1(13)	3.5(12)	5.9(13)
C13	22.9(15)	38.8(18)	34.6(17)	1.4(14)	6.0(12)	3.5(13)
C14	35.1(17)	33.8(17)	23.6(13)	-1.8(12)	7.0(12)	-3.8(13)
C15	43.1(17)	24.8(13)	25.0(13)	2.7(14)	2.3(11)	1.4(16)
C16	28.8(16)	31.2(16)	25.5(14)	2.1(12)	-0.9(11)	6.8(13)
C17	41(2)	44(2)	42.8(19)	-0.5(16)	12.2(15)	-11.2(16)
O1	31.3(10)	25.0(11)	24.7(9)	1.4(9)	1.6(7)	-3.8(9)
O2	20.9(13)	71(2)	68.7(19)	32.3(16)	2.0(12)	5.5(13)
S1	23.3(3)	38.9(4)	28.5(3)	6.7(4)	-1.8(2)	-2.9(4)

Table 4 Bond Lengths for 15m_mb2_memory2mzz216_0f.

Atom	Atom	Length/Å	Atom	Atom	Length/Å
C1	C2	1.521(4)	C11	C12	1.391(4)
C1	C6	1.532(4)	C11	C16	1.385(4)
C1	O1	1.473(3)	C11	S1	1.789(3)
C2	C3	1.522(4)	C12	C13	1.382(5)
C3	C4	1.525(5)	C13	C14	1.400(5)
C3	C7	1.525(4)	C14	C15	1.391(4)
C4	C5	1.527(4)	C14	C17	1.505(5)
C5	C6	1.537(4)	C15	C16	1.395(5)
C6	C8	1.538(4)	O1	S1	1.626(2)
C8	C9	1.516(5)	O2	S1	1.469(3)
C8	C10	1.532(5)			

Table 5 Bond Angles for 15m_mb2_memory2mzz216_0f.

Atom	Atom	Atom	Angle/°	Atom	Atom	Atom	Angle/°
C2	C1	C6	112.0(2)	C12	C11	S1	119.4(2)
O1	C1	C2	107.1(2)	C16	C11	C12	120.6(3)
O1	C1	C6	108.2(2)	C16	C11	S1	119.8(2)
C1	C2	C3	112.0(3)	C13	C12	C11	119.8(3)
C2	C3	C4	109.9(2)	C12	C13	C14	121.1(3)
C2	C3	C7	111.4(3)	C13	C14	C17	120.8(3)
C7	C3	C4	111.8(3)	C15	C14	C13	118.0(3)
C3	C4	C5	111.4(3)	C15	C14	C17	121.2(3)
C4	C5	C6	112.2(3)	C14	C15	C16	121.7(3)
C1	C6	C5	108.1(2)	C11	C16	C15	118.8(3)

C1	C6	C8	113.9(2)	C1	O1	S1	116.54(17)
C5	C6	C8	114.0(3)	O1	S1	C11	93.62(12)
C9	C8	C6	113.8(3)	O2	S1	C11	105.71(16)
C9	C8	C10	110.4(3)	O2	S1	O1	109.46(15)
C10	C8	C6	110.9(3)				

Table 6 Torsion Angles for 15m_mb2_memory2mzz216_0f.

A	B	C	D	Angle/°	A	B	C	D	Angle/°
C1	C2	C3	C4	55.1(3)	C11	C12	C13	C14	0.8(5)
C1	C2	C3	C7	179.5(3)	C12	C11	C16	C15	0.9(4)
C1	C6	C8	C9	-67.0(4)	C12	C11	S1	O1	-57.9(3)
C1	C6	C8	C10	167.8(3)	C12	C11	S1	O2	-169.3(3)
C1	O1	S1	C11	149.9(2)	C12	C13	C14	C15	-0.4(5)
C1	O1	S1	O2	-102.0(2)	C12	C13	C14	C17	178.9(3)
C2	C1	C6	C5	56.4(3)	C13	C14	C15	C16	0.2(4)
C2	C1	C6	C8	-175.8(2)	C14	C15	C16	C11	-0.5(4)
C2	C1	O1	S1	-113.8(2)	C16	C11	C12	C13	-1.1(5)
C2	C3	C4	C5	-54.9(3)	C16	C11	S1	O1	126.5(3)
C3	C4	C5	C6	57.3(4)	C16	C11	S1	O2	15.2(3)
C4	C5	C6	C1	-56.5(3)	C17	C14	C15	C16	-179.0(3)
C4	C5	C6	C8	175.8(3)	O1	C1	C2	C3	-175.9(2)
C5	C6	C8	C9	57.7(4)	O1	C1	C6	C5	174.2(2)
C5	C6	C8	C10	-67.5(4)	O1	C1	C6	C8	-58.0(3)
C6	C1	C2	C3	-57.4(3)	S1	C11	C12	C13	-176.6(2)
C6	C1	O1	S1	125.2(2)	S1	C11	C16	C15	176.4(2)
C7	C3	C4	C5	-179.0(3)					

Table 7 Hydrogen Atom Coordinates (Å×10⁴) and Isotropic Displacement Parameters (Å²×10³) for 15m_mb2_memory2mzz216_0f.

Atom	*x*	*y*	*z*	U(eq)
H1	1897.9	7986.25	2590.6	26
H2A	-917.96	8586.4	2513.57	32
H2B	-1073.29	7347.85	1658.63	32
H3	574.16	11375.78	1926.82	35
H4A	1107.53	11409.11	532.36	39
H4B	203.7	9135.05	403.95	39
H5A	3148.95	9751.32	1349.83	38
H5B	3020.49	8546.69	487.58	38
H6	1445.57	5771.58	1060.85	28
H7A	-2346.78	10677.47	982.86	62
H7B	-1468.04	12968.91	1104.17	62
H7C	-2266.54	11799.39	1861.17	62

H8	3405.79	4013.3	1908.88	38
H9A	5330.52	7817.26	1804.8	77
H9B	5954.68	5559.01	2175.3	77
H9C	4585.56	6897.66	2621.87	77
H10A	4854.48	5738.88	495.54	66
H10B	3532.15	3847.03	456.53	66
H10C	5249.97	3443.85	908.32	66
H12	-2067.92	5062.67	3356.53	35
H13	-4238.02	2864.68	3678.12	38
H15	-1130.06	-1762.83	4495.93	37
H16	1065.58	426.82	4168.67	34
H17A	-4349.74	-1196.09	4946.07	63
H17B	-4194.81	-2528.87	4117.16	63
H17C	-5327.45	-430.5	4139.66	63

Experimental

Single crystals of $C_{17}H_{26}O_2S$ **[15m_mb2_memory2mzz216_0f]** were **[]**. A suitable crystal was selected and **[]** on a **'Bruker APEX-II CCD'** diffractometer. The crystal was kept at 173.15 K during data collection. Using Olex2 [1], the structure was solved with the ShelXT [2] structure solution program using Intrinsic Phasing and refined with the ShelXL [3] refinement package using Least Squares minimisation.

1. Dolomanov, O.V., Bourhis, L.J., Gildea, R.J, Howard, J.A.K. & Puschmann, H. (2009), J. Appl. Cryst. 42, 339-341.
2. Sheldrick, G.M. (2015). Acta Cryst. A71, 3-8.
3. Sheldrick, G.M. (2015). Acta Cryst. C71, 3-8.

Crystal structure determination of [15m_mb2_memory2mzz216_0f]

Crystal Data for $C_{17}H_{26}O_2S$ (M =294.44 g/mol): monoclinic, space group $P2_1$ (no. 4), a = 8.2724(5) Å, b = 6.1759(4) Å, c = 16.4324(9) Å, β = 91.941(4)°, V = 839.04(9) Å^3, Z = 2, T = 173.15 K, μ(MoKα) = 0.193 mm^{-1}, *Dcalc* = 1.165 g/cm^3, 7354 reflections measured (4.926° ≤ 2Θ ≤ 55.996°), 3973 unique (R_{int} = 0.0297, R_{sigma} = 0.0421) which were used in all calculations. The final R_1 was 0.0437 (I > 2σ(I)) and wR_2 was 0.1154 (all data).

Refinement model description

Number of restraints - 1, number of constraints - unknown.

Details:

```
1. Fixed Uiso
 At 1.2 times of:
  All C(H) groups, All C(H,H) groups
 At 1.5 times of:
  All C(H,H,H) groups
2.a Ternary CH refined with riding coordinates:
 C1(H1), C3(H3), C6(H6), C8(H8)
2.b Secondary CH2 refined with riding coordinates:
 C2(H2A,H2B), C4(H4A,H4B), C5(H5A,H5B)
2.c Aromatic/amide H refined with riding coordinates:
 C12(H12), C13(H13), C15(H15), C16(H16)
2.d Idealised Me refined as rotating group:
 C7(H7A,H7B,H7C), C9(H9A,H9B,H9C), C10(H10A,H10B,H10C), C17(H17A,H17B,H17C)
```

This report has been created with Olex2, compiled on 2018.05.29 svn.r3508 for OlexSys. Please let us know if there are any errors or if you would like to have additional features.

Crystal structure for compound 137

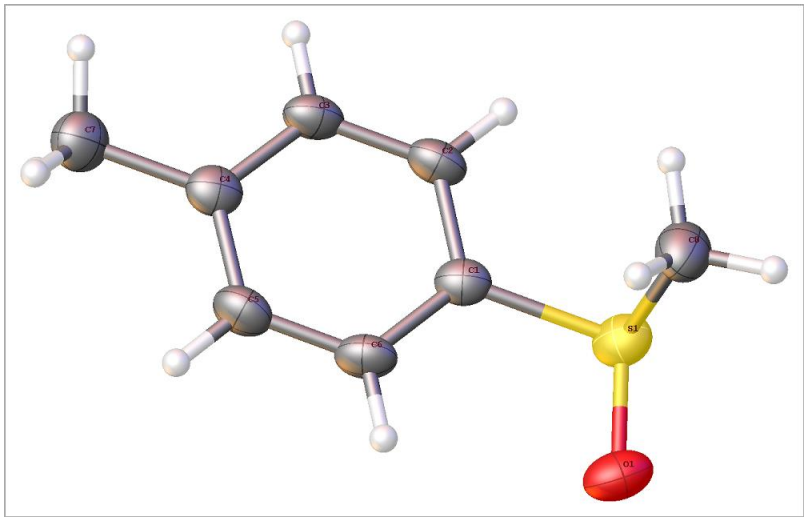


Table 1 Crystal data and structure refinement for 16m_mb1_memory1mzz232_0f.

Identification code	16m_mb1_memory1mzz232_0f
Empirical formula	$C_8H_{10}OS$
Formula weight	154.22
Temperature/K	173.15
Crystal system	orthorhombic
Space group	$P2_12_12_1$
a/Å	5.75756(9)
b/Å	8.58241(13)
c/Å	16.2747(3)
α/°	90
β/°	90
γ/°	90
Volume/Å^3	804.19(2)
Z	4
ρ_{calc}g/cm^3	1.274
μ/mm^{-1}	0.330
F(000)	328.0
Crystal size/mm^3	0.39 × 0.15 × 0.09
Radiation	MoKα (λ = 0.71073)
2Θ range for data collection/°	5.006 to 55.946
Index ranges	$-7 \leq h \leq 7$, $-11 \leq k \leq 11$, $-20 \leq l \leq 21$
Reflections collected	15634
Independent reflections	1945 [R_{int} = 0.0276, R_{sigma} = 0.0152]
Data/restraints/parameters	1945/0/93
Goodness-of-fit on F^2	1.073
Final R indexes [I>=2σ (I)]	R_1 = 0.0271, wR_2 = 0.0732
Final R indexes [all data]	R_1 = 0.0305, wR_2 = 0.0754
Largest diff. peak/hole / e Å^{-3}	0.28/-0.12
Flack parameter	0.02(2)

Table 2 Fractional Atomic Coordinates (×10^4) and Equivalent Isotropic Displacement Parameters (Å^2×10^3) for 16m_mb1_memory1mzz232_0f. U_{eq} is defined as 1/3 of of the trace of the orthogonalised U_{IJ} tensor.

Atom	*x*	*y*	*z*	U(eq)
C1	6274(3)	2193(2)	6975.2(11)	29.3(4)
C2	5493(4)	3025(2)	7656.7(11)	33.1(4)
C3	6819(4)	3055(2)	8366.3(12)	33.3(4)
C4	8915(3)	2241(2)	8415.9(12)	31.4(4)
C5	9639(4)	1400(2)	7730.4(12)	35.0(4)
C6	8346(3)	1377(2)	7012.9(12)	33.2(4)
C7	10327(4)	2260(3)	9196.1(12)	42.4(5)
C8	5211(4)	4028(2)	5684.6(14)	45.2(5)
O1	5627(3)	995.2(17)	5495.1(9)	44.0(4)
S1	4514.5(9)	2129.9(6)	6070.5(3)	35.56(15)

Table 3 Anisotropic Displacement Parameters (Å^2×10^3) for 16m_mb1_memory1mzz232_0f. The Anisotropic displacement factor exponent takes the form: -2π^2[h^{2}a*^{2}U_{11}+2hka*b*U_{12}+…].

Atom	U_{11}	U_{22}	U_{33}	U_{23}	U_{13}	U_{12}
C1	29.5(8)	25.1(8)	33.2(9)	-1.0(8)	6.4(7)	-4.3(8)
C2	31.6(9)	27.4(8)	40.4(10)	-0.6(7)	9.2(8)	5.3(9)
C3	39.7(11)	27.3(9)	33.0(9)	-1.5(7)	11.0(8)	4.0(8)
C4	35.3(9)	25.8(8)	33.1(9)	4.0(7)	6.4(7)	-2.8(8)
C5	29.8(9)	32.2(9)	42.9(10)	-0.5(8)	7.9(9)	5.2(9)
C6	31.4(9)	30.0(9)	38.1(10)	-7.1(8)	10.9(8)	0.5(8)
C7	49.1(12)	42.4(11)	35.7(10)	5.3(8)	1.7(9)	2.2(11)
C8	55.1(14)	34.2(10)	46.2(11)	3.6(9)	-11.4(12)	-1.5(10)
O1	55.1(9)	37.8(7)	39.1(7)	-10.7(6)	5.8(8)	-8.2(8)
S1	31.2(2)	36.5(3)	39.0(2)	-5.6(2)	2.4(2)	-7.9(2)

Table 4 Bond Lengths for 16m_mb1_memory1mzz232_0f.

Atom	Atom	Length/Å	Atom	Atom	Length/Å
C1	C2	1.393(3)	C4	C5	1.392(3)
C1	C6	1.385(3)	C4	C7	1.508(3)
C1	S1	1.788(2)	C5	C6	1.385(3)
C2	C3	1.385(3)	C8	S1	1.791(2)
C3	C4	1.397(3)	O1	S1	1.4951(16)

Table 5 Bond Angles for 16m_mb1_memory1mzz232_0f.

Atom	Atom	Atom	Angle/°	Atom	Atom	Atom	Angle/°
C2	C1	S1	119.23(15)	C5	C4	C7	121.27(18)
C6	C1	C2	120.11(19)	C6	C5	C4	121.48(18)
C6	C1	S1	120.61(15)	C1	C6	C5	119.55(17)
C3	C2	C1	119.70(18)	C1	S1	C8	97.72(9)
C2	C3	C4	121.01(17)	O1	S1	C1	107.03(9)
C3	C4	C7	120.59(18)	O1	S1	C8	106.07(10)
C5	C4	C3	118.13(18)				

Table 6 Torsion Angles for 16m_mb1_memory1mzz232_0f.

A	B	C	D	Angle/°	A	B	C	D	Angle/°
C1	C2	C3	C4	-1.1(3)	C4	C5	C6	C1	-0.7(3)
C2	C1	C6	C5	-0.3(3)	C6	C1	C2	C3	1.2(3)
C2	C1	S1	C8	77.98(17)	C6	C1	S1	C8	−104.53(17)
C2	C1	S1	O1	−172.53(15)	C6	C1	S1	O1	4.96(18)
C2	C3	C4	C5	0.2(3)	C7	C4	C5	C6	179.92(18)
C2	C3	C4	C7	−179.02(18)	S1	C1	C2	C3	178.67(15)
C3	C4	C5	C6	0.7(3)	S1	C1	C6	C5	−177.76(15)

Table 7 Hydrogen Atom Coordinates (Å×10⁴) and Isotropic Displacement Parameters (Å²×10³) for 16m_mb1_memory1mzz232_0f.

Atom	*x*	*y*	*z*	U(eq)
H2	4057.45	3568.91	7634.52	40
H3	6295.59	3638.22	8826.53	40
H5	11051.05	830.03	7755.4	42
H6	8877.24	805.76	6549.69	40
H7A	9922.79	1352.94	9532.46	64
H7B	9992.85	3216.21	9503.58	64
H7C	11984.09	2224.73	9059.39	64
H8A	6877.1	4083.38	5564.55	68
H8B	4810.84	4814.36	6097.46	68
H8C	4326.82	4223.96	5180.58	68

Experimental

Single crystals of $C_8H_{10}OS$ **[16m_mb1_memory1mzz232_0f]** were **[]**. A suitable crystal was selected and **[]** on a **'Bruker APEX-II CCD'** diffractometer. The crystal was kept at 173.15 K during data collection. Using Olex2 [1], the structure was solved with the ShelXT [2] structure solution program using Intrinsic Phasing and refined with the ShelXL [3] refinement package using Least Squares minimisation.

1. Dolomanov, O.V., Bourhis, L.J., Gildea, R.J, Howard, J.A.K. & Puschmann, H. (2009), J. Appl. Cryst. 42, 339-341.
2. Sheldrick, G.M. (2015). Acta Cryst. A71, 3-8.
3. Sheldrick, G.M. (2015). Acta Cryst. C71, 3-8.

Crystal structure determination of [16m_mb1_memory1mzz232_0f]

Crystal Data for $C_8H_{10}OS$ (M =154.22 g/mol): orthorhombic, space group $P2_12_12_1$ (no. 19), a = 5.75756(9) Å, b = 8.58241(13) Å, c = 16.2747(3) Å, V = 804.19(2) Å^3, Z = 4, T = 173.15 K, μ(MoKα) = 0.330 mm^{-1}, *Dcalc* = 1.274 g/cm^3, 15634 reflections measured (5.006° ≤ 2Θ ≤ 55.946°), 1945 unique (R_{int} = 0.0276, R_{sigma} = 0.0152) which were used in all calculations. The final R_1 was 0.0271 (I > 2σ(I)) and wR_2 was 0.0754 (all data).

Refinement model description

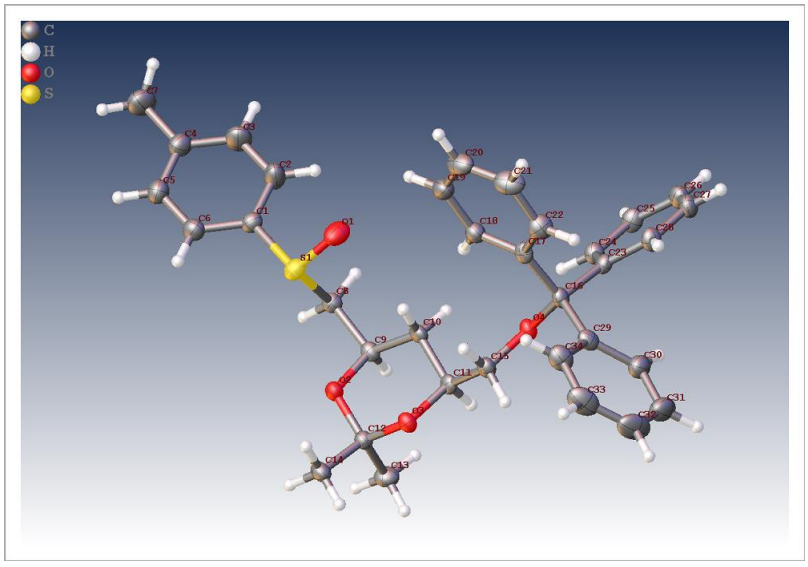
Number of restraints - 0, number of constraints - unknown.

Details:

```
1. Fixed Uiso
 At 1.2 times of:
  All C(H) groups
 At 1.5 times of:
  All C(H,H,H) groups
2.a Aromatic/amide H refined with riding coordinates:
 C2(H2), C3(H3), C5(H5), C6(H6)
2.b Idealised Me refined as rotating group:
 C7(H7A,H7B,H7C), C8(H8A,H8B,H8C)
```

This report has been created with Olex2, compiled on 2018.05.29 svn.r3508 for OlexSys. Please let us know if there are any errors or if you would like to have additional features.

Crystal structure for compound 124



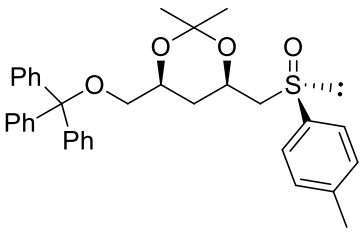


Table 1 Crystal data and structure refinement for 18a_mb2_MZZ432_0f.

Identification code	18a_mb2_MZZ432_0f
Empirical formula	$C_{34}H_{36}O_4S$
Formula weight	540.69
Temperature/K	173.15
Crystal system	orthorhombic
Space group	$P2_12_12_1$
a/Å	9.2972(3)

b/Å	15.1161(5)
c/Å	20.4356(7)
α/°	90
β/°	90
γ/°	90
Volume/Å^3	2871.97(17)
Z	4
ρ_{calc}g/cm^3	1.250
μ/mm^{-1}	0.150
F(000)	1152.0
Crystal size/mm^3	0.48 × 0.08 × 0.05
Radiation	MoKα (λ = 0.71073)
2Θ range for data collection/°	3.352 to 50.99
Index ranges	-11 ≤ h ≤ 11, -18 ≤ k ≤ 18, -24 ≤ l ≤ 24
Reflections collected	27581
Independent reflections	5356 [R_{int} = 0.0706, R_{sigma} = 0.0524]
Data/restraints/parameters	5356/0/353
Goodness-of-fit on F^2	1.036
Final R indexes [I>=2σ (I)]	R_1 = 0.0403, wR_2 = 0.0818
Final R indexes [all data]	R_1 = 0.0549, wR_2 = 0.0879
Largest diff. peak/hole / e Å^{-3}	0.18/-0.25
Flack parameter	0.04(5)

Table 2 Fractional Atomic Coordinates (×10^4) and Equivalent Isotropic Displacement Parameters (Å^2×10^3) for 18a_mb2_MZZ432_0f. U_{eq} is defined as 1/3 of of the trace of the orthogonalised U_{IJ} tensor.

Atom	*x*	*y*	*z*	U(eq)
C1	3721(4)	4821(2)	5139.7(15)	27.5(7)
C2	4784(4)	4459(2)	4745.8(19)	45.2(10)
C3	5037(4)	3558(2)	4778(2)	48.1(10)
C4	4257(4)	3006(2)	5179.7(17)	36.8(9)
C5	3195(4)	3385(2)	5568.5(16)	36.3(8)
C6	2925(4)	4283(2)	5545.7(16)	32.7(8)
C7	4534(5)	2020(2)	5196(2)	54.8(12)
C8	4865(3)	6423(2)	5426.4(15)	23.4(7)
C9	4789(3)	7421(2)	5520.1(14)	21.9(7)
C10	4631(3)	7935.0(19)	4887.2(14)	22.4(7)
C11	4283(3)	8899.4(19)	5010.1(14)	21.7(6)
C12	3302(3)	8500.6(19)	6061.9(14)	22.1(7)
C13	4497(4)	8903(2)	6468.6(16)	31.7(8)
C14	1875(4)	8538(2)	6415.0(15)	28.1(7)
C15	3761(3)	9363(2)	4396.5(14)	24.0(7)
C16	4512(3)	9527(2)	3255.3(14)	21.7(7)
C17	3555(3)	8808(2)	2953.7(14)	22.6(7)
C18	3579(4)	7958(2)	3203.3(15)	27.4(8)

C19	2811(4)	7277(2)	2913.8(17)	36.1(9)
C20	2028(4)	7440(3)	2351.5(17)	40.4(9)
C21	2027(4)	8273(3)	2084.9(18)	40.3(9)
C22	2768(4)	8958(2)	2384.0(15)	33.9(8)
C23	5940(3)	9478(2)	2881.9(15)	21.4(7)
C24	7096(3)	8998(2)	3129.9(15)	25.7(7)
C25	8357(3)	8919(2)	2772.1(16)	29.3(7)
C26	8476(4)	9305(2)	2165.1(16)	31.1(8)
C27	7327(4)	9765(2)	1903.3(16)	31.1(8)
C28	6074(4)	9852(2)	2261.0(16)	28.5(8)
C29	3843(4)	10452(2)	3248.1(15)	26.1(7)
C30	4714(4)	11202(2)	3240.5(16)	35.3(9)
C31	4133(5)	12045(2)	3299.5(18)	46.5(11)
C32	2671(6)	12143(3)	3383.1(19)	54.2(12)
C33	1793(5)	11411(3)	3399.3(18)	49.1(11)
C34	2363(4)	10572(2)	3328.0(16)	36.2(9)
O1	3219(3)	6181.1(14)	4366.8(10)	38.0(6)
O2	3563(2)	7582.1(13)	5931.9(9)	23.0(5)
O3	3096(2)	8964.9(13)	5461.5(9)	22.7(4)
O4	4884(2)	9315.4(13)	3924.4(9)	22.3(5)
S1	3232.4(8)	5960.8(5)	5079.2(4)	26.76(19)

Table 3 Anisotropic Displacement Parameters ($Å^2×10^3$) for 18a_mb2_MZZ432_0f. The Anisotropic displacement factor exponent takes the form: $-2\pi^2[h^2a^{*2}U_{11}+2hka^*b^*U_{12}+\ldots]$.

Atom	U_{11}	U_{22}	U_{33}	U_{23}	U_{13}	U_{12}
C1	26.2(17)	25.5(17)	31.0(18)	-2.2(14)	0.6(16)	-0.1(14)
C2	52(3)	31(2)	53(2)	3.6(18)	23(2)	1.3(19)
C3	51(2)	36(2)	57(3)	-3.6(19)	20(2)	9.7(19)
C4	48(2)	27.2(19)	35(2)	1.5(16)	0.2(18)	1.9(17)
C5	41(2)	30.8(19)	37.4(19)	2.5(16)	4.0(19)	-4.1(18)
C6	32(2)	31(2)	35.1(18)	-2.4(15)	6.3(16)	-0.4(15)
C7	74(3)	33(2)	57(3)	0.3(19)	12(2)	11(2)
C8	20.2(16)	26.5(18)	23.5(16)	0.6(13)	-1.1(14)	2.2(14)
C9	16.0(15)	29.0(18)	20.7(15)	0.6(13)	-0.7(14)	0.0(13)
C10	17.9(16)	28.0(17)	21.3(15)	-1.5(13)	5.8(14)	-0.3(13)
C11	13.4(13)	25.1(16)	26.5(16)	-0.1(15)	4.4(13)	-2.7(12)
C12	22.6(16)	23.0(16)	20.8(15)	-0.2(13)	1.7(14)	-0.9(15)
C13	29.8(19)	36(2)	29.2(17)	-7.0(16)	-4.1(15)	-1.1(16)
C14	28.0(18)	33.5(19)	22.7(16)	-2.6(14)	4.9(15)	-4.2(16)
C15	20.9(16)	25.3(17)	25.7(16)	2.1(13)	5.5(14)	2.5(13)
C16	21.4(17)	22.5(17)	21.0(16)	5.6(13)	1.9(14)	2.1(13)
C17	11.7(15)	28.2(18)	27.9(16)	1.7(13)	3.4(13)	0.8(12)
C18	27.7(19)	29.9(19)	24.8(16)	-0.1(14)	3.3(15)	-0.1(15)

C19	39(2)	34(2)	35(2)	-5.9(16)	11.0(18)	-6.0(17)
C20	29(2)	49(2)	43(2)	-15.5(18)	3.8(18)	-8.6(18)
C21	26(2)	55(3)	39(2)	-10.6(18)	-9.7(17)	5.1(18)
C22	29.2(19)	37(2)	35.6(18)	3.3(17)	-3.2(15)	5.7(17)
C23	19.2(16)	19.2(16)	25.7(16)	1.4(13)	-0.1(13)	-2.4(13)
C24	22.9(17)	27.1(17)	27.1(16)	2.4(14)	-0.1(13)	0.7(15)
C25	20.2(17)	28.1(18)	39.5(18)	3.0(15)	-0.6(15)	3.4(15)
C26	26.4(19)	30.9(19)	36.0(18)	2.1(15)	9.0(16)	0.1(15)
C27	36(2)	29(2)	28.6(18)	5.9(15)	7.2(16)	-2.0(16)
C28	26.8(19)	28.4(19)	30.2(18)	7.2(15)	0.2(16)	3.4(15)
C29	28.7(18)	29.7(19)	20.1(16)	4.1(14)	0.3(15)	6.9(15)
C30	45(2)	28(2)	32.9(19)	2.9(16)	2.7(17)	0.7(17)
C31	70(3)	27(2)	43(2)	0.8(18)	5(2)	5(2)
C32	82(4)	36(2)	44(2)	4.5(19)	3(2)	31(2)
C33	47(2)	55(3)	45(2)	6.7(19)	5(2)	28(2)
C34	34(2)	39(2)	36(2)	6.8(17)	2.4(17)	11.3(17)
O1	49.6(15)	31.9(13)	32.4(13)	0.2(10)	-14.3(12)	-2.9(12)
O2	22.3(12)	23.1(12)	23.7(11)	0.7(9)	4.5(9)	-0.9(9)
O3	18.7(10)	27.7(11)	21.7(10)	2.1(9)	3.0(9)	1.2(10)
O4	19.2(11)	26.2(12)	21.5(11)	4.9(9)	3.1(9)	0.6(9)
S1	21.4(4)	23.9(4)	35.0(4)	-1.4(4)	-1.2(4)	0.6(3)

Table 4 Bond Lengths for 18a_mb2_MZZ432_0f.

Atom	Atom	Length/Å	Atom	Atom	Length/Å
C1	C2	1.387(5)	C16	C29	1.530(4)
C1	C6	1.378(5)	C16	O4	1.446(3)
C1	S1	1.786(3)	C17	C18	1.382(4)
C2	C3	1.384(5)	C17	C22	1.394(4)
C3	C4	1.377(5)	C18	C19	1.385(5)
C4	C5	1.391(5)	C19	C20	1.383(5)
C4	C7	1.512(5)	C20	C21	1.372(5)
C5	C6	1.382(5)	C21	C22	1.385(5)
C8	C9	1.522(4)	C23	C24	1.392(4)
C8	S1	1.815(3)	C23	C28	1.395(4)
C9	C10	1.516(4)	C24	C25	1.387(4)
C9	O2	1.438(3)	C25	C26	1.375(4)
C10	C11	1.514(4)	C26	C27	1.382(5)
C11	C15	1.516(4)	C27	C28	1.382(5)
C11	O3	1.441(3)	C29	C30	1.394(5)
C12	C13	1.515(4)	C29	C34	1.397(5)
C12	C14	1.512(4)	C30	C31	1.390(5)
C12	O2	1.434(4)	C31	C32	1.377(6)
C12	O3	1.426(3)	C32	C33	1.376(6)

C15	O4	1.423(3)	C33	C34	1.382(5)
C16	C17	1.534(4)	O1	S1	1.494(2)
C16	C23	1.533(4)			

Table 5 Bond Angles for 18a_mb2_MZZ432_0f.

Atom	Atom	Atom	Angle/°	Atom	Atom	Atom	Angle/°
C2	C1	S1	121.5(3)	C18	C17	C16	120.1(3)
C6	C1	C2	119.9(3)	C18	C17	C22	117.8(3)
C6	C1	S1	118.3(3)	C22	C17	C16	121.7(3)
C3	C2	C1	118.9(4)	C17	C18	C19	121.7(3)
C4	C3	C2	122.3(4)	C20	C19	C18	119.6(3)
C3	C4	C5	117.7(3)	C21	C20	C19	119.6(3)
C3	C4	C7	121.3(4)	C20	C21	C22	120.6(3)
C5	C4	C7	121.0(3)	C21	C22	C17	120.6(3)
C6	C5	C4	121.0(3)	C24	C23	C16	120.9(3)
C1	C6	C5	120.2(3)	C24	C23	C28	118.2(3)
C9	C8	S1	113.0(2)	C28	C23	C16	120.7(3)
C10	C9	C8	113.9(2)	C25	C24	C23	120.4(3)
O2	C9	C8	106.2(2)	C26	C25	C24	120.5(3)
O2	C9	C10	109.6(2)	C25	C26	C27	120.0(3)
C11	C10	C9	111.9(2)	C28	C27	C26	119.7(3)
C10	C11	C15	112.1(2)	C27	C28	C23	121.2(3)
O3	C11	C10	109.6(2)	C30	C29	C16	120.5(3)
O3	C11	C15	104.6(2)	C30	C29	C34	117.9(3)
C14	C12	C13	111.5(2)	C34	C29	C16	121.2(3)
O2	C12	C13	111.5(3)	C31	C30	C29	121.3(4)
O2	C12	C14	105.9(2)	C32	C31	C30	119.5(4)
O3	C12	C13	111.9(2)	C33	C32	C31	120.2(4)
O3	C12	C14	105.9(2)	C32	C33	C34	120.5(4)
O3	C12	O2	109.9(2)	C33	C34	C29	120.6(4)
O4	C15	C11	107.6(2)	C12	O2	C9	114.0(2)
C23	C16	C17	105.5(2)	C12	O3	C11	114.5(2)
C29	C16	C17	114.1(3)	C15	O4	C16	117.0(2)
C29	C16	C23	113.1(3)	C1	S1	C8	97.53(15)
O4	C16	C17	111.2(2)	O1	S1	C1	106.53(14)
O4	C16	C23	104.7(2)	O1	S1	C8	107.58(15)
O4	C16	C29	108.0(2)				

Table 6 Torsion Angles for 18a_mb2_MZZ432_0f.

A	B	C	D	Angle/°	A	B	C	D	Angle/°
C1	C2	C3	C4	1.0(6)	C18	C19	C20	C21	0.4(5)
C2	C1	C6	C5	0.9(5)	C19	C20	C21	C22	-1.9(5)

C2	C1	S1	C8	-70.3(3)	C20	C21	C22	C17	1.4(5)
C2	C1	S1	O1	40.7(3)	C22	C17	C18	C19	-2.1(5)
C2	C3	C4	C5	-0.8(6)	C23	C16	C17	C18	89.3(3)
C2	C3	C4	C7	178.8(4)	C23	C16	C17	C22	-83.4(3)
C3	C4	C5	C6	0.7(5)	C23	C16	C29	C30	-32.6(4)
C4	C5	C6	C1	-0.8(5)	C23	C16	C29	C34	155.1(3)
C6	C1	C2	C3	-1.0(6)	C23	C16	O4	C15	176.4(2)
C6	C1	S1	C8	115.7(3)	C23	C24	C25	C26	-0.7(5)
C6	C1	S1	O1	-133.3(3)	C24	C23	C28	C27	-1.1(5)
C7	C4	C5	C6	-178.9(4)	C24	C25	C26	C27	-1.0(5)
C8	C9	C10	C11	169.4(2)	C25	C26	C27	C28	1.5(5)
C8	C9	O2	C12	-178.6(2)	C26	C27	C28	C23	-0.5(5)
C9	C8	S1	C1	-174.3(2)	C28	C23	C24	C25	1.7(5)
C9	C8	S1	O1	75.7(2)	C29	C16	C17	C18	-145.9(3)
C9	C10	C11	C15	-165.8(2)	C29	C16	C17	C22	41.3(4)
C9	C10	C11	O3	-50.0(3)	C29	C16	C23	C24	138.6(3)
C10	C9	O2	C12	-55.2(3)	C29	C16	C23	C28	-46.7(4)
C10	C11	C15	O4	-60.7(3)	C29	C16	O4	C15	55.6(3)
C10	C11	O3	C12	54.4(3)	C29	C30	C31	C32	1.6(6)
C11	C15	O4	C16	165.8(2)	C30	C29	C34	C33	-0.2(5)
C13	C12	O2	C9	-66.3(3)	C30	C31	C32	C33	-0.8(6)
C13	C12	O3	C11	66.5(3)	C31	C32	C33	C34	-0.4(6)
C14	C12	O2	C9	172.2(2)	C32	C33	C34	C29	1.0(6)
C14	C12	O3	C11	-171.8(2)	C34	C29	C30	C31	-1.0(5)
C15	C11	O3	C12	174.8(2)	O2	C9	C10	C11	50.6(3)
C16	C17	C18	C19	-175.1(3)	O2	C12	O3	C11	-57.9(3)
C16	C17	C22	C21	173.5(3)	O3	C11	C15	O4	-179.5(2)
C16	C23	C24	C25	176.6(3)	O3	C12	O2	C9	58.3(3)
C16	C23	C28	C27	-176.1(3)	O4	C16	C17	C18	-23.6(4)
C16	C29	C30	C31	-173.5(3)	O4	C16	C17	C22	163.7(3)
C16	C29	C34	C33	172.2(3)	O4	C16	C23	C24	21.3(4)
C17	C16	C23	C24	-96.1(3)	O4	C16	C23	C28	-163.9(3)
C17	C16	C23	C28	78.7(3)	O4	C16	C29	C30	82.7(3)
C17	C16	C29	C30	-153.2(3)	O4	C16	C29	C34	-89.5(4)
C17	C16	C29	C34	34.5(4)	S1	C1	C2	C3	-174.9(3)
C17	C16	O4	C15	-70.2(3)	S1	C1	C6	C5	175.0(3)
C17	C18	C19	C20	1.7(5)	S1	C8	C9	C10	-63.5(3)
C18	C17	C22	C21	0.6(5)	S1	C8	C9	O2	57.2(3)

Table 7 Hydrogen Atom Coordinates (Å×10^4) and Isotropic Displacement Parameters (Å^2×10^3) for 18a_mb2_MZZ432_0f.

Atom	*x*	*y*	*z*	U(eq)
H2	5329.15	4822.8	4459.21	54

H3	5775.15	3310.8	4513.1	58
H5	2648.07	3020.86	5854.23	44
H6	2187.84	4530.36	5810.66	39
H7A	4574.33	1791.67	4747.09	82
H7B	3756.32	1724.73	5434.34	82
H7C	5452.01	1904.93	5415.53	82
H8A	5050.95	6139.57	5854.99	28
H8B	5684.39	6281.48	5134.87	28
H9	5677.62	7623.95	5751.49	26
H10A	5537.39	7893.57	4634.75	27
H10B	3855.53	7666.86	4621.02	27
H11	5143.83	9211.28	5190.91	26
H13A	4605.58	8567.56	6875.85	48
H13B	5399.8	8883.59	6221.59	48
H13C	4258.2	9519.31	6571.44	48
H14A	1953.62	8227.25	6834.16	42
H14B	1611.82	9157.17	6493.68	42
H14C	1133.14	8255.34	6146.06	42
H15A	2883.81	9070.12	4227.58	29
H15B	3527.8	9988.41	4493.95	29
H18	4135.2	7838.17	3582.89	33
H19	2823.03	6701.55	3100.38	43
H20	1493.81	6978.42	2150.88	49
H21	1512.33	8381.75	1691.25	48
H22	2739.29	9533.94	2199.09	41
H24	7021.31	8723.65	3546.73	31
H25	9144.04	8595.52	2947.42	35
H26	9348.23	9255.67	1925.73	37
H27	7398.99	10019.96	1479.75	37
H28	5288.88	10171.81	2080.69	34
H30	5725.13	11135.7	3193.96	42
H31	4738.81	12550.76	3282.3	56
H32	2268.86	12717	3429.66	65
H33	786.26	11482.09	3460.01	59
H34	1743.84	10071.94	3333.4	43

Experimental

Single crystals of $C_{34}H_{36}O_4S$ **[18a_mb2_MZZ432_0f]** were **[]**. A suitable crystal was selected and **[]** on a **'Bruker APEX-II CCD'** diffractometer. The crystal was kept at 173.15 K during data collection. Using Olex2 [1], the structure was solved with the ShelXT [2] structure solution program using Intrinsic Phasing and refined with the ShelXL [3] refinement package using Least Squares minimisation.

1. Dolomanov, O.V., Bourhis, L.J., Gildea, R.J, Howard, J.A.K. & Puschmann, H. (2009), J. Appl. Cryst. 42, 339-341.
2. Sheldrick, G.M. (2015). Acta Cryst. A71, 3-8.
3. Sheldrick, G.M. (2015). Acta Cryst. C71, 3-8.

Crystal structure determination of [18a_mb2_MZZ432_0f]

Crystal Data for $C_{34}H_{36}O_4S$ (*M* =540.69 g/mol): orthorhombic, space group $P2_12_12_1$ (no. 19), *a* = 9.2972(3) Å, *b* = 15.1161(5) Å, *c* = 20.4356(7) Å, *V* = 2871.97(17) Å^3, *Z* = 4, *T* = 173.15 K, μ(MoKα) = 0.150 mm^{-1}, *Dcalc* = 1.250 g/cm^3, 27581 reflections measured (3.352° ≤ 2Θ ≤ 50.99°), 5356 unique (R_{int} = 0.0706, R_{sigma} = 0.0524) which were used in all calculations. The final R_1 was 0.0403 (I > 2σ(I)) and wR_2 was 0.0879 (all data).

Refinement model description

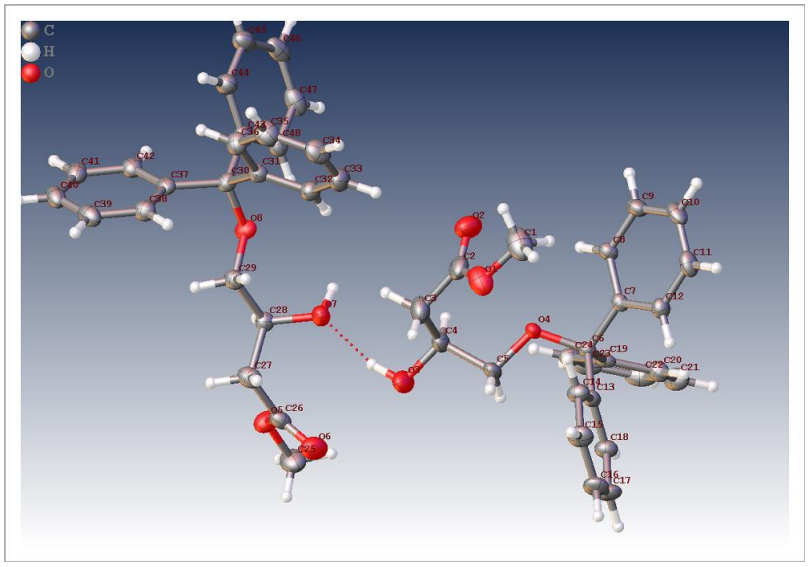
Number of restraints - 0, number of constraints - unknown.

Details:

```
1. Fixed Uiso
 At 1.2 times of:
  All C(H) groups, All C(H,H) groups
 At 1.5 times of:
  All C(H,H,H) groups
2.a Ternary CH refined with riding coordinates:
 C9(H9), C11(H11)
2.b Secondary CH2 refined with riding coordinates:
 C8(H8A,H8B), C10(H10A,H10B), C15(H15A,H15B)
2.c Me refined with riding coordinates:
 C13(H13A,H13B,H13C), C14(H14A,H14B,H14C)
2.d Aromatic/amide H refined with riding coordinates:
 C2(H2), C3(H3), C5(H5), C6(H6), C18(H18), C19(H19), C20(H20), C21(H21),
 C22(H22), C24(H24), C25(H25), C26(H26), C27(H27), C28(H28), C30(H30), C31(H31),
  C32(H32), C33(H33), C34(H34)
2.e Idealised Me refined as rotating group:
 C7(H7A,H7B,H7C)
```

This report has been created with Olex2, compiled on 2018.05.29 svn.r3508 for OlexSys. Please let us know if there are any errors or if you would like to have additional features.

Crystal structure for compound 142



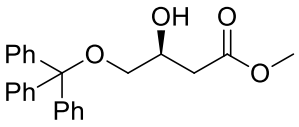


Table 1 Crystal data and structure refinement for 18dbv_mzz_527_xtal2_0s.

Identification code	18dbv_mzz_527_xtal2_0s
Empirical formula	$C_{24}H_{24}O_4$
Formula weight	376.43
Temperature/K	173.15
Crystal system	monoclinic
Space group	$P2_1$
a/Å	13.9337(11)
b/Å	9.0460(7)

c/Å	16.2618(13)
α/°	90
β/°	105.718(2)
γ/°	90
Volume/Å^3	1973.1(3)
Z	4
ρ_{calc}g/cm^3	1.267
μ/mm^{-1}	0.085
F(000)	800.0
Crystal size/mm^3	0.37 × 0.25 × 0.24
Radiation	MoKα (λ = 0.71073)
2Θ range for data collection/°	6.074 to 56.782
Index ranges	-18 ≤ h ≤ 18, -12 ≤ k ≤ 12, -21 ≤ l ≤ 21
Reflections collected	44143
Independent reflections	9805 [R_{int} = 0.0328, R_{sigma} = 0.0238]
Data/restraints/parameters	9805/2/513
Goodness-of-fit on F^2	1.058
Final R indexes [I>=2σ (I)]	R_1 = 0.0437, wR_2 = 0.1052
Final R indexes [all data]	R_1 = 0.0491, wR_2 = 0.1087
Largest diff. peak/hole / e Å^{-3}	0.58/-0.23
Flack parameter	0.04(19)

Table 2 Fractional Atomic Coordinates (×10^4) and Equivalent Isotropic Displacement Parameters (Å^2×10^3) for 18dbv_mzz_527_xtal2_0s. U_{eq} is defined as 1/3 of of the trace of the orthogonalised U_{IJ} tensor.

Atom	*x*	*y*	*z*	U(eq)
C1	9973(2)	6941(5)	5089(2)	54.8(9)
C2	8297(2)	6261(4)	4886.6(15)	39.4(6)
C3	7264(2)	6838(4)	4809.8(18)	44.6(7)
C4	6900.5(17)	6518(3)	5604.0(16)	30.4(5)
C5	7566.5(16)	7202(3)	6403.7(16)	28.0(5)
C6	9124.5(15)	6607(2)	7467.5(13)	19.0(4)
C7	10133.0(15)	6001(2)	7408.8(13)	20.0(4)
C8	10147.7(16)	4638(2)	7008.3(14)	24.3(4)
C9	11045.2(18)	4039(3)	6951.4(16)	31.0(5)
C10	11928.8(17)	4783(3)	7282.1(16)	33.1(6)
C11	11922.6(17)	6134(3)	7679.5(16)	32.8(5)
C12	11028.9(16)	6735(3)	7751.1(15)	26.5(5)
C13	9170.9(15)	8265(2)	7658.2(14)	20.9(4)
C14	9496.8(19)	9215(3)	7114.2(15)	28.2(5)
C15	9530(2)	10724(3)	7250.0(17)	33.6(5)
C16	9231(2)	11323(3)	7928.8(18)	34.7(5)
C17	8886(2)	10400(3)	8454.6(18)	35.5(6)
C18	8851.6(19)	8877(3)	8320.4(16)	28.2(5)
C19	8789.8(16)	5673(2)	8129.2(14)	21.4(4)

C20	9399.4(18)	5579(3)	8961.9(15)	29.1(5)
C21	9129(2)	4697(3)	9559.4(18)	38.7(6)
C22	8243(2)	3908(3)	9339(2)	41.0(7)
C23	7637(2)	3994(3)	8520(2)	38.2(6)
C24	7908.8(18)	4861(3)	7912.8(17)	28.9(5)
O5	2669.4(14)	6182(2)	4666.5(11)	34.7(4)
O6	3818.9(15)	7934(2)	5053.2(14)	45.4(5)
O7	4863.2(14)	5285(2)	4174.1(12)	37.2(4)
O8	4358.1(12)	3700.2(18)	2588.4(10)	26.3(3)
C25	2492(2)	6278(4)	5496.6(18)	44.8(7)
C26	3357.1(18)	7083(3)	4528.6(17)	29.2(5)
C27	3478(2)	6874(3)	3640.3(17)	33.6(5)
C28	3933.6(15)	5377(2)	3545.4(14)	22.8(4)
C29	4057.4(18)	5186(3)	2656.3(15)	27.5(5)
C30	4665.9(17)	3310(2)	1840.0(13)	23.1(4)
C31	5659.4(17)	4064(2)	1852.8(15)	24.1(4)
C32	6343.1(18)	4382(3)	2627.8(15)	28.7(5)
C33	7269.8(19)	4977(3)	2651.6(18)	36.8(6)
C34	7529.9(19)	5261(3)	1907.2(19)	38.8(6)
C35	6866(2)	4917(3)	1131.7(18)	37.5(6)
C36	5941.2(19)	4315(3)	1105.2(16)	31.4(5)
C37	3818.1(16)	3664(3)	1035.8(14)	23.9(4)
C38	3730.5(19)	5066(3)	663.3(15)	29.6(5)
C39	2933(2)	5387(3)	-42.5(16)	35.6(6)
C40	2220.1(19)	4339(3)	-374.9(16)	34.9(6)
C41	2290.6(18)	2960(3)	1.1(15)	32.3(5)
C42	3084.7(17)	2622(3)	703.8(15)	27.3(5)
C43	4895.7(16)	1643(3)	1940.4(15)	25.8(4)
C44	5124.8(19)	862(3)	1279.2(16)	32.7(5)
C45	5407(2)	-617(3)	1379.6(19)	37.5(6)
C46	5468.9(18)	-1326(3)	2143(2)	38.9(6)
C47	5245.9(19)	-555(3)	2803.9(19)	37.5(6)
C48	4958.9(17)	922(3)	2707.3(16)	30.6(5)
O1	8952.2(15)	7371(3)	4977.4(13)	45.4(5)
O2	8511.9(17)	4984(3)	4857.1(15)	55.8(6)
O3	5951.2(14)	7146(3)	5486.1(14)	47.4(5)
O4	8468.6(11)	6351.1(17)	6627.4(9)	22.4(3)

Table 3 Anisotropic Displacement Parameters ($Å^2×10^3$) for 18dbv_mzz_527_xtal2_0s. The Anisotropic displacement factor exponent takes the form: $-2\pi^2[h^2a^{*2}U_{11}+2hka^*b^*U_{12}+\ldots]$.

Atom	U_{11}	U_{22}	U_{33}	U_{23}	U_{13}	U_{12}
C1	37.8(14)	81(3)	48.9(17)	22.2(17)	18.3(13)	1.4(16)
C2	35.1(13)	60.1(18)	21.4(11)	-3.6(12)	5.1(9)	2.9(13)

C3	32.3(13)	65(2)	32.4(13)	2.5(13)	2.2(11)	5.9(13)
C4	21.7(10)	31.7(13)	33.7(12)	-6.0(10)	0.7(9)	2.7(9)
C5	21.7(10)	24.5(11)	34.7(12)	-5.9(10)	2.1(9)	6.4(9)
C6	19.1(9)	15.9(9)	22.4(9)	-0.9(7)	6.1(7)	-0.2(7)
C7	18.4(9)	20.5(10)	22.1(9)	5.0(8)	7.1(7)	1.5(7)
C8	22.1(10)	22.3(10)	29.2(11)	0.7(9)	8.4(8)	2.2(8)
C9	31.6(12)	31.5(12)	32.2(12)	1.1(10)	12.6(10)	10.6(10)
C10	22.3(10)	48.4(16)	32.2(12)	11.6(11)	13.7(9)	11.8(10)
C11	18.7(10)	42.3(14)	35.7(12)	9.5(11)	4.4(9)	-2.6(10)
C12	23.2(10)	26.6(11)	28.6(11)	1.3(9)	5.1(9)	-1.4(9)
C13	19.5(9)	17.5(10)	24.8(10)	-0.7(8)	4.7(8)	0.1(7)
C14	35.7(12)	23.2(11)	28.2(11)	1.7(9)	12.9(10)	1.4(9)
C15	43.7(14)	20.2(11)	40.0(13)	3.9(10)	16.5(11)	-1.6(10)
C16	42.7(14)	16.4(10)	46.2(14)	-3.4(10)	13.8(11)	1.6(10)
C17	46.2(15)	25.5(12)	39.8(13)	-7.8(10)	20.1(11)	2.8(11)
C18	33.8(12)	22.0(11)	32.3(12)	-0.7(9)	15.1(10)	0.7(9)
C19	23.0(10)	14.9(9)	29.8(10)	0.0(8)	12.9(8)	3.0(8)
C20	29.5(11)	27.8(12)	31.3(12)	4.6(9)	10.6(9)	1.7(9)
C21	52.7(16)	34.5(14)	32.3(13)	8.9(11)	17.6(12)	7.5(12)
C22	60.4(18)	24.5(12)	51.9(16)	5.9(11)	38.7(15)	1.1(12)
C23	41.8(14)	23.4(12)	59.7(17)	-5.6(11)	31.4(13)	-7.6(11)
C24	29.5(11)	21.7(11)	39.2(13)	-5.5(9)	15.8(10)	-2.2(9)
O5	36.6(9)	39.3(10)	32.1(9)	-5.0(8)	15.9(7)	-7.0(8)
O6	37.9(10)	39.8(11)	58.5(13)	-14.3(10)	12.9(9)	-4.2(9)
O7	34.5(9)	37.1(10)	32.8(9)	-6.1(8)	-3.2(7)	11.1(8)
O8	33.4(8)	25.4(8)	23.3(7)	2.3(6)	13.0(6)	-1.8(7)
C25	45.9(16)	59.0(19)	36.0(14)	2.5(13)	22.1(12)	7.7(14)
C26	25.4(11)	23.9(11)	39.1(13)	0.4(10)	10.2(10)	4.7(9)
C27	36.3(13)	32.6(13)	36.9(13)	8.7(10)	18.7(11)	5.8(10)
C28	21.6(10)	22.5(10)	24.9(10)	1.3(8)	7.1(8)	-3.9(8)
C29	30.3(11)	26.6(11)	27.8(11)	4.5(9)	11.7(9)	2.8(9)
C30	25.9(10)	23.9(11)	20.9(10)	1.2(8)	8.9(8)	-2.8(8)
C31	24.9(10)	21.4(11)	27.7(11)	2.3(8)	9.8(9)	0.3(8)
C32	29.2(11)	29.1(12)	28.4(11)	-1.6(9)	8.6(9)	0.4(9)
C33	28.6(12)	40.1(14)	39.2(13)	-7.9(12)	4.7(10)	-2.7(11)
C34	27.6(12)	37.0(14)	54.8(16)	0.7(12)	16.6(11)	-4.9(11)
C35	35.7(13)	41.0(14)	41.1(14)	10.0(12)	19.4(11)	-1.5(11)
C36	31.7(12)	36.1(13)	27.6(11)	6.1(10)	10.3(9)	-1.8(10)
C37	24.4(10)	29.3(11)	20.4(10)	1.4(8)	10.1(8)	2.4(9)
C38	33.8(12)	28.3(12)	29.1(11)	4.1(9)	12.9(10)	1.3(10)
C39	39.8(13)	38.5(14)	32.2(12)	11.0(11)	15.9(11)	12.3(11)
C40	28.4(12)	50.9(16)	27.1(12)	6.3(11)	10.3(10)	11.3(11)
C41	25.7(11)	44.7(15)	28.2(11)	-3.0(11)	10.1(9)	0.2(10)
C42	27.5(11)	31.1(12)	26.1(11)	2.2(9)	12.0(9)	0.8(9)
C43	21.6(10)	24.2(11)	30.7(11)	2.0(9)	5.4(8)	-3.6(8)

C44	33.7(12)	30.6(13)	34.1(12)	0.2(10)	9.4(10)	2.2(10)
C45	31.1(12)	29.7(13)	50.6(16)	-6.2(12)	8.9(11)	0.0(10)
C46	22.4(11)	24.5(12)	66.7(19)	3.9(12)	6.6(11)	-2.6(9)
C47	25.8(11)	34.6(13)	50.0(15)	17.5(12)	6.8(11)	-1.6(10)
C48	24.2(11)	33.6(13)	33.0(12)	6.3(10)	6.2(9)	-3.6(9)
O1	37.2(10)	58.3(13)	43.4(11)	16.3(10)	15.8(9)	2.7(10)
O2	46.3(12)	60.7(15)	57.8(14)	-26.3(12)	9.8(10)	2.7(11)
O3	25.7(9)	61.7(14)	49.4(12)	-19.8(11)	1.0(8)	6.5(9)
O4	19.0(7)	21.2(7)	24.6(7)	-3.3(6)	1.7(6)	5.5(6)

Table 4 Bond Lengths for 18dbv_mzz_527_xtal2_0s.

Atom	Atom	Length/Å	Atom	Atom	Length/Å
C1	O1	1.437(4)	O5	C25	1.439(3)
C2	C3	1.504(4)	O5	C26	1.323(3)
C2	O1	1.338(4)	O6	C26	1.199(3)
C2	O2	1.198(4)	O7	C28	1.419(3)
C3	C4	1.537(4)	O8	C29	1.421(3)
C4	C5	1.510(3)	O8	C30	1.440(3)
C4	O3	1.404(3)	C26	C27	1.511(4)
C5	O4	1.434(3)	C27	C28	1.521(3)
C6	C7	1.535(3)	C28	C29	1.512(3)
C6	C13	1.529(3)	C30	C31	1.538(3)
C6	C19	1.537(3)	C30	C37	1.540(3)
C6	O4	1.442(2)	C30	C43	1.542(3)
C7	C8	1.397(3)	C31	C32	1.389(3)
C7	C12	1.390(3)	C31	C36	1.394(3)
C8	C9	1.389(3)	C32	C33	1.390(4)
C9	C10	1.378(4)	C33	C34	1.379(4)
C10	C11	1.384(4)	C34	C35	1.383(4)
C11	C12	1.392(3)	C35	C36	1.388(4)
C13	C14	1.395(3)	C37	C38	1.397(3)
C13	C18	1.387(3)	C37	C42	1.387(3)
C14	C15	1.382(3)	C38	C39	1.395(4)
C15	C16	1.391(4)	C39	C40	1.374(4)
C16	C17	1.372(4)	C40	C41	1.381(4)
C17	C18	1.394(3)	C41	C42	1.392(3)
C19	C20	1.393(3)	C43	C44	1.394(3)
C19	C24	1.391(3)	C43	C48	1.389(3)
C20	C21	1.386(3)	C44	C45	1.391(4)
C21	C22	1.387(4)	C45	C46	1.379(4)
C22	C23	1.373(4)	C46	C47	1.386(4)
C23	C24	1.392(4)	C47	C48	1.391(4)

Table 5 Bond Angles for 18dbv_mzz_527_xtal2_0s.

Atom	Atom	Atom	Angle/°	Atom	Atom	Atom	Angle/°
O1	C2	C3	111.0(3)	O5	C26	C27	111.0(2)
O2	C2	C3	125.2(3)	O6	C26	O5	123.3(2)
O2	C2	O1	123.9(3)	O6	C26	C27	125.7(2)
C2	C3	C4	113.0(2)	C26	C27	C28	111.5(2)
C5	C4	C3	112.4(2)	O7	C28	C27	107.66(19)
O3	C4	C3	108.7(2)	O7	C28	C29	111.36(18)
O3	C4	C5	106.75(19)	C29	C28	C27	110.93(19)
O4	C5	C4	106.88(18)	O8	C29	C28	107.12(18)
C7	C6	C19	107.66(16)	O8	C30	C31	110.69(17)
C13	C6	C7	111.96(17)	O8	C30	C37	109.36(17)
C13	C6	C19	113.68(17)	O8	C30	C43	104.53(17)
O4	C6	C7	103.86(16)	C31	C30	C37	113.59(17)
O4	C6	C13	109.33(16)	C31	C30	C43	105.77(18)
O4	C6	C19	109.88(17)	C37	C30	C43	112.50(18)
C8	C7	C6	118.26(19)	C32	C31	C30	119.9(2)
C12	C7	C6	122.83(19)	C32	C31	C36	118.2(2)
C12	C7	C8	118.9(2)	C36	C31	C30	121.7(2)
C9	C8	C7	120.2(2)	C31	C32	C33	120.6(2)
C10	C9	C8	120.6(2)	C34	C33	C32	120.7(2)
C9	C10	C11	119.7(2)	C33	C34	C35	119.2(2)
C10	C11	C12	120.2(2)	C34	C35	C36	120.2(2)
C7	C12	C11	120.4(2)	C35	C36	C31	121.0(2)
C14	C13	C6	118.60(19)	C38	C37	C30	120.9(2)
C18	C13	C6	122.96(19)	C42	C37	C30	120.3(2)
C18	C13	C14	118.3(2)	C42	C37	C38	118.6(2)
C15	C14	C13	120.7(2)	C39	C38	C37	120.2(2)
C14	C15	C16	120.5(2)	C40	C39	C38	120.7(2)
C17	C16	C15	119.2(2)	C39	C40	C41	119.5(2)
C16	C17	C18	120.5(2)	C40	C41	C42	120.5(2)
C13	C18	C17	120.8(2)	C37	C42	C41	120.5(2)
C20	C19	C6	119.57(19)	C44	C43	C30	119.9(2)
C24	C19	C6	121.8(2)	C48	C43	C30	121.0(2)
C24	C19	C20	118.5(2)	C48	C43	C44	118.9(2)
C21	C20	C19	120.5(2)	C45	C44	C43	120.9(2)
C20	C21	C22	120.5(3)	C46	C45	C44	120.0(3)
C23	C22	C21	119.4(2)	C45	C46	C47	119.5(2)
C22	C23	C24	120.5(2)	C46	C47	C48	120.9(3)
C19	C24	C23	120.6(2)	C43	C48	C47	119.9(3)
C26	O5	C25	116.0(2)	C2	O1	C1	115.7(3)
C29	O8	C30	117.32(17)	C5	O4	C6	116.17(16)

Table 6 Torsion Angles for 18dbv_mzz_527_xtal2_0s.

A	B	C	D	Angle/°	A	B	C	D	Angle/°
C2	C3	C4	C5	59.7(3)	C25	O5	C26	C27	179.7(2)
C2	C3	C4	O3	177.7(2)	C26	C27	C28	O7	-57.5(3)
C3	C2	O1	C1	177.8(2)	C26	C27	C28	C29	-179.6(2)
C3	C4	C5	O4	-72.8(3)	C27	C28	C29	O8	−172.38(19)
C4	C5	O4	C6	−167.21(18)	C29	O8	C30	C31	68.9(2)
C6	C7	C8	C9	-179.1(2)	C29	O8	C30	C37	-57.0(2)
C6	C7	C12	C11	180.0(2)	C29	O8	C30	C43	−177.63(18)
C6	C13	C14	C15	178.6(2)	C30	O8	C29	C28	−171.05(17)
C6	C13	C18	C17	-178.4(2)	C30	C31	C32	C33	175.9(2)
C6	C19	C20	C21	-177.5(2)	C30	C31	C36	C35	-176.2(2)
C6	C19	C24	C23	178.3(2)	C30	C37	C38	C39	-177.2(2)
C7	C6	C13	C14	55.7(3)	C30	C37	C42	C41	176.9(2)
C7	C6	C13	C18	-128.0(2)	C30	C43	C44	C45	175.1(2)
C7	C6	C19	C20	58.1(3)	C30	C43	C48	C47	-174.8(2)
C7	C6	C19	C24	-119.3(2)	C31	C30	C37	C38	-36.8(3)
C7	C6	O4	C5	−161.08(18)	C31	C30	C37	C42	147.8(2)
C7	C8	C9	C10	-0.5(4)	C31	C30	C43	C44	-69.4(3)
C8	C7	C12	C11	1.3(3)	C31	C30	C43	C48	105.3(2)
C8	C9	C10	C11	0.4(4)	C31	C32	C33	C34	0.0(4)
C9	C10	C11	C12	0.5(4)	C32	C31	C36	C35	-2.3(4)
C10	C11	C12	C7	-1.4(4)	C32	C33	C34	C35	-1.5(4)
C12	C7	C8	C9	-0.4(3)	C33	C34	C35	C36	1.1(4)
C13	C6	C7	C8	−162.19(19)	C34	C35	C36	C31	0.8(4)
C13	C6	C7	C12	19.1(3)	C36	C31	C32	C33	1.9(4)
C13	C6	C19	C20	-66.6(3)	C37	C30	C31	C32	153.0(2)
C13	C6	C19	C24	116.1(2)	C37	C30	C31	C36	-33.2(3)
C13	C6	O4	C5	-41.4(2)	C37	C30	C43	C44	55.2(3)
C13	C14	C15	C16	-0.5(4)	C37	C30	C43	C48	-130.1(2)
C14	C13	C18	C17	-2.0(4)	C37	C38	C39	C40	0.7(4)
C14	C15	C16	C17	-1.1(4)	C38	C37	C42	C41	1.5(3)
C15	C16	C17	C18	1.1(4)	C38	C39	C40	C41	0.7(4)
C16	C17	C18	C13	0.4(4)	C39	C40	C41	C42	-1.0(4)
C18	C13	C14	C15	2.1(4)	C40	C41	C42	C37	-0.1(4)
C19	C6	C7	C8	72.2(2)	C42	C37	C38	C39	-1.7(3)
C19	C6	C7	C12	-106.5(2)	C43	C30	C31	C32	-83.1(2)
C19	C6	C13	C14	177.97(19)	C43	C30	C31	C36	90.7(2)
C19	C6	C13	C18	-5.7(3)	C43	C30	C37	C38	-156.9(2)
C19	C6	O4	C5	84.0(2)	C43	C30	C37	C42	27.7(3)
C19	C20	C21	C22	-0.7(4)	C43	C44	C45	C46	-0.3(4)

C20 C19 C24 C23	1.0(3)	C44 C43 C48 C47	-0.1(3)
C20 C21 C22 C23	0.7(4)	C44 C45 C46 C47	0.1(4)
C21 C22 C23 C24	0.1(4)	C45 C46 C47 C48	0.2(4)
C22 C23 C24 C19	-1.0(4)	C46 C47 C48 C43	-0.2(4)
C24 C19 C20 C21	-0.1(3)	C48 C43 C44 C45	0.3(4)
O5 C26 C27 C28	-68.3(3)	O1 C2 C3 C4	-109.0(3)
O6 C26 C27 C28	111.1(3)	O2 C2 C3 C4	72.2(4)
O7 C28 C29 O8	67.7(2)	O2 C2 O1 C1	-3.4(4)
O8 C30 C31 C32	29.6(3)	O3 C4 C5 O4	168.1(2)
O8 C30 C31 C36	-156.7(2)	O4 C6 C7 C8	-44.3(2)
O8 C30 C37 C38	87.4(2)	O4 C6 C7 C12	137.0(2)
O8 C30 C37 C42	-88.0(2)	O4 C6 C13 C14	-58.8(2)
O8 C30 C43 C44	173.7(2)	O4 C6 C13 C18	117.5(2)
O8 C30 C43 C48	-11.6(3)	O4 C6 C19 C20	170.54(19)
C25 O5 C26 O6	0.3(4)	O4 C6 C19 C24	-6.8(3)

Table 7 Hydrogen Atom Coordinates (Å×10^4) and Isotropic Displacement Parameters (Å^2×10^3) for 18dbv_mzz_527_xtal2_0s.

Atom	*x*	*y*	*z*	U(eq)
H1A	10391.29	7826.06	5149.13	82
H1B	10194.95	6329.63	5602.87	82
H1C	10027.11	6373.5	4589.89	82
H3A	6795.05	6382.62	4304.8	54
H3B	7256.02	7919.89	4714.78	54
H4	6861.91	5425.73	5683.19	36
H5A	7712.98	8244.84	6297.52	34
H5B	7237.65	7174.49	6872.18	34
H8	9542.22	4120.11	6774.19	29
H9	11049.94	3108.28	6682.2	37
H10	12539.47	4369.79	7237.33	40
H11	12529.9	6653.21	7904.15	39
H12	11031.33	7652.73	8035.78	32
H14	9697.73	8820.21	6645.41	34
H15	9759.2	11357.56	6877.06	40
H16	9265.75	12359.59	8027.23	42
H17	8668.95	10801.81	8913.36	43
H18	8606.66	8250.27	8686.7	34
H20	10004.69	6122.77	9121.5	35
H21	9554.25	4632.21	10123.95	46
H22	8056.17	3313	9752.38	49
H23	7028.78	3457.03	8366.34	46
H24	7488.73	4900.05	7345.43	35
H25A	1972.74	5569.61	5532.36	67

H25B	3108.43	6049.11	5937.01	67
H25C	2273.82	7281.21	5585.66	67
H27A	3911.47	7665.48	3519.42	40
H27B	2819.03	6956.08	3217.63	40
H28	3484.14	4581.28	3653.04	27
H29A	3419.92	5389.5	2223.01	33
H29B	4568.6	5878.31	2563.63	33
H32	6175.7	4191.98	3146.65	34
H33	7729.3	5189.25	3186.77	44
H34	8158.34	5689.05	1926.85	47
H35	7042.31	5092.37	615.48	45
H36	5493.96	4070.02	569.29	38
H38	4215.28	5802.91	891.34	35
H39	2882.86	6340.13	-295.96	43
H40	1682.8	4560.95	-859.69	42
H41	1793.65	2237.09	-221.17	39
H42	3124.61	1670.83	958.07	33
H44	5087.38	1345.35	752.94	39
H45	5558.05	-1137.19	922.6	45
H46	5662.5	-2335.18	2214.46	47
H47	5289.64	-1041.91	3330.44	45
H48	4806.37	1436.38	3165.36	37
H3	5490(20)	6590(40)	5040(20)	63(11)
H7	5020(30)	4240(30)	4280(30)	73(13)

Experimental

Single crystals of $C_{24}H_{24}O_4$ **[18dbv_mzz_527_xtal2_0s]** were **[]**. A suitable crystal was selected and **[]** on a **'Bruker APEX-II CCD'** diffractometer. The crystal was kept at 173.15 K during data collection. Using Olex2 [1], the structure was solved with the ShelXT [2] structure solution program using Intrinsic Phasing and refined with the ShelXL [3] refinement package using Least Squares minimisation.

1. Dolomanov, O.V., Bourhis, L.J., Gildea, R.J, Howard, J.A.K. & Puschmann, H. (2009), J. Appl. Cryst. 42, 339-341.
2. Sheldrick, G.M. (2015). Acta Cryst. A71, 3-8.
3. Sheldrick, G.M. (2015). Acta Cryst. C71, 3-8.

Crystal structure determination of [18dbv_mzz_527_xtal2_0s]

Crystal Data for $C_{24}H_{24}O_4$ (M =376.43 g/mol): monoclinic, space group $P2_1$ (no. 4), a = 13.9337(11) Å, b = 9.0460(7) Å, c = 16.2618(13) Å, β = 105.718(2)°, V = 1973.1(3) Å^3, Z = 4, T = 173.15 K, μ(MoKα) = 0.085 mm^{-1}, *Dcalc* = 1.267 g/cm^3, 44143 reflections measured (6.074° ≤ 2Θ ≤ 56.782°), 9805 unique (R_{int} = 0.0328, R_{sigma} = 0.0238) which were used in all calculations. The final R_1 was 0.0437 (I > 2σ(I)) and wR_2 was 0.1087 (all data).

Refinement model description

Number of restraints - 2, number of constraints - unknown.

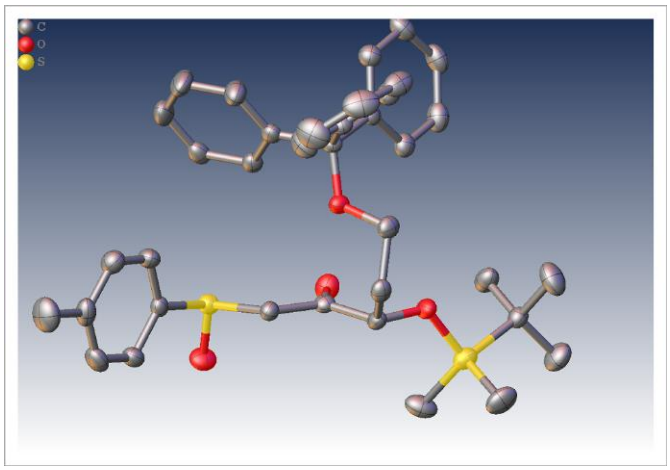
Details:

```
1. Fixed Uiso
 At 1.2 times of:
  All C(H) groups, All C(H,H) groups
 At 1.5 times of:
  All C(H,H,H) groups
2. Restrained distances
 O7-H7 ≈ O3-H3
 with sigma of 0.001
```

```
3.a Ternary CH refined with riding coordinates:
 C4(H4), C28(H28)
3.b Secondary CH2 refined with riding coordinates:
 C3(H3A,H3B), C5(H5A,H5B), C27(H27A,H27B), C29(H29A,H29B)
3.c Me refined with riding coordinates:
 C1(H1A,H1B,H1C), C25(H25A,H25B,H25C)
3.d Aromatic/amide H refined with riding coordinates:
 C8(H8), C9(H9), C10(H10), C11(H11), C12(H12), C14(H14), C15(H15), C16(H16),
 C17(H17), C18(H18), C20(H20), C21(H21), C22(H22), C23(H23), C24(H24), C32(H32),
  C33(H33), C34(H34), C35(H35), C36(H36), C38(H38), C39(H39), C40(H40),
 C41(H41), C42(H42), C44(H44), C45(H45), C46(H46), C47(H47), C48(H48)
```

This report has been created with Olex2, compiled on 2018.05.29 svn.r3508 for OlexSys. Please let us know if there are any errors or if you would like to have additional features.

Crystal structure for compound 144



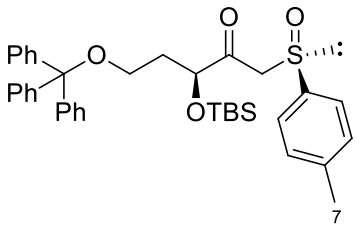


Table 1 Crystal data and structure refinement for 19m_mb1_MZZ534B_0s.

Identification code	19m_mb1_MZZ534B_0s
Empirical formula	$C_{37}H_{44}O_4S_2$
Formula weight	616.84
Temperature/K	173.15
Crystal system	monoclinic
Space group	$P2_1$
a/Å	14.4049(4)
b/Å	7.5907(2)
c/Å	16.9364(5)
α/°	90
β/°	112.0590(10)
γ/°	90
Volume/Å^3	1716.32(8)
Z	2
ρ_{calc}g/cm^3	1.194
μ/mm^{-1}	0.192
F(000)	660.0
Crystal size/mm^3	0.407 × 0.391 × 0.208
Radiation	MoKα (λ = 0.71073)

2Θ range for data collection/°	2.594 to 56.816
Index ranges	$-19 \leq h \leq 19$, $-10 \leq k \leq 10$, $-22 \leq l \leq 21$
Reflections collected	24077
Independent reflections	8570 [R_{int} = 0.0519, R_{sigma} = 0.0615]
Data/restraints/parameters	8570/1/395
Goodness-of-fit on F^2	1.011
Final R indexes [I>=2σ (I)]	R_1 = 0.0473, wR_2 = 0.1088
Final R indexes [all data]	R_1 = 0.0679, wR_2 = 0.1200
Largest diff. peak/hole / e $Å^{-3}$	0.35/-0.51
Flack parameter	0.15(8)

Table 2 Fractional Atomic Coordinates (×10^4) and Equivalent Isotropic Displacement Parameters ($Å^2$×10^3) for 19m_mb1_MZZ534B_0s. U_{eq} is defined as 1/3 of of the trace of the orthogonalised U_{IJ} tensor.

Atom	*x*	*y*	*z*	U(eq)
C1	8762(2)	5268(4)	5751.6(18)	24.8(6)
C2	9397(2)	6358(5)	6374.6(19)	31.5(7)
C3	9079(3)	7080(5)	6969(2)	38.8(8)
C4	8126(3)	6758(5)	6959(2)	37.3(8)
C5	7503(3)	5668(5)	6329(2)	36.2(8)
C6	7812(2)	4899(5)	5729(2)	32.3(7)
C7	7765(3)	7579(7)	7609(2)	56.1(11)
C8	8531(2)	6049(4)	4185.9(18)	24.2(6)
C9	8559(2)	5695(4)	3323.2(19)	24.8(6)
C10	8212(2)	7227(4)	2698.6(18)	26.2(6)
C11	7176(2)	7930(4)	2592(2)	28.3(7)
C12	6323(2)	6650(4)	2193(2)	30.1(7)
C13	10348(3)	7022(5)	2306(2)	43.8(9)
C14	8877(3)	9793(5)	1280(3)	46.7(9)
C15	8769(2)	6095(4)	523.3(19)	27.2(7)
C16	8856(3)	4122(5)	738(2)	39.8(8)
C17	7691(3)	6480(7)	-87(2)	51.3(11)
C18	9490(3)	6541(6)	91(2)	47.0(10)
C19	5705(2)	3888(4)	2579.0(18)	23.3(6)
C20	5633(2)	2676(4)	1827.7(18)	25.2(6)
C21	6322(2)	2777(5)	1437.8(19)	30.3(7)
C22	6251(3)	1623(5)	775(2)	38.8(8)
C23	5519(3)	343(5)	522(2)	38.6(9)
C24	4850(3)	215(5)	925(2)	37.3(8)
C25	4913(2)	1372(5)	1571(2)	30.5(7)
C26	6037(2)	2685(4)	3371.3(18)	26.6(7)
C27	7011(2)	2082(4)	3701.9(18)	26.2(6)
C28	7332(3)	924(5)	4387(2)	32.9(7)
C29	6666(3)	346(5)	4743(2)	44.1(10)
C30	5697(3)	917(6)	4419(2)	51.6(11)

C31	5374(3)	2086(6)	3735(2)	42.1(9)
C32	4746(2)	4921(5)	2448.3(19)	28.2(7)
C33	3964(2)	5095(5)	1662(2)	31.3(7)
C34	3176(3)	6238(5)	1566(3)	41.6(9)
C35	3150(3)	7199(6)	2244(3)	52.0(11)
C36	3914(3)	7022(6)	3032(3)	54.1(11)
C37	4702(3)	5909(6)	3127(2)	42.5(9)
O1	10262.5(16)	4764(3)	5241.5(14)	35.2(6)
O2	8855.3(17)	4324(3)	3139.1(14)	34.6(5)
O3	8211.0(16)	6732(3)	1897.6(13)	30.3(5)
O4	6505.2(15)	5154(3)	2753.5(12)	25.3(4)
S1	9173.6(5)	4373.5(10)	4955.2(4)	25.30(17)
S2	9059.0(6)	7408.8(11)	1526.7(5)	31.8(2)

Table 3 Anisotropic Displacement Parameters ($Å^2×10^3$) for 19m_mb1_MZZ534B_0s. The Anisotropic displacement factor exponent takes the form: $-2\pi^2[h^2a^{*2}U_{11}+2hka^*b^*U_{12}+\ldots]$.

Atom	U_{11}	U_{22}	U_{33}	U_{23}	U_{13}	U_{12}
C1	29.6(16)	21.9(15)	21.2(14)	2.5(12)	7.4(12)	-0.1(13)
C2	31.9(17)	30.3(18)	28.2(16)	-2.2(14)	6.4(14)	-6.4(14)
C3	47(2)	35(2)	27.7(16)	-8.0(15)	5.8(15)	-4.0(16)
C4	56(2)	30.6(18)	26.7(16)	1.7(14)	17.0(16)	3.8(17)
C5	39.4(19)	35(2)	37.7(18)	-0.3(15)	18.3(15)	-3.0(15)
C6	31.8(17)	34.2(19)	29.2(16)	-3.7(14)	9.6(13)	-9.4(14)
C7	72(3)	60(3)	43(2)	-9(2)	28(2)	10(2)
C8	23.5(14)	24.9(15)	23.7(14)	2.4(12)	8.3(12)	-0.8(13)
C9	19.0(14)	27.2(17)	28.7(15)	0.1(13)	9.5(12)	-1.8(12)
C10	30.1(15)	26.9(16)	24.0(14)	-1.7(13)	12.9(12)	-6.6(13)
C11	37.3(18)	19.7(16)	27.7(15)	2.1(12)	12.0(14)	2.9(13)
C12	26.8(16)	28.4(17)	32.4(16)	8.6(14)	8.1(13)	4.4(13)
C13	27.3(17)	41(2)	55(2)	-10.6(18)	5.8(16)	0.6(15)
C14	54(2)	26(2)	68(2)	9.2(18)	31(2)	3.4(16)
C15	27.0(16)	28.8(17)	27.9(15)	2.8(13)	12.8(13)	0.2(13)
C16	57(2)	31(2)	37.5(18)	-5.0(15)	24.9(17)	-8.8(17)
C17	43(2)	70(3)	33.4(19)	-1.4(19)	5.2(17)	14(2)
C18	54(2)	50(3)	51(2)	1.7(19)	35(2)	-3(2)
C19	20.4(14)	23.5(16)	25.5(14)	-0.6(12)	8.1(12)	0.2(11)
C20	23.3(14)	27.5(17)	22.0(14)	0.9(12)	5.4(11)	4.2(13)
C21	29.0(16)	32.5(19)	28.9(16)	4.2(13)	10.4(13)	5.3(14)
C22	42(2)	46(2)	31.4(17)	4.4(16)	17.4(15)	12.4(17)
C23	43(2)	43(2)	26.7(16)	-6.6(15)	8.9(15)	10.2(17)
C24	34.4(18)	36.9(19)	33.1(17)	-8.8(15)	4.2(14)	3.0(16)
C25	27.6(16)	30.7(18)	32.9(16)	-0.6(14)	11.1(14)	1.6(14)
C26	30.7(16)	24.0(17)	23.3(14)	-4.0(12)	8.1(12)	-4.6(13)

C27	32.6(16)	19.5(16)	25.3(14)	-2.7(12)	9.5(12)	-3.1(12)
C28	37.3(18)	24.8(17)	28.6(15)	-2.0(13)	3.2(14)	-1.0(14)
C29	55(2)	40(2)	29.8(17)	10.0(16)	7.7(16)	-6.6(18)
C30	45(2)	68(3)	43(2)	19(2)	19.2(18)	-9(2)
C31	34.0(19)	58(3)	34.1(17)	9.8(18)	12.4(15)	-3.3(18)
C32	23.7(15)	30.0(17)	32.4(16)	-0.1(13)	12.2(13)	1.3(13)
C33	26.7(16)	33.4(18)	34.0(17)	4.0(14)	11.6(14)	4.0(14)
C34	26.9(17)	38(2)	59(2)	13.1(18)	14.8(17)	8.0(15)
C35	33(2)	43(2)	85(3)	0(2)	28(2)	10.5(18)
C36	52(2)	52(3)	62(2)	-18(2)	26(2)	8(2)
C37	40(2)	49(2)	38.2(19)	-9.4(17)	14.8(16)	5.1(18)
O1	20.9(11)	38.0(15)	43.1(13)	2.4(11)	7.8(9)	4.4(10)
O2	39.9(13)	31.8(13)	37.7(12)	0.6(11)	20.9(10)	7.6(12)
O3	31.4(12)	37.9(13)	25.0(10)	-3.3(10)	14.5(9)	-9.1(10)
O4	23.2(10)	22.5(11)	27.4(10)	3.6(9)	6.3(8)	-0.3(9)
S1	23.8(4)	23.3(4)	26.7(3)	0.7(3)	7.0(3)	1.2(3)
S2	30.9(4)	27.7(4)	38.9(4)	3.1(4)	15.6(3)	0.0(3)

Table 4 Bond Lengths for 19m_mb1_MZZ534B_0s.

Atom	Atom	Length/Å	Atom	Atom	Length/Å
C1	C2	1.382(4)	C19	C26	1.543(4)
C1	C6	1.384(4)	C19	C32	1.532(4)
C1	S1	1.798(3)	C19	O4	1.443(4)
C2	C3	1.367(5)	C20	C21	1.385(4)
C3	C4	1.388(5)	C20	C25	1.381(4)
C4	C5	1.382(5)	C21	C22	1.397(5)
C4	C7	1.518(5)	C22	C23	1.378(6)
C5	C6	1.381(5)	C23	C24	1.378(5)
C8	C9	1.501(4)	C24	C25	1.378(5)
C8	S1	1.807(3)	C26	C27	1.379(4)
C9	C10	1.524(4)	C26	C31	1.393(5)
C9	O2	1.209(4)	C27	C28	1.390(4)
C10	C11	1.531(4)	C28	C29	1.382(5)
C10	O3	1.407(3)	C29	C30	1.364(6)
C11	C12	1.512(5)	C30	C31	1.394(5)
C12	O4	1.439(4)	C32	C33	1.390(4)
C13	S2	1.854(3)	C32	C37	1.394(5)
C14	S2	1.854(4)	C33	C34	1.388(5)
C15	C16	1.535(5)	C34	C35	1.374(6)
C15	C17	1.537(5)	C35	C36	1.381(6)
C15	C18	1.517(4)	C36	C37	1.376(6)
C15	S2	1.877(3)	O1	S1	1.487(2)
C19	C20	1.541(4)	O3	S2	1.651(2)

Table 5 Bond Angles for 19m_mb1_MZZ534B_0s.

Atom	Atom	Atom	Angle/°	Atom	Atom	Atom	Angle/°
C2	C1	C6	120.4(3)	C25	C20	C21	118.5(3)
C2	C1	S1	119.3(2)	C20	C21	C22	119.9(3)
C6	C1	S1	120.3(2)	C23	C22	C21	120.6(3)
C3	C2	C1	119.6(3)	C22	C23	C24	119.4(3)
C2	C3	C4	121.5(3)	C25	C24	C23	119.9(3)
C3	C4	C7	121.7(3)	C24	C25	C20	121.6(3)
C5	C4	C3	117.9(3)	C27	C26	C19	119.0(3)
C5	C4	C7	120.4(4)	C27	C26	C31	118.3(3)
C6	C5	C4	121.7(3)	C31	C26	C19	122.5(3)
C5	C6	C1	118.8(3)	C26	C27	C28	121.2(3)
C9	C8	S1	112.5(2)	C29	C28	C27	119.8(3)
C8	C9	C10	114.7(3)	C30	C29	C28	119.8(3)
O2	C9	C8	123.1(3)	C29	C30	C31	120.6(4)
O2	C9	C10	122.2(3)	C26	C31	C30	120.3(3)
C9	C10	C11	113.5(2)	C33	C32	C19	123.3(3)
O3	C10	C9	110.3(3)	C33	C32	C37	117.9(3)
O3	C10	C11	109.3(2)	C37	C32	C19	118.3(3)
C12	C11	C10	114.9(3)	C34	C33	C32	120.3(3)
O4	C12	C11	107.3(2)	C35	C34	C33	120.8(3)
C16	C15	C17	108.4(3)	C34	C35	C36	119.6(4)
C16	C15	S2	109.5(2)	C37	C36	C35	119.7(4)
C17	C15	S2	109.4(2)	C36	C37	C32	121.7(3)
C18	C15	C16	108.9(3)	C10	O3	S2	123.38(19)
C18	C15	C17	109.6(3)	C12	O4	C19	117.2(2)
C18	C15	S2	111.0(2)	C1	S1	C8	92.93(14)
C20	C19	C26	105.5(2)	O1	S1	C1	106.55(14)
C32	C19	C20	114.1(2)	O1	S1	C8	106.65(14)
C32	C19	C26	113.4(2)	C13	S2	C15	112.53(16)
O4	C19	C20	111.6(2)	C14	S2	C13	109.54(19)
O4	C19	C26	104.7(2)	C14	S2	C15	110.49(17)
O4	C19	C32	107.2(2)	O3	S2	C13	111.47(16)
C21	C20	C19	121.5(3)	O3	S2	C14	109.10(16)
C25	C20	C19	119.8(3)	O3	S2	C15	103.55(13)

Table 6 Torsion Angles for 19m_mb1_MZZ534B_0s.

A	B	C	D	Angle/°	A	B	C	D	Angle/°
C1	C2	C3	C4	-0.7(5)	C20	C19	O4	C12	77.4(3)
C2	C1	C6	C5	1.3(5)	C20	C21	C22	C23	-2.0(5)
C2	C1	S1	C8	-97.7(3)	C21	C20	C25	C24	-1.9(5)
C2	C1	S1	O1	10.6(3)	C21	C22	C23	C24	0.3(5)

C2	C3	C4	C5	0.5(5)	C22	C23	C24	C25	0.6(5)
C2	C3	C4	C7	-179.0(4)	C23	C24	C25	C20	0.2(5)
C3	C4	C5	C6	0.6(5)	C25	C20	C21	C22	2.8(5)
C4	C5	C6	C1	-1.5(5)	C26	C19	C20	C21	-108.8(3)
C6	C1	C2	C3	-0.3(5)	C26	C19	C20	C25	66.5(3)
C6	C1	S1	C8	80.9(3)	C26	C19	C32	C33	-135.4(3)
C6	C1	S1	O1	-170.8(3)	C26	C19	C32	C37	52.5(4)
C7	C4	C5	C6	-179.9(4)	C26	C19	O4	C12	-168.9(2)
C8	C9	C10	C11	-53.6(3)	C26	C27	C28	C29	0.6(5)
C8	C9	C10	O3	-176.6(2)	C27	C26	C31	C30	0.5(5)
C9	C8	S1	C1	-172.6(2)	C27	C28	C29	C30	0.0(6)
C9	C8	S1	O1	79.2(2)	C28	C29	C30	C31	-0.3(6)
C9	C10	C11	C12	-65.2(3)	C29	C30	C31	C26	0.1(6)
C9	C10	O3	S2	-105.9(3)	C31	C26	C27	C28	-0.8(5)
C10	C11	C12	O4	62.0(3)	C32	C19	C20	C21	126.1(3)
C10	O3	S2	C13	51.5(3)	C32	C19	C20	C25	-58.6(4)
C10	O3	S2	C14	-69.6(3)	C32	C19	C26	C27	-161.6(3)
C10	O3	S2	C15	172.7(2)	C32	C19	C26	C31	22.7(4)
C11	C10	O3	S2	128.7(2)	C32	C19	O4	C12	-48.2(3)
C11	C12	O4	C19	169.8(2)	C32	C33	C34	C35	-0.7(6)
C16	C15	S2	C13	61.1(3)	C33	C32	C37	C36	0.2(6)
C16	C15	S2	C14	-176.1(3)	C33	C34	C35	C36	-0.2(6)
C16	C15	S2	O3	-59.4(3)	C34	C35	C36	C37	1.1(7)
C17	C15	S2	C13	179.8(3)	C35	C36	C37	C32	-1.2(7)
C17	C15	S2	C14	-57.4(3)	C37	C32	C33	C34	0.7(5)
C17	C15	S2	O3	59.3(3)	O2	C9	C10	C11	128.2(3)
C18	C15	S2	C13	-59.1(3)	O2	C9	C10	O3	5.2(4)
C18	C15	S2	C14	63.7(3)	O3	C10	C11	C12	58.4(3)
C18	C15	S2	O3	-179.6(3)	O4	C19	C20	C21	4.4(4)
C19	C20	C21	C22	178.1(3)	O4	C19	C20	C25	179.6(3)
C19	C20	C25	C24	-177.3(3)	O4	C19	C26	C27	-45.1(3)
C19	C26	C27	C28	-176.6(3)	O4	C19	C26	C31	139.3(3)
C19	C26	C31	C30	176.1(3)	O4	C19	C32	C33	109.6(3)
C19	C32	C33	C34	-171.4(3)	O4	C19	C32	C37	-62.5(4)
C19	C32	C37	C36	172.8(4)	S1	C1	C2	C3	178.3(3)
C20	C19	C26	C27	72.8(3)	S1	C1	C6	C5	-177.3(3)
C20	C19	C26	C31	-102.9(3)	S1	C8	C9	C10	-168.6(2)
C20	C19	C32	C33	-14.5(4)	S1	C8	C9	O2	9.6(4)
C20	C19	C32	C37	173.4(3)					

Table 7 Hydrogen Atom Coordinates (Å×10⁴) and Isotropic Displacement Parameters (Å²×10³) for 19m_mb1_MZZ534B_0s.

Atom	***x***	***y***	***z***	**U(eq)**

H2	10049.91	6604.67	6389.68	38
H3	9521.38	7818.09	7399.83	47
H5	6845.65	5441.22	6307.26	43
H6	7378.99	4130.41	5308.92	39
H7A	7386.89	8654.97	7371.81	84
H7B	8342.6	7870.46	8126.17	84
H7C	7331.99	6742.91	7749.99	84
H8A	7824.99	6112.43	4135.83	29
H8B	8845.85	7206.43	4392.56	29
H10	8704.46	8209.59	2921.03	31
H11A	7186.78	8276.13	3158.8	34
H11B	7041.37	9005.34	2235.27	34
H12A	5677	7210.05	2125.32	36
H12B	6296.23	6277.03	1624.99	36
H13A	10514.36	7908.42	2759.16	66
H13B	10822.39	7108.83	2017.63	66
H13C	10389.93	5844.15	2554.3	66
H14A	8275.61	9964.19	764.49	70
H14B	9461.07	10261.72	1186.27	70
H14C	8796.83	10413.36	1757.73	70
H16A	9543.55	3849.29	1118.46	60
H16B	8683.35	3434.66	212.39	60
H16C	8394.65	3821.38	1020.73	60
H17A	7227.55	6214.1	198	77
H17B	7526.32	5744.95	-597.17	77
H17C	7630.66	7725.37	-250.38	77
H18A	9406.98	7779.75	-85.27	71
H18B	9350.41	5788.87	-411.04	71
H18C	10179.57	6343.3	489.35	71
H21	6842.02	3630.5	1620.74	36
H22	6711.33	1720.44	497.01	47
H23	5475.35	-442.9	72.7	46
H24	4346.43	-668.72	759.04	45
H25	4449.55	1268.54	1846.29	37
H27	7470.65	2465.11	3456.59	31
H28	8007.55	529.96	4610.58	39
H29	6881.72	-446.66	5211.13	53
H30	5239.42	514.05	4662.33	62
H31	4697.52	2476.02	3514.87	51
H33	3968.28	4428.71	1188.7	38
H34	2649.83	6357.75	1023.96	50
H35	2609.02	7980.81	2171.86	62
H36	3894.86	7665.89	3507.08	65
H37	5230.9	5812.25	3669.21	51

Experimental

Single crystals of $C_{37}H_{44}O_4S_2$ **[19m_mb1_MZZ534B_0s]** were **[]**. A suitable crystal was selected and **[]** on a **'Bruker APEX-II CCD'** diffractometer. The crystal was kept at 173.15 K during data collection. Using Olex2 [1], the structure was solved with the ShelXT [2] structure solution program using Intrinsic Phasing and refined with the ShelXL [3] refinement package using Least Squares minimisation.

1. Dolomanov, O.V., Bourhis, L.J., Gildea, R.J, Howard, J.A.K. & Puschmann, H. (2009), J. Appl. Cryst. 42, 339-341.
2. Sheldrick, G.M. (2015). Acta Cryst. A71, 3-8.
3. Sheldrick, G.M. (2015). Acta Cryst. C71, 3-8.

Crystal structure determination of [19m_mb1_MZZ534B_0s]

Crystal Data for $C_{37}H_{44}O_4S_2$ (M =616.84 g/mol): monoclinic, space group $P2_1$ (no. 4), a = 14.4049(4) Å, b = 7.5907(2) Å, c = 16.9364(5) Å, β = 112.0590(10)°, V = 1716.32(8) Å^3, Z = 2, T = 173.15 K, μ(MoKα) = 0.192 mm^{-1}, *Dcalc* = 1.194 g/cm^3, 24077 reflections measured (2.594° ≤ 2Θ ≤ 56.816°), 8570 unique (R_{int} = 0.0519, R_{sigma} = 0.0615) which were used in all calculations. The final R_1 was 0.0473 (I > 2σ(I)) and wR_2 was 0.1200 (all data).

Refinement model description

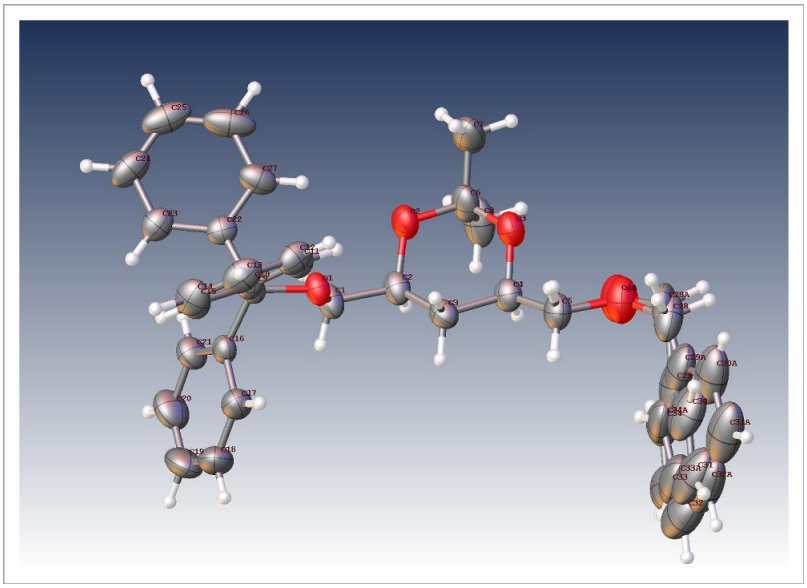
Number of restraints - 1, number of constraints - unknown.

Details:

```
1. Twinned data refinement
 Scales: 0.85(8)
 0.15(8)
2. Fixed Uiso
 At 1.2 times of:
  All C(H) groups, All C(H,H) groups
 At 1.5 times of:
  All C(H,H,H) groups
3.a Ternary CH refined with riding coordinates:
 C10(H10)
3.b Secondary CH2 refined with riding coordinates:
 C8(H8A,H8B), C11(H11A,H11B), C12(H12A,H12B)
3.c Aromatic/amide H refined with riding coordinates:
 C2(H2), C3(H3), C5(H5), C6(H6), C21(H21), C22(H22), C23(H23), C24(H24),
 C25(H25), C27(H27), C28(H28), C29(H29), C30(H30), C31(H31), C33(H33), C34(H34),
  C35(H35), C36(H36), C37(H37)
3.d Idealised Me refined as rotating group:
 C7(H7A,H7B,H7C), C13(H13A,H13B,H13C), C14(H14A,H14B,H14C), C16(H16A,H16B,
 H16C), C17(H17A,H17B,H17C), C18(H18A,H18B,H18C)
```

This report has been created with Olex2, compiled on 2018.05.29 svn.r3508 for OlexSys. Please let us know if there are any errors or if you would like to have additional features.

Crystal structure for compound 152



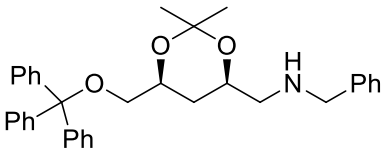


Table 1 Crystal data and structure refinement for 17mv_moira3_mzz_325_0f.

Identification code	17mv_moira3_mzz_325_0f
Empirical formula	$C_{34}H_{36}O_4$
Formula weight	508.63
Temperature/K	173.15
Crystal system	monoclinic
Space group	$P2_1$
a/Å	8.9936(5)
b/Å	11.0745(6)
c/Å	15.0150(8)
α/°	90
β/°	90.4235(18)
γ/°	90
Volume/Å^3	1495.45(14)
Z	2
ρ_{calc}g/cm^3	1.130
μ/mm^{-1}	0.073
F(000)	544.0
Crystal size/mm^3	0.66 × 0.07 × 0.06
Radiation	MoKα (λ = 0.71073)
2Θ range for data collection/°	6.422 to 51.996
Index ranges	$-11 \leq h \leq 11$, $-12 \leq k \leq 13$, $-18 \leq l \leq 18$
Reflections collected	24429
Independent reflections	5247 [R_{int} = 0.0482, R_{sigma} = 0.0414]
Data/restraints/parameters	5247/206/388
Goodness-of-fit on F^2	1.069
Final R indexes [I>=2σ (I)]	R_1 = 0.0592, wR_2 = 0.1585
Final R indexes [all data]	R_1 = 0.0853, wR_2 = 0.1744
Largest diff. peak/hole / e Å^{-3}	0.66/-0.27
Flack parameter	-0.2(5)

Table 2 Fractional Atomic Coordinates ($\times 10^4$) and Equivalent Isotropic Displacement Parameters ($Å^2 \times 10^3$) for 17mv_moira3_mzz_325_0f. U_{eq} is defined as 1/3 of of the trace of the orthogonalised U_{IJ} tensor.

Atom	*x*	*y*	*z*	U(eq)
C1	7436(4)	5359(5)	5622(2)	45.8(10)
C2	7146(4)	5338(4)	6607(2)	44.8(10)
C3	5671(4)	4807(4)	6879(2)	44.4(10)
C4	5515(4)	4892(4)	7878(2)	46.4(10)
C5	4011(5)	4531(5)	8209(3)	55.8(12)
C6	7115(5)	6651(5)	7882(3)	56.4(12)
C7	6950(7)	7969(6)	8076(3)	80.9(18)
C8	8434(5)	6075(7)	8373(3)	79.5(19)
C9	6469(4)	6060(4)	4223(2)	35.6(8)
C10	4936(4)	6336(4)	3805(2)	37.5(9)
C11	3750(4)	6699(4)	4327(3)	41.6(9)
C12	2382(4)	6968(5)	3926(3)	51.5(11)
C13	2194(5)	6893(5)	3021(3)	58.1(13)
C14	3385(5)	6562(5)	2498(3)	57.0(12)
C15	4736(4)	6283(4)	2883(2)	46.5(10)
C16	7169(4)	4953(4)	3796(2)	37.8(9)
C17	6292(5)	3952(5)	3613(3)	54.8(12)
C18	6914(7)	2888(5)	3292(3)	70.8(15)
C19	8379(8)	2811(6)	3165(4)	79.7(17)
C20	9309(6)	3778(6)	3353(4)	73.4(16)
C21	8696(5)	4845(5)	3669(3)	50.6(11)
C22	7369(4)	7224(4)	4137(3)	38.6(9)
C23	8066(4)	7550(4)	3342(3)	48.7(11)
C24	8763(5)	8653(5)	3256(4)	61.9(14)
C25	8796(5)	9456(5)	3955(5)	73.3(16)
C26	8124(6)	9156(5)	4741(5)	75.6(17)
C27	7404(5)	8035(5)	4839(3)	53.6(12)
O1	6183(3)	5805(3)	5143.9(15)	40.0(7)
O2	7260(3)	6552(3)	6941.0(17)	52.2(8)
O3	5750(3)	6117(3)	8162.3(17)	50.9(8)
O4	3840(40)	4480(60)	9183(9)	84(3)
C28	2370(30)	4118(17)	9480(20)	80(4)
C29	2163(12)	2798(9)	9293(8)	79(4)
C30	730(11)	2405(13)	9098(9)	106(5)
C31	460(15)	1188(14)	8940(10)	125(6)
C32	1620(20)	363(10)	8977(9)	127(6)
C33	3058(16)	756(10)	9171(7)	105(5)

C34	3328(10)	1974(10)	9329(8)	84(4)
O4A	4120(40)	4500(80)	9184(10)	84(3)
C28A	2600(40)	4330(20)	9510(30)	81(6)
C29A	1806(16)	3146(13)	9380(9)	92(5)
C30A	270(16)	3074(16)	9460(9)	112(6)
C31A	-451(17)	1979(19)	9320(9)	130(7)
C32A	360(20)	956(16)	9102(10)	135(8)
C33A	1900(20)	1028(13)	9022(10)	129(7)
C34A	2621(17)	2123(15)	9161(10)	101(6)

Table 3 Anisotropic Displacement Parameters ($Å^2×10^3$) for 17mv_moira3_mzz_325_0f. The Anisotropic displacement factor exponent takes the form: $-2\pi^2[h^2a^{*2}U_{11}+2hka^*b^*U_{12}+\ldots]$.

Atom	U_{11}	U_{22}	U_{33}	U_{23}	U_{13}	U_{12}
C1	41(2)	63(3)	33(2)	-0.2(18)	-1.6(15)	15(2)
C2	42(2)	58(3)	34(2)	3.1(18)	-1.8(15)	10.5(19)
C3	49(2)	46(3)	38(2)	-1.9(17)	-3.7(16)	9(2)
C4	47(2)	56(3)	36(2)	2.9(19)	-5.0(16)	2(2)
C5	58(3)	70(4)	39(2)	7(2)	1.5(18)	-1(2)
C6	59(3)	78(4)	32(2)	-6(2)	-2.9(17)	-17(2)
C7	108(4)	84(5)	51(3)	-19(3)	8(3)	-35(4)
C8	58(3)	139(6)	42(2)	-2(3)	-7(2)	-16(3)
C9	33.2(18)	43(2)	30.8(17)	-1.9(15)	-0.1(14)	1.3(16)
C10	34.1(18)	41(3)	37.2(19)	0.4(16)	-1.0(14)	-7.8(17)
C11	32.6(18)	49(3)	43(2)	5.2(18)	0.8(15)	-2.7(18)
C12	34(2)	52(3)	69(3)	11(2)	0.3(18)	-3.6(19)
C13	41(2)	59(3)	74(3)	12(2)	-20(2)	-12(2)
C14	54(3)	70(4)	46(2)	3(2)	-17.9(19)	-10(2)
C15	45(2)	57(3)	38(2)	2.3(19)	-5.3(16)	-5(2)
C16	42(2)	43(3)	28.1(17)	0.5(15)	0.7(14)	-1.1(18)
C17	62(3)	51(3)	51(3)	-3(2)	7(2)	-8(2)
C18	97(4)	47(3)	69(3)	-11(2)	14(3)	-13(3)
C19	116(5)	52(4)	72(3)	-14(3)	17(3)	18(4)
C20	69(3)	82(5)	69(3)	-9(3)	15(2)	25(3)
C21	47(2)	56(3)	49(2)	-5(2)	5.1(18)	9(2)
C22	29.7(18)	41(2)	45(2)	1.5(17)	-7.4(15)	2.0(17)
C23	38(2)	54(3)	54(2)	8(2)	-6.1(18)	-5(2)
C24	40(2)	61(4)	85(4)	23(3)	-10(2)	-13(2)
C25	44(3)	47(3)	129(5)	16(3)	-24(3)	-7(2)
C26	57(3)	53(4)	116(5)	-31(3)	-35(3)	7(3)
C27	43(2)	54(3)	64(3)	-18(2)	-10.7(19)	3(2)
O1	35.5(13)	56(2)	28.6(13)	0.7(12)	-0.7(10)	6.8(12)
O2	61.4(18)	63(2)	31.9(13)	-2.4(13)	-0.3(11)	-7.2(16)
O3	51.2(16)	64(2)	37.1(14)	-3.0(13)	3.6(11)	0.0(15)

O4	81(10)	111(4)	60(2)	11(2)	12(3)	-5(10)
C28	67(8)	113(9)	60(9)	34(9)	14(7)	18(8)
C29	85(6)	118(8)	33(6)	30(6)	0(5)	-7(6)
C30	96(8)	147(11)	74(9)	53(8)	-19(7)	-21(8)
C31	146(12)	150(12)	78(10)	56(9)	-35(9)	-64(10)
C32	175(14)	121(11)	84(9)	34(9)	-25(9)	-52(9)
C33	147(11)	110(8)	58(7)	10(6)	7(7)	-18(8)
C34	94(8)	106(8)	50(7)	4(6)	9(6)	-6(6)
O4A	81(10)	111(4)	60(2)	11(2)	12(3)	-5(10)
C28A	87(11)	103(10)	53(10)	10(9)	32(8)	-13(8)
C29A	106(10)	122(11)	49(8)	28(8)	-3(8)	-35(9)
C30A	108(9)	178(15)	50(8)	20(9)	-13(7)	-52(10)
C31A	127(13)	199(17)	63(9)	28(10)	-21(8)	-78(11)
C32A	181(16)	165(14)	58(10)	26(10)	-17(10)	-102(13)
C33A	189(16)	131(13)	69(9)	14(10)	26(11)	-69(12)
C34A	137(14)	113(11)	53(9)	1(9)	27(10)	-57(9)

Table 4 Bond Lengths for 17mv_moira3_mzz_325_0f.

Atom	Atom	Length/Å	Atom	Atom	Length/Å
C1	C2	1.504(5)	C18	C19	1.336(8)
C1	O1	1.420(4)	C19	C20	1.388(9)
C2	C3	1.510(6)	C20	C21	1.389(7)
C2	O2	1.438(6)	C22	C23	1.399(6)
C3	C4	1.511(5)	C22	C27	1.386(6)
C4	C5	1.499(6)	C23	C24	1.379(7)
C4	O3	1.437(6)	C24	C25	1.376(9)
C5	O4	1.472(14)	C25	C26	1.371(9)
C5	O4A	1.467(16)	C26	C27	1.408(8)
C6	C7	1.496(9)	O4	C28	1.459(15)
C6	C8	1.531(7)	C28	C29	1.501(18)
C6	O2	1.425(5)	C29	C30	1.3900
C6	O3	1.429(5)	C29	C34	1.3900
C9	C10	1.541(5)	C30	C31	1.3900
C9	C16	1.522(6)	C31	C32	1.3900
C9	C22	1.528(6)	C32	C33	1.3900
C9	O1	1.437(4)	C33	C34	1.3900
C10	C11	1.387(5)	O4A	C28A	1.464(17)
C10	C15	1.395(5)	C28A	C29A	1.507(18)
C11	C12	1.398(6)	C29A	C30A	1.3900
C12	C13	1.370(7)	C29A	C34A	1.3900
C13	C14	1.382(7)	C30A	C31A	1.3900
C14	C15	1.377(6)	C31A	C32A	1.3900
C16	C17	1.387(6)	C32A	C33A	1.3900

C16	C21	1.393(5)	C33A	C34A	1.3900
C17	C18	1.391(8)			

Table 5 Bond Angles for 17mv_moira3_mzz_325_0f.

Atom	Atom	Atom	Angle/°	Atom	Atom	Atom	Angle/°
O1	C1	C2	111.1(3)	C18	C19	C20	121.0(5)
C1	C2	C3	115.5(3)	C19	C20	C21	119.1(5)
O2	C2	C1	108.4(4)	C20	C21	C16	120.9(5)
O2	C2	C3	109.3(3)	C23	C22	C9	122.1(4)
C2	C3	C4	109.4(3)	C27	C22	C9	119.4(4)
C5	C4	C3	113.8(3)	C27	C22	C23	118.3(4)
O3	C4	C3	109.9(3)	C24	C23	C22	121.0(5)
O3	C4	C5	106.5(4)	C25	C24	C23	120.6(5)
O4	C5	C4	116.1(12)	C26	C25	C24	119.5(5)
O4A	C5	C4	106.5(14)	C25	C26	C27	120.6(5)
C7	C6	C8	113.0(5)	C22	C27	C26	120.0(5)
O2	C6	C7	106.2(4)	C1	O1	C9	114.0(3)
O2	C6	C8	111.6(4)	C6	O2	C2	114.3(3)
O2	C6	O3	110.2(3)	C6	O3	C4	115.3(3)
O3	C6	C7	105.1(4)	C28	O4	C5	115(2)
O3	C6	C8	110.5(4)	O4	C28	C29	109(3)
C16	C9	C10	111.1(3)	C30	C29	C28	117.3(12)
C16	C9	C22	115.0(3)	C30	C29	C34	120.0
C22	C9	C10	105.7(3)	C34	C29	C28	122.6(12)
O1	C9	C10	105.4(2)	C29	C30	C31	120.0
O1	C9	C16	108.9(3)	C32	C31	C30	120.0
O1	C9	C22	110.3(3)	C31	C32	C33	120.0
C11	C10	C9	121.1(3)	C32	C33	C34	120.0
C11	C10	C15	118.6(3)	C33	C34	C29	120.0
C15	C10	C9	120.2(3)	C28A	O4A	C5	106(3)
C10	C11	C12	119.7(4)	O4A	C28A	C29A	121(4)
C13	C12	C11	121.1(4)	C30A	C29A	C28A	120.6(17)
C12	C13	C14	119.3(4)	C30A	C29A	C34A	120.0
C15	C14	C13	120.4(4)	C34A	C29A	C28A	119.4(17)
C14	C15	C10	120.9(4)	C31A	C30A	C29A	120.0
C17	C16	C9	119.4(3)	C30A	C31A	C32A	120.0
C17	C16	C21	117.6(4)	C33A	C32A	C31A	120.0
C21	C16	C9	122.6(4)	C32A	C33A	C34A	120.0
C16	C17	C18	121.1(5)	C33A	C34A	C29A	120.0
C19	C18	C17	120.2(5)				

Table 6 Torsion Angles for 17mv_moira3_mzz_325_0f.

A	B	C	D	Angle/°
C1	C2	C3	C4	-177.8(4)
C1	C2	O2	C6	-175.7(3)
C2	C1	O1	C9	169.1(4)
C2	C3	C4	C5	172.8(4)
C2	C3	C4	O3	53.5(4)
C3	C2	O2	C6	57.6(4)
C3	C4	C5	O4	174(3)
C3	C4	C5	O4A	172(4)
C3	C4	O3	C6	-54.1(4)
C4	C5	O4	C28	-180(3)
C4	C5	O4A	C28A	171(4)
C5	C4	O3	C6	-177.8(3)
C5	O4	C28	C29	71(5)
C5	O4A	C28A	C29A	70(6)
C7	C6	O2	C2	-168.7(4)
C7	C6	O3	C4	167.8(4)
C8	C6	O2	C2	67.8(5)
C8	C6	O3	C4	-70.1(5)
C9	C10	C11	C12	178.6(4)
C9	C10	C15	C14	-178.1(4)
C9	C16	C17	C18	-174.6(4)
C9	C16	C21	C20	174.0(4)
C9	C22	C23	C24	174.3(4)
C9	C22	C27	C26	-174.6(4)
C10	C9	C16	C17	-41.9(5)
C10	C9	C16	C21	145.4(4)
C10	C9	C22	C23	-80.3(4)
C10	C9	C22	C27	94.3(4)
C10	C9	O1	C1	171.5(4)
C10	C11	C12	C13	-0.7(7)
C11	C10	C15	C14	-1.2(6)
C11	C12	C13	C14	-1.0(7)
C12	C13	C14	C15	1.5(7)
C13	C14	C15	C10	-0.4(7)
C15	C10	C11	C12	1.8(6)
C16	C9	C10	C11	139.5(4)
C16	C9	C10	C15	-43.8(5)
C16	C9	C22	C23	42.7(5)
C16	C9	C22	C27	-142.7(4)
C16	C9	O1	C1	52.3(4)
C16	C17	C18	C19	0.7(8)
C17	C16	C21	C20	1.2(6)
C17	C18	C19	C20	0.5(9)
C18	C19	C20	C21	-0.8(9)
C21	C16	C17	C18	-1.5(6)
C22	C9	C10	C11	-95.1(4)
C22	C9	C10	C15	81.6(4)
C22	C9	C16	C17	-161.9(3)
C22	C9	C16	C21	25.3(5)
C22	C9	O1	C1	-74.8(4)
C22	C23	C24	C25	0.4(7)
C23	C22	C27	C26	0.2(6)
C23	C24	C25	C26	-0.2(7)
C24	C25	C26	C27	0.0(7)
C25	C26	C27	C22	0.0(7)
C27	C22	C23	C24	-0.4(6)
O1	C1	C2	C3	46.6(5)
O1	C1	C2	O2	-76.4(4)
O1	C9	C10	C11	21.6(5)
O1	C9	C10	C15	-161.6(4)
O1	C9	C16	C17	73.7(4)
O1	C9	C16	C21	-99.0(4)
O1	C9	C22	C23	166.3(3)
O1	C9	C22	C27	-19.1(5)
O2	C2	C3	C4	-55.3(4)
O2	C6	O3	C4	53.8(5)
O3	C4	C5	O4	-65(3)
O3	C4	C5	O4A	-67(4)
O3	C6	O2	C2	-55.4(5)
O4	C28	C29	C30	-148.3(16)
O4	C28	C29	C34	34(3)
C28	C29	C30	C31	-178.1(17)
C28	C29	C34	C33	178.0(18)
C29	C30	C31	C32	0.0
C30	C29	C34	C33	0.0
C30	C31	C32	C33	0.0
C31	C32	C33	C34	0.0
C32	C33	C34	C29	0.0
C34	C29	C30	C31	0.0
O4A	C28A	C29A	C30A	-163(2)
O4A	C28A	C29A	C34A	16(4)
C28A	C29A	C30A	C31A	178(2)
C28A	C29A	C34A	C33A	-178(2)
C29A	C30A	C31A	C32A	0.0
C30A	C29A	C34A	C33A	0.0
C30A	C31A	C32A	C33A	0.0
C31A	C32A	C33A	C34A	0.0
C32A	C33A	C34A	C29A	0.0

C19	C20	C21	C16	-0.1(8)	C34A	C29A	C30A	C31A	0.0

Table 7 Hydrogen Atom Coordinates (Å×10⁴) and Isotropic Displacement Parameters (Å²×10³) for 17mv_moira3_mzz_325_0f.

Atom	*x*	*y*	*z*	U(eq)
H1A	8307.97	5878.47	5500.73	55
H1B	7670.07	4532.4	5414.96	55
H2	7950.35	4849.05	6896.17	54
H3A	5614.7	3951.82	6690.37	53
H3B	4850.41	5253.32	6583.97	53
H4	6283.52	4365.25	8165.29	56
H5AA	3269.5	5108.22	7968.47	67
H5AB	3767.8	3725.46	7962.36	67
H5BC	3250.12	5123.3	8015.18	67
H5BD	3732.29	3726.12	7974.86	67
H7A	6687.47	8079.34	8703.38	121
H7B	6164.43	8309.1	7696.51	121
H7C	7891.02	8382.8	7956.23	121
H8A	9354.59	6483.96	8200.53	119
H8B	8497.17	5217.97	8215.46	119
H8C	8295.35	6154.66	9017.1	119
H11	3867.06	6763.24	4954.13	50
H12	1570.38	7207.87	4286.04	62
H13	1255.64	7066.68	2756.17	70
H14	3270.62	6526.43	1869.03	68
H15	5543.96	6052.15	2516.57	56
H17	5250.33	3992.99	3706.89	66
H18	6294.2	2214.91	3164.29	85
H19	8789.92	2081.85	2941.36	96
H20	10351.39	3712.24	3267.06	88
H21	9326.62	5510.81	3800.01	61
H23	8059.5	7003.74	2854.33	58
H24	9224.85	8859.07	2709.91	74
H25	9279.63	10213.45	3892.58	88
H26	8145.19	9709.58	5224.76	91
H27	6942.06	7835.29	5386.88	64
H28A	1597.45	4593.85	9170.81	96
H28B	2279.21	4267.9	10132.2	96
H30	-66.15	2968.47	9073.61	127
H31	-519.71	918.96	8807.31	150
H32	1440.43	-468.74	8868.49	152
H33	3854.15	193.06	9195.98	126
H34	4307.74	2242.58	9462.29	100

H28C	1975.9	4962.7	9222.89	97
H28D	2613.52	4504.71	10153.59	97
H30A	-287.01	3772.9	9609.07	134
H31A	-1501.17	1930.09	9374.65	156
H32A	-129.05	208.07	9006.34	162
H33A	2457.25	328.86	8872.46	155
H34A	3671.45	2171.66	9106.89	121

Table 8 Atomic Occupancy for 17mv_moira3_mzz_325_0f.

Atom	*Occupancy*	Atom	*Occupancy*	Atom	*Occupancy*
H5AA	0.540(19)	H5AB	0.540(19)	H5BC	0.460(19)
H5BD	0.460(19)	O4	0.540(19)	C28	0.540(19)
H28A	0.540(19)	H28B	0.540(19)	C29	0.540(19)
C30	0.540(19)	H30	0.540(19)	C31	0.540(19)
H31	0.540(19)	C32	0.540(19)	H32	0.540(19)
C33	0.540(19)	H33	0.540(19)	C34	0.540(19)
H34	0.540(19)	O4A	0.460(19)	C28A	0.460(19)
H28C	0.460(19)	H28D	0.460(19)	C29A	0.460(19)
C30A	0.460(19)	H30A	0.460(19)	C31A	0.460(19)
H31A	0.460(19)	C32A	0.460(19)	H32A	0.460(19)
C33A	0.460(19)	H33A	0.460(19)	C34A	0.460(19)
H34A	0.460(19)				

Experimental

Single crystals of $C_{34}H_{36}O_4$ **[17mv_moira3_mzz_325_0f]** were **[]**. A suitable crystal was selected and **[]** on a **'Bruker APEX-II CCD'** diffractometer. The crystal was kept at 173.15 K during data collection. Using Olex2 [1], the structure was solved with the ShelXT [2] structure solution program using Intrinsic Phasing and refined with the ShelXL [3] refinement package using Least Squares minimisation.

1. Dolomanov, O.V., Bourhis, L.J., Gildea, R.J, Howard, J.A.K. & Puschmann, H. (2009), J. Appl. Cryst. 42, 339-341.
2. Sheldrick, G.M. (2015). Acta Cryst. A71, 3-8.
3. Sheldrick, G.M. (2015). Acta Cryst. C71, 3-8.

Crystal structure determination of [17mv_moira3_mzz_325_0f]

Crystal Data for $C_{34}H_{36}O_4$ (M =508.63 g/mol): monoclinic, space group $P2_1$ (no. 4), a = 8.9936(5) Å, b = 11.0745(6) Å, c = 15.0150(8) Å, β = 90.4235(18)°, V = 1495.45(14) Å^3, Z = 2, T = 173.15 K, μ(MoKα) = 0.073 mm^{-1}, *Dcalc* = 1.130 g/cm^3, 24429 reflections measured (6.422° ≤ 2Θ ≤ 51.996°), 5247 unique (R_{int} = 0.0482, R_{sigma} = 0.0414) which were used in all calculations. The final R_1 was 0.0592 (I > 2σ(I)) and wR_2 was 0.1744 (all data).

Refinement model description

Number of restraints - 206, number of constraints - unknown.

Details:

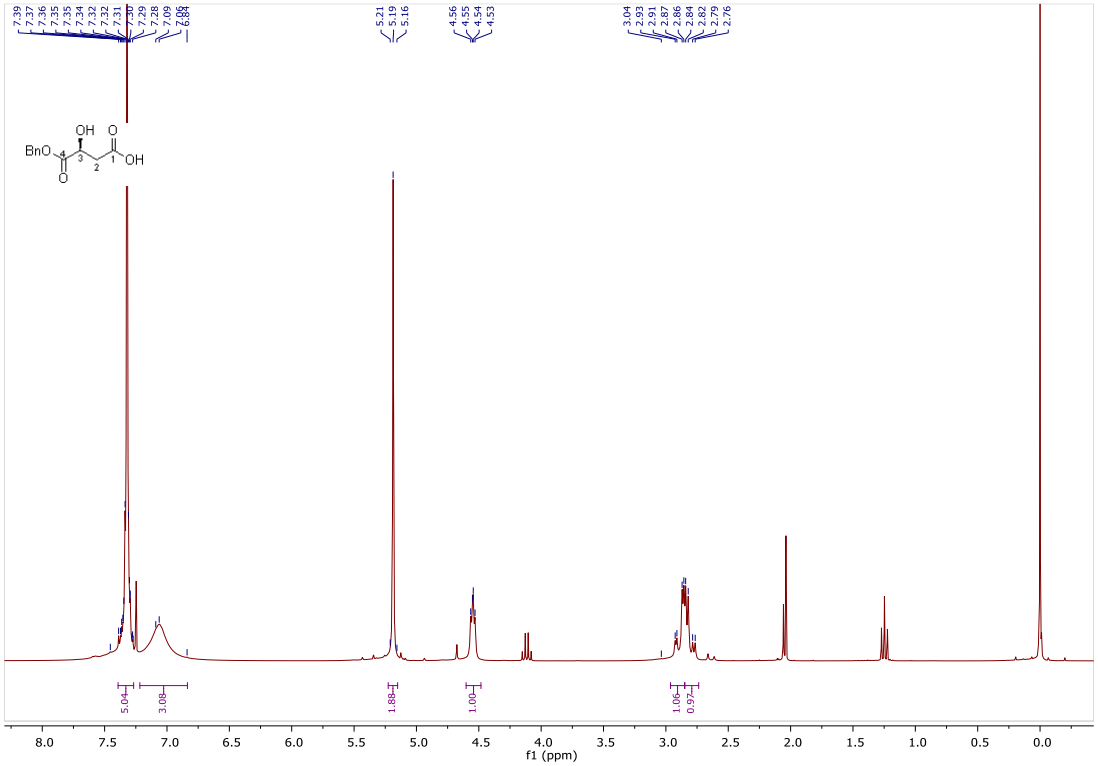
```
1. Fixed Uiso
 At 1.2 times of:
  All C(H) groups, All C(H,H) groups, All C(H,H,H,H) groups
 At 1.5 times of:
  All C(H,H,H) groups
2. Restrained distances
 C5-O4 ≈ C5-O4A ≈ O4A-C28A ≈ O4-C28
 with sigma of 0.02
```

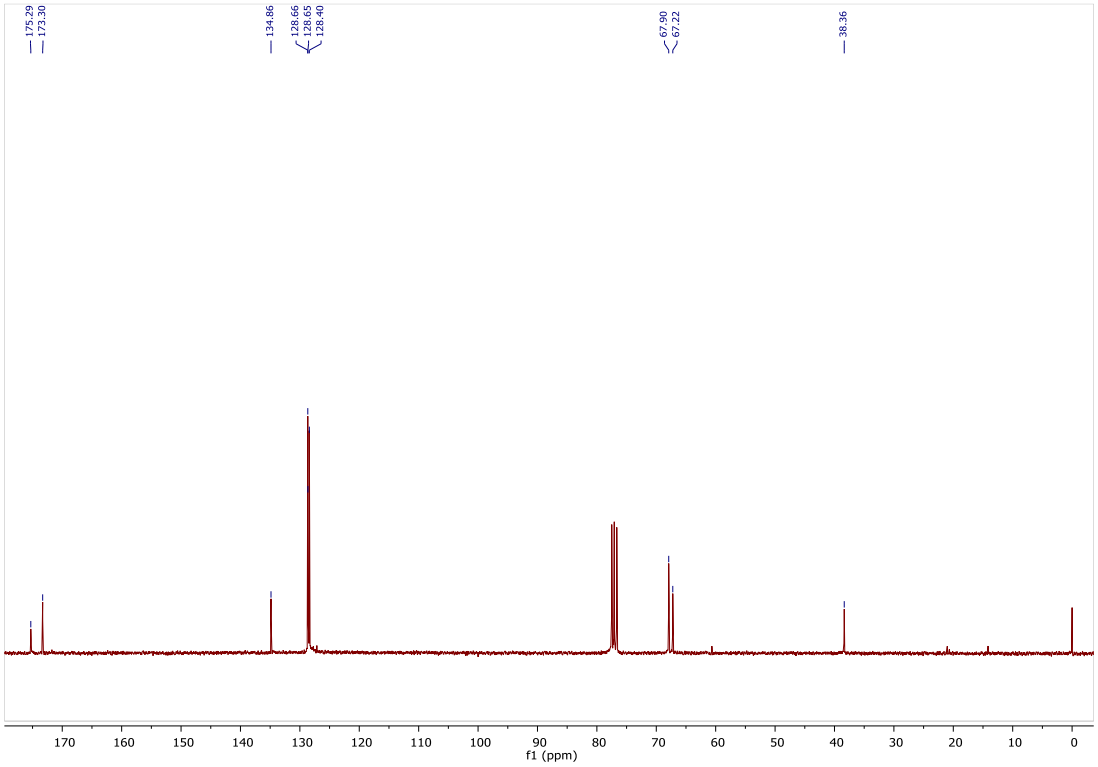
```
 C28-C29 ≈ C28A-C29A
 with sigma of 0.02
3. Uiso/Uaniso restraints and constraints
O4 ≈ C28 ≈ C29 ≈ C30 ≈ C31 ≈ C32 ≈ C33 ≈ C34:
within 2A with sigma of 0.02 and sigma for terminal atoms of 0.04
O4A ≈ C28A ≈ C29A ≈ C30A ≈ C31A ≈ C32A ≈ C33A ≈
C34A: within 2A with sigma of 0.02 and sigma for terminal atoms of 0.04
Uanis(O4) = Uanis(O4A)
4. Rigid body (RIGU) restrains
 O4, C28, C29, C30, C31, C32, C33, C34
 with sigma for 1-2 distances of 0.004 and sigma for 1-3 distances of 0.004
 O4A, C28A, C29A, C30A, C31A, C32A, C33A, C34A
 with sigma for 1-2 distances of 0.004 and sigma for 1-3 distances of 0.004
5. Others
 Sof(H5BC)=Sof(H5BD)=Sof(O4A)=Sof(C28A)=Sof(H28C)=Sof(H28D)=Sof(C29A)=
 Sof(C30A)=Sof(H30A)=Sof(C31A)=Sof(H31A)=Sof(C32A)=Sof(H32A)=Sof(C33A)=
 Sof(H33A)=Sof(C34A)=Sof(H34A)=1-FVAR(1)
 Sof(H5AA)=Sof(H5AB)=Sof(O4)=Sof(C28)=Sof(H28A)=Sof(H28B)=Sof(C29)=Sof(C30)=
 Sof(H30)=Sof(C31)=Sof(H31)=Sof(C32)=Sof(H32)=Sof(C33)=Sof(H33)=Sof(C34)=
 Sof(H34)=FVAR(1)
6.a Ternary CH refined with riding coordinates:
 C2(H2), C4(H4)
6.b Secondary CH2 refined with riding coordinates:
 C1(H1A,H1B), C3(H3A,H3B), C5(H5AA,H5AB), C5(H5BC,H5BD), C28(H28A,H28B),
 C28A(H28C,H28D)
6.c Aromatic/amide H refined with riding coordinates:
 C11(H11), C12(H12), C13(H13), C14(H14), C15(H15), C17(H17), C18(H18),
 C19(H19), C20(H20), C21(H21), C23(H23), C24(H24), C25(H25), C26(H26), C27(H27),
  C30(H30), C31(H31), C32(H32), C33(H33), C34(H34), C30A(H30A), C31A(H31A),
 C32A(H32A), C33A(H33A), C34A(H34A)
6.d Fitted hexagon refined as free rotating group:
 C29(C30,C31,C32,C33,C34), C29A(C30A,C31A,C32A,C33A,C34A)
6.e Idealised Me refined as rotating group:
 C7(H7A,H7B,H7C), C8(H8A,H8B,H8C)
```

This report has been created with Olex2, compiled on 2018.05.29 svn.r3508 for OlexSys. Please let us know if there are any errors or if you would like to have additional features.

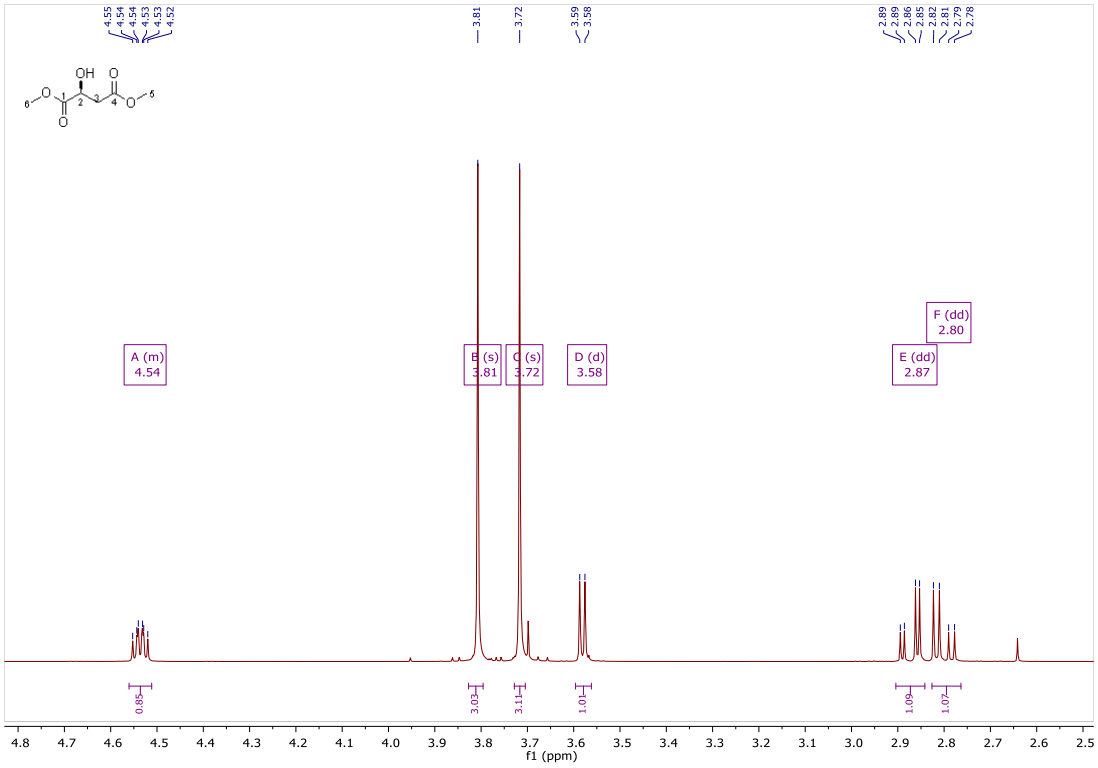
^{1}H & ^{13}C NMR SPECTRA

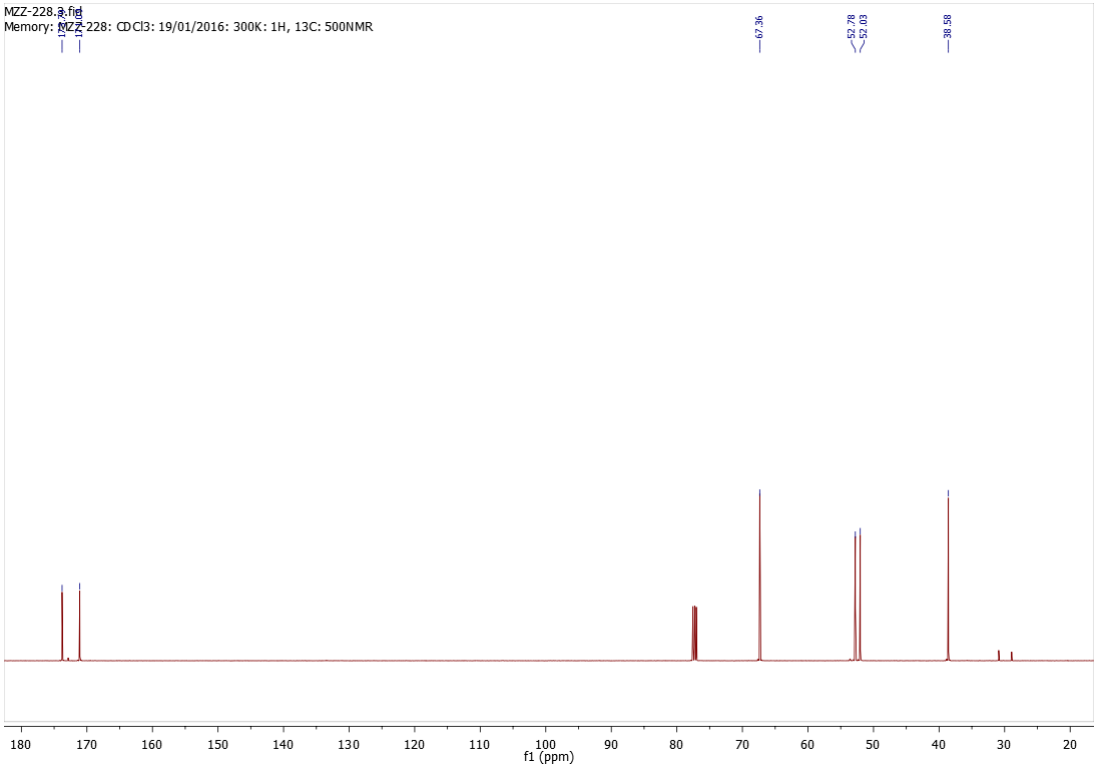
Compound 126



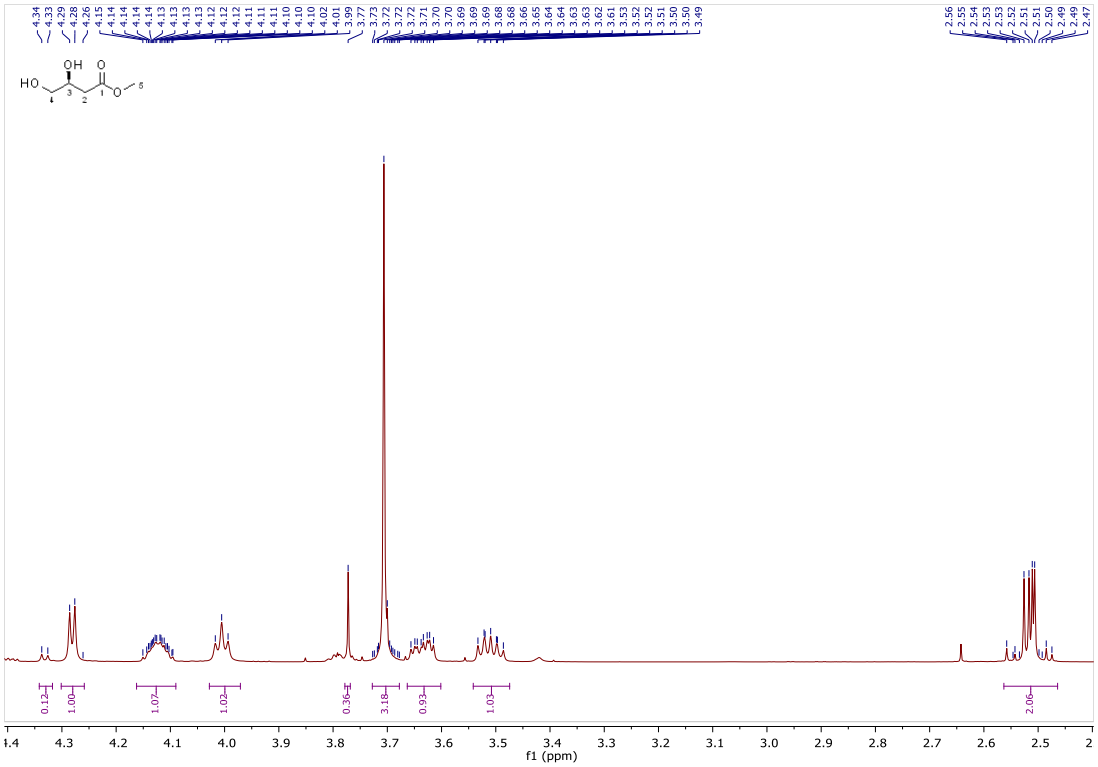


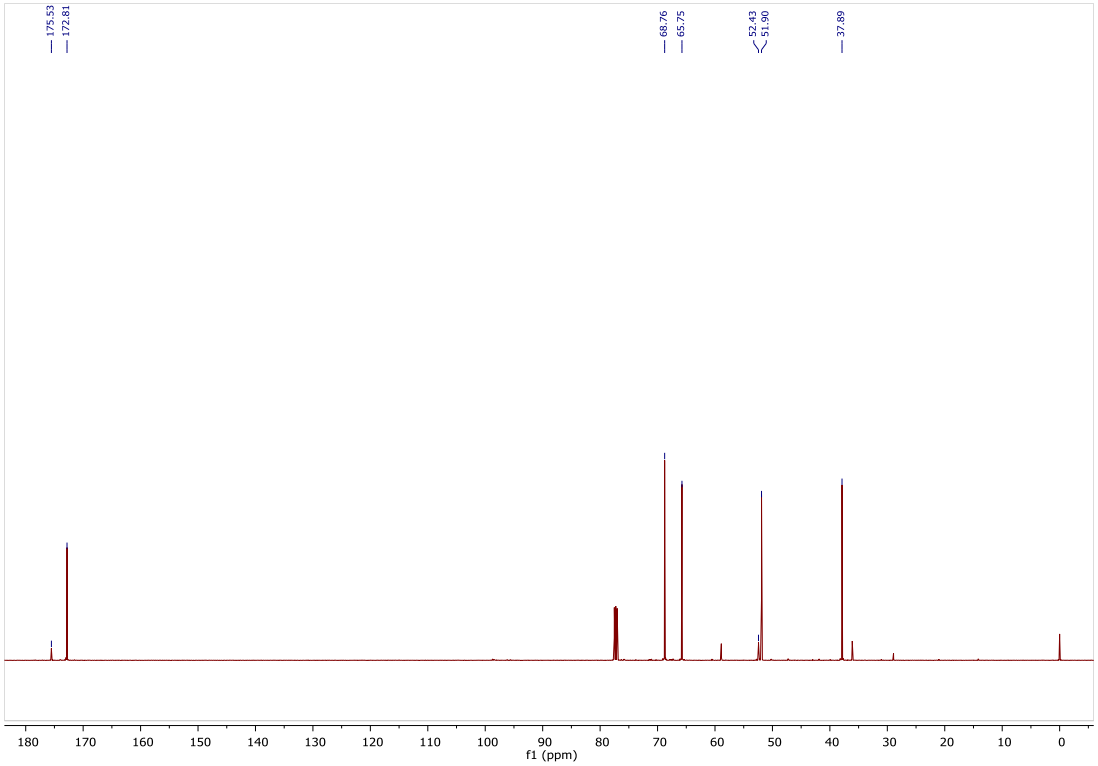
Compound 128

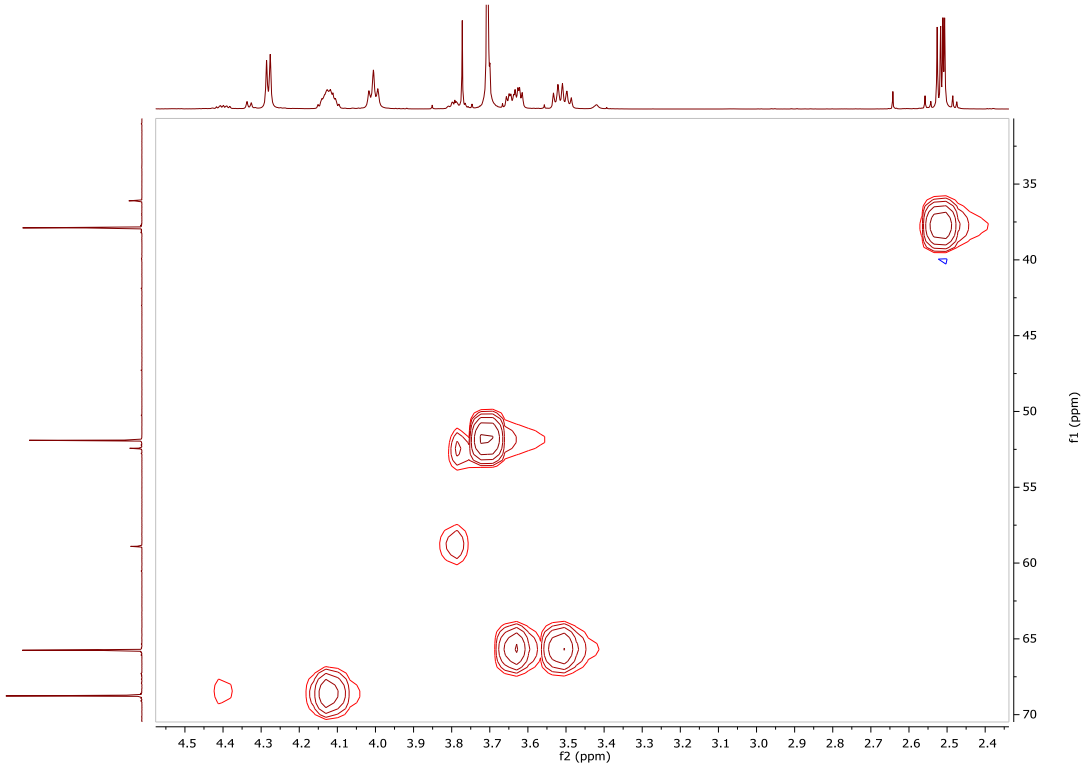




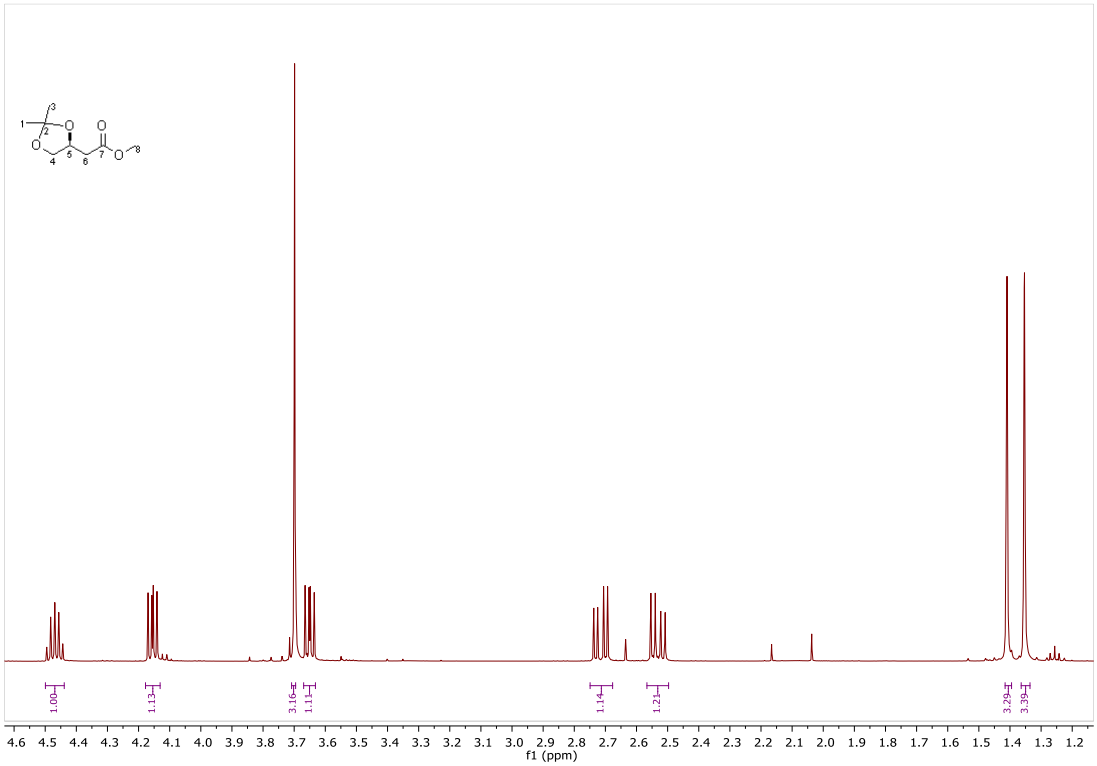
Compound 129

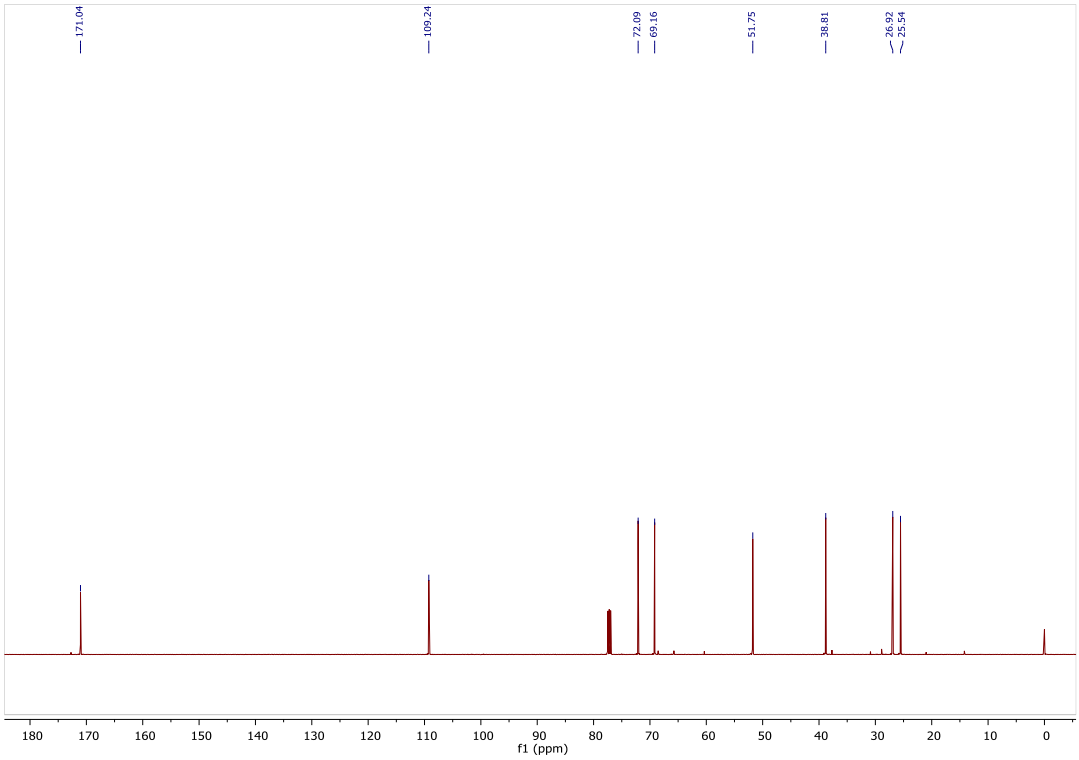


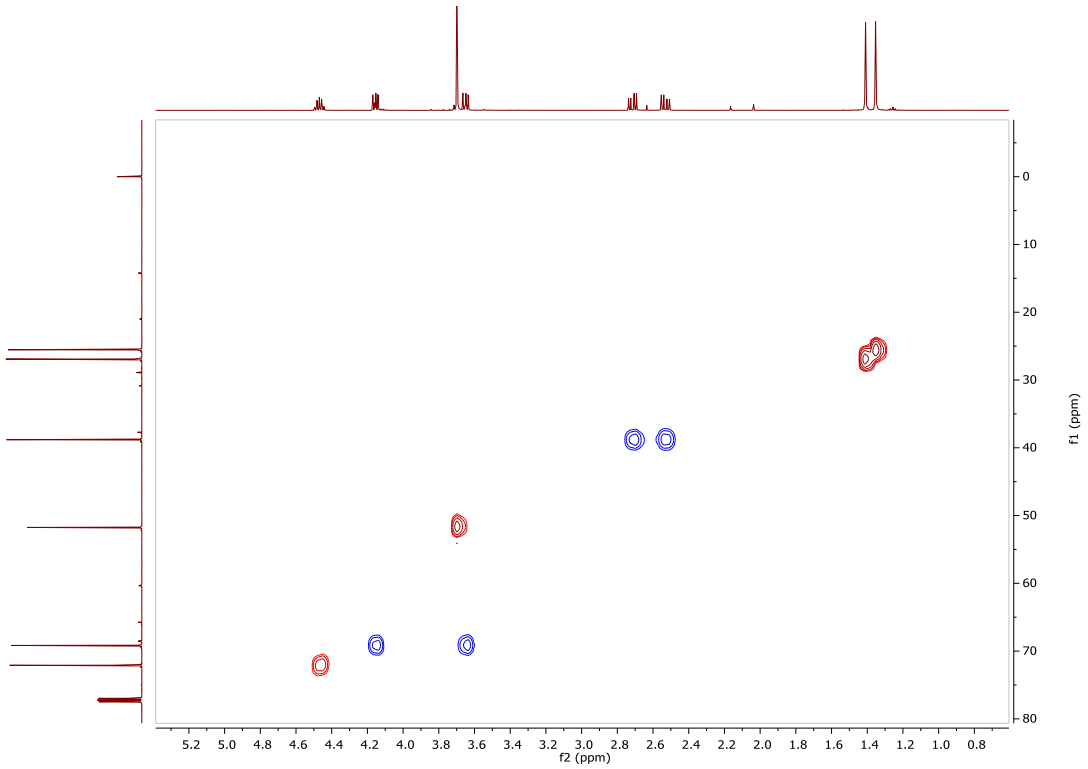




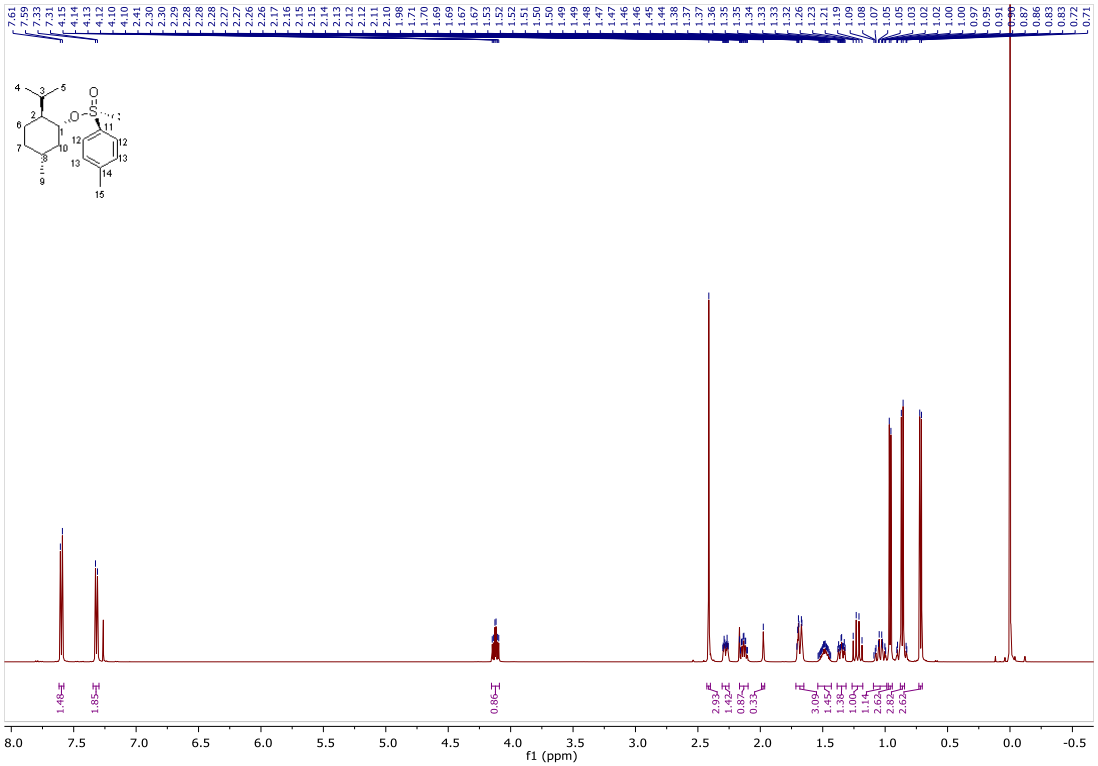
Compound 132

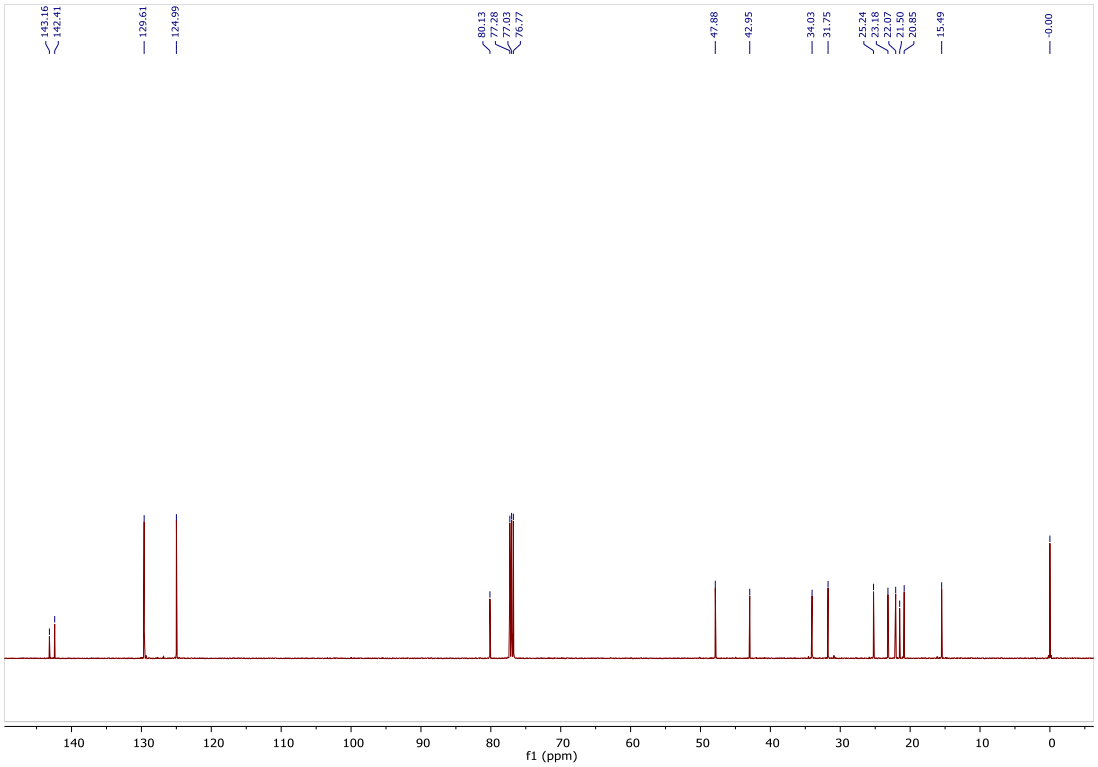


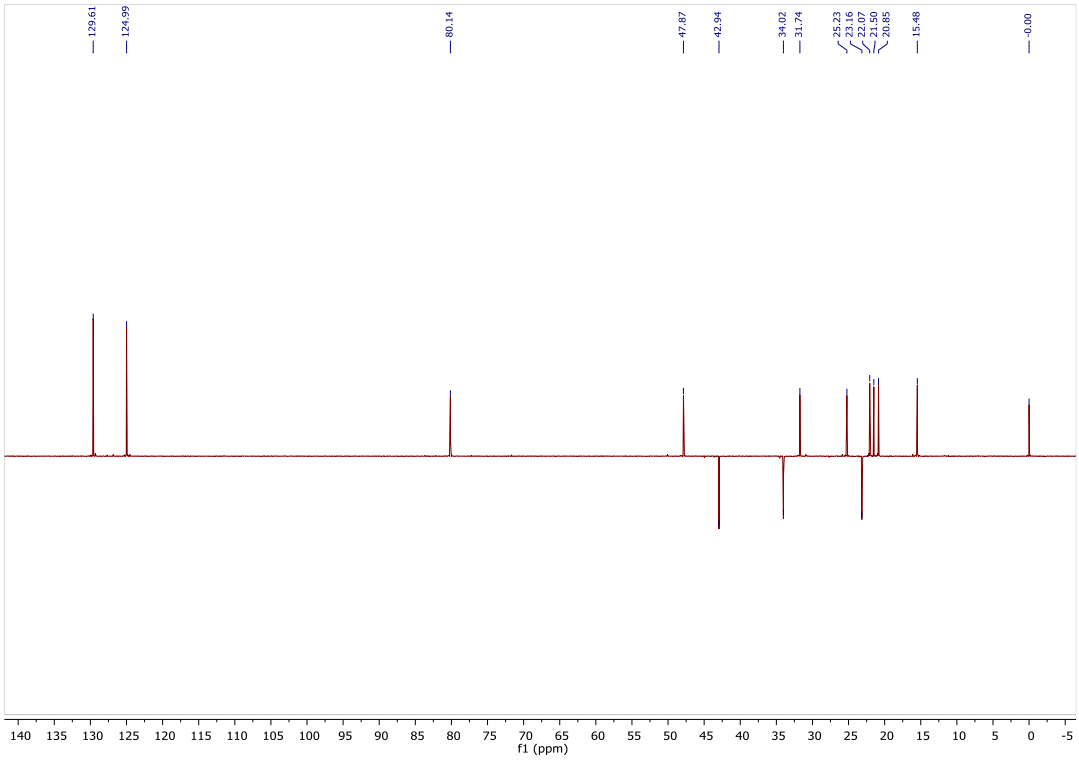

171.04
109.24
72.09
69.16
51.75
38.81
26.92
25.54
f1 (ppm)

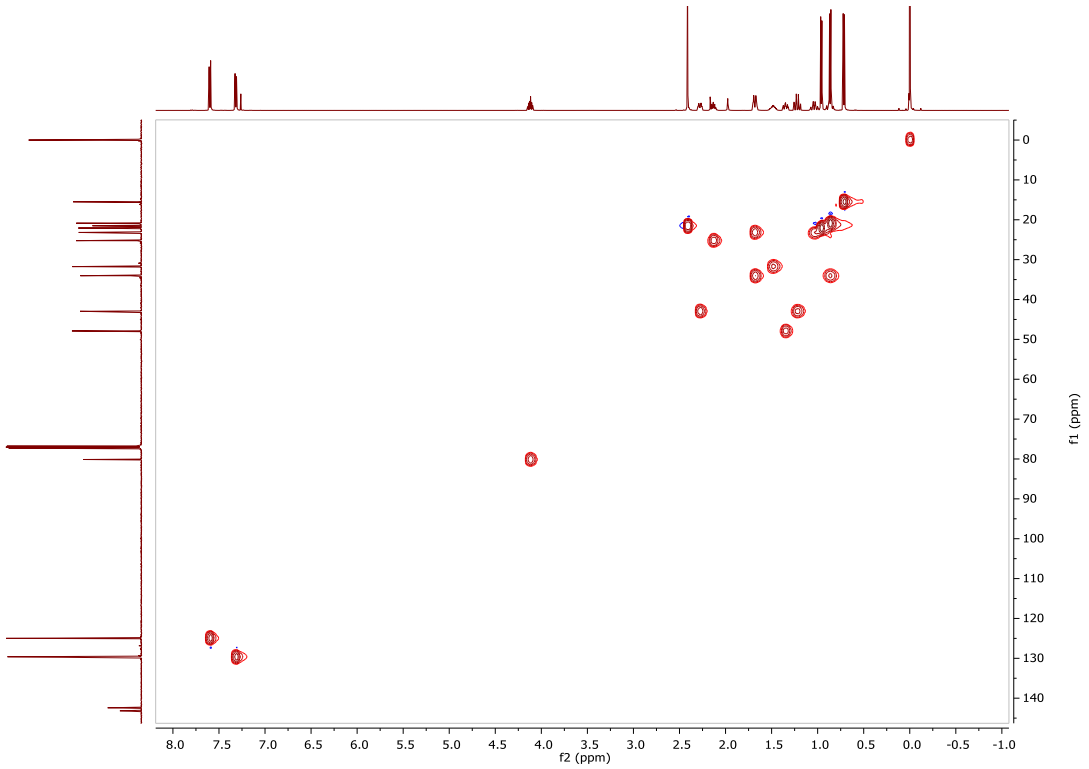

f2 (ppm)
f1 (ppm)

Compound 136

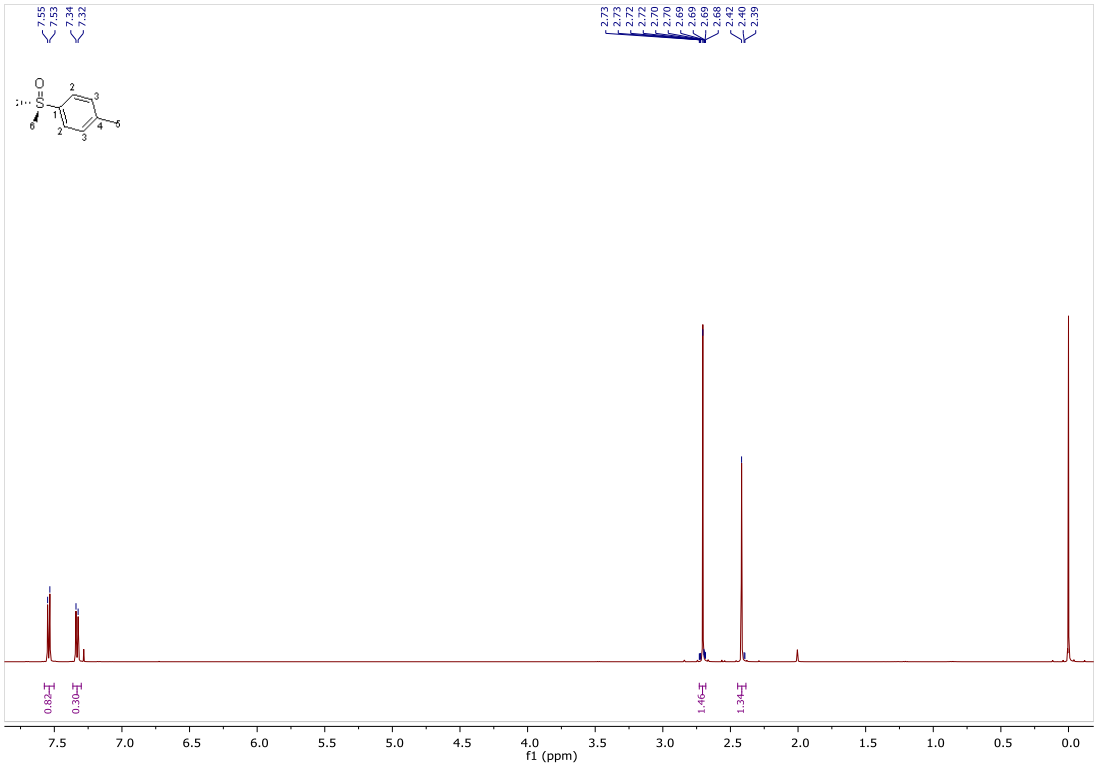


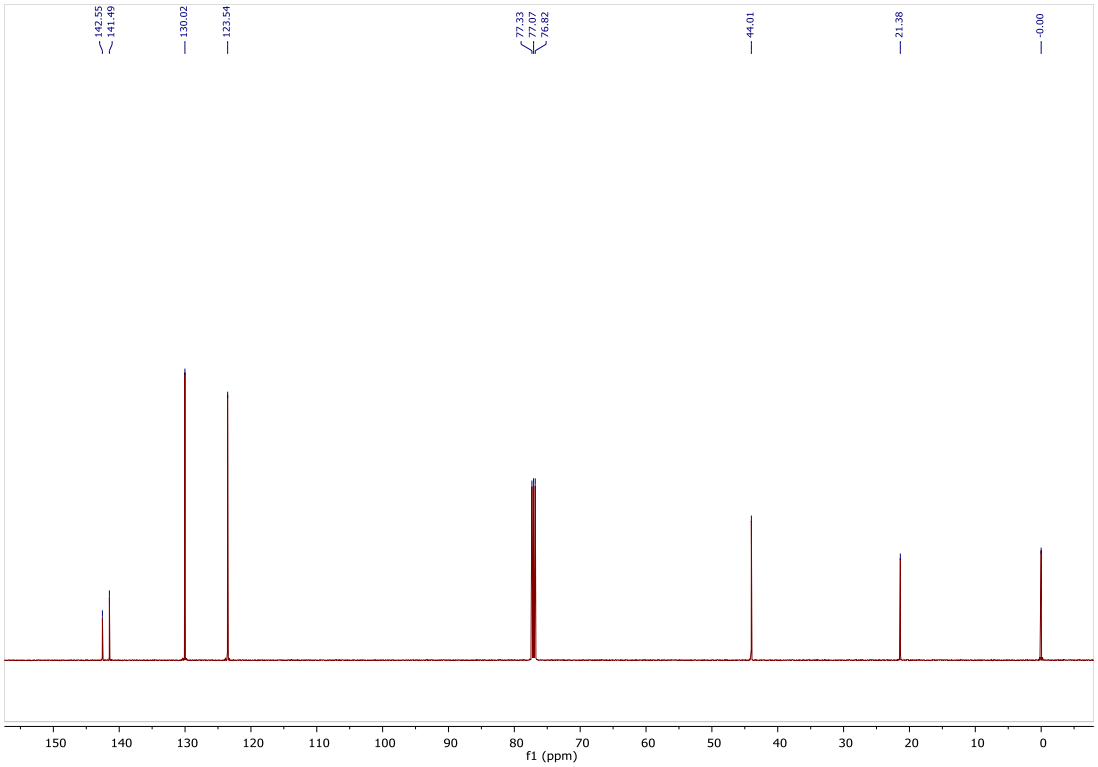



129.61
124.99
80.14
47.87
42.94
34.02
31.74
25.23
23.16
22.07
21.50
20.85
15.48
-0.00
f1 (ppm)

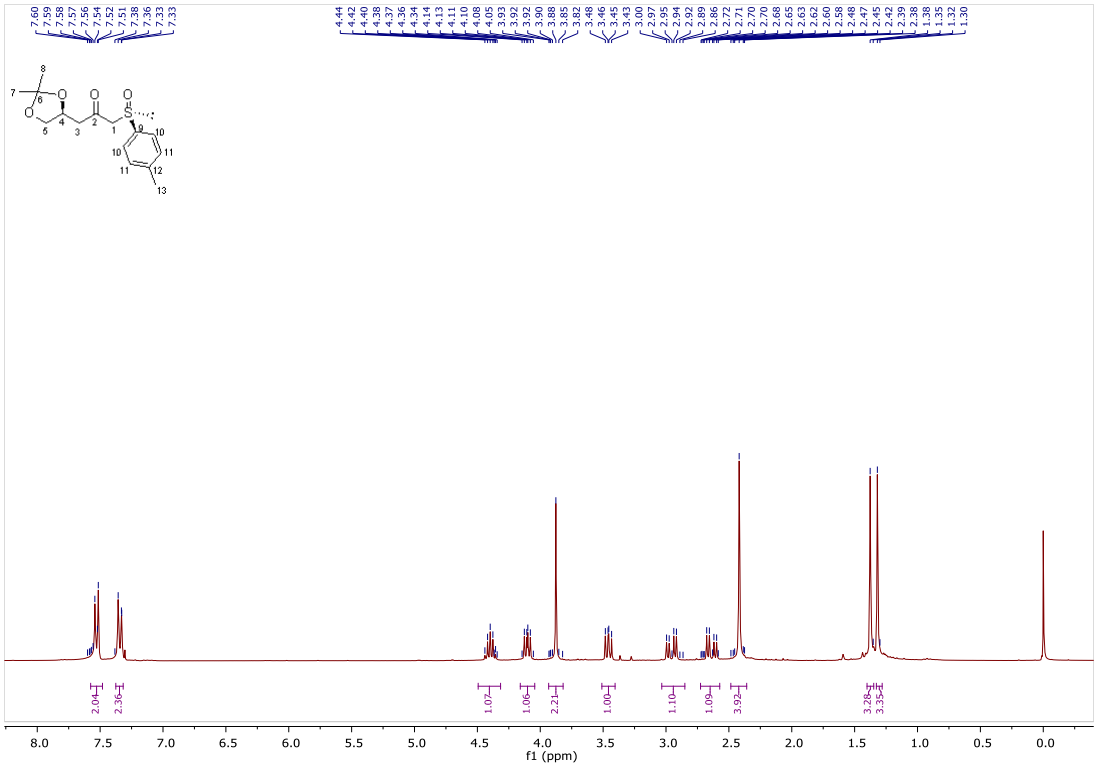

f2 (ppm)
f1 (ppm)

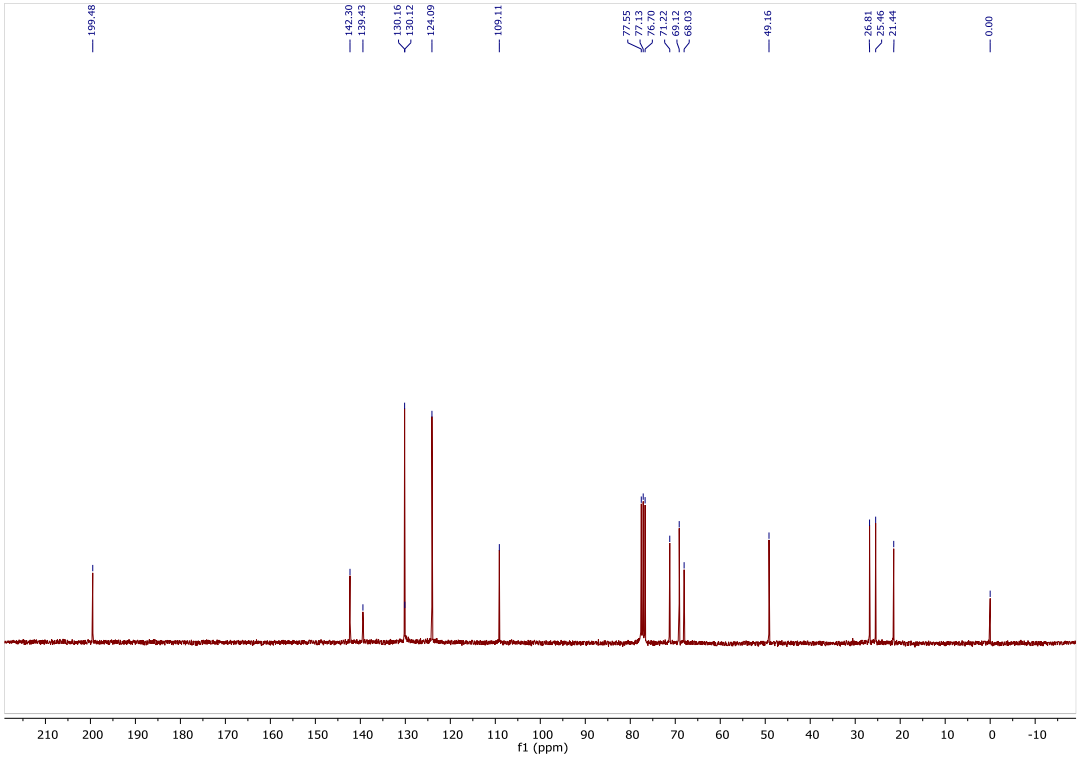
Compound 137

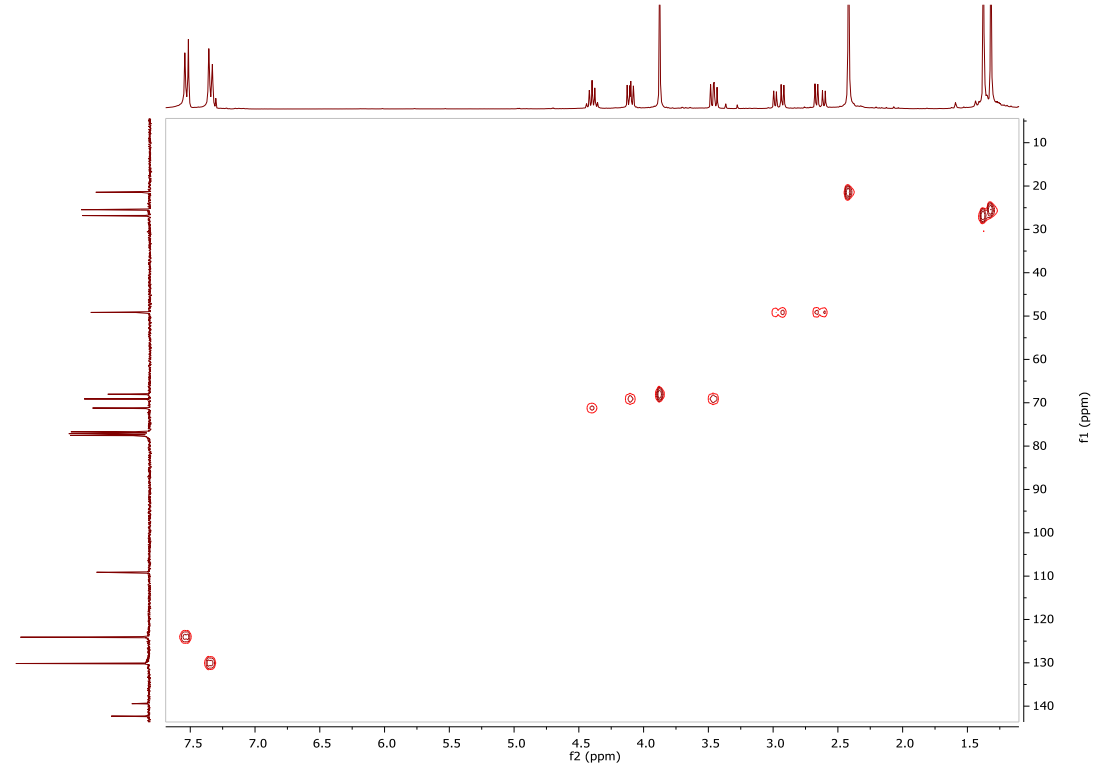


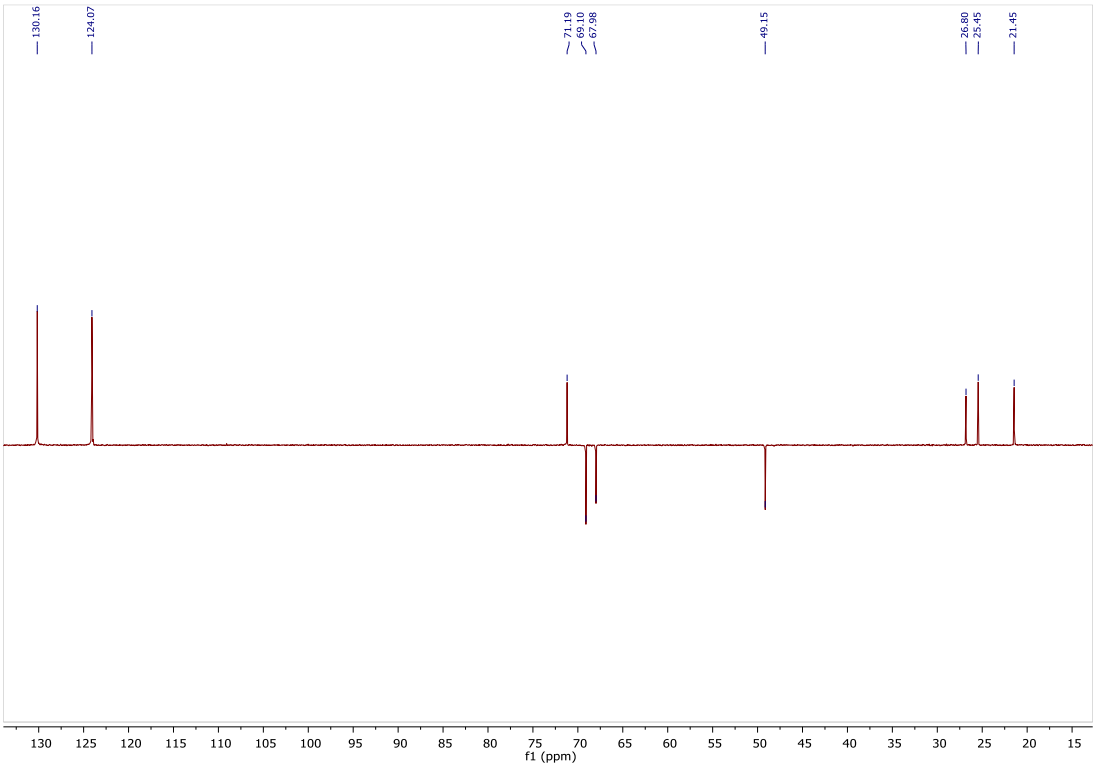


Compound 138

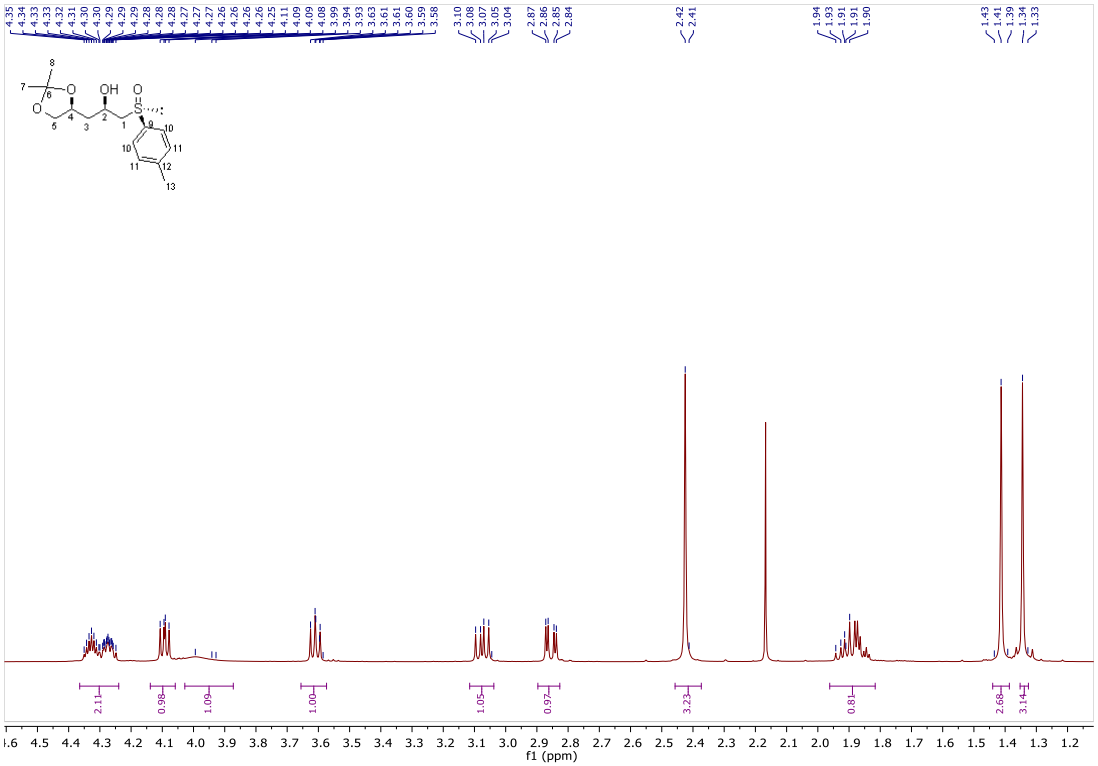


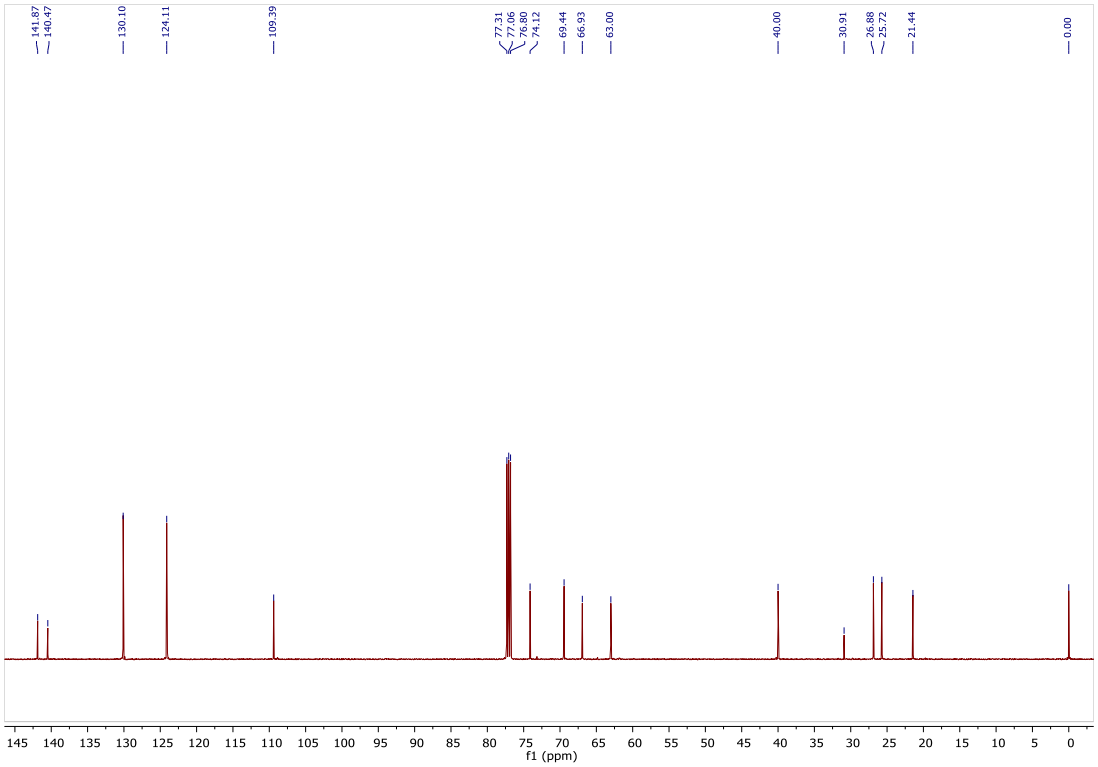


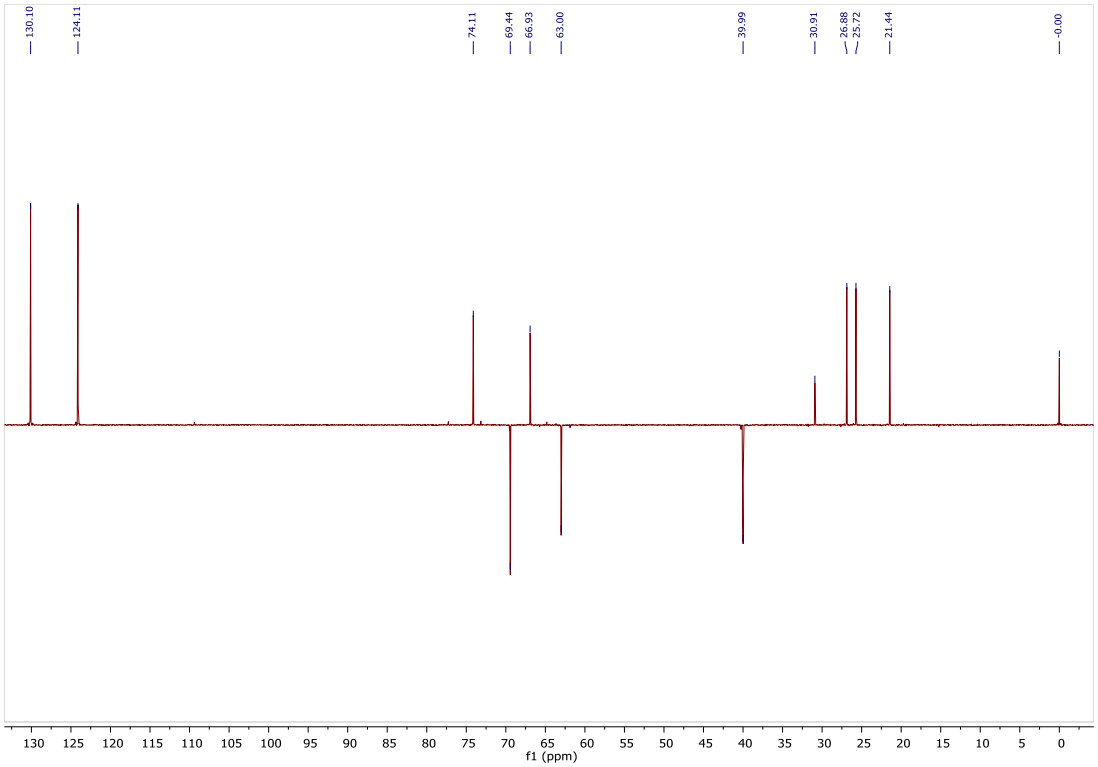

f2 (ppm)
f1 (ppm)

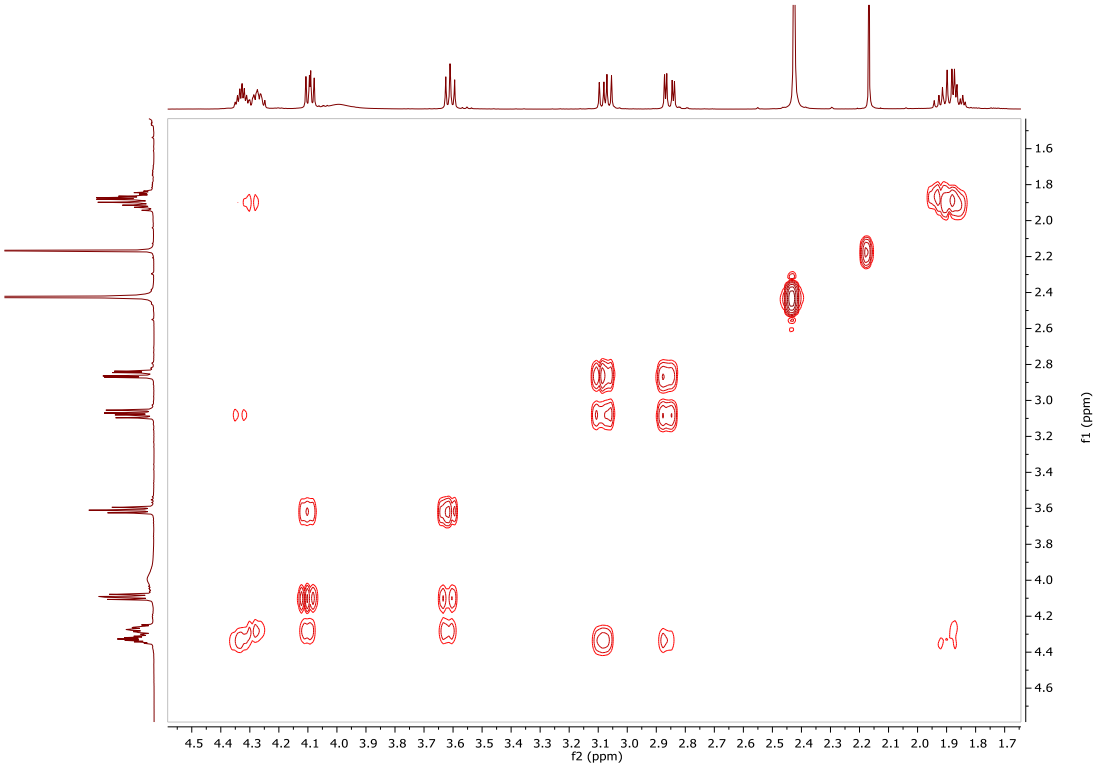

130.16
124.07
71.19
69.10
67.98
49.15
26.80
25.45
21.45
f1 (ppm)

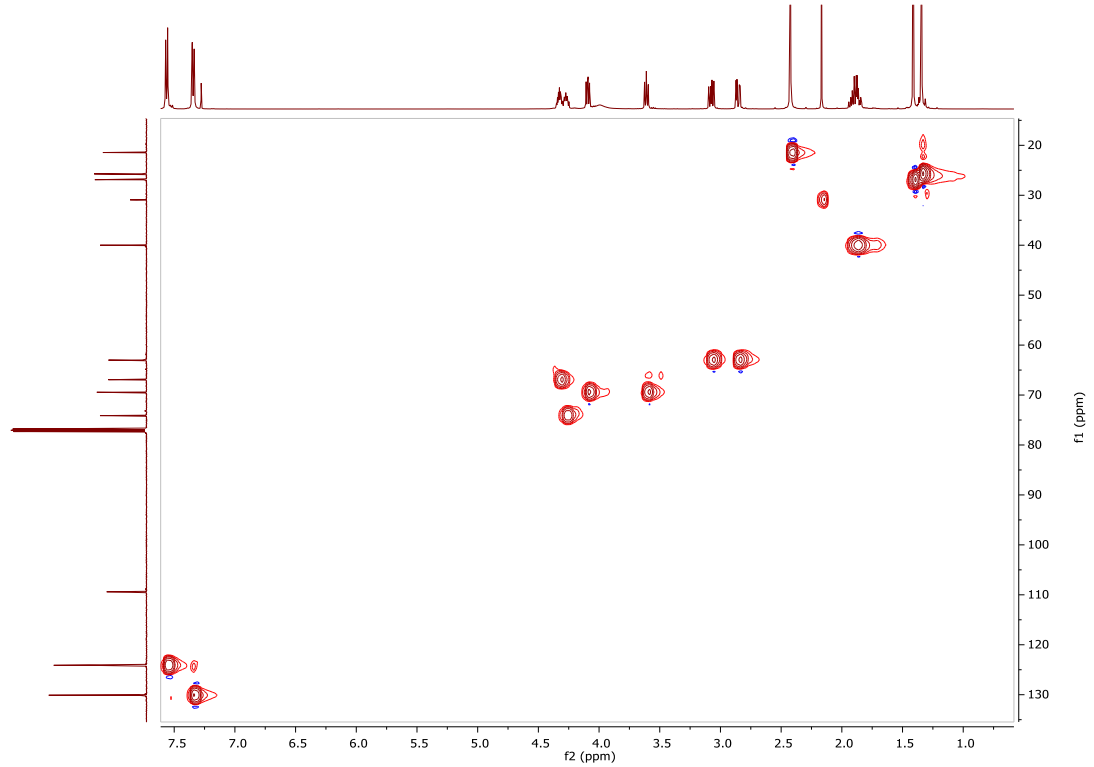
Compound 139



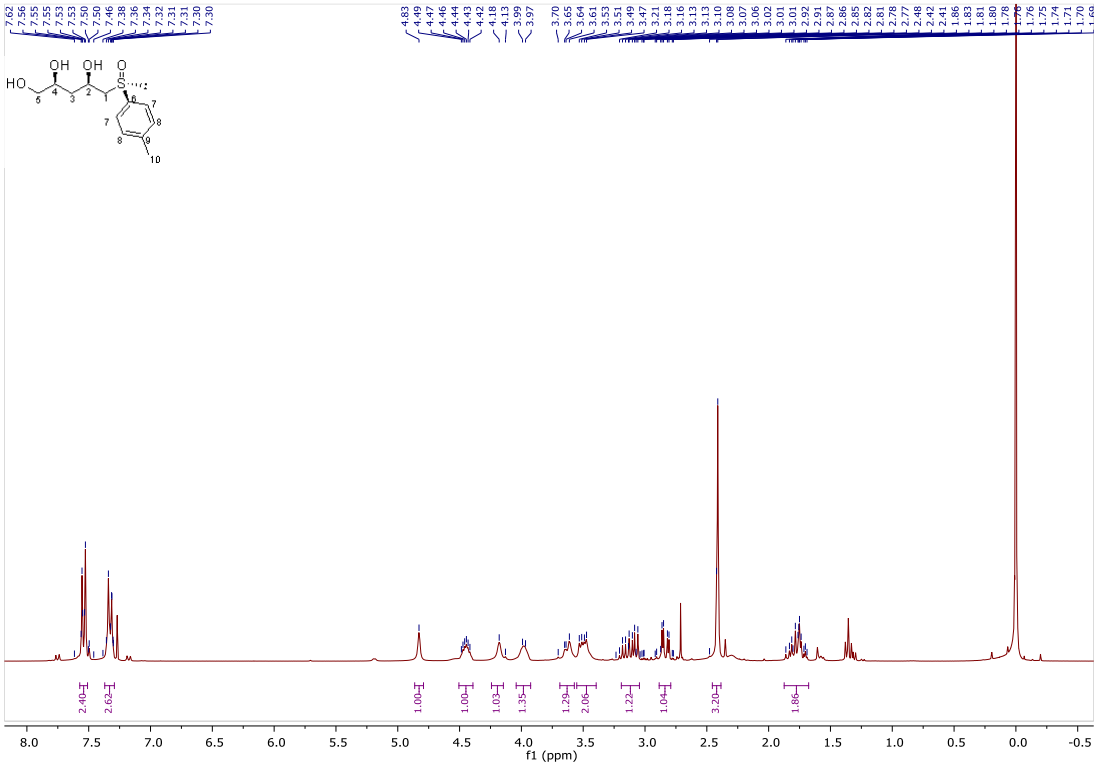


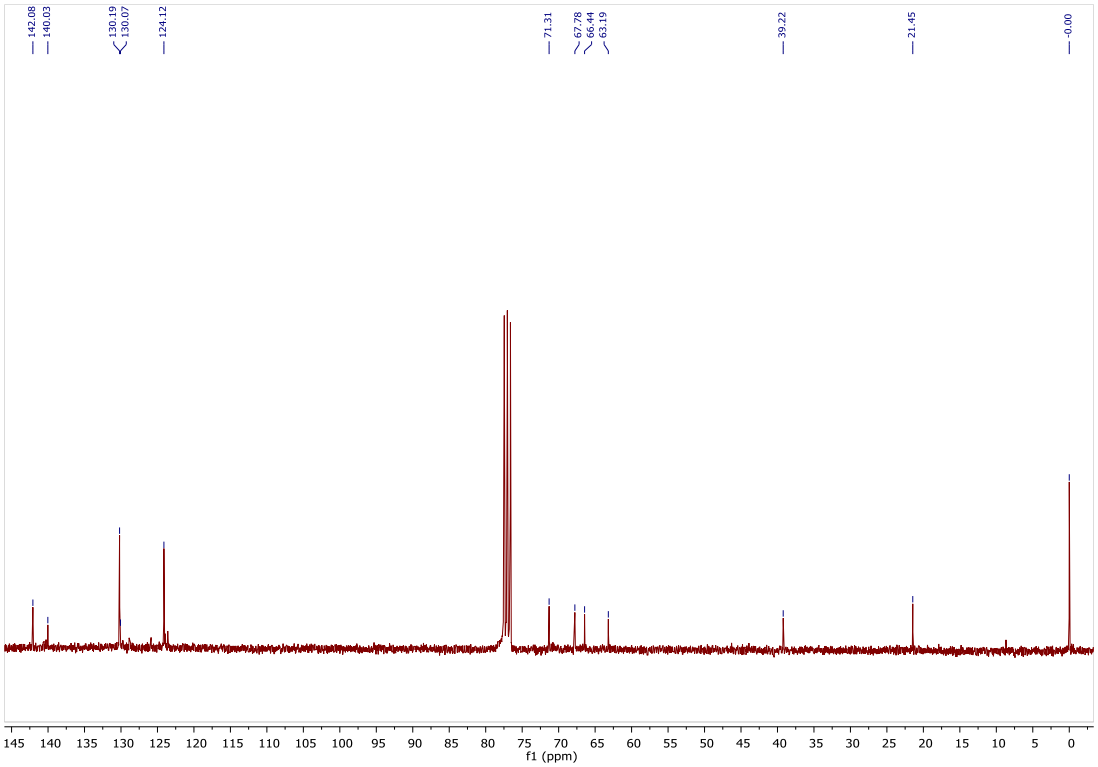

130.10
124.11
74.11
69.44
66.93
63.00
39.99
30.91
26.88
25.72
21.44
0.00
f1 (ppm)

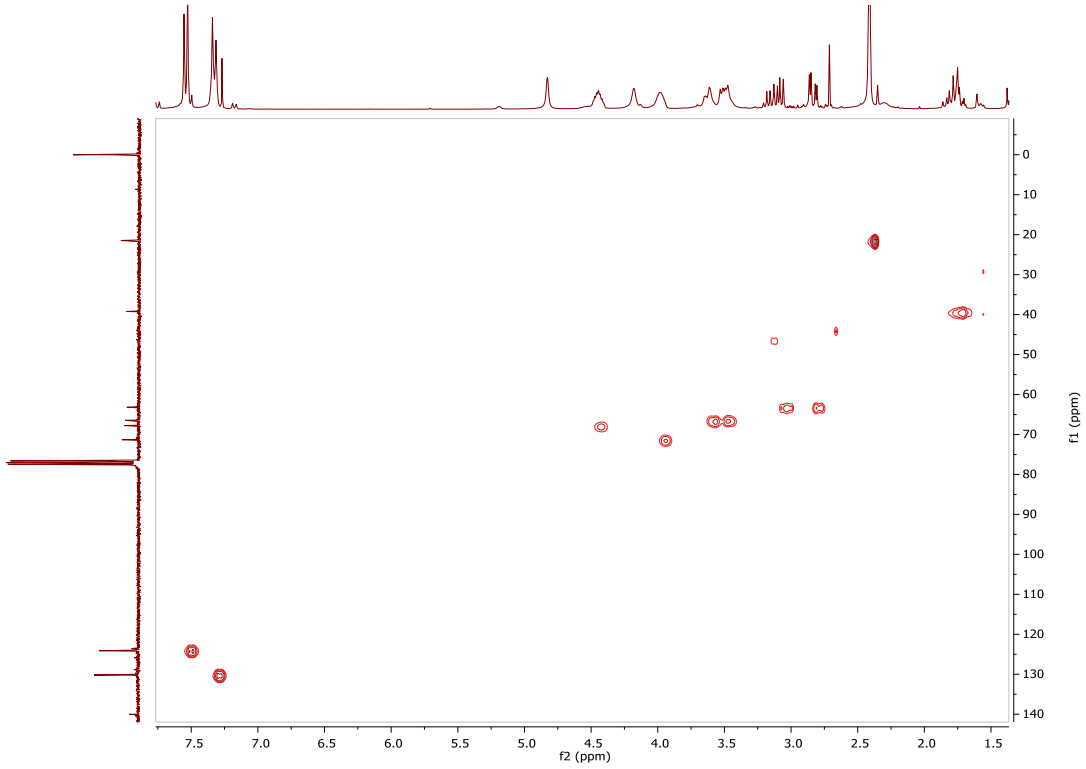

f1 (ppm)
f2 (ppm)



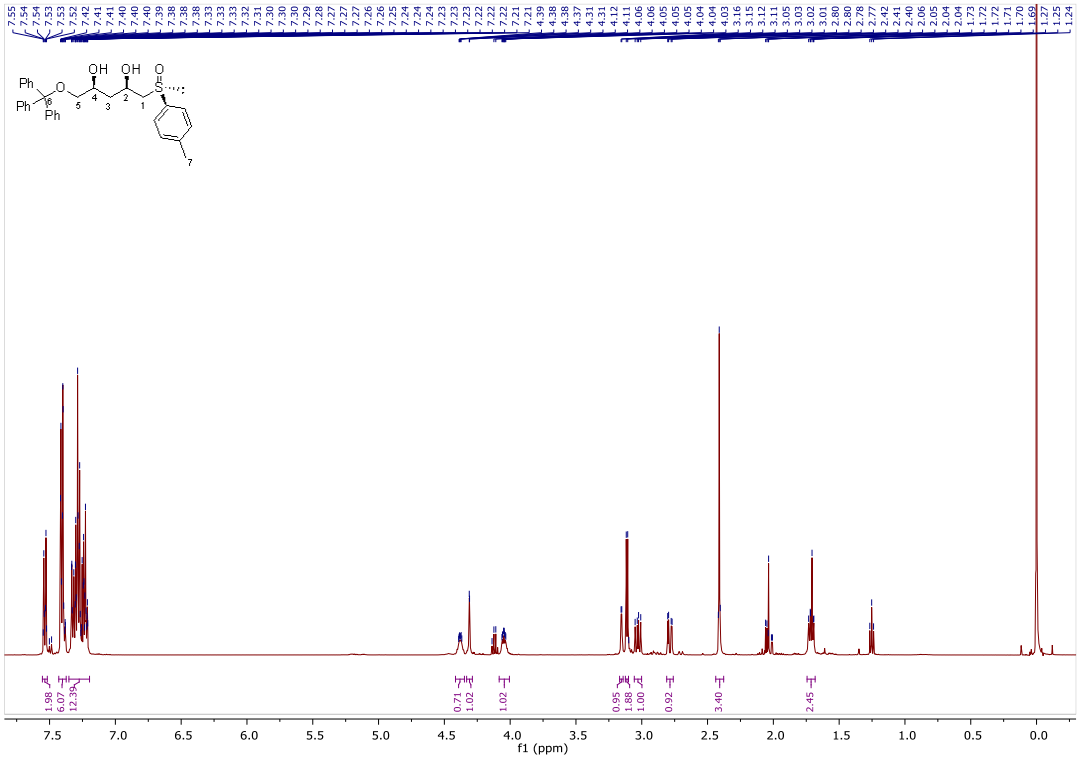
Compound 140

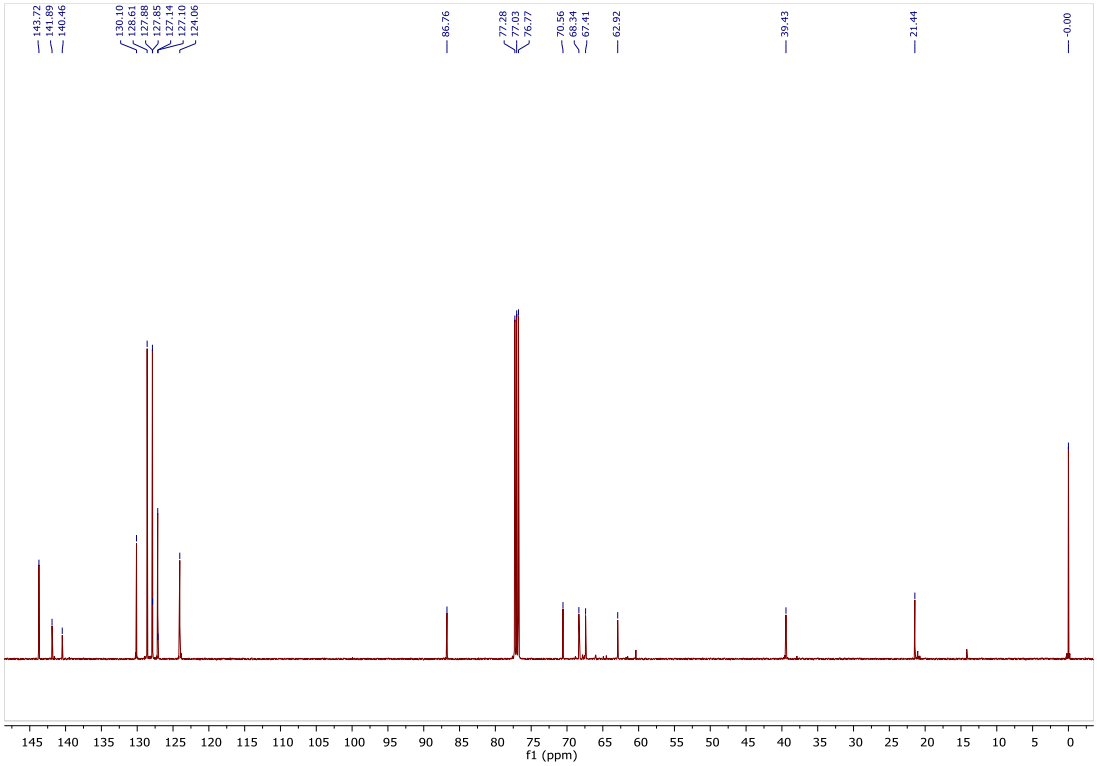


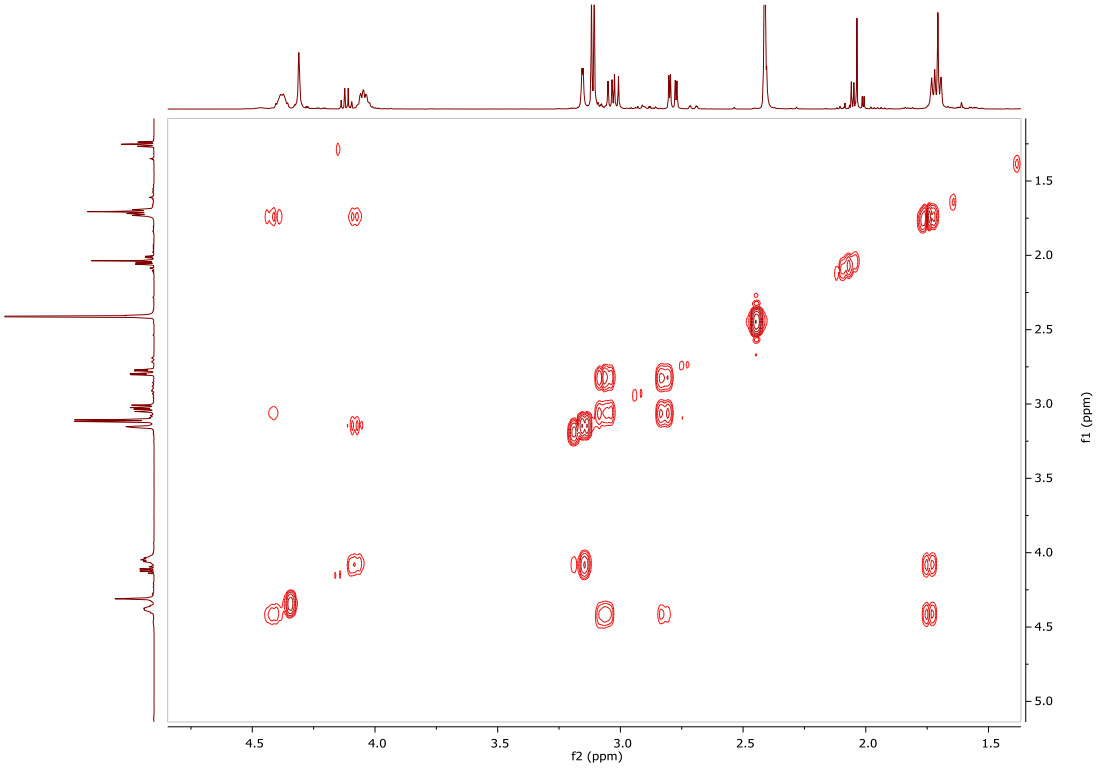

142.08
140.03
130.19
130.07
124.12
71.31
67.78
66.44
63.19
39.22
21.45
0.00
f1 (ppm)

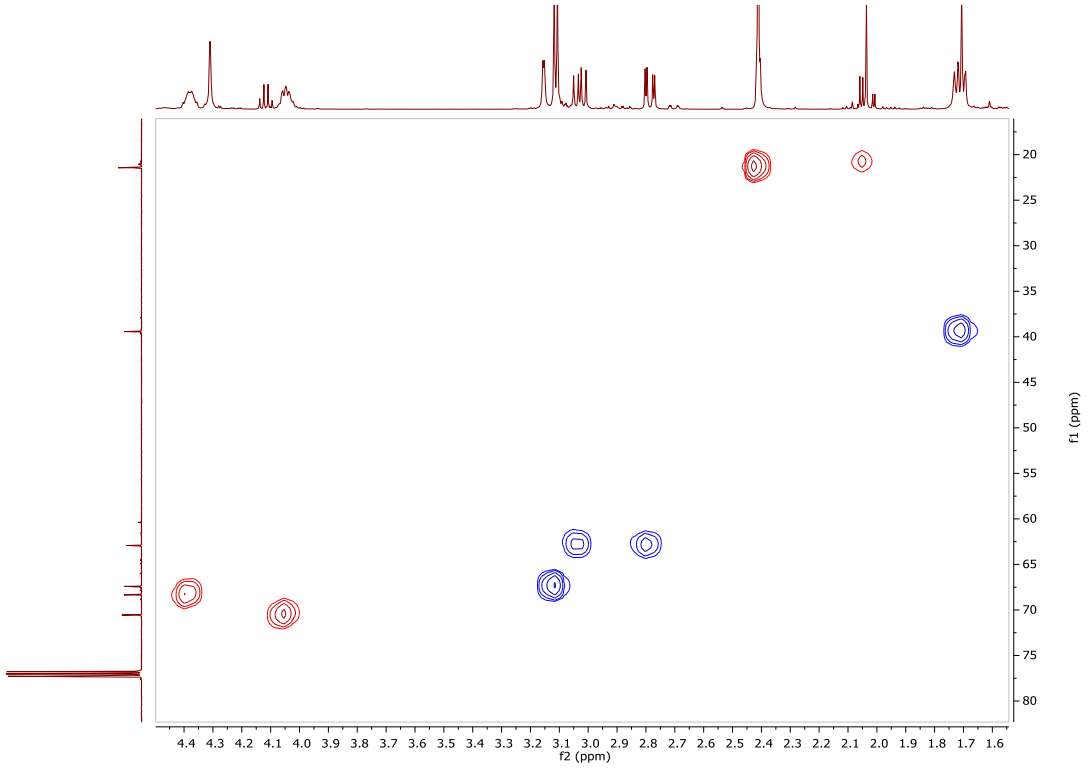

f2 (ppm)
f1 (ppm)

Compound 141

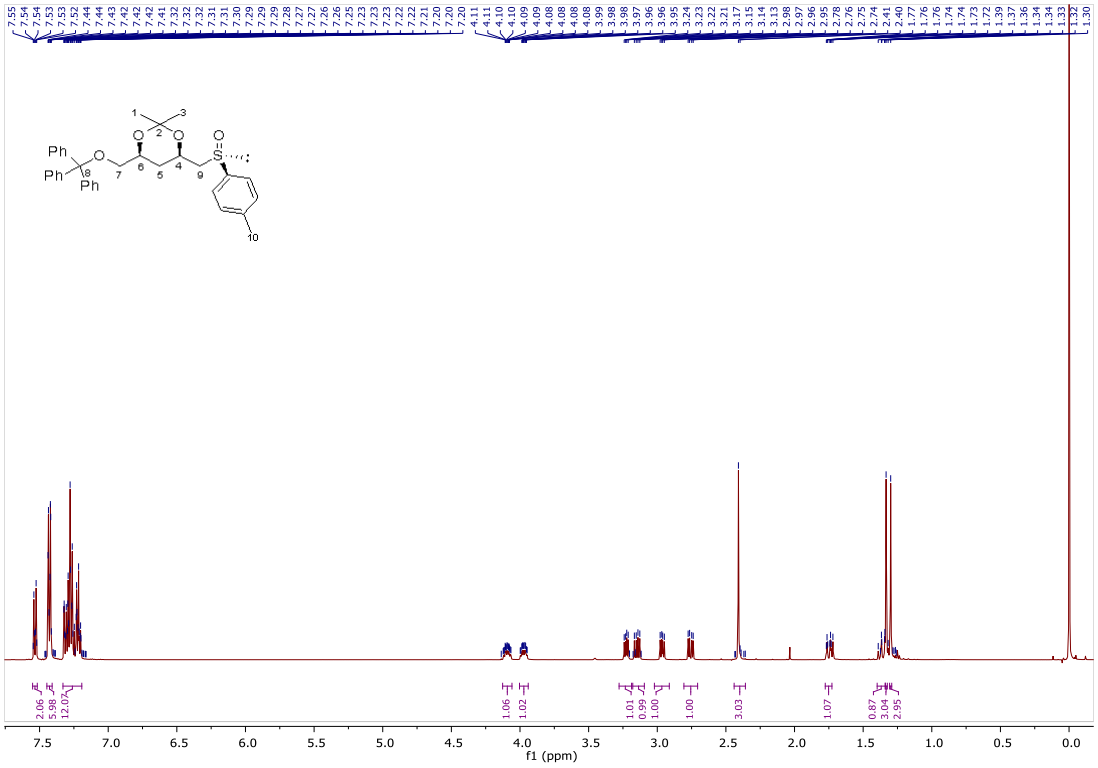


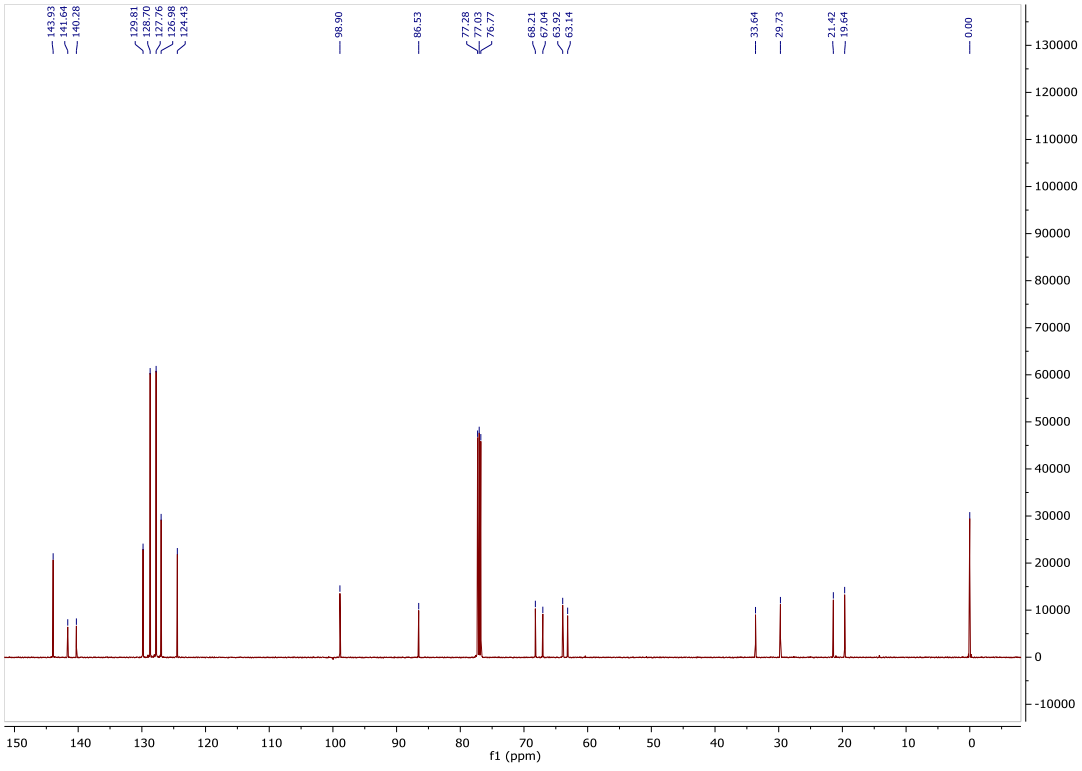


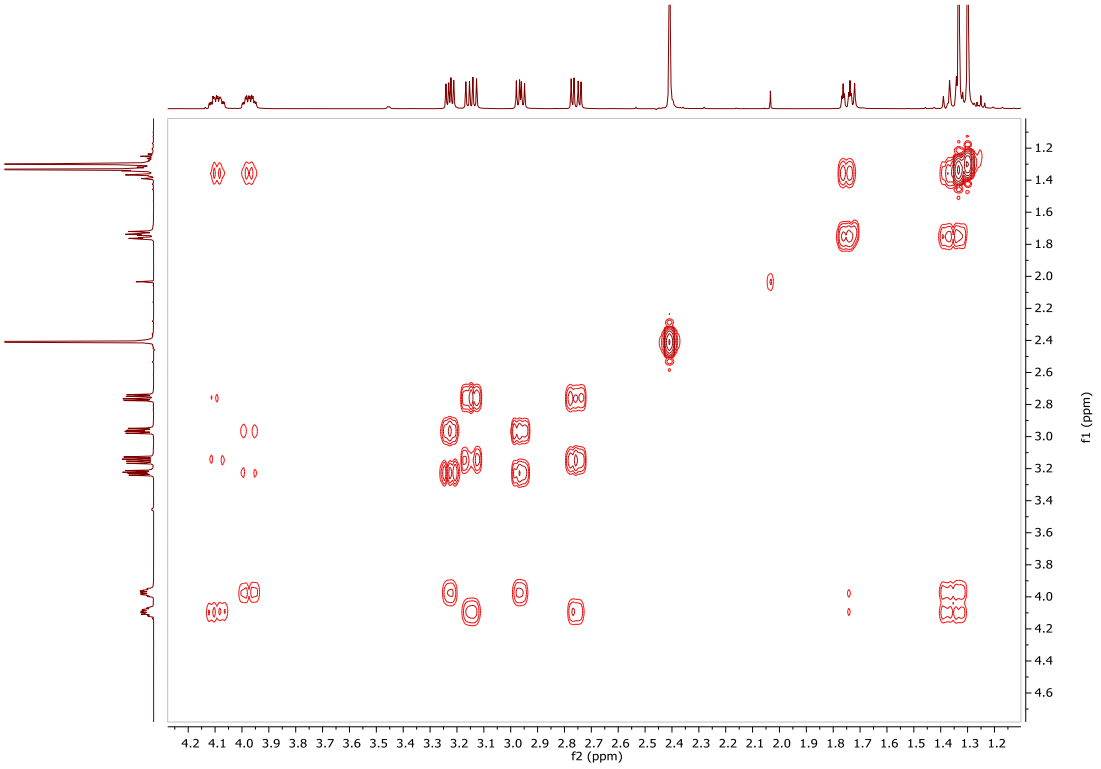

1.5
2.0
2.5
3.0
3.5
4.0
4.5
5.0
f1 (ppm)
4.5
4.0
3.5
3.0
2.5
2.0
1.5
f2 (ppm)

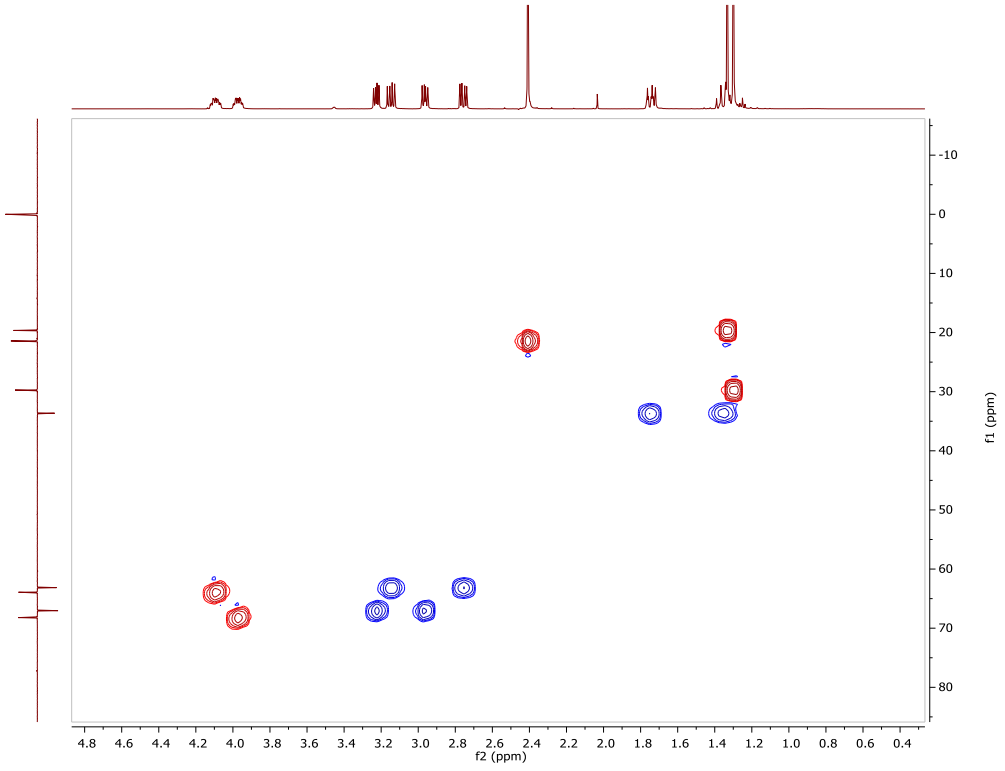

20
25
30
35
40
45
50
55
60
65
70
75
80
f1 (ppm)
4.4 4.3 4.2 4.1 4.0 3.9 3.8 3.7 3.6 3.5 3.4 3.3 3.2 3.1 3.0 2.9 2.8 2.7 2.6 2.5 2.4 2.3 2.2 2.1 2.0 1.9 1.8 1.7 1.6
f2 (ppm)

Compound 124

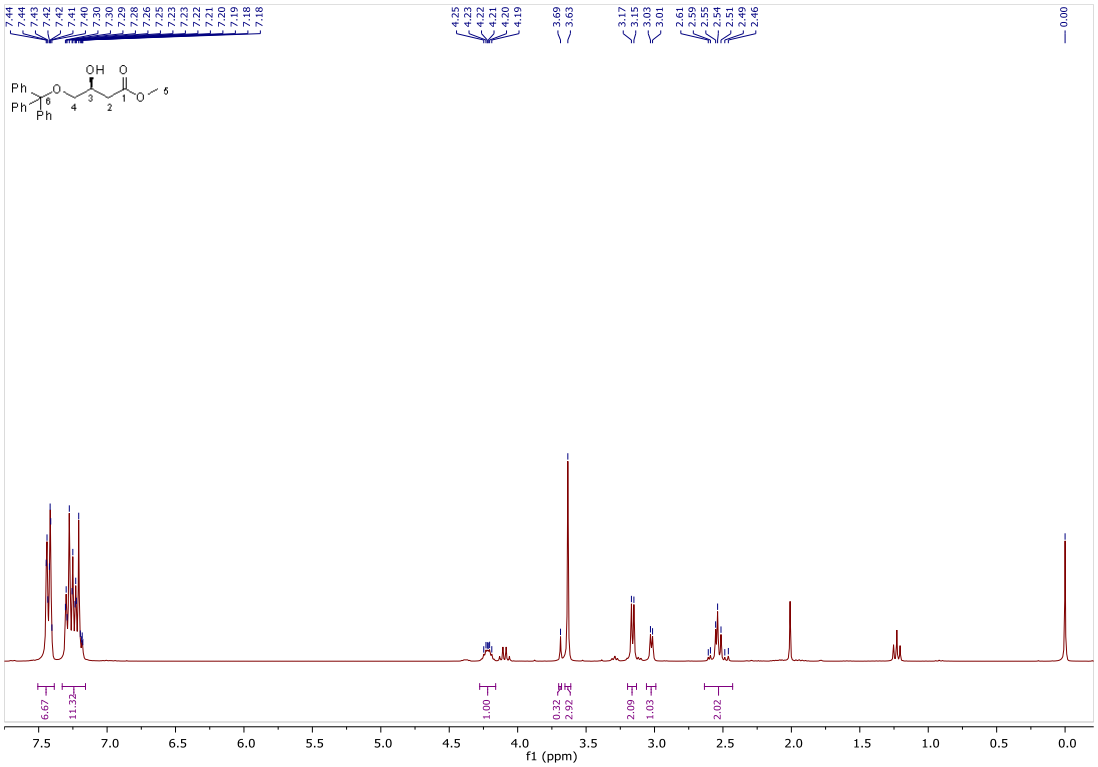


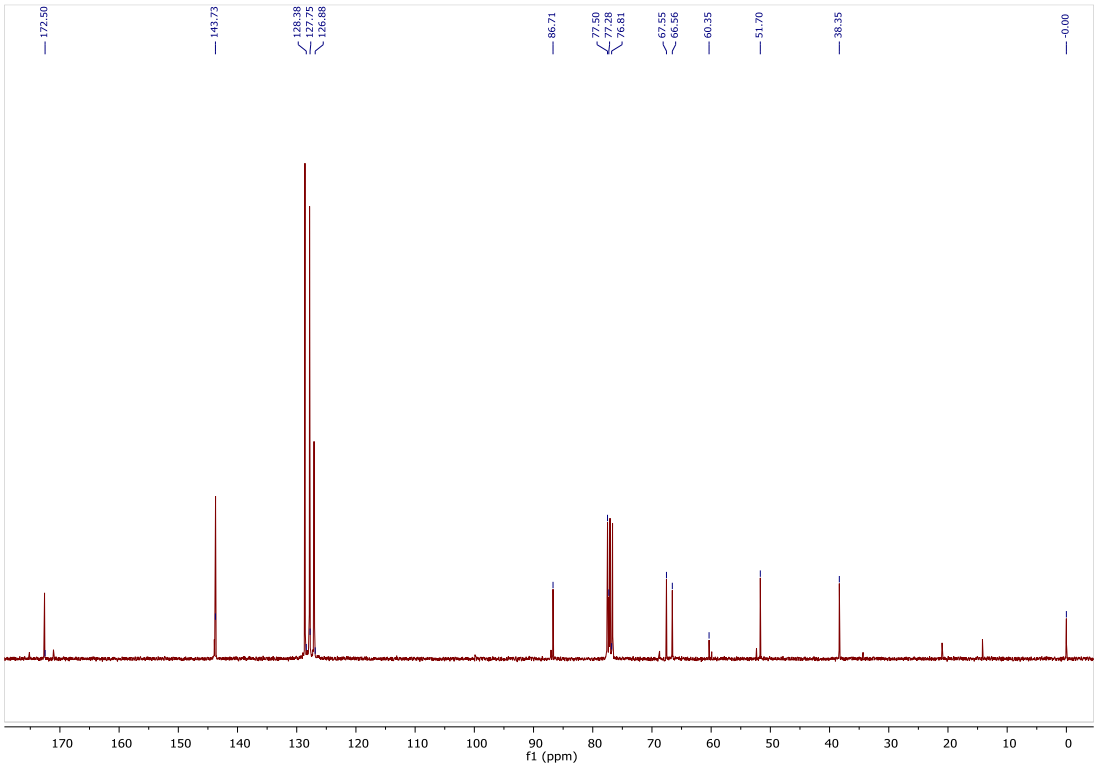




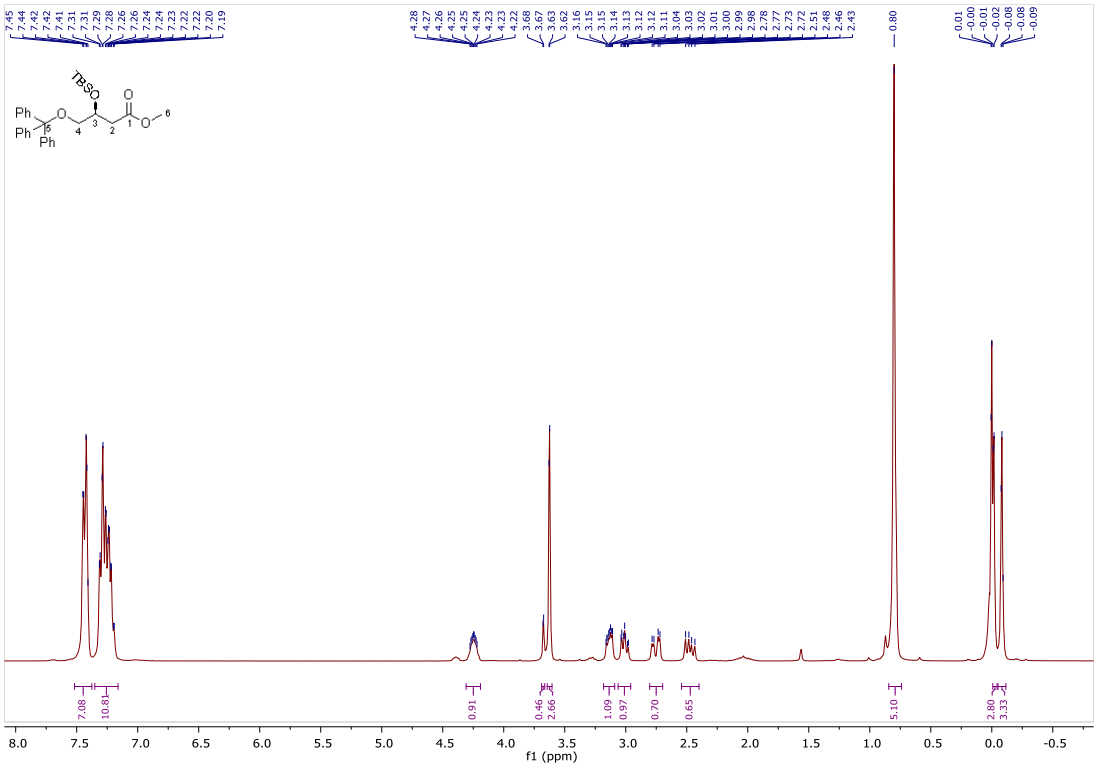


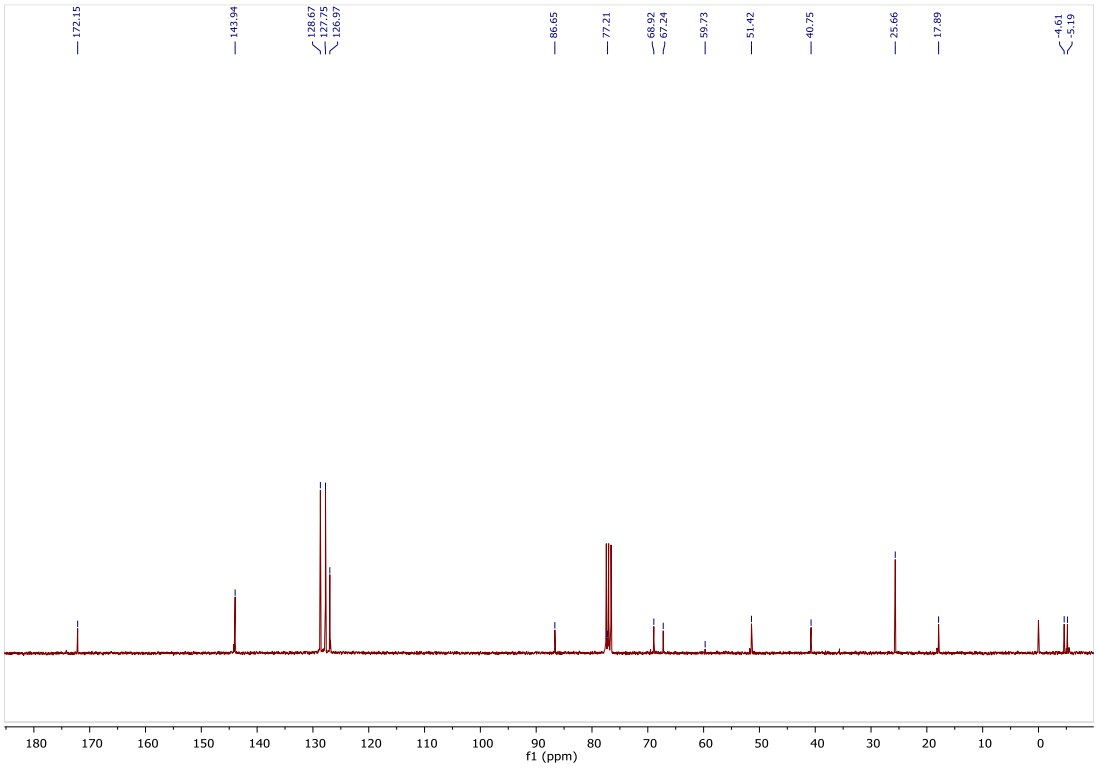
Compound 142



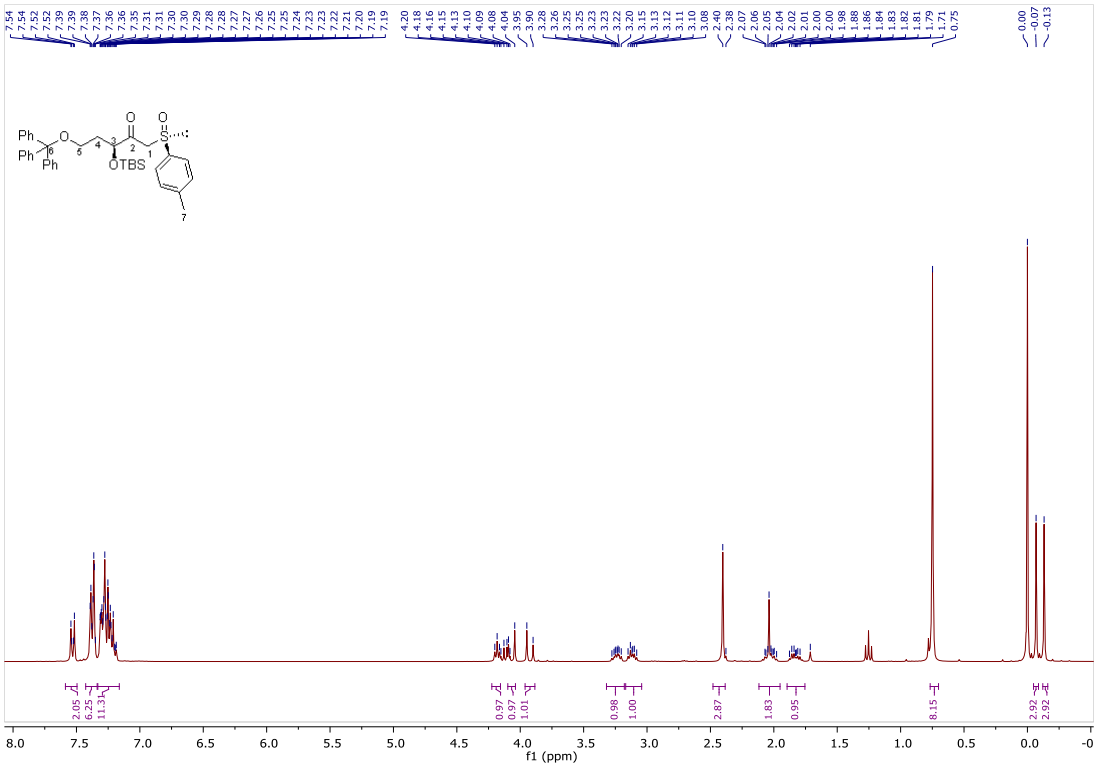


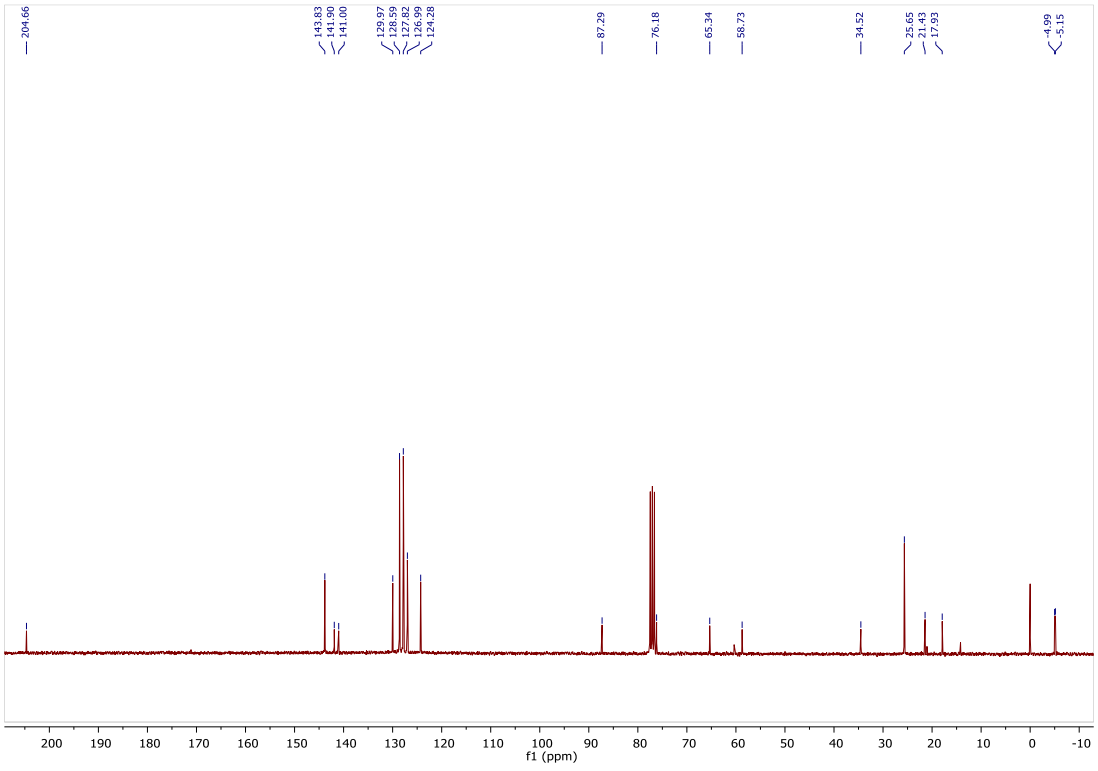
Compound 143



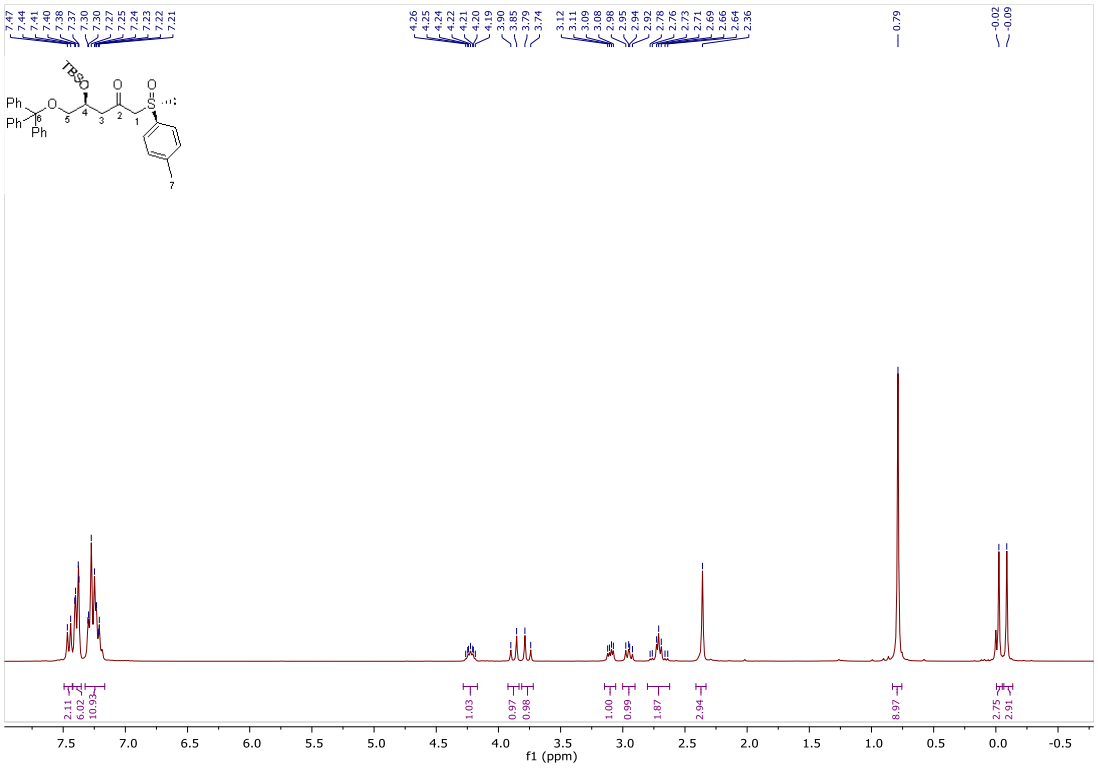


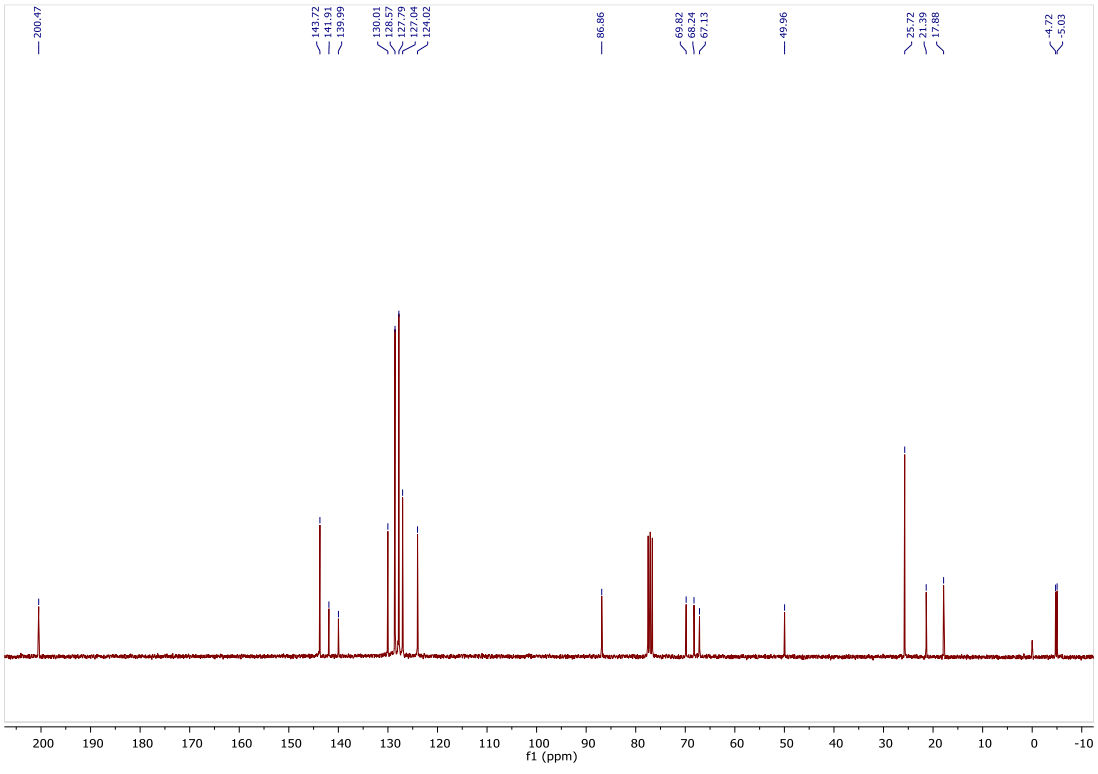
Compound 144



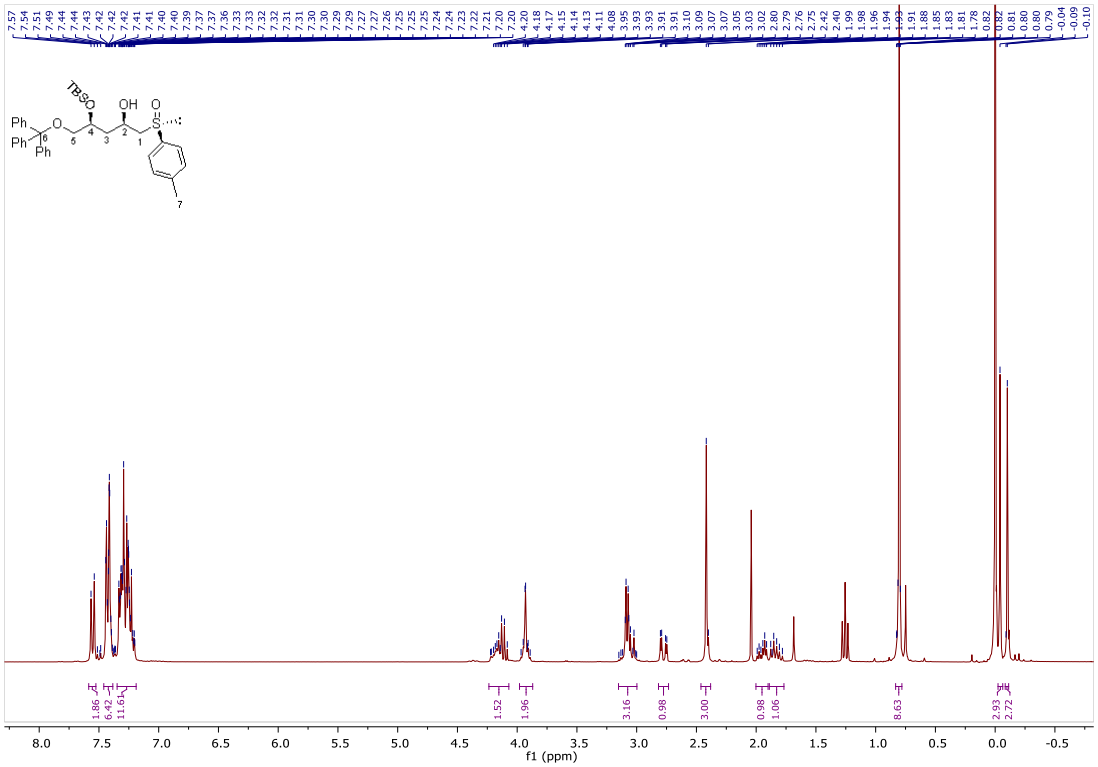


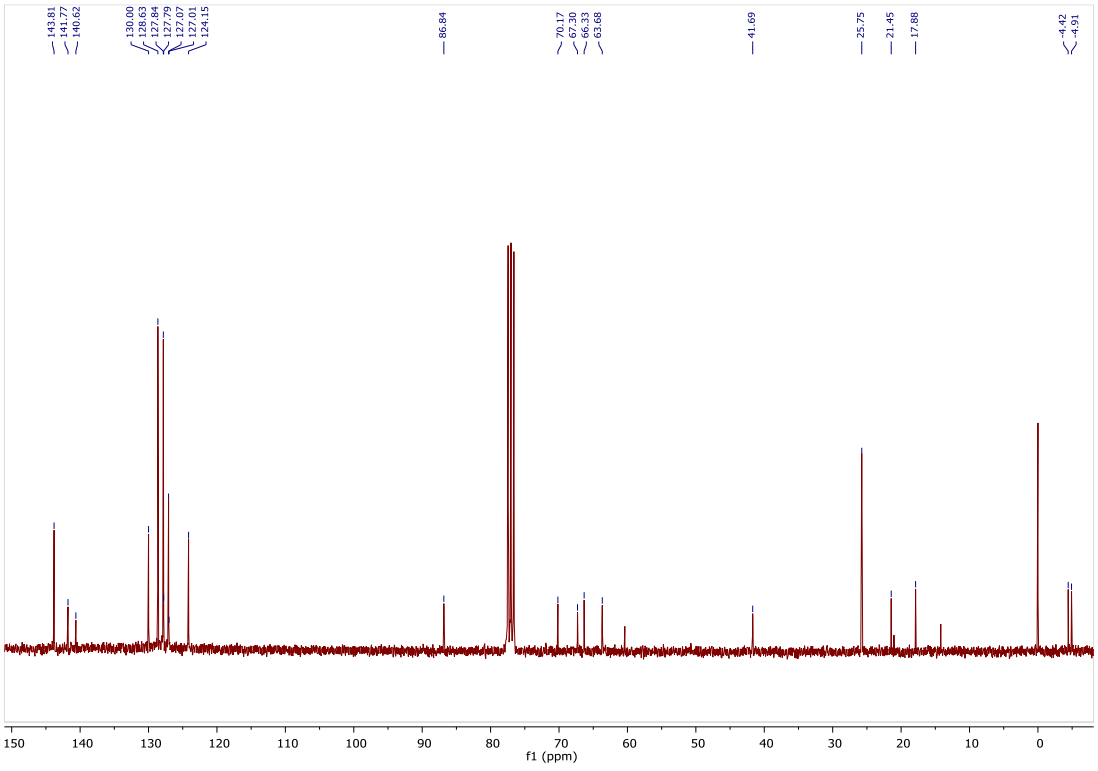
Compound 145



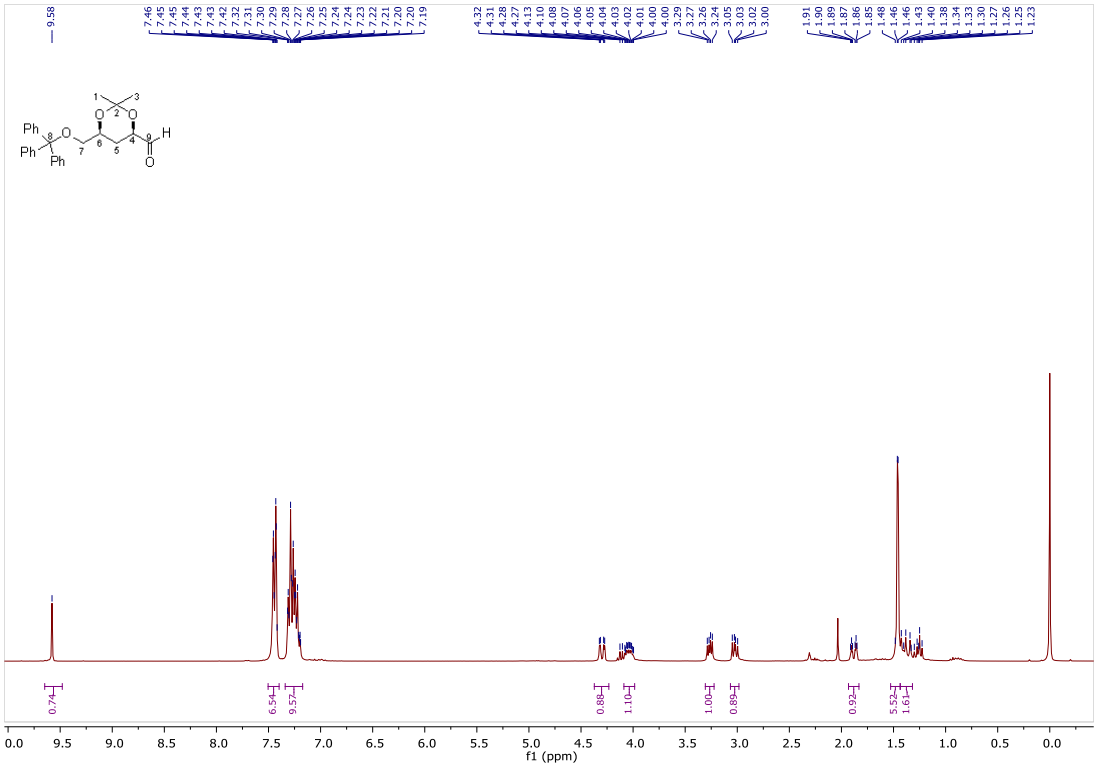


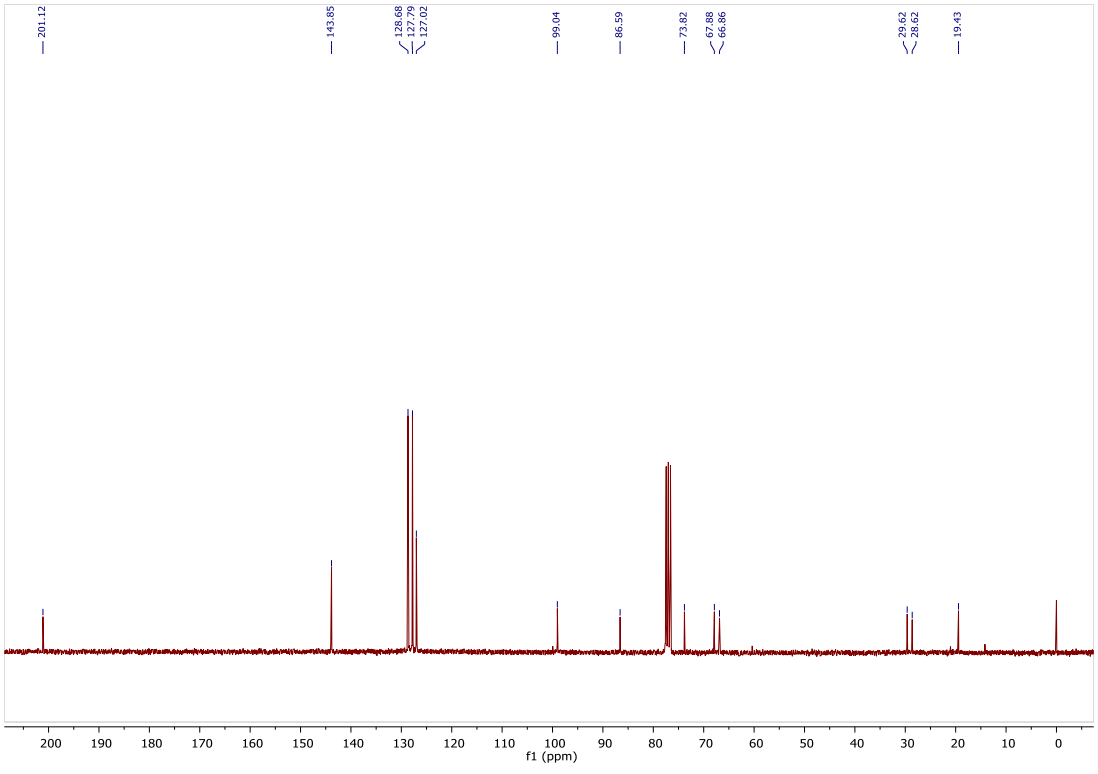
Compound 150



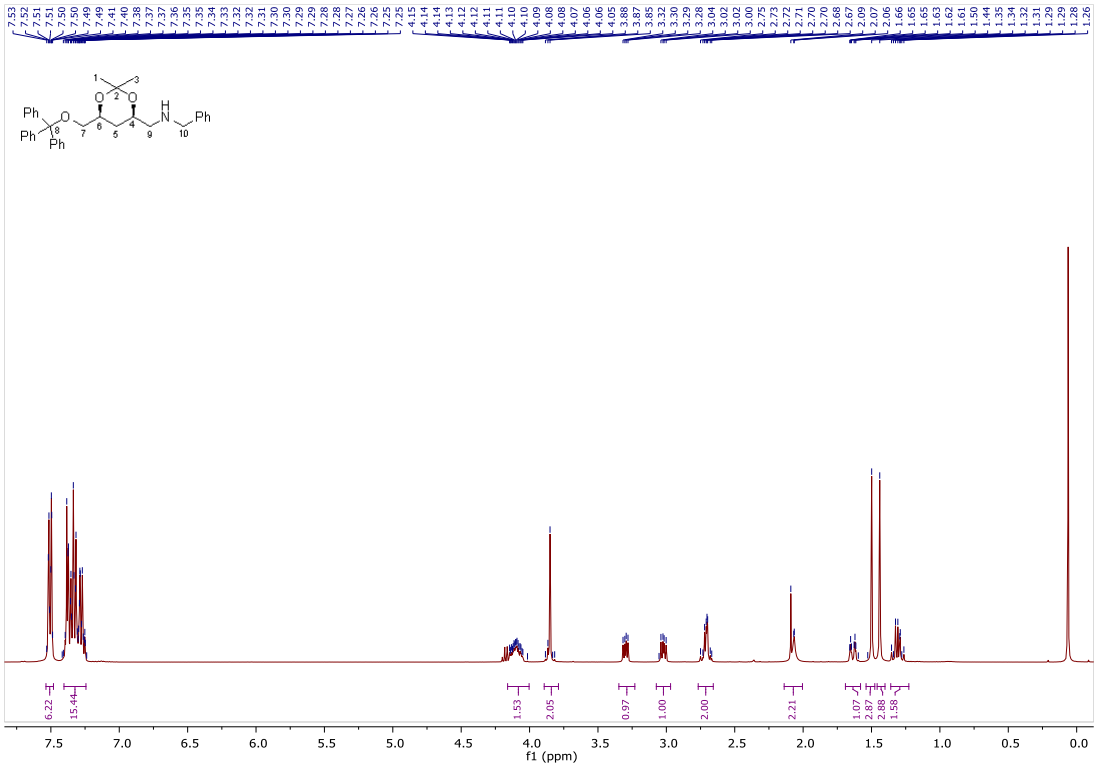


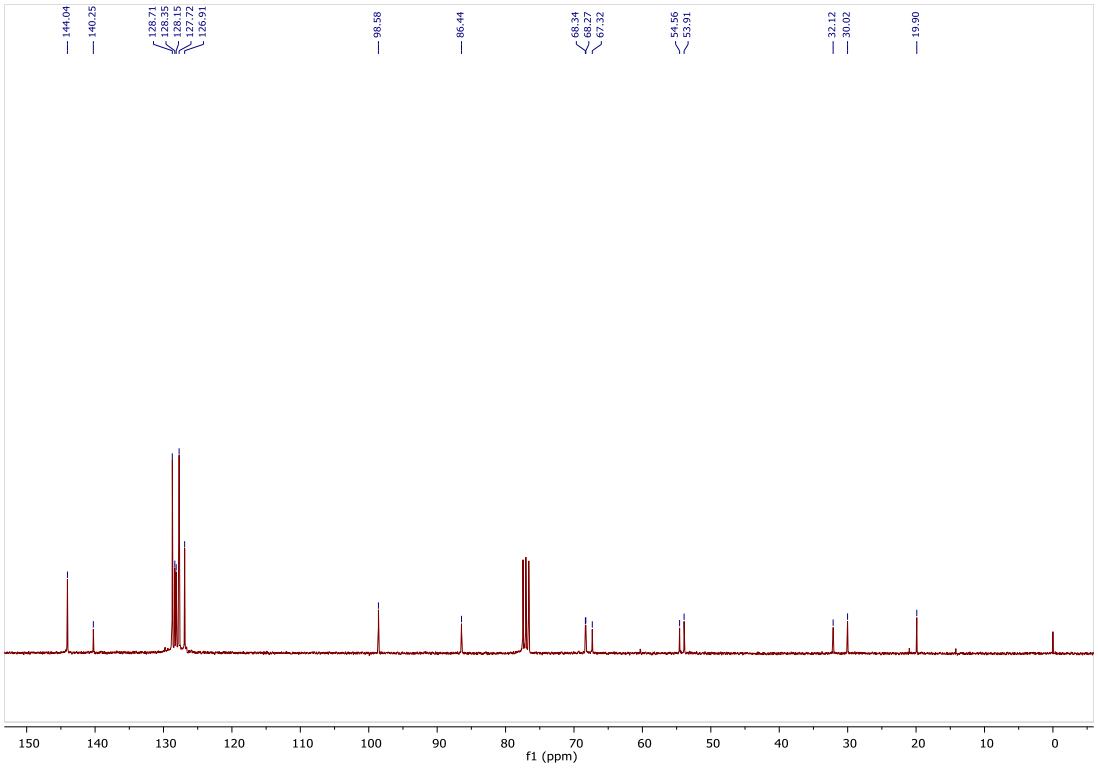
Compound 151



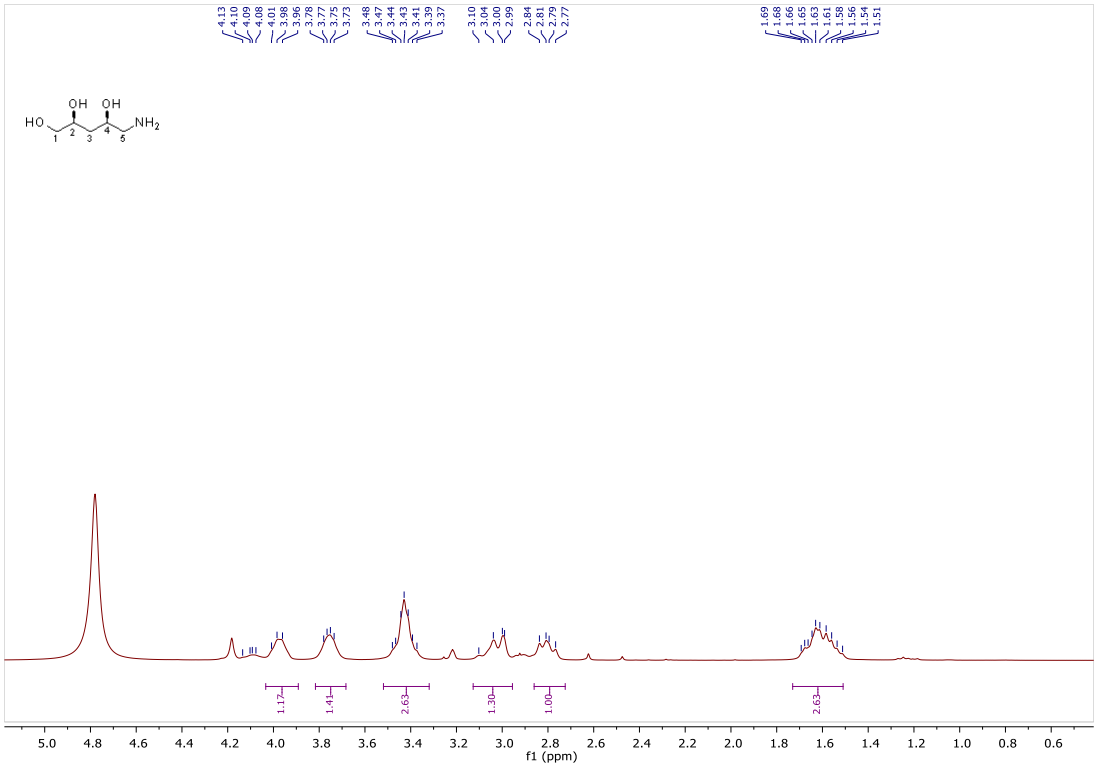


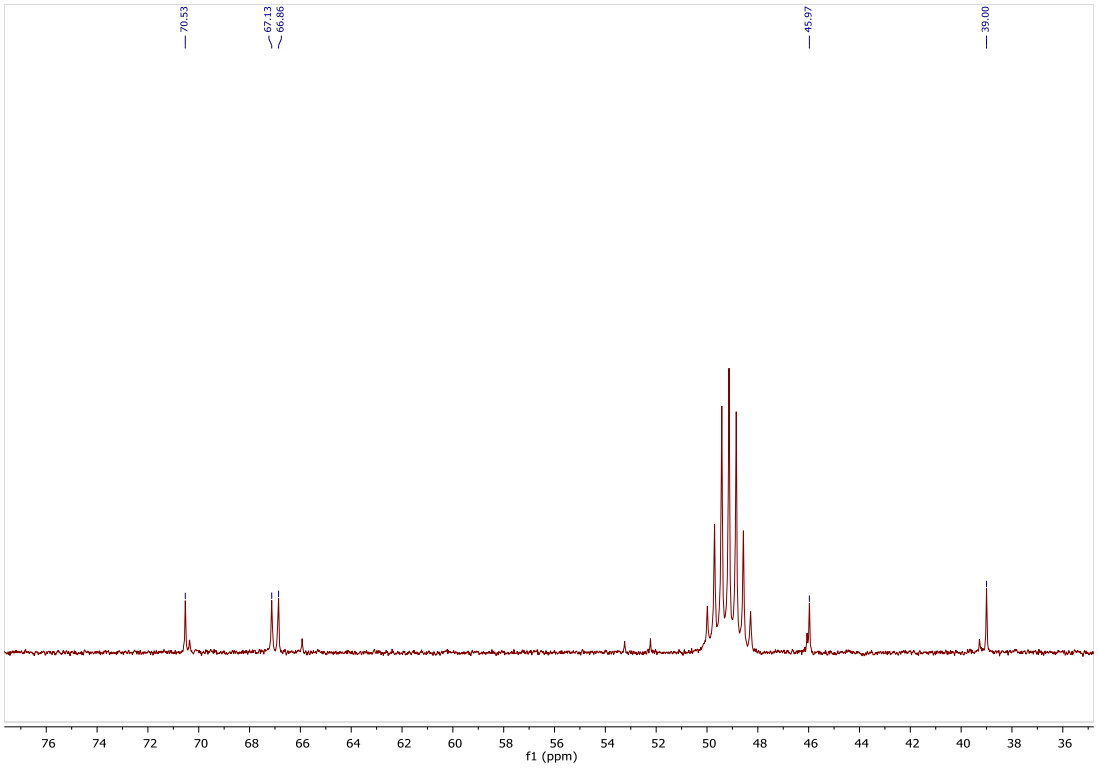
Compound 152



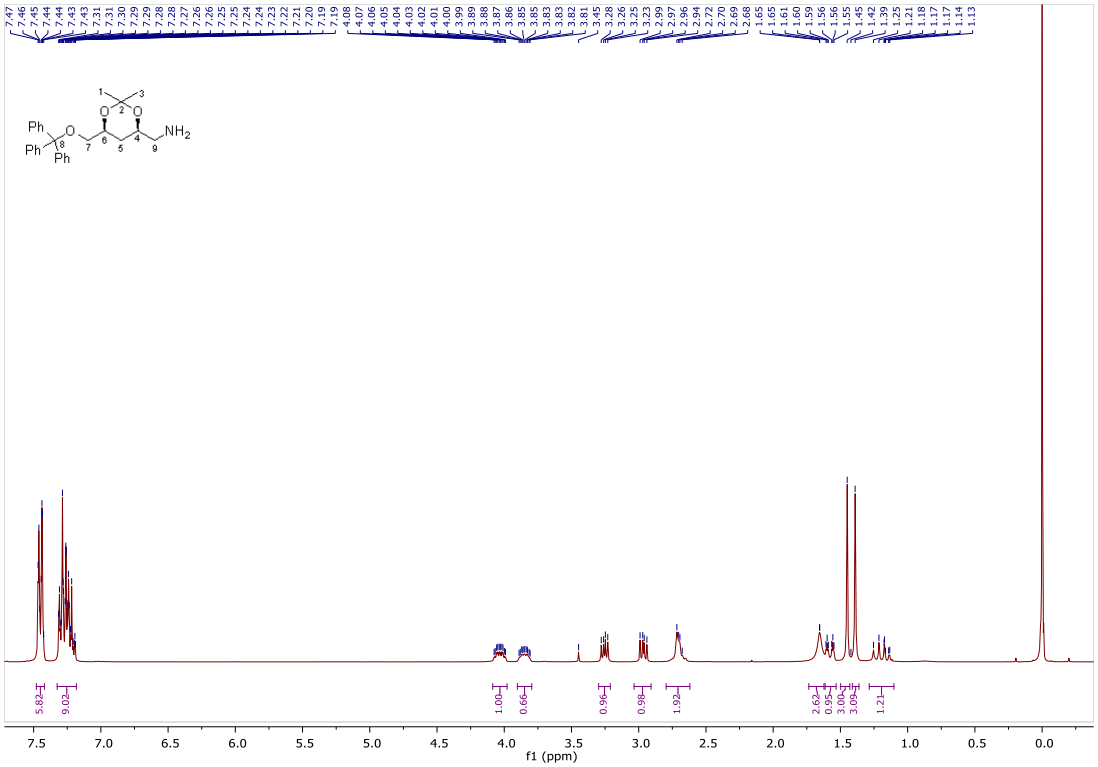


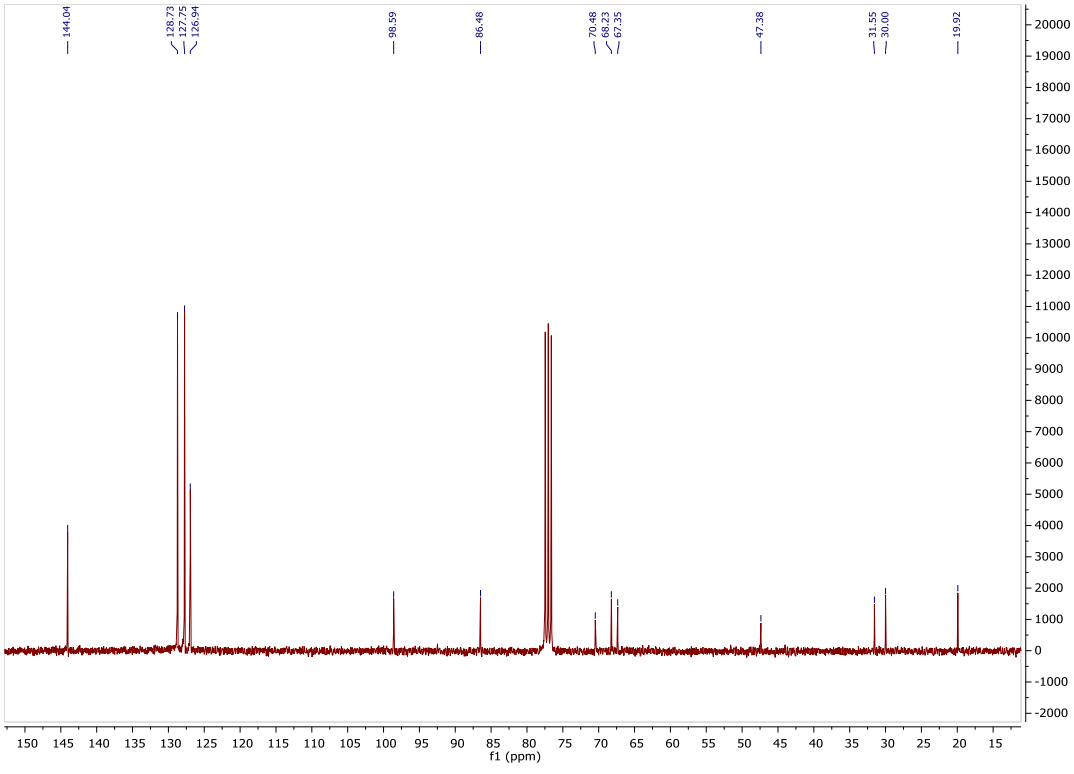
Compound 153



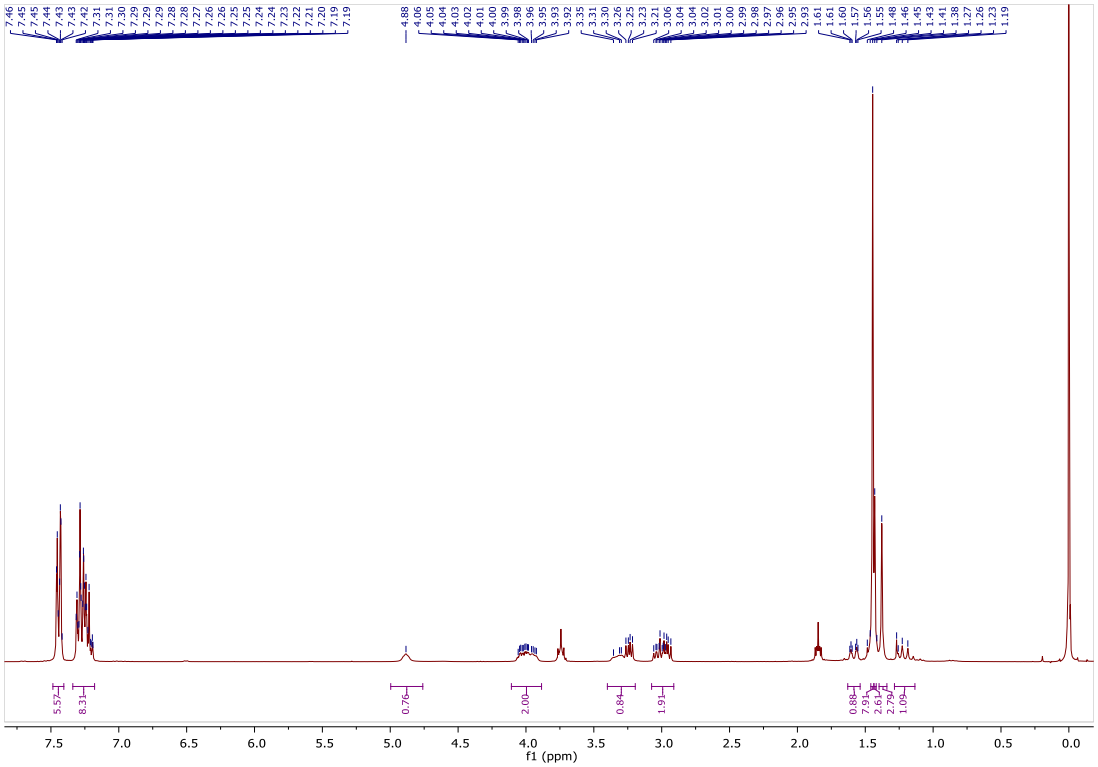


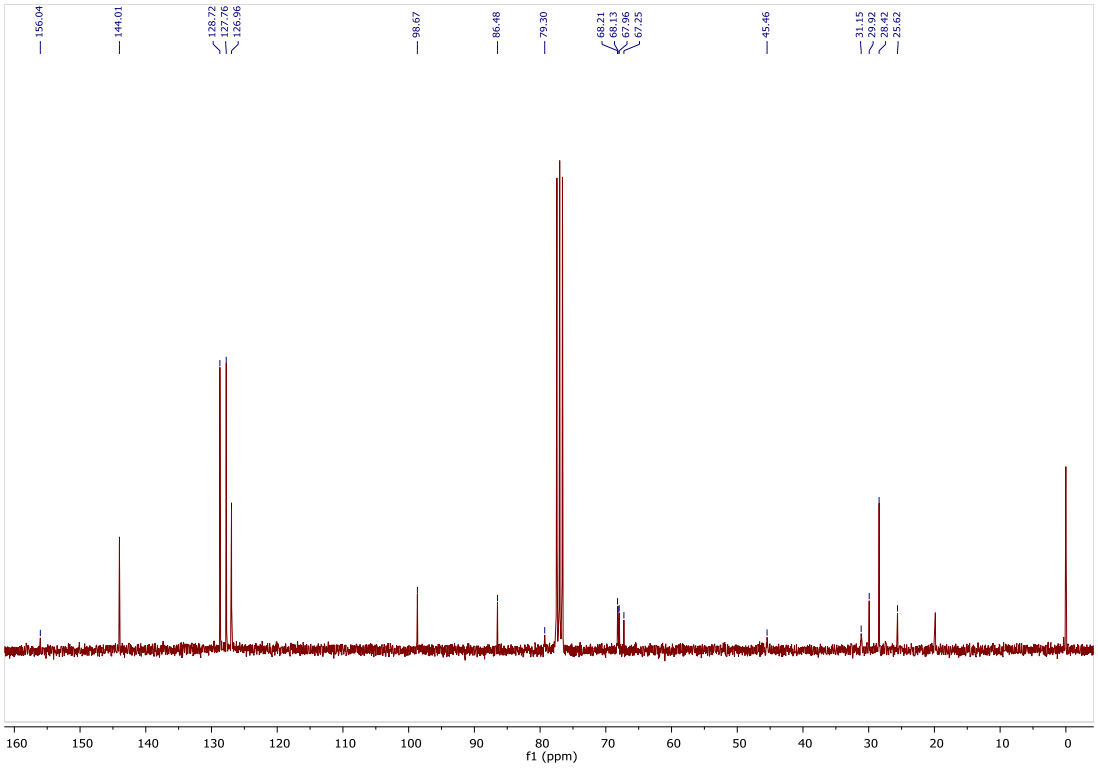
Compound 154



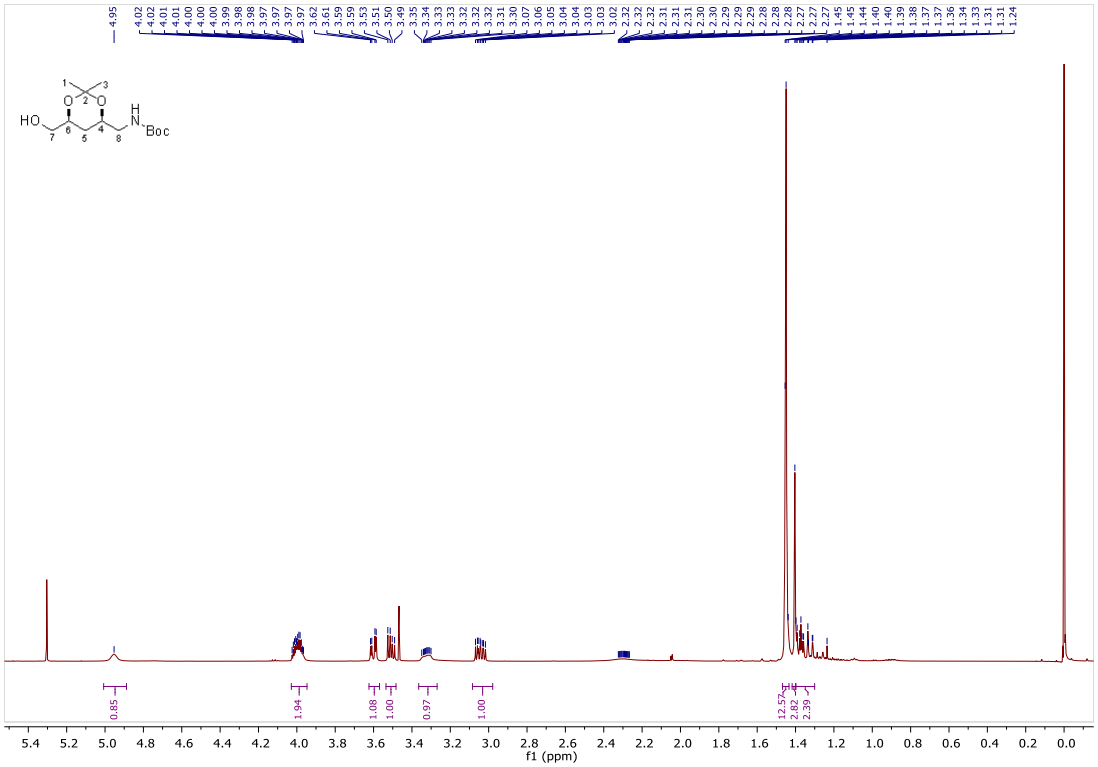


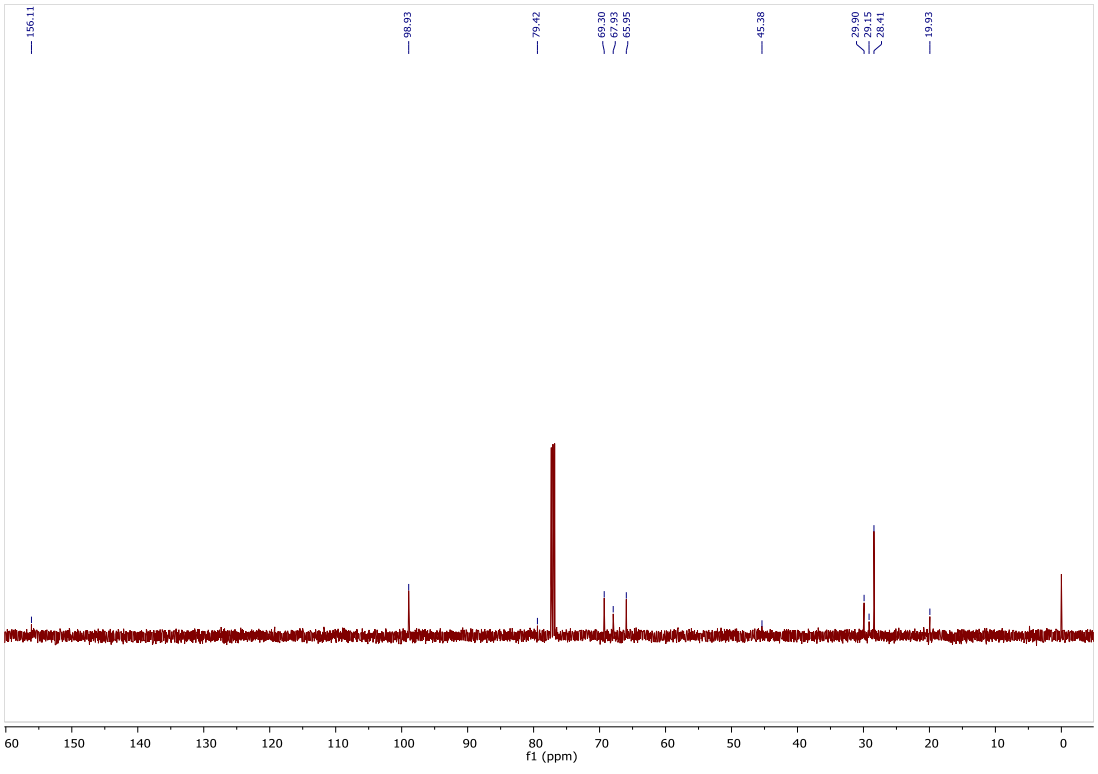
Compound 155



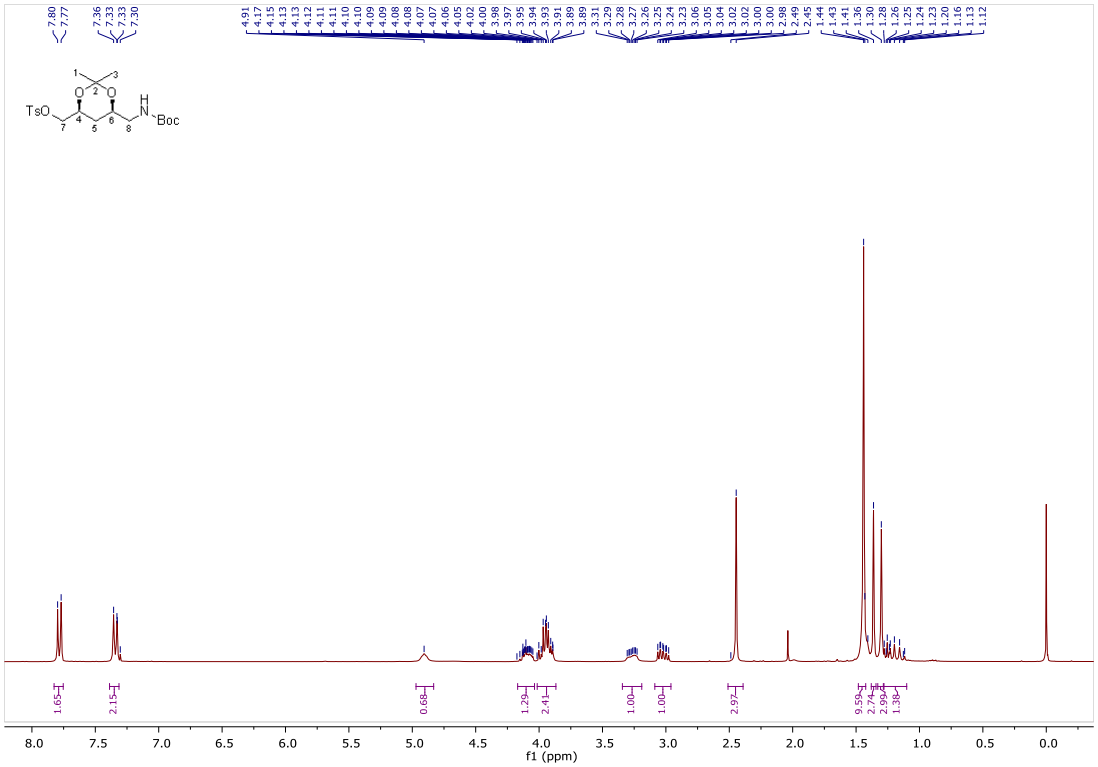


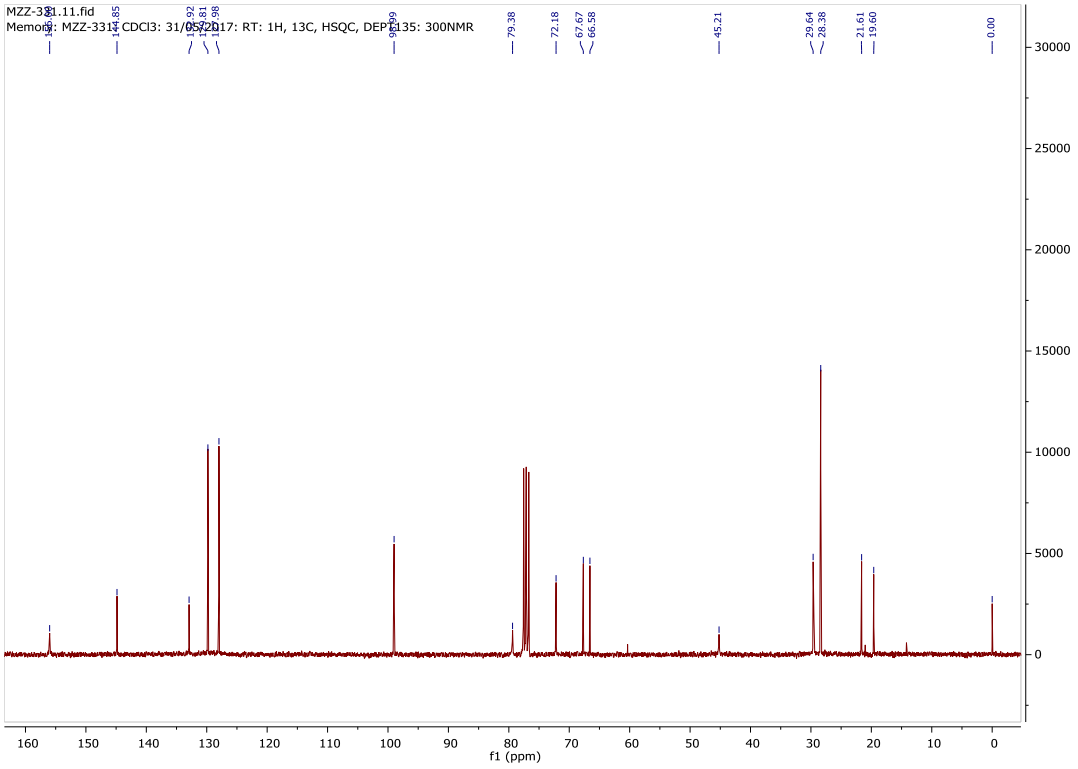
Compound 156



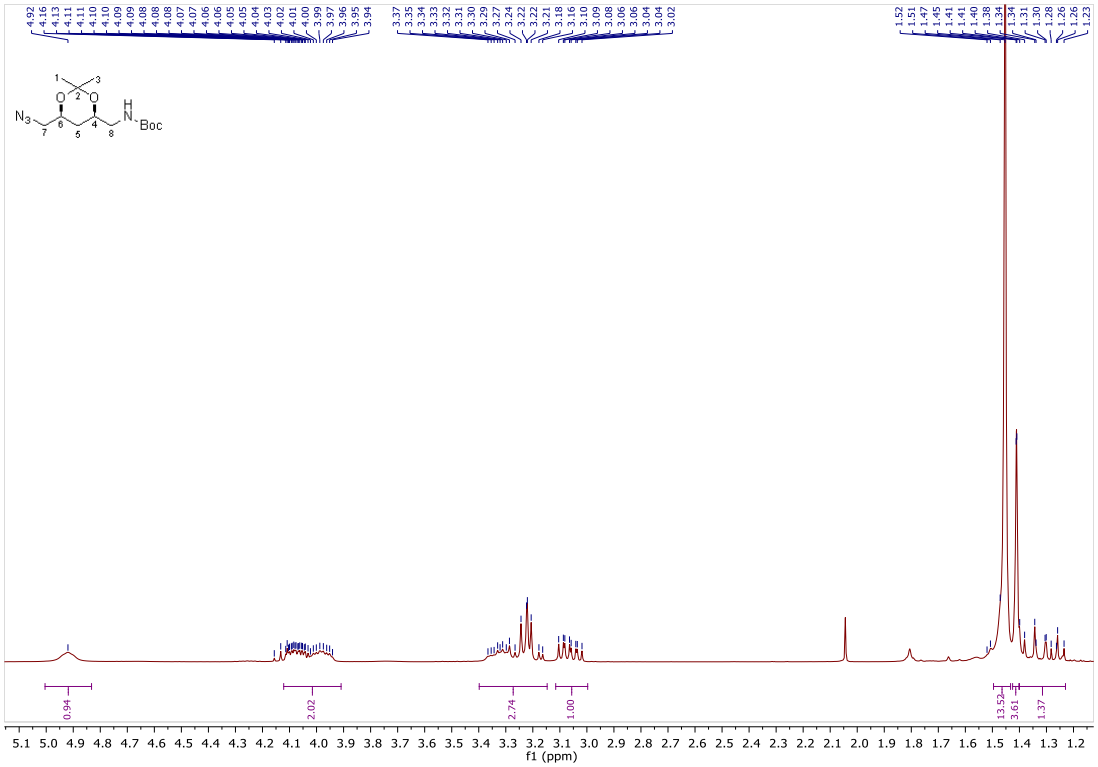


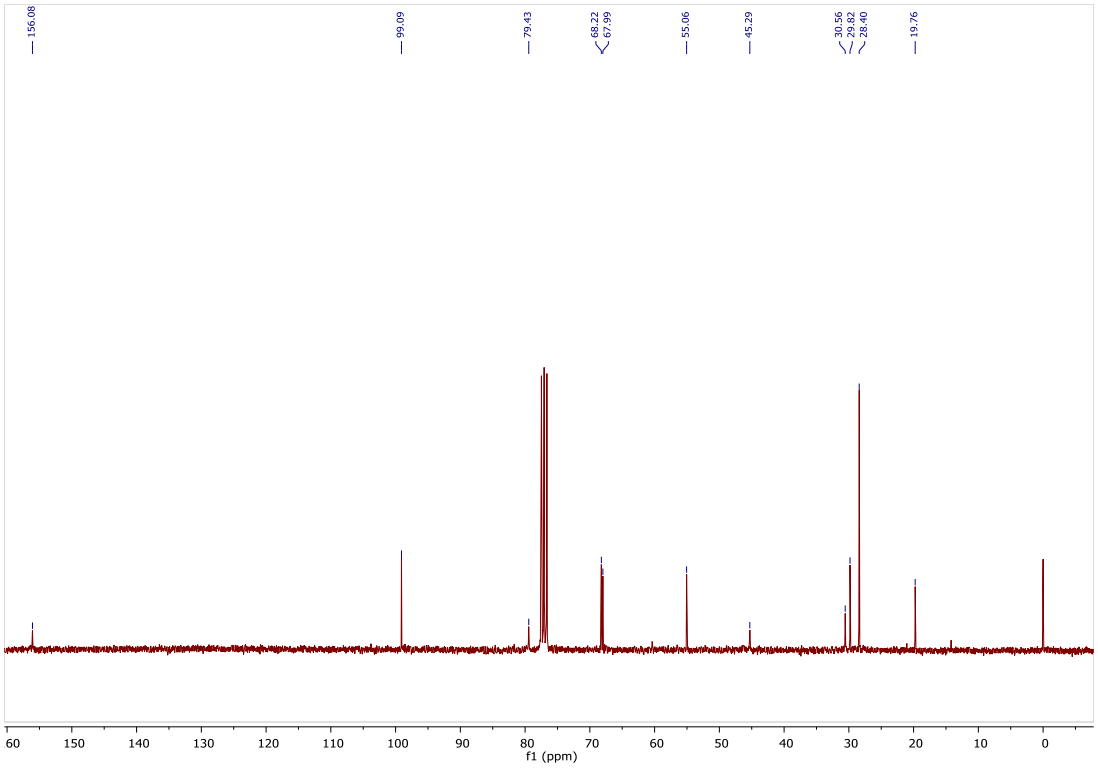
Compound 157



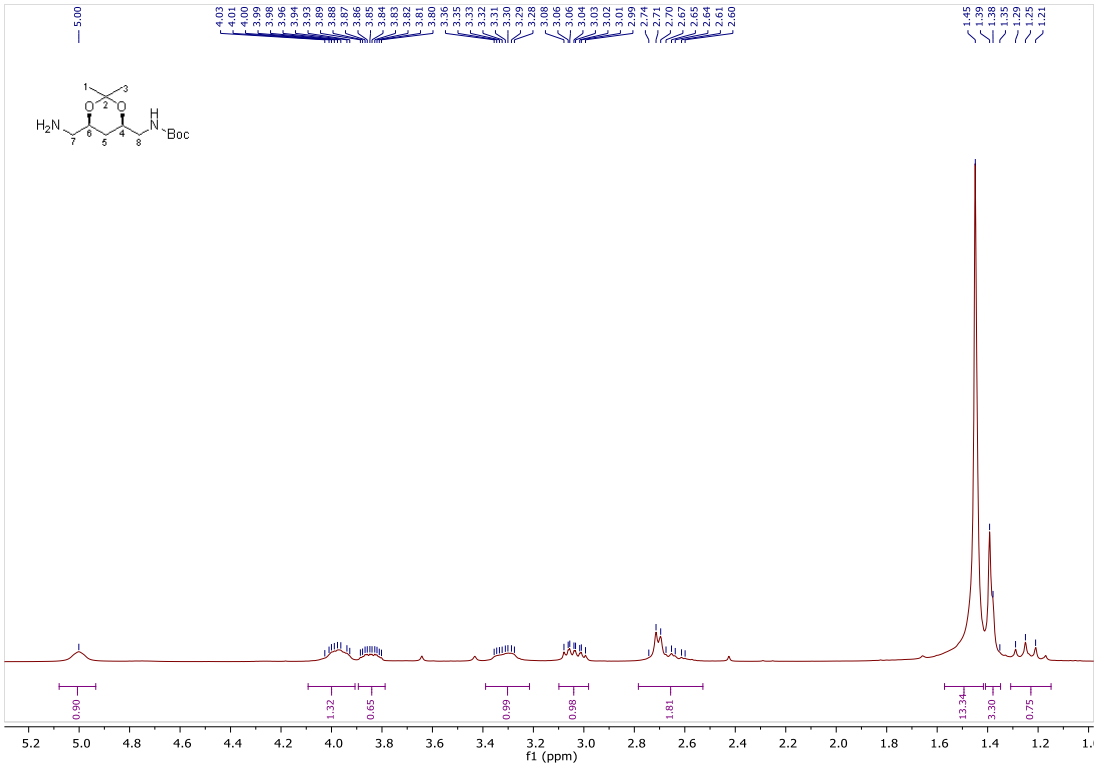


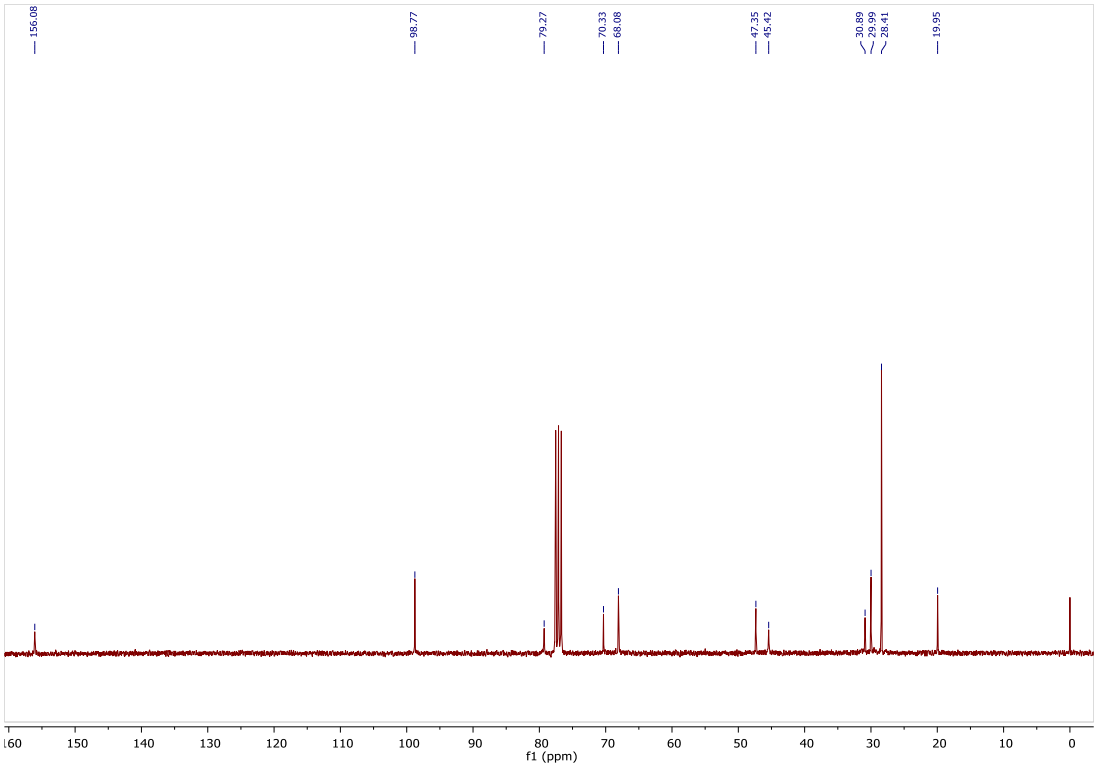
Compound 158



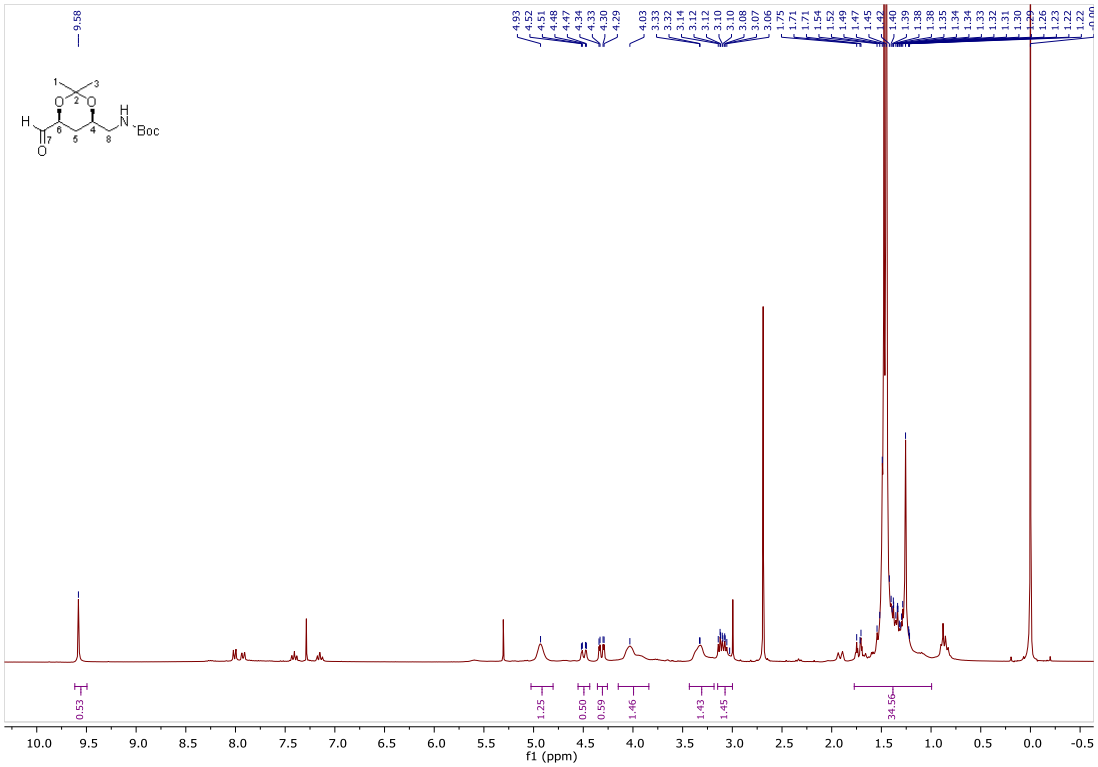


Compound 159

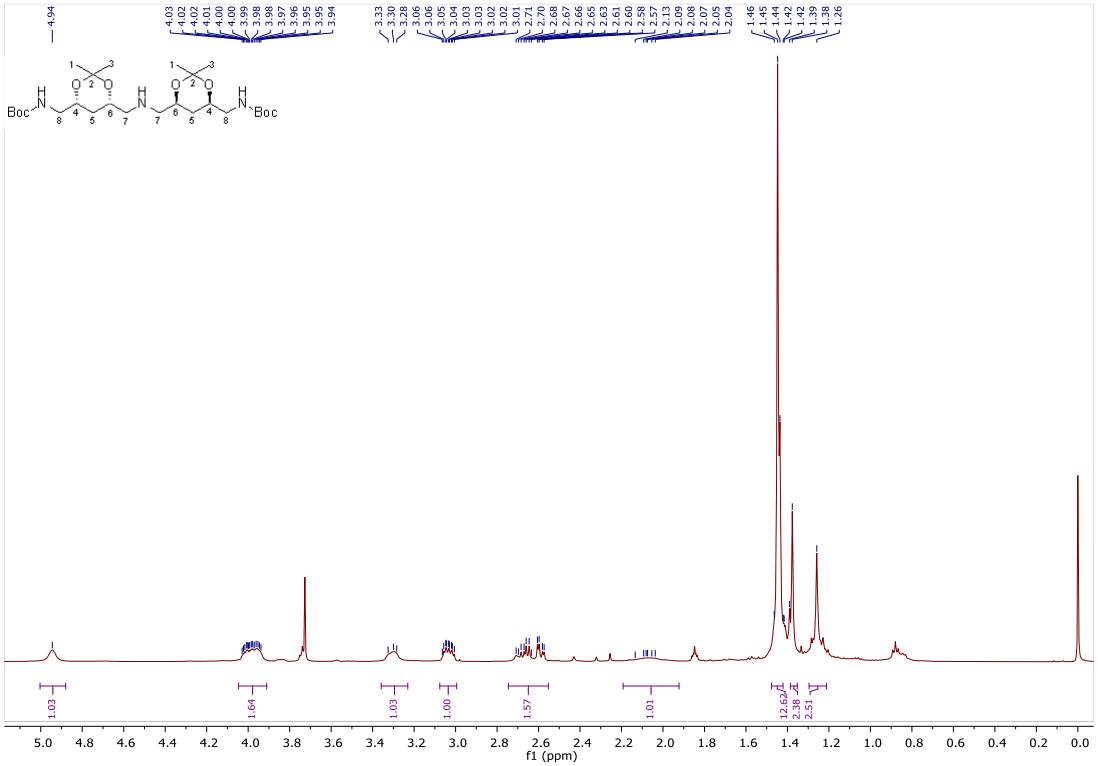


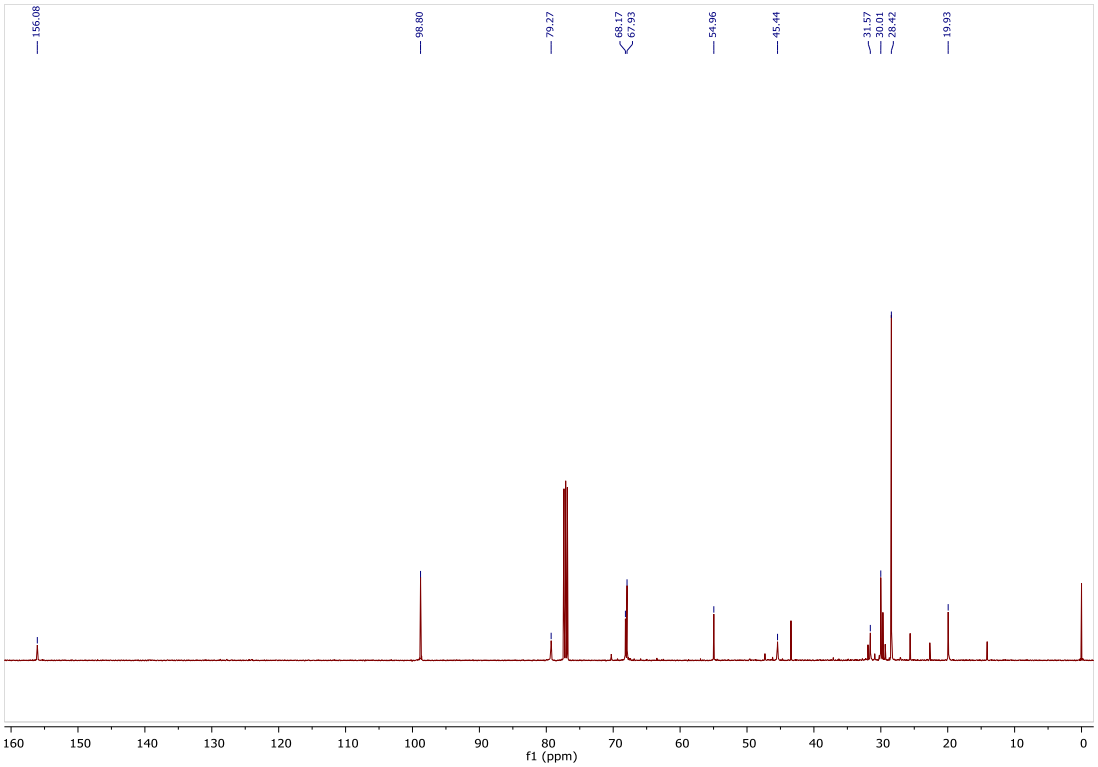


Compound 160

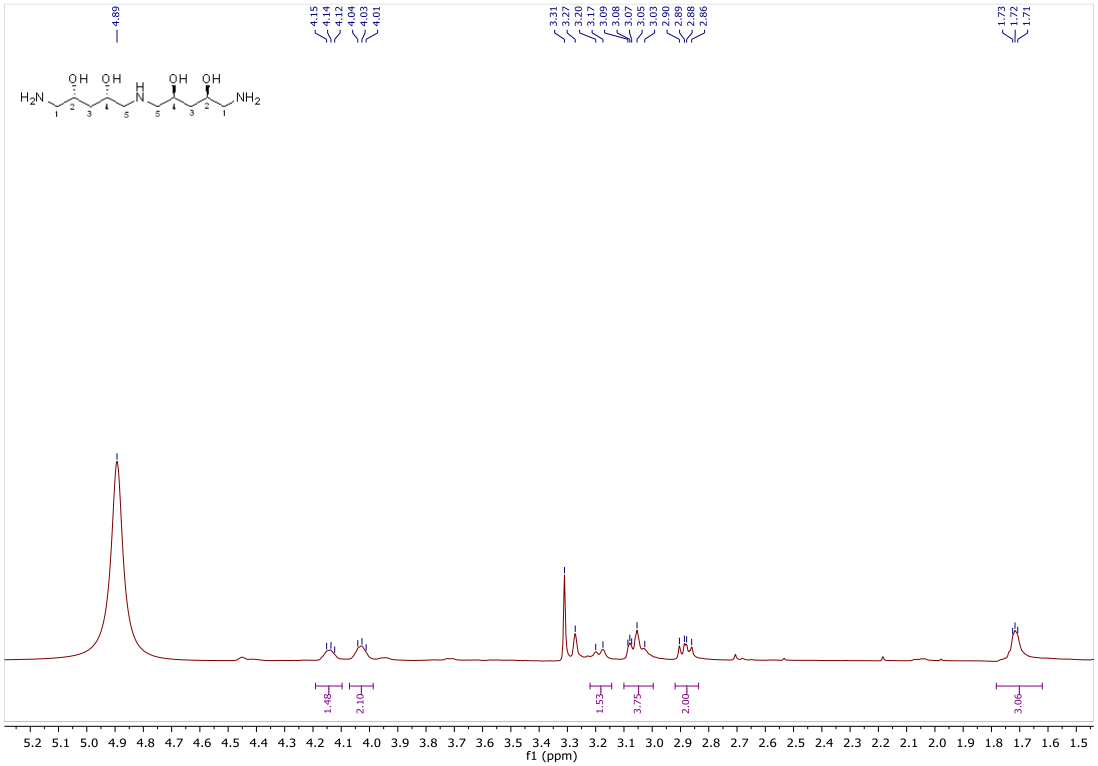


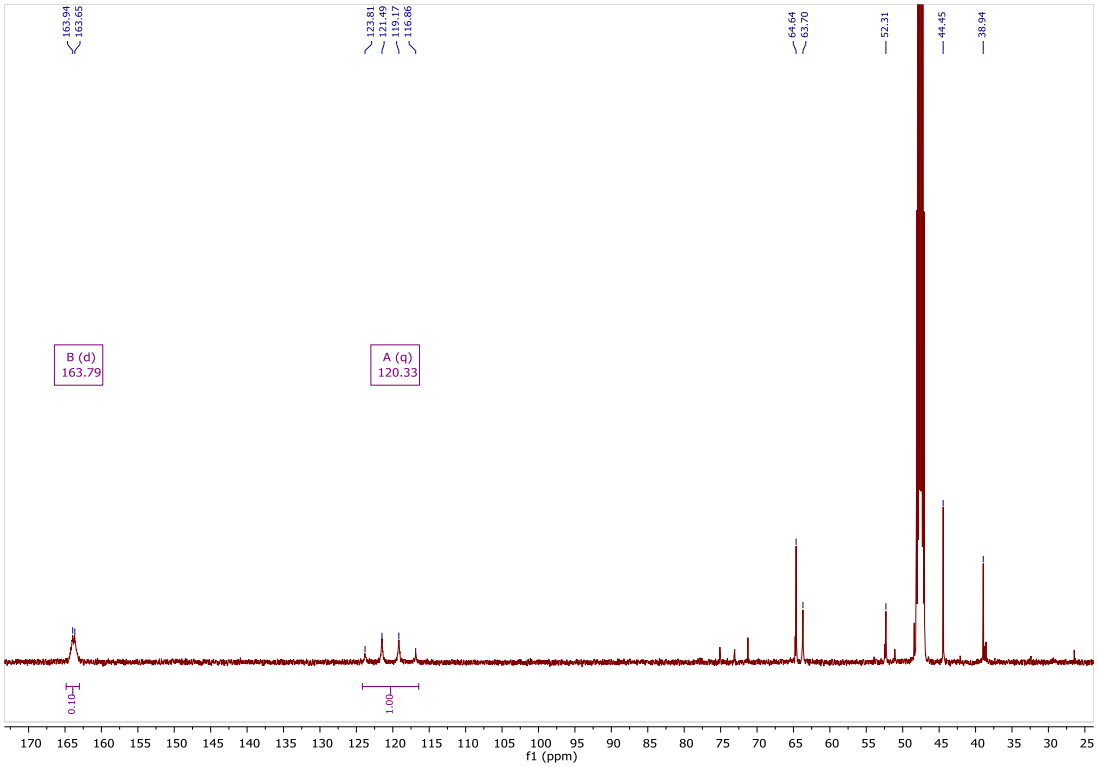
Compound 161



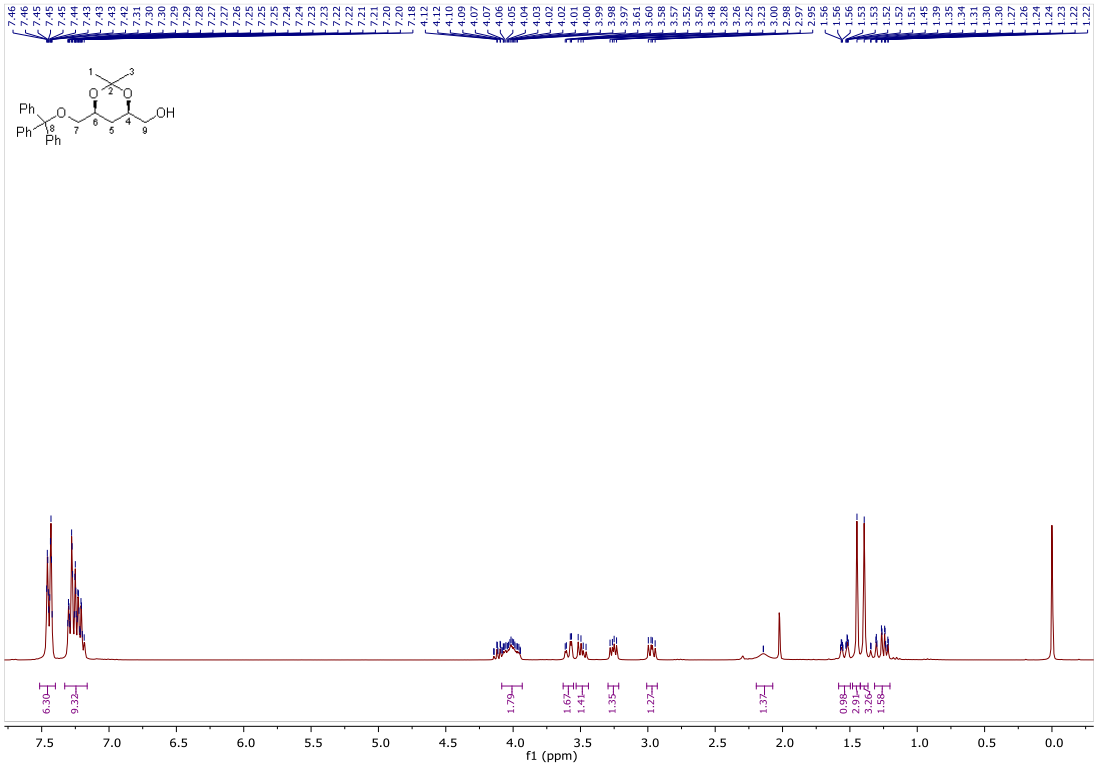


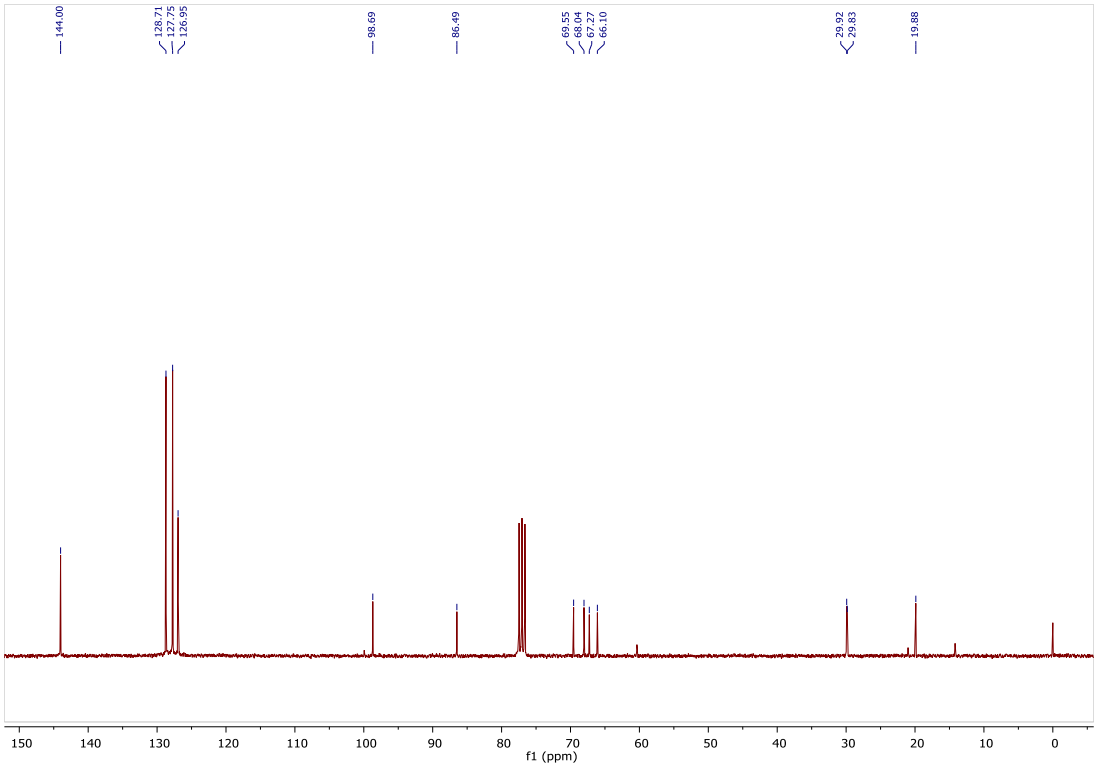
Compound 112



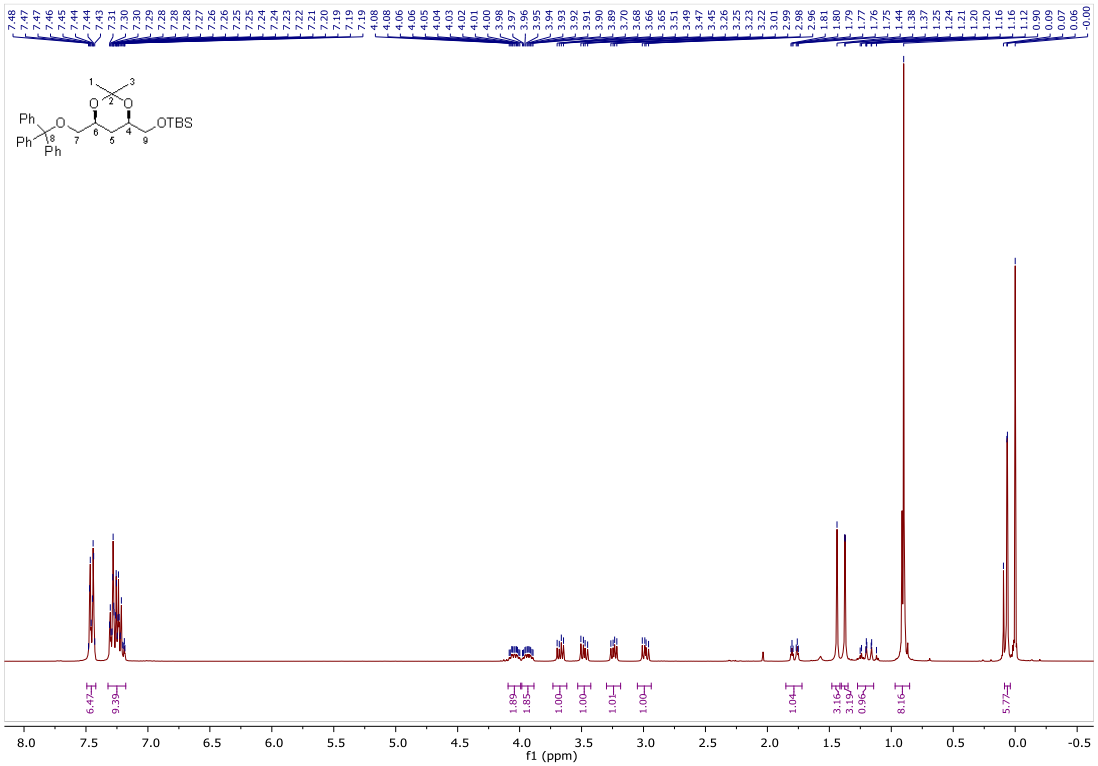


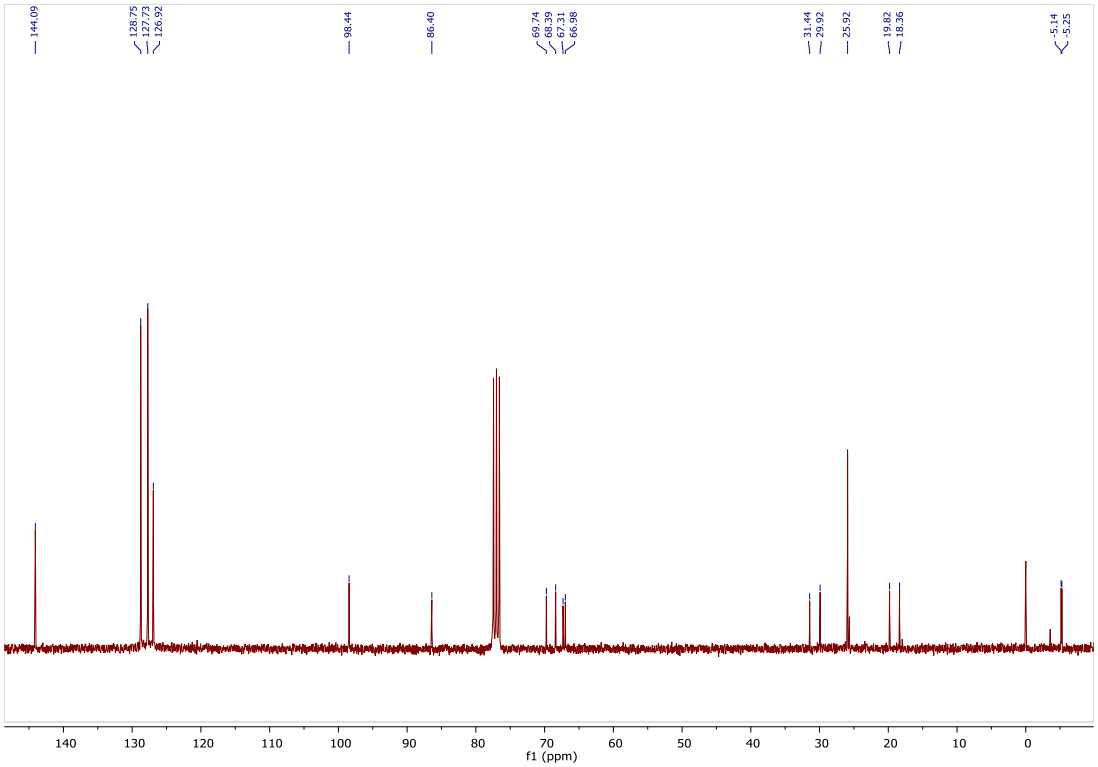
Compound 162



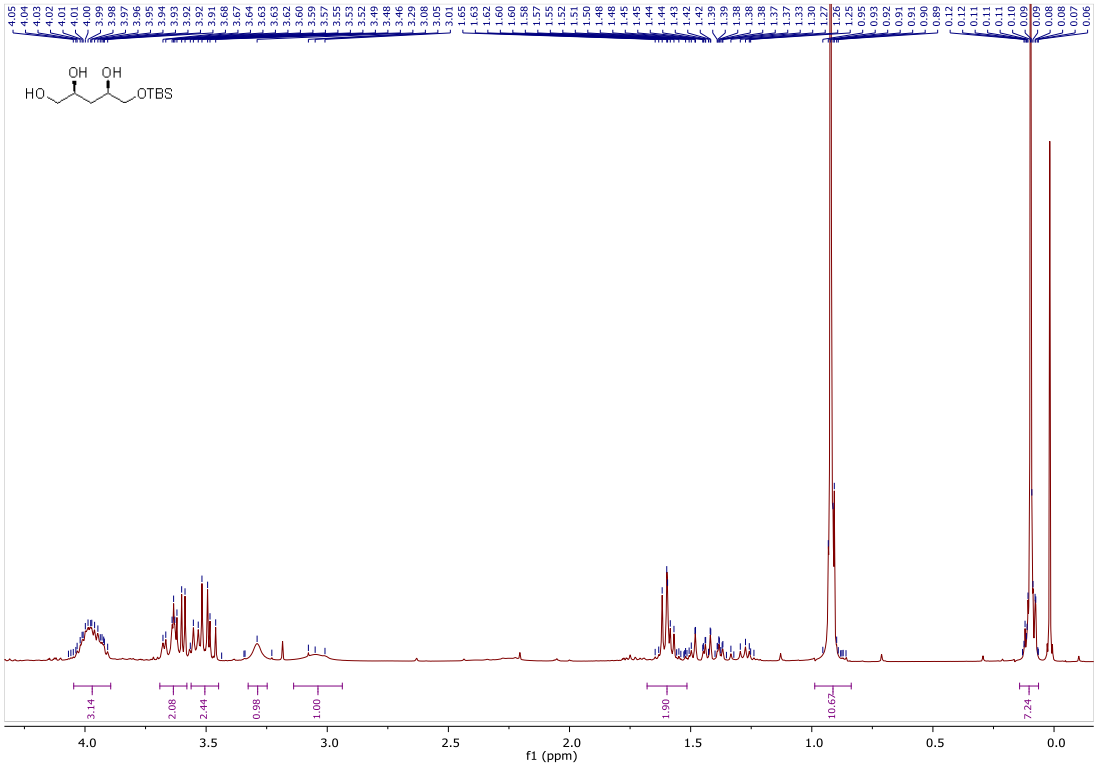


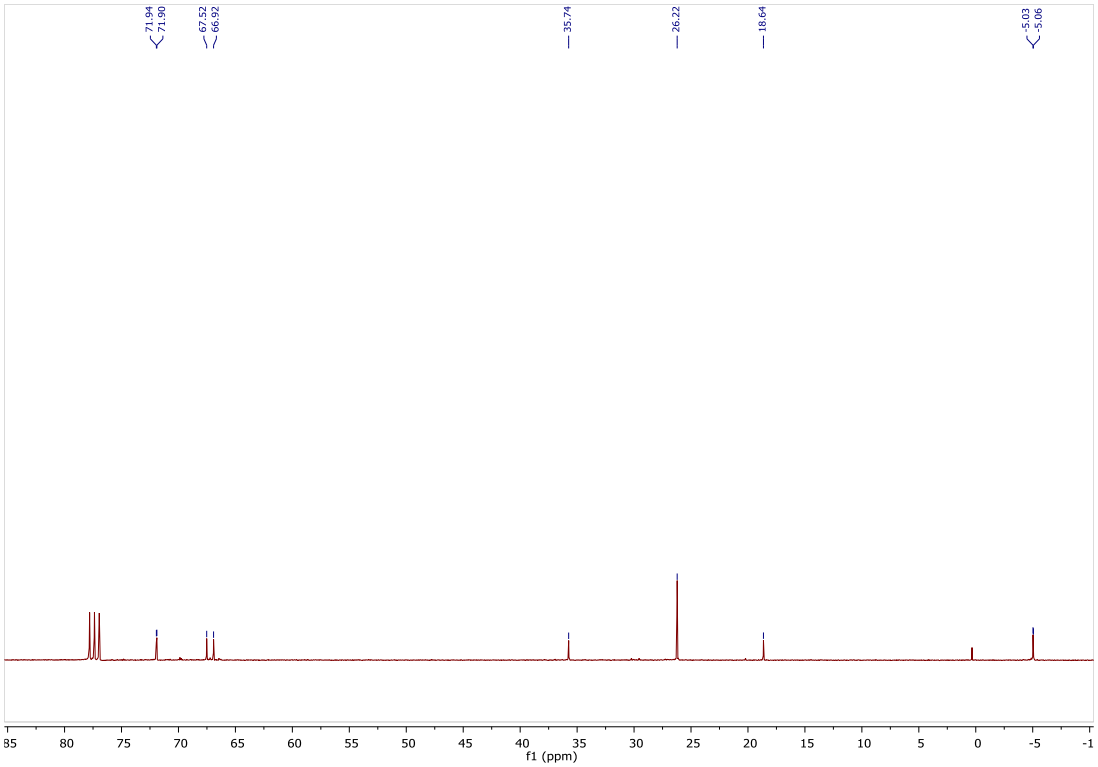
Compound 163



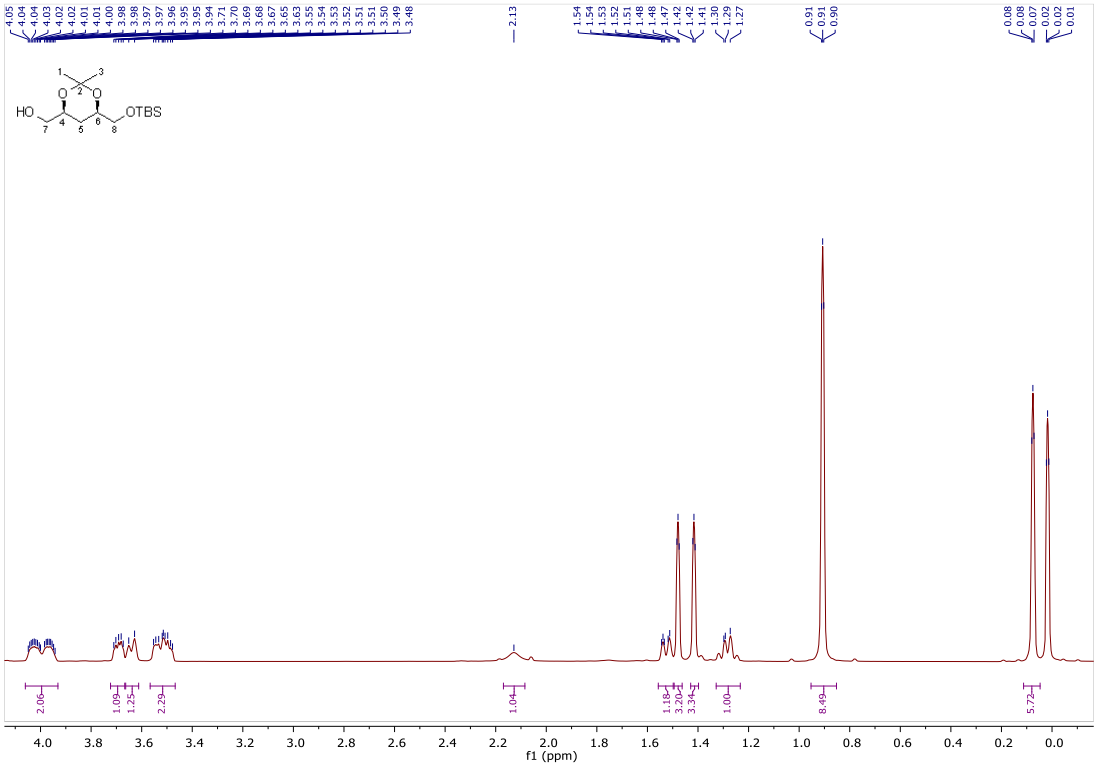


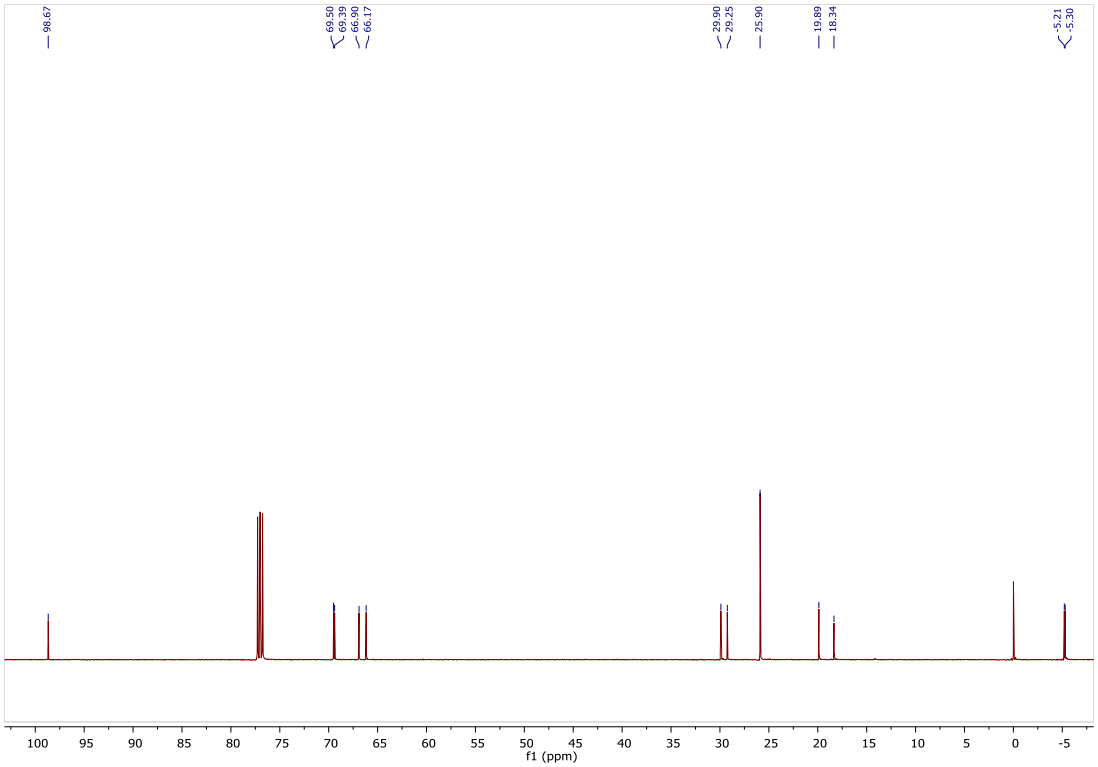
Compound 164



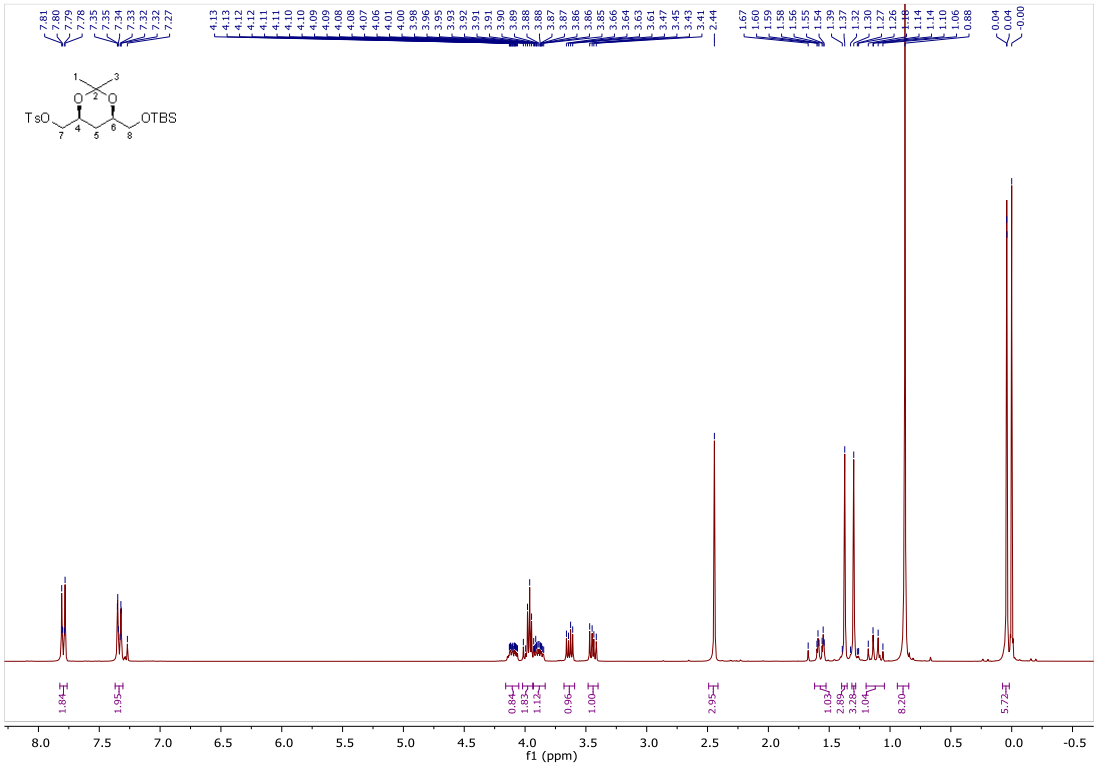


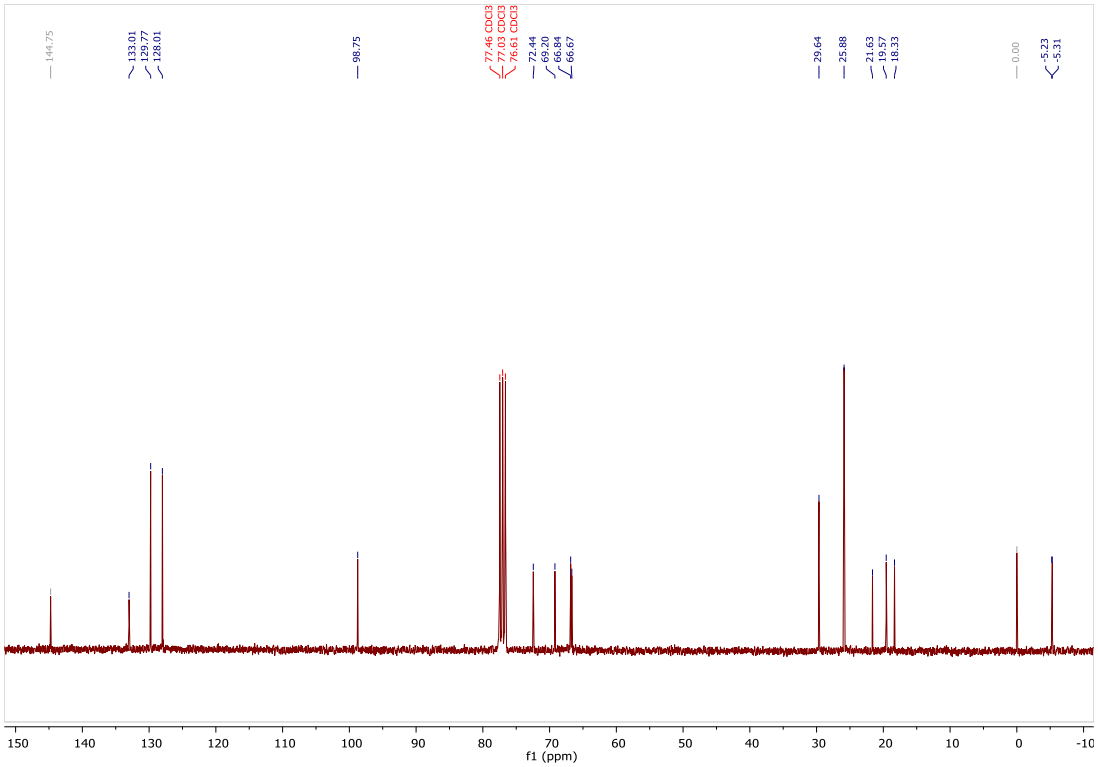
Compound 165



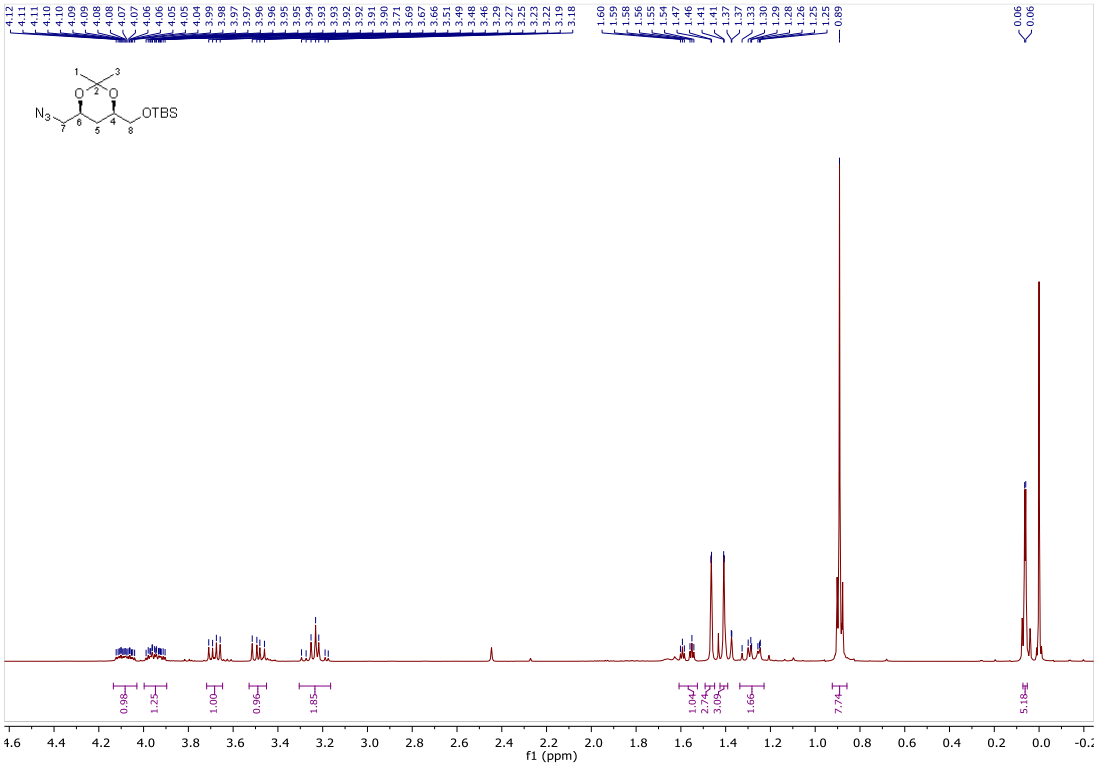


Compound 166

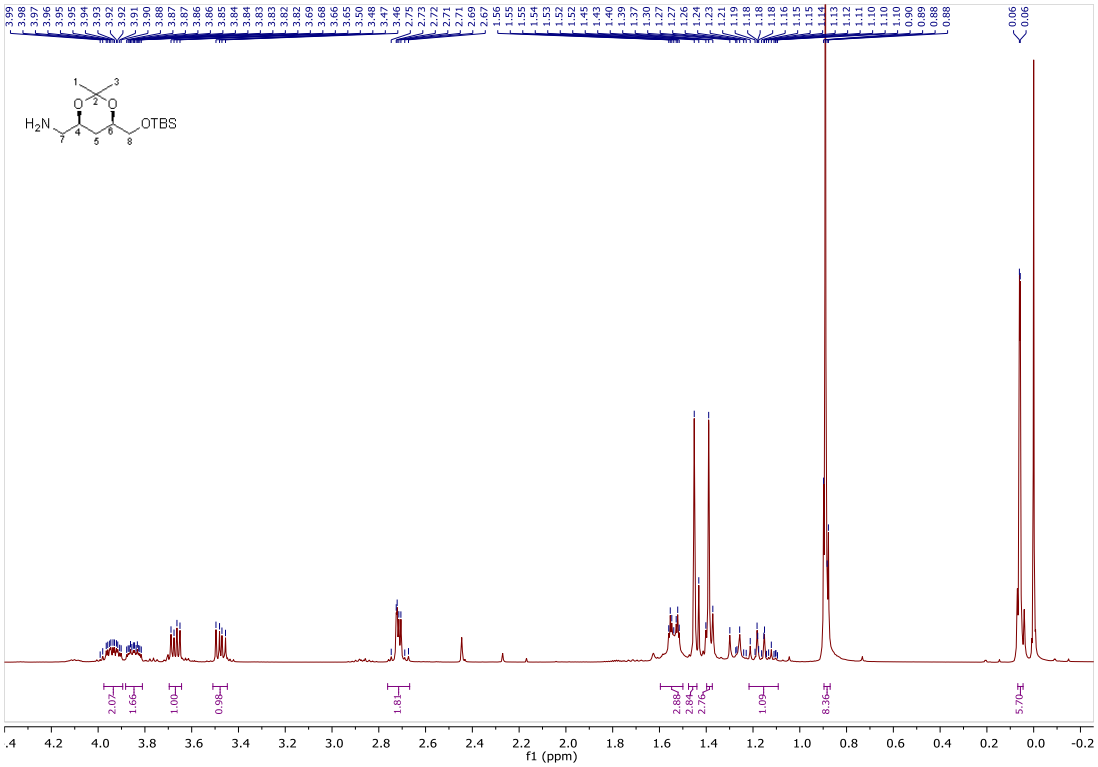


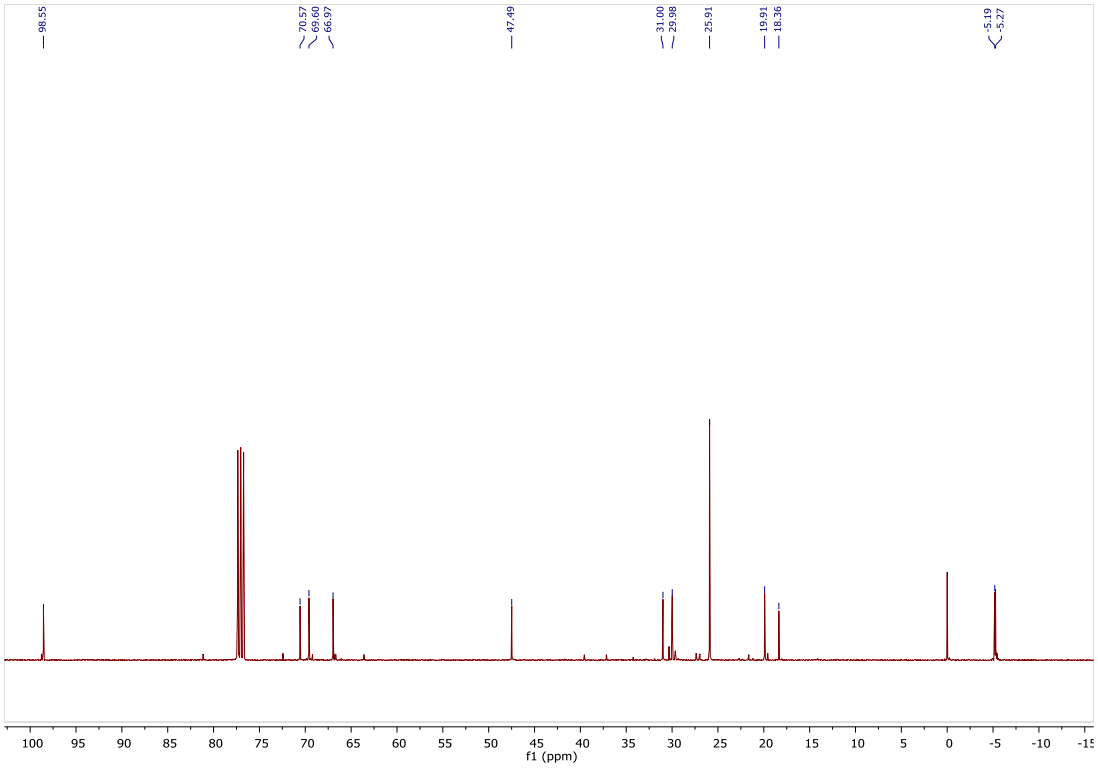


Compound 167

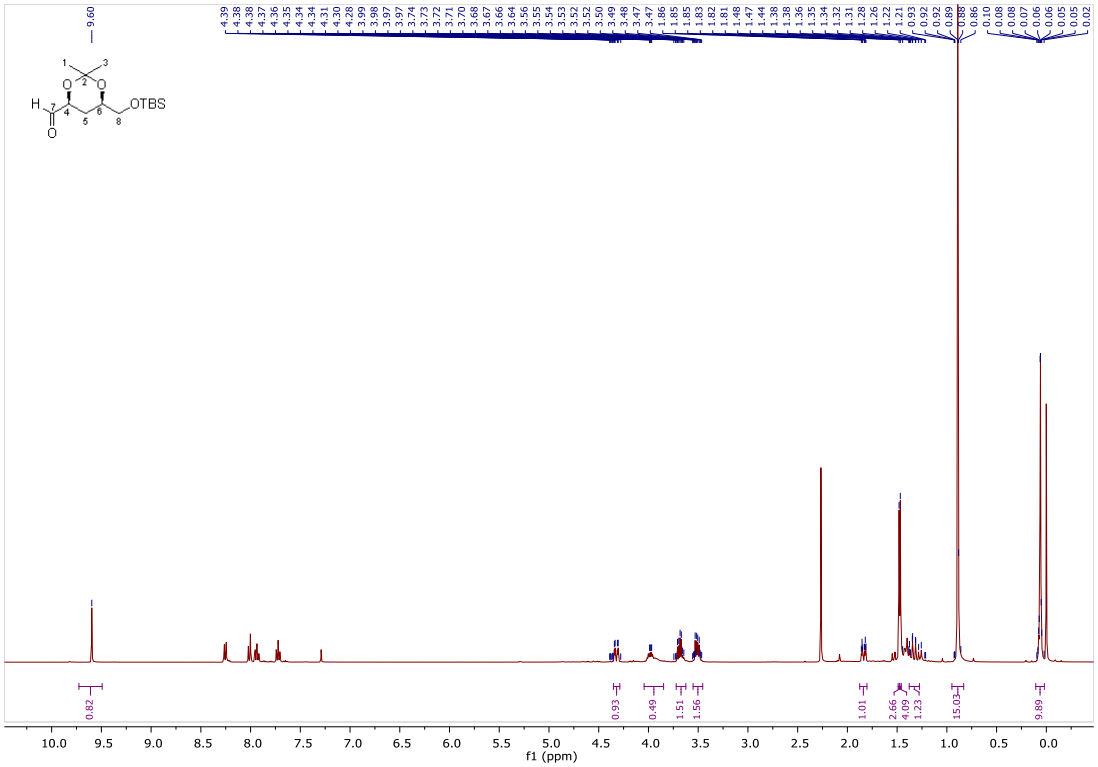


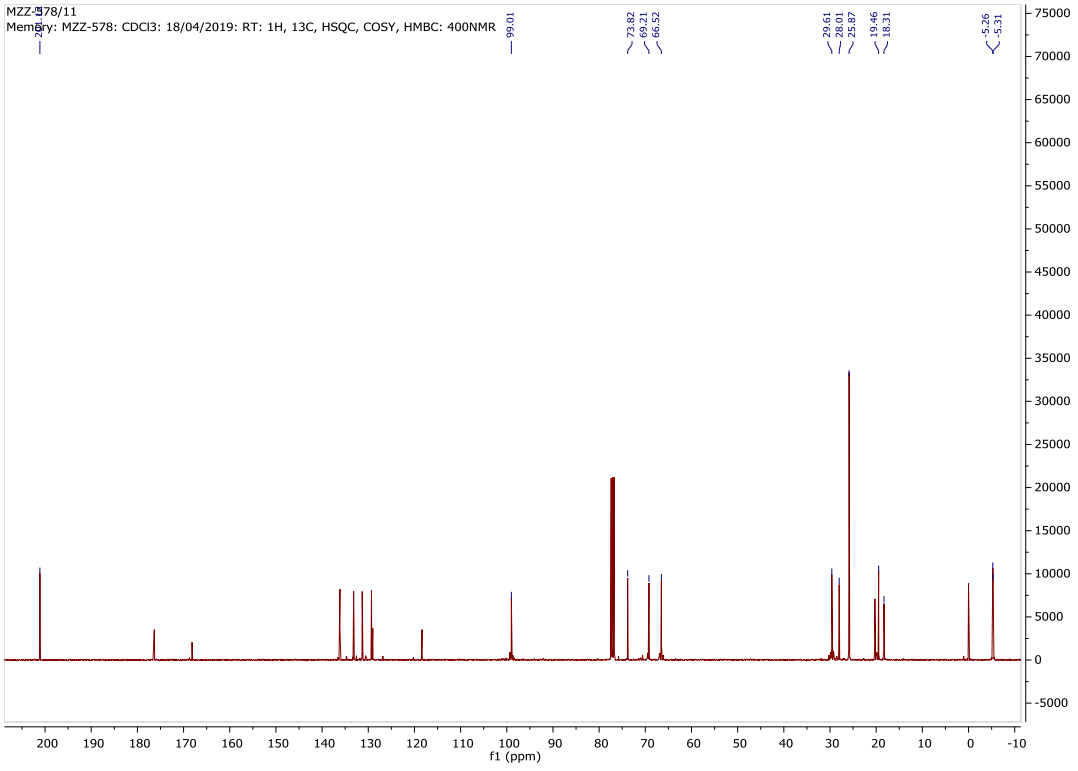
Compound 168



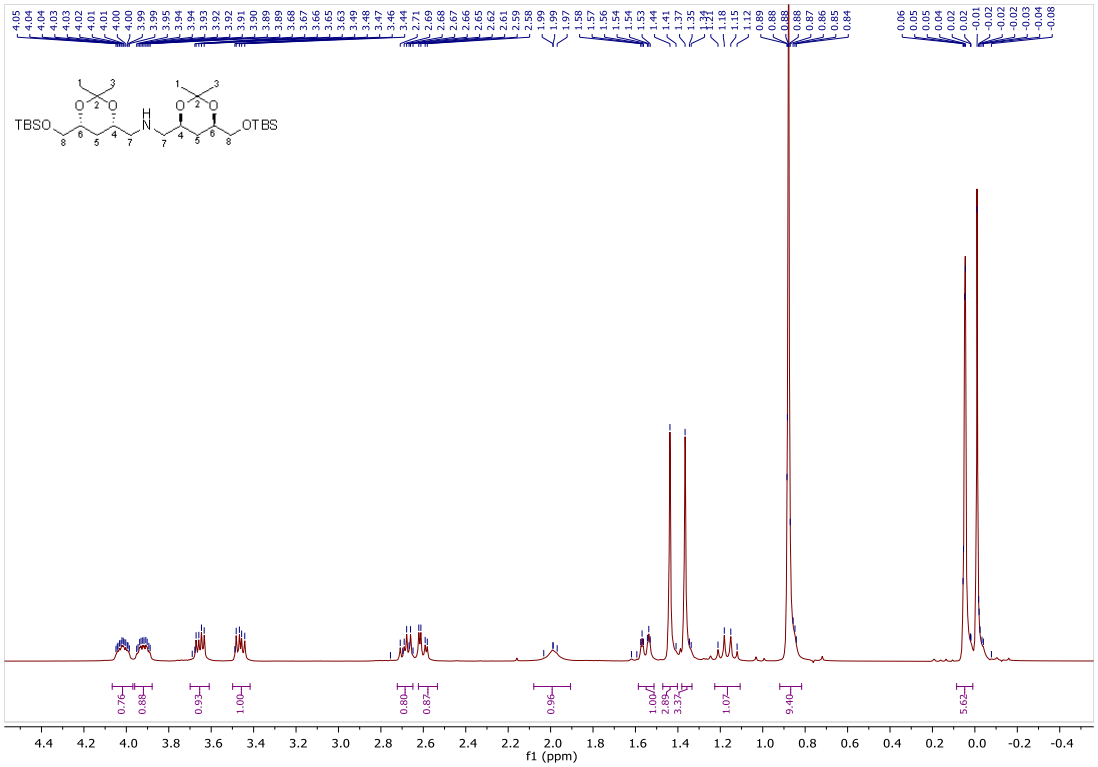


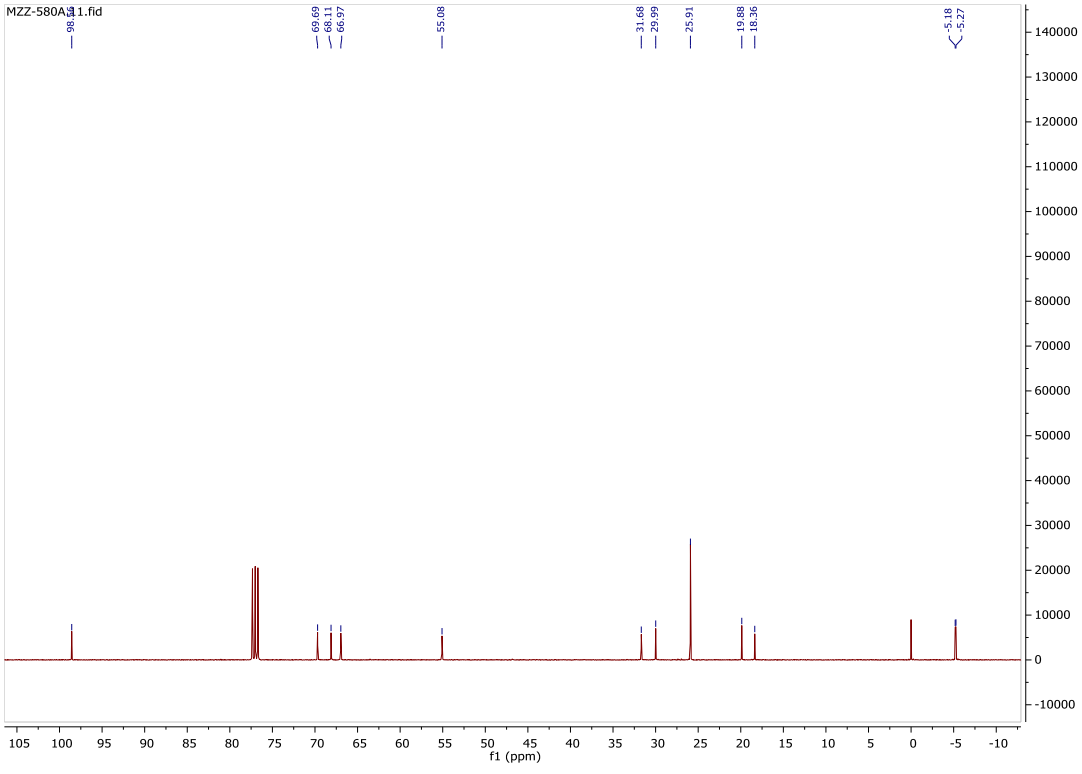
Compound 170



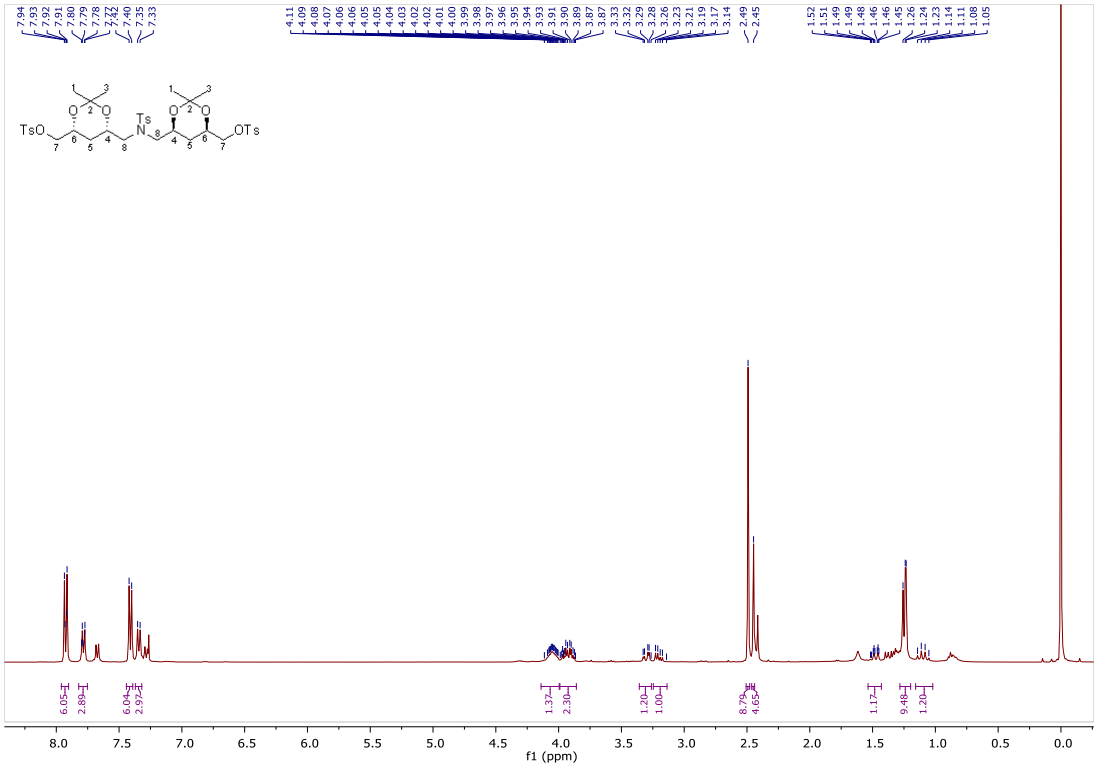


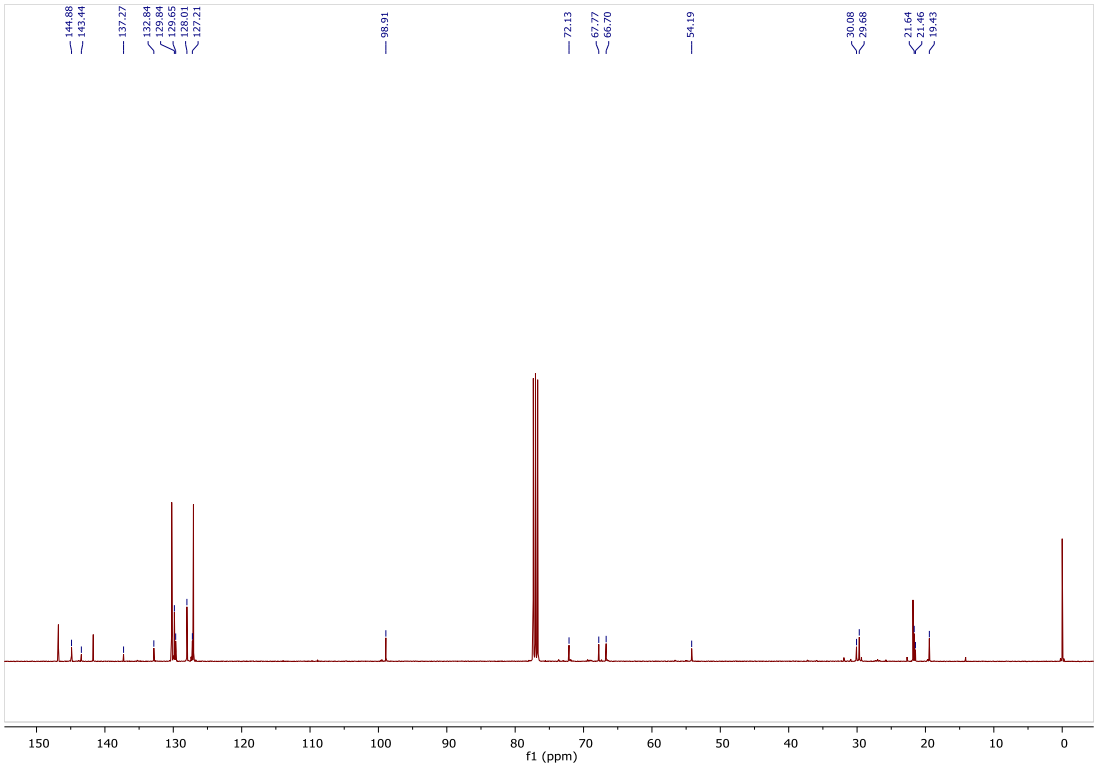
Compound 171



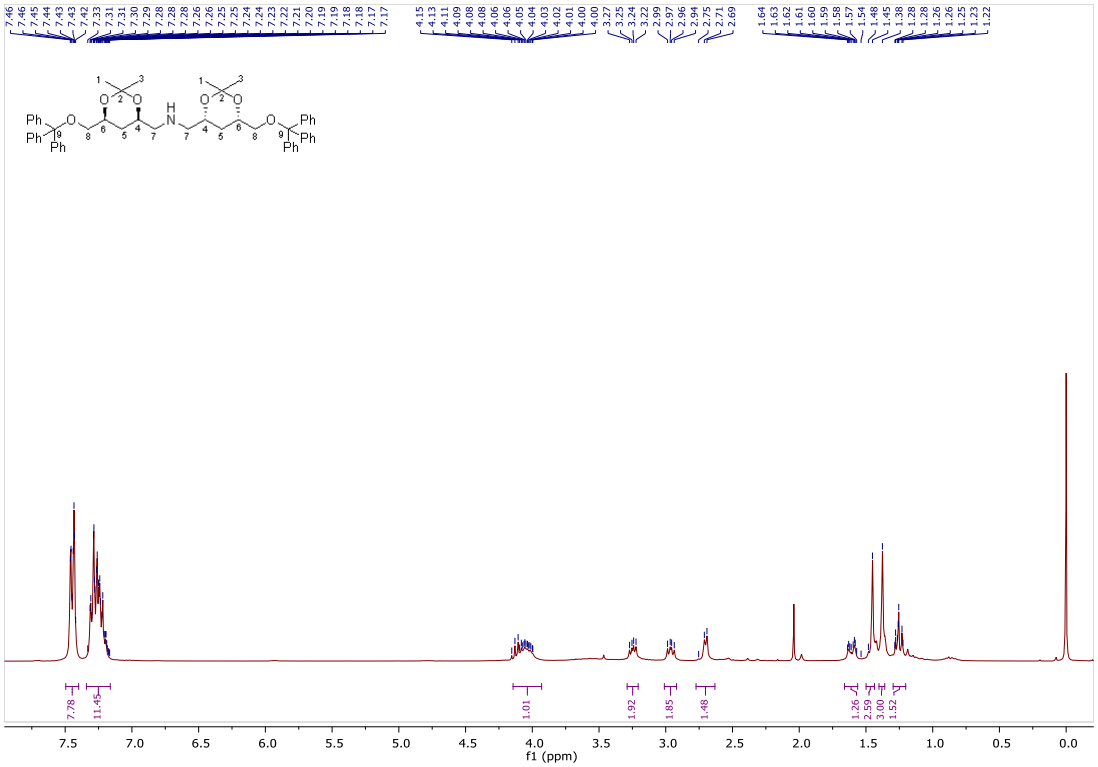


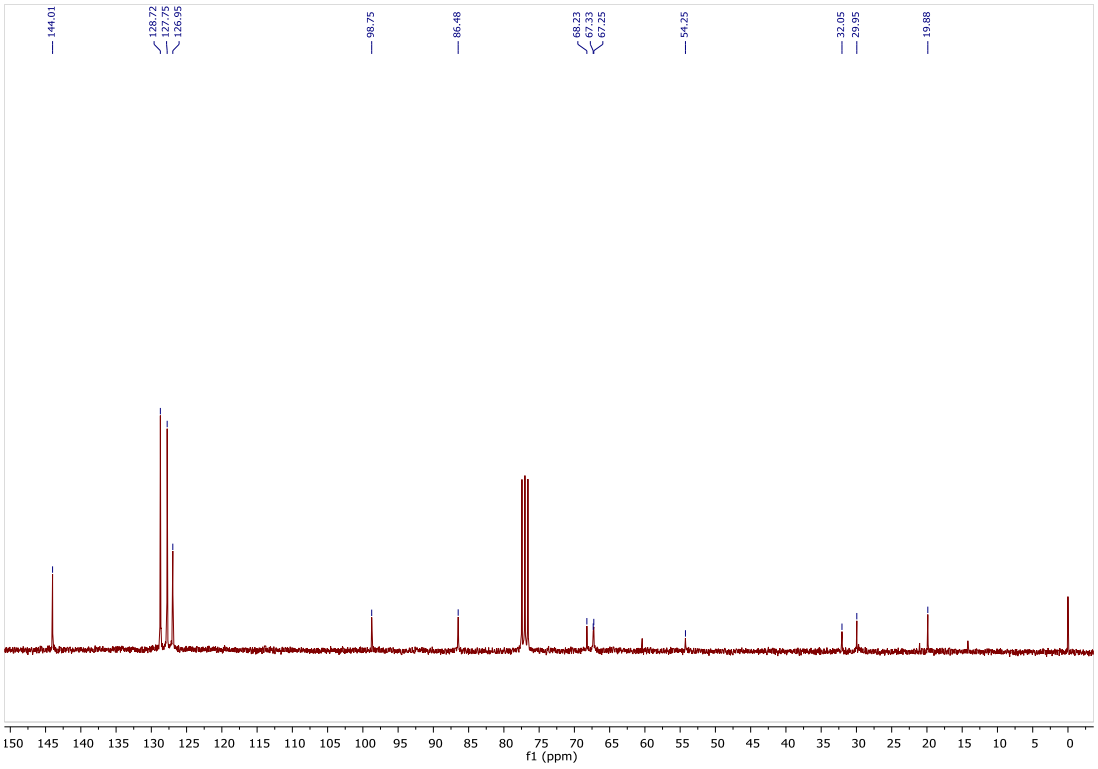
Compound 173



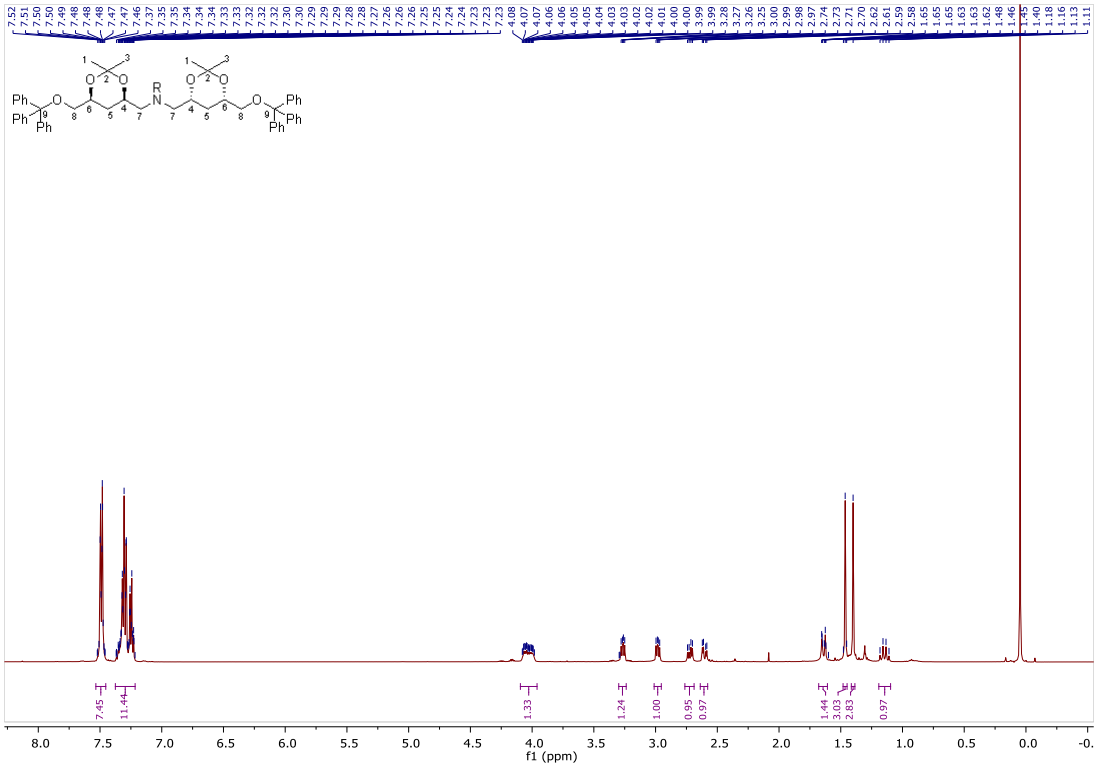


Compound 177

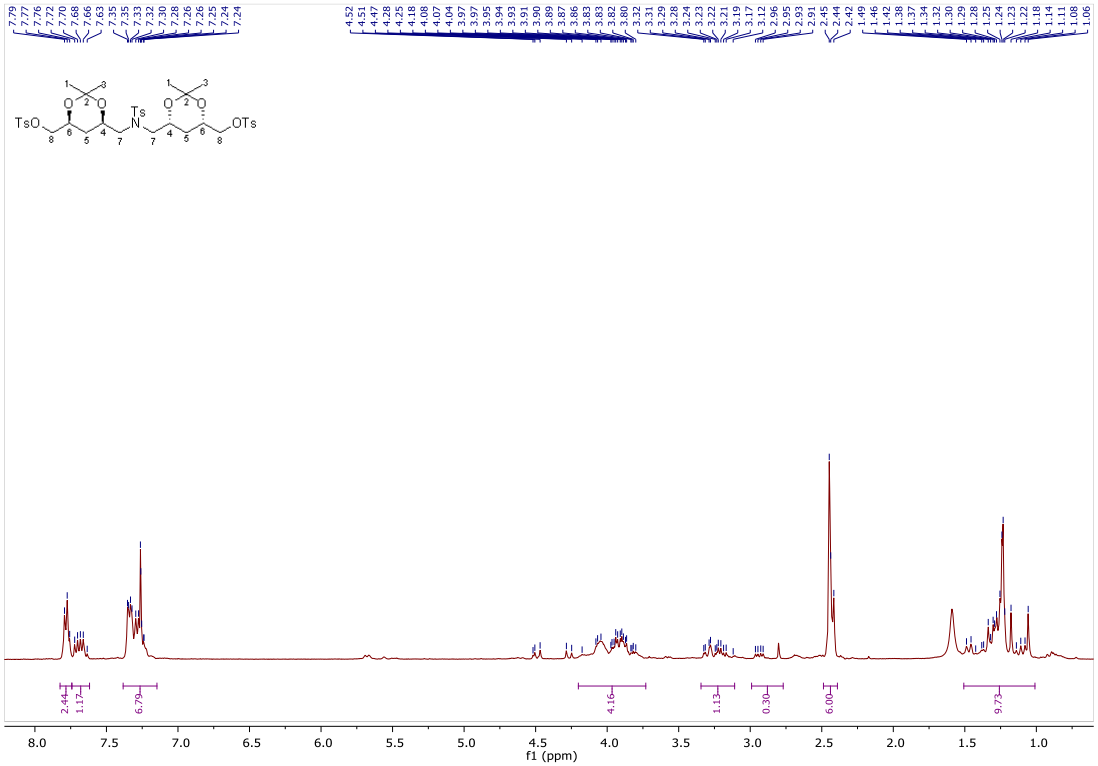


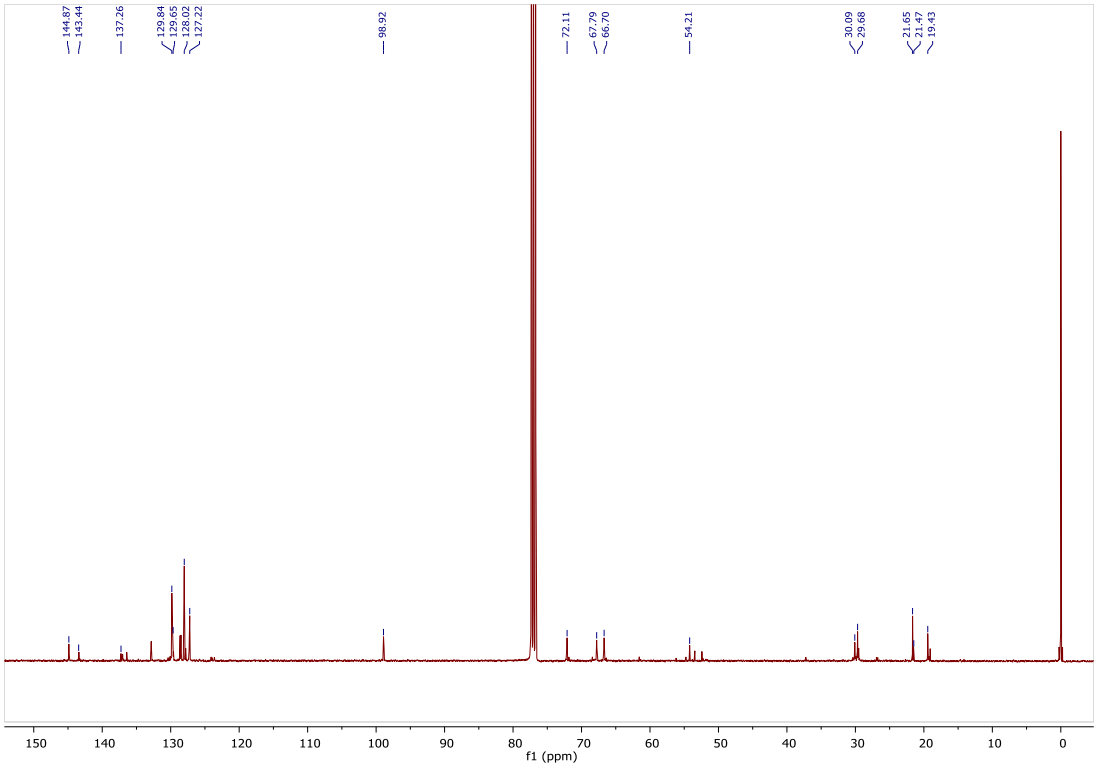


Compound 178

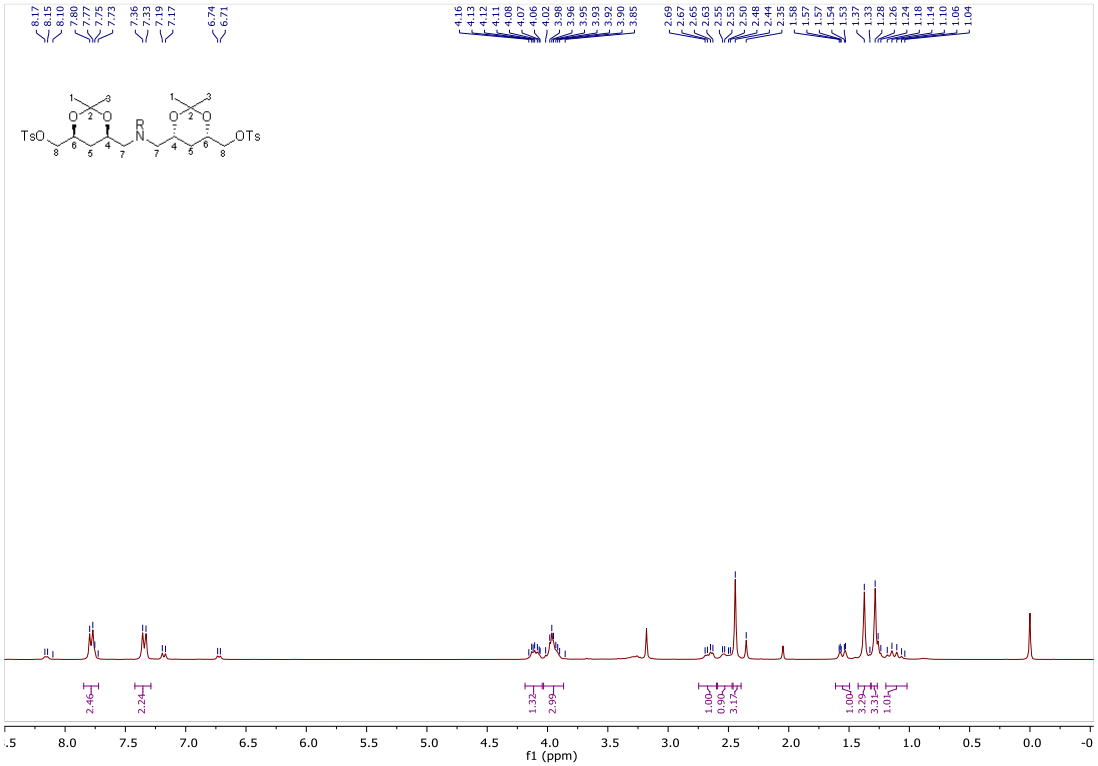


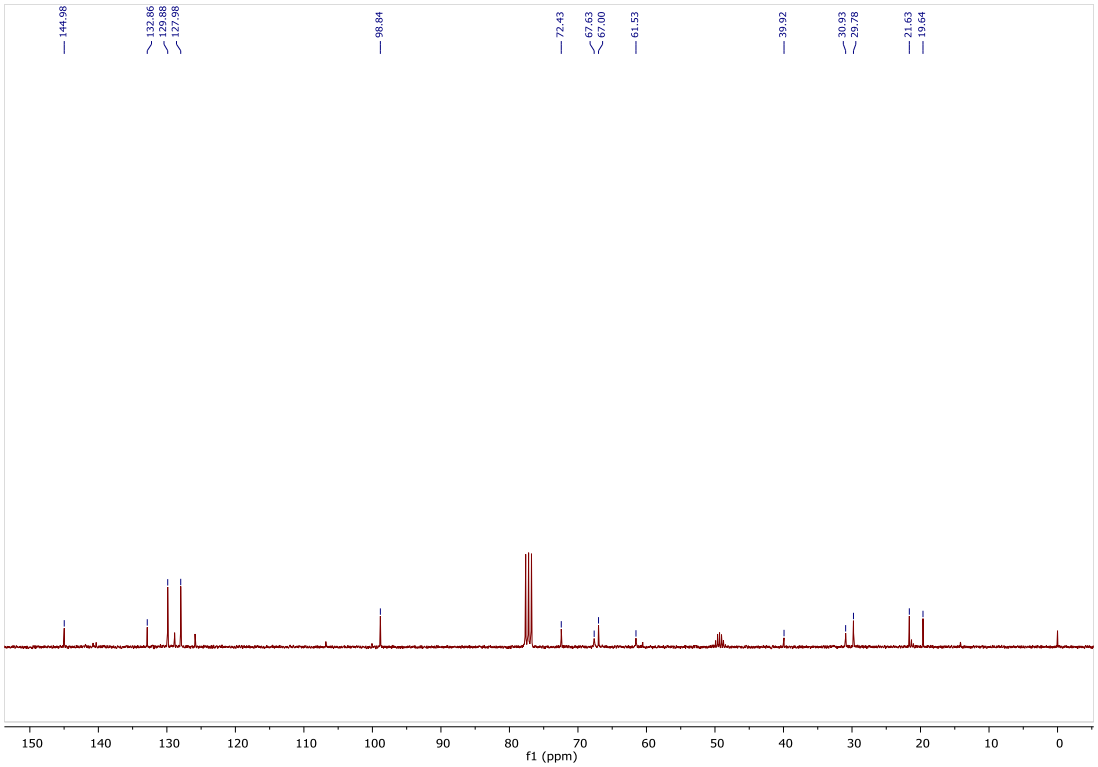
Compound 180



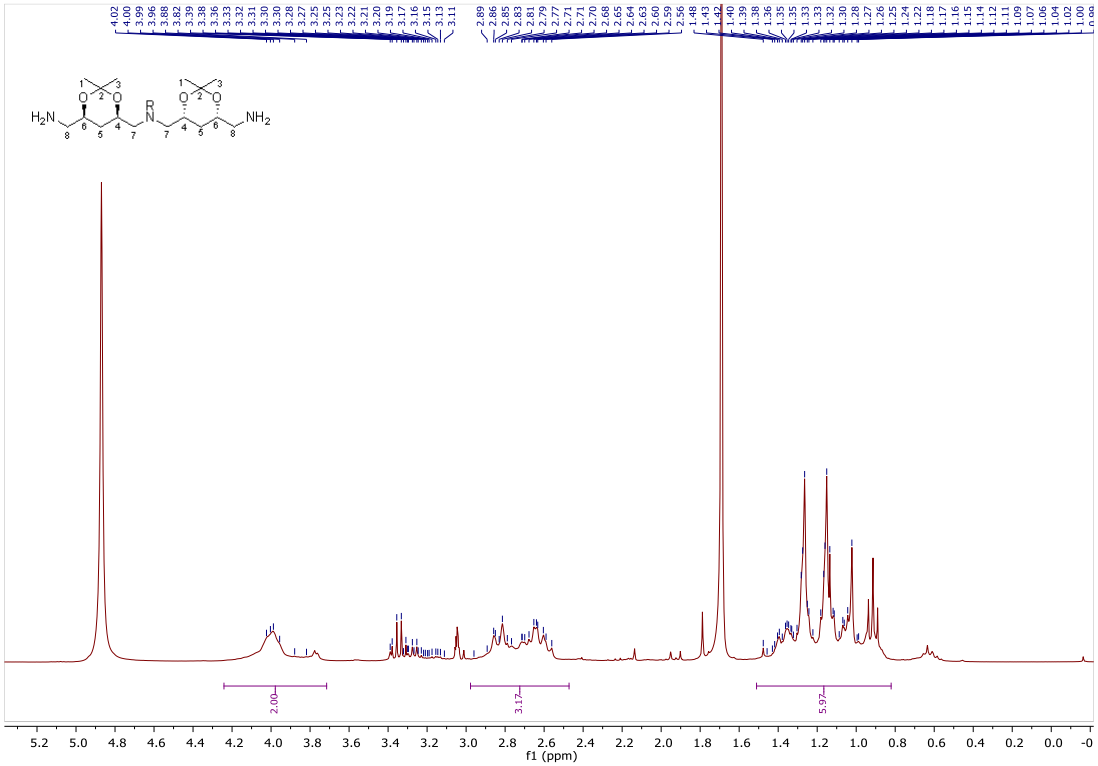


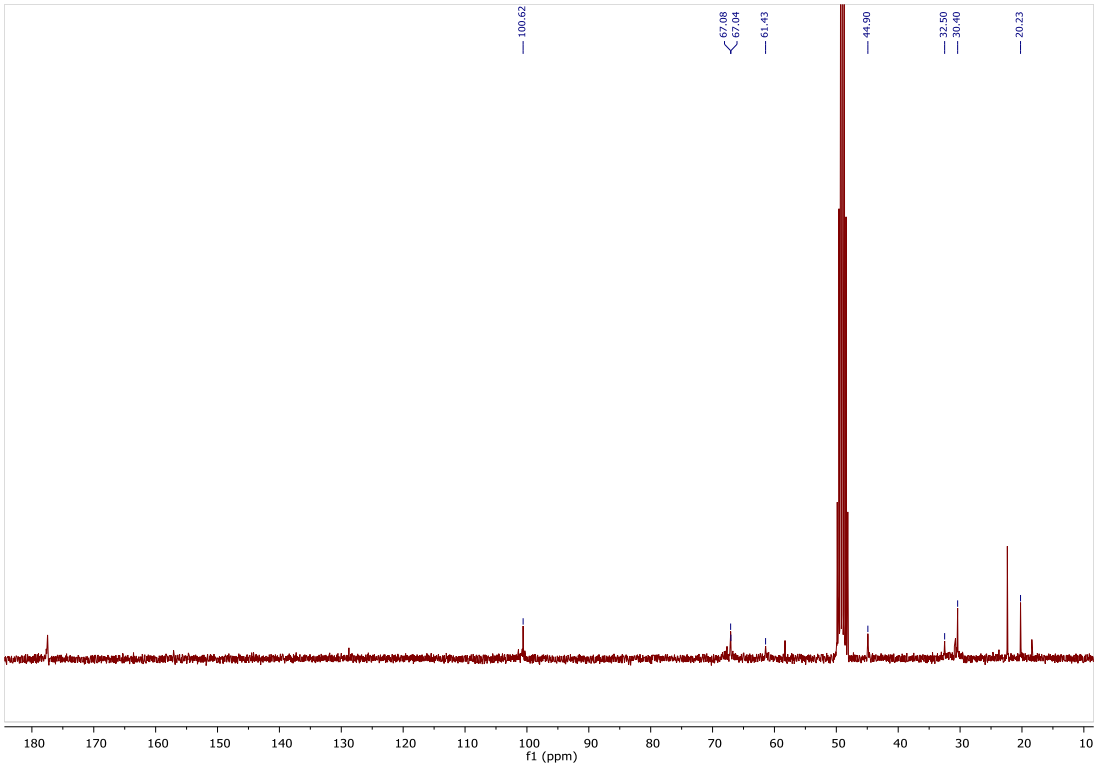
Compound 182



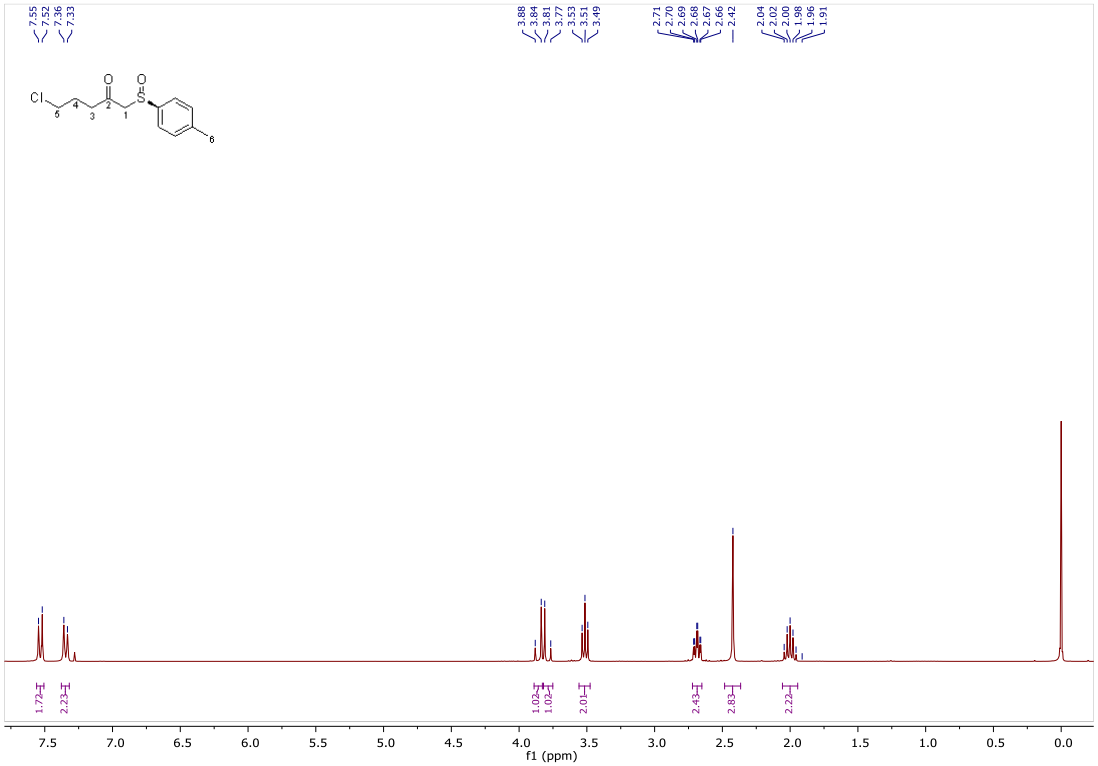


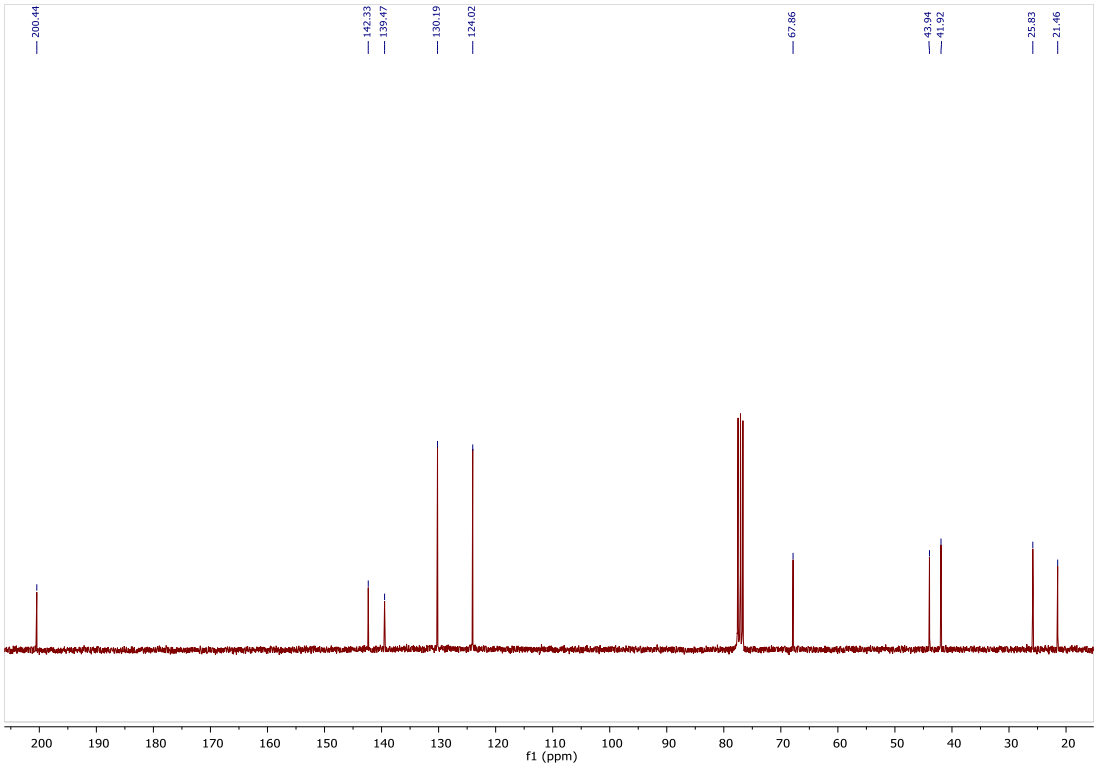
Compound 184



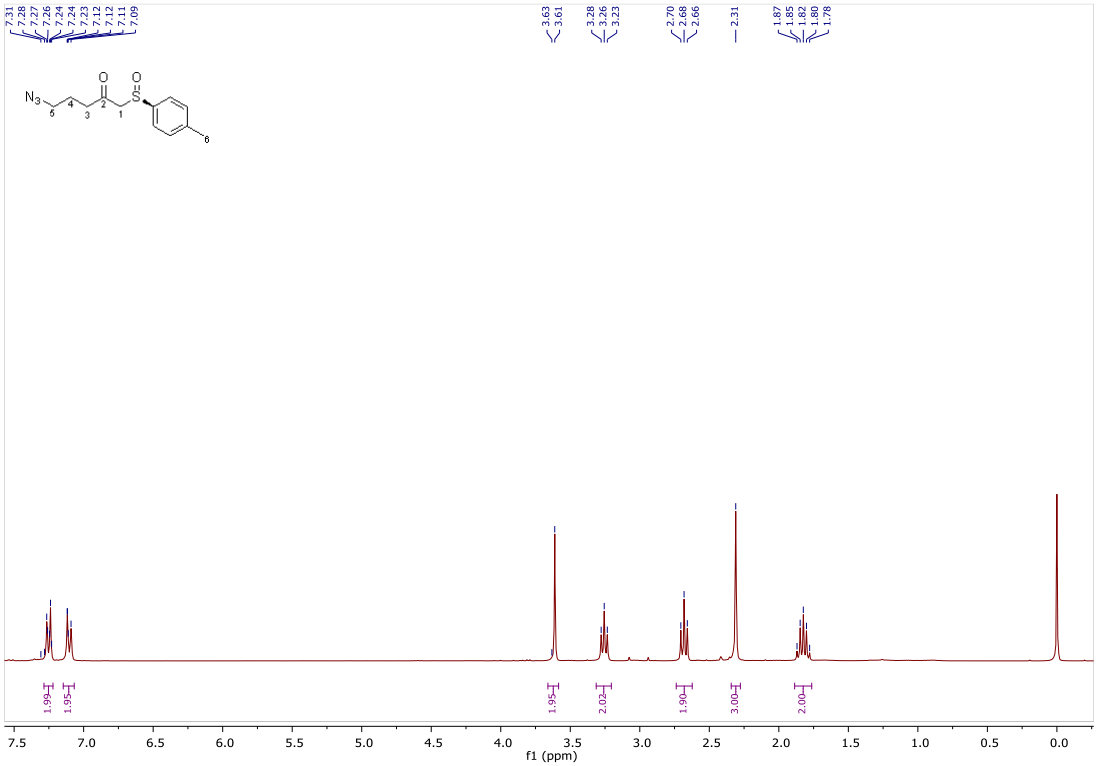


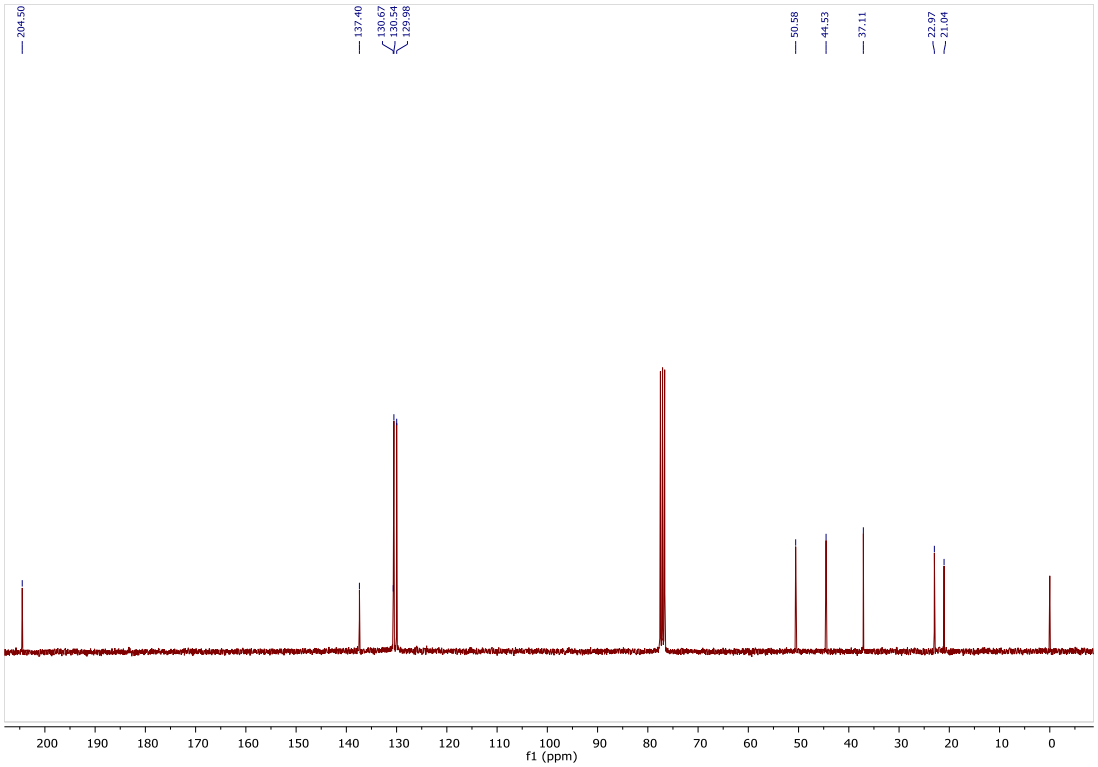
Compound 192



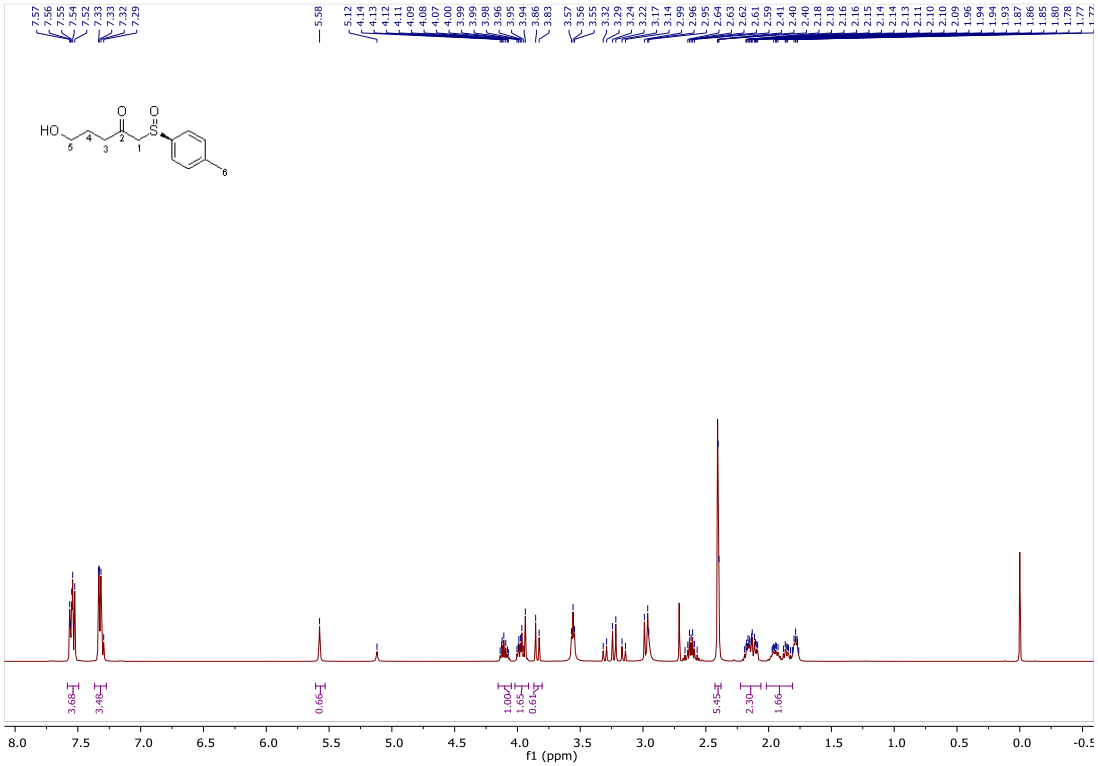


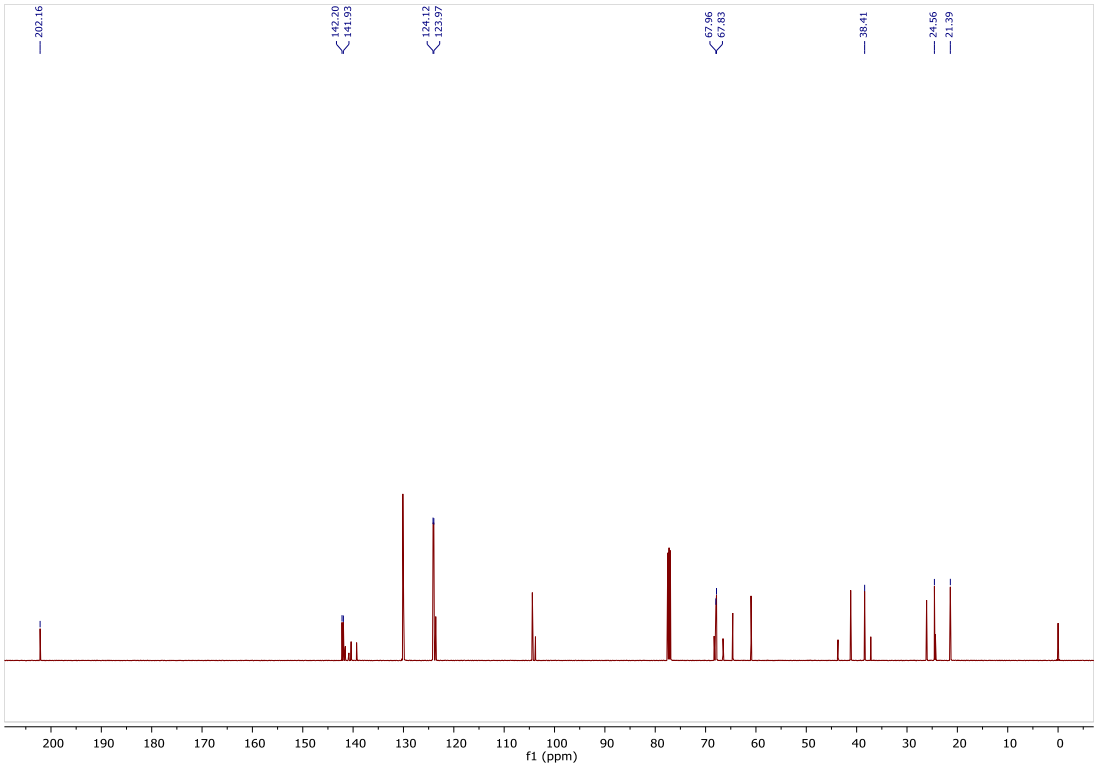
Compound 193



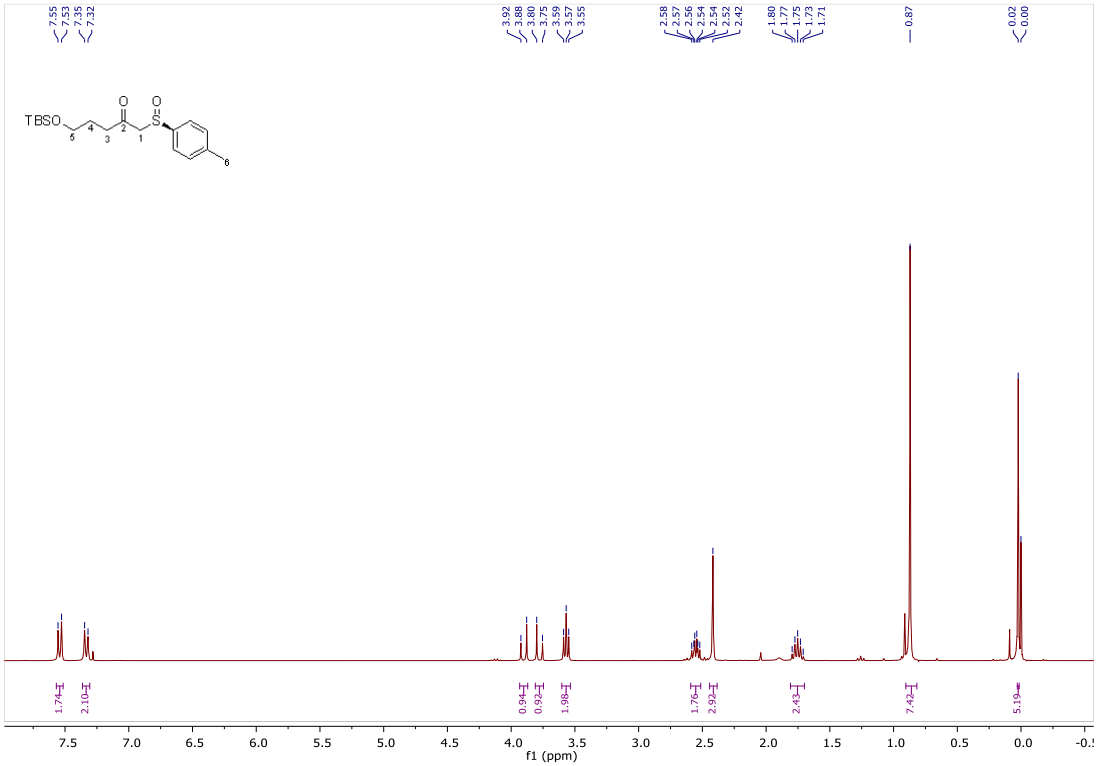


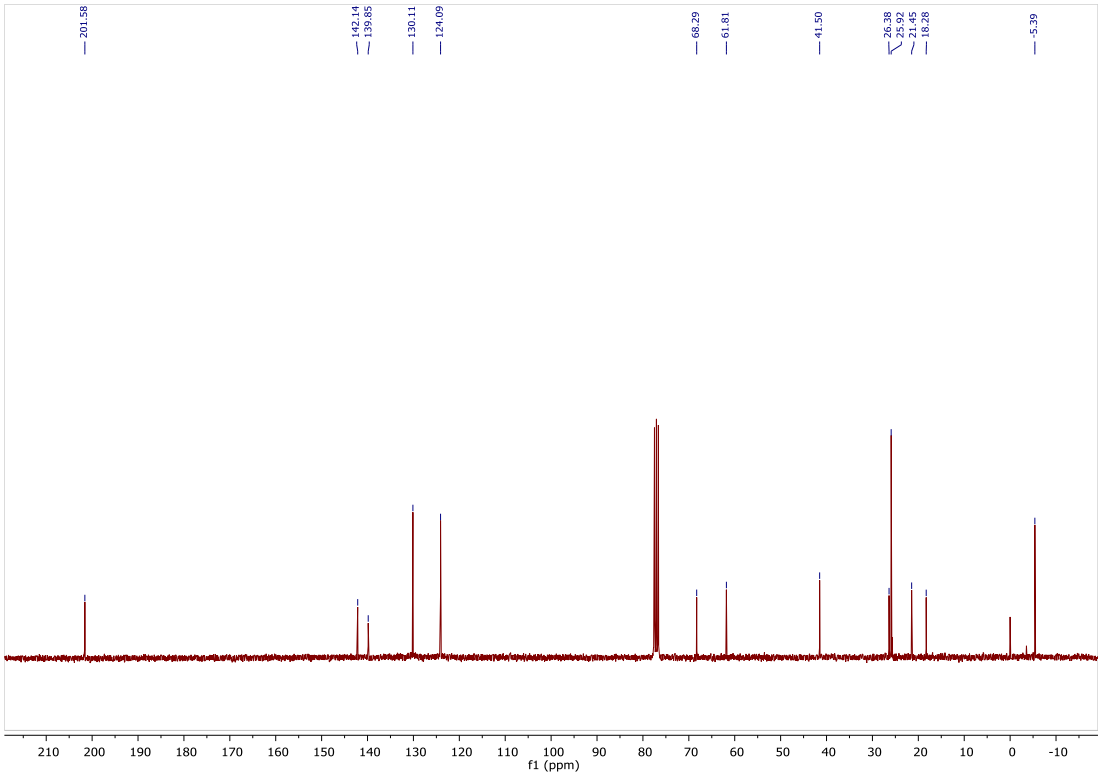
Compound 195



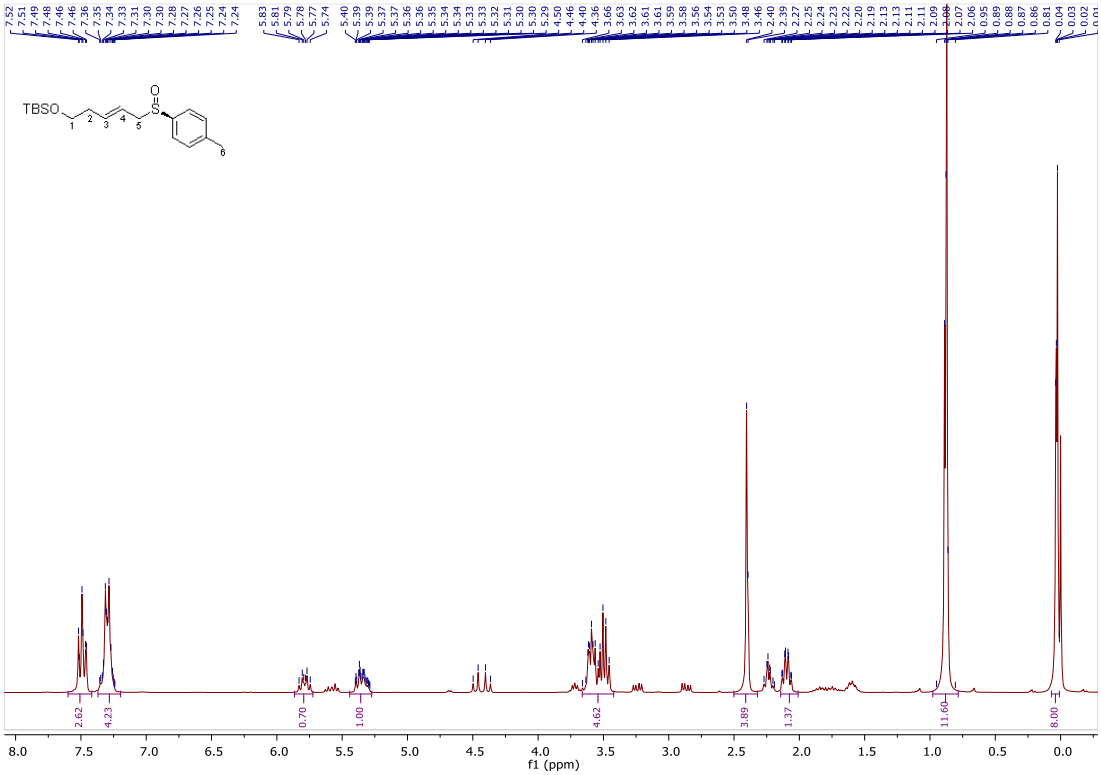


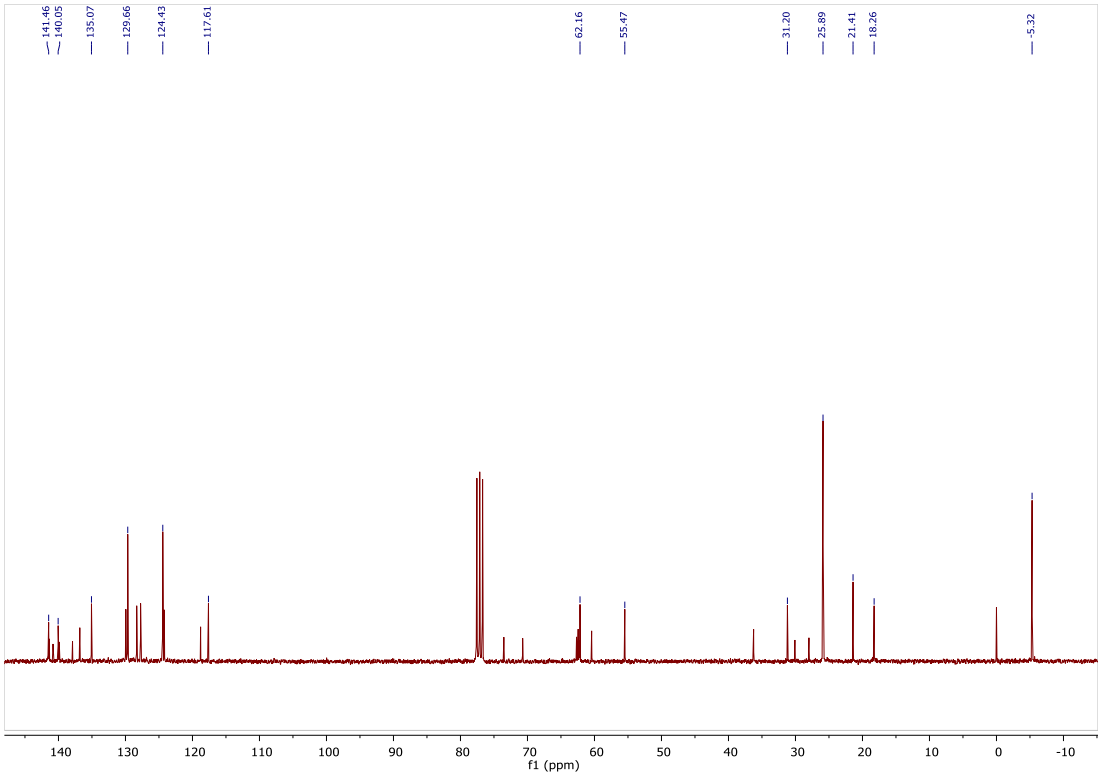
Compound 196



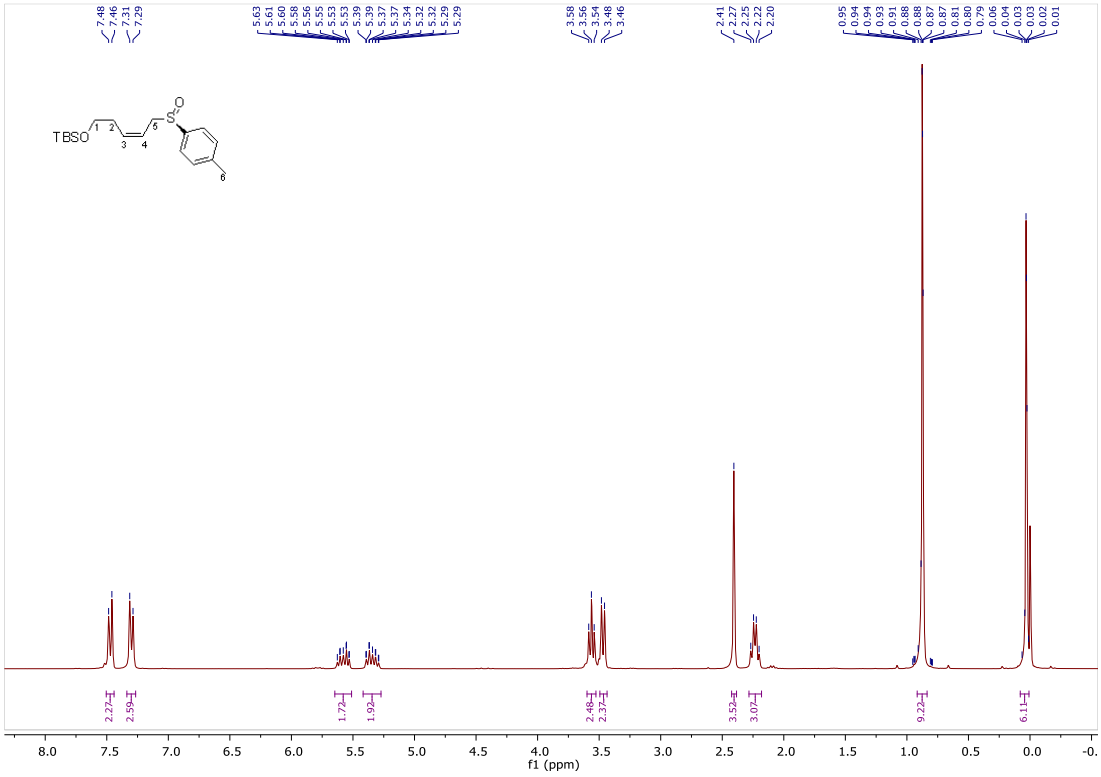


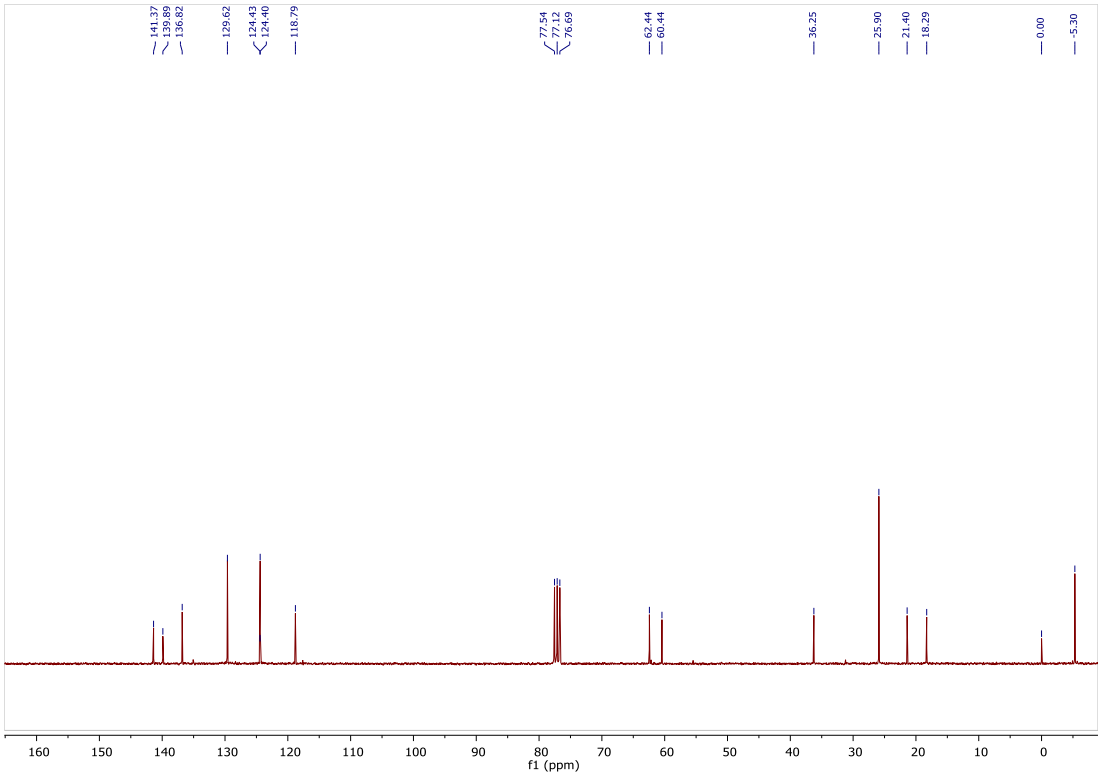
Compound 198



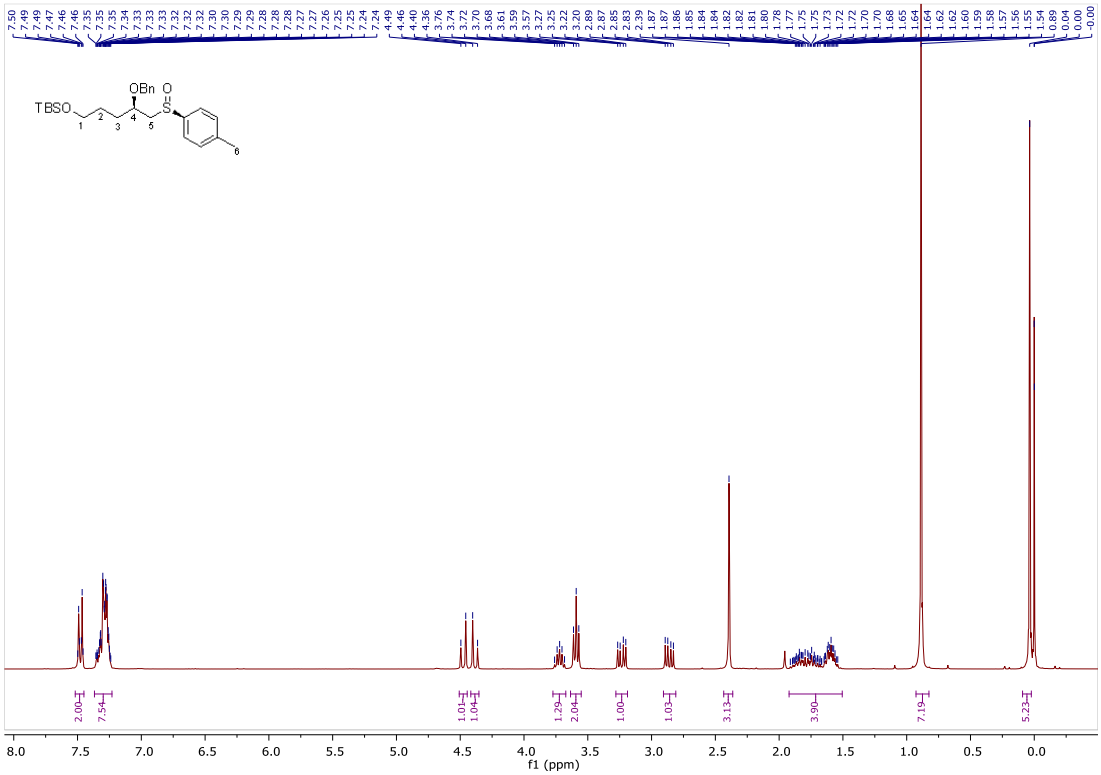


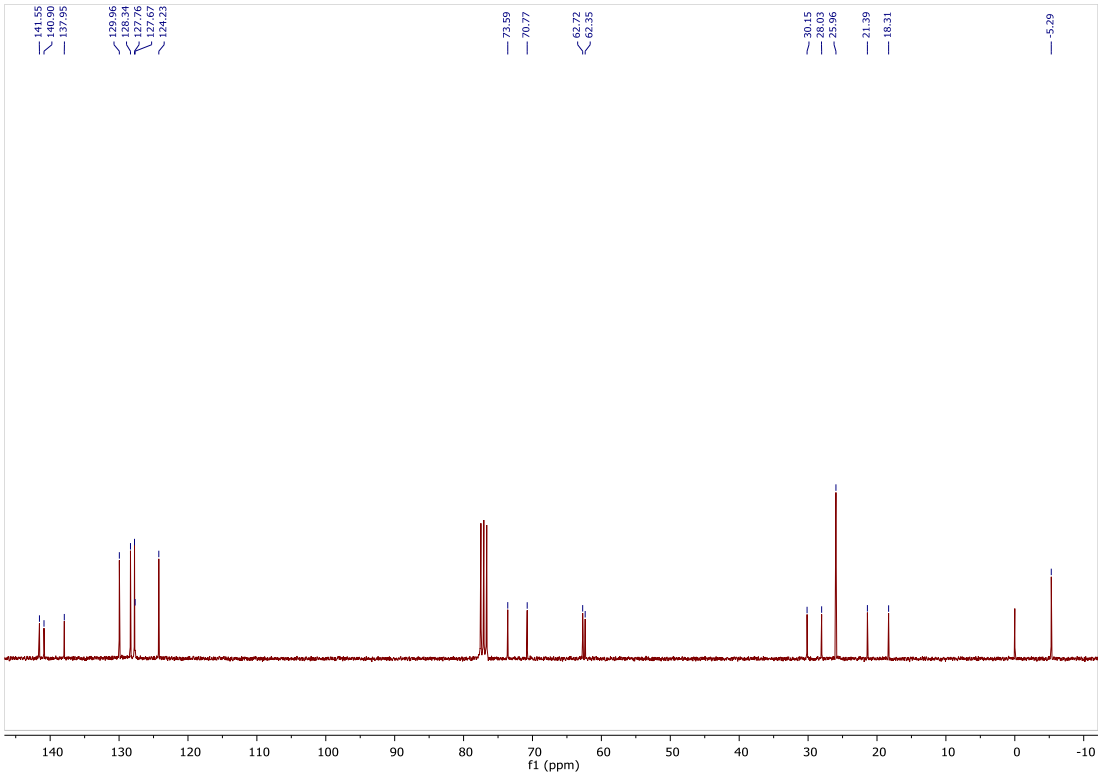
Compound 199



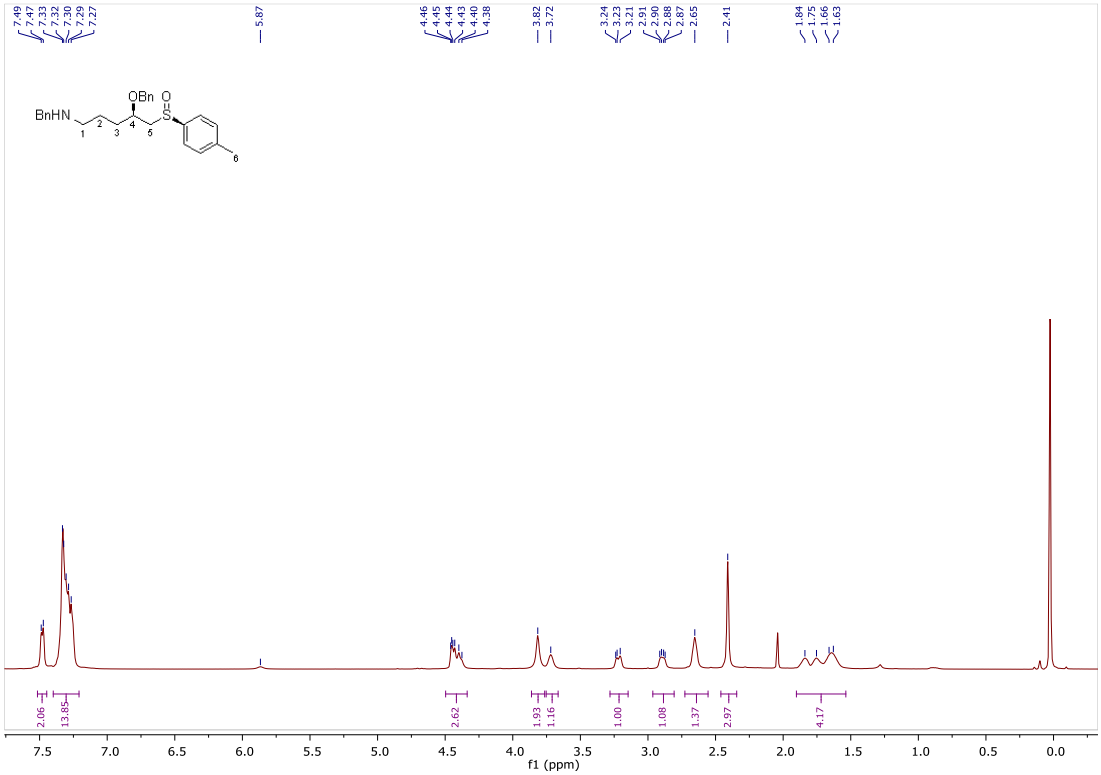


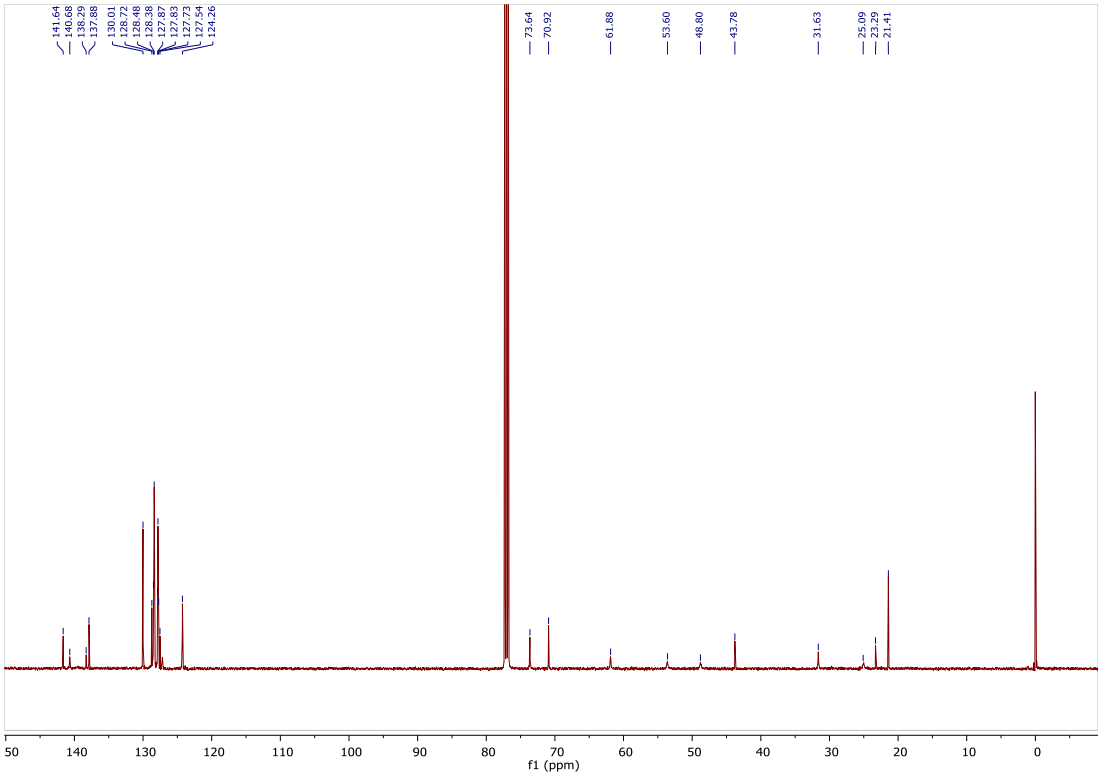
Compound 200



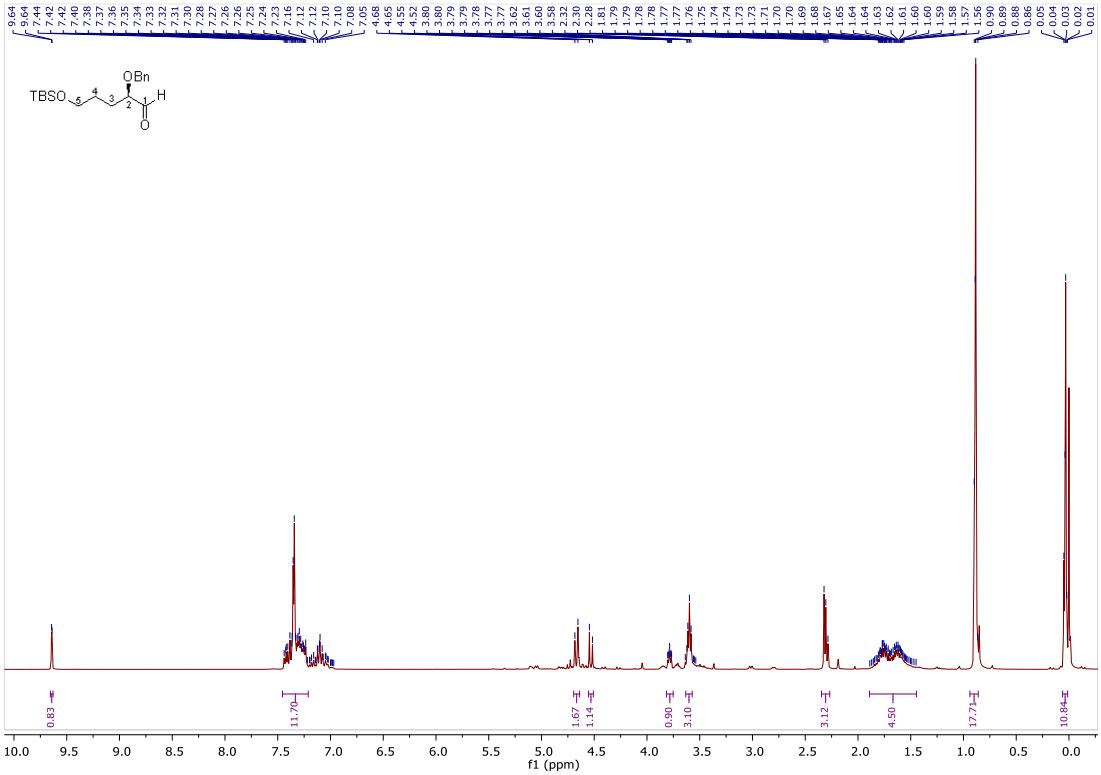


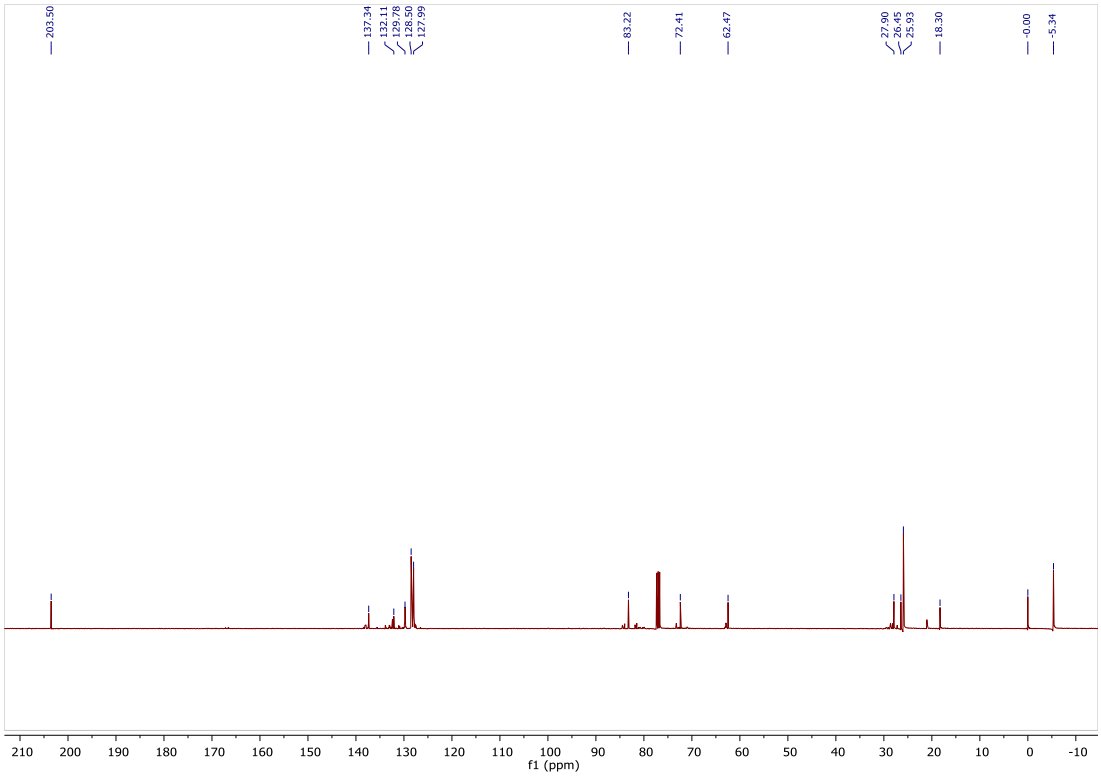
Compound 203



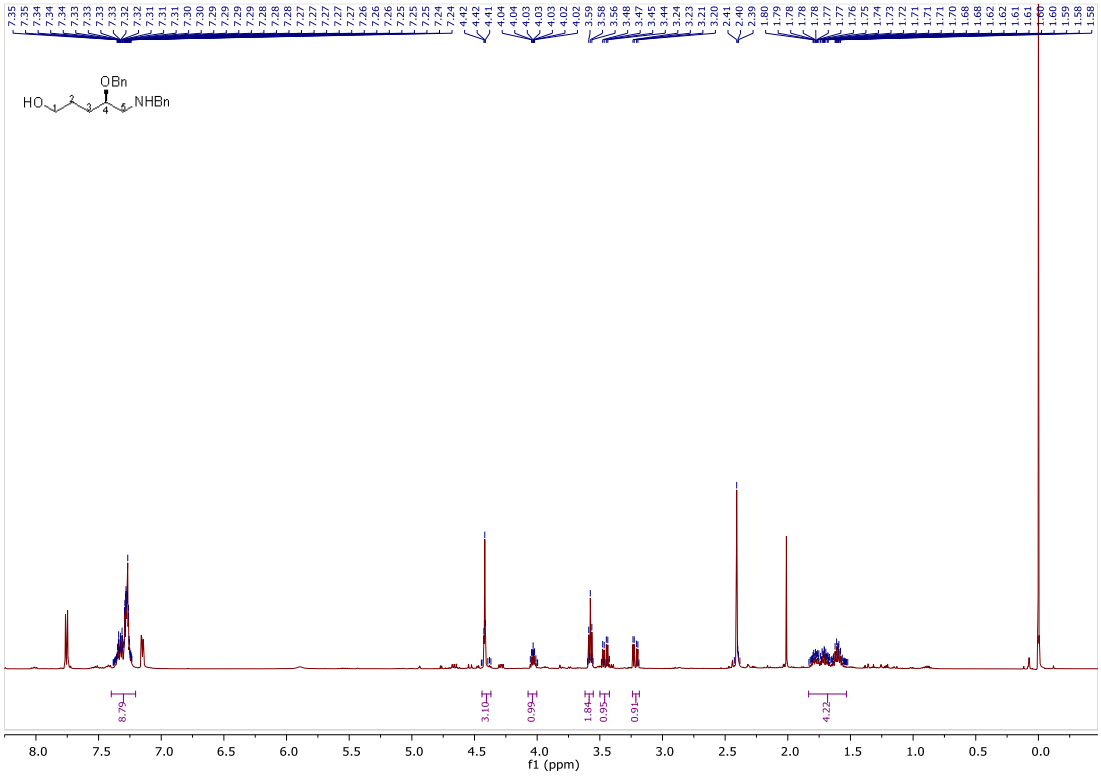


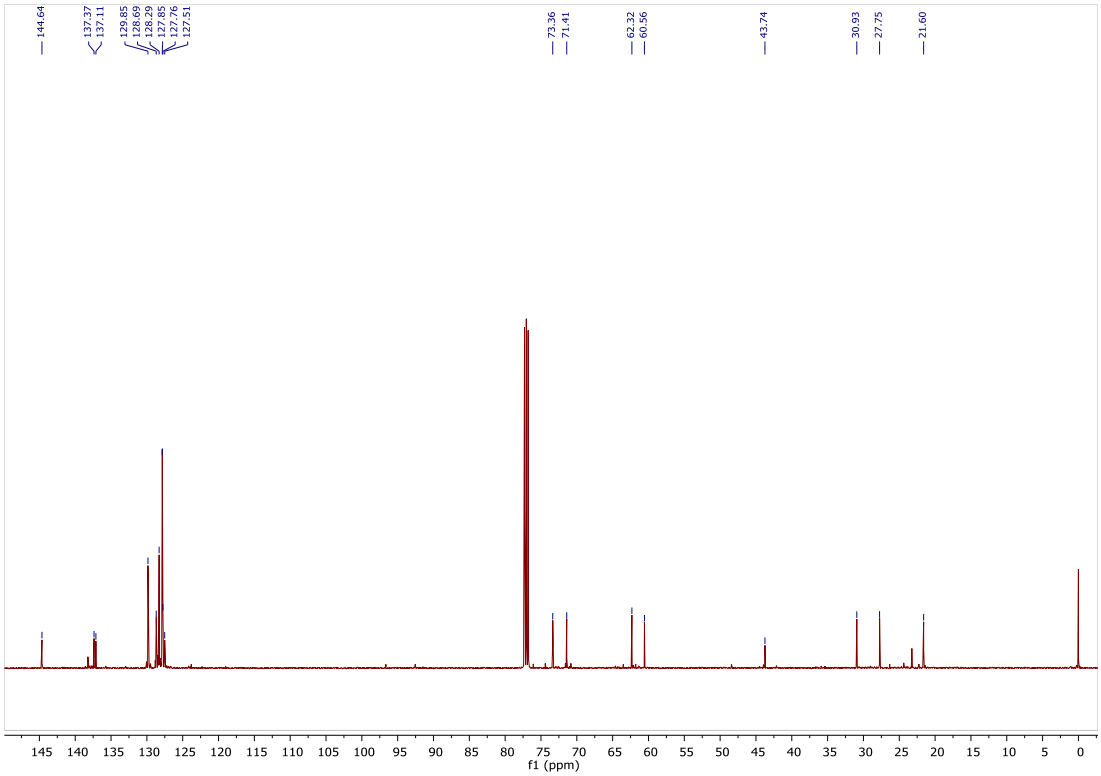
Compound 204



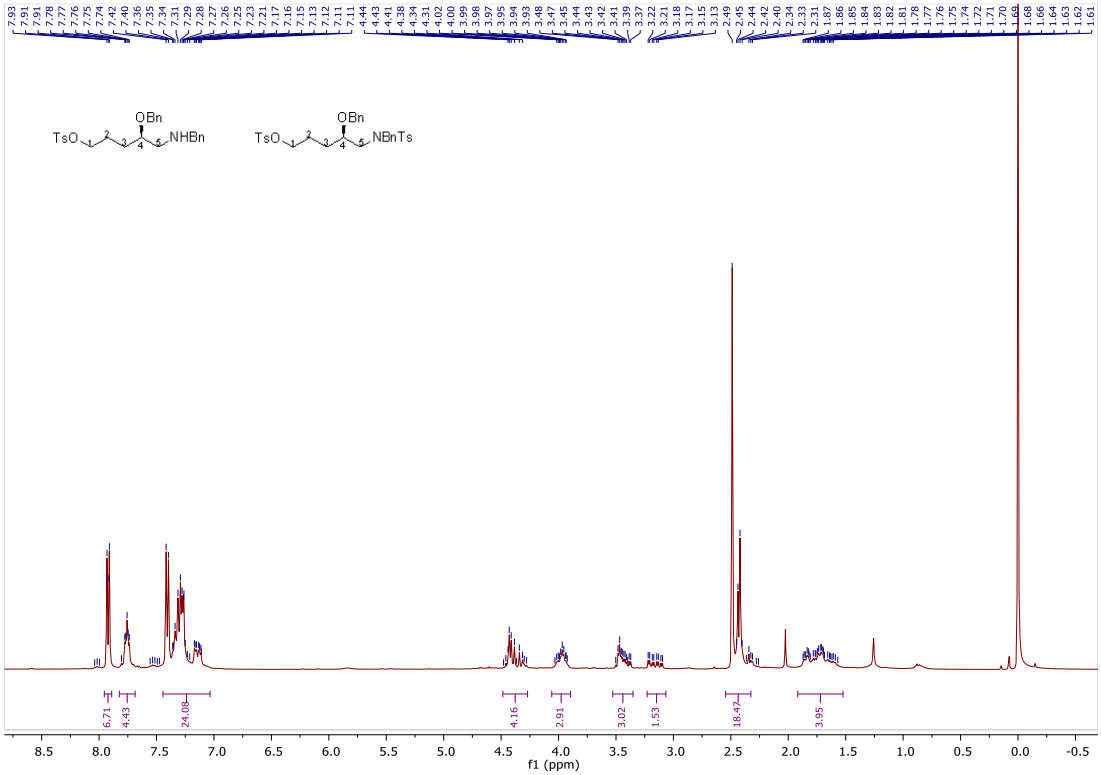


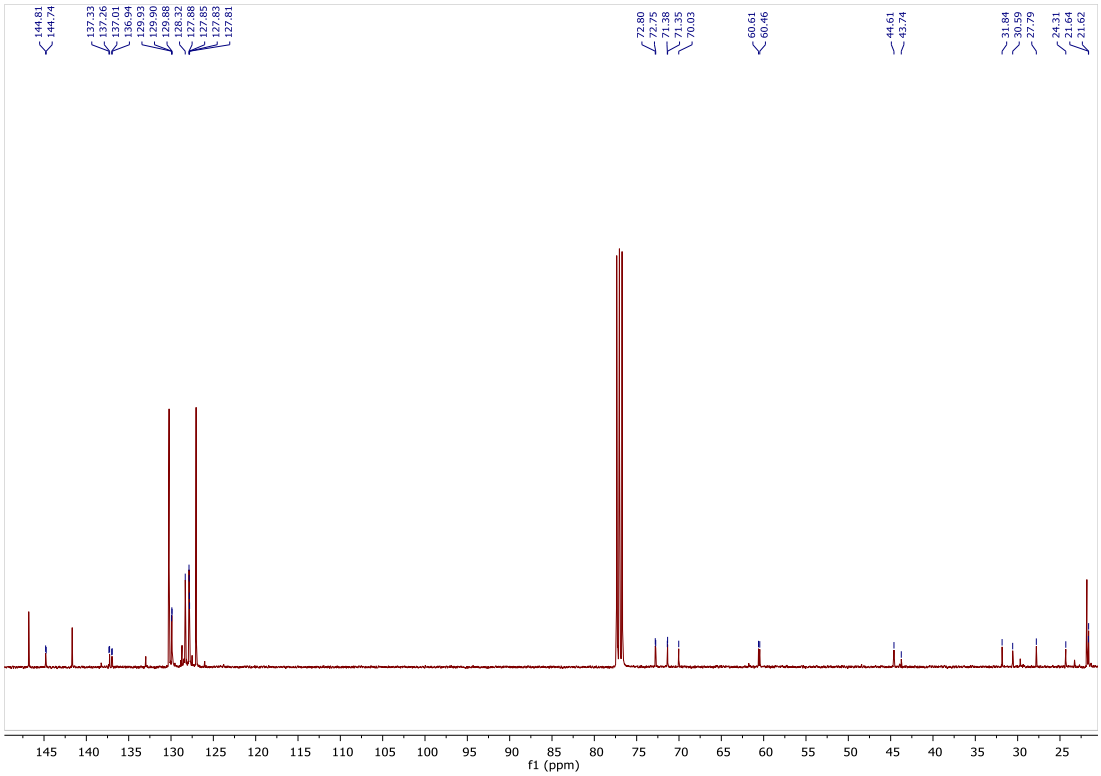
Compound 205



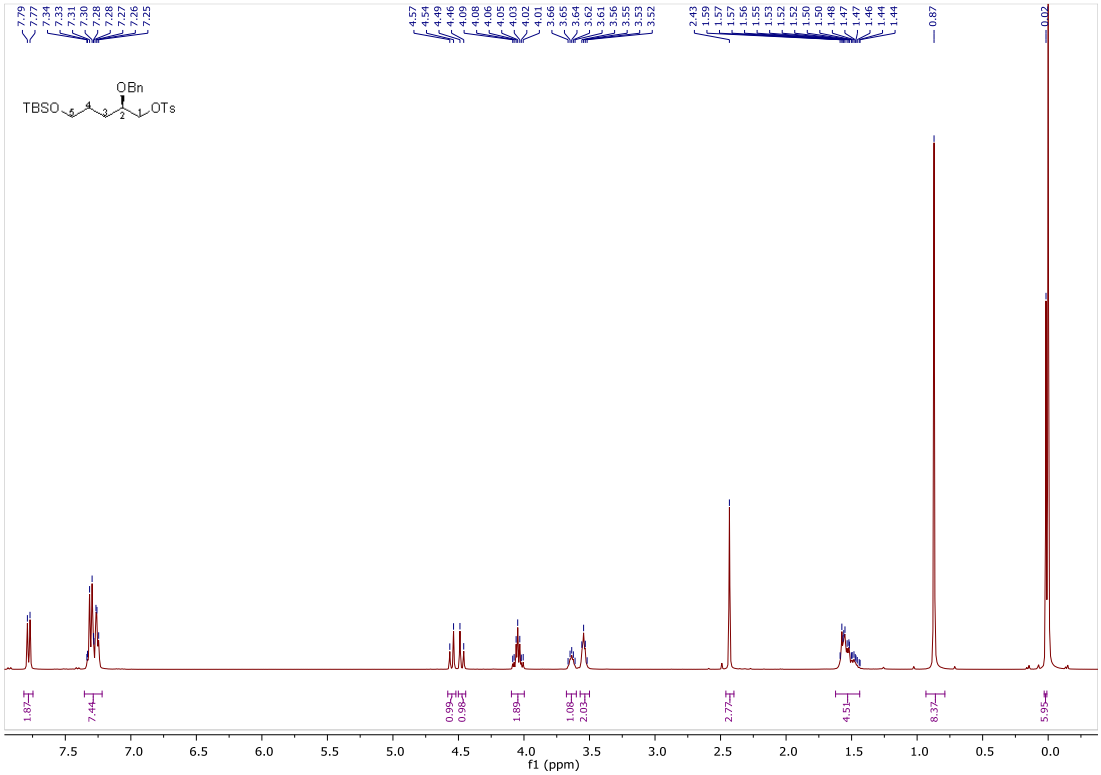


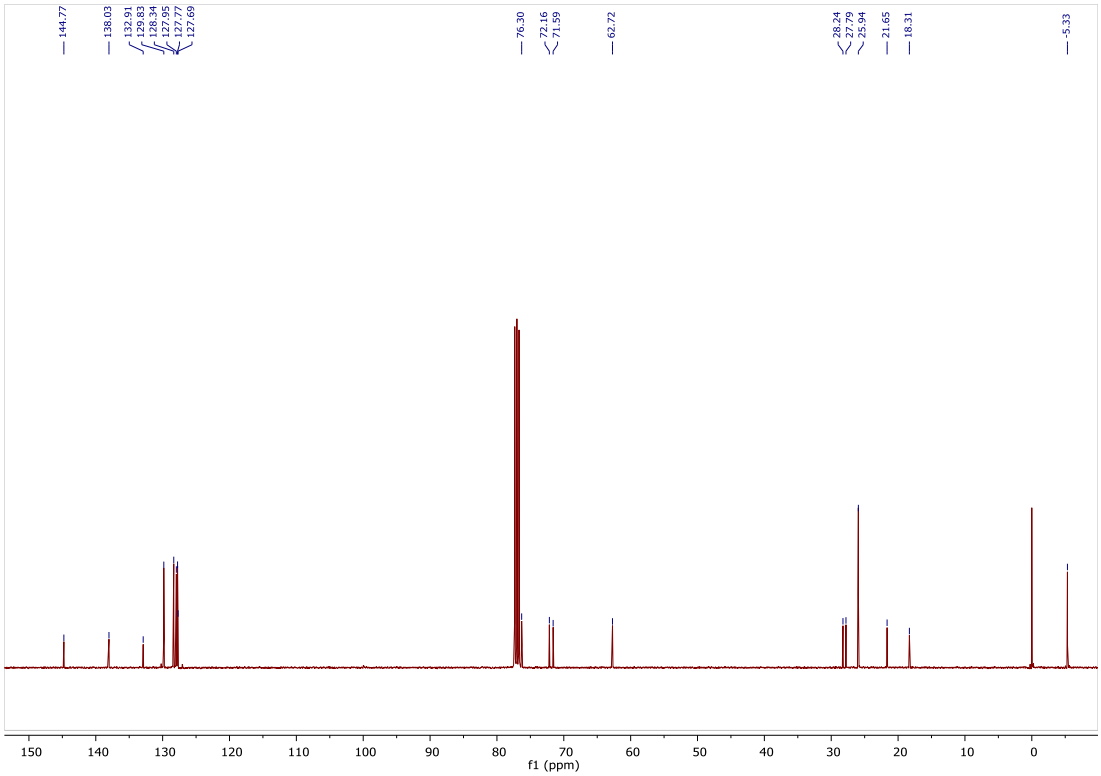
Compound 206 and 207



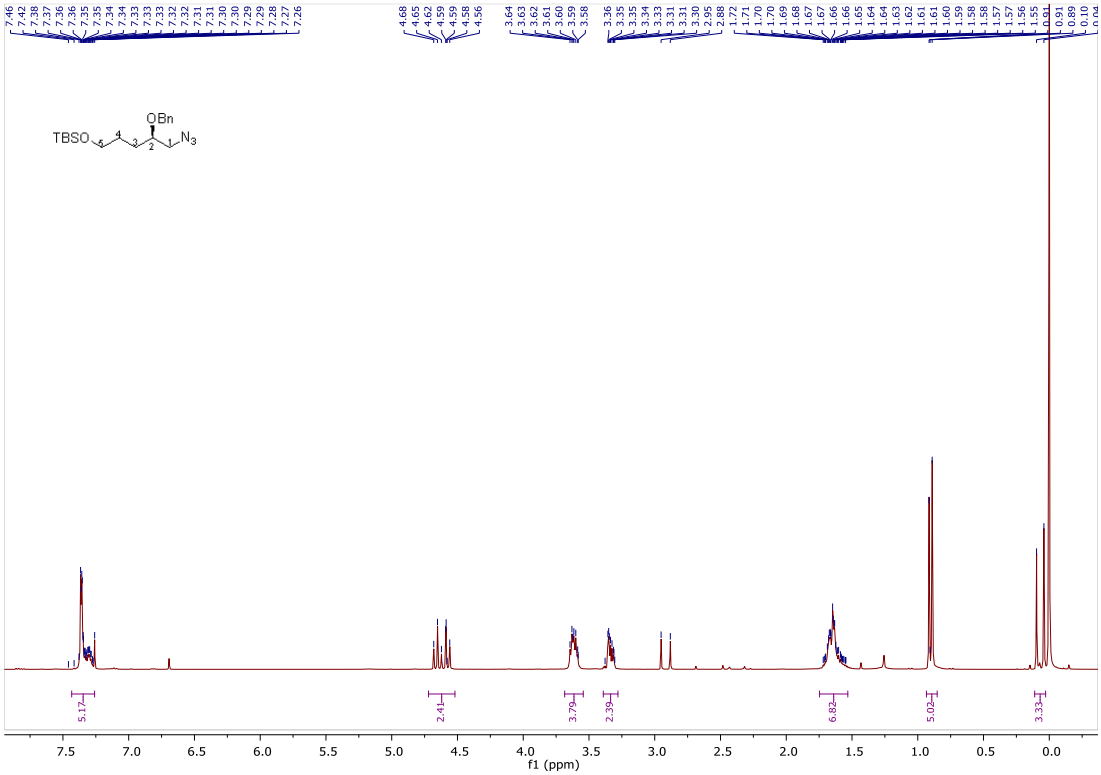


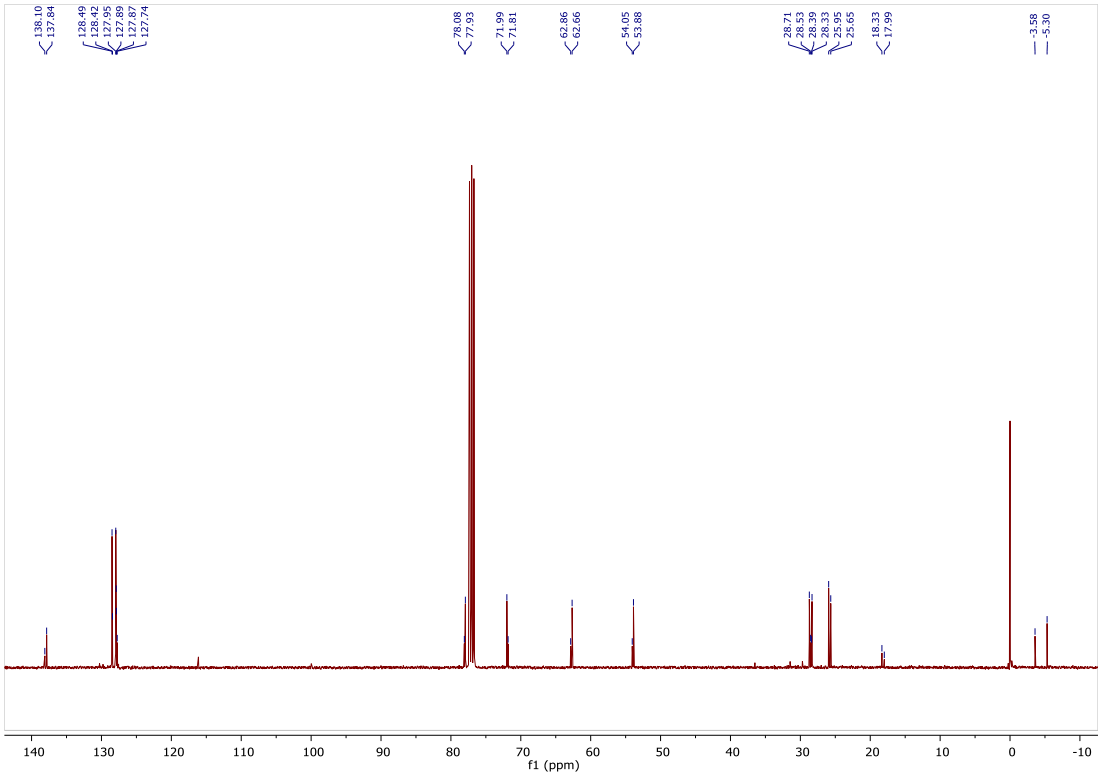
Compound 211



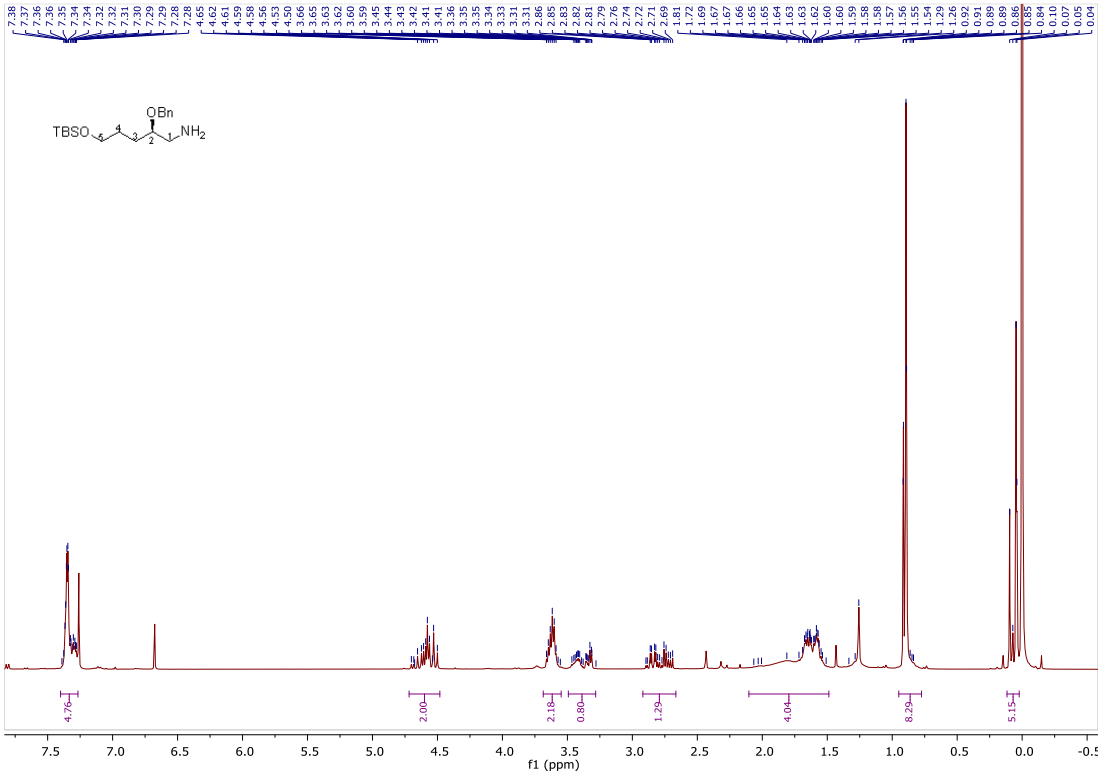


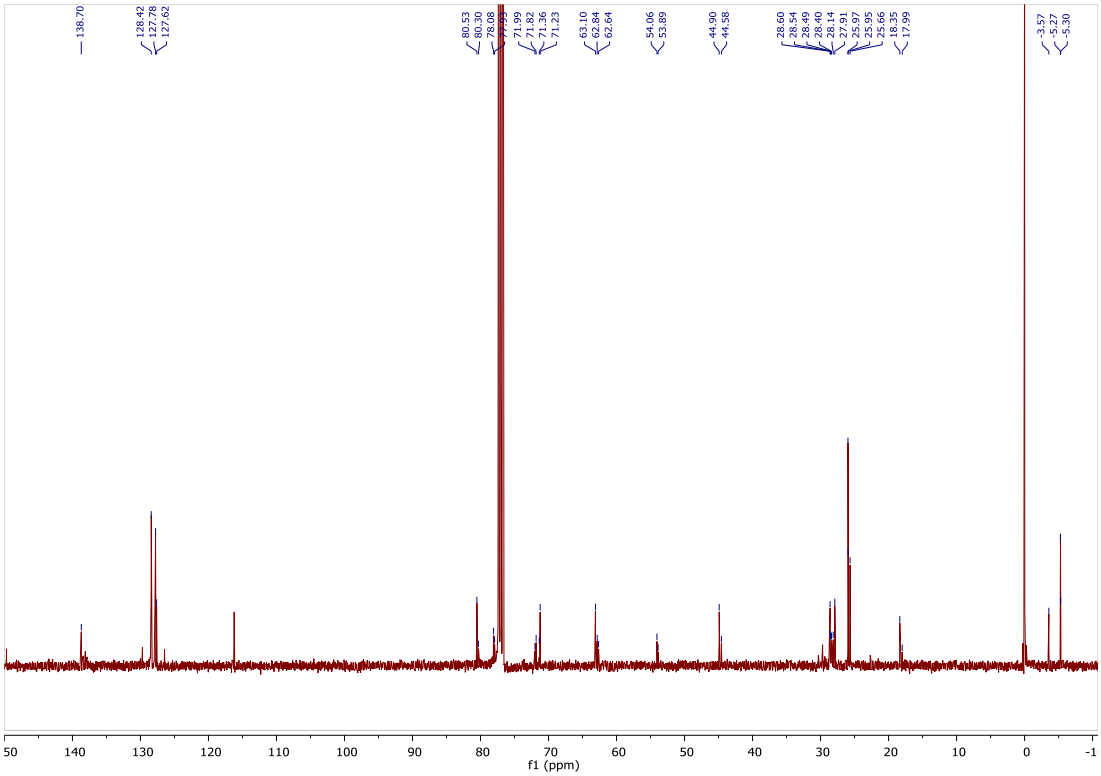
Compound 212



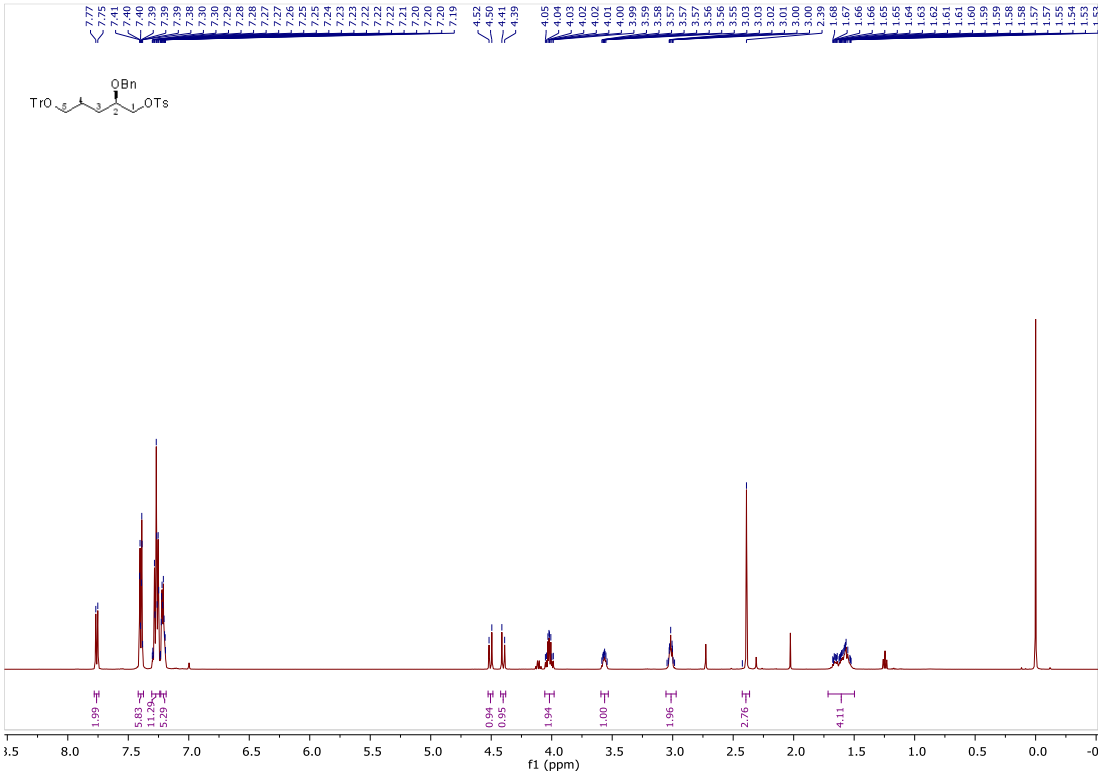


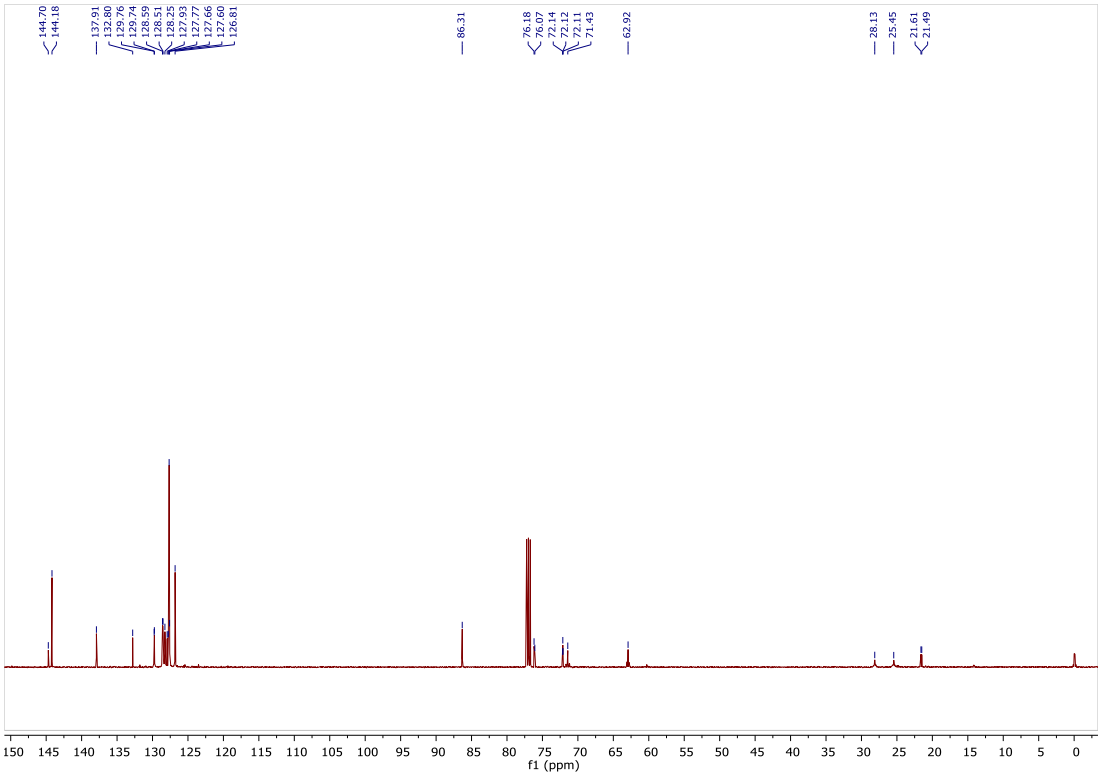
Compound 213



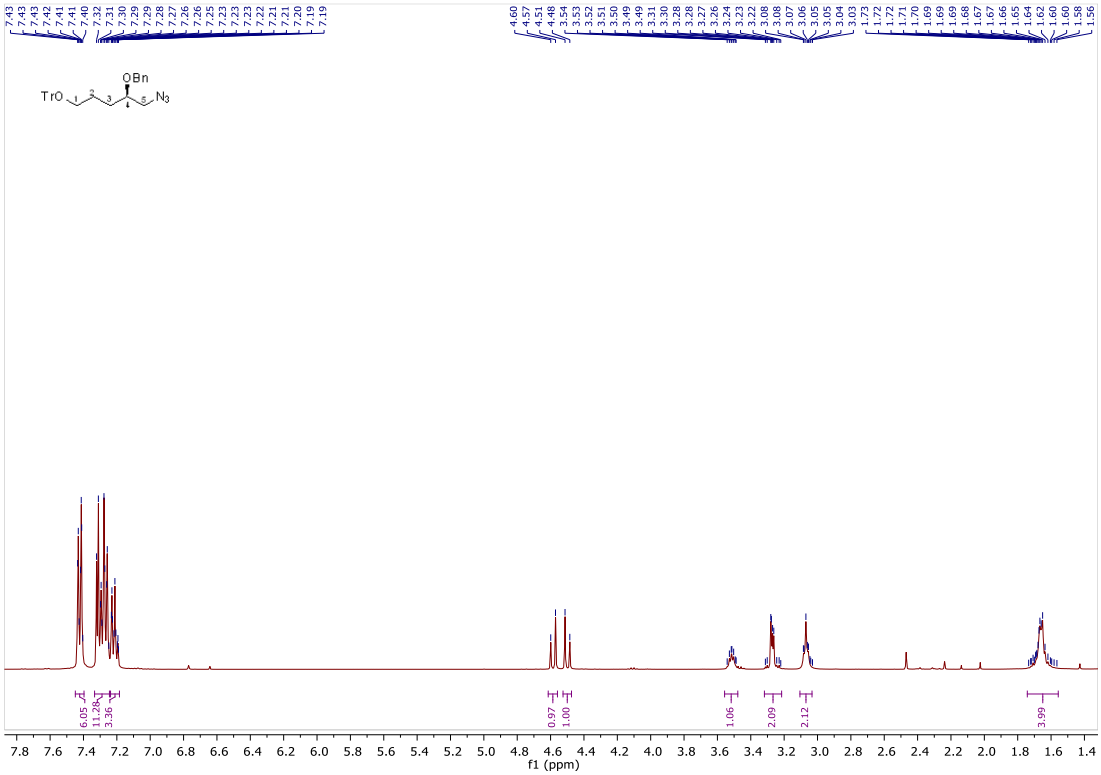


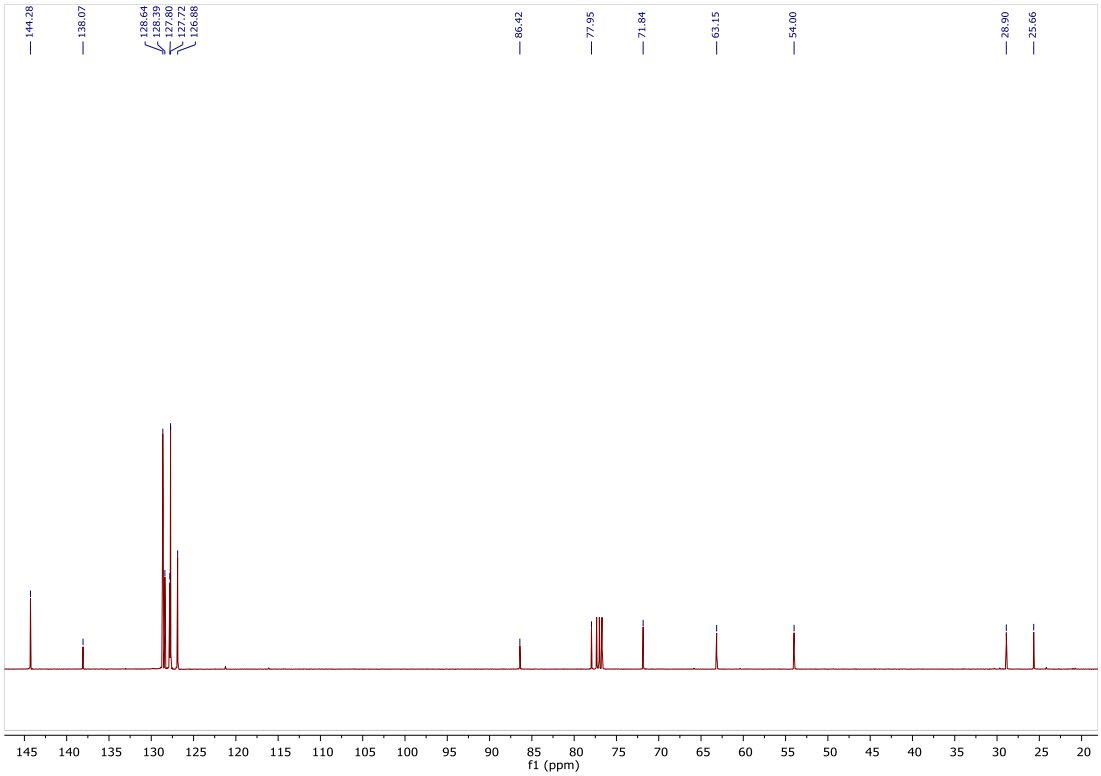
Compound 216



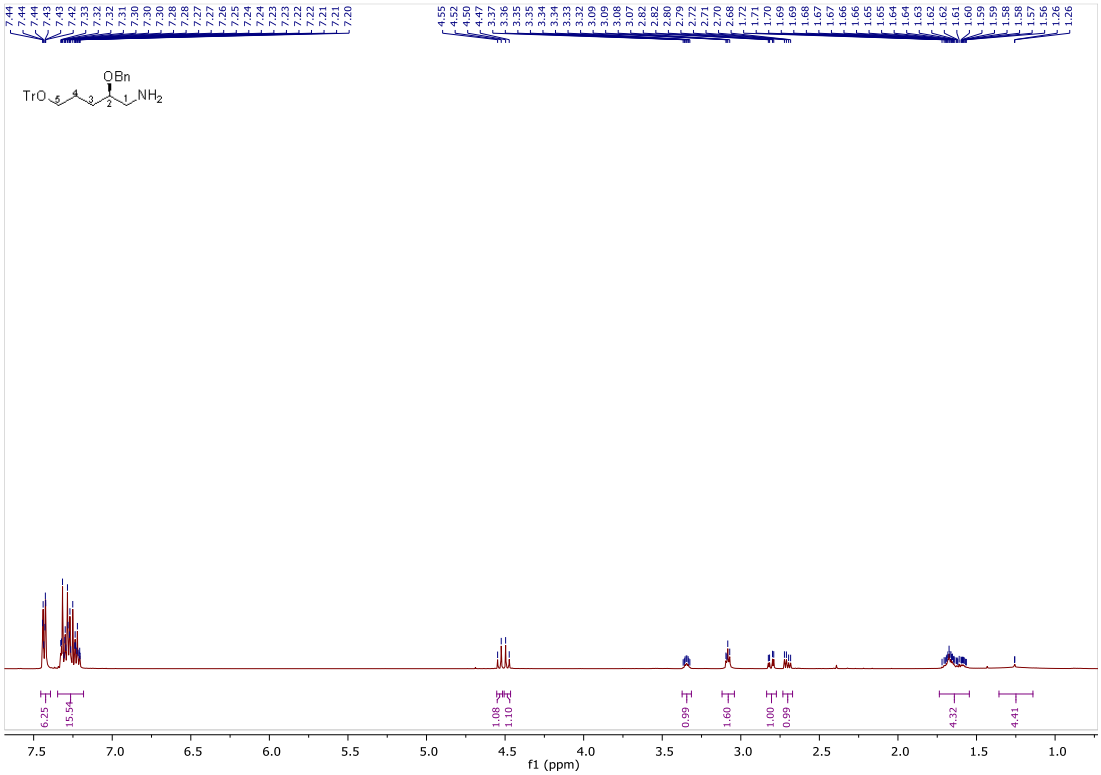


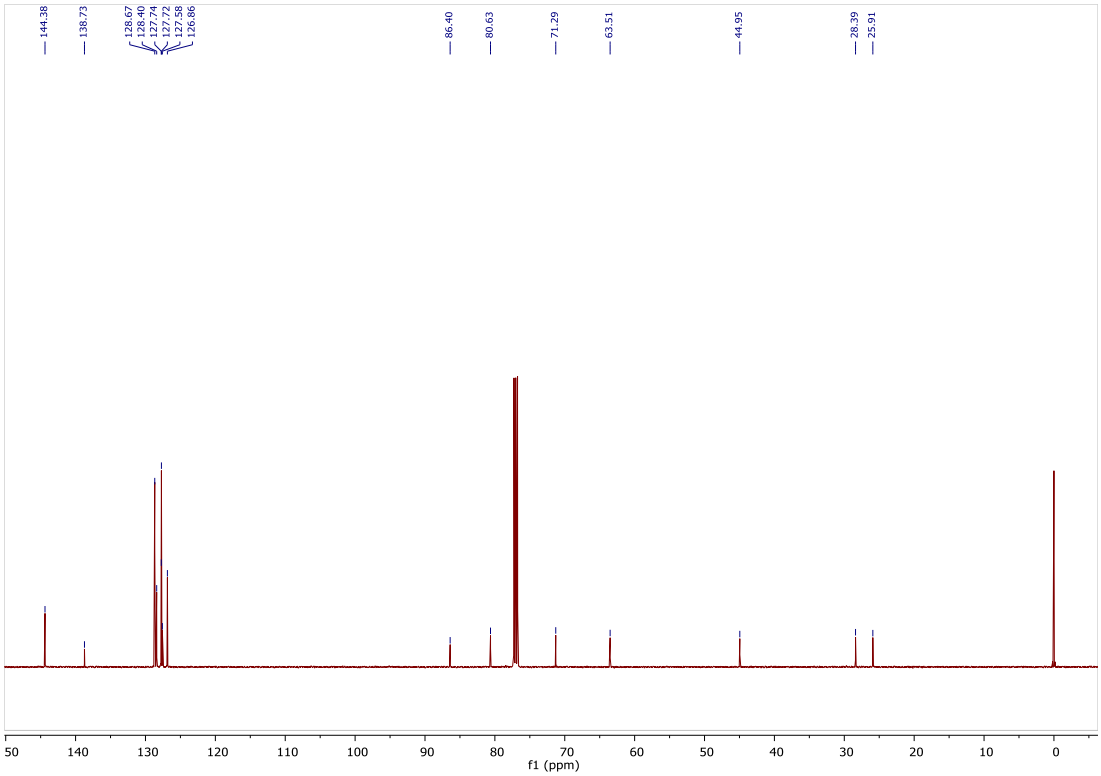
Compound 217



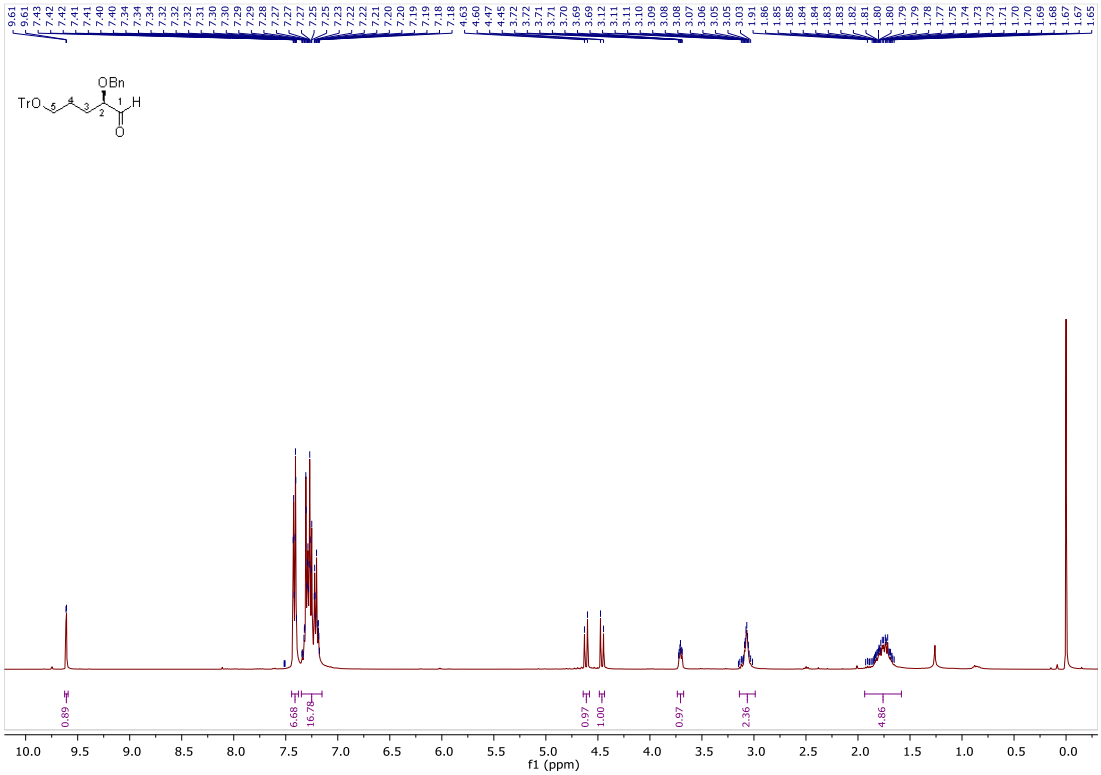


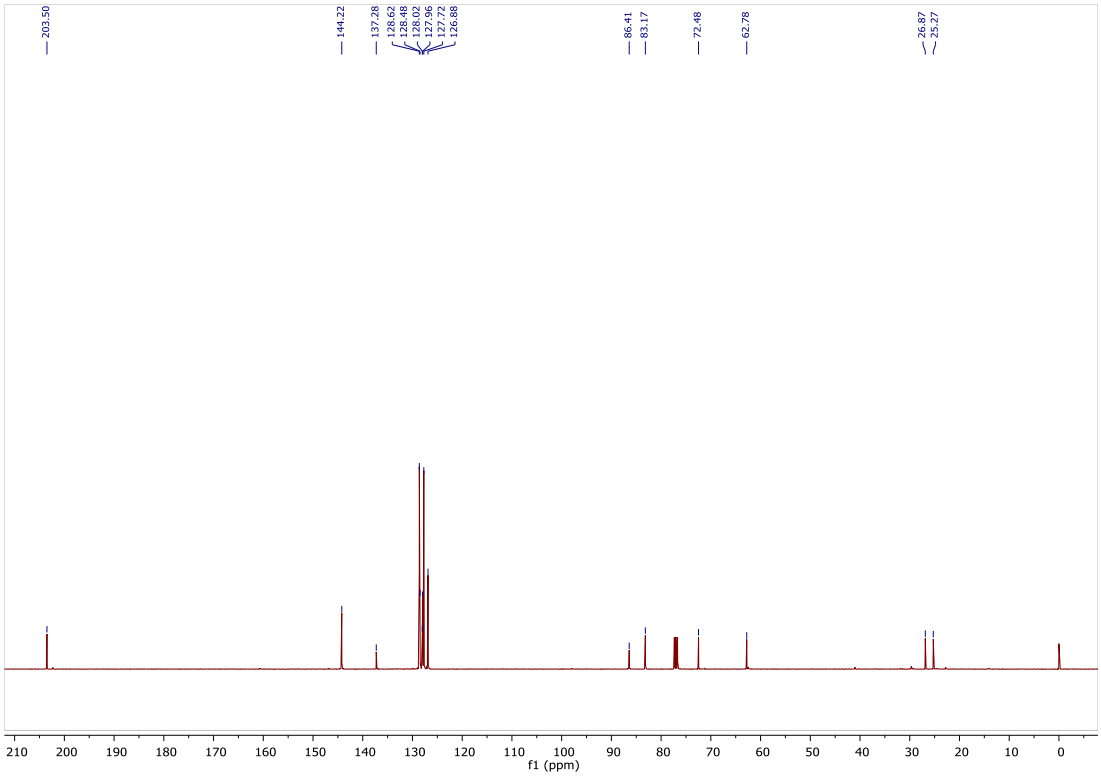
Compound 218



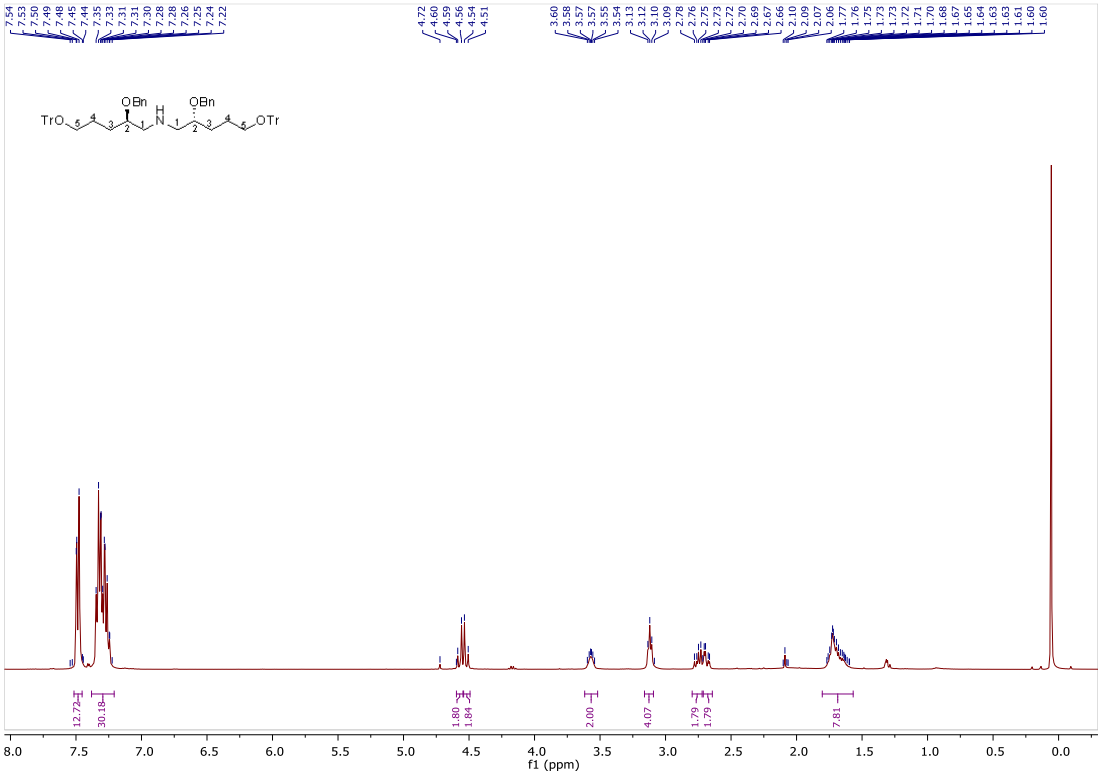


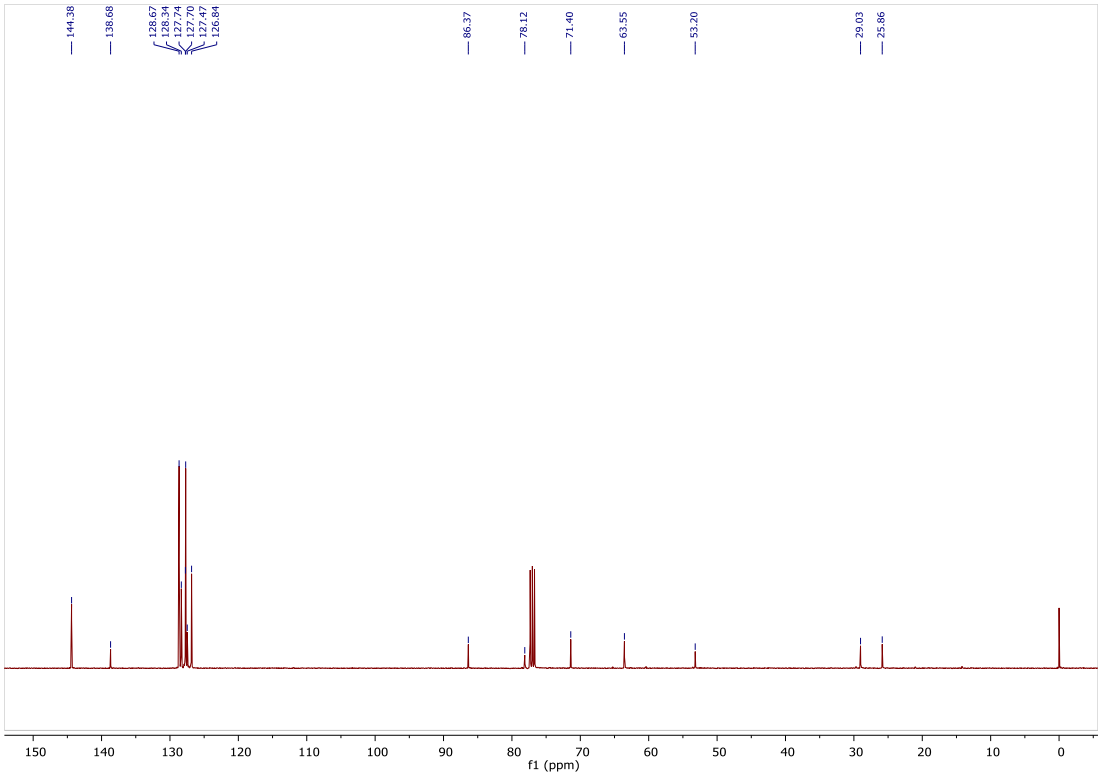
Compound 219



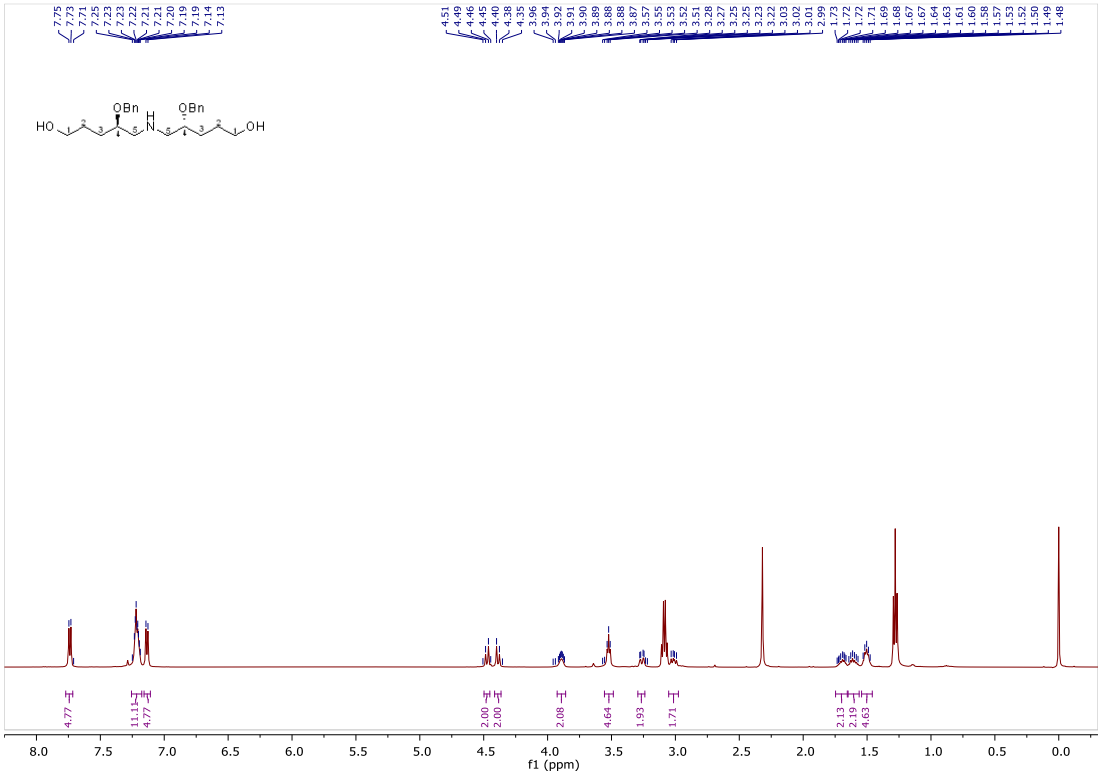


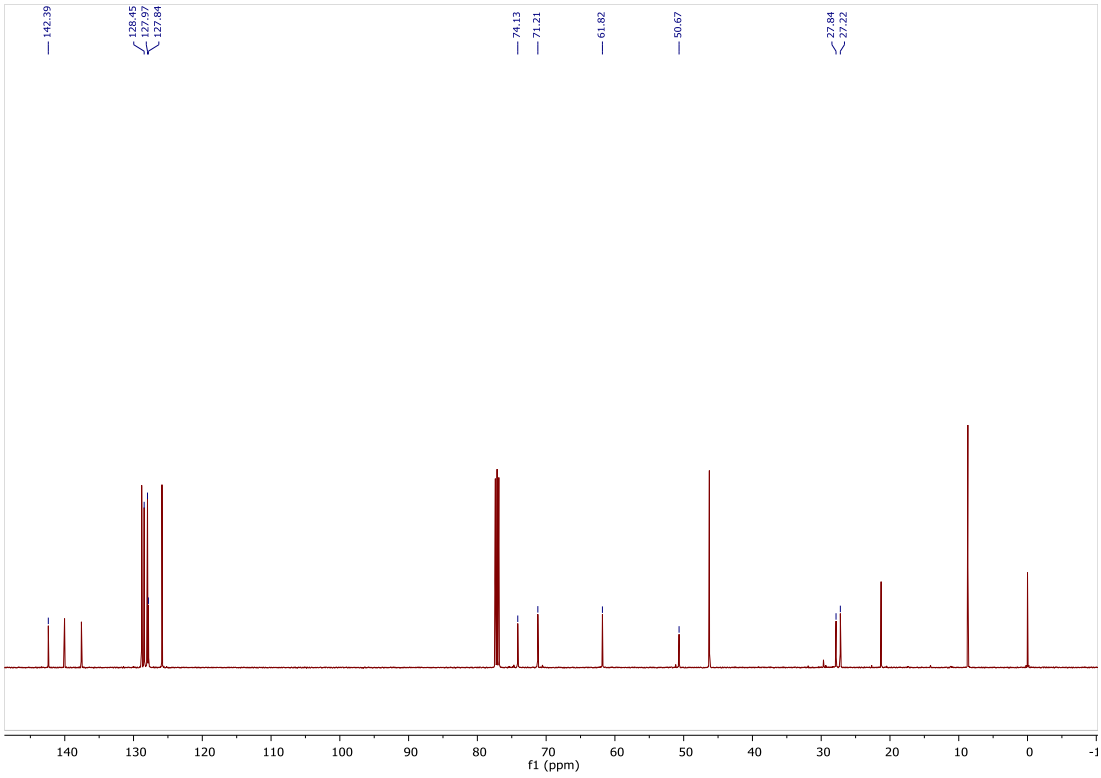
Compound 220





Compound 221




142.39
128.45
127.97
127.84
74.13
71.21
61.82
50.67
27.84
27.22
140
130
120
110
100
90
80
70
60
50
40
30
20
10
0
f1 (ppm)